THE 22TH EUROPEAN MODELING & SIMULATION SYMPOSIUM

OCTOBER 13-15 2010
FES, MOROCCO

EDITED BY
AGOSTINO BRUZZONE
CLAUDIA FRYDMAN
FRANCESCO LONGO
KHALID MEKOUAR
MIQUEL ANGEL PIERA

PRINTED IN FES, OCTOBER 2010

ISBN 2-9524747-8-8
EAN 9782952474788

THE 22TH EUROPEAN MODELING & SIMULATION SYMPOSIUM

OCTOBER 13-15 2010

FES, MOROCCO

ORGANIZED BY

DIPTEM – UNIVERSITY OF GENOA

LIOPHANT SIMULATION

ECOLE SUPERIEURE D'INGENIERIE EN SCIENCES APPLIQUEES

UNIVERSITY OF AIX-MARSEILLE - LSIS MARSEILLE

MECHANICAL DEPARTMENT, UNIVERSITY OF CALABRIA

MSC-LES, MODELING & SIMULATION CENTER, LABORATORY OF ENTERPRISE SOLUTIONS

LOGISIM – AUTONOMOUS UNIVERSITY OF BARCELONA

SPONSORED BY

ACADEMIC, INSTITUTES, INDUSTRY AND SOCIETIES SPONSORS

SIMULATION TEAM

MISS – MCLEOD INSTITUTE OF SIMULATION SCIENCE

M&SNET – MODELING & SIMULATION NETWORK

IMCS – INTERNATIONAL MEDITERRANEAN & LATIN AMERICAN COUNCIL OF SIMULATION

UNIVERSITY OF LA LAGUNA

MISS LATVIAN CENTER – RIGA TECHNICAL UNIVERSITY

LOGISIM, MISS SPANISH CENTER - UAB

UNIVERSITY OF PERUGIA

MAST – MANAGEMENT AND ADVANCED SOLUTIONS AND TECHNOLOGIES

LAMCE, UFRJ

CIFASIS: CONICET - UNR - UPCAM

EDITORS

AGOSTINO BRUZZONE
MISS-DIPTEM, UNIVERSITY OF GENOA
VIA OPERA PIA 15
16145 GENOVA, ITALY
agostino@itim.unige.it
http://st.itim.unige.it

CLAUDIA FRYDMAN
LSIS - LABORATOIRE DES SCIENCES DE L'INFORMATION ET DES SYSTEMES
UNIVERSITE AIX-MARSEILLE (U3)
DOMAINE UNIVERSITAIRE DE SAINT-JEROME, AVENUE ESCADRILLE NORMANDIE-NIEMEN,
13397 MARSEILLE CEDEX 20, FRANCE
claudia.frydman@lsis.org
www.lsis.org

FRANCESCO LONGO
MSC-LES, MODELING & SIMULATION CENTER – LABORATORY OF ENTERPRISE SOLUTIONS
MECHANICAL DEPARTMENT
UNIVERSITY OF CALABRIA
VIA P. BUCCI – 87036, RENDE (CS), ITALY
flongo@unical.it
www.msc-les.org

KHALID MEKOUAR
ECOLE SUPERIEURE D'INGENIERIE EN SCIENCES APPLIQUEES
29 BIS AV IBN KHATIB ROUTE D'IMMOUZZER
FES, MOROCCO
k.mekouar@esisa.ma
http://esisa.ac.ma/

MIQUEL ANGEL PIERA
LOGISIM, DEPARTMENT OF TELECOMUNICATIONS AND SYSTEM ENGINEERING
UNIVERSITY AUTONOMOUS OF BARCELONA
08193- BELLATERRA- SPAIN
MiquelAngel.Piera@uab.es
www.uab.es

THE INTERNATIONAL MEDITERRANEAN AND LATIN AMERICAN MODELING MULTICONFERENCE, I3M 2010

GENERAL CO-CHAIRS

AGOSTINO BRUZZONE, *MISS DIPTEM, UNIVERSITY OF GENOA, ITALY*
CLAUDIA FRYDMAN, *LSIS, UNIVERSITY OF AIX-MARSEILLE, FRANCE*

PROGRAM CHAIR

KHALID MEKOUAR, *ESISA, MOROCCO*
MIQUEL ANGEL PIERA, *AUTONOMOUS UNIVERSITY OF BARCELONA, SPAIN*

THE 22TH EUROPEAN MODELING & SIMULATION SYMPOSIUM, EMSS 2010

GENERAL CO-CHAIRS

FRANCESCO LONGO, *MSC-LES, UNIVERSITY OF CALABRIA, ITALY*
MIQUEL ANGEL PIERA, *AUTONOMOUS UNIVERSITY OF BARCELONA, SPAIN*

PROGRAM CO-CHAIRS

AGOSTINO BRUZZONE, *MISS DIPTEM, UNIVERSITY OF GENOA, ITALY*
CLAUDIA FRYDMAN, *LSIS, UNIVERSITY OF AIX-MARSEILLE*

EMSS 2010 International Program Committee

Michael Affenzeller, *Upper Austrian Univ. of AS, Austria*
Rosa Mª Aguilar, *University of La Laguna, Spain*
Andreas Beham, *Upper Austrian Univ. of AS, Austria*
Enrico Bocca, *Liophant Simulation, Italy*
Yeray Callero, *University of la Laguna, Spain*
Agostino Bruzzone, *University of Genoa, Italy*
Iván Castilla Rodriguez, *University of La Laguna, Spain*
Antonio Cimino, *MSC-LES*, *University of Calabria, Italy*
Idalia Flores, *National Autonomous Univ. of Mexico, Mexico*
Claudia Frydman, *LSIS, France*
Toni Guasch, *UPC, Spain*
Witold Jacak, *Upper Austrian Univ. of AS, Austria*
Emilio Jiménez, University of la Rioja, Spain
Francesco Longo, *MSC-LES, University of Calabria, Italy*
Marina Massei, *Simulationteam, Italy*
Yuri Merkuryev, *Riga Technical University, Latvia*
Giovanni Mirabelli, *University of Calabria, Italy*
Roberto Muñoz González, *University of La Laguna, Spain*
Mercedes Elizabeth Narciso, *UAB, SPain*
Tudor Niculiu, *University of Bucharest, Romania*
Tuncer Ören, M&SNet, *University of Ottawa, Canada*
Mercedes Perez, University of la Rioja, Spain
Miquel Angel Piera, *UAB, Spain*
Cesar de Prada, *Universidad de Valladolid, Spain*
Juan Jose Ramos, *UAB, Spain*
José L. Risco-Martín, Complutense Univ. of Madrid, Spain
Stefano Saetta, *University of Perugia, Italy*
Alberto Tremori, *Simulationteam, Italy*
Levent Yilmaz, *Auburn University, USA*
Stefan Wagner, *Upper Austrian Univ. of AS, Austria*
Gabriel Wainer, *Carleton University, Canada*
Ann Wellens, National Autonomous Univ. of Mexico, Mexico

Tracks and Workshop Chairs

Workshop on Soft Computing and Modeling & Simulation
Chairs: Witold Jacak, Michael Affenzeller**,** *Upper Austrian University of Applied Sciences, (Austria)*

Continous and Hybrid Simulation
Chair: Cesar De Prada, *Universidad de Valladolid, (Spain)*

Industrial Engineering
Chair: Giovanni Mirabelli, MSC-LES, University of Calabria, Italy

Agent Directed Simulation
Chairs: Tuncer Ören, *University of Ottawa (Canada)*; Levent Yilmaz, *Auburn University (USA)*

Simulation and Artificial Intelligence
Chair: Tudor Niculiu, *University "Politehnica" of Bucharest, (Romania)*

Modeling & Simulation with Petri Nets
Chair: Emilio Jiménez, University of La Rioja (Spain)

DEVS Modelling & Simulation
Chairs: Gabriel Wainer, *Carleton University (Canada), José L. Risco-Martín, Universidad Complutense de Madrid (Spain)*

Optimization Methods and Simulation Tools for Dynamic Systems
Chairs: Idalia Flores, Universidad Nacional Autónoma de México (Mexico); Ann Wellens, Universidad Nacional Autónoma de México (Mexico)

CHAIRS' MESSAGE

WELCOME TO EMSS 2010

Building on the long success of 21 editions, the 22nd European Modeling & Simulation Symposium (also known since 1996 as "Simulation in Industry") is an important forum to discuss theories, practices and experiences on M&S (Modelling & Simulation).

EMSS 2010 brings together people from Academia, Agencies and Industries from all over the world, despite the Symposium name refers just to Europe; in fact EMSS 2010 represents an unique opportunity within I3M2010 framework to share experiences and ideas and to generate a new archival source for innovative papers on M&S-related topics.

The Symposium is also meant to provide information, identify directions for further research and to be an ongoing framework for knowledge sharing; the structure of the conferences, strongly based on Tracks, allows synergies among different groups keeping pretty sharp each framework to be created. The quality of the papers is the stronghold of this event and even this year it was possible to apply severe selection on the submissions and to guarantee top level papers.

Another strong feature for the edition 2010 of EMSS is the venue: in fact the event is located in the beautiful and historic city of Fes, one of four "imperial cities" (with Marrakech, Meknes and Rabat, and the largest existing Medina in the world).

The EMSS 2010 Program, Presentations, People and Place make it a professionally worthwhile and a personally enjoyable experience: so welcome to EMSS 2010

Miquel Angel Piera, Autonomous University of Barcelona, Spain

Claudia Frydman, LSIS, Marseille, France

ACKNOWLEDGEMENTS

The EMSS 2010 International Program Committee selected the papers for the Conference among many submissions and we expected a very successful event based on their efforts; so we would like to thank all the authors as well as the IPCs and reviewers for their review process.
A special thank to the organizations, institutions and societies that are supporting and technically sponsoring the event: University of Genoa, Liophant Simulation, Ecole Supérieure d'Ingénierie en Sciences Appliquées, University of Aix-Marseille, Autonomous University of Barcelona, University of Calabria, Modeling & Simulation Center – Laboratory of Enterprise Solutions (MSC-LES), McLeod Institute of Simulation Science (MISS), Modeling & Simulation Network (M&SNet), International Mediterranean & Latin American Council of Simulation (IMCS), Management and Advanced Solutions and Technologies (MAST). Finally, we would like to thank all the Conference Organization Supporters.

Table of Contents

Soft Computing and Modelling & Simulation

FEATURE SELECTION IN THE ANALYSIS OF TUMOR MARKER DATA USING EVOLUTIONARY ALGORITHMS

Stephan M. Winkler [(a)], Michael Affenzeller [(b)], Gabriel Kronberger [(c)], Michael Kommenda [(d)], Stefan Wagner [(e)], Witold Jacak [(f)], Herbert Stekel [(g)]

[(a – f)] Upper Austria University of Applied Sciences
School for Informatics, Communications, and Media
Heuristic and Evolutionary Algorithms Laboratory
Softwarepark 11, 4232 Hagenberg, Austria

[(g)] General Hospital Linz
Central Laboratory
Krankenhausstraße 9, 4021 Linz, Austria

[(a)] stephan.winkler@fh-hagenberg.at, [(b)] michael.affenzeller@fh-hagenberg.at , [(c)] gabriel.kronberger@fh-hagenberg.at, [(d)] michael.kommenda@fh-hagenberg.at, [(e)] stefan.wagner@fh-hagenberg.at, [(f)] witold.jacak@fh-hagenberg.at , [(g)] herbert.stekel@akh.linz.at

ABSTRACT
In this paper we describe the use of evolutionary algorithms for the selection of relevant features in the context of tumor marker modeling. Our aim is to identify mathematical models for classifying tumor marker values AFP and CA 15-3 using available patient parameters; data provided by the General Hospital Linz are used. The use of evolutionary algorithms for finding optimal sets of variables is discussed; we also define fitness functions that can be used for evaluating feature sets taking into account the number of selected features as well as the resulting classification accuracies.

In the empirical section of this paper we document results achieved using an evolution strategy in combination with several machine learning algorithms (linear regression, k-nearest-neighbor modeling, and artificial neural networks) which are applied using cross-validation for evaluating sets of selected features. The identified sets of relevant variables as well as achieved classification rates are compared.

Keywords: Evolutionary Algorithms, Medical Data Analysis, Tumor Marker Modeling, Data Mining, Machine Learning, Classification, Statistical Analysis

1. INTRODUCTION AND SCIENTIFIC GOALS

In general, tumor markers are substances found in humans (especially blood and / or body tissues) that can be used as indicators for certain types of cancer. There are several different tumor markers which are used in oncology to help detect the presence of cancer; elevated tumor marker values can indicate the presence of cancer, but there can also be other causes. As a matter of fact, elevated tumor marker values themselves are not diagnostic, but rather only suggestive; tumor markers can be used to monitor the result of a treatment (as for example chemotherapy). Literature discussing tumor markers, their identification, their use, and the application of data mining methods for describing the relationship between markers and the diagnosis of certain cancer types can be found for example in (Koepke, 1992) (where an overview of clinical laboratory tests is given and different kinds of such test application scenarios as well as the reason of their production are described) and (Yonemori et al., 2006).

The general goal of the research work described here is to identify models for estimating selected tumor marker values on the basis of routinely available blood values; in detail, estimators for the tumor markers AFP and CA 15-3 have been identified. The documented tumor marker values are classified as “normal”, “slightly elevated”, “highly elevated”, and “beyond plausible”; our goal is to design classifiers for the 2-class-classification problem classifying samples into “normal” vs. “elevated”, “highly elevated”, or “beyond plausible”.

In the research work reported on in this paper we use evolutionary algorithms for optimizing the selection of features that are used by machine learning algorithms for modeling the given target values. This approach is closely related to the method described in (Alba, García-Nieto, Jourdan, and Talbi 2007) where the authors compared the use of a particle swarm optimization (PSO) and a genetic algorithm (GA), both augmented with support vector machines, for the classification of high dimensional microarray data.

2. DATA BASE

Data of thousands of patients of the General Hospital (AKH) Linz, Austria, have been analyzed in order to identify mathematical models for tumor markers. We have used a medical data base compiled at the Central

Laboratory of the General Hospital Linz, Austria, in the years 2005 – 2008: 28 routinely measured blood values of thousands of patients are available as well as several tumor markers; not all values are measured for all patients, especially tumor marker values are determined and documented if there are indications for the presence of cancer.

The blood data measured at the AKH in the years 2005-2008 have been compiled in a data base storing each set of measurements (belonging to one patient): Each sample in this data base contains an unique ID number of the respective patient, the date of the measurement series, the ID number of the measurement, and several other clinical parameters; standard blood parameters are stored as well as tumor marker values. Data that could identify patients uniquely (as for example name, date of birth, …) where at no time available to the authors except the head of the laboratory.

In total, information about 20,819 patients is stored in 48,580 samples. Please note that of course not all values are available in all samples; there are many missing values simply because not all blood values are measured during each examination.

In (Winkler, Affenzeller, Jacak, and Stekel 2010) the authors give further details about the data used in the research work described here; background information about the blood parameters given in the following two subsections as well as references to important literature on these clinical parameters can be found there, too.

2.1. Input Data

The following features are available in the AKH data base and are potential inputs for modeling the given tumor marker values: ALT (lanine transaminase), AST (aspartate transaminase), BSG1 (the erythrocyte sedimentation rate), BUN (blood urea nitrogen), CBAA (basophil granulocytes), CEOA (eosinophil granulocytes), CH37 (cholinesterase), CHOL (cholesterol), CLYA (lymphocytes), CMOA (monocytes), CNEA (neutrophils), CRP (c-reactive protein), FE (iron), FER (ferritin), GT37 (γ-glutamyltransferase), HB (hemoglobin), HDL (high-density lipoprotein), HKT (hematocrit), HS (uric acid), KREA (creatinine), LD37 (lactate dehydrogenase) MCV (mean corpuscular / cell volume), PLT (thrombocytes), RBC (erythrocytes), TBIL (bilirubin), TF (transferring), WBC (leukocytes), and finally the age and the sex of the patients.

2.2. Target Data

In addition to the features listed in the previous section, the following tumor markers are also documented in the AKH data base: AFP (alpha-fetoprotein), CA 125 (cancer antigen 125), CA 15-3 (mucin 1), CEA (carcinoembryonic antigen), CYFRA (fragments of cytokeratin 19), and PSA (prostate-specific antigen).

The two tumor markers analyzed in this work can be described in the following way:

- ***AFP:*** Alpha-fetoprotein is a protein found in the blood plasma; during fetal life it is produced by the yolk sac and the liver. For example, AFP values of pregnant women can be used in screening tests for developmental abnormalities as increased values might for example indicate open neural tube defects, decreased values might indicate Down syndrome. AFP is also often measured and used as a marker for a set of tumors, especially endodermal sinus tumors (yolk sac carcinoma), neuroblastoma, hepatocellular carcinoma, and germ cell tumors (Duffy and Crown, 2008).
- ***CA 15-3:*** Mucin 1 (MUC1), also known as cancer antigen 15-3 (CA 15-3), is a protein found in humans; it is used as a tumor marker in the context of monitoring certain cancers (Niv, 2008), especially breast cancer.

2.3. Data Preprocessing

Before analyzing the data and using them for training classifiers we have preprocessed the available data:

First, all variables have been linearly scaled to the interval [0;1]: For each variable v_i, the (predefined) minimum value min_i is subtracted from all contained values and the result divided by the difference between min_i and the (also predefined) maximum plausible value $maxplau_i$; all values greater than the given maximum plausible value are replaced by 1.0. Then, all samples belonging to the same patient with not more than one day difference with respect to the measurement data have been merged. This has been done in order to decrease the number of missing values in the data matrix. In rare cases, more than one value might thus be available for a certain variable; in such a case, the first value is used.

Additionally, all measurements have been sample-wise re-arranged and clustered according to the patients' IDs; this has been done in order to prevent data of certain patients being included in the training as well as in the test data.

Before using modeling algorithms for training classifiers we have compiled separate data sets for each analyzed target tumor marker tm_i: First, all samples containing measured values for tm_i are extracted. Second, all variables are removed from the resulting data set that contain values in less than 80% of the remaining samples. Third, all samples are removed that still contain missing values. This procedure results in a specialized data set $dstm_i$ for each tumor marker tm_i.

Details about these data preprocessing steps can be found in (Winkler, Affenzeller, Jacak, and Stekel 2010).

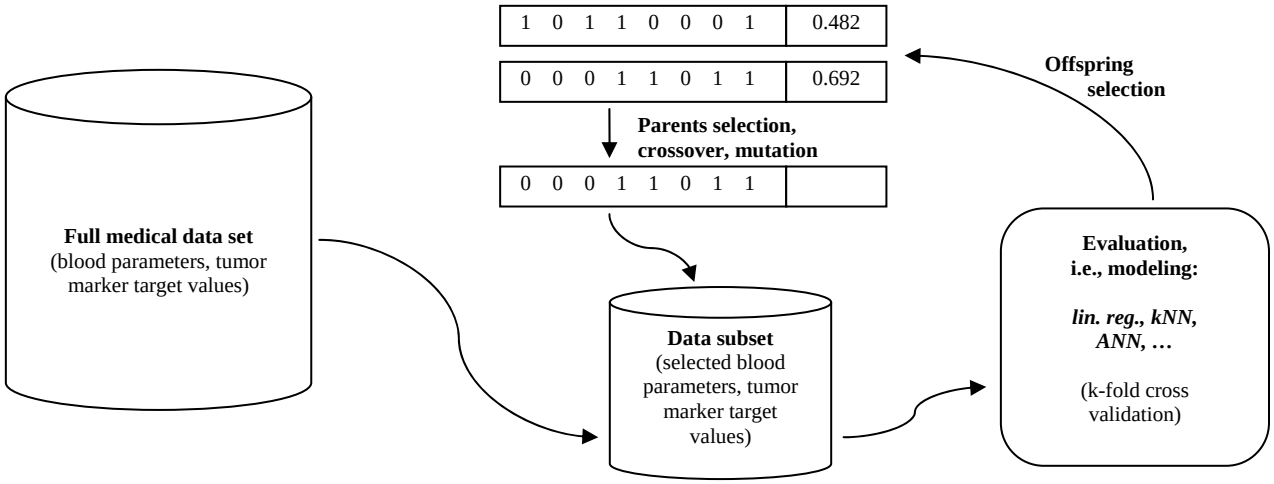

Figure 1: A hybrid evolutionary algorithm for feature selection in the context of tumor marker modeling. Machine learning algorithms are applied for evaluating feature sets.

3. MODELING APPROACH

As for example discussed in detail in (Alba, García-Nieto, Jourdan, and Talbi 2007), feature selection is often considered an essential step in data analysis as this method can reduce the dimensionality of the datasets and often conducts to better analyses.

Given a set of features $F = \{f_1, f_2, \ldots, f_n\}$, our goal here is to find a subset $F' \subseteq F$ that is on the one hand as small as possible and on the other hand allows modeling methods to identify models that estimate given target values as well as possible. This implies that we have to deal with a tradeoff situation as in most cases we will see that more complex models (i.e., models using more features) show better fit on data.

This optimization approach is schematically shown in Figure 1.

The fitness of a feature selection F_k is calculated in the following way: We use a machine learning method (linear regression, k-nearest-neighbor modeling, artificial neural networks, SVMs, or any other kind of training algorithm) for estimating predicted target values est_k and compare those to the original target values *orig*; the *coefficient of determination* (R^2) function is used for calculating the quality of the estimated values, i.e., we calculate the quality of the model produced using F_k, $r^2(F_k)$: $r^2(F_k) = r^2(est_k,orig)$. Additionally, we also calculate the ratio of selected features a as $a(F_k,F) = ||F_k||/||F||$. Finally, using a weighting factor α, we calculate the fitness of the set of features F_k:

$$fitness(F_k) = \alpha * a(F_k,F) + (1- \alpha) * (1-r^2(F_k)) \quad (1)$$

As an alternative to the coefficient of determination function we can also use a classification specific function that calculates the ratio of correctly classified samples, either in total or as the average of all classification accuracies of the given classes (as for example described in (Winkler 2009), Section 8.2):

For all samples that are to be considered we know the original classifications *origClass*, and using (predefined or dynamically chosen) thresholds we get estimated classifications $estClass_k$ for estimated target values est_k (calculated using features set F_k). The total classification accuracy ca_k is calculated as

$$ca(F_k) = ||\{j: estClass_k[j] = origClass[j]\}|| / ||estClass|| \quad (2)$$

Class-wise classification accuracies *cwca* are calculated as the average of all classification accuracies for each given class $c \in C$, $ca_{k,c}$, separately:

$$ca_{k,c} = ||\{j: estClass_k[j] = origClass[j] \; \& \; origClass[j] = c\}|| / ||j: origClass[j] = c|| \quad (3)$$

$$cwca(F_k) = \Sigma_{c \in C}(ca_{k,c}) / ||C|| \quad (4)$$

We can now define the classification specific fitness of feature selection Fk as

$$fitness_{class}(F_k) = \alpha * a(F_k,F) + (1- \alpha) * (1-ca(F_k)) \quad (5)$$

or

$$fitness_{class}(F_k) = \alpha * a(F_k,F) + (1- \alpha) * (1-cwca(F_k)) \quad (6)$$

We use evolutionary algorithms for search for solutions that minimize the given fitness functions. Evolutionary algorithms are used for generating solutions consisting of bit vectors b_j, where $b_j(m)$ denotes whether variable m is used by solution candidate j or not. This rather simple definition of solution candidates enables the use of standard genetic operators for crossover and mutation of bit vectors: We use uniform, single point, and 2-point crossover operators for binary vectors and bit flip mutation that flips each of the given bits with a given probability. Explanations of these operators can for example be found in (Holland 1975) and (Eiben and Smith, 2003).

We have implemented and tested several EAs for guiding the search for optimal feature sets, especially evolution strategies (ES) (Rechenberg 1973; Schwefel 1994) and genetic algorithms (GAs) (Holland 1975).

When applying the ES based approach, populations consisting of μ individuals are used; in each generation, λ children are generated using random parent selection, recombination (which is optional) and mutation, and then the μ best solutions (selected from

the children, if the *comma* strategy is chosen, or from parents and children, if the *plus* strategy is chosen) become the next generation's members. Additionally, the ratio of successful mutations (i.e., mutations that lead to an improvement of the solutions' qualities) is monitored; if this ratio is less than 1/5, then the mutation operator's flip probability is (in our implementation) multiplied by 0.9, and if it is greater than 1/5, then it is divided by 0.9.

The GA approaches used in the authors' research work include the application of parents selection (proportional or linear rank, e.g.), crossover, and mutation. Optionally, offspring selection can also be applied: After generating new solutions by crossover and mutation, these new solutions are inserted into the next generation's population only if they are better than their parents. Details about this procedure can for example be found in (Affenzeller, Winkler, Wagner, and Beham 2009).

4. IMPLEMENTATION

The approach described in this paper (including the evolutionary algorithms used for optimizing feature selection as well as the machine learning methods used for evaluating feature sets) have been implemented using the HeuristicLab (HL) framework (http://www.heuristiclab.com; (Wagner 2009)), a framework for prototyping and analyzing optimization techniques for which both generic concepts of evolutionary algorithms and many functions to evaluate and analyze them are available; we have used these implementations for producing the results summarized in the following section.

5. EMPIRICAL TESTS AND RESULTS

5.1. Test Series Setup

In this section we document modeling results for tumor markers AFP and CA 15-3. We have applied the evolutionary modeling and feature selection approach described in Section 3 using an (10+100) evolution strategy (without recombination, only using mutation); the number of evaluations (of the ES algorithm) was for some test runs limited to 1,000 and for others to 10,000, and the parameter α (which weights the ratio of selected features, see Section 3) was in some cases set to 0.2 and in other to 0.5. Initially, each feature was selected by each solution candidate with 20% probability. When mutating a solution candidate, the initial bit flip probability (i.e., the probability of changing the information about using a certain feature) for each feature was set to 0.5, and this bit flip probability was (as described in Section 3) modified with respect to success ratio; the minimum value for the bit flip probability was set to 0.1.

We have tested each algorithm setting 5 times using different machine learning algorithms (with varying algorithm specific parameter settings); 5-fold cross validation was applied. Linear regression (linReg), k-nearest-neighbor (kNN) learning, and artificial neural networks (ANNs) have been used as machine learning algorithms; details about their implementation in HL can for example be found in (Winkler, Affenzeller, Jacak, and Stekel 2010). The number of neighbors (*k*) considered in kNN classification was varied and set to 3, 5, and 10, respectively; for training ANNs the number of hidden nodes was set to 10, and 30% of the available training samples were used as validation set, i.e., the network that performed best on validation samples was eventually presented as result of the learning process.

For evaluating modeling results, the fitness function (1) given in Section 3 was used. In the following subsections we summarize the results documented for these test parameters; for each tumor marker and each modeling scenario we list the input features selected by the evolutionary process (features not selected in each test run are given in brackets) as well as average best fitness values (which are used by the evolutionary algorithm and are calculated using validation samples) and test classification accuracies (i.e., the ratios of correctly classified samples that were not considered during the learning process).

5.2. Test Results for AFP

Table 1: Results for AFP (linReg; $\alpha = 0.2$)

Evaluations	Selected features	Best fitness	Avg. test accuracy
1,000	(AGE), AST, (CH37), (HKT), (KREA), (PLT),	0.6867	80.73%
10,000	AST, CH37, (HKT)	0.6677	80.33%

Table 2: Results for AFP (kNN; $\alpha = 0.2$)

k	Evaluations	Selected features	Best fitness	Avg. test accuracy
3	1,000	(AGE), AST, CH37, GT37, HB, (HKT), (PLT), (TBIL), (WBC)	0.8574	78.38%
	10,000	AST, CH37, (HKT), (WBC)	0.8226	77.93%
5	1,000	AST, (BUN), CH37, GT37, (HB), (TBIL)	0.7822	79.02%
	10,000	AST, (BUN), CH37, GT37, (HB)	0.7687	79.30%
10	1,000	AST, (BUN), CH37, (HB)	0.7149	80.87%
	10,000	AST, (BUN), CH37, (HB)	0.7149	80.03%

Table 3: Results for AFP (ANN; $\alpha = 0.2$)

Evaluations	Selected features	Best fitness	Avg. test accuracy
1,000	AST, CH37, (HKT)	0.6482	82.54%
10,000	AST, CH37	0.6475	82.49%

Table 4: Results for AFP (linReg; $\alpha = 0.5$)

Evaluations	Selected features	Best fitness	Avg. test accuracy
1,000	AST, (CH37), (HB), (PLT)	0.4636	79.24%
10,000	AST	0.4556	78.91%

Table 5: Results for AFP (kNN; $\alpha = 0.5$)

k	Evalu-ations	Selected features	Best fitness	Avg. test accuracy
3	1,000	AST	0.5872	75.90%
	10,000	AST	0.5872	75.90%
5	1,000	AST	0.5289	77.86%
	10,000	AST	0.5289	77.86%
10	1,000	AST, (CH37), (HKT), (WBC)	0.5385	79.93%
	10,000	AST	0.5055	78.84%

Table 6: Results for AFP (ANN; $\alpha = 0.5$)

Evalu-ations	Selected features	Best fitness	Avg. test accuracy
1,000	AST	0.4384	79.53%
10,000	AST	0.4384	79.53%

5.3. Test Results for CA 15-3

Table 7: Results for CA 15-3 (linReg; $\alpha = 0.2$)

Evalu-ations	Selected features	Best fitness	Avg. test accuracy
1,000	(AGE), AST, (CH37), (HKT), (KREA), (PLT),	0.6867	80.73%
10,000	AST, CH37	0.6677	80.33%

Table 8: Results for CA 15-3 (kNN; $\alpha = 0.2$)

k	Evalu-ations	Selected features	Best fitness	Avg. test accuracy
3	1,000	(AST), (BUN), (CEOA), (CMOA), (CNEA), (HKT), LD37	0.8979	67.90%
	10,000	(AST), (BUN), (CEOA), (CNEA), (HKT), LD37	0.8847	67.73%
5	1,000	(CEOA), (CMOA), (CRP), (GT37), (HKT), LD37, (WBC)	0.8149	70.44%
	10,000	(CEOA), (CMOA), (CRP), (HB), LD37	0.8104	70.23%
10	1,000	(BUN), (CEOA), (CMOA), (CRP), (HB), (HKT), LD37	0.7568	72.01%
	10,000	(BUN), (CEOA), (CMOA), (CRP), (HB), (HKT), LD37	0.7522	71.37%

Table 9: Results for CA 15-3 (ANN; $\alpha = 0.2$)

Evalu-ations	Selected features	Best fitness	Avg. test accuracy
1,000	(AST), (CBAA), (CNEA), HB, LD37, (GT37), (PLT), (SEX)	0.7030	73.91%
10,000	(AST), (CNEA), (GT37), (HB), LD37	0.6793	73.18%

Table 10: Results for CA 15-3 (linReg; $\alpha = 0.5$)

Evalu-ations	Selected features	Best fitness	Avg. test accuracy
1,000	AST, (CH37), (HB), (PLT)	0.4636	79.24%
10,000	AST	0.4556	78.91%

Table 11: Results for CA 15-3 (kNN; $\alpha = 0.5$)

k	Evalu-ations	Selected features	Best fitness	Avg. test accuracy
3	1,000	(CMOA), (HKT), LD37	0.6196	65.80%
	10,000	(CMOA), (HKT), LD37	0.5878	65.45%
5	1,000	(CMOA), (HKT), (CRP), (LD37)	0.5860	65.97%
	10,000	(CMOA), (HKT), (CRP), (LD37)	0.5731	65.23%
10	1,000	(CEOA), (CEA), (GT37), LD37, (RBC)	0.5602	70.46%
	10,000	(CEOA), (GT37), LD37, (RBC)	0.5488	70.21%

Table 12: Results for CA 15-3 (ANN; $\alpha = 0.5$)

Evalu-ations	Selected features	Best fitness	Avg. test accuracy
1,000	(LD37), (AST), (HB)	0.4863	70.94%
10,000	AST, HB	0.4674	72.35%

6. CONCLUSIONS AND OUTLOOK

From the tables given in Section 5 we see that in most cases rather small feature sets are sufficient for achieving satisfying classification results: The test classification accuracies documented here are in most cases comparable to those summarized in (Winkler, Affenzeller, Jacak, and Stekel 2010); as expected, the best classifiers are here produced using ANNs. Obviously, setting α=0.5 leads to very strong parsimony pressure, whereas setting α=0.2 seems to be the better choice as it leads to better classification results using only comparably small feature sets. Furthermore, we also see that the test results documented after 1,000 evaluations are in many cases better than those documented after 10,000 evaluations.

On the one hand, future work should deal with the identification of feature sets and models for other tumor markers which are already available in the data based used in this research work; on the other hand, the authors will also try to identify estimation models for tumor diagnoses based on tumor marker information as well as standard blood parameters.

ACKNOWLEDGMENTS

The work described in this paper was done within the Josef Ressel Centre for Heuristic Optimization *Heureka!* (http://heureka.heuristiclab.com/) sponsored by the Austrian Research Promotion Agency (FFG).

REFERENCES

Affenzeller, M., Winkler, S., Wagner, S., A. Beham, 2009. *Genetic Algorithms and Genetic Programming - Modern Concepts and Practical Applications*. Chapman & Hall/CRC. ISBN 978-1584886297. 2009.

Alba, E., García-Nieto, J., Jourdan, L., Talbi, E.-G., 2005. Gene selection in cancer classification using PSO/SVM and GA/SVM hybrid algorithms. *IEEE Congress on Evolutionary Computation 2007*, pp. 284 – 290.

Duffy, M. J. and Crown, J., 2008. A personalized approach to cancer treatment: how biomarkers can help. *Clinical Chemistry*, 54(11), pp. 1770–1779

Eiben, A.E. and Smith, J.E. 2003. Introduction to Evolutionary Computation. *Natural Computing Series*, Springer-Verlag Berlin Heidelberg.

Holland, J.H., 1975. *Adaption in Natural and Artifical Systems.* University of Michigan Press.

Koepke, J.A., 1992. Molecular marker test standardization. *Cancer*, 69, pp. 1578–1581.

Niv, Y., 2008. Muc1 and colorectal cancer pathophysiology considerations. *World Journal of Gastroenterology*, 14(14), pp. 2139–2141.

Rechenberg, I., 1973. *Evolutionsstrategie.* Friedrich Frommann Verlag.

Schwefel, H.-P., 1994. *Numerische Optimierung von Computer-Modellen mittels der Evolutions-strategie.* Basel: Birkhäuser Verlag.

Wagner, S., 2009. *Heuristic Optimization Software Systems - Modeling of Heuristic Optimization Algorithms in the HeuristicLab Software Environment*. PhD Thesis, Institute for Formal Models and Verification, Johannes Kepler University Linz, Austria.

Winkler, S., Affenzeller, M., Jacak, W., Stekel, H., 2010. Classification of Tumor Marker Values Using Heuristic Data Mining Methods. *Proceedings of Genetic and Evolutionary Computation Conference 2010, Workshop on Medical Applications of Genetic and Evolutionary Computation*, pp. 1915–1922.

Winkler, S., 2009. *Evolutionary System Identification - Modern Concepts and Practical Applications.* Schriften der Johannes Kepler Universität Linz, Reihe C: Technik und Naturwissenschaften. Universitätsverlag Rudolf Trauner. ISBN 978-3-85499-569-2.

Yonemori, K., Ando, M., Taro, T. S., Katsumata, N., Matsumoto, K., Yamanaka, Y., Kouno, T., Shimizu, C., Fujiwara, Y., 2006. Tumor-marker analysis and verification of prognostic models in patients with cancer of unknown primary, receiving platinum-based combination chemotherapy. *Journal of Cancer Research and Clinical Oncology*, 132(10), pp. 635–642.

AUTHORS BIOGRAPHIES

STEPHAN M. WINKLER received his PhD in engineering sciences in 2008 from Johannes Kepler University (JKU) Linz, Austria. His research interests include genetic programming, nonlinear model identification and machine learning. Since 2009, Dr. Winkler is professor at the Department for Medical and Bioinformatics at the Upper Austria University of Applied Sciences (UAS), Campus Hagenberg.

MICHAEL AFFENZELLER has published several papers, journal articles and books dealing with theoretical and practical aspects of evolutionary computation, genetic algorithms, and meta-heuristics in general. In 2001 he received his PhD in engineering sciences and in 2004 he received his habilitation in applied systems engineering, both from the Johannes Kepler University of Linz, Austria. Michael Affenzeller is professor at UAS, Campus Hagenberg, and head of the Josef Ressel Center *Heureka!* at Hagenberg.

GABRIEL KRONBERGER is a research associate at the UAS Research Center Hagenberg. His research interests include genetic programming, machine learning, and data mining and knowledge discovery. Currently he works on practical applications of data-based modeling methods for complex systems within *Heureka!*.

MICHAEL KOMMENDA finished his studies in bioinformatics at Upper Austria University of Applied Sciences in 2007. Currently he is a research associate at the UAS Research Center Hagenberg working on data-based modeling algorithms for complex systems within *Heureka!*.

STEFAN WAGNER received his PhD in engineering sciences in 2009 from JKU Linz, Austria; he is professor at the Upper Austrian University of Applied Sciences (Campus Hagenberg). Dr. Wagner's research interests include evolutionary computation and heuristic optimization, theory and application of genetic algorithms, and software development.

WITOLD JACAK received his PhD in electric engineering in 1977 from the Technical University Wroclaw, Poland, where he was appointed Professor for Intelligent Systems in 1990. Since 1994 Prof. Jacak is head of the Department for Software Engineering at the Upper Austrian University of Applied Sciences (Campus Hagenberg) where he currently also serves as Dean of the School of Informatics, Communications and Media.

HERBERT STEKEL received his MD from the University of Vienna in 1985. Since 1997 Dr. Stekel is chief physician at the General Hospital Linz, Austria, where Dr. Stekel serves as head of the central laboratory.

PREDICTION OF BLOOD DEMANDS IN A HOSPITAL

Christian Fischer [(a)], Lukas Bloder [(b)], Christoph Neumüller [(c)], Sebastian Pimminger [(d)], Michael Affenzeller [(e)], Stephan M. Winkler [(f)], Herbert Stekel [(g)], Rupert Frechinger [(h)]

[(a – f)] Upper Austria University of Applied Sciences
School for Informatics, Communications, and Media
Heuristic and Evolutionary Algorithms Laboratory
Softwarepark 11, 4232 Hagenberg, Austria

[(g – h)] General Hospital Linz
[(g)] Central Blood Laboratory / [(h)] Medical Controlling
Krankenhausstraße 9, 4021 Linz, Austria

[(a)] christian.fischer@students.fh-hagenberg.at, [(b)] lukas.bloder@students.fh-hagenberg.at,
[(c)] christoph.neumueller@students.fh-hagenberg.at, [(d)] sebastian.pimminger@students.fh-hagenberg.at,
[(e)] michael.affenzeller@fh-hagenberg.at, [(f)] stephan.winkler@fh-hagenberg.at,
[(g)] herbert.stekel@akh.linz.at, [(h)] rupert.frechinger@akh.linz.at

ABSTRACT
In this paper we describe the use of genetic programming for the prediction of blood demands. As blood bags for Hospitals are provided by blood banks on demand, predicting the needed amount of those should be as precise as possible. In order to achieve such an accurate prediction we have used genetic programming for data based modeling in order to find a mathematical model which predicts the blood bag demand of a hospital. This model should allow the hospital to minimize storage costs and the probability of running out of certain types of blood bags. In addition to the anonymized patient data provided by the General Hospital Linz, Austria we have also considered supplemental data such as weather and historical data such as the blood demand of the last few days which might lead to a more accurate model.

Keywords: blood demand prediction, machine learning, regression, structure identification

1. INTRODUCTION

1.1. Blood Demand in a Hospital

Every hospital needs a certain amount of blood bags for various medical activities throughout a day or a week. This blood consumption consists of demands from scheduled events (e.g. such as planned surgeries, ...) and from unpredicted events (e.g. some type of traffic accident followed by a treatment in the emergency room).

The blood bags are provided by a blood bank operated by the Austrian Red Cross on a "by demand" basis. If the hospital needs blood bags they are delivered by the blood donation service. In every hospital there is a need to predict the optimal demand of blood bags to minimize storage cost and the risk to run out of certain types of blood bags.

1.2. Research Goal

The research goal was to create a model which is able to predict the amount of blood bags of a specific type. There are different types of blood bag demands to predict, like demand per day, demand per week or demand per medical activity.

In this paper we present the research results achieved by analyzing the data of thousands of medical activities in the General Hospital Linz, Austria using data based modeling methods (namely genetic programming with offspring selection) in order to identify mathematical models for predicting blood bag demands.

In the following section (Section 2) we describe the data basis we have used for our research work. In Section 2.2 we describe the data preprocessing steps we performed to make the data more useful and complete for the model identification task. In Section 3 we give an overview over the modeling methods used in this project as well as the parameter settings applied, and in Section 4 we present and analyze the modeling results we have achieved. In the last section (Section 5) we give a conclusion of this project.

2. DATA BASIS

2.1. Available Patient Data

The data is provided by the Central Blood Laboratory of the General Hospital Linz, Austria and has been measured in the years 2005-2009. The following data tables are being used for the blood demand prediction:

- Laboratory Data: Contains every single blood value measured with a unique id for every pa-

tient, the label and the date of the value as well as the value itself. There are 27 routinely measured blood values of thousands of patients available, but not all values are measured at one examination.

- Medical Activities: Contains data about which medical activities were performed in which treatment. One treatment is identified by a case ID. A treatment can last several days or weeks and a number of blood measurements can be made during a treatment. A treatment typically ends by the discharge of the patient from the hospital.
- Blood Consumption: Contains records about the amount and type of the used blood bags in one treatment. However there is no direct connection between one medical activity and the used types of blood bags. Our approach to solve this problem is described in Section 2.2.1.

Patients' personal data (as for example name, date of birth and so on) where at no time available to the authors except the head of the laboratory and medical controlling.

2.2. Data Preprocessing

For most heuristic classification and regression tasks, the preprocessing of the raw input data has a big impact on the final model quality. The preprocessed data should end up containing both meaningful and complete information which is suitable for model identification using heuristic methods. Depending on the domain and the quality of the raw data, this can be quite a challenging task.

Figure 1 shows a brief overview of all the steps performed in the data preprocessing stage. Selected steps are described in one of the following sections. After all the input data is converted, the actual model identification can be performed. The desired prediction model should estimate the demand of blood bags for the General Hospital Linz for a given day or week as precisely as possible.

In the first preprocessing stage there are a number of input files, which contain multiple file types and have inconsistent column naming. For the modeling phase, the output of this stage should be a comma separated file, which has a consistent column naming and is usable for further processing and modeling tasks.

As a very practical problem, it appeared that the input data is scattered among multiple spreadsheet files with possibly different column names or even file formats. This problem is solved by a tool, which can merge an arbitrary number of heterogeneous spreadsheet files while taking into account that equivalent – but differently named – columns have to be merged. Those equivalences have to be defined manually.

Another problem is that in the laboratory data, every record represents one measured blood value. For blood demand prediction, one record has to represent an entire blood examination. For this reason, the records are transposed in a way that one record contains all blood values from a single examination.

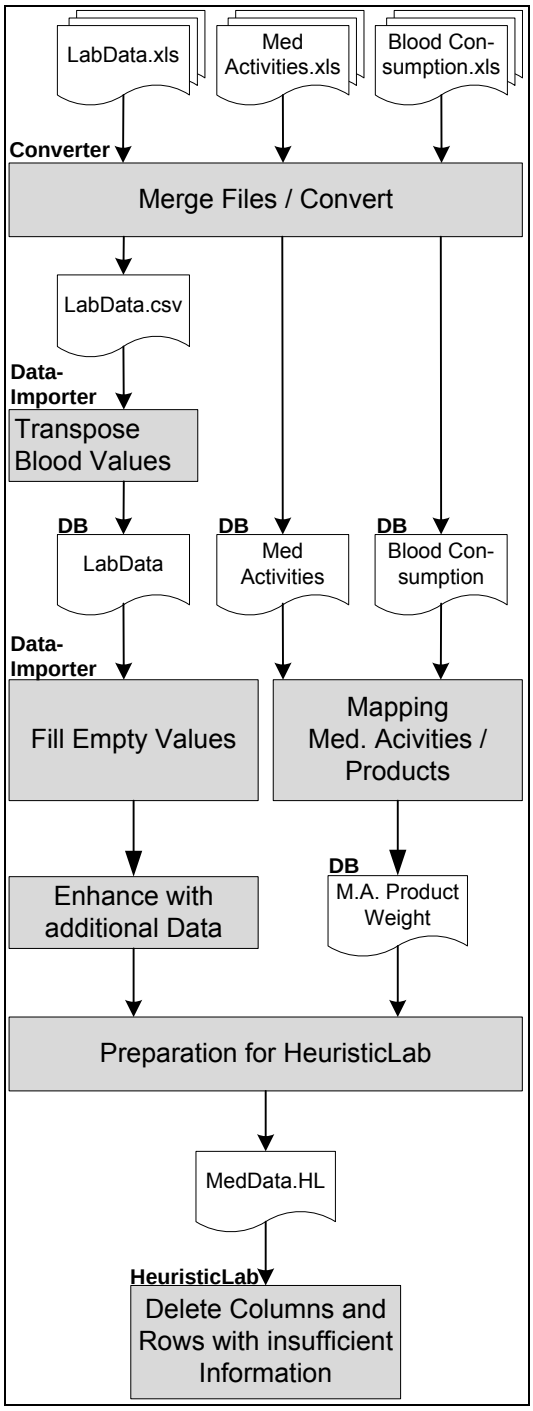

Figure 1: Workflow of data preprocessing phase

2.2.1. Mapping Medical Activities to Blood Products

For application of the blood demand prediction in the hospital a schedule of medical activities in the next days or week, for example derived from the planned surgeries, can be used as input data. The desired output is the amount of certain blood bags, grouped by different blood products.

In the data provided by the General Hospital Linz, Austria there is currently no unique mapping between

medical activities and issued blood products. But by using a schedule of medical activities as input for the blood demand prediction such a mapping is deemed necessary.

Therefore we distinguish the data in two sets: already unique mappings and non-unique mappings. For the first set we calculate a weight based on the amount of issued blood bags and the number of different patients who received these blood bags. For the second set we assign a constant weight of one and then combine the two sets again. With this new mapping we can bridge the gap between medical activities and different blood products to enable a blood demand prediction grouped by different blood products as desired.

2.3. Strategies for Improving Data Completion

In order to overcome the problem of empty feature values, samples from within a certain time span are used to fill up the missing values. This time span, e.g. one day, is used by a search function that determines which samples belong together and thus can provide features to each other.

Two strategies namely fill and merge, can be used to populate missing feature values of the given samples. The fill strategy fills up missing feature values for a given sample if a value exists within the list of samples chosen by the time span function. This strategy does not delete any samples but allows more complete samples to be increased in weight as their values are used more often. In contrast to that the merge strategy merges the selected samples to one. This results in fewer samples but does not favor feature-rich samples. The two strategies can be combined with one of the following aggregation functions which define how to compute the new value if more than one values are found by the search function:

- Min: fills up the missing values with the smallest value found in search space
- Max: fills up the missing values with the greatest value found in search space
- Mean: fills up the missing values with the mean value found in search space
- First (Merge only): takes the value from the sample with the oldest timestamp found in search space
- Last (Merge only): takes the value from the sample with the youngest timestamp found in search space
- Nearest (Fill only): takes the value with the minimum time distance to the empty value

Table 1: Input Data

Pat ID	Date	Val.1	Val.2	Val.3	Val.4
1	20/12/08		35		25
1	21/12/08	8.6		19	
2	21/12/08	10		30	8
2	22/12/08	5	15		13

Table 2: Merge-Max

Pat ID	Date	Val.1	Val.2	Val.3	Val.4
1	20/12/08	8.6	35	19	25
2	21/12/08	10	15	30	13

Table 3: Fill-Max

Pat ID	Date	Val.1	Val.2	Val.3	Val.4
1	20/12/08	8.6	35	19	25
1	21/12/08	8.6	35	19	25
2	21/12/08	10	15	30	8
2	22/12/08	5	15	30	13

The algorithm can be parameterized with a threshold which defines the size of the search space in days and a number of grouping columns, which also constrain the search space. In the case of Laboratory Data, the Patient ID would be such a grouping column, since only samples from the same patient shall be merged or filled.

3. MODELING METHODS

3.1. Artificial Neural Networks

Besides the use of genetic programming (GP) for system identification also artificial neural networks (ANN) can be utilized. For a regression or classification task a feed-forward neural network with one output neuron and backpropagation can be used; theoretical background and details can for example be found in (Gurney 1997, Priddy 2005).

But in contrast to GP, where the actual size and height of the tree containing the operators and feature variables can grow and shrink during the run, the number of neurons and their connections however has to be fixed before each training of an ANN. In addition an activation function for each neuron or for all neurons in each layer has to be chosen for ANN, whereas the operators in the tree for GP are chosen randomly during initialization.

We limited our work to GP in finding a model for the prediction of blood demands. The various modeling approaches are discussed in the following section.

3.2. Genetic Programming

Our main approach towards the blood demand prediction is genetic programming (GP). This section gives a theoretical background on genetic programming and shows how it can be applied to solve problems.

3.2.1. Introduction to Genetic Programming

Genetic programming is inspired by the Darwinian principles of selection, crossover and mutation. It can be seen as a specialized form of genetic algorithms (GA) to generate computer programs and therefore to solve problems automatically.

Historically the field of genetic programming began with the evolutionary algorithms. In the 1990s, John R. Koza pioneered the application of genetic programming. Over the years the idea was expanded and gained foothold both in the academic and industrial

field. As described in (Koza 1992) virtually all problems in artificial intelligence, machine learning, adaptive systems, and genetic programming provides a way to successfully conduct the search in space of computer programs.

As mentioned before, GP is a specialization of genetic algorithms. Each individual is a computer program that receives input, performs computations and generates output. In (Buchberger et al. 2009) GP is described as a machine learning technique used to optimize a population of computer programs according to a fitness landscape determined by a program's ability to perform the given task. The concept of GP is domain-independent, so it is important to find a good problem representation schema that can be effectively manipulated by the two main operators, namely crossover and mutation. This is critical to the success of genetic programming. The most common representation type is the point-labeled structure tree as seen for example in (Koza 1992; Koza 1994; Koza et al. 1999; Koza et al. 2003; Langdon and Poli 2002).

The crossover operator is applied on individuals to exchange a node of the structure tree with another node in another population. Due to the tree representation this can mean that a whole branch is replaced. As an effect the resulting new program structure can differ strongly from its parents.

The mutation operator is applied on a randomly chosen node. It can either alter the information of a node, or replace it completely, depending on the problem and tree representation.

3.2.2. Data Based Modeling and Structure Identification

In structure identification, solution candidates represent mathematical models; these models are applied to the given training data and the so generated output values are compared to the original target data. The left part of Figure 2 visualizes how the GP cycle works: As in every evolutionary process, new individuals (in GP's case, new programs) are created and tested, and the fitter ones in the population succeed in creating children of their own; unfit ones die and are removed from the population (Langdon and Poli 2002).

Within the last years the Josef Ressel Centre for Heuristic Optimization has set up an enhanced and problem domain independent GP based structure identification framework that has been successfully used in the context of various different kinds of identification problems for example in mechatronics, medical data analysis, and the analysis of steel production processes. One of the most important problem independent concepts used in this implementation of GP-based structure identification is offspring selection (Affenzeller et al. 2005), an enhanced selection model that has enabled genetic algorithms and genetic programming implementations to produce superior results for various kinds of optimization problems. As in the case of conventional GAs or GP, offspring are generated by parent selection, crossover, and mutation. In a second (strict offspring) selection step (as shown in the right part of Figure 2), only those children become members of the next generation's population that outperform their own parents; the algorithm repeats the process of creating new children until the number of successful offspring is sufficient to create the next generation's population (Winkler et al. 2009).

"Using Genetic Programming for data-based modeling has the advantage that we are able to design an identification process that automatically incorporates variables selection, structural identification and parameters optimization in one process" (Buchberger et al. 2009).

3.2.3. Modeling for Blood Demand Prediction

For our blood demand prediction we follow two approaches:

1. Blood Bag demand per medical activity (grouped by day and blood product)
2. Blood bag demand per day (grouped by blood product)

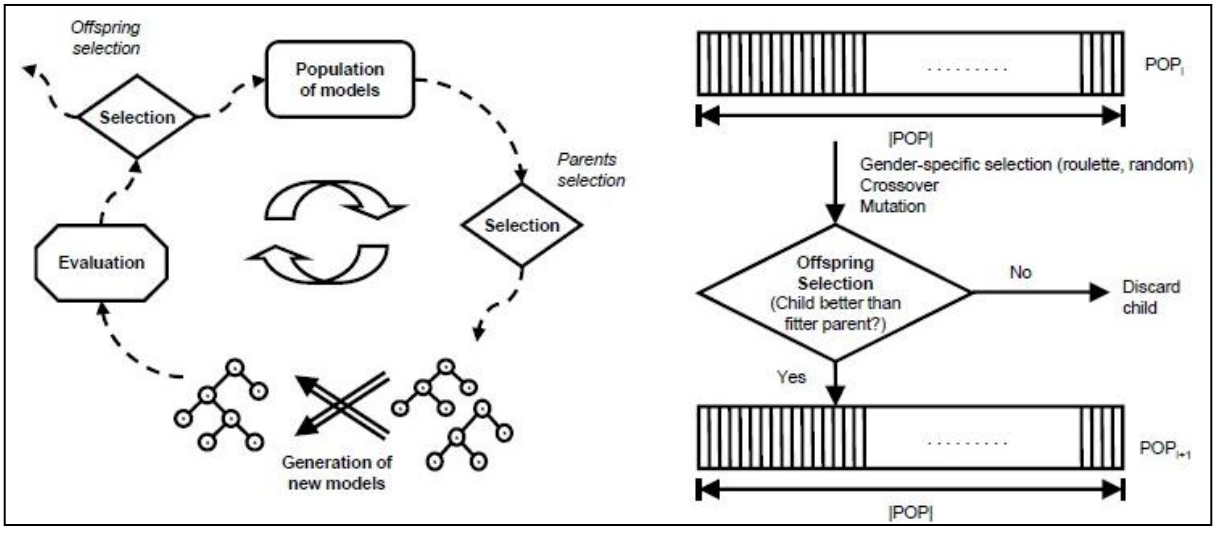

Figure 2: Left: The extended genetic programming cycle including offspring selection; Right: Strict offspring selection as used here within the GP process

Since the prediction depends on the blood product, both approaches are based on the mapping from medical activities to blood products described in Section 2.2.1. An additional feature with historical data is added, which sums up the blood consumption in the last one and last seven days. Now it should be possible to predict for example the blood demand for the next day.

In addition to splitting the given data into training and test data, the GP based training algorithm in HeuristicLab (Affenzeller et al. 2009, Wagner 2009) has been implemented in such a way that a part of the given training data is not used for training the model and serves as validation set; in the end, the algorithm returns those models that perform best on validation data. This approach has been chosen because it is assumed to help to cope with overfitting; it is also applied in other GP based machine learning algorithms as for example described in (Banzhaf and Lasarczyk 2004).

4. RESULTS

In this section we report the best test results we have achieved. Table 4 shows the most promising parameter settings for each scenario, which were found by running a number of test runs using different parameter settings. The parameters have been determined experimentally, since there is no golden rule for the optimal settings.

The tree complexity of the models has been restricted by defining an upper limit for tree height and tree size. This was done to keep the solutions interpretable and to avoid overfitting. Scenario 1 represents blood bags per day and Scenario 2 blood bags per medical activity.

Table 4: Parameter settings for test runs

Parameter	Scenario 1	Scenario 2
Population size	500	500
Mutation rate	0.05	0.05
Parents selection	Random & Proportional	Random & Proportional
Offspring selection	Strict	Strict
1-Elitism	Yes	Yes
Selection Pressure	200	300
Generations	1,000	1,000
Tree Size / Height	70 / 8	100 / 10

The results displayed in table 5 and 6 show the mean value and standard deviation of the model qualities achieved in nine test runs. In scenario 1 the 60,784 available samples were partitioned in 2,000 training, 43,589 validation and 15,195 test samples. In scenario 2 the 59,968 available samples were partitioned in 2,000 training, 42,977 validation and 14,991 test samples**.**

Table 5: Results Blood bags per day

	μ	σ
Training %	2.1929	0.0268
Validation %	1.5244	0.0027
Test %	1.8746	0.0151

Table 6: Results Blood bags per medical activity

	μ	σ
Training %	1.1897	0.0444
Validation %	1.2678	0.0388
Test %	1.1514	0.0311

5. CONCLUSION AND OUTLOOK

In this paper we have described the use of genetic programming to identify structure models that describe the blood bag demands in a hospital. The used data was provided by the General Hospital Linz, Austria. We have also described the necessary preprocessing steps in order to prepare the data to be useable for structure identification with genetic programming.

As seen in the results the introduction of features representing a medical activity leads to a significant improvement of the model quality.

Future goals in this research project include new modeling scenarios like the prediction of blood demand per week and for other time intervals. Additionally, further parameter optimization will be conducted.

ACKNOWLEDGMENTS

The work described in this paper was done within the Josef Ressel Centre for Heuristic Optimization *Heureka!* (http://heureka.heuristiclab.com/) sponsored by the Austrian Research Promotion Agency (FFG).

REFERENCES

Affenzeller, M., Wagner, S., Winkler, S., 2005. Goal-oriented preservation of essential genetic information by offspring selection. *In Proceedings of the Genetic and Evolutionary Computation Conference (GECCO), volume 2*, pages 1595–1596. June 25-29, 2005, Washington DC, USA.

Affenzeller, M., Winkler, S., Wagner, S., Beham, A., 2009. *Genetic Algorithms and Genetic Programming - Modern Concepts and Practical Applications*. Chapman & Hall/CRC. ISBN 978-1584886297.

Banzhaf, W., Lasarczyk, C., 2004. Genetic programming of an algorithmic chemistry. In O'Reilly, U., Yu, T., Riolo, R., Worzel, B., eds. *Genetic Programming Theory and Practice II*. Ann Arbor, pages 175-190.

Buchberger, B., Affenzeller, M., Ferscha, A., Haller, M., Jebelean, T., Klement, E.P., Paule, P., Pomberger, G., Schreiner, W., Stubenrauch, R., Wagner, R., Weiß, G., Windsteiger, W., 2009. *Hagenberg Research. 1st edition*. Dordrecht, Heidelberg, London, New York: Springer, ISBN 978-3-642-02126-8.

Gurney, K., 1997. *An introduction to neural networks*. London: CRC Press.

Koza, J. R., 1992. *Genetic Programming: On the Programming of Computers by Means of Natural Selection*. The MIT Press.

Koza, J. R., 1994. *Genetic Programming II: Automatic Discovery of Reusable Programs*. The MIT Press.

Koza, J. R., Bennett III, F.H., Andre, D., Keane, M.A., 1999. *Genetic Programming III: Darvinian Invention and Problem Solving*. Morgan Kaufmann Publishers.

Koza, J.R., Keane, M.A., Streeter, M.J., Mydlowec, W., Yu, J., Lanza, G., 2003. *Genetic Programming IV: Routine Human-Competitive Machine Learning*. Kluwer Academic Publishers.

Langdon, W.B., Poli, R., 2002. *Foundations of Genetic Programming*. Berlin, Heidelberg, New York: Springer Verlag.

Priddy, K.L., Keller, P.E., 2005. *Artificial neural networks: an introduction*. Washington: The International Society for Optical Engineering.

Wagner, S., 2009. *Heuristic Optimization Software Systems - Modeling of Heuristic Optimization Algorithms in the HeuristicLab Software Environment*. PhD thesis, Johannes Kepler University Linz.

Winkler, S., Hirsch, M., Affenzeller, M., Re, L., Wagner, S. 2009. Virtual Sensors for Emissions of a Diesel Engine. *Produced by Evolutionary System Identification. In Computer Aided Systems theory (EUROCAST)*, February 15-20, 2009, Las Palmas de Gran Canaria, Spain.

AUTHORS BIOGRAPHIES

CHRISTIAN FISCHER received his BSc in software engineering in 2009 from the Upper Austria University of Applied Sciences, Campus Hagenberg. He is currently pursuing studies for his master's degree. In the course of his studies he is involved in the project team for the prediction of blood demands in a hospital in cooperation with the Josef Ressel Centre Heureka! and the General Hospital Linz.

LUKAS BLODER received his BSc in internet technologies in 2009 from the Joanneum University of Applied Sciences, Kapfenberg. He is currently pursuing studies for his master's degree in software engineering. In the course of his studies he is involved in the project team for the prediction of blood demands in a hospital in cooperation with the Josef Ressel Centre Heureka! and the General Hospital Linz.

CHRISTOPH NEUMÜLLER received his BSc in software engineering in 2010 from the Upper Austria University of Applied Sciences, Campus Hagenberg. He is currently pursuing studies for his master's degree. In the course of his studies he is involved in the project team for the prediction of blood demands in a hospital in cooperation with the Josef Ressel Centre Heureka! and the General Hospital Linz.

SEBASTIAN PIMMINGER received his BSc in software engineering in 2009 from the Upper Austria University of Applied Sciences, Campus Hagenberg. He is currently pursuing studies for his master's degree. In the course of his studies he is involved in the project team for the prediction of blood demands in a hospital in cooperation with the Josef Ressel Centre Heureka! and the General Hospital Linz.

MICHAEL AFFENZELLER has published several papers and journal articles dealing with theoretical aspects of evolutionary computation and genetic algorithms. In 2001 he received his PhD in engineering sciences from JKU Linz, Austria. Dr. Affenzeller is professor at the Upper Austria University of Applied Sciences, Campus Hagenberg, and head of the Josef Ressel Center *Heureka!* at Hagenberg.

STEPHAN M. WINKLER received his MSc in computer science in 2004 and his PhD in engineering sciences in 2008, both from Johannes Kepler University (JKU) Linz, Austria. His research interests include genetic programming, nonlinear model identification and machine learning. Since 2009, Dr. Winkler is professor at the Department for Medical and Bioinformatics at the Upper Austria University of Applied Sciences, Campus Hagenberg.

HERBERT STEKEL received his MD from the University of Vienna in 1985. Since 1997 Dr. Stekel is chief physician at the General Hospital Linz, Austria, where Dr. Stekel serves as head of the central laboratory.

RUPERT FRECHINGER received his MD from the University of Vienna. He obtained his apprenticeship as general practitioner at the hospitals of Upper Austria. Subsequently Dr. Frechinger was consultant at the Computer Science Cooperation Austria. Since 2000 he has been the head of medical controlling department at the General Hospital Linz, Austria.

SYMBOLIC REGRESSION WITH SAMPLING

Michael Kommenda[a], Gabriel K. Kronberger[b], Michael Affenzeller[c], Stephan M. Winkler[d], Christoph Feilmayr[e], Stefan Wagner[f]

[a – d, f] Upper Austria University of Applied Sciences
School for Informatics, Communications, and Media
Heuristic and Evolutionary Algorithms Laboratory
Softwarepark 11, 4232 Hagenberg, Austria

[e] voestalpine Stahl GmbH
Research & Development Ironmaking
4020 Linz, Austria

[a] michael.kommenda@fh-hagenberg.at, [b] gabriel.kronberger@fh-hagenberg.at, [c] michael.affenzeller@fh-hagenberg.at, [d] stephan.winkler@fh-hagenberg.at, [e] christoph.feilmayr@voestalpine.com, [f] stefan.wagner@fh-hagenberg.at,

ABSTRACT
In this paper a way of improving the performance of genetic programming (GP) for regression tasks is presented. In general, most of the execution time is consumed during the evaluation step of an individual. Hence reducing the number of samples which are evaluated during the learning phase of the algorithm significantly reduces its execution time. A reduction of the available training samples might hamper the algorithm in its capability to learn the desired correlation. For this reason our approach evaluates each solution only on a randomly chosen part of all training samples, which is selected before the evaluation step. In the result section runs with different parameter settings of our approach and traditional genetic programming algorithms are compared regarding the solution quality and execution time to each other.

Keywords: Genetic Programming, Symbolic Regression, Sampling, Machine Learning, Performance Analysis

1. INTRODUCTION

1.1. Regression

Regression analysis is the task of modeling a relationship between a dependent (target) variable y and several independent (input) variables *x* in a dataset. Thus we want to get function f which calculates the target variable *y* using the input variables *x* and different weights *w* (1). The identified model is all the better the smaller the error term ε.

$$y = f(x, w) + \varepsilon \quad (1)$$

Regression analysis is often performed using supervised machine learning algorithms such as support vector machines (SVMs), artificial neuronal networks (ANNs) and genetic programming (GP) or statistical methods such as linear and polynomial regression. All of these methods have in common that available data is divided into a training and test partition. The training partition is used to learn the model and afterwards the generalization capabilities of the selected models are evaluated on the test partition, which must not have been used during the training. Some algorithms additionally take a part of the training partition for parameter optimization or model selection. This part of the training partition is referred to as validation partition.

After the identification of a model its performance must be measured. This is mostly done using the mean squared error (MSE) between the predicted and the original values of the target variable. Other correlation measures like the Pearson correlation coefficient (R^2), Spearman's rank correlation coefficient or variations of the MSE are also commonly used.

1.2. Symbolic Regression by Genetic Programming

Genetic programming (GP), an extension of genetic algorithms, was first studied at length by John Koza (1992). In contrast to the goal of genetic algorithms, finding a fixed length vector of predefined symbols, GP tries to find a variable length program to solve a given problem. The identified program is often represented as structure tree of a computer program, similar to symbolic-expressions of functional programming languages. Since GP evolves variable length programs no assumption about the structure of the programs needs to be made. GP is regarded as an evolutionary and population based optimization technique and the algorithmic steps are described in the following.

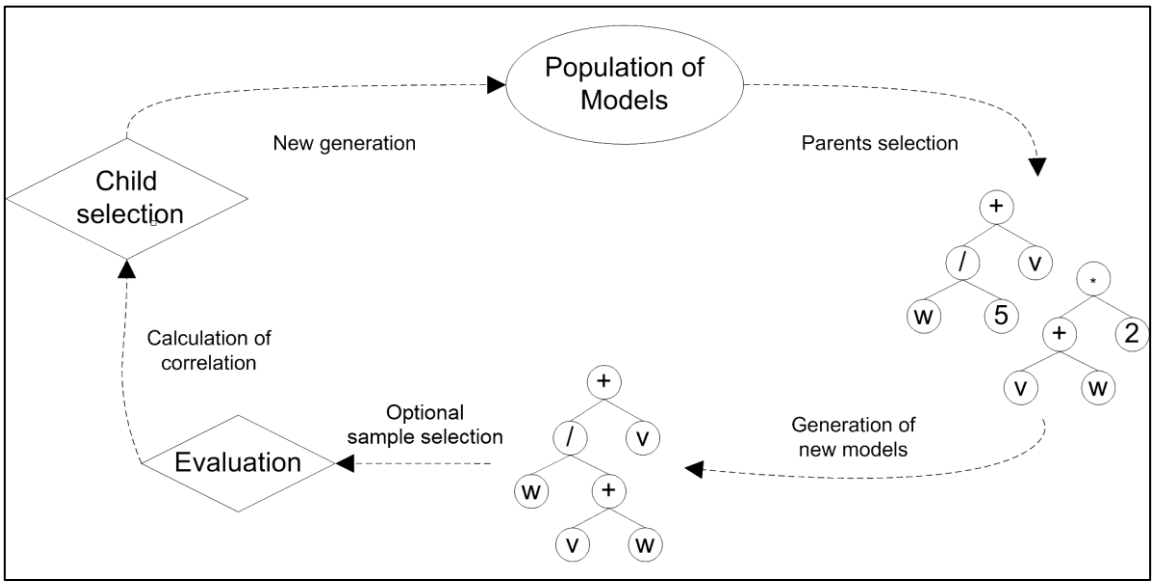

Figure 1: Schematic Representation of the GP algorithm

The population is first initialized with random individuals (structure trees), whose quality is calculated by a problem dependent fitness function. In the case of symbolic regression the MSE is mostly used as fitness function. Every generation parts of the population are replaced by new child individuals, created by combining the information of two parent individuals, e.g., merging parts of the parent structure trees. Afterwards the newly created child individual is mutated with a given probability to induce additional diversity in the population. The probability for an individual to be selected as parent is usually correlated to its fitness. The algorithm finishes if a given termination criterion is meet, e.g. a maximum number of generations has been evaluated. A schematic representation of a GP algorithm is shown in Figure 1.

When using GP for regression tasks the individuals are represented as structure trees, where each non terminal node represents a mathematical function and each terminal node represents either an input variable or a constant. Therefore the whole tree represents a mathematical formula as described in formula 1. During the evaluation step of the algorithm the estimated values of the target variable must be calculated for each created model. As this step is very time consuming, especially for large datasets, reducing the number of evaluated samples without losing predictive power is advantageous.

2. ALGORITHM EXTENSIONS

We introduced the relative number of evaluated samples as an additional parameter in the GP algorithm. This parameter ranges from [0, 1] and states the relative number of samples of the training partition that should be used in the algorithm. For example if the relative number of evaluated samples is 0.2 only 1/5 of the training partition is considered during the evaluation of the model. But overall the algorithm considers the whole information present in the trainings data, because this 1/5 is chosen repeatedly.

There are two possibilities how this reduction of the training partition could be implemented. In the first algorithmic extension all individuals are evaluated on the same part of the training in each generation. The selected training samples are changed only during the generational step of the genetic algorithm. In contrast to this, the other possibility is to evaluate all individuals on a different part of the training set by randomly selecting the training samples before each evaluation.

If every individual should be evaluated on the same training samples, the training partition is shuffled in every generation. The shuffling was implemented using a Fisher-Yates algorithm as described by Richard Durstenfeld (1964). Every individual is afterwards evaluated on the first *K* samples of the shuffled dataset. *K* defines the number of samples that should be used for evaluation and is calculated as the total number of training samples *N* multiplied with the relative number of evaluated samples.

The other possibility is that every individual is evaluated on a different, randomly chosen, part of the training samples. In this case it would be inefficient to shuffle the whole training data before each evaluation. Therefore we select a sequence of K unique samples between the training samples start and end. This problem is equivalent to the problem of picking *K* items from a collection of *N* items and can be efficiently solved using the selection sampling technique described by Knuth (1997). The selection sampling technique works by iterating over all samples until *K* samples are selected and is shown in Table 1; *N* defines the total number of samples, *n* the number of remaining samples, *K* the number of samples to select and *k* the number of already selected samples.

Table 1: Pseudo Code of the Selection Sampling Technique

```
While k < K
    Select actual sample with probability (K-k) / n
    If sample is selected
        Increase k
    Decrease n
    Step to next sample
End
```

It can be shown that this algorithm produces an unbiased random subset of the total samples by varying the probability to select a sample. The probability is equal to the relative number of evaluated samples for the first sample. It increases while the number of remaining samples *n* decreases and decreases if a sample got selected. All samples are selected with the same probability and exactly *K* samples are selected.

These two approaches to reduce the number of evaluated samples are only used for the training partition and so for the learning phase of the GP. In contrast all generated models are always evaluated on the whole validation partition, because the best performing model on the validation partition is returned as the result of the algorithm. Therefore the comparison value (MSE on the validation partition) must not be falsified, which forbids virtually reducing the size of the validation partition. Reducing the size of the test partition is also not reasonable, because it would change the estimation of the generalization capabilities of a model.

The reasons why reducing the number of evaluations is desirable are listed in Poli and McPhee (2008). In the first place the execution time of the GP algorithm is drastically reduced and in addition it is less likely that a specialized individual dominates the whole population. We could verify these advantages by achieving a significant speed up in terms of execution time and no drawback in terms of the quality of the identified solutions.

3. EXPERIMENTAL SETUP

The tests for these algorithm adaptations were performed on a regression dataset from Dow Chemical. The dataset was used in the symbolic regression competition, a side event of the EvoStar 2010 conference, and is publicly available at http://casnew.iti.upv.es/index.php/evocompetitions/105-symregcompetition. It contains 57 different input variables of a chemical real world process at Dow Chemical and 1066 samples. The sizes of the different partitions were 375 samples for training, 375 for validation and 316 for testing.

Furthermore we prepared a second dataset that contains data collected from an iron ore reduction process of our project partner voestalpine. It contains 5449 samples and 23 input variables describing the input material, products and the state of the blast furnace. A detailed description of the blast furnace process can be found in Kronberger et al. (2009). In this larger dataset 1900 samples were used for training, as well as 1900 for validation and 1800 samples for the test partition.

3.1. Experiments

We tested the described improvements on the Dow Chemical and on the voestalpine dataset. The major difference between the different algorithm runs was the population size parameter, which was chosen 1000 or 5000 respectively. The population size directly affects the execution time of the run because the number of evaluations during the algorithm run depends on the population size and on the number of generations. In addition the relative number of evaluated samples was varied between 0.1, 0.5, and 1.0. The parameter settings of the GP algorithm are summarized in Table 2.

These two changing parameters led to six different parameter combinations which were tested with the two algorithmic adaptations; whether all samples are evaluated on a differently chosen part of the training samples or if the part of the training samples is fixed during each generation.

Table 2: GP Algorithm Parameters

Population size	1000, 5000
Generations	300
Relative number of evaluated samples	0.1, 0.5 ,1
Mutation rate	0.15
Max tree height	10
Max tree size	100
Elites	1
Crossover	SubTreeCrossover
Selection	Tournament selection
Tournament size	5

3.2. Implementation

The approaches described in this paper have been implemented using the most recent version (3.3) of HeuristicLab (Wagner, 2009). HeuristicLab is a generic framework for modeling, executing and comparing different heuristic optimization techniques and provides plenty of functions for result analysis and evaluation. Another advantage is that all operators necessary for using GP for symbolic regression are already available. A binary version of HeuristicLab is available at http://dev.heuristiclab.com/trac/hl/core.

4. RESULTS

In this section the results regarding the execution time of the algorithm and the solution quality (MSE on the test partition of the best model per algorithm) on the Dow Chemical and the voestalpine dataset are shown. The main parameters were the sample selection strategy (every generation or every evaluation), the relative number of evaluated samples, and the population size. As the GP process is stochastic we repeated each parameter setting 40 times.

4.1. Execution time

Figure 2 shows a boxplot of the different execution times of the algorithm with a population size of 1000. The x-axis indicates the sample selection strategy, whether the training samples were the same for one generation or if the training samples varied for every evaluation, and the relative number of evaluated samples parameter value. The y-axis shows the execution time of all 40 repetitions as boxes. The results regarding the execution time for GP algorithms with a population size of 5000 are shown in Figure 3. It is noticeable that the execution time of runs that use the same 10% of the training partition for all models in a generation (Figure 3, first box), spreads strongly, but the median (dotted line in the boxplot) is as expected lower than the median of the runs which use more samples of the training partition. The results on the voestalpine dataset are shown in Figure 4 and 5. The runs illustrate the same correlation between the relative number of evaluated samples and the execution time, except that the average execution time is longer because of the larger training, validation, and test partitions.

Whenever only parts of training set are used, the runtime drops significantly. The validation and test partition have the same amount of samples for every algorithmic setting. Additionally, every structure tree must be interpreted before it can be evaluated. The interpretation is only dependent on the tree size and so it is not affected by the reduction of the evaluated samples. These two factors specify a lower bound on the execution time.

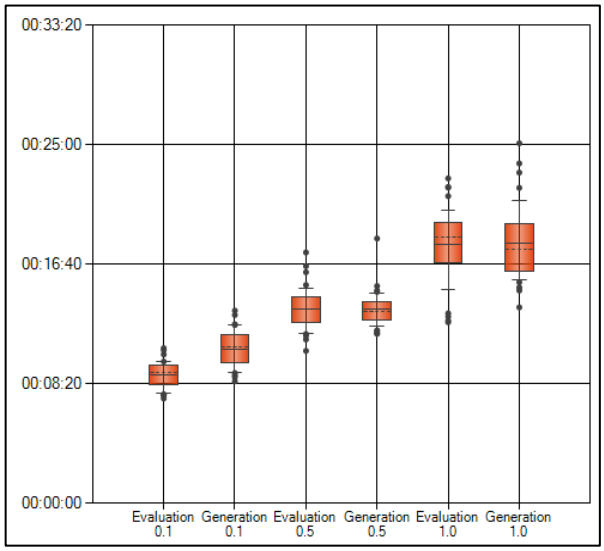

Figure 2: Boxplot of the Execution Times of GP Runs on the Dow Chemical Dataset with Population Size 1000

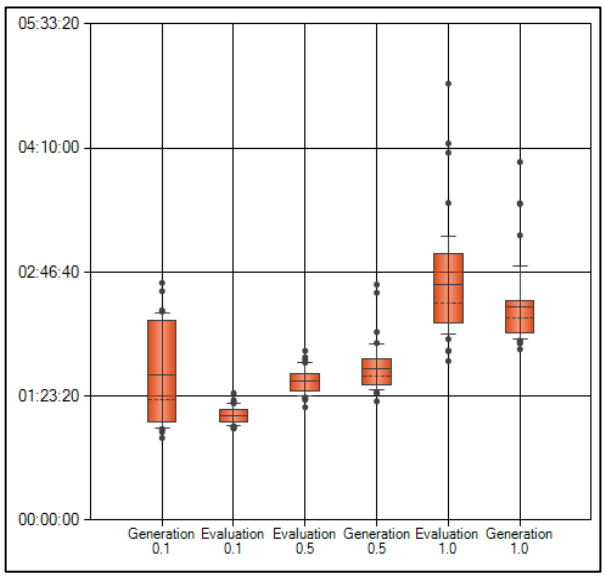

Figure 3: Boxplot of the Execution Times of GP Runs on the Dow Chemical Dataset with Population Size 5000

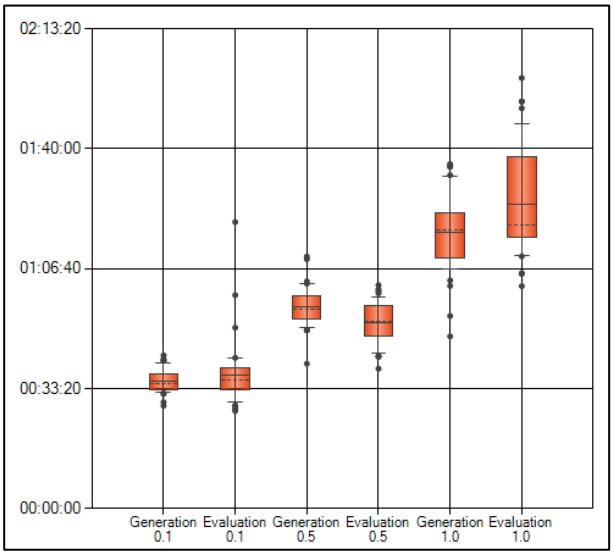

Figure 4: Boxplot of the Execution Times of GP Runs on the voestalpine Dataset with Population Size 1000

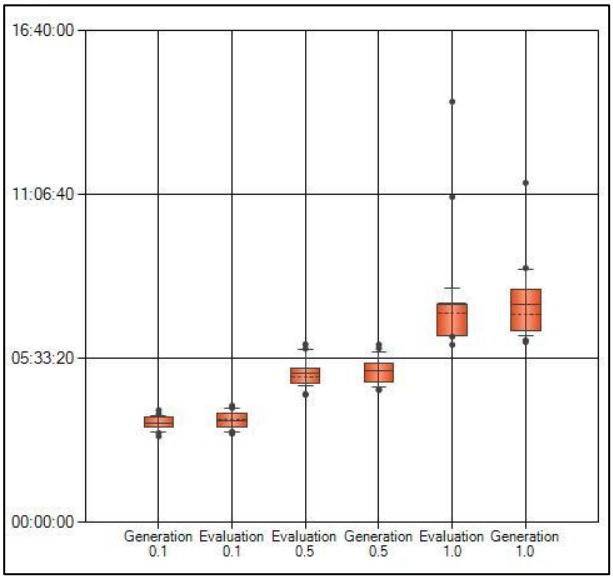

Figure 5: Boxplot of the Execution Times of GP Runs on the voestalpine Dataset with Population Size 5000

As it is shown in the figures above the runtime is drastically affected by the number of evaluated samples in each generation. However, the reduction would be useless, if the achieved quality was not competitive to the quality achieved by evaluating all available training samples.

4.2. Generalization error

The generalization error of the identified models is estimated by evaluating the models on the test partition. The validation partition could not be used for this task because the identified model is selected as the best performing model on the validation partition. The median MSE and its standard deviation of all 40 algorithm runs, per sample selection strategy and population size on the Dow Chemical dataset, are listed in Table 2. There is no obvious difference when only parts of the training partition are used to learn the models. Additionally the standard deviation of the MSE is bigger when more samples are used for training (relative number of evaluated samples 1.0). The reason for this is that it is more likely that the models are overfitted when using more training samples.

Table 2: Median and the standard deviation of the MSE on the test partition of the Dow Chemical dataset

Sample selection strategy	Population size	Median (MSE)	StDev (MSE)
Generation 0.1	1000	0.0578	0.0080
	5000	0.0520	0.0078
Generation 0.5	1000	0.0637	0.0091
	5000	0.0571	0.0329
Generation 1.0	1000	0.0609	0.2512
	5000	0.0598	0.0085
Evaluation 0.1	1000	0.0560	0.0032
	5000	0.0523	0.0056
Evaluation 0.5	1000	0.0623	0.0171
	5000	0.0620	0.0088
Evaluation 1.0	1000	0.0622	0.0130
	5000	0.0598	2.0066

Table 3: Median and the Standard Deviation of the MSE on the Test Partition of the voestalpine Dataset

Sample selection strategy	Population size	Median (MSE)	StDev (MSE)
Generation 0.1	1000	162.17	53.65
	5000	168.49	38.34
Generation 0.5	1000	169.83	58.68
	5000	158.09	49.99
Generation 1.0	1000	178.63	67.41
	5000	189.69	59.44
Evaluation 0.1	1000	198.03	90.25
	5000	184.79	61.48
Evaluation 0.5	1000	169.08	67.04
	5000	183.01	44.45
Evaluation 1.0	1000	160.42	71.94
	5000	159.75	47.77

The results on the voestalpine dataset are shown in Table 3. On this dataset runs that use more samples for training have a slightly lower median MSE. However, the differences between the MSEs are not significant, when compared with the standard deviation.

5. CONCLUSIONS AND OUTLOOK

Not surprisingly a reduction of the evaluated samples decreases the execution time of the GP runs. In addition the result section also shows that runs which use fewer training samples perform as good as runs that use all the available training samples to learn the models. Therefore it is better to use fewer evaluated samples, because the saving of the execution time enables the user to do more test runs or to integrate more advanced, time extensive concepts in the GP algorithm.

Another interesting approach to virtually reducing the number of training samples is using sliding windows in combination with GP (Winkler, Affenzeller and Wagner 2007). An advantage of this technique is that it can be used to predict time-dependent features, which is not possibly with the adaptations described in this paper.

The next step is the integration of an automatically adaption of the relative number of evaluated samples parameter during the algorithm run to improve the achieved qualities while minimizing the necessary execution time. Another interesting approach is stated in the work of Gathercole and Ross (1994). They suggest weighting every sample according to its age (how long the sample has not been used for training) and its difficulty to be predicted correctly. They showed that this method outperforms random subset selection on classification problems and it would be interesting if their method could be adapted for symbolic regression problems.

ACKNOWLEDGMENTS

The work described in this paper was done within the Josef Ressel Centre for Heuristic Optimization *Heureka!* (http://heureka.heuristiclab.com/) sponsored by the Austrian Research Promotion Agency (FFG).

REFERENCES

Durstenfeld, R., 1964, Algorithm 235: Random permutation, *Communications of the ACM*, 7 (7), pp. 420

Gathercole, C., Ross, P., 1994, Dynamic Training Subset Selection for Supervised Learning in Genetic Programming, *Parallel problem solving from nature III*, pp 312- 321, 09-14 October, Jerusalem, Israel

Knuth, D., 1997, *The Art of Computer Programming Volume 2 Seminumerical Algorithms*¸ 3rd Edition, Addison-Wesley Professional, pp 142 - 148

Koza, J. R., 1992, *Genetic Programming: On the Programming of Computers by Means of Natural Selection.* MIT Press.

Kronberger, G., Feilmayr, C., Kommenda, M., Winkler, S., Affenzeller, M., Bürgler T., 2009, System Identification of Blast Furnace Processes with Genetic Programming, *Proceedings of the IEEE 2nd International Symposium on Logistics and Industrial Informatics (Lindi 2009)*, pp. 63-68, September 10-11, Linz, austria

Poli, R., Langdon, W.B., McPhee, N.F., 2008, *A field guide to genetic programming*. Published via http://lulu.com and freely available at http://www.gp-field-guide.org.uk, (with contributions by J. R. Koza).

Wagner, S., 2009, *Heuristic Optimization Software Systems - Modeling of Heuristic Optimization Algorithms in the HeuristicLab Software Environment*. Thesis (PhD), Johannes Kepler University Linz, Austria.

Winkler, S. M., Affenzeller, M., Wagner, S., 2007, Selection Pressure Driven Sliding Window Behavior in Genetic Programming Based Structure Identification, *Computer Aided Systems Theory – EUROCAST 2007*, pp. 788-795, February 12-16, Las Palmas de Gran Canaria, Spain.

AUTHORS BIOGRAPHIES

MICHAEL KOMMENDA finished his studies in bioinformatics at Upper Austria University of Applied Sciences in 2007. Currently he is a research associate at the UAS Research Center Hagenberg working on data-based modeling algorithms for complex systems within *Heureka!*.

GABRIEL KRONBERGER is a research associate at the UAS Research Center Hagenberg. His research interests include genetic programming, machine learning, and data mining and knowledge discovery. Currently he works on practical applications of data-based modeling methods for complex systems within Josef Ressel Center *Heureka!*.

MICHAEL AFFENZELLER has published several papers, journal articles and books dealing with theoretical and practical aspects of evolutionary computation, genetic algorithms, and meta-heuristics in general. In 2001 he received his PhD in engineering sciences and in 2004 he received his habilitation in applied systems engineering, both from the Johannes Kepler University of Linz, Austria. Michael Affenzeller is professor at the Upper Austria University of Applied Sciences, Campus Hagenberg, and head of the Josef Ressel Center *Heureka!* at Hagenberg.

STEPHAN M. WINKLER received his MSc in computer science in 2004 and his PhD in engineering sciences in 2008, both from Johannes Kepler University (JKU) Linz, Austria. His research interests include genetic programming, nonlinear model identification and machine learning. Since 2009, Dr. Winkler is professor at the Department for Medical and Bioinformatics at the Upper Austria University of Applied Sciences, Campus Hagenberg.

CHRISTOPH FEILMAYR finished his diploma studies in chemical engineering at Technical University of Vienna in 2003. From that time he has worked as research engineer at voestalpine and has been mainly engaged with projects dealing with blast furnace iron making.

STEFAN WAGNER received his MSc in computer science in 2004 and his PhD in engineering sciences in 2009, both from Johannes Kepler University (JKU) Linz, Austria; he is professor at the Upper Austrian University of Applied Sciences (Campus Hagenberg). Dr. Wagner's research interests include evolutionary computation and heuristic optimization, theory and application of genetic algorithms, machine learning and software development.

GENERAL PURPOSE DATA MONITORING SOFTWARE FOR PLATFORM INDEPENDENT REMOTE VISUALIZATION

Andreas Gschwandtner[(a)], Michael Bogner [(b)], Franz Wiesinger[(c)], Martin Schwarzbauer [(d)]

[(a, b, c, d)]Upper Austria University of Applied Sciences, Hagenberg Austria,
Hardware/Software Design & Embedded Systems Design

[(a)]andreas.gschwandtner@fh-hagenberg.at, [(b)]michael.bogner@fh-hagenberg.at,
[(c)]franz.wiesinger@fh-hagenberg.at, [(d)]martin.schwarzbauer@fh-hagenberg.at

ABSTRACT

This paper presents a novel general purpose data monitoring software for remote visualization. This tool can be used broadly in practical applications to record, trace, and display measurement information from any data source. It covers a wide range of use cases through the support of various chart types such as line graphs, pie charts, and bar graphs. Although designed as general purpose monitoring tool, it was specially intended for dedicated applications as embedded devices with limited resources with possibly no graphical output interface. The underlying idea is to develop a tool that can process data from any device, completely independent from its hardware, operating system, or software. Next to data monitoring, it can be used as central recording platform where the data will be evaluated later. This feature is especially useful during the development and debugging phase. Measurements, in particular erroneous values, can be easily detected using visual support.

Keywords: visualization, embedded system, remote, network

1. INTRODUCTION

"A picture is worth a thousand words" (Barnard, F., 1927) is an often used phrase that emerged in the USA in the early part of the 20th century. The meaning of it is that a picture tells a story just as well as a large amount of descriptive text. The advantages of information visualization compared to information description are as follows (Colin Ware, 2004):

1. Images can provide simultaneous information.
2. Images have expressions that are linguistically hard to describe.
3. Images can condense information very strong.
4. Images can easily identify or focus on important information.

The fictive example in Fig. 1 shall depict the difference in data visualization opposing a diagram to a tabular presentation form. The introduced example consists of a random voltage profile of an electronic component recorded by an embedded system. On the left side of the figure we can see the tabular presentation of the individual voltage levels over time. On the right, the same information is presented, but in difference visually processed (Otto-von-Guericke, 2008). In fact, the line diagram is much easier to comprehend.

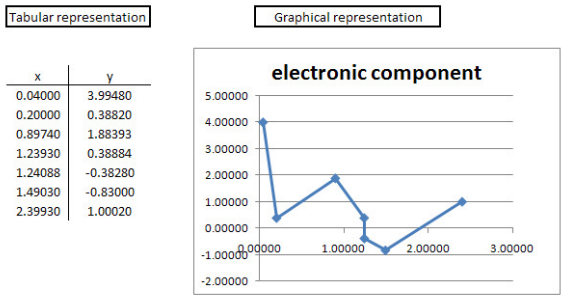

Figure 1: Different types of data visualization; tabular presentation (left), diagram presentation (right).

Due the fact, that human beings are more familiar with visually processed information, the line chart in Fig. 1 is the preferred method to turn the data into information. Furthermore, information has nothing to do with the amount of data; it is all about the appropriate representation (Schwarz, 2008). The main aim of this paper is the development of a platform independent visualization tool for displaying any kind of data. It can capture continuous, discrete, and instantaneous values. In order to be a general purpose tool, the supported chart types can be freely configured by the data source. The DataMonitor is not only tied to technical issues, but also generally usable. There exists no limitation of the visualization, which corresponds to semantics or meaning of data. This flexibility can be practical in many other fields, e.g.:

1. Automotive development (motor speed, exhaust gas temperature, torque measurements, system diagnostic, oil pressure...)
2. Chemistry and Biology
3. Geography (elevation profile)

4. Weather information (water level standings, CO2 emissions, temperature patterns...)
5. Home Automation (heating curves, heating duration…)
6. Financial economic (stock data)

2. COMMUNICATION

In computing, inter-process communication (IPC) is a set of techniques for the exchange of data among multiple threads in one or more processes. These processes may also run on different devices connected by a network. Due to the fact that we cover a large scope of applications, the platform independency is an important requirement of the visualization tool. The main objective was to support local and remote devices across heterogeneous platforms. Therefore we will basically focus on remote IPC techniques (Koch, 1993). After deeper investigations on different communication techniques (Microsoft Corporation, 2005), four main requirements were figured out. Tab. 1 shows an overview of the results of the elaboration of remote IPC methods.

Table 1: Rating of communication methods.

criteria	Remote procedure call	Named Pipe	Socket
flexibility	-	X	X
duplex operation	X	X	X
Connection-orientated	X	X	X
platform independent	-	-	X

Recently, to meet the required independency of the platform, the socket communication is prioritized. In particular, the socket communication (BSDZone, 2008) meets all criteria as shown in Tab.1. However, the software can be extended by other communications such as serial (RS232) or USB interfaces. In difference to common workstations where the serial port has largely been replaced by USB, embedded systems still count on this interface because of the low resource consumption. The advantage of the DataMontitor is the extensibility for other communication devices to support especially limited devices with different kinds of communication ports.

3. VISUALIZATION

Data visualization is the study of the visual representation of data. The main goal of data visualization is to communicate information in a clear and effective way through graphical means (Gregory, Hagen, Müller, 1997). It helps to provide insights into a rather sparse and complex data set by communicating its key aspects in a more intuitive way. With the support of graphical illustration of data, key-aspects can be filtered, meaning a simplification to the user. In general the different representations can be divided into conventional and innovative techniques:

1. Conventional techniques of data visualization are graph-based diagrams (as tree diagrams and flowcharts), chart types (as pie charts, beam diagrams and line diagrams) and many other variations and types of diagrams (e.g. exploded view, density map). Fig. 2 and Fig. 3 show three chart-like diagrams and an analog display. These kinds of diagrams display the relationship between two variables that take either discrete continuous or instantaneous values.
2. Innovative techniques are often in conjunction with scientific visualization and used for specific applications.

The fundamental idea of this work was to create a general purpose tool. In fact, it is focused on conventional presentation techniques.

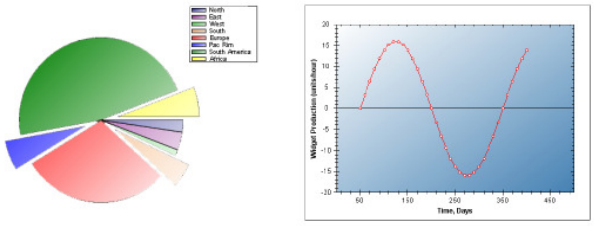

Figure 2: pie chart (left), line chart (right)

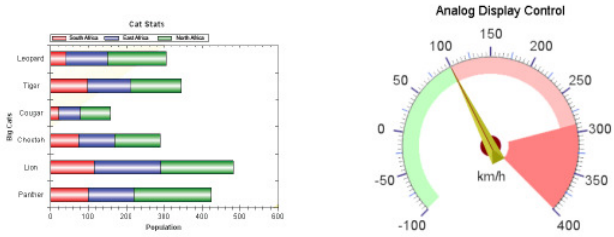

Figure 3: bar chart (left), analog display (right)

The DataMonitor supports commonly used chart-like diagrams and analog/digital display controls. In terms of flexibility, the tool can be easily extended to support further charts and remains backward compatibility. Because of the modular design concept, specific chart types can be easily integrated into the system. Moreover it doesn't interfere with the existing applications.

4. DESIGN AND IMPLEMENTATION

The software was designed as client/server system to assist in the creation of a platform independent system. The design consists essentially of two parts: the communication and the visualization.

4.1. Communication

To meet the requirements of an easy-to-use application, we use an ordinary communication protocol without request acknowledgments. The communication protocol implemented in this design is a TLV-protocol (Type, Length, and Value) to fulfill the communication and the data transfer. On the one hand, the TLV is a simple and sparse protocol, but on the other hand it allows the creation of a very flexible design. Because of the modular design of the TLV, we can integrate new features in the packet by using the value part of it, where another TLV packet can be inserted. Furthermore, we can generate new keywords (e.g. for specific charts) to extend the functionality and still remain backward compatibility.

In order to keep the effort for configuration at a minimum, there were only a few keywords defined for setting up a communication channel between the server and the client. This makes the DataMonitor applicable especially for limited devices with low memory and restricted communication resources. As described before, the server doesn't send an acknowledgment after a request at all. If the communication protocol was misinterpreted by the data source, the data sink will discard incoming data. In figure 4, the directed stream (one way) from the data source to the data sink can be seen. As the Internet Protocol (IP) defines a standard network byte order used for numeric values, we intend to use the same Big Endian format too. By default, the software supports socket communication over TCP/IP, but to be backward compatible to earlier software applications of the "Upper Austria University of Applied Sciences" the tool also supports the remote procedure call communication (RPC). The application is capable to switch the communication on the fly without the need to restart the program. The integration of other communication channels as RS232 or USB is described later in the implantation section.

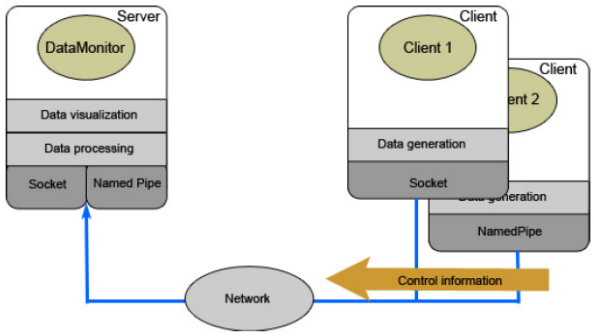

Figure 4: The DataMonitor mainly supports communication either via sockets or via RPC.

Next to the well-defined and easy-to-use protocol, we developed a class called ProtocolBuilder in C++. This class should ease the first use of the DataMontitor. It supports the user working with our predefined protocol. Every configuration can be set by functions provided by the ProtocolBuilder. Once familiar with all the settings, the user can easily change the system, the application and the programming language.

4.2. Visualization

The monitoring tool supports different kinds of charts and displays. The data source can configure the desired chart by sending the appropriate control info to the data sink. Visual controls such as analog and digital displays, line charts, bar charts, scatter plots, and pie charts are supported. Instantaneous values are visualized either with the self written analog or digital display. Visualization of the continuous values is accomplished by the use of the free ZedGraph-Graphic library. This library supports a various amount of different chart types. As stated in previous section, the DataMonitor basically supports common chart types, as shown in Fig. 5. Although different applications got different demands on data presentation, the DataMonitor covers a wide range of diagrams. In order to enhance it by a new feature, it has to be integrated in data sink and the data source. Although the monitoring tool was modified, existing applications are not affected by that.

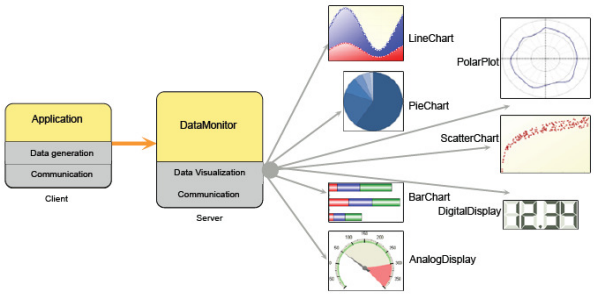

Figure 5: Overview of the system and its supported chart types.

4.3. Implementation

The basic structure of the design is shown in Fig. 6. The design has a clear separation between the communication and the visualization part. Only by that, we can ensure a modular and thus extendable application.

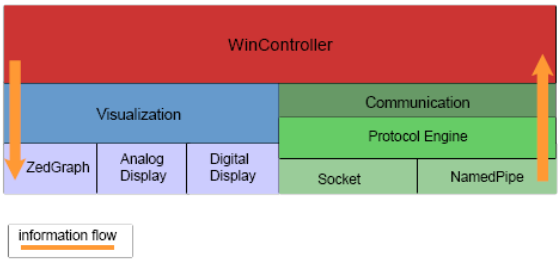

Figure 6: Internal structure and information flow of the DataMonitor.

The core of the software design is the class WinController. It is responsible for controlling the communication and the visualization. Moreover it

contains the state machine shown in Fig. 7.

The state diagram of the defined protocol is as follows:

1. *NoChart*
   Transition from *NoChart* state to *ChartCreated* by NewChart.
2. *ChartCreated*
   Sending measurement data. State remains until CloseChart.

The initial state *NoChart* is reached after the software has been initialized and started up correctly. It is then waiting for incoming requests delivered by the data source. While the server is in the initial state, the only acceptable transition is the creation of a new chart. All other incoming data will be discarded. When creating a new chart, the data source can set the type, the range of the axis, labels, and the amount of input sources, colors, and a few more parameters. While the system is in the *Chartcreated* state, the data source can send chart values, recreate a new chart or close the chart in order to quit or interrupt the measurement phase.

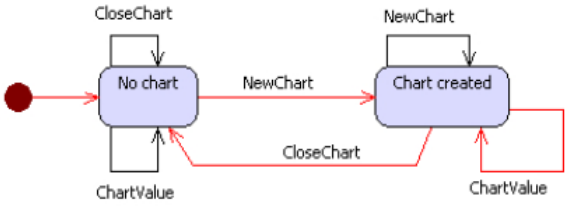

Figure 7: State diagram of the monitoring tool.

The controller acts as a master for the visualization and as a slave for the communication as shown in the information flow in Fig. 6 by the orange arrows.
The communication concept uses the Strategy pattern (Gamma, Helm, Johnson, Vlissides, 1994) in order to select the different interfaces at runtime. Thus it is possible to swap dynamically between the implemented interfaces. After the desired interface was selected and the server started, a thread within the chosen communication object begins running and waits for incoming data. Incoming requests are handed over the protocol engine, which only checks the correctness and the semantic (e.g. keywords, hierarchical order and proper nesting) of the TLV packets. Wrong data is discarded and if the TLV packet was incomplete, the server closes the connection to the client. In every other case, the WinController gets informed about arriving data packets. The new data is processed by the WinController in form of a transition in the internal state machine on the condition of possible transitions. The development of the state machine provides us on the one hand with a clearly structured control sequence and on the other hand makes it is to maintain and extend for future purpose. In order to extend the DataMonitor by a new communication interface, the ICommIF in Fig. 8 has to be implemented.

```
1 public interface ICommIF : IDisposable
2 {
3   event StatusChangedEventHandler StatusChanged;
4   event DataReceivedEventHandler DataReceived;
5   event DataSentEventHandler DataSent;
6   event ErrorEventHandler Error;
7
8   void Start();
9   void Send(string msg);
10  void SendBytes(byte[] buf);
11  void Stop();
12 }
```

Figure 8: Interface definition for communication classes.

The interface consists mainly of two functions to start and stop the communication port. Next to these, there are two more functions for sending data, which are currently obsolete but integrated for future purpose (e.g. extension of bidirectional communication). Incoming data or occurring errors are signaled by three events: StatusChanged, DataReceived and Error. The fourth event DataSent is currently obsolete, because of the unidirectional communication. These signals are either captured by the ProtocolEngine or the WinController. By using the Observer (Gamma, Helm, Johnson, Vlissides, 1994) pattern, we can define this one-to-many dependency between objects so that when one object changes (e.g. new data arrived), all its dependents are notified and updated automatically. Because of this design pattern, the DataMonitor receives data in a non-blocking way.
The visualization component consists of three different libraries: analog display control library, digital display control library, and the ZedGraph library. The analog and digital display controls were developed specifically as dial indicators for speed (analog control) and time (digital control). Nevertheless, the analog control can be used to display pressure values, static state values like ON/OFF and other measurement data (e.g. voltage level). In addition, the digital display control can be used to present textual information as running text (e.g. error messages during a system test, which can be very useful in terms of failures). With the integration of the Open-Source library ZedGraph (ZedGraph, 2008), the functional range could be greatly expanded by many different diagrams. Although it is very powerful, you can create diagrams with a few parameters. This approach fits perfectly into the overall concept of our design – little configuration effort, but a large spectrum of diagrams. For the addition of new charts, the ZedGraph library still offers enough potential. For further details we refer to the online documentation.

5. EXPERIMENTAL RESULTS

In order to provide some results, we intend to give a simple example on the usage of this tool. The example code snippets show, that a few lines suffice to produce well-to-understand visualization of measurement data. Before the client can connect to the server, the desired communication interface has to be selected. After that, the client can start the control sequence to generate a diagram. Fig. 9 shows us the connection routine for a client using socket

communication.

```
Socket mSock = new Socket(AddressFamily.InterNetwork, SocketType.Stream,
    ProtocolType.Tcp);
mSock.Connect("192.168.0.200", 8001); // connect
// start sending data to DataMonitor...
mSock.Close(); // close connection
```

Figure 9: Connect to the server using socket communication.

After the connection to the server was established, the client can send control information to the DataMonitor. In the example shown in Fig. 10, a bar chart with main title, axis title, bar count and elements is created. This information is send to the DataMonitor.

```
BarChart bchart = new BarChart();
bchart.title = "Jahresentwicklung der Rohoelpreise";
bchart.bar_direction = eBarDirection.Vertical;
bchart.x_title = "Jahr";
bchart.y_title = "Euro/Barrel";

bchart.bar_count = 1;
BarElement[] b = new BarElement[bchart.bar_count];
b[0].bar_name = "Euro";
b[0].bar_color = eColor.Green;
bchart.bars = b;

// use ProtocolBuilder
byte[] senddata = ProtocolBuilder.NewChart(bchart.GetBytes());
mSock.Send(senddata, 0, senddata.Length, SocketFlags.None); // send
```

Figure 10: Creation of a bar chart.

When the DataMonitor receives the NewChart control information, the visualization configures the corresponding diagram and the diagram configuration can immediately be check by the user. At this point, the DataMonitor state machine is ready for receiving measurement values. In a few lines, Fig. 11 shows how to generate and send the measurement values to DataMonitor.

```
BarValues bval = new BarValues();

for (int i = 0; i < 8; i++)
{
    // retrieve barchart value from any internal/external source
    ...
    senddata = ProtocolBuilder.ChartValue(bval.GetBytes());
    mSock.Send(senddata, 0, senddata.Length, SocketFlags.None);
}
```

Figure 11: Generation of measurement values.

The result of the presented lines of code is shown in Fig. 12. There you see all labels, the configured coloring and some random bars.

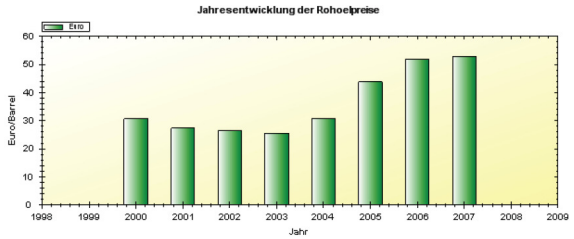

Figure 12: Generation of measurement values.

6. CONCLUSION

The main aim of this work was the development of an easy-to-use, remote and simple to integrate and access (so to speak platform independent) visualization tool. Because of the modular concept of the software design and the user-friendly handling, we assume that the DataMonitor is in addition to the technology field useful in many other areas. Whenever embedded devices, especially restricted devices or so called display-less devices, are used, the need for output types except textual increases. The DataMonitor has been developed exactly for this purpose.

A typical use case for embedded systems in combination with the monitoring tool is to process system information as processor utilization, memory utilization, and power consumption. While running performance tests to identify the maximum throughput of embedded systems, computationally intensive visualization or communication tracers will influence the result. Compared to other common interfaces like Ethernet, the communication effort for data transfer is far less with the simple protocol and will therefore hardly influence the trace of the performance counters.

REFERENCES

BSDZone, 2008. *Berkely Software Distribution*. University of California. Available from: http://www.bsdzone.org [accessed April 2008]

Gamma, E., Helm, R., Johnson, R., Vlissides, J.M., 1994. *Design Patterns. Elements of Reusable Object-Oriented Software.*, 1st ed, Addison-Wesley.

Otto-von-Guericke, 2008. *Grundlagen Visualisierung und Wahrnehmung*. University of Magdeburg. Available from: http://wwwisg.cs.unimagdeburg.de/cv/lehre/VisualAnalytics/material/Bade_Grundlagen-Vis-Wahrnehmung+Infovis.pdf [accessed April 2008]

Colin Ware, 2004. *Information Visualization – Perception for design*, 2nd ed, Kaufman.

Microsoft Corporation, 2005. *Interprocess communications*. Available from: http://msdn.microsoft.com/en-us/library/aa365574(VS.85).aspx [accessed June 2008]

Schwarz, D., 2008. *Mehr Information durch Visualisierung von Daten?* University library Bochum. Available from: http://www.b-i-t-online.de/ [accessed June 2008]

Koch, A., 1993. *Offene Systeme – Interprozesskommunikation in verteilten Systemen*. Springer Verlag.

Barnard, F., 1927. *One picture is worth a thousand words.* Printers' Ink trade journal, pp. 114-115.

Gregory M.N., Hagen, H., Müller, H., 1997. *Scientific Visualization: Overview, Methodologies, and Techniques.* IEEE Computer Society, 1997.

ZedGraph, 2008. *Zegraph – Overview, Samples and Class Documentation* from: http://zedgraph.org/wiki/index.php?title=MainPage [accessed June 2008]

OPTIMIZATION OF KEYWORD GROUPING IN BIOMEDICAL INFORMATION RETRIEVAL USING EVOLUTIONARY ALGORITHMS

Viktoria Dorfer [a], Stephan M. Winkler [b], Thomas Kern [c], Gerald Petz [d], Patrizia Faschang [e]

[a,b,c] Upper Austria University of Applied Sciences
School of Informatics, Communications and Media
Softwarepark 11, 4232 Hagenberg/Mühlkreis, Austria

[d,e] Upper Austria University of Applied Sciences
School of Management
Wehrgrabengasse 1-3, 4400 Steyr, Austria

[a]viktoria.dorfer@fh-hagenberg.at, [b]stephan.winkler@fh-hagenberg.at, [c]thomas.kern@fh-hagenberg.at,
[d]gerald.petz@fh-steyr.at, [e]patrizia.faschang@fh-steyr.at,

ABSTRACT
The amount of data available in the field of life sciences is growing exponentially; therefore, intelligent information search strategies are required to find relevant information as fast and correctly as possible. In this paper we propose a document keyword clustering approach: On the basis of a given set of documents, we identify groups of keywords found in the given documents. Having developed those clusters, the complexity of the data base can be handled much easier: Future user queries can be extended with terms found in the same clusters as those originally defined by the user.

In this paper we present a framework for representing and evaluating keyword clusters on a given data basis as well as a simple evolutionary algorithm (based on an evolution strategy) that shall find optimal keyword clusters. In the empirical section of this paper we document first results obtained using a data set published at the TREC-9 conference.

Keywords: Information Retrieval, Evolutionary Algorithms, Keyword Identification, Document Clustering, Bioinformatics

1. INTRODUCTION

In the year 2009 on average 63.000 new papers per month have been added to PubMed (see www.ncbi.nlm.nih.gov/pubmed), at the moment containing more than 19 million citations. Physicians, biologists, people working in the field of life sciences have to stay up-to-date, regarding for example new therapies, to be able to carry out their work as good as possible. As this huge amount of data cannot be processed manually, intelligent search strategies are necessary to be able to extract as much information as possible for an existing question.

This special field of research is called information retrieval (IR). Many different approaches have already been developed in IR to design intelligent search strategies, including relevance feedback, clustering, parsing and regression analyses (Rocchio 1971; Salton 1988; Schank 1975; Lenat and Guha 1989; Fontaine 1995). The quality of an information retrieval approach can be measured through precision and recall; precision is given by the number of retrieved relevant documents divided by the number of totally retrieved documents, whereas recall is the ratio of the number of relevant retrieved documents and the number of totally relevant documents (see Figure 1). Since it is not trivial to determine the number of relevant documents, certain approximations have to be used.

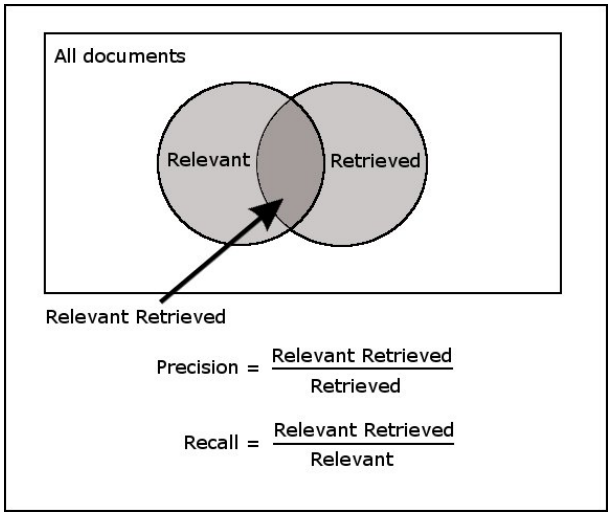

Figure 1: Result Set: Relevant Retrieved, Relevant, and Retrieved (Grossman and Frieder 2004)

However, it is not trivial to find a perfect information retrieval solution (Grossman and Frieder 2004). One reason might be that the approaches were tested with limited data sets, as they were unable to cope with the amount of available data. Still, we cannot make a statement about the performance of a certain approach unless we consider representative data sets (Grossman and Frieder 2004; Hersh 2003).

In this paper we present a method based on evolutionary algorithms that identifies optimal sets of document keywords: The given training sets of documents are analyzed and groups of keywords that are frequently found in combination are generated. Using the produced sets of keywords, future user queries can be updated (extended or transformed) automatically in order to find sets of appropriate documents more efficiently.

2. SCIENTIFIC GOALS

Document clustering is one of the approaches in information retrieval that are used to reduce complexity. Here, documents are divided in groups and the query terms are only matched against the groups assumed to be relevant (Grossman and Frieder, 2004).

Much research has been performed on document clustering, mostly using k-means clustering (Willet 1990; Steinbach, Karypis, and Kumar 2000), but only a few have worked with evolutionary algorithms (Gordon 1991; Robertson and Willet 1994; Jones, Robertson, Santimetvirul, and Willet 1995). Gordon (1991) developed a user based approach where document descriptions are adjusted over time. In contrast, Robertson and Willet (1994) proposed a method to generate groups of words being similarly frequent. Jones, Robertson, Santimetvirul, and Willet (1995) described an approach to search document cluster centers through genetic algorithms.

Apart from the information retrieval scope, work on document clustering based on heuristics has also been carried out, e.g. by Jian-Xian, Huai, Yue-Hong, and Xin-Ning (2009), who worked on a clustering method with known cluster count to optimize classification.

In the context of our research project, the main goal is to identify a document clustering algorithm that is able to cope with a big data base. The idea is to design an algorithm that identifies clusters of documents with respect to sets of keywords that occur in the documents. With these document clusters we now want to adapt queries by adding new relevant terms; these terms are taken from the clusters that seem to be relevant. This approach shall help to improve information retrieval by finding new relevant documents.

In order to reach these goals we have to cope with complex combinatorial problems; we have therefore decided to apply evolutionary algorithms. Details about this approach are given in the following section.

3. APPROACH

3.1. Evolutionary Algorithms

In order to solve complex problems, for which there is no exact and efficient way to find a solution in acceptable time, heuristic methods can be applied. Heuristic methods provide a reasonable tradeoff between achievable solution quality and required computing time, as they employ intelligent rules to scan only a fraction of a highly complex search space. For efficiently scanning complex and exponentially growing search spaces, only heuristic methods can be considered for solving problems in dimensions relevant in real-world applications.

One of the most prominent representatives of heuristics is the class of evolutionary algorithms (EAs): Starting from an (in most cases randomly created) initial population, new solution candidates (individuals) are repeatedly generated by combining attributes of existing solution candidates (which are selected using parent selection operators). These new solutions are optionally modified using a certain mutation routine. The two probably best known types of EAs are the genetic algorithm (GA; Holland 1975) and the evolution strategy (ES; Rechenberg 1973, Schwefel 1994); a detailed overview of evolutionary algorithms, especially genetic algorithms and genetic programming, can be found in Affenzeller, Winkler, Wagner, and Beham (2009).

In the research work described in this paper we have used evolution strategies: Populations consisting of μ individuals are used; in each generation, λ children are generated using random parent selection and mutation. Then the μ best solutions (selected from the children, if the *comma* strategy is chosen, or from parents and children, if the *plus* strategy is chosen) become the next generation's members. We have designed and implemented problem specific mutation operators that are used for modifying solution candidates in order to create new solutions; these operators are described in the next subsection.

3.2. Definition of Solution Candidates

In this work solution candidates represent sets of keywords. These clusters can be initialized either randomly or with keywords based on known statistical information. Mutation can be applied with the implemented problem specific mutation operators: Given a solution candidate c, mutants are created by generating a copy of c and modifying the sets of keywords stored in c. There are several ways how this modification can be done: Randomly chosen keywords might be added to a cluster, keywords of a cluster or even a whole cluster might be removed, a new (randomly generated) cluster could be inserted, or a cluster might be split into two separate clusters.

Neither the total number of clusters nor the number of keywords describing one cluster is fixed. Figure 2 gives a graphical illustration of this idea: Keywords KW_{ij} form cluster C_i; each solution candidate consists of arbitrarily many clusters C_k.

In this context it is very important that the calculated clusters are directly usable: As mentioned previously, the overall goal is to design a framework for biomedical information retrieval which should first cluster document keywords and then use these clusters to extend queries. Provided with the clusters as depicted in Figure 2, it is possible to extend user queries with

terms found in those clusters containing also the original user query terms.

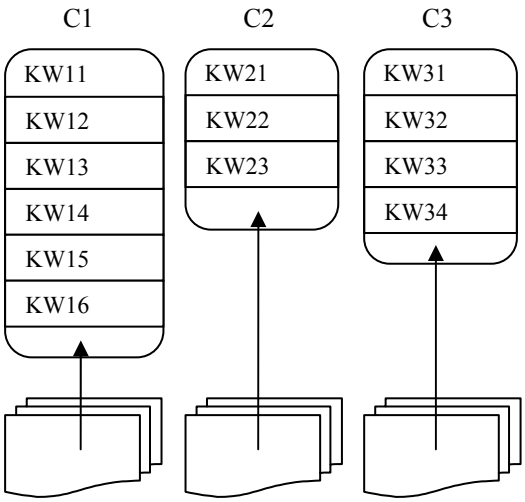

Figure 2: Keyword Clusters Defined by one Solution Candidate

3.3. Fitness of Solution Candidates

The quality of a solution candidate depends on the specificity of the clusters it represents: The better the separation of clusters, the higher the fitness of the candidate. Beside the specificity parts of a cluster we also consider other issues in our fitness function. These aspects cover the number and the distribution of documents assigned to a cluster, or the total number of documents assigned to the clusters. It is also not prohibited that a document belongs to more than one cluster.

Two slightly different fitness functions were tested, each of them considering the following features:

- *A* (range [-∞; 1]): In parameter *A* the ratio of the number of total assigned documents (*At*) to the number of distinct assigned documents (*Ad*) is incorporated; the smaller *A,* the fewer documents are assigned to more than one cluster. In the optimal case the value for *A* would be 1, where every assigned document is assigned to only one cluster.
- *B* (range [0; 1]): Parameter *B* represents the ratio of the number of distinct assigned documents (*Ad*) to the total number of documents (*N*). In the optimal case the value for *B* would be 1, where all documents in the data base are assigned to a cluster.
- *C* (range [0; 1]): Parameter *C* is the mean average cluster confidence, i.e., how good do the documents assigned to a cluster C_i fit to the cluster C_i. The cluster confidence of a cluster C_i ($cConf(C_i)$) is calculated in the following way: For all documents in cluster C_i we calculate the ratio of the number of keywords present in document *d* as well as in cluster C_i, and the number of keywords present in document *d*. These ratios are summed up over all documents in cluster C_i. In the optimal case the value of *C* would be 1, where all documents fit perfectly to their assigned clusters, meaning every document *d* assigned to cluster C_i contains only keywords also present in C_i, whereas C_i can contain more keywords than present in *d*.
- *D* (range [0; 1]): Parameter *D* is the mean average document confidence of each document in each cluster ($dConf(d_j, C_i)$); *D* is a measure how good a cluster fits to a specific document. The document confidence of a document d_j in Cluster C_i is calculated as the ratio of the number of keywords present in d_j as well as in C_i, and the number of keywords of C_i. In the optimal case the value of *D* would be 1, where all clusters fit perfectly to their documents, meaning every cluster C_i contains only keywords which are represented in each document assigned to cluster C_i, whereas document d_j assigned to C_i can contain more keywords than present in C_i.
- *E* (range [-∞; 1]): Parameter *E* considers the standard deviation of the number of documents in the clusters. In the optimal case the value for *E* would be 1, i.e., the same number of documents is assigned to every cluster.
- *G* (range [-∞; 1]): Parameter *G* represents the squared difference of the number of generated clusters to the favored number of clusters (which is defined as a multiple of the logarithm of the number of documents). In the optimal case the value for *G* would be 1, i.e., the number of generated clusters is the same as the number of favored clusters.

$$A = 1 - \left(\frac{At}{Ad} - 1\right) \tag{1}$$

$$B = \left(\frac{Ad}{N}\right) \tag{2}$$

$$cConf(C_i) = \frac{\sum_{d \in d_{C_i}} \frac{|KW:KW \in KW(d)\ \&\ KW \in C_i|}{|KW(d)|}}{\left|d_{C_i}\right|} \tag{3}$$

$$C = \frac{\sum_{i=1}^{CK} cConf(C_i)}{CK} \tag{4}$$

$$dConf(d_j, C_i) = \frac{|KW:KW \in KW_j\ \&\ KW \in C_i|}{|KW(C_i)|} \tag{5}$$

$$D = \frac{\sum_{i=1}^{CK}\left(\frac{\sum_{d_j \in d_{C_i}} dConf(d_j, C_i)}{\left|d_{C_i}\right|}\right)}{CK} \tag{6}$$

$$E = 1 - \sqrt{\frac{1}{CK-1}\sum_{i=1}^{CK}\left(N_{C_i} - \overline{N_C}\right)^2} \tag{7}$$

$$G = 1 - \left(\frac{|CK - \varphi * \log N|}{\varphi * \log N}\right)^2 \tag{8}$$

These parameters yield to the following fitness functions, both to be maximized:

$$F_1 = \alpha \cdot A + \beta \cdot B + \gamma \cdot C + \delta \cdot D + \varepsilon \cdot E + \zeta \cdot G \quad (9)$$

$$F_2 = -(\alpha \cdot \log(z - A) + \beta \cdot \log(z - B) + \gamma \cdot \log(z - C) + \delta \cdot \log(z - D) + \varepsilon \cdot \log(z - E) + \zeta \cdot \log(z - G)) \quad (10)$$

(z has to be greater than 1, thus z:= 1.1 or 2.0, e.g.)

The second fitness function is motivated by the approach of multiplying the logarithm of the punishment factors of each parameter, preventing an unfair high fitness value if only one parameter gets very high (which could be a possible problem when using fitness function F_1).

The optimal fitness value for F_1 is $\alpha+\beta+\gamma+\delta+\varepsilon+\zeta$; the maximum fitness value for F_2 is $-(\alpha \cdot log(x) + \beta \cdot log(x) + \gamma \cdot log(x) + \delta \cdot log(x) + \varepsilon \cdot log(x) + \zeta \cdot log(x))$ where $x=z-1$; in the case of $z=2$ the fitness value of an optimal solution becomes 0 (if F_2 is used).

4. DATA BASES

The data used is part of the ohsumed data file of the TREC-9 conference in the year 2000 and has been used in the filtering track (Vorhees and Harman 2000). To be exact, the file used is "ohsumed89.tar.gz", downloaded from http://trec.nist.gov/data/t9_filtering.html, containing references from MEDLINE (Pubmed 2010) of the year 1989, including title, abstract, MeSH (Medical Subject Headings) terms, authors, source, and publication type. MeSH is the U.S. National Library of Medicine's controlled vocabulary used for indexing articles for MEDLINE/PubMed (NCBI 2010). We extracted 36.890 data sets out of the mentioned data file.

Initially we performed some data preprocessing on the extracted sets for better comparability; we have applied stemming and have removed stop words. Stemming is the reduction of words to their stem. We used a simple stemming algorithm, following the algorithm by Harman (1991), but adapted it slightly: The third rule in the Harman algorithm is to trim words ending with "s", except those ending with "us" or "ss". We added the exception "is" to the rule in order not to trim words like "meiosis" or "synthesis", e.g. The stop word list used was taken from Lewis (2004) to remove common English words such as for example "a", "the", "our", or "usually" in order not to distort the clustering.

5. RESULTS

We tested both fitness functions with various settings, each setting with different numbers of generations (5000, 10000, 20000, 50000, and 70000) and each generation setting was tested 5 times.

Six different parameter settings including different setups for μ and λ have been used in the test series documented here. All in all, the algorithm delivered meaningful results and found useful clusters in different parts of the solution space. Examples for meaningful clusters are the combination of "male", "female", "human", "gov" and "support" or the combination of "spider" and "arachnidism".

Figure 3 gives an overview of the weighting factor settings used in examples 1 to 6, Figures 4 and 5 summarize the results that were retrieved in the respective test series. In test series 1 to 3 fitness function F_1 has been applied, test series 4 to 6 were executed using F_2. μ was set to 20 for examples 2 and 3, and to 1 for all other tests; λ was set to 100 for example 1, to 50 for examples 2 and 3, and to 10 for all other runs.

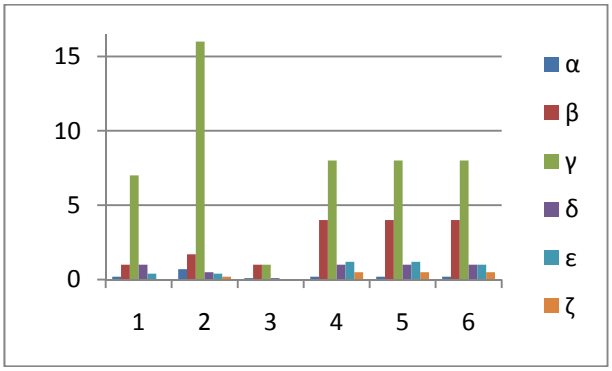

Figure 3: Test Setup (Weighting Factor Settings) of Test Runs 1 – 6

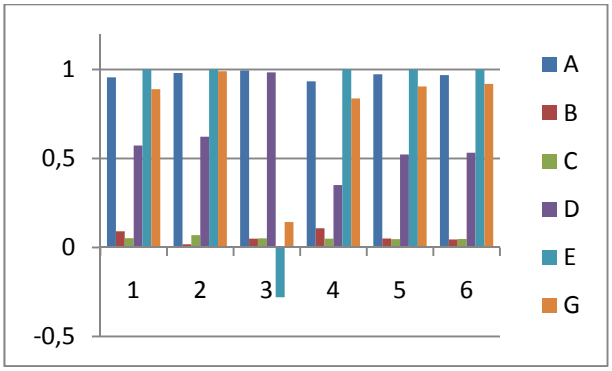

Figure 4: Results of Parameters A-G of Test Series 1 – 6 Retrieved Using Weighting Factors Depicted in Figure 3

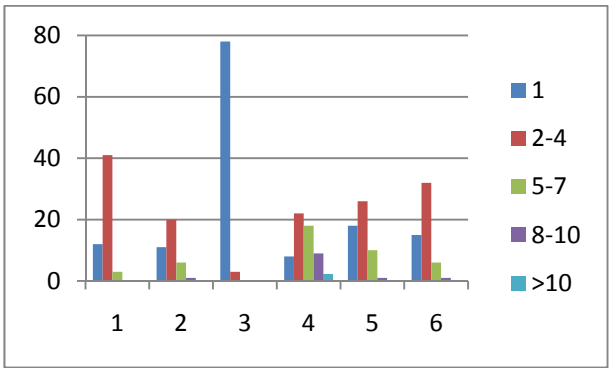

Figure 5: Keyword Histogram for Examples 1 – 6: For Each Example We Give the Number of Clusters Containing 1, 2-4, 5-7, 8-10, or more than 10 Keywords

6. DISCUSSION AND OUTLOOK

6.1. Discussion, Algorithmic Improvements

Even though parts of optimal solutions have been identified, one clearly sees that the presented method is not yet robust if the quality of the given training data set is not ideal (i.e., if the given document keywords are not easily separable into distinct clusters) or the algorithmic parameters are chosen in a suboptimal way. At the moment we suggest combining the results of separate optimization runs and use a combination of their most significant clusters.

As we have not yet been able to find the "optimal" parameter settings, future work will include more parameter tuning and algorithm testing. The authors plan to improve the mutation operators and will also define crossover operators.

6.2. Usage of Text Terms

For future work we also want to use not only the keywords of the documents but all the words of the text for clustering. To filter the significant words we plan to use a commonly used weighting scheme (as described for example in Grossman and Frieder 2004):

$$d_{ij} = tf_{ij} \times idf_j \tag{11}$$

where tf_{ij} is the number of occurrences of term t_j in document D_i – the term frequency – and idf_j is the inverse document frequency, calculated as

$$idf_j = \log\left(\frac{d}{df_j}\right) \tag{12}$$

where df_j is the document frequency, i.e., the number of documents that contain term t_j, and d is the number of documents.

6.3. Implementation

The IR preprocessing approach described in this paper shall be integrated in the HeuristicLab framework (http://www.heuristiclab.com; Wagner et al. 2008; Wagner 2009), a framework for prototyping and analyzing optimization techniques for which generic concepts of evolutionary algorithms as well as many functions to evaluate and analyze them are available. The HeuristicLab framework has been designed and developed by members of the Heuristic and Evolutionary Algorithms Laboratory (HEAL, http://heal.heuristiclab.com/) at the Upper Austria University of Applied Sciences; it is also used as the main framework for the research project *Heureka!* (http://heureka.heuristiclab.com/).

6.4. Biomedical Information Retrieval Framework

As mentioned in Section 2 the authors plan to integrate the clustering algorithm in a biomedical information retrieval framework. This framework shall be used to extend user queries with terms which are members of those clusters also containing the user query terms.

ACKNOWLEDGMENTS

The work performed in this paper was done within *TSCHECHOW*, a research project funded by the basic research funding program of Upper Austria University of Applied Sciences.

REFERENCES

Affenzeller, M., Winkler, S., Wagner, S., A. Beham, 2009. *Genetic Algorithms and Genetic Programming - Modern Concepts and Practical Applications*. Chapman & Hall/CRC. ISBN 978-1584886297. 2009.

Fontaine, A., 1995. *Sub-element indexing and probabilistic retrieval in the POSTGRES database system.* Master thesis. University of California Berkeley.

Gordon, M., 1991. User-based document clustering by redescribing subject description with a genetic algorithm. *Journal of the American Society for Information Science*, 42 (5), 311-322.

Grossman, D.A., Frieder, O., 2004. *Information Retrieval – Algorithms and Heuristics*. 2nd ed. Dordrecht: Springer

Harman, D., 1991. How effective is suffixing? *Journal of the American Society for Information Science*, 42, 7-15.

Hersh, W.R., 2003. *Information Retrieval: a health and biomedical perspective*. 2nd ed. New York: Springer

Holland, J.H., 1975. *Adaption in Natural and Artifical Systems.* University of Michigan Press

Jian-Xiang, W., Huai, L., Yue-hong, S., Xin-Ning, S., 2009. Application of Genetic Algorithm in Document Clustering. *ITCS '09: Proceedings of the 2009 International Conference on Information Technology and Computer Science*, 145-148. July 25-26, Kiev (Ukraine)

Jones, G., Robertson A.M., Santimetvirul, C., Willet, P., 1995. Non-hierarchic document clustering using a genetic algorithm. *Information Research,* 1(1), Available from: http://InformationR.net/ir/1-1/paper1.html [accessed 1 April 2010]

Lenat, D., Guha, R., 1989. *Building Large Knowledge-Based Systems - Representation and Inference in the Cyc Project.* Boston: Addison-Wesley Longman Publishing Co., Inc.

Lewis, D.D., Yang, Y., Rose, T., Li, F., 2004. A New Benchmark Collection for Text Categorization Research. *Journal of Machine Learning Research.* 5, 361-397. Stop word list available from: http://jmlr.csail.mit.edu/papers/volume5/lewis04a/a11-smart-stop-list/english.stop [accessed 1 April 2010]

NCBI, 2010. http://www.ncbi.nlm.nih.gov/mesh [accessed 20 July 2010]

PubMed, 2010. http://www.ncbi.nlm.nih.gov/pubmed

Rechenberg, I., 1973. *Evolutionsstrategie.* Friedrich Frommann Verlag

Rocchio, J.J., 1971. Relevance Feedback in Information Retrieval. In: Salton, G., eds. *The SMART retrieval system - experiments in automatic document processing*. Englewood Cliffs: Prentice-Hall, Inc., 313-323.

Robertson, A.M, Willet, P., 1994. Generation of equifrequent groups of words using a genetic algorithm. *Journal of Documentation*, 50 (3), 213-232.

Salton, G., 1988. *Automatic Text Processing*. Boston: Addison-Wesley Longman Publishing Co., Inc.

Schank, R.C., 1975. *Conceptual Information Processing*. New York: Elsevier Science Inc.

Schwefel, H.-P., 1994. *Numerische Optimierung von Computer-Modellen mittels der Evolutionsstrategie*. Basel: Birkhäuser Verlag

Steinbach, M., Karypis, G., Kumar, V., 2000. *A Comparison of Document Clustering Techniques*. Technical Report. University of Minnesota, Department of Computer Science and Engineering

Vorhees, E.M., Harman, D.K., 2000. *NIST Special Publication 500-249: The Ninth Text REtrieval Conference (TREC-9)*. Gaithersburg, Maryland: Department of Commerce, National Institute of Standard and Technology.

Wagner, S., Kronberger, G., Beham, A., Winkler, S., Affenzeller, M., 2008. Modeling of heuristic optimization algorithms. *Proceedings of the 20th European Modeling and Simulation Symposium (EMSS2008)*, pp.106-111.

Wagner, S., 2009. *Heuristic Optimization Software Systems - Modeling of Heuristic Optimization Algorithms in the HeuristicLab Software Environment*. PhD Thesis, Institute for Formal Models and Verification, Johannes Kepler University Linz, Austria.

Willet, P., 1990. Document clustering using an inverted file approach. *Journal of Information Science*, 2, 223-231.

AUTHORS BIOGRAPHIES

VIKTORIA DORFER is a senior researcher in the field of Bioinformatics at the Research Center Hagenberg, School of Informatics, Communications and Media. After finishing the diploma degree of bioinformatics in 2007 she was a team member of various projects in the field of informatics and bioinformatics. She is currently working on information retrieval within the TSCHECHOW project.

STEPHAN M. WINKLER received his MSc in computer science in 2004 and his PhD in engineering sciences in 2008, both from Johannes Kepler University (JKU) Linz, Austria. His research interests include genetic programming, nonlinear model identification and machine learning. Since 2009, Dr. Winkler is professor at the Department for Medical and Bioinformatics at the Upper Austria University of Applied Sciences, Campus Hagenberg.

THOMAS KERN is head of the Research Center Hagenberg, School of Informatics, Communications and Media, Upper Austria University of Applied Sciences (UAS). He finished his studies in Software Engineering in 1998. After some work experience in industry he started his academic career at UAS in autumn 2000 as research associate and lecturer for algorithms and data structures, technologies for knowledge based systems, semantic systems and information retrieval. Since 2003 he has conducted several application oriented R&D projects in the fields of bioinformatics and software engineering.

GERALD PETZ is director of the degree course "Marketing and Electronic Business" at the University of Applied Sciences in Upper Austria, School of Management in Steyr. His main research areas are Web 2.0, electronic business and electronic marketing; he has also conducted several R&D projects in these research fields. Before starting his academic career he was project manager and CEO of an internet company.

PATRIZIA FASCHANG received her bachelor degree in electronic business and is a junior researcher at the Research Center Steyr, School of Management, in the area of digital economy. She has worked on several small projects in the field of marketing and electronic business and is currently working on Opinion Mining and Web 2.0 methods within the TSCHECHOW project.

ON-LINE PARAMETER OPTIMIZATION STRATEGIES FOR METAHEURISTICS

Michael Affenzeller, Lukas Pöllabauer, Gabriel Kronberger, Erik Pitzer, Stefan Wagner, Stephan M. Winkler, A. Beham, M. Kofler

Upper Austria University of Applied Sciences
School for Informatics, Communications, and Media
Heuristic and Evolutionary Algorithms Laboratory
Softwarepark 11, 4232 Hagenberg, Austria

michael.affenzeller@fh-hagenberg.at , lukas.poellabauer@fh-hagenberg.at, gabriel.kronberger@heuristiclab.com, erik.pitzer@heuristiclab.com, stefan.wagner@heuristiclab.com, stephan.winkler@fh-hagenberg.at, andreas.beham@heuristiclab.com, monika.kofler@heuristiclab.com

ABSTRACT
In this paper we describe different aspects of parameter tuning strategies for meta-heuristic algorithms. In contrast to many automated parameter adjustment methods in the field, special attention is given to parameter tuning strategies which are able to be applied during the run of a meta-heuristics. The basic idea we are using for this approach steams from self adaptive evolution strategies and this paper discusses different adaptations to this idea in order to find out, to which extent this concept can be transformed to other meta-heuristics.

Keywords: Meta-heuristic Optimization, Evolutionary Algorithms, Parameter Tuning.

1. INTRODUCTION

Heuristic methods provide a reasonable tradeoff between achieved solution quality and required computing time, as they employ intelligent rules to scan only a fraction of a highly complex search space. Typical applications of heuristic methods can be found in production optimization; for example, heuristic algorithms are applied in machine scheduling and logistics optimization. For efficiently scanning such highly complex and exponentially growing search spaces, only heuristic methods can be considered for solving problems in dimensions which are relevant for real-world applications.

The step from heuristics to meta-heuristics is an essential one: While heuristics are often designed and tuned for some specific problem, meta-heuristics offer generic strategies for solving arbitrary problems. The implementation of concrete solution manipulation operators still depends on the problem representation, but the optimization strategy itself is problem-independent.

The success of meta-heuristics is based on an interplay between phases of diversification and intensification, but in order to achieve a beneficial equilibrium, fine-tuning is necessary for each problem instance depending on its fitness landscape characteristics (Affenzeller et al., 2009).

One of the most prominent representatives of meta-heuristics is the class of evolutionary algorithms (Eiben and Smith, 2003): New solution candidates (individuals) are generated by combining attributes of existing solution candidates (crossover) and afterwards they are slightly modified with a certain probability (mutation); parent individuals are chosen by means of nature inspired selection techniques (Holland, 1975). A second well-known example of a rather simple meta-heuristic is simulated annealing (Kirkpatrick et al., 1983): This approach is closely related to local search strategies such as hill climbing/descending and generates new solutions iteratively, starting from a usually randomly initialized solution. In contrast to simple hill climbing/descending, moves to worse solutions are permitted with a certain probability which decreases during the heuristic search process; by this means the algorithm first performs exploration (diversification), and later tends to focus on promising regions (intensification).

A multitude of other meta-heuristics has been described in the literature, such as for example particle swarm optimization (Eberhardt et al., 2001), tabu search (Glover, 1997) and iterated local search (Lourenco et al., 2003). The evolution of so many diverse meta-heuristics results from the fact that no single method outperforms all others for all possible problems. To be a bit more precise, the so-called No-Free-Lunch theorem postulates that a general-purpose universal optimization strategy is impossible and that the only way how one strategy can outperform another is to be more specialized to the structure of the tackled problem. The No-Free-Lunch theorem basically says that, given two arbitrary meta-heuristics (including random search), there always exist search spaces for which the first meta-heuristic will perform better than the second and vice versa.

This means that even for the most sophisticated meta-heuristic a fitness landscape can be constructed for

which it performs worse than ordinary random search. Therefore, it always takes qualified algorithm experts to select, parameterize and tune a meta-heuristic algorithm for a concrete application.

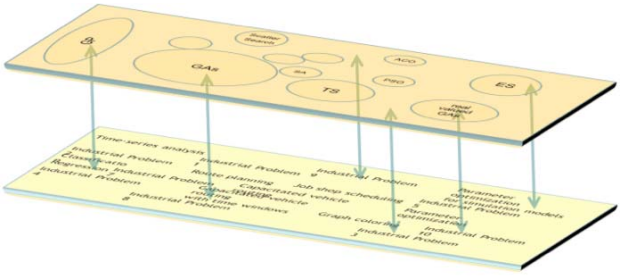

Figure 1: Schematic representation of the ordered relation between problem instances (lower layer) and potentially well suited meta-heuristics (upper layer).

This situation is illustrated in Figure 1 where the lower layer represents the problem instances with their associated fitness landscape characteristics and the upper layer shows the meta-heuristic methods under certain parameterizations. There exist some rough rules of thumb derived from empirical testing that indicate which meta-heuristics should be chosen for certain problem characteristics. However, picking an appropriate method for a certain problem instance is a non-trivial task. On the one hand, fitness landscape characteristics may change remarkably for different problem dimensions; on the other hand, the characteristics of a certain meta-heuristic may considerably vary for different parameter settings.

The problem of choosing an appropriate method and to find a beneficial set of parameters for a given optimization task is usually a challenging and time consuming task which takes an experienced algorithm expert. Alternatively, some automated approaches have been proposed that try chose the method or its parameter setting automatically. However, these approaches usually all suffer from enormous runtime consumption as it is necessary to run a set of parameter settings for the meta-heuristics to be optimized in order to evaluate only one single solution candidate of the optimization method which is responsible for optimizing the parameter tuning. The approach of optimizing the parameters of a meta-heuristics for a certain problem is often referred to as meta-optimization of meta-heuristics and is usually done with a meta-heuristics itself. Unfortunately, it is also no good idea to optimize the parameters applied to a small problem instance of the problem class to be solved in terms of parameter adjustment, as fitness landscape characteristics are usually totally different for different problem instance of the same problem class and therefore require different parameter settings. Summarizing all these considerations, it can be concluded that the application of meta optimization strategies for the parameter optimization task of a modern meta-heuristics applied to a challenging problem to be solved is a very time consuming task and therefore usually not applied in practice where up-to date hardware environment is already on its limits just for solving the problem to be solved.

In this paper we aim to introduce a general purpose lazy meta-optimization approach which is able to adapt certain parameter setting of a meta-heuristic algorithm during its run. The basic idea is inspired by the general idea, how self adaptive evolution strategies handle componentwise adjustment of the strategy parameters during the run (Schwefel, 1975). The main advantage of this strategy is, that, even if it is not so powerful than pure meta-optimization approaches, that it should be quite easily applicable to even quite time consuming problem instances as the runtime requirements are not much higher than in the case of a standard meta-heuristics.

The paper is organized as follows: Sections 2 and 3 describe the theoretical foundations for the new lazy meta-optimization approach which is introduced in section 4. In section 5 first results of the lazy meta-optimization are shown exemplarily for genetic algorithms with and without offspring selection (Affenzeller and Wagner, 2005). Finally, section 6 concludes the main characteristics of the proposed approach and touches on some ideas about future application areas of the proposed ideas.

2. META OPTIMIZATION

As stated in the introduction, the choice of a certain meta-heuristics as well as the parameter tuning process is highly dependent on the problem instance which is to be optimized. With the No-Free-Lunch theorem in mind there is also strong theoretical evidence that a universal solver meta-heuristics cannot be realized.

Meta meta-heuristics, in which meta-heuristics are used for the parameter tuning process of a meta-heuristics, has have already been discussed for a long period of time. In (Grefenstette, 1986), for example, a genetic algorithm has been used for tuning the parameters of a genetic algorithm.

A severe drawback of such approaches is that for the fitness evaluation of a high-level (meta-meta level) solution candidate a complete run of the low level algorithm has to be performed; considering the fact that reams of thousands of evaluations are usually required for achieving satisfying results and that each evaluation on the high level requires a full run on the low-level meta-heuristics it becomes easy to follow that this approach is still rather restricted to solve rather simple (low dimensional) problems. A crucial fact concerning this approach is also that it is not advantageous to identify good algorithm parameters on the basis of low dimensional problems and apply them on higher dimensional problems because the fitness landscape characteristics are drastically changing even for different problem instances of the same problem class.

A comprehensive review of parameter control strategies for evolutionary algorithms is stated in (Eiben et al., 1999).

A similar flavor which is driven by the availability of parallel hardware systems is given by hyper-heuristics (Burke et al., 2003). The goal here is, that hyper-heuristics should be able to adapt to the fitness landscape characteristics associated with a certain problem. However, the approach is quite different: Hyper-heuristics operate on a higher level of abstraction: they choose a certain meta-heuristics out from a set of available meta-heuristics depending on the actual performance which may be measured on the basis of CPU-time and the change in fitness. Even this approach seems to be quite simple and also quite efficient to handle especially in a parallel environment, it is not able to tune the parameters of the certain meta-heuristics themselves.

In the following sections we will propose a new attempt which may be seen as some kind of compromise of meta-meta heuristics and hyper heuristics. In this approach, the tuning of parameters should be done during the run of a single algorithm in way which is inspired by the way evolution strategies adaptively handle step-width regulation according to (Beyer and Schwefel, 2002).

3. SELF-ADAPTIVE ES

With the 1/5 success-rule, Rechenberg introduced a regulator for the mutation strength depending on the ratio of successful mutants in a certain generation (Rechenberg, 1973). If the ratio of successful mutants is high (>1/5) it is rather easy to achieve improvements and the optimum is considered to be far away. Therefore, the mutation strength (step-width) is increased. In case of too little successful mutants (<1/5) mutation strength is decreased because it is argued that the algorithm may jump around an optimum without detecting it.

Following basically the same idea, Schwefel introduced a self-adaptive step-width regulation which is applied individually to each dimension of the parameter vector for each solution candidate of the ES population (Schwefel, 1975). Technically, this is done in the following way:

The dimension of an *n*-dimensional parameter vector is doubled resulting in a parameter vector of dimension *2n*. The additional *n* dimensions store the actual standard deviation of the usually normal distributed mutation step-width for each dimension of the parameter vector.

$$X = ((x_1, x_2, \ldots x_n), (\sigma_1, \sigma_2, \ldots, \sigma_n))$$
$$x_i' = x_i + N(0, \sigma_i') \text{ (mutation)}$$

Consequently, also the mutation step-widths have to be mutated as well. This is usually done by adding some Gaussian noise around 0 with a constant term and a term which depends on the dimension.

The aspect of this adaptive parameter tuning strategy which is quite unique is the fact that the mutation step-widths σ_i are implicitly optimized even if we do not have an explicit fitness function for them. In other word this means that this strategy operates under the assumption that above average solution candidates are more likely to have emerged with advantageous parameters (step-width variances).

The main idea of the present contribution is to consider, how and to which extent this idea can be transferred to other meta-heuristics. The next two chapters exemplarily point out some concrete strategies about how such an ES-inspired lazy meta-optimization strategy may be transferred to genetic algorithms and give some preliminary results.

4. LAZY META-OPTIMIZATION

In this section we consider which parameter of a standard genetic algorithm (SGA), an island model parallel genetic algorithm (PGA), and an offspring selection genetic algorithm (OSGA) can be optimized implicitly during the run of the algorithm.

Basically, offspring selection is defined in the following way: After generating new solutions by crossover and mutation, these new solutions are inserted into the next generation's population only if they are better than their parents. The decision whether a child is considered better than its parents depends on the so-called comparison factor *cf* (*cf* ∈ [0, 1]) parameter: If *cf=0* then a child is already considered better if it surpasses the fitness of the worse parent, if *cf=1* then a child has to be better than both parents for being considered successful. Additionally, the parameter *success ratio* defines the ratio of successful individuals in the next population; the rest of the population is filled up with children that do not necessarily have to be successful. Details about this procedure can for example be found in (Affenzeller and Wagner, 2005) or in (Affenzeller et al., 2009).

For the considered GA variants the following parameter values have to be adjusted:

- Population size
- Selection operator
- Elitism
- Crossover operator
- Mutation operator
- Mutation rate
- Additionally for PGAs
  - Communication topology
  - Migration scheme
  - Migration rate
  - Migration interval
- Additionally for OSGAs
  - Comparision factor
  - Success ratio
  - Maximum selection pressure

The only parameters that can be considered in a sense that they were relevant for the evolvement of a certain individual are the choice of the crossover operator and the mutation operator.

Parameters like the mutation rate have to be analyzed with respect to the evolvement of the population.

So far we have analyzed combinations of different crossover and mutation operators which are stored together with the individual (the individual stores the operator by which it has been evolved). Due to the sexual recombination aspect, a local family tournament is applied when the two parent individuals are carrying different crossover operators in their parameter knapsack. If mutation is to be applied in the actual reproduction step, the family tournament has to be extended for up to four potential offspring solution candidates that may arise, if both parents have used different crossover and mutation operators.

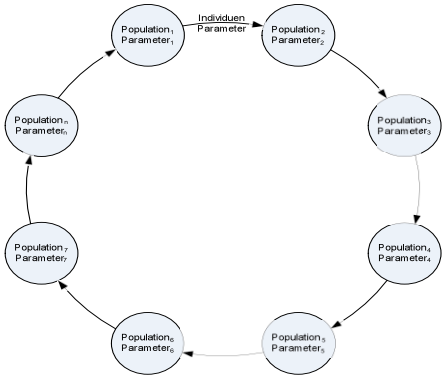

Figure 2: Migration of parameters (and) individuals in the topology of a unidirectional ring.

Concerning the online-optimization of strategy parameters that have to be interpreted on the population level several more challenging questions arise – especially in the context of genetic algorithms. In contrast to standard meta-optimization approaches, here we want to evaluate the actual potential of the population in terms of achievable solution quality during the run of the algorithm. Therefore, it becomes necessary to define some measure for the potential of the population with respect to achievable solution quality. Having in mind the building block theory for genetic algorithms (e.g. in Affenzeller et al, 2009) the achievable solution quality of a genetic algorithm mainly depends on the distribution of essential genetic information over the individuals in a certain population and how the available genetic operators are able to combine this essential genetic information to better and better solution candidates.

The evaluation function for the actual potential of a population may be defined in terms of a measure which calculates the relative ratio of successful offspring of a random sample taken from the actual population where an offspring is considered successful if its fitness is better than the fitness of the better two parents which can be evolved using the actual set of parameters and operators. However, the question remains how the parameters which are relevant for the evolvement of a population can be compared amongst each other. For this purpose we propose an architecture which is similar to a course grained parallel GA. The only difference to an island model GA is that the concept of migration is adapted for the exchange of advantageous parameter settings between the subpopulations as indicated in Figure 2.

5. RESULTS

In this section first results of lazy meta-optimization are shown for genetic algorithms considering the performance of different crossover operators for the *ch130* travelling salesman benchmark problem taken from the TSPLib. The experiments have been performed with the framework HeuristicLab 3.3[1] using the set of parameters shown in Table 1 and Table 2. A detailed description of the listed GA parameters and operators can be found in (Affenzeller et al., 2009).

Parameter	Value
Generations	2000
Population size	100
Selection operator	Proportional
Mutation operator	Inversion
Mutation rate	5%
Elitism strategy	1-elitism
Crossover operators	Family tournament using the following set of crossover operators: AbsolutePositionTopologicalCrossover OrderBasedCrossover PositionBasedCrossover CyclicCrossover OrderCrossover EdgeRecombinationCrossover MaximalPreservativeCrossover PariallyMatchedCrossover CosaCrossover

Table1: Parameters for the experiments shown in Figure 3 and Figure 4.

Figure 3 shows that when using a standard GA basically only two (ERX and Cosa) out of the nine available crossover operators turn out to be successful where ERX becomes even more successful in the final (almost converged) stage when the goal is to achieve still minor improvements.

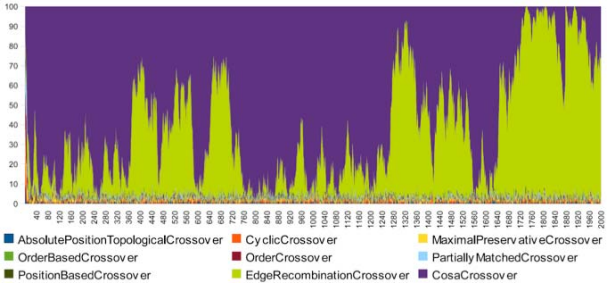

Figure 3: Distribution of crossover operators when using a standard GA.

[1] https://dev.heuristiclab.com/trac/hl/core

Parameter	Value
Generations	500
Success Ratio	1
Comparison Factor	1
Max. selection pressure	100

Table 2: Additional (offspring selection) parameters for the experiments shown in Fig. 4.

The remaining seven crossover operators turn out to be ineffective for the given problem and are therefore practically not used even if some survival strategy is implemented in order to avoid the total disappearance of an operator.

When using an offspring selection GA (additional parameters are given in Table 2) the dominance of single operators becomes even more evident and it is especially the ERX operator which extensively outperforms the other operators; only the Cosa operator can contribute in some stages of the algorithm.

Even if we can only show some snapshot results in this paper, the basic characteristics (dominance of ERX and Cosa) explained here are characteristic for other TSP experiments. When experimenting with other problem instances or even other problems the characteristics are different of course which is one of the main motivations for meta-meta or hyper-heuristics.

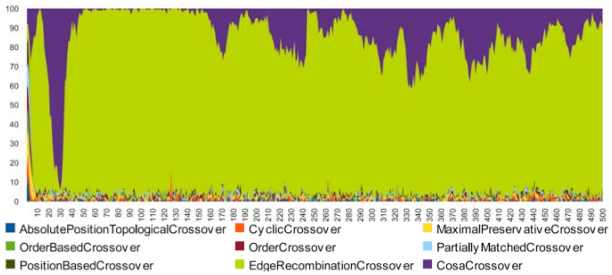

Figure 4: Distribution of crossover operators when using an offspring selection GA.

Concerning the experiments it has to be pointed out that the results shown here are only exemplarily and many other experimental setups are to be addressed in the future. Some suggestions are given in the conclusion. Furthermore, the main goal of the experiments of this paper was not focused on solution quality but rather on indicating the potential of the proposed lazy meta-optimization approach. However, the achieved results are close (within a 5% range) to the global optimal solution and comparable or better than with any single operator.

6. CONCLUSION

In this paper we have proposed several aspects for a lazy meta-optimization approach which is inspired by the implicit strategy parameter optimization of evolution strategies with adaptive step-width regulation according to (Schwefel, 1975). Concretely, it has been considered, which parameters of several genetic algorithm variants may be optimized following this strategy. First exemplary results of this approach have been shown.

However, many aspects should be analyzed in more detail: Open topics for future research in this field concern the mentioned family tournament. Alternatively also random operators of the two parent individuals could be used analyzing the effects concerning performance and expressiveness. Also the analysis of different migration strategies (for the exchange of parameters relevant for the performance of subpopulations) need to be studied in more detail.

Furthermore, the evaluation of the actual potential of a GA population is a challenging research topic of its own. As an alternative to the proposed potential evaluation, also a combined measure could be used considering the best and average individual fitness combined with a diversity potential.

ACKNOWLEDGMENTS

The work described in this paper was done within the Josef Ressel Centre for Heuristic Optimization *Heureka!* (http://heureka.heuristiclab.com/) sponsored by the Austrian Research Promotion Agency (FFG).

REFERENCES

Affenzeller, M. and Wagner, S., 2005. Offspring selection: A new self-adaptive selection scheme for genetic algorithms. *Adaptive and Natural Computing Algorithms*, Springer Computer Science, pp. 218-221.

Affenzeller, M., Winkler, S., Wagner, S., A. Beham, 2009. *Genetic Algorithms and Genetic Programming - Modern Concepts and Practical Applications*. Chapman & Hall/CRC. ISBN 978-1584886297.

Beyer, H-G. and Schwefel. *Evolution strategies – A Comprehensive Introduction*. Natural Computing 1(1). 2002. pp. 3 – 52.

Burke, E., Kendall, G., Newall, J., Hart, E., Ross P., Schulenburg S., 2003. Hyper-heuristics: An Emerging Direction in Modern Search Technology. In: F. Golver and G.A. Kochenberger, ed. *Handbook of Metaheuristics*. Kluwer Academic Publishers: pp. 457–474.

Eberhardt, R. C., Shi, Y, Kennedy, J., 2001. Swarm Intelligence. *The Morgan Kaufmann Series in Artificial Intelligence.*

Eiben, A.E, Hinterding, R., Michaelwicz Z. 1999. Parameter Control in Evolutionary Algorithms. *IEEE Transactions on Evolutionary Computation 3(2)*, IEEE Press, pp 124 - 141.

Eiben, A.E. and Smith, J.E. 2003. Introduction to Evolutionary Computation. *Natural Computing Series*, Springer-Verlag Berlin Heidelberg.

Glover, F. ,1997. Tabu Search and Adaptive Memory Programming – Advances, Applications, and Challenges. *Advances in Metaheuristics, Optimization and Stochastic Modeling Technologies* 7, Springer, pp. 1-75.

Grefenstette, J. ,1986. Optimization of control parameters for genetic algorithms. *IEEE Transactions on Systems, Man and Cybernetics 16 (1)*, IEEE Press, pp. 122-128.

Holland, J.H., 1975. *Adaption in Natural and Artifical Systems.* University of Michigan Press

Kirkpatrick, S., Gelatt Jr., C. D., Vecchi, M. P., 1983. Optimization by Simulated Annealing, *Science* 220(4598): 671-680.

Lourenco, H. R., Martin, O. C., Stützle, T., 2003 Iterated Local Search, Handbook of Metaheuristics (57), Kluwer 321 – 352.

Rechenberg, I., 1973. *Evolutionsstrategie.* Friedrich Frommann Verlag

Schwefel, H.-P., 1975. *Evolutionsstrategie und Numerische Optimierung.* Technische Universität Berlin, Fachbereich Verfahrenstechnik: Dr.-Ing., Dissertation.

Schwefel, H.-P., 1994. *Numerische Optimierung von Computer-Modellen mittels der Evolutionsstrategie.* Basel: Birkhäuser Verlag

AUTHORS BIOGRAPHIES

MICHAEL AFFENZELLER has published several papers, journal articles and books dealing with theoretical and practical aspects of evolutionary computation, genetic algorithms, and meta-heuristics in general. In 2001 he received his PhD in engineering sciences and in 2004 he received his habilitation in applied systems engineering, both from the Johannes Kepler University of Linz, Austria. Michael Affenzeller is professor at the Upper Austria University of Applied Sciences, Campus Hagenberg, and head of the Josef Ressel Center *Heureka!* at Hagenberg.

LUKAS PÖLLABAUER studied Software Engineering at the Upper Austrian University of Applied Sciences (Campus Hagenberg) and received his MSc in 2009. His research interests include heuristic optimization methods and parameter optimization of metaheuristics. He is currently employed as a software developer at DHL Express Austria.

GABRIEL KRONBERGER authored and co-authored numerous papers in the area of evolutionary algorithms, genetic programming, machine learning and data mining. Currently he is a research associate at the Research Center Hagenberg of the Upper Austria University of Applied Sciences working on data-based modeling algorithms for complex systems within the Josef-Ressel Centre for Heuristic Optimization Heureka!.

ERIK PITZER received his diploma in software engineering in 2004 at the Upper Austria University of Applied Sciences. Since 2004 he has been working as a research associate at the Research Center Hagenberg of the Upper Austria University of Applied Sciences and at the Decision Systems Group of Harvard Medical School in Boston. Erik Pitzer is currently working on his PhD thesis in the field of fitness landscape analysis for the design and analysis of meta-heuristic algorithms.

STEFAN WAGNER received his MSc in computer science in 2004 and his PhD in engineering sciences in 2009, both from Johannes Kepler University (JKU) Linz, Austria; he is professor at the Upper Austrian University of Applied Sciences (Campus Hagenberg). Dr. Wagner's research interests include evolutionary computation and heuristic optimization, theory and application of genetic algorithms, machine learning and software development.

STEPHAN M. WINKLER received his MSc in computer science in 2004 and his PhD in engineering sciences in 2008, both from Johannes Kepler University (JKU) Linz, Austria. His research interests include genetic programming, nonlinear model identification and machine learning. Since 2009, Dr. Winkler is professor at the Department for Medical and Bioinformatics at the Upper Austria University of Applied Sciences, Campus Hagenberg.

ANDREAS BEHAM received his MSc in computer science in 2007 from Johannes Kepler University (JKU) Linz, Austria. His research interests include heuristic optimization methods and simulation-based as well as combinatorial optimization. Currently he is a research associate at the Research Center Hagenberg of the Upper Austria University of Applied Sciences (Campus Hagenberg).

MONIKA KOFLER studied Medical Software Engineering at the Upper Austrian University of Applied Sciences, Campus Hagenberg, Austria, from which she received her diploma's degree in 2006. She is currently employed as a research associate at the Research Center Hagenberg and pursues her PhD in engineering sciences at the Johannes Kepler University Linz, Austria.

EFFECTS OF MUTATION BEFORE AND AFTER OFFSPRING SELECTION IN GENETIC PROGRAMMING FOR SYMBOLIC REGRESSION

Gabriel K. Kronberger[(a)], Stephan M. Winkler[(b)], Michael Affenzeller[(c)], Michael Kommenda[(d)], Stefan Wagner[(e)]

[(a – e)] Upper Austria University of Applied Sciences
School for Informatics, Communications, and Media
Heuristic and Evolutionary Algorithms Laboratory
Josef Ressel Centre for Heuristic Optimization - Heureka!
Softwarepark 11, 4232 Hagenberg, Austria

[(a)] gabriel.kronberger@fh-hagenberg.at, [(b)] stephan.winkler@fh-hagenberg.at ,
[(c)] michael.affenzeller@fh-hagenberg.at , [(d)] michael.kommenda@fh-hagenberg.at ,
[(e)] stefan.wagner@fh-hagenberg.at

ABSTRACT
In evolutionary algorithms mutation operators increase the genetic diversity in the population. Mutations are undirected and have only a low probability to improve the quality of the manipulated solution. Offspring selection determines if a newly created solution is added to the next generation of the population. By definition, offspring selection is applied after mutation and the effects of mutation are directed and quality-driven.

In this paper we propose an alternative variant of genetic programming with offspring selection where mutation is applied to increase genetic diversity after offspring selection. We compare the solution quality achieved by the original algorithm and the new algorithm when applied to a symbolic regression problem. We observe that solutions produced by the new variant have a smaller generalization error and conclude that the proposed variant is better for symbolic regression with linear scaling.

Keywords: Genetic Programming, Symbolic Regression, Mutation Operators

1. INTRODUCTION

In evolutionary algorithms mutation operators are used to manipulate existing solutions. Usually mutations are non-deterministic, local and undirected and have only a minor effect on the quality of the solution candidate (e.g., the single point mutation operator for genetic algorithms with binary encoding changes a single bit in the binary string representing the solution). The probability that a random mutation improves the quality of a solution is rather small. In genetic algorithms the purpose of mutation operators is to increase the genetic diversity of the population which often has a beneficial effect on the overall dynamics of the algorithm and the final solution quality.

For some problem formulations mutation operators or recombination operators are more natural or more efficient, but most evolutionary algorithms described recently use a combination of both, recombination and mutation, to generate new solution candidates from existing ones.

1.1. Offspring Selection

Offspring selection (Affenzeller and Wagner 2005) is an additional selection step in evolutionary algorithms which is applied after parental selection, recombination and mutation. Offspring selection adds a newly created solution to the next generation only if it fulfills a success criterion. Most often the success criterion is that the newly created child solution must have a better quality than its parents. It has been shown that offspring selection can improve the final solution quality found by genetic algorithms on different benchmark problems (Affenzeller, Winkler, Wagner and Beham 2009).

If offspring selection is applied after mutation, mutations become directed and quality-driven. In this configuration the mutation operator can be compared to a local first-improvement optimization step after recombination that is applied to a small percentage of the generated individuals determined by the mutation rate parameter.

The two algorithm variants studied in this paper can be directly related to the two possible perspectives of mutation in the theory of evolutionary algorithms. In the perspective of population genetics as also pursued by (Beyer and Schwefel 2002) mutation affects the genotype before selection. This is also concordant to the original formulation of offspring selection. In the perspective of genetic algorithms the role of mutation is to increase the genetic diversity of the population through random undirected changes of the genotype that are not driven by solution quality (Holland 1975).

1.2. Genetic Programming

Genetic programming (Koza 1992) is a heuristic problem solving method that uses the principles of evolution to evolve programs that solve the original

problem when executed. The core of genetic programming is an evolutionary algorithm that evolves computer programs in generational steps using selection, recombination and manipulation operations, starting from a randomly initialized population. Solution candidates represent computer programs that are most often encoded as symbolic expression trees where the root node is the program entry point. The set of symbols that can be used in the tree and the interpretation of the symbolic expression tree is problem specific.

One possible problem that can be solved by genetic programming is symbolic regression. In the case of symbolic regression the goal of genetic programming is to find a functional expression to predict the value of a target variable from values of input variables, given a set of observed or measured values for each input variable and the target variable. The functional expression is encoded as a symbolic expression tree that contains basic arithmetic operations (+, -, /, *) in internal tree nodes. In terminal nodes only two types of symbols are allowed: either a terminal node represents an input variable or a constant value.

The task of symbolic regression is a very constrained and simple form of genetic programming that makes this task ideal as a test-bed for more theoretical research. The scope of problems that can be solved be genetic programming is much larger. If it is possible to formulate a language for problem solutions and a fitness function for such solutions can be defined it is possible to use genetic programming to evolve solutions for the problem using the constructs defined in the language. Genetic programming has been used to find novel and human competitive solutions (Koza 2010).

1.3. Mutation in Genetic Programming

The role of mutation in genetic programming is uncertain (Poli, Langdon and McPhee 2008, Langdon and Poli 2002). Koza showed that mutation is not necessary for GP (Koza 1992, 1994) and crossover is sufficient to search the solution space. However, for certain problems it has been shown that GP with mutation performs better than GP with only crossover (Harries and Smith 1997, Luke and Spector 1997). The effect of mutation often depends on the problem and on the GP system (Luke and Spector 1997). This work is the first in which the effects of mutation in combination with offspring selection are studied.

2. EXPERIMENTAL SETUP

The main aim of this paper is to compare two genetic programming variants using offspring selection. The first algorithm applies mutation before offspring selection (BeforeOS), the second algorithm applies mutation after offspring selection (AfterOS).

We ran a number of experiments to answer the following two questions: How many mutated solution candidates are successful and accepted into the next generation if offspring selection is applied after mutation? Is the solution quality better or worse if the algorithm is changed so that mutation is applied after offspring selection?

Many different mutation operators for genetic programming with symbolic expression encoding have been described in the literature. We picked four different mutation operators and applied both algorithm variants each time with a different manipulation operator on a symbolic regression problem. For each configuration 20 independent runs were executed. The results shown in the next section are based on 160 independent genetic programming runs.

2.1. Symbolic Regression Problem

In the experiments we use a dataset from a real world chemical process at Dow Chemical that contains 57 cheap process measurements, such as temperatures, pressures, and flows (inputs) and noisy lab data of a chemical composition which is expensive to measure (http://dces.essex.ac.uk/research/evostar/competitions.html). This data set has been made public by Arthur Kordon, Dow Chemical for the symbolic regression competition which was a side event of the EvoStar 2010 conference. Unfortunately, no details have been published about the chemical plant and the process from which this dataset was created.

The dataset contains a total of 747 measurements of the 58 variables and was split into three partitions: training set (0-400), validation set (400-600) and test set (600-747). The validation set is used by the algorithm for model selection. The best solution determined by the algorithm in each run is evaluated on the test set in order to get an expected value for the unknown generalization error of the model on unseen data.

Each solution candidate considered by the algorithm was linearly scaled before evaluation (Keijzer 2004). Linear scaling transforms the output values generated by the symbolic regression models to the same offset and scale as the original target values; linear scaling has been shown to improve the final solution quality produced by genetic programming (Keijzer 2004).

2.2. Mutation Operators

The following mutation operators are used in the experiments:

ChangeNodeType: This operator selects a single node of the solution that has been selected for manipulation, and replaces the symbol in the selected node with a random symbol from the function library. Symbols are selected with uniform probability. The original symbol is included in the list of available symbols. When a terminal node is manipulated the replacement symbol must be a terminal symbol (either variable or constant).

OnePointShaker: This operator selects a single terminal node of the solution that has been selected for manipulation, and applies a shaking operation to the parameter values of the terminal node. If the selected node is a constant a normally distributed with ($N(0,1)$)

value is added to the current constant value. If the selected node is a variable node a normally distributed (*N(0,1)*) value is added to the weighting factor of the variable and the referenced input variable is selected randomly from the set of all allowed input variables.

FullTreeShaker: This operator applies the shaking operation executed by the *OnePointShaker* on all terminal nodes of the solution that has been selected for manipulation.

SubsituteSubTree: This operator randomly selects a branch in the solution that has been selected for manipulation and replaces the whole branch starting at the selected node with a new random tree of the same size. Random trees are generated with the PTC2 operator (Luke 2000), the same operator that is used for generation of the initial population.

2.3. Parameter Settings

We used the same parameter settings for all experiments, only the manipulation operator was exchanged. These settings are well-proven settings that have been used to generate high quality solutions in a number of real world applications of GP. The upper limit of 500.000 evaluated solutions was used as stopping criterion.

Table 1: GP algorithm parameter values for all experiments.

Parameter	Value
Population size	1000
Max tree size	100
Max tree height	10
Mutation rate	15%
Comparison factor	1
Success ratio	1
Crossover	Sub-tree swapping (Koza 1992)
Initialization	PTC2 (Luke 2000)
Selection	50%: Random 50%: Proportional
Evaluation wrapper	Linear scaling (Keijzer 2004)

3. IMPLEMENTATION

The following tables show the pseudo-code of a genetic programming algorithm with offspring selection. Inside the offspring selection loop solution candidates are evaluated only on the training set. The output of the solution candidate is scaled linearly to match the offset and scale of the original target variables (Keijzer 2004).

Table 2 shows the first algorithm (BeforeOS) where mutation is applied inside the offspring selection loop. Thus only mutations which do not have a negative effect on the solution quality are accepted.

Table 3 shows the proposed algorithm variant (AfterOS). The difference to the first algorithm is that the mutation operator is applied after the next generation has been populated via repeated application of selection and crossover in the offspring selection step. The solution candidates which are manipulated have to be evaluated a second time on the training set.

Table 2: Algorithm I: BeforeOS

```
Initialization:
    i ← 0
    Best-Solution_i ← Ø
    Pop_i ← Create-Random-Individuals_PTC2 (PopSize)
    Evaluate_training ( Pop_i )
Repeat (Main Loop):
    Pop_i+1 ← Ø
    Repeat (Offspring Selection):
        Parent_male ← Selection_male (Pop_i)
        Parent_female ← Selection_female (Pop_i)
        Child = Crossover (Parent_male Parent_female)
        Conditional on Mutation Rate
            Mutate (Child)
        Quality_child ← Evaluate_training (Child)
        if Quality_child ≤ Min(Quality_male, Quality_female)
            Pop_i+1 ← Pop_i+1 ∪ {Child }
        Else
            Discard Child
    Until |Pop_i+1| = PopSize
    Best-Solution_i+1 ←
        argmin_solution (Evaluate_validation (solution)),
        where solution ∈ Pop_i+1 ∪ { Best-Solution_i }
    i ← i + 1
Until Stopping-Criterion = true
Output ( Solution_best )
```

Table 3: Algorithm II: AfterOS

```
Initialization:
    i ← 0
    Best-Solution_i ← Ø
    Pop_i ← Create-Random-Individuals_PTC2 (PopSize)
    Evaluate_training ( Pop_i )
Repeat (Main Loop):
    Pop_i+1 ← Ø
    Repeat (Offspring Selection):
        Parent_male ← Selection_male (Pop_i)
        Parent_female ← Selection_female (Pop_i)
        Child = Crossover (Parent_male Parent_female)
        Quality_child ← Evaluate_training (Child)
        if Quality_child ≤ Min(Quality_male, Quality_female)
            Pop_i+1 ← Pop_i+1 ∪ {Child }
        Else
            Discard Child
    Until |Pop_i+1| = PopSize
    For each solution ∈ Pop_i+1
        Conditional on Mutation-Rate
            Mutate (solution)
            Quality_solution ← Evaluate_training (solution)
    Best-Solution_i+1 ←
        argmin_solution (Evaluate_validation (solution)),
        where solution ∈ Pop_i+1 ∪ { Best-Solution_i }
    i ← i + 1
Until Stopping-Criterion = true
Output ( Solution_best )
```

Both algorithms have been implemented using an internal pre-release version of HeuristicLab (http://dev.heuristiclab.com) (Wagner 2009), a generic and paradigm independent framework for heuristic optimization.

4. RESULTS

The results of the experiments show that when offspring selection is applied after mutation the number of mutated individuals that are accepted into the next generation is high in the beginning stages of the algorithm, but drops later. There is no significant difference in the solution quality on the training data, however, the solutions generated by the algorithm with mutation after offspring selection are better on the validation data-set.

4.1. Effective Mutation Rates

Figure 1 shows the effective mutation rate for all mutation operators. In the first generations of the run almost all mutations improve the solution quality; in the later stages the probability sinks, but is still rather high. All mutation operators except for the *FullTreeShaker* have a probability greater than 30% to produce successful solutions even at end of the run.

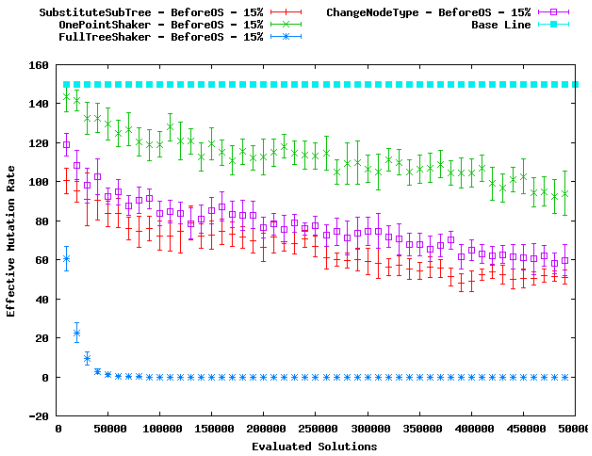

Figure 1: Number of mutated individuals in the population of manipulation operators when applied before offspring selection (averages over 20 runs for each mutation operator; error bars indicate the 95% confidence interval.)

4.2. Training Error

In Figure 2 the best training and validation quality of solutions generated by genetic programming with mutation before offspring selection are shown. Each data point is the best training/validation quality (y-axis) found after the number of evaluated solutions (x-axis) averaged over 20 independent runs (error bars indicate the 95% confidence interval). After the first few generations the algorithm generations solutions that are increasingly worse on the validation set, while the quality on the training set steadily increases. In Figure 3 the same effect can be observed, however the effect is not so strong when mutation is applied after offspring selection. The overfitting effect can be attributed to the linear scaling operation applied to all solutions. Only the training data-set is considered for the scaling operation, this leads to bad performance on the validation set and also on the test set. Based on this observation linear scaling of solution candidates should always be used in combination with an internal validation data-set for model selection. Figures 2 and 3 also show that there is no significant difference in the final solution quality of the two algorithm variants if only the training quality is considered.

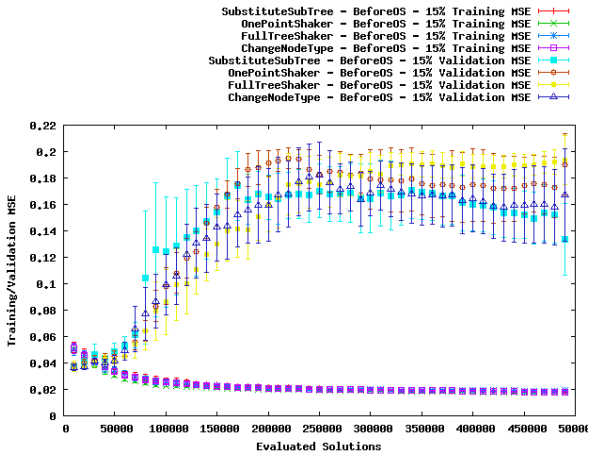

Figure 2: Best training and validation quality averaged over 20 independent runs for each mutation operator when applied before offspring selection (error bars indicate the 95% confidence interval.)

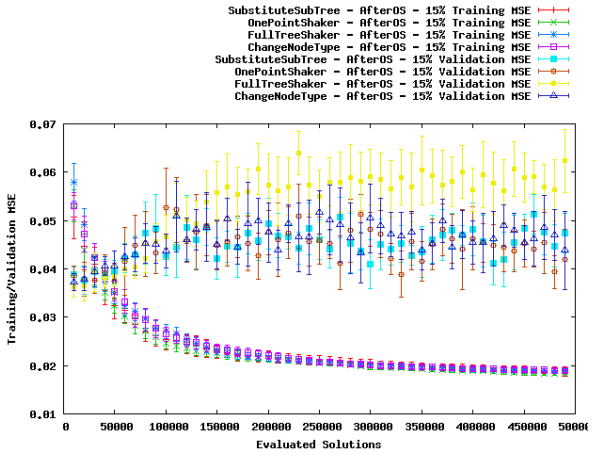

Figure 3: Best training and validation quality averaged over 20 independent runs for each mutation operator when applied after offspring selection (error bars indicate the 95% confidence interval).

4.3. Generalization Error

For the symbolic regression task the quality on unseen data is more relevant than the solution quality achieved while training because it is a better estimate for the quality of the model when applied to unseen data.

Table 4 shows the generalization error of the models selected as final result (best model on the

validation set over the whole run) for all mutation operators and different mutation rates (5%, 10%, 15%). The values are averages over 20 independent GP runs. Statistical significance was tested with the two-tailed non-parametric Mann-Whitney-U test (null hypothesis: the medians are equal). Significant results are given in bold face (p-Value < 0.01). Overfitting on the validation set occurs in both configurations for all mutation operators. This can be seen by the fact that the generalization error is very high in comparison to the average training MSE of the best on validation solutions which is 0.08 and the average validation MSE which is 0.03 over all runs.

Table 4: Generalization error (mean squared error on test set) of models generated by the GP variants averaged over 20 independent runs.

Operator	Rate	Test MSE (beforeOS)	Test MSE (afterOS)
ChangeNodeType	0.05	0.240	0.252
	0.15	0.253	0.235
	0.25	0.276	**0.121**
FullTreeShaker	0.05	0.265	0.219
	0.15	0.220	0.208
	0.25	0.205	0.216
OnePointShaker	0.05	0.263	0.208
	0.15	0.221	0.170
	0.25	0.281	**0.165**
SubstituteTree	0.05	0.237	0.209
	0.15	0.251	**0.141**
	0.25	0.204	0.165

Table 5: Best solution (on validation set) generation (median value of 20 independent runs).

Operator	Rate	Generation (beforeOS)	Generation (afterOS)
ChangeNodeType	0.05	4	**10.5**
	0.15	4	**31.5**
	0.25	5	**28**
FullTreeShaker	0.05	4	**6**
	0.15	4	4.5
	0.25	3	**11**
OnePointShaker	0.05	5	**26**
	0.15	3.5	**23.5**
	0.25	4	**22**
SubstituteTree	0.05	4	**22.5**
	0.15	3	**28.5**
	0.25	3.5	**23.5**

In Table 5 the median value of the generation when the best solution on the validation set was found is shown. From the table it can be seen that if mutation is applied before offspring selection the best solution is found in the first few generations and no improved solution is found over the rest of the GP run. If mutation is applied after OS this effect is reduced.

These observations strongly suggest that mutation should be applied after offspring selection in order to reduce overfitting if linear scaling is used. The results also raise the following questions which should be pursued in further experiments. What causes the observed overfitting effect with linear scaling and which countermeasures effectively prevent it? Does linear scaling cause a loss of genetic diversity and premature convergence? Further experiments should include an analysis of the genetic diversity in order to get an insight about the effects of linear scaling on the genetic diversity.

5. CONCLUSIONS

In this paper we have analyzed a variant of genetic programming with offspring selection where mutation is applied after offspring selection. In the original formulation of offspring selection it is applied after mutation. Both variants were used to solve a symbolic regression problem. In the experiments we observed that even when offspring selection is applied after the mutation operator a large percentage of mutated individuals are accepted into the next generation. This means that mutation has a high probability to improve solution quality. This is a bit surprising because mutations are usually undirected random changes and should intuitively have a low probability to improve solution quality. We attribute this behavior to the linear scaling operator which is a local optimization step before evaluation and improves the model quality on the training data-set. We also observed that the *FullTreeShaker* manipulation operator almost never improves the solution quality and thus has no effect when it is applied before offspring selection.

The results show that linear scaling leads to overfitting on the training data-set. This is clearly seen when the solution candidates are evaluated on the test data-set. Thus linear scaling should be used in combination with a model selection step to make sure that the final solution is not overfit on the training, for instance by tracking the best solution on an internal validation set.

Interestingly the overfitting effect of the linear scaling operation is less problematic if mutation is applied after offspring selection. In some configurations the application of mutation after offspring selection produced significantly better results regarding the generalization error.

The results of our experiments suggest that the overfitting effect is related to a kind of premature convergence to highly fit but small solutions. The cause for this is unfortunately not directly apparent from our experiments. In further research the experiments should also include analysis of the genetic diversity in order to get an insight about the effects of linear scaling on the genetic diversity.

From the results described in this work we conclude that if linear scaling is used in OSGP then mutation should be applied after offspring selection to reduce the probability of overfitting.

ACKNOWLEDGMENTS

The work described in this paper was done within the Josef Ressel Centre for Heuristic Optimization *Heureka!* (http://heureka.heuristiclab.com/) sponsored by the Austrian Research Promotion Agency (FFG).

REFERENCES

Affenzeller, M. and Wagner, S., 2005. *Offspring selection: A new self-adaptive selection scheme for genetic algorithms*. Proceedings of ICANNGA 2005, pp. 218–221. 21st–23rd March 2005, Coimbra, Portugal.

Affenzeller, M., Winkler, S.M., Wagner, S. and Beham, A., 2009. *Genetic algorithms and genetic programming – Modern concepts and practical applications*. Boca Raton: CRC Press.

Beyer, H. G., and Schwefel, H.-P., 2002. Evolution Strategies: A Comprehensive Introduction. In Natural Computing, 1:1, pp. 3 – 52.

Harries, K. and Smith, P., 1997. Exploring alternative operators and search strategies in genetic programming. In J. R. Koza, et al., editors, *Genetic Programming 1997: Proceedings of the Second Annual Conference*, pp. 147 – 155, Stanford University, CA, USA, 1997.

Holland, J. H., 1975. *Adaption in Natural and Artificial Systems*, University of Michigan Press, Ann Harbor.

Keijzer, M., 2004. *Scaled Symbolic Regression*. Genetic Programming and Evolvable Machines 5:3 (September 2004), pp. 259 – 269.

Koza, J. R., 1992. *Genetic Programming: On the Programming of Computers by Means of Natural Selection.* MIT Press.

Koza, J. R., 1994. *Genetic Programming II: Automatic Discovery of Reusable Programs.* MIT Press.

Koza, J. R., 2010. Human-competitive results produced by genetic programming. In J. Miller, et al., editors, *Tenth Anniversary Issue: Progress in Genetic Programming and Evolvable Machines*, Vol. 11, No. 3-4, pp. 251 – 284. Springer Netherlands.

Langdon, W. B. and Poli, R., 2002. *Foundations of Genetic Programming*. Springer-Verlag.

Luke, S. 2000. *Two fast tree-creation algorithms for genetic programming.* In IEEE Transactions on Evolutionary Computation 4:3 (September 2000), 274-283. IEEE.

Luke, S. and Spector L., 1997. A comparison of crossover and mutation in genetic programming. In J. R. Koza, et al., editors, *Genetic Programming 1997: Proceedings of the Second Annual Conference*, pp. 147 – 155, Stanford University, CA, USA, 1997.

Poli, R., Langdon, W. B., and McPhee N., 2008. *A field guide to genetic programming.* Published via http://lulu.com and freely available at http://www.gp-field-guide.org.uk, (with contributions by J. R. Koza).

Wagner, S., 2009. *Heuristic Optimization Software Systems - Modeling of Heuristic Optimization Algorithms in the HeuristicLab Software Environment*. Thesis (PhD), Johannes Kepler University Linz, Austria.

AUTHORS BIOGRAPHIES

GABRIEL KRONBERGER is a research associate at the UAS Research Center Hagenberg. His research interests include genetic programming, machine learning, and data mining and knowledge discovery. Currently he works on practical applications of data-based modeling methods for complex systems within the Josef Ressel Centre Heureka!.

STEPHAN M. WINKLER received his PhD in engineering sciences in 2008 from Johannes Kepler University (JKU) Linz, Austria. His research interests include genetic programming, nonlinear model identification and machine learning. Since 2009, Dr. Winkler is professor at the Department for Medical and Bioinformatics at the Upper Austria University of Applied Sciences (UAS), Campus Hagenberg.

MICHAEL AFFENZELLER has published several papers, journal articles and books dealing with theoretical and practical aspects of evolutionary computation, genetic algorithms, and meta-heuristics in general. In 2001 he received his PhD in engineering sciences and in 2004 he received his habilitation in applied systems engineering, both from the Johannes Kepler University of Linz, Austria. Michael Affenzeller is professor at the Upper Austria University of Applied Sciences, Campus Hagenberg, and head of the Josef Ressel Center *Heureka!* at Hagenberg.

MICHAEL KOMMENDA finished his studies in bioinformatics at Upper Austria University of Applied Sciences in 2007. Currently he is a research associate at the UAS Research Center Hagenberg working on data-based modeling algorithms for complex systems within *Heureka!*.

STEFAN WAGNER his PhD in engineering sciences in 2009 from Johannes Kepler University (JKU) Linz, Austria; he is professor at the Upper Austrian University of Applied Sciences (Campus Hagenberg). Dr. Wagner's research interests include evolutionary computation and heuristic optimization, theory and application of genetic algorithms, machine learning and software development.

MUTATION EFFECTS IN GENETIC ALGORITHMS WITH OFFSPRING SELECTION APPLIED TO COMBINATORIAL OPTIMIZATION PROBLEMS

Stefan Wagner[(a)], Michael Affenzeller[(b)], Andreas Beham[(c)], Gabriel Kronberger[(d)], Stephan M. Winkler[(e)]

[(a – e)] Upper Austria University of Applied Sciences
School for Informatics, Communications, and Media – Hagenberg
Josef Ressel-Centre *Heureka!* for Heuristic Optimization
Heuristic and Evolutionary Algorithms Laboratory
Softwarepark 11, A-4232 Hagenberg, Austria

[(a)]stefan.wagner@fh-hagenberg.at, [(b)]michael.affenzeller@fh-hagenberg.at, [(c)]andreas.beham@fh-hagenberg.at, [(d)]gabriel.kronberger@fh-hagenberg.at, [(e)]stephan.winkler@fh-hagenberg.at

ABSTRACT
In this paper the authors describe the effects of mutation in genetic algorithms when used together with offspring selection to solve combinatorial optimization problems. In the initial definition of offspring selection stated by Affenzeller et al., offspring selection is applied to each solution after its creation using crossover and optional mutation. Thereby a solution is immediately accepted for the next generation only if it is able to outperform its parental solutions in terms of quality.

It has been shown in several publications by Affenzeller et al. that this additional selection step leads to a better maintenance of high quality alleles and therefore to a better convergence behavior and a superior final solution quality.

Due to the application of offspring selection after crossover and mutation, both operations become directed by the quality of the created solutions. This is in fact a different interpretation of mutation compared to classical genetic algorithms where mutation is used in an undirected way to introduce new genetic information into the search process.

In this contribution the authors propose a new version of offspring selection by applying it after crossover, but before mutation. In a series of experiments the similarities and differences of these two approaches are shown and the interplay between mutation and offspring selection is analyzed.

Keywords: Genetic Algorithms, Combinatorial Optimization, Selection

1. INTRODUCTION

Selection for reproduction represents the main driving force in genetic algorithms that guides the search process through the solution space. By selecting solutions of above average fitness and applying crossover and optionally mutation, genetic algorithms try to combine alleles of high quality in order to obtain better and better solutions. During the search process genetic diversity is usually decreased step by step so that the algorithm is able to converge to solutions of high quality in the end.

However, due to the effects of genetic drift high quality (i.e., relevant) alleles which are required to reach global optimal solutions might be lost in the whole population. This leads to so-called premature convergence which describes a state in which the algorithm is no longer able to create better solutions although it has not reached a global optimum so far (Fogel 1994; Affenzeller 2005). This situation can be compared to the effect of getting stuck in a local optimum in neighborhood-based meta-heuristics.

In general the following three aspects can be identified as the main reasons for the loss of relevant alleles (Affenzeller 2005; Affenzeller, Wagner, and Winkler 2010):

- Some relevant alleles might not be included in the initial population. This especially might be the case if the population size is rather small.
- Relevant alleles might be lost due to the stochastic nature of selection and genetic drift. This is frequently the case in an early phase of the algorithm, when relevant alleles are included in solutions of rather bad quality.
- For many applications of genetic algorithms the applied crossover operators cannot guarantee that the created children are exact combinations of the genetic information of the parents as new alleles might have to be introduced in order to create feasible solutions.

In classical genetic algorithms the only approach to counteract the loss of relevant alleles and therefore to avoid premature convergence is mutation. However, as mutation is used as an undirected operator, the probability to get back relevant alleles by lucky mutations decreases rapidly when trying to solve problems of larger size.

Additionally to mutation, some other ideas are also discussed in literature to reduce the negative effects of premature convergence. Among them the most common representative are preselection (Cavicchio 1970), crowding (De Jong 1975), and fitness-sharing (Goldberg 1989). The main idea of these approaches is to maintain genetic diversity by replacing solutions more frequently which occupy similar regions of the search space (preselection, crowding) or the reduce the fitness value of solutions which are located in densely populated regions of the search space (fitness-sharing). All these three approaches require the definition of a distance measure in order to be able to calculate the similarity of solutions in the search space, and fitness-sharing is additionally quite restricted to fitness proportional selection. As a consequence, these approaches are not applicable in each case. Furthermore, they do not really address the problem of loosing relevant alleles but try to reduce the loss of genetic diversity in general.

In order to develop a more general technique to counteract the loss of relevant alleles and therefore to prolongate premature convergence the authors introduced offspring selection (Affenzeller and Wagner 2005; Affenzeller, Wagner, and Winkler 2010; Affenzeller, Winkler, Wagner, and Beham 2009). The basic idea of this selection model is to consider not only the fitness of the parents when creating new solutions. Additionally, the fitness value of each new child solution created by crossover and optionally mutation is compared with the fitness values of its parents. The child is immediately accepted for the next generation if and only if it outperforms its parents' fitness. This strategy guarantees that the search process is continued mainly with crossover results that were able to mix the properties of their parents in an advantageous way and/or with mutation results that contain relevant alleles. In other words, offspring selection supports *survival of the fittest alleles rather than survival of the fittest chromosomes*. This is a very essential concept concerning the preservation of relevant genetic information stored in the individuals of a population.

2. OFFSPRING SELECTION

In general, offspring selection consists of the following steps (Affenzeller and Wagner 2005):

At first parents are selected for reproduction either randomly or in any other well-known way of genetic algorithms (e.g., fitness proportional selection, linear rank selection, tournament selection). After crossover and optionally mutation have been applied to create a new child solution, another selection step is introduced which considers the success of the applied reproduction procedure. The goal of this second selection step (i.e. the offspring selection step) is to continue the search process mainly with successful offspring which surpass their parents' quality. Therefore, a new parameter called success ratio (*SuccRatio*) is introduced. The success ratio defines the relative amount of members in the next population that have to be generated by successful mating (crossover, mutation).

Additionally, it has to be defined when a solution is considered to be successful: Is a child solution better than its parents, if it surpasses the fitness of the weaker, the better, or some kind of mean value of both? For this purpose a parameter called comparison factor (*CompFactor*) is used to define the success criterion for each created solution as a weighted average of the quality of the worse and better parent (i.e., if the comparison factor is 0, successful solutions at least have to be better than the worse parent, and if it is 1 they have to outperform the better parent).

Based on the comparison factor, the authors decided to introduce a cooling strategy which is similar to simulated annealing. Following the basic principle of simulated annealing, an offspring only has to surpass the fitness value of the worse parent in order to be successful at the beginning of the search process (*CompFactor* is initialized with 0 or a rather small value). While evolution proceeds solutions have to be better than a fitness value continuously increasing between the fitness of the weaker and the better parent (*CompFactor* is increased in each generation until it reaches 1 or a rather high value). As in the case of simulated annealing, this strategy leads to a broader search at the beginning, whereas at the end the search process becomes more and more directed.

After the amount of successful solutions in the next generation has reached the success ratio, the remaining solutions for the next generation (i.e., (1-*SuccRatio*)·|*POP*|) are taken from the pool of solutions which were also created by crossover and mutation but did not necessarily reach the success criterion. The actual selection pressure *ActSelPress* at the end of a single generation is defined by the quotient of individuals that had to be created until the success ratio was reached and the number of individuals in the population:

$$ActSelPress = \frac{|POP| \cdot SuccRatio + |POOL|}{|POP|} \quad (1)$$

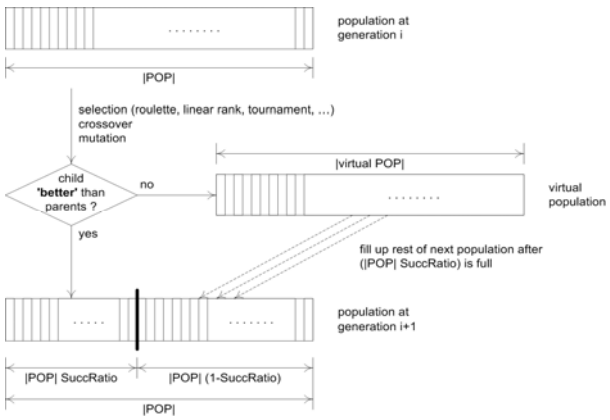

Figure 1: Flowchart of a Classical Genetic Algorithm Extended by Offspring Selection

Figure 1 shows these basic steps of offspring selection and how they are embedded into a classical genetic algorithm.

Furthermore, an upper limit for the selection pressure (*MaxSelPress*) can be defined as another parameter which states the maximum number of children (as a multiple of the population size) that might be created in order to fulfill the success ratio. With this additional parameter offspring selection also provides a precise detector for premature convergence: If the algorithm cannot create a sufficient number of successful solutions ($SuccRatio \cdot |POP|$) even after $MaxSelPress \cdot |POP|$ solutions have been created, premature convergence has occurred and the algorithm can be stopped.

As a basic principle of offspring selection, higher success ratio and comparison factor cause higher selection pressure. Nevertheless, a higher selection pressure does not necessarily cause premature convergence when using offspring selection, as offspring selection also supports the preservation of relevant alleles and not only the preservation of fitter solutions as a whole.

3. OFFSPRING SELECTION AND MUTATION

In its original definition offspring selection is applied to each solution after it has been created by crossover and optionally manipulated by mutation. Thereby offspring selection assures that the search process is continued mainly with solutions which contain a promising combination of the genetic information of their parents (assembled by the crossover operator) and/or which contain high quality alleles that have been added by mutation. This approach leads to a strong direction of the search process. Several experiments have shown that a genetic algorithm with offspring selection is also able to achieve results of high quality, even if selection for reproduction is done randomly and only offspring selection is used to guide the search (Affenzeller 2005; Affenzeller, Wagner, and Winkler 2010).

This is in fact a slightly different interpretation of crossover and mutation compared to classical genetic algorithms. In a classical genetic algorithm the crossover operator is responsible for combining alleles to longer and longer building blocks and mutation is used as an undirected manipulation operator whose purpose is to add new alleles to the population in order to keep the search process alive (Holland 1975). When applying offspring selection both operators, crossover and mutation, are always considered in combination and are directed by the success criterion which has to be fulfilled by the created solutions. Consequently, the mutation operator does not longer serve as an undirected manipulation operator, as it is followed by an additional selection step. This interpretation of mutation is concordant with the way mutation is considered in population genetics and also in evolution strategies (Beyer and Schwefel 2002) where it affects the genotype before and not after selection.

As an alternative, a new version of offspring selection can be easily defined by applying the success criterion after crossover has created a new solution but before the mutation operator is optionally used to manipulate it. In this new version of offspring selection a stronger focus is put on the crossover operator by checking if it was able to combine the genetic information of the parents in a successful way and the mutation operator turns into an undirected operator again. This interpretation of the roles of crossover and mutation is more similar to the classical view on genetic algorithms in which their search process is considered as hyperplane sampling (Whitley 1994).

4. EXPERIMENTAL RESULTS AND ANALYSIS

In order to evaluate and compare the two versions of offspring selection described in the previous sections and to gain a deeper insight into the interplay of offspring selection and mutation, the authors carried out a series of test runs with the ch130 instance of the Traveling Salesman Problem (TSP) taken from the TSPLIB (Reinelt 1991). For all tests HeuristicLab 3.3 (Wagner 2009) was used which provides both versions of offspring selection and can be downloaded from the HeuristicLab homepage at http://dev.heuristiclab.com.

Table 1: Parameter Settings

Parameter	Value
Population Size	500
Parent Selection	Random
Crossover Operators	OX ERX MPX OX, ERX and MPX
Mutation Operators	2-opt 3-opt 2-opt and 3-opt
Mutation Probabilities	1% 5% 10% 20%
Elites	1
Offspring Selection	Before Mutation After Mutation
Success Ratio (*SuccRatio*)	1.0
Comparison Factor (*CompFactor*)	1.0
Maximum Generations	1000
Maximum Selection Pressure (*MaxSelPress*)	250

In Table 1 the algorithm's parameter settings are shown which have been used for the tests. In order to highlight the effects of offspring selection before and after mutation, random parent selection and a success ratio and a comparison factor of 1.0 have been applied. Furthermore, several typical crossover and mutation operators for solving the TSP (Larranaga 1999) have been used in combination with different mutation

probabilities. The crossover and mutation operators have also been applied in combination which means that each time a crossover or mutation operator had to be applied, it was chosen randomly.

Table 2: Relative Difference to the Optimal Solution (Offspring Selection after Mutation)

Mut. Op.	Mut. Prob.	Mean	Standard Deviation
2-opt	1%	0,1359	0,1160
	5%	0,0840	0,0726
	10%	0,1052	0,1005
	20%	0,1038	0,1020
3-opt	1%	0,1288	0,1150
	5%	0,1388	0,1201
	10%	0,1410	0,1262
	20%	0,1455	0,1140
2-opt and 3-opt	1%	0,1400	0,1263
	5%	0,0829	0,0851
	10%	0,1226	0,1152
	20%	**0,0671**	0,0744

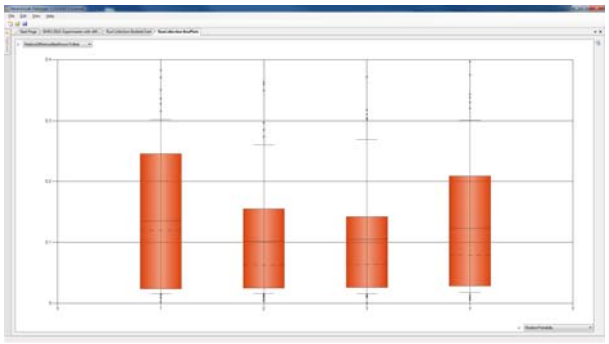

Figure 2: Relative Difference to the Optimal Solution for 1%, 5%, 10% and 20% Mutation Probability (Offspring Selection after Mutation)

Table 3: Relative Difference to the Optimal Solution (Offspring Selection before Mutation)

Mut. Op.	Mut. Prob.	Mean	Standard Deviation
2-opt	1%	0,1307	0,1212
	5%	0,0933	0,0701
	10%	0,0409	0,0325
	20%	0,0222	0,0103
3-opt	1%	0,1525	0,1258
	5%	0,1054	0,1002
	10%	0,0540	0,0684
	20%	0,0240	0,0139
2-opt and 3-opt	1%	0,1156	0,1017
	5%	0,0928	0,0836
	10%	0,0683	0,0799
	20%	**0,0190**	0,0099

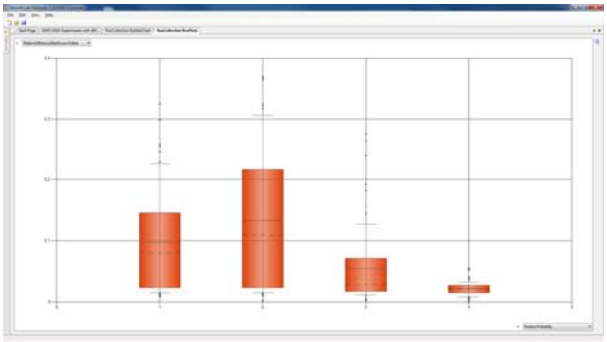

Figure 3: Relative Difference to the Optimal Solution for 1%, 5%, 10% and 20% Mutation Probability (Offspring Selection before Mutation)

For each parameter configuration, 5 independent runs have been executed which gives a total sum of 480 runs. In Table 2 and Figure 2 the relative difference of the best found solution to the global optimal solution is analyzed for the case when offspring selection is done after mutation (classical offspring selection); Table 3 and Figure 3 show the same results for applying offspring selection before mutation (new version).

Furthermore, also the number of evaluated solutions is analyzed for both cases in Table 4, Figure 4, Table 5 and Figure 5.

Table 4: Evaluated Solutions (Offspring Selection after Mutation)

Mut. Op.	Mut. Prob.	Mean	Standard Deviation
2-opt	1%	1.567.880,00	429.171,66
	5%	1.722.365,00	380.228,61
	10%	1.705.435,00	387.580,38
	20%	1.809.925,00	415.801,80
3-opt	1%	1.648.370,00	476.494,38
	5%	1.643.395,00	442.052,44
	10%	1.693.385,00	462.979,53
	20%	1.686.315,00	426.681,99
2-opt and 3-opt	1%	1.633.605,00	515.648,60
	5%	1.773.865,00	436.819,40
	10%	1.621.055,00	393.168,40
	20%	1.929.205,00	480.513,97

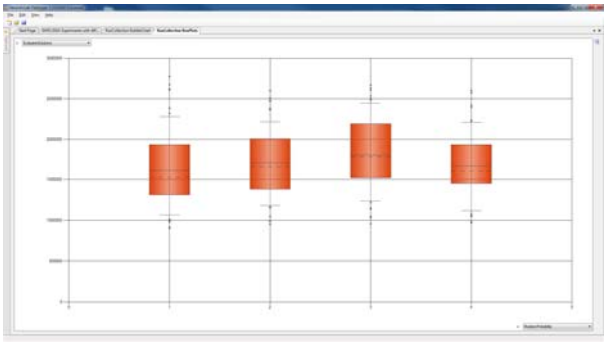

Figure 4: Evaluated Solutions for 1%, 5%, 10% and 20% Mutation Probability (Offspring Selection after Mutation)

Table 5: Evaluated Solutions
(Offspring Selection before Mutation)

Mut. Op.	Mut. Prob.	Mean	Standard Deviation
2-opt	1%	1.637.656,75	405.592,54
	5%	1.857.213,60	382.548,56
	10%	4.957.905,00	4.498.932,66
	20%	31.470.516,65	6.134.381,08
3-opt	1%	1.624.311,45	464.574,57
	5%	1.997.821,55	524.652,97
	10%	18.435.419,90	17.615.456,28
	20%	24.561.314,80	4.869.505,18
2-opt and 3-opt	1%	1.697.508,60	416.604,78
	5%	1.883.439,00	444.074,17
	10%	6.812.471,10	10.224.809,35
	20%	27.093.109,30	3.656.663,69

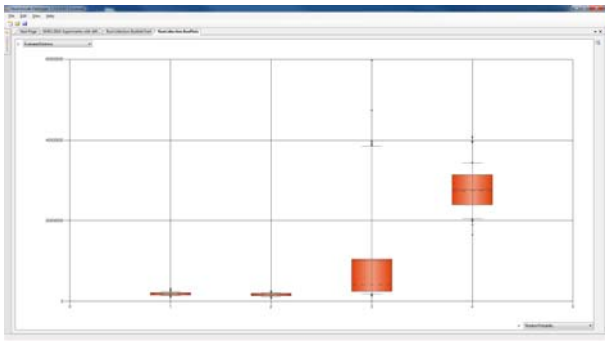

Figure 5: Evaluated Solutions for 1%, 5%, 10% and 20% Mutation Probability
(Offspring Selection before Mutation)

Obviously the algorithm's behavior changes if offspring selection is applied before mutation, especially when working with high mutation probabilities. In the classical version of offspring selection (offspring selection after mutation) changing the mutation rate does not make much difference. The relative difference to the optimal solution as well as the number of evaluated solutions do not change notably (see Table 2, Figure 2, Table 4, Figure 4). However, when applying offspring selection before mutation, the mean value and the standard deviation of the relative difference to the optimal solution decrease significantly and the mean value and the standard deviation of the number of evaluated solutions increase significantly when increasing the mutation probability (see Table 3, Figure 3, Table 5, Figure 5).

These results show that applying offspring selection before mutation and using rather high mutation probabilities leads to a longer execution time, more solution evaluations and more robust algorithms. In fact, this is quite reasonable and consistent with the theory of genetic algorithms. In the classical version of offspring selection the effects of mutation are dominated by the offspring selection step. Therefore, mutation is not undirected anymore and its characteristics as diversification method are lost.

In the new version of offspring selection (offspring selection before mutation) mutation is more used in a way similar to standard genetic algorithms as the result of a mutation is not going through an additional selection process anymore. By this means, mutation becomes a diversification method again which leads to a longer run time, a broader search in the solution space, significantly more solution evaluations, but also more robust results.

5. CONCLUSIONS

In this contribution the authors focused on offspring selection which has been proposed by Affenzeller et al. to counteract the loss of relevant alleles and to prolongate premature convergence. A new version of offspring selection was presented in which the offspring selection step is not applied after mutation but before mutation.

In a series of tests the authors analyzed the similarities and differences of these two versions of offspring selection when solving the Traveling Salesman Problem.

It was shown for the original version of offspring selection (offspring selection after mutation) that the effects of mutation are dominated by the offspring selection step and that mutation therefore does not act as a diversification method anymore. However, when applying offspring selection before mutation the algorithm's behavior is significantly different, especially when using high mutation probabilities. As in this case the result of a mutation is not going through an additional selection process anymore, mutation is applied in an undirected way again and therefore leads to a diversification of the search process. By this means, the algorithm evaluates more solutions and becomes more robust when applying offspring selection before and not after mutation.

In the future the authors are going to focus on a comparison of the robustness of both offspring selection versions when evaluating approximately the same number of solutions. Furthermore, additional test series with other TSP instances and also other combinatorial optimization problems should be done to enable an even more reliable analysis and interpretation.

ACKNOWLEDGMENTS

The work described in this paper was done within the Josef Ressel-Centre *Heureka!* for Heuristic Optimization (http://heureka.heuristiclab.com) sponsored by the Austrian Research Promotion Agency (FFG).

REFERENCES

Affenzeller, M. and Wagner, S., 2005. Offspring selection: A new self-adaptive selection scheme for genetic algorithms. *Proceedings of ICANNGA 2005*, pp. 218–221. 21st–23rd March 2005, Coimbra, Portugal.

Affenzeller, M., 2005. *Population genetics and evolutionary computation: Theoretical and practical aspects*. Linz: Trauner Verlag.

Affenzeller, M., Wagner, S. and Winkler, S.M., 2010. Effective allele preservation by offspring selection: An empirical study for the TSP. *International Journal of Simulation and Process Modelling*, 6 (1), 29–39.

Affenzeller, M., Winkler, S.M., Wagner, S. and Beham, A., 2009. *Genetic algorithms and genetic programming – Modern concepts and practical applications*. Boca Raton: CRC Press.

Beyer, H.G. and Schwefel, H.P., 2002. Evolution strategies: A Comprehensive Introduction. *Natural Computing*, 1 (1), 3–52.

Cavicchio, D.J., 1970. *Adaptive search using simulated evolution*. Thesis (PhD). University of Michigan.

De Jong, K., 1975. *An analysis of the behavior of a class of genetic adaptive systems*. Thesis (PhD). University of Michigan.

Fogel, D., 1994. An introduction to simulated evolutionary optimization. *IEEE Transactions on Neural Networks*, 5 (1), 3–14.

Goldberg, D.E., 1989. *Genetic algorithms in search, optimization and machine learning*. Addison-Wesley.

Holland, J.H., 1975. *Adaption in Natural and Artificial Systems*, University of Michigan Press, Ann Harbor.

Larranaga, P., Kuijpers, C.M.H., Murga, R.H., Inza, I. and Dizdarevic, D., 1999. Genetic algorithms for the traveling salesman problem: A review of representations and operators. *Artificial Intelligence Review*, 13, 129–170.

Reinelt, G., 1991. *TSPLIB – A traveling salesman problem library*. ORSA Journal on Computing, 3, 376–384.

Wagner, S., 2009. *Heuristic optimization software systems – Modeling of heuristic optimization algorithms in the HeuristicLab software environment*. Thesis (PhD). Johannes Kepler University Linz.

Whitley, D., 1994. *A Genetic Algorithm Tutorial*. Statistics and Computing, 4, 65–85.

AUTHORS BIOGRAPHIES

STEFAN WAGNER received his MSc in computer science in 2004 and his PhD in engineering sciences in 2009, both from Johannes Kepler University (JKU) Linz, Austria; he is professor at the Upper Austria University of Applied Sciences (Campus Hagenberg). Dr. Wagner's research interests include evolutionary computation and heuristic optimization, theory and application of genetic algorithms, model driven software development and software engineering.

MICHAEL AFFENZELLER has published several papers, journal articles and books dealing with theoretical and practical aspects of evolutionary computation, genetic algorithms, and meta-heuristics in general. In 2001 he received his PhD in engineering sciences and in 2004 he received his habilitation in applied systems engineering, both from the Johannes Kepler University of Linz, Austria. Michael Affenzeller is professor at the Upper Austria University of Applied Sciences, Campus Hagenberg, and head of the Josef Ressel Center *Heureka!* at Hagenberg.

ANDREAS BEHAM received his MSc in computer science in 2007 from Johannes Kepler University (JKU) Linz, Austria. His research interests include heuristic optimization methods and simulation-based as well as combinatorial optimization. Currently he is a research associate at the Research Center Hagenberg of the Upper Austria University of Applied Sciences (Campus Hagenberg).

GABRIEL K. KRONBERGER received his MSc. in computer science in 2005 from Johannes Kepler University Linz, Austria. His research interests include parallel evolutionary algorithms, genetic programming, machine learning and data mining. Currently he is a research associate at the Research Center Hagenberg of the Upper Austria University of Applied Sciences.

STEPHAN M. WINKLER received his MSc in computer science in 2004 and his PhD in engineering sciences in 2008, both from Johannes Kepler University (JKU) Linz, Austria. His research interests include genetic programming, nonlinear model identification and machine learning. Since 2009, Dr. Winkler is professor at the Department for Medical and Bioinformatics at the Upper Austria University of Applied Sciences, Campus Hagenberg.

BAUOPTIMIZER: MODELLING AND SIMULATION TOOL FOR ENERGY AND COST OPTIMIZATION IN BUILDING CONSTRUCTION PLAN DESIGN

Gerald Zwettler[(a)], Florian Waschaurek[(b)], Paul Track[(c)], Elmar Hagmann[(b,d)], Richard Woschitz[(c.d)], Stefan Hinterholzer[(e)]

[(a)]Research and Development Department, University of Applied Sciences Upper Austria, Softwarepark 11, 4232 Hagenberg, AUSTRIA
[(b)]Dipl. Ing. Wilhelm Sedlak GmbH, Quellenstraße 163, 1100 Wien, AUSTRIA
[(c)]RWT PLUS ZT GmbH, Karlsplatz 2/6-7, 1010 Wien, AUSTRIA
[(d)]ARGE Innovation Bautechnik und Bauprozessoptimierung OG, Quellenstraße 163, 1100 Wien, AUSTRIA
[(e)]School of Informatics, Communication and Media, University of Applied Sciences Upper Austria, Softwarepark 11, 4232 Hagenberg, AUSTRIA

[(a)]gerald.zwettler@fh-hagenberg.at, [(b)]{waschaurek|hagmann}@sedlak.co.at, [(c)]{p.track|r.woschitz}@rwt.at, [(e)]stefan.hinterholzer@fh-hagenberg.at

ABSTRACT

In the light of increasing energy prices and declining fossil resources, energy efficient design is an important aspect of building construction planning. Software application *BauOptimizer* supports the planner in calculating, monitoring and optimizing both energy demand and cost aspects from the very first planning phase until the final architecture improving economic and ecologic properties of the building design. Furthermore the number of required planning phases is reduced as normative limits are kept considered right from the beginning.

Costs for building hull creation and expected energy costs for the next decades are linked together as efficiency measure and all planning variants applicable for a concrete construction area are automatically evaluated, covering different material at different thicknesses, the window ratio, roof modality, and many more aspects.

Within this full construction variants coverage, the planner optimizes his architectural design and building physics aspect to approximate efficiency optimum with respect to economy and ecology.

Keywords: energy and cost efficiency, economy, ecology, construction design optimization

1. INTRODUCTION

For the architectural and conception planning of buildings several perspectives on the desired outcome exist. The architect himself wants to act out his inspiration with jutties, alignments and shifted walls whereas the building owner desires reduced construction costs and a maximum exploitation of the building development regulations with respect to net floor area. Another fundamental aspect to consider is energy efficiency of the building. Investments into increased insulation measurements are connected with increased construction costs per square meters but are intended to reduce the energy demand and all associated costs for heating and air conditioning, see Fig. 1. Furthermore the legislative body states prescriptive limits with relevance for awarding a grant.

All of these aspects must be considered in a balanced building construction plan. As there is no tool supporting for cost and energy demand calculations in the early architectural planning phase, several cost intensive design iterations are often required before all relevant criterions are met, see Fig. 2.

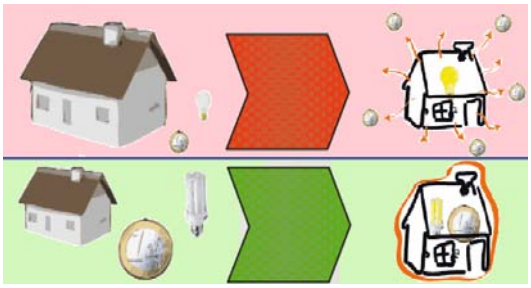

Figure 1: Focus on cheap building construction (top) leads to increased energy demand, whereas setting the focus on energy efficiency (bottom) leads to reduced energy costs at operation.

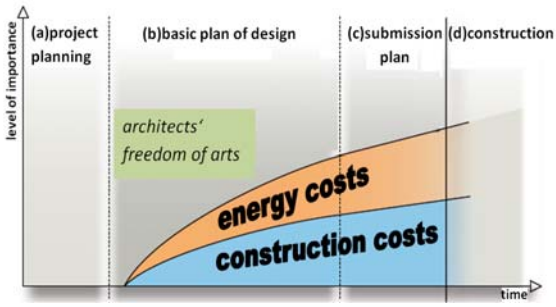

Figure 2: Delineation of the several planning phases. First the architects' design idea is a focal point whereas restrictions for construction and energy costs are considered later.

For linking and balancing the different, partially oppositional, planning criterions, a common basis for comparison must be developed. Therefore the term efficiency is intended to both cover economy and ecology and preserve a common base for comparison. Increase investments into energy demand reduction can redeem within a period of amortization. Consequently investment costs can be offset against reduction in energy demand.

The objective of project *BauOptimizer* is to develop a software tool for supporting architects and building owners in construction cost, energy demand, funding, normative limits and an efficiency evaluation, from the very beginning planning phase until the finalization of the building construction plan. Furthermore the current plan can be positioned relative to the theoretically best and worst result of economy / ecology. Thereby the stakeholders and authorities can assess the current plans distance to the global most efficient plan optimized for the particular building site and the restrictions to be considered.

2. MODELLING ARCHITECTURE, COST AND ENERGY ASPECTS

Before creating the efficiency model, all relevant parameters must be identified and their influence on costs and energy demand must be investigated on, see Fig. 3. In the following sections all parameters relevant for our efficiency model are enlisted and described in detail.

2.1. Building Site and Climate Parameters

When starting an optimization project, the planner has to specify the building site dimensions at first. Thereby the maximum constructible length, width and height as well as tolerance extents in this regard must be specified. The tolerance extent refers to local legally binding land-use plan and is relevant for e.g. jutties, loft conversions or keeping the building lines.

The climate properties comprising the country, region, sea level and orientation are inevitable for precise evaluation of solar gains and the heating demand in addition to the expected monthly average temperatures based on regional climate statistics. For calculation of the required energy demand, the difference from *20* Kelvin must be compensated by external energy supply at all times to ensure constant room air. As this tool is intended for modeling and optimizing the construction plans and choice of the building materials, the heating and ventilation system itself as well as air conditioning aspects are not being considered.

2.2. Modeling Building Geometrics and Design

The ground plan for each floor of the building can be specified by a polyline defined by arbitrarily oriented points on a regular grid of precision *0.5* meters, see Fig. 4. All defined walls are orthonormally positioned above the fundament at a floor-specific height. Copy-paste and arithmetic functions allow the user to propagate floor templates for fast entire building capture, even if there is a large number of floors to construct. That way the modeling of the building's architectonic character requires only little user interaction but provides sufficient accuracy for precise evaluations.

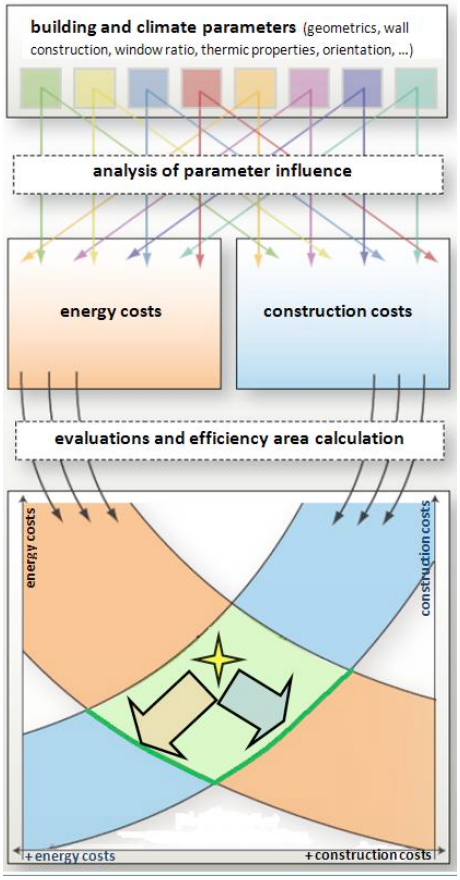

Figure 3: Higher investments into construction lead to reduced energy demand and vice versa. The parameters of the model have influence on energy costs, construction costs or both. The current planning solution (yellow star) can be optimized towards efficiency areas (arrows).

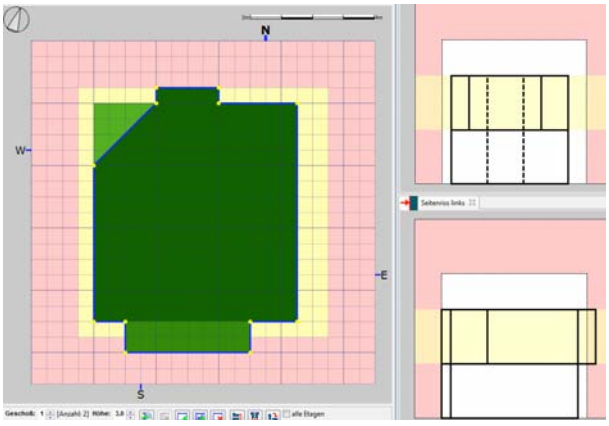

Figure 4: Floor-by-floor modeling of the building geometrics. The red area refers to the so called tolerance area. Wall jutties, offsets, ground and roof areas are displayed in shades of green. A front and a side projection provide an overview for the user.

2.3. Specifying the Wall Modalities

After creating the floor plan, for each wall the modality, i.e. properties towards the outside, with respect to specific thermal resistances, can be specified. For walls possible modalities with relevance for building physics are in extracts:

- towards surrounding air
- towards heated outbuilding
- towards unheated outbuilding
- towards soil

The modalities all show different properties relevant for heat conductance value calculation. The modality selection influences thermal resistivity from the building inside to the wall (R_{si}) as well as wall to the outside (R_{se}) and a specific temperature correction factor *F*.

Concerning the ground, roof, jutty and offset regions a modality has to be specified too. For the house top the type of the roof, like platform, gable or mono-pitch roof, has to be chosen. For the ground there is a significant difference whether there is a cellar, coil or air at raised standing buildings below the ground floor.

Another aspect to handle via modality assignation is the window ratio in percent or square meters as well as the shading strategy, like no shading, marquee, roller shutter, and so on. Depending on the wall's orientation, the window percentage strongly affects the solar gains to achieve. Consequently at the south front, larger window fronts are to be planned compared to the north front.

2.4. Selection of the wall and window construction

A catalogue of categorized and plausible wall constructions with up-to-date cost parameters is imported. For each different assignable wall modality, the planner can pick one single wall construction, see Fig. 5. That way the entire building physics aspect of the construction plan can be modeled. Up-to-now there are more than 300 of the most relevant wall, ground and roof construction sets contained in the catalogue but the coverage will be iteratively expanded.

A discrete wall or floor construction exists of several different material layers, as listed in Table 1, Table 2 and Table 3 for floor, wall and roof construction parts, where the bold-marked insulation and construction layers can be altered in thickness and material choice. These two main components, construction and insulation, can be individually altered by the planner, thus influencing thermic conductance and construction costs.

Window construction selection is specified in a quite similar way. For each different selected shading modality, a certain window type with respect to the heat conductance value can be chosen, see Fig. 6. For the window U-values, the g-value (solar energy transmittance) and the construction costs per m² are the deciding criterions used for categorization besides the window frame material (wood, plastic, aluminum,…).

Table 1: ground floor construction above soil with a total thickness of 0.634 metres, a thermal resistivity ($R_{si}+R_{se}$) of 0.17 and a construction-dependent total resisity R[m²K/W] of 2.673 leading to an U-value[W/m²K] of 0.374

	material	d[m]	λ[W/mK]
1	**foam glass granules**	**0.160**	**0.085**
2	PAE insulation film	0.002	0.230
3	**steel reinfoced concrete plate**	**0.300**	**2.500**
4	bituminous primer	0.000	---
5	optional ground sealing	0.005	---
6	polysterene concrete	0.060	---
7	subsonic noise insulation	0.020	0.040
8	PAE insulation film	0.002	0.230
9	screed	0.070	---
10	lining	0.015	

Table 2: insulated outer wall construction with a total thickness of 0.360 meters, a thermal resistivity ($R_{si}+R_{se}$) of 0.17 and a construction-dependent total resisity R[m²K/W] of 3.257 leading to an U-value[W/m²K] of 0.307

	material	d[m]	λ[W/mK]
1	exterior plaster	0.015	---
2	**EPS-F (expanded polystyrene)**	**0.120**	**0.040**
3	adhesive putty	0.010	---
4	**steel reinforced concrete wall**	**0.200**	**2.300**
5	inner wall plastering	0.015	---

Table 3: insulated flat roof construction with a total thickness of 0.465 meters, a thermal resistivity ($R_{si}+R_{se}$) of 0.14 and a construction-dependent total resisity R[m²K/W] of 5.311 leading to an U-value[W/m²K] of 0.188

	material	d[m]	λ[W/mK]
1	PVC-film [UV-resistant]	0.004	0.020
2	**EPS-W**	**0.200**	**0.040**
3	moisture barrier film	0.000	0.250
4	concrete for leveling	0.060	0.980
5	**steel reinforced concrete**	**0.200**	**2.300**
6	plastering	0.001	1.400

Figure 5: Modeling the building physics. The outer walls are constructed with 25cm brick stones and insulated with 14cm mineral rock wood. The construction-cost-ratio (CCR) and the energy-ratio (ER) illustrate the cost-to-energy balance with respect to the building hull proportion of each part. The color-coded state in the last column row reflects, whether normative limits are kept or not.

part	window type	*	category	*	U-value	*	ratio	CCR	ER	s	#v
window	wood windows	☑	in free-standing building	☑	0,7W/m2K	☑	4,86	10,08	3,90		56
window	wood-aluminum w…	☐	in vacant lot	☐	0,6W/m2K	☑	8,88	26,31	4,61		7
window	wood windows	☐	in free-standing building	☐	0,9W/m2K	☐	5,53	7,77	1,70		1

Figure 6: Modeling the windows with respect to assigned shading modalities. The window quality is defined via U-value category. For each wall, ground, roof and window, construction and insulation aspects can be defined as variable or fixed via check-box selection for later variant calculation. The number of variants for each part is announced in the last column.

3. EFFICIENCY DEFINITION

3.1. Key model results and parameters

The two key results to directly compute based on the planning model are the expected energy demand in *kWh* per *m²* (square meters) and year as well as the costs for constructing the building's hull in Euro.

For calculating the annual energy demand per square meter gross floor area, the building physics calculation algorithm by Pöhn (Pöhn, et al. 2010), used for energy certificate calculations in Austria, is adapted for use with arbitrarily detailed construction plans. The calculation algorithm is conforming the Austrian policies *ÖNORM H 5055*, *ÖNORM B 8110-3* and implementing the initiating EU act in law 2002/91/EG (Pöhn, 2008).

3.2. Defining and Calculating the Efficiency

As common calculation basis costs in Euro are chosen. Therefore the *ΔkWh/m²/a* to achieve by increased investments in insulation for instance must be expressed as benefit in Euro. Several financial mathematics models have been presented in the past, covering amortization periods, energy cost rates, interest rates and inflation (U.S. Congress 1992; Jakob and Jochem 2004).

Our efficiency model observes an amortization period of *t=20* years. In that period the increased investment costs charged interest are opposed to the cost savings due to reduced energy demand. The financial mathematics model covers debit and credit rates and a progressive energy cost indicator. Each model parameter can be adjusted to fit changed business conditions. Energy saving devaluation due to inflation is not considered to be relevant.

The expected construction costs per m² and the predicted energy savings in Euro per m² over the next 20 years of amortization are combined at equal weights yielding a total efficiency parameter.

As a common basis for planning variants comparison is given, automated estimation of the minimal and maximal efficiency to achieve for a certain building construction plan becomes technically feasible. Furthermore all variants of choosing different wall, ground, roof and window types can be automatically evaluated for predicting the possible changes in efficiency to achieve as distribution.

4. VARIANTS CALCULATION FOR SIMULATION AND PLAN EVALUATION

Based on the floor plans and assigned modalities defining the building geometry, we can simulate different planning variants and evaluate their predicted efficiency. Thereby for example an outer wall constructed of 20cm brick stones is to be compared to a wall constructed of 22cm brick stones or 18cm concrete. A large number of permutations designated as variants can be evaluated. The user has to decide which aspects of the building physics plan should be considered for variant calculation and which not. On a top level view the building parts can be permutated: *walls* × *grounds* × *roofs* × *windows* × *windowRatios*. For the construction group "walls", all different assigned modalities can be permutated, for example *outerWall* × *partitionWall*. The wall bordering an adjacent building can be further decomposed, e.g. according to the chosen category like fire wall or insulated wall. For each of these sub-categories variants can be arranged as *constructionMaterial* × *constructionThickness* × *insulationMaterial* × *insulationThickness* ending up in a large number of total permutations. The dimensionality of the solution space is defined by the cumulated numbers of distinctive modalities for walls (W), roofs (R), grounds (G), window shadings (WS) and window ratios (WR) used in the plan, for example $D = \overline{W} + \overline{R} + \overline{G} + \overline{WR} + \overline{WS} = 7$ defines the solution space:

$$S = \begin{pmatrix} W_{outerWall} \\ W_{flatRoof} \\ R_{shedRoof} \\ G_{groundOnSoil} \\ WS_{marquee} \\ WR_{North\_windowRatio} \\ WR_{SouthWest\_windowRatio} \end{pmatrix}$$

with $W_{outerWall}$ for example covering all permutations of *constructionMaterial* × *constructionThickness* × *insulationMaterial* × *insulationThickness* as

$$W_{outerWall} = \left\{ \begin{pmatrix} concrete \\ brickstone \\ wood \end{pmatrix} \times \begin{pmatrix} 20cm \\ 25cm \\ 30cm \\ 35cm \end{pmatrix} \times \begin{pmatrix} EPS \\ XPS \\ MWPT \end{pmatrix} \times \begin{pmatrix} 8cm \\ 10cm \\ 12cm \\ 14cm \end{pmatrix} \right\}$$

resulting in a set of 144 discrete wall constructions for walls with modality *outerWall*:

$$W_{outerWall} = \{c20EPS8, c20EPS10, \ldots w35MWPT14\}.$$

The window ratio variations can be performed for walls in one of the eight main orientation intervals. For the discrete variation of the window-ratio per orientation, the lower and upper boundaries as well as

the increment can be parameterized, see Fig. 7. For application of the target window-ratio, two strategies are available:

- to assign the target window-ratio to all window-walls in the orientation interval or
- to preserve the orientation intra-group-ratio and preserve the different proportions of the walls to process. E.g. if the two equally-sized north walls with 10% and 20% window ratio and a cumulated window-ratio of 15% should be applied a total window ratio of 30%, the wall-ratios are set to 20% and 40% to keep the intra-group ratios.

window ratio	area in m²	total ratio [%]	relative ratio [%]	min	max	step width	*	#var
south-east	49,20	36,44	36,44	20	60	10	☑	6
south-west	64,80	56,84	56,84	30	55	15	☐	1
north-west	24,00	17,78	25,00	5	75	20	☑	5

Figure 7: The window-ratio of all orientation-groups can be considered for variant calculation. The relative window ratio, comprising all walls with windows at a certain orientation, is variegated in the interval [min;max] at defined step width.

If there are no fixed parameters defined as restrictions for variant calculation, a solution space with several billions of single efficiency evaluations might have to be evaluated. As the plan has to comply with legal requirements, the number can be significantly reduced. Furthermore the planner might further more restrict the problem dimension according to his or the construction owner's specifications or sequentially work on the optimization by e.g. first varying the window aspects, later on the walls and finally the roof construction. For a real world planning problem a search space of only around 10 million discrete variants will remain at the most if the optimization is performed in a sequential way, see Fig. 8.

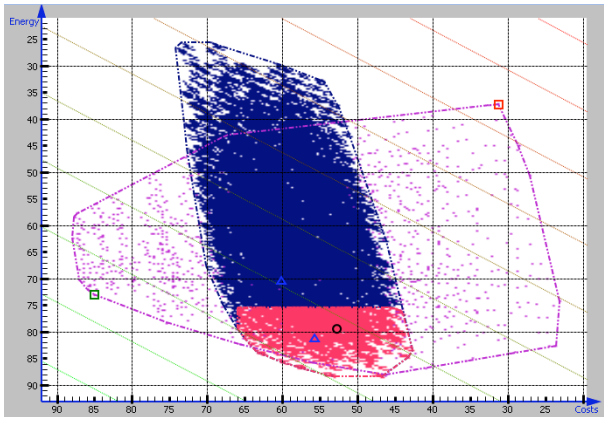

Figure 8: Results of sequentially evaluating more than 10 million variants in total. The x-axis shows the expected costs for construction the building hull as cost-efficiency percentage and the y-axis the energy costs for the next 20 years of amortization as energy-efficiency, both comparing with the defined norm building. Besides the current solution, prior planning variants and the best/worst variant are displayed.

Each construction part with all of its components can be chosen for variant calculation by the user defining the total number of solutions to evaluate, see Fig. 10. Within the variants chart the most and least efficient solution are marked with green and red quadrates respectively. The position of the current chosen construction plan is marked as black circle. The diagonal blue auxiliary lines refer to efficiency categories; the closer the results are to the origin, the higher the efficiency is. Furthermore, the variant solution space can be viewed ad arbitrary detail level by allowing continuous zoom-support.

Utilizing the variant chart, the planner can track the consequences of on-the-fly changes on the construction parts to optimize towards the optimum. Furthermore one can gain information about the parameter configurations beneath the charted efficiency results to obtain information on how to improve the plan at best, after clicking on a chart position, see Fig. 9. If performing several variant calculation runs, the planner can decide which results to present in the chart, see Fig. 10.

cost efficiency: 69,62% energy efficiency: 78,574% **total efficiency: 81,334%**

modality	variant	max efficiency	min efficiency
wall adjacent air	**brick 18cm EPS-F 20cm**	**brick 18cm EPS-F 20cm**	brick 18cm MW-PT 10cm
roof flat roof	concrete 20cm XPS-G 20cm	concrete 20cm XPS-G 36cm	concrete 25cm XPS-G 20cm
window-ratio south-east	**20%**	**20%**	60%

Figure 9: Single variant selected from the chart. For each varied parameter, the possibly best and worst are compared to the current chosen parametrization.

description	num of elements	color	show	hull curve
calculation#4	48	(7,252,41)	☐	☐
windows	1732	(183,3,206)	☑	☑
walls, ground, roof	39043	(0,0,128)	☑	☑
insulation thickness	10761	(249,40,104)	☑	☑

Figure 10: Each variant calculation run can be added a description label and a display color. Furthermore, each variant calculation run can be shown or hidden in the chart. Option *hull curve* (Preparata and Hong 1977) draws the surrounding polyline for the discrete variant results in the chart.

5. REFERENCE PLAN AS BASIS OF COMPARISON

Although construction costs and the expected energy demand can be evaluated very precisely, it is not the primary goal of BauOptimizer software to represent a cost calculation tool or a tool for energy demand approximation, precisely taking into account arbitrary architectural variations like wall ledges or jutties. Instead, comparison of different planning designs and an optimization of efficiency are achieved by efficiency definition and specification of a reference plan.

Consequently, a comparative basis for construction costs, energy demand and efficiency is required. Instead of absolute construction cost parameters in €/m² and energy demands in kWh/m²a, only relative values are presented to the planner, e.g. costs of 85.2% in the range of [0;100]% derived from the best and worst possible planning design. Energy and efficiency are

only represented as quantitative comparison to the reference plan, too.

The reference plan characterizes the planning design, that best takes advantage of the given building site with respect to given preconditions and requirements, like keeping the building lines, considering restrictions like fitting into a vacant construction lot and many more. The reference plan is the simplest geometric shape to fit the construction lot without any architectonical variations but modeling the constraints, like modalities for walls to neighboring buildings, as precisely as possible.

Concerning the construction and insulation material of the ground, the walls, the roof and the windows, a preferably unrestricted wide range of construction variants is allowed.

Based on the reference plan geometrics, the best and worst plan concerning construction costs, energy demand and efficiency must be found. As the solutions for walls, roof, windows and ground are independent from each other, they can be optimized with respect to min/max construction costs, energy demand and efficiency one-by-one. Consequently, for optimization, the permutations of these groups can be additively combined as *walls + grounds + roofs + windows*, thus significantly reducing the dimension of the solution space that has to be searched for reference plan evaluation.

Only the window ratio cannot be seen isolated from the other part-by-part optimization. As the choice of the window ratio directly influences choice of the window type, for entire reference plan optimization, the following search space is defined as:
(walls + grounds + roofs + windows) × windowRatios.
With the minimum and maximum construction costs, the reference plan range of [100;0]% for comparison with other planning results is defined. The same intervals are created for energy demand and efficiency criterion. That way a relative metric for cost efficiency, energy efficiency and the cumulated total efficiency has been defined.

6. IMPLEMENTATION

BauOptimizer planning software is implemented utilizing Eclipse RCP framework for plug-in based application development (McAffer and Lemieux 2005). The charting functionality and parameter editing composites are implemented with *SWT* and *JFace* technology (Daum 2007).

Specification of the floor plans, wall construction assignment and the variant calculations can be performed in a perspective-specific configured editor. All charting and numeric results as well as 2D projections on the building geometry are implemented as viewers.

New wall construction parts, changed cost parameters or additive materials to consider can be handled via proper importers.

Concerning time-intensive variant calculation, we pursue a strategy that primarily necessitates only the recalculation of specific terms of the heating demand and cost calculations by factoring invariant sub-results, thus significantly reducing runtime. Moreover the permutations must be arranged in a sequential order to minimize the required recalculations from variant to variant.

7. RESULTS

7.1. Model Validation

We are currently validating the cost, energy and efficiency results by modeling and simulating real-world planning projects already constructed. Thereby we have to identify the aspects of the entire model that are inexact. Exemplarily the λ-values for material-specific heat conductance value calculation turned out to be modeled too restrictive. As a consequence we have introduced a concept to configure several λ-values at certain thickness intervals for each material. This allows us to add composite construction aspects to our wall construction catalogue.

Besides the abstraction precision to be evaluated and validated on real-world projects, all sub-calculations for energy demand, costs and variant optimization have already been validated separately.

7.2. Calculation of the Cost and Energy Demand Extreme Points

Theoretic considerations and evaluations showed that most of parameters are invariant towards the others. So e.g. the most expensive roof configuration will definitely be the roof for the overall most expensive building configuration as its independent to the ground and walls to choose.

Consequently only very few calculations are to be performed for calculating the best and worst plan with respect to the construction and energy costs, thus defining the 2D range within optimization can take place. This fact is taken advantage of for reference plan evaluation and range pre-calculations before each variant calculation run.

7.3. Variant Calculation Performance

Runtime tests utilizing a 32-*bit Intel Pentium 4* CPU with *2.79 GHz* processing frequency and 1*GHz RAM* an average processing speed of around 190 variant calculations per ms can be timed, see Table 4. The variant calculation task is not parallelized thus only one processor is used for processing on multi-core architectures.

Due to intensive optimization work on the heating demand and cost calculation algorithms, runtime has been reduced by a factor of 10 compared to the first implementations to reach the speed presented in Table 4. In the course of runtime optimization, method calls were replaced by inline assignments, constant terms were pre-calculated and time-consuming exponential function call, that had accounted 60% of the total runtime, was replaced by an approximation based on

floating-point shift-operations and Newton's method (Deuflhard 2004, Ankerl 2007).

Table 4: Average calculation speed at different numbers of variants to calculate. Calculation throughput increases with the number of variants to calculate due to communication overhead and constant initializations.

number of variants	calculation time [ms]	calculations per ms
252	31	7.875
2,016	32	65.032
24,192	219	110.466
96,768	860	112.521
290,304	1,875	154.829
2,032,128	11,797	172.258
12,192,768	65,031	187.491
156,473,856	810,136	193.145

7.4. Findings concerning Material Choice

Besides planning project-specific optimization of the building construction material, several findings concerning general material choice guidelines and rules of action can be derived. One aspect even very surprising for the architects and building physicians is that a common brick stone wall generally outperforms a wall made of concrete by far and that thermal insignificant parts of the building, e.g. a partition wall to a heated adjacent building, have a deciding potential for cost reduction.

Analysis of the hull curves resulting from variant calculations show, that planning results of a certain energetic quality can be achieved at different material choices, thus leading to a broad cost spectrum for construction, see Fig. 11 and Fig. 12.

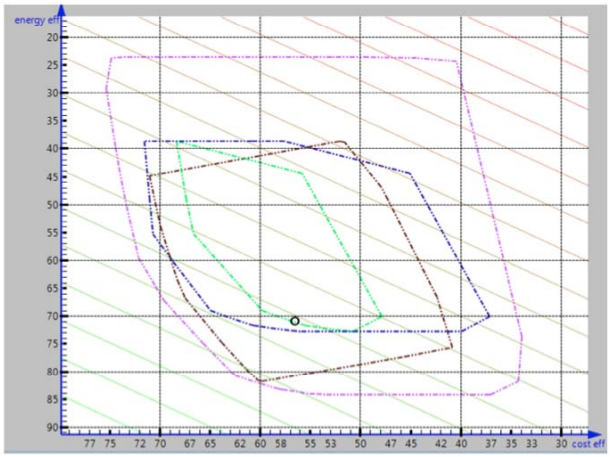

Figure 11: Results of varying construction and insulation material and thickness. The broadly based hull curves illustrate, that results in the same energy efficiency class can be achieved by solutions at a wide spectrum of cost efficiency.

The theoretical inverse correlation of cost and energy efficiency cannot be observed in variant calculation. Increased construction costs do not automatically lead to a reduced energy demand and higher energy efficiency can also be achieved by cheaper material respectively. For window choice, the g-value quality is another deciding factor besides costs and U-value as energy criterion.

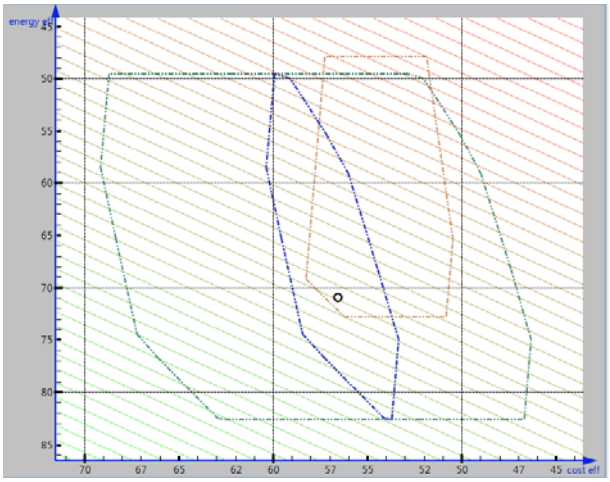

Figure 12: Results of varying window type and quality. The horizontally oriented borders of the hull curves indicate, that the same energy efficiency intervals can be achieved at window constructions at very different costs.

7.5. Trend-Chart for Energy-Cost Correlation Analysis of the Variant Optimization Space

The findings discussed in the prior section raise the demand for detailed analysis of the variant optimization space. Each single variant solution is sorted according to cumulated efficiency value and charted with respect to energy and cost efficiency. The distribution of the solutions in the variant optimization is modeled as color-coded intensities, see Fig. 13 and Frig. 15.

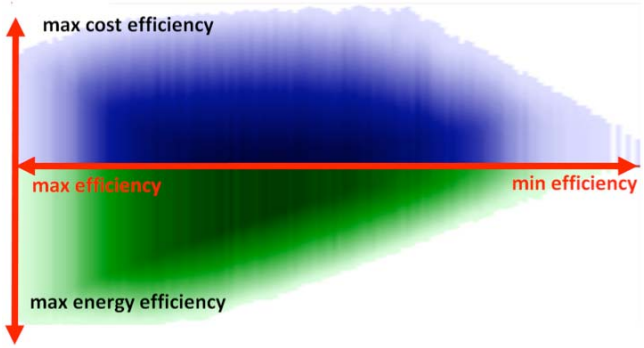

Figure 13: Trend-chart for variation of insulation material and thickness. The y+ axis plots cost efficiency, whereas the y- axis plots the energy efficiency for each single variant solution cumulated efficiency x axis position. Comparing costs and energy at high intensity values in the midst of the efficiency spectrum illustrates, that there is a linear correlation between energy and cumulated efficiency optimization, whereas the cost aspect shows slightly indifferent tendency. The maximum cumulated efficiency at the very left shows higher energy efficiency compared to the costs. At the very right solutions can be found, that show both, low cost and low energy efficiency.

If analysis of single efficiency intervals must be performed, normalization allows filtering-out the distribution-based intensity variation to facilitate analysis of the energy-to-cost efficiency ratio at different intervals, see Fig. 14 and Fig. 16.

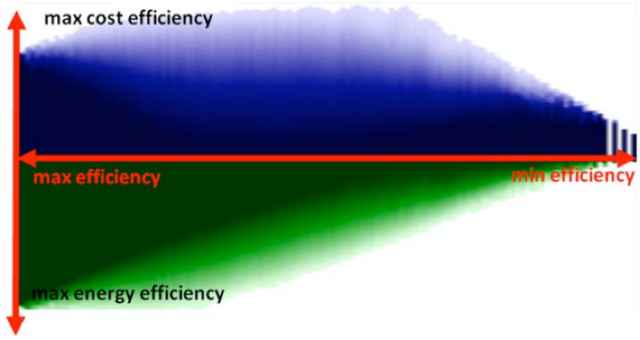

Figure 14: Trend-chart on same variant results data as plotted in Fig. 13. To equalize the distribution-based variation, normalization has been performed to independently handle the color-coding intensities of each cumulated efficiency slot. The sample above shows high variability of the cost efficiency in the midst results and less variability for the energy efficiency. Maximizing energy efficiency leads to the best results whereas solutions with high cost efficiencies are slightly ranked at back.

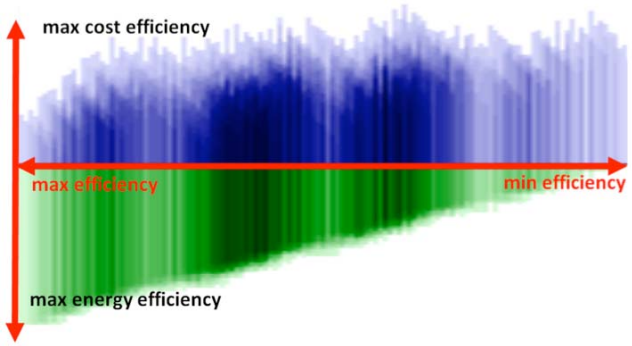

Figure 15: Trend-chart for variation of window frame material and window glass insulation quality. A strong linear correlation between energy efficiency and the solution quality can be observed. The expensive window solutions are at the first ranks, whereas the cheaper windows can be found at the lower end of the efficiency range.

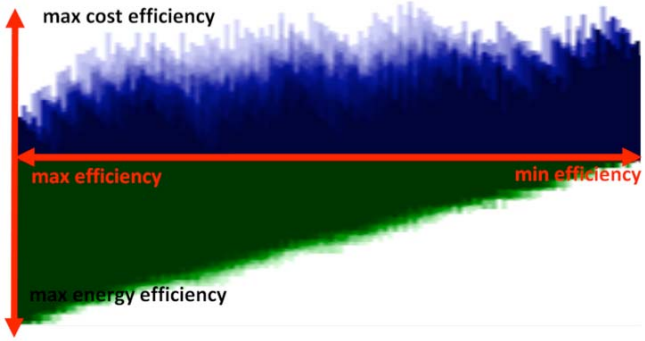

Figure 16: Trend-chart on same variant results data as plotted in Fig. 15 with normalized intensities.

7.6. Evaluation based on Real-World Reference Planning Projects

Evaluation and validation of the described modeling and analysis software must be performed based on real-world reference planning and construction projects carried out in the past. There are several aspects to validate:

- is the 0.5m grid accurate enough for modeling the building geometrics?
- does the construction material catalogue have a sufficient extensiveness for modeling arbitrary construction strategies and concepts?
- is the geometrics-dependent energy demand calculation valid?
- is the cost-approximation valid?

By now two major planning projects have undergone detailed analysis. As building-hull dependent energy demand and building-hull dependent cost fraction are no common parameters to survey in architecture and construction engineering, they have been approximated for the two projects to evaluate. Accurate cost parameters for constructing the building-hull will be collected for future projects from now.

7.6.1. Reference Planning Project I

Construction area dimension *22.5m* × *35m* × *10.5m*, orientation *4°* north was covered with a 5 floor building and total net dwelling area of *3,041.25m²* at a sphericity of *33.98%*, see Fig. 17. The chosen plan shows a total efficiency of *32.71%* (cost efficiency 53.44% with 233.94€/m² and energy efficiency 20.96% with 23.55 kWh/m²a) compared to the reference building. The possibly best, optimized building design would show a total efficiency of *64.461%* (cost efficiency 41.26% and energy efficiency 81.94%), see Fig. 18.

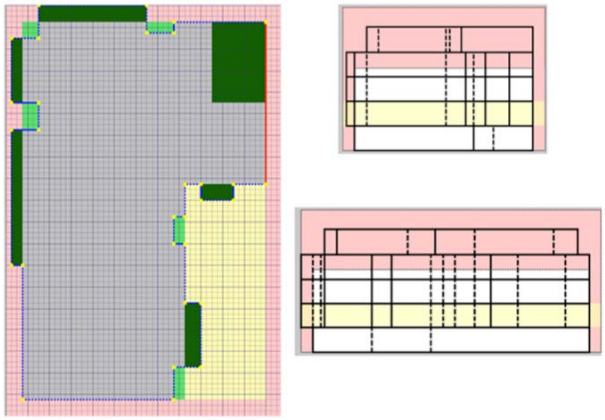

Figure 17: Horizontal, front and side projection of the reference planning project I construction design.

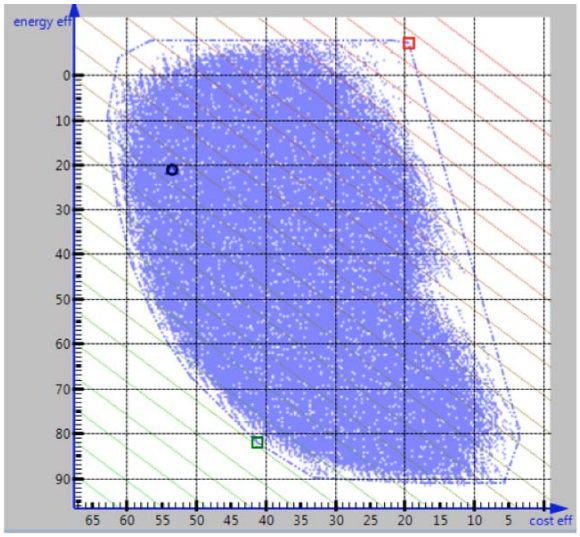

Figure 18: The chosen planning solution at [53.44;20.96] could approach the achievable optimum at [41.26;81.94] by increasing insulation and window quality and decreasing the window ratio at north walls. The increased construction costs are over-compensated by the energy savings.

7.6.2. Reference Planning Project II

Construction area dimension *15.5m* × *15m* × *16m*, orientation *40°* north was covered with a 7 floor building and total net dwelling area of *1,370.12m²* at a sphericity of *38.64%*, see Fig. 19. The chosen plan shows a total efficiency of *18.34%* (cost efficiency 41.42% with 248.09€/m² and energy efficiency 10.60% with 21.25 kWh/m²a) compared to the reference building. The possibly best, optimized building design would show a total efficiency of *70.291%* (cost efficiency 45.20% and energy efficiency 90.37%), see Fig. 20.

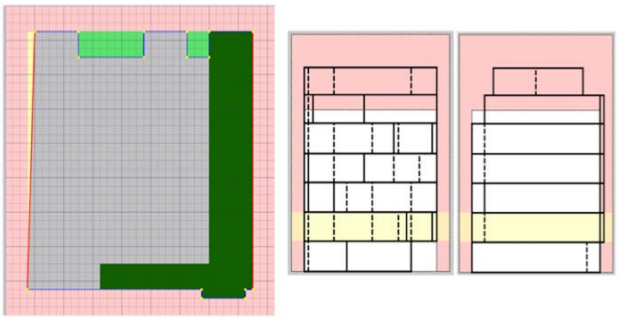

Figure 19: Horizontal, front and side projection of the reference planning project II construction design.

7.6.3. Conclusions from the Reference Planning Projects

The 0.5m grid offers sufficient precision and the construction material catalogue contained the required wall, ground and roof construction concepts for precisely modeling the reference planning project designs.

Energy demand calculation and hull-specific construction costs have been compared to results of conventional energy demand calculation and the hull cost approximation. The marginal deviance results from floor-plan-specific energy demand calculation in our application, whereas common software of building physics cannot handle the exact geometry and can only give a rougher approximation.

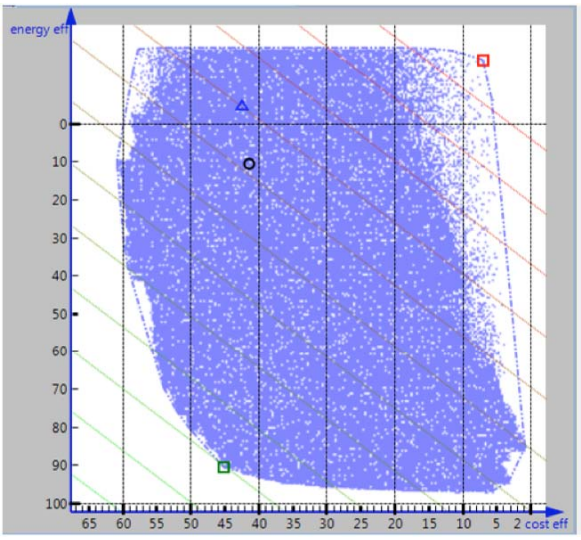

Figure 20: The chosen planning solution at [41.42;10.60] could approach the achievable optimum at [45.20;90.37] by increasing insulation and window quality and decreasing the window ratio at north walls. The increased construction costs are over-compensated by the energy savings.

8. DISCUSSION

We have developed and presented a planning tool already appropriate for precise modeling of the different construction planning aspects and ready to perform automated optimization with respect to cost and energy efficiency.

For the first time changes on the building geometry, like adding or removing a jutty can be evaluated towards cost and energy demand consequences on-the-fly.

Furthermore the legislative body can check the permission plan not only for keeping the normative limits but also for exhausting the construction-site specific potential in future. Consequently future financial promotion for building projects might not only depend on the normative limits of the single construction parts but also on the distance from the optimal achievable limit with respect to efficiency.

For construction companies usage of the planning software is expected to take advantage of cost reduction potentials when competing with rival applicants in the course of award procedures.

A future field of application is planning thermal rehabilitation activities. Thereby the simulation could predict how many years it will take to redeem the investment costs and which measurements have the highest payoff. Not every investment instigated in the light of energy saving and CO2 reduction for ecology might effectively be worth a consideration. Up to now thermal rehabilitation activities are not planned

according to highest efficiency but highest energy savings to achieve and best-practice manuals (Gabriel and Ladener 2009) instead considering the required investment cost.

ACKNOWLEDGMENTS

The project was financially supported by the FFG, the Austrian Research Funding Agency, base funding program.

REFERENCES

Ankerl, M., 2007. *Optimized pow() approximation for java and c/c++*, available from http://martin.ankerl.com/2007/10/04/optimized-pow-approximation-for-java-and-c-c/

Daum, B., 2007. *Rich-Client-Entwicklung mit Eclipse 3.3*. 3rd ed. dpunkt Verlag

Deuflhard, P., 2004. Newton Methods for Nonlinear Problems – Affine Invariance and Adaptive Algorithms. Berlin: *Springer Series in Computational Mathematics*, vol. 35.

Gabriel, I. and Ladener, H. (eds.) 2009. *Vom Altbau zum Niedrigenergie- und Passivhaus*. 8th ed., Ökobuch Verlag.

Jakob, M. and Jochem, E. 2004. *Kosten und Nutzen-Wärmeschutz bei Wohnbauten*. Bern: Centre for Energy Policy and Economics, Swiss Federal Institutes of Technology, available from http://www.cepe.ch/download/staff/martin/WaermeschutzWohnbautenKosten_Nutzen.pdf [08.04.2010]

McAffer, J. and Lemieux, J.-M., 2005. *Eclipse Rich Client Platform: Designing, Coding and Packaging Java Applications*. Amsterdam: Addison-Wesley Longman

Pöhn, C., 2008. *Die EU-Gebäuderichtlinie*. Magistratsabteilung MA39, available from http://www.bauxund.at/fileadmin/user_upload/media/service/nachhaltigKrankenhaus08/Poehn_vortrag_KAV080618.pdf [08.04.2010]

Pöhn, C., Pech, A., Bednar, T. and Streicher, W., 2010. *Bauphysik Erweiterung 1: Energiesparung und Wärmeschutz. Energieausweis – Gesamtenergieeffizient*. 2nd ed. Wien: Springer.

Preparata, F.P and Hong, S.J., 1977. Convex Hulls of Finite Sets of Points in Two and Three Dimensions, *Commun. ACM*, 20(2), 87-93.

U.S. Congress, 1992. *Building Energy Efficiency, Office of Technology Assessment*. Washington: U.S. Government Printing, available from http://www.fas.org/ota/reports/9204.pdf [08.04.2010]

AUTHORS BIOGRAPHY

Gerald A. Zwettler was Born in Wels, Austria and attended the Upper Austrian University of Applied Sciences, Campus Hagenberg where he studied *software engineering for medicine* and graduated Dipl.-Ing.(FH) in 2005 and his follow up master studies in *software engineering* in 2009. In 2010 he has started his PhD studies at the University of Vienna at the faculty of Computer Sciences. Since 2005 he is working as research and teaching assistant at the Upper Austrian University of Applied Sciences at the school of informatics, communications and media at the Campus Hagenberg in the field of medical image analysis and software engineering with focus on computer-based diagnostics support and medical applications. His e-mail address is gerald.zwettler@fh-hagenberg.at and the research web page of the Research&Development department at campus Hagenberg he is employed at can be found under the link http://www.fh-ooe.at/fe/forschung.

Stefan Hinterholzer has finished his doctoral studies at the Johannes Kepler University Linz in 1992, graduating Mag. Dr. rer. soc. oec. Since then he has been working as professor for business, accountancy and management at the school of informatics, communications and media at Campus Hagenberg, Upper Austrian University of Applied Sciences. His e-mail address is stefan.hinterholzer@fh-hagenberg.at and the faculty web page can be accessed via link http://www.fh-ooe.at/campus-hagenberg/.

Richard Woschitz was born in Oberpullendorf, Austria and has studied construction engineering at the Technical-University of Vienna, receiving a Diploma-Engineer degree in 1991. In 1996 he received doctor's degree Dr. tech. from Technical-University of Vienna. Since then he has been teaching as university lector and guest-professor at several European universities. In 1996 he has set up his company for civil engineering that is now registered as RWT plus ZT GmbH. In 2009 he has founded the enterprise ARGE innovation GmbH together with Dipl.-Ing. Wilhelm Sedlak. His e-mail address is r.woschitz@rwt.at and RWT plus ZT GmbH company homepage can be accessed via link http://www.rwt-plus.at/.

Elmar Hagmann was born in Vienna and studied construction engineering at the Technical-University of Vienna, receiving a Diploma-Engineer degree in 2000 and MBA in 2005. Since then he has been working as civil engineer, consultant for construction engineering and master-builder. In 2008 he became a certified authority for building construction, sworn in court, and became an authorized officer at the Dipl.-Ing. Wilhelm Sedlak GmbH, where he had started his career as expert for building engineering in 2002. His e-mail address is hagmann@sedlak.co.at and Dipl.-Ing. Wilhelm Sedlak GmbH company homepage can be accessed via link http://www.sedlak.co.at.

ON THE BENEFITS OF A DOMAIN-SPECIFIC LANGUAGE FOR MODELING METAHEURISTIC OPTIMIZATION ALGORITHMS

Stefan Vonolfen[(a)], Stefan Wagner[(b)], Andreas Beham[(c)] , Michael Affenzeller[(d)]

[(a)(b)(c)(d)] Upper Austria University of Applied Sciences, Campus Hagenberg
School of Informatics, Communication and Media
Heuristic and Evolutionary Algorithms Laboratory
Softwarepark 11, A-4232 Hagenberg, Austria

[(a)]stefan.vonolfen@heuristiclab.com, [(b)]stefan.wagner@heuristiclab.com, [(c)]andreas.beham@heuristiclab.com,
[(d)]michael.affenzeller@heuristiclab.com

ABSTRACT
This work provides a case-study of how metaheuristic optimization algorithms can be developed using a domain-specific language as a separate modeling layer. A separation of the modeling process from the implementation of the algorithmic concepts improves the communication and collaboration of practitioners, optimization experts and programmers. This is achieved by providing a higher level of abstraction compared to a general-purpose programming language. A generic and extensible modeling concept is presented and several example algorithm models are illustrated.

Keywords: metaheuristics, modeling, domain specific language

1. INTRODUCTION

Metaheuristics are general search strategies that can be used to calculate approximate solutions for many different kinds of problems in diverse application areas. They guide the search process and can be seen as an algorithmic framework with the ability to be tailored to different problem environments (cf. Blum and Roli 2003). Many metaheuristic search strategies are inspired by nature. For an overview of metaheuristic techniques see for example Talbi (2009).

However according to Wolpert and Macready (1995) there is no general search strategy that performs well for all kinds of problems. This implies that even though metaheuristics are general search strategies, tailoring has to be done in order to generate good and feasible solutions for a given problem.

According to Talbi (2009) there are three major approaches for the development of metaheuristics: From scratch, code reuse and both design and code reuse. A software framework provides reusable code and also a reusable design (cf. Johnson and Foote 1988). The goal of using a metaheuristic framework is to be able to build on as much existing code and design elements as possible when developing a new optimization solution. There are many different frameworks available in that area - examples are Templar (Jones 2000), HotFrame (Voss and Woodruff 2002), ParadisEO (Talibi 2009) or HeuristicLab (Wagner, Winkler, Braune, Kronberger, Beham, Affenzeller 2007; Wagner 2009).

When using such frameworks - however - the user generally needs an in depth-knowledge of the framework since according to (Talibi 2009) currently a white-box approach is more suited to metaheuristics than a black-box approach. This means that the user often needs to know implementation details of the framework and needs to have programming skills.

White-box reuse means that a very low level of abstraction (i.e. the source code level) has to be provided to the user in order to tailor an algorithm to a certain problem. There are some approaches to build an additional level of abstraction on top of the frameworks including EASEA (Collete, Luttion, Schoenauer and Louchet 2000) and GUIDE (Da Costa and Schoenauer 2009). However these approaches are either limited to a particular optimization paradigm or very close to an actual programming language.

The scope of this work is to raise this level of abstraction by developing a modeling layer for metaheuristic optimization techniques which is independent of the underlying implementation. This is accomplished by providing black-box reuse without losing the flexibility to tailor the algorithm. Black-box reuse means that components (building-blocks) are provided that have a well defined interface and can be combined in a well-defined way.

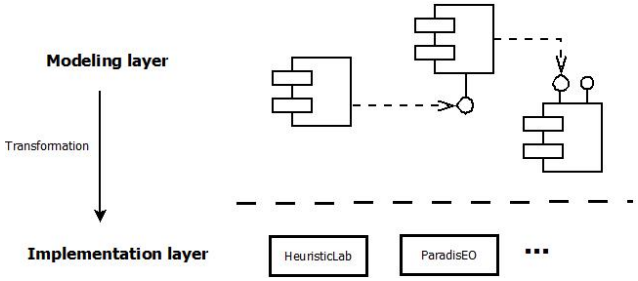

Figure 1: Separation of the modeling layer from the implementation layer

The modeling layer is separated from the implementation layer as illustrated in Figure 1. In the modeling layer algorithm models can be built by combining algorithm building blocks. These building blocks are then executed in the implementation layer, for example by transforming them to code using an underlying framework.

The created models are written according to a specification - an extensible domain specific language (DSL) for metaheuristic optimization. This language consists of all building blocks that are available to the modeler and can be extended by adding new components. In that way for example new algorithmic concepts or problem-specific parts can be incorporated. The models can be validated according to the specification.

There are various benefits a separate modeling layer yields which are examined in this work. First of all additional layers of abstraction can be built where the implementation details can be abstracted and the requirement of programming skills can be removed. Second of all different frameworks or framework versions can be used to transform the models into an executable representation. Apart from that various artifacts can be generated from the models including for example textual descriptions.

When building this modeling layer both, top-down and bottom-up, approaches are possible. Top-down means that the modeler starts by defining abstract components that the algorithm is built of. Then by using stepwise refinement these components are mapped to the according implementation concepts. Bottom-up means that more abstract components are defined starting from an existing implementation layer.

2. BENEFITS

The level of abstraction that is provided by current frameworks is raised by providing a separate modeling layer above existing frameworks and consequently the implementation layer is separated from the modeling layer. This yields several benefits:

- **Communication:** In heuristic optimization projects there are usually different types of stakeholders. When implementing a solution, an expert in the field of heuristic optimization algorithms usually needs to have programming skills since most of the available frameworks are whitebox oriented. A separate modeling layer could improve the communication between experts in the field of optimization and programmers.

- **Collaboration:** By proving a common model, algorithm designers and programmers can work together more efficiently because both, top-down and bottom-up, modeling approaches are possible. On the one hand, in a top-down approach an algorithm designer would first specify the abstract algorithm building blocks and model the algorithm, then the programmer maps these building blocks to an existing framework or implements them from scratch. On the other hand, in a bottom-up approach the programmer first maps existing implementations to modeling building blocks that the algorithm designer can then use to design new algorithmic variants. Of course, also mixed approaches are possible where certain building blocks are provided and new ones are added later on by the programmer.

- **Abstraction:** Algorithms can be modeled independently and the implementation details are abstracted. As a result, no internal knowledge of the underlying framework is necessary and no programming skills are required. During the modeling process the technical details are hidden. Furthermore higher layers of abstraction can be created, than it is possible to realize within a programming language. This can be achieved for example by using coarse grained components.

- **Generation:** Various artifacts can be generated from the models. For example different frameworks or framework versions can be supported for the actual implementation and execution of the algorithmic model, since it is independent of the implementation. Apart from that for example textual descriptions of the algorithm or graphical representations can be generated. In terms of communication and collaboration it is also important that the generated executable representations can be easily executed and algorithm runs can be easily analyzed by the domain expert. The generated executable representations of the algorithms are all unified, which means that for example coding standards are followed and the design is standardized. This is often very difficult to achieve when writing hand-crafted code, especially when parts are written by different developers.

- **Model validation:** Since the model is defined according to a meta-model, various validations can be included. This validation is often only performed on the syntactical level in current frameworks. An example would be that the operators actually fit together and work on the same type of problem representation.

- **Flexibility:** Apart from providing the before mentioned benefits, the modeling layer should provide full flexibility. This means that it should not be restricted to a certain paradigm and the algorithmic structure should be fully modifiable.

3. EXISTING MODELING LAYERS

There are already some approaches of providing a modeling layer for heuristic optimization. For example some domain specific languages for local search strategies have been developed which are mostly based on constraint programming according to Fink and Voss (2001). Other examples of modeling layers are EASEA (Collete, Luttion, Schoenauer and Louchet 2000), GUIDE (Collete, Luttion, Schoenauer and Louchet 2000) and the HotFrame configurator (Fink and Voss 2001) which are examined in the following. Also the HeuristicLab environment (Wagner, Winkler, Braune, Kronberger, Beham, Affenzeller 2007; Wagner 2009) can be regarded as a modeling tool.

In this section the existing modeling layers are evaluated according to the benefits that are discussed in section 2. Table 1 gives an overview of the evaluation criteria. A √ symbol means that the criterion is fulfilled; a o symbol means that a criterion is partially met and a × symbol means that the criterion is not met. The − symbol means that a certain criterion is not applicable to a modeling layer.

Table 1: Evaluation

Criterion	EASEA	GUIDE	HotFrame Configurator	HeuristicLab
Communication	×	o	o	√
Collaboration	×	o	o	√
Abstraction	o	√	o	o
Generation	√	√	√	−
Model validation	×	−	−	−/×
Flexibility	o	×	×	√

EASEA is a scripting language for evolutionary computation and is close to a programming language. This means that even though it abstracts the actual programming language and framework, the communication and collaboration between implementers and domain experts is not supported. This is because programming skills are required to use EASEA efficiently. However, one benefit of using EASEA is certainly that code generation for different frameworks is possible. Model validation is not supported. In terms of flexibility, EASEA is designed for evolutionary computation. However, since EASEA is very close to an actual programming language, one could argue that additional paradigms can be incorporated.

GUIDE provides a graphical user interface for building evolutionary algorithms based on an algorithm template. Its graphical user interface is intuitive and reflects the terms used in the evolutionary computation community. This enables communication between programmers and domain experts. In terms of collaboration building blocks based on a certain framework can be defined and offered to the modeler. However, in terms of communication and collaboration the analysis of algorithm runs is not supported directly. All framework and implementation details are abstracted and code can be generated for various frameworks. Model validation is not required, since the tool does not allow the construction of invalid models. However in terms of flexibility GUIDE is limited to evolutionary algorithms and the underlying algorithm structure cannot be modified.

Similar to GUIDE, the HotFrame configurator is designed as a configuration tool. It hides all implementation details by providing a configuration language to the user which improves the communication. In terms of collaboration, programmers can provide configurable building blocks to the domain expert. From the configuration an executable representation is generated. However, the analysis of algorithm runs is not supported. In terms of abstraction, the HotFrame configurator is limited to the HotFrame framework. There is no need for model validation since it only allows the user to create valid models. When it comes to flexibility, the HotFrame configurator is limited to the configuration of the algorithms; the algorithm structure cannot be modified.

Regarding HeuristicLab, one great benefit is certainly the communication and collaboration between domain experts and programmers. In the current release (version 3.3) communication and collaboration between programmers and domain experts is supported using a model-driven approach which is described by Wagner (2009). Apart from building the algorithms using pre-defined building blocks, algorithm runs can be executed and analyzed within the HeuristicLab environment. The details of the underlying programming language are abstracted completely by providing a generic modeling concept. However, this layer of abstraction is tied to the HeuristicLab framework and right now it cannot be used to generate code for other frameworks. This means that the framework details are not abstracted. As a result the modeling and execution layer are not separated and no generation is needed to execute the models. In terms of flexibility, there exist two different types of algorithms in the HeuristicLab framework: pre-defined and user-defined algorithms. Pre-defined algorithms can be parameterized (similar to the HotFrame configurator) and thus there is no need for model validation, since the user cannot construct invalid models. User-defined algorithms provide a full degree of flexibility. However, for these algorithms no fully-fledged meta-layer exists right now. This means that the control and data flow cannot be validated when constructing custom algorithms.

4. MODELING CONCEPT

As stated in section 1, the developed modeling concept is a black-box oriented approach. This allows the definition and combination of well defined building blocks. These building blocks are components that represent a specific encapsulated functionality which is part of a metaheuristic optimization algorithm. This functionality can be realized on different levels of abstraction.

The elementary components that the algorithm is built of are operators, similar to the modeling concept proposed by Wagner (2009). However the level of abstraction is higher and less focused on

implementation and execution than the algorithm models of the examined frameworks. The modeling layer is separated from the implementation/execution layer.

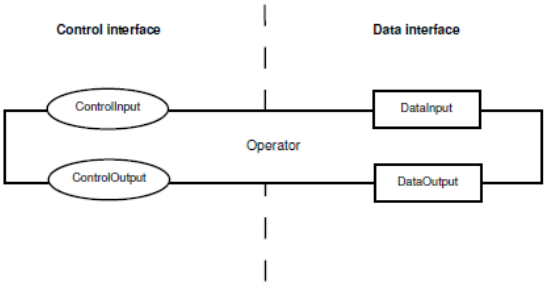

Figure 2: Interface of an operator

Following a component-based approach, these building blocks have a well defined interface. This interface determines how building blocks can be combined. As illustrated in Figure 2 an operator has a control interface and a data interface. The control interface can be used to model the control flow, the data interface to model the data flow of the algorithm. This separation allows a high level of flexibility. The control and data interfaces consist of input and output ports that can be connected to each other.

4.1. Control Flow

By connecting the control ports of the operators, the control flow of the algorithm can be modeled. Each operator has exactly one control input and zero or more control outputs. A connection between the control output of an operator A and a control input of an operator B means that operator B is called by operator A. Each algorithm has a start operator that has no control input and one control output that triggers the execution of the algorithm.

Whenever multiple control output ports are connected to one control input port, the control flows are joined at that point. The semantic of a join is that the execution of all previous operators has to be finished before the called operator is executed. Finished means that all previous operators either have finished execution or are not executed.

4.2. Data Flow

Whenever an operator is executed, the parameters from the input data ports are processed and the results are written to the output data ports. An operator can have zero or more data input and zero or more data output ports. The data input ports store the current value until a new value is set. The value of each data input port is set to empty at the beginning of the execution of an algorithm. A data output port can be connected to an arbitrary number of data input ports. The value of the data output port is written to all connected data input ports.

5. IMPLEMENTATION

To provide means of formulating the models, a domain specific language (DSL) for metaheuristic optimization algorithms is developed. The design and implementation of the modeling layer is based on the general modeling concept that is outlined in the previous section. Several design choices were made to create a modeling system that meets the benefits described in section 2.

First of all it was decided that an external graphical DSL should be developed. The main reason for that is raising the level of abstraction and hiding the implementation details. Furthermore, to enhance the communication between domain experts and programmers, a graphical concrete syntax was chosen.

To achieve a high level of flexibility the vocabulary of the DSL should not be fixed but definable by the user. The user should be able to define new building blocks and that way add a new vocabulary to the modeling language. The developed DSL should be highly extensible.

As a result, actually two graphical editors are developed: One editor to define the algorithmic building blocks and one editor to model the algorithms. That way, new building blocks for the modeling of algorithms can be created and the vocabulary can be easily extended.

The DSL to define algorithmic building blocks provides a specification of the algorithmic components. It is used to create toolbox models which provide a set of components that can be used in an algorithm. In principal these two DSLs can be used by the same or by different users. For example one user could create certain building blocks and then provide them to another user. The first user that defines the components could be a programmer and the second user that builds the algorithm models using the second editor could be a domain expert in heuristic optimization. That way the communication between these two user groups could be enhanced.

Both languages were implemented as graphical editors using the Microsoft Visual Studio Visualization and Modeling SDK[1]. Both designers are integrated into the Visual Studio environment.

6. RESULTS

Using the developed modeling tools, several example algorithm models were created. Figure 3 shows a genetic algorithm model solving the traveling salesman problem using a permutation encoding. In that case, high-level building blocks which are defined in the corresponding toolboxes are combined with each other.

[1] http://code.msdn.microsoft.com/vsvmsdk

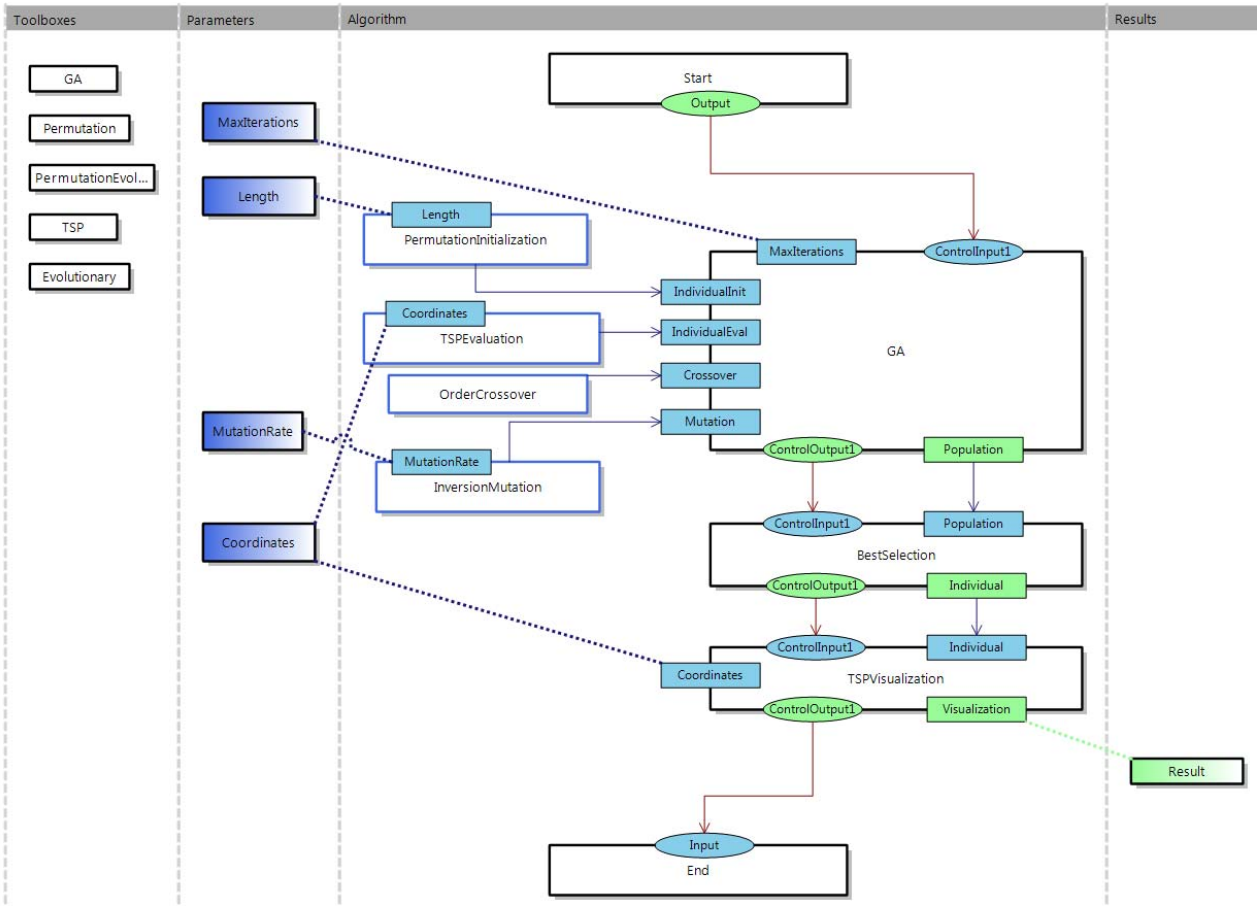

Figure 3: Genetic algorithm model solving the TSP

These high-level building blocks are defined in toolboxes. Some can be directly mapped to a framework, others are defined as finer-grained algorithm models. For example the *GA* building block is defined by a finer-grained GA building block that includes operations such as evaluation, selection and reproduction following the abstract GA specification.

In the example model, the problem-specific *TSP* toolbox is combined with the encoding-specific *Permutation* toolboxes and the general *Evolutionary* and *GA* toolbox.

Due to data flow validation, only building blocks that fit together can be combined; for example no real-vector operations can be used in conjunction with permutation operations.

These algorithm models can be converted to executable HeuristicLab algorithms using the HeuristicLab code generator. The targeted HeuristicLab version is 3.3.0 (http://dev.heuristiclab.com).

The runtime and quality of generated solutions for different problem instances retrieved from the TSPLIB [Rei91] has been measured and analyzed. These results are compared to the standard GA implementation included in the HeuristicLab 3.3.0 release which is hand-crafted.

All test runs where done using a population size of 100, a mutation rate of 5% and one-elitism. For all instances 10 independent test runs were done and the mean value and standard deviation was calculated.

The quality of the best solution after 100 iterations is examined to make sure that the generated code produces correct results. The results are listed in table 3. All deltas between the results of the hand-crafted GA and the generated GA are in the range of the standard deviation which shows the correctness of the approach.

Table 3: Best solution quality analysis

Instance	Handcrafted μ	Handcrafted σ	Generated μ	Generated σ
eil51	936.8	46.2	941.0	54.3
ch130	30438.1	670.4	30952.7	1082.3
rl5934	39008794.3	106313.8	39122368.0	246800.6
rl11849	82537969.2	235147.2	82545883.2	299712.9
d18512	56920526.6	151996.7	56985640.1	80526.1

7. CONCLUSION

Concluding, a prototype of the modeling environment has been developed and several benefits have been met and also some drawbacks were identified:

- **Communication**: It has been shown that these algorithm models are close to the abstract algorithmic specification found in the literature. This illustrates that a domain-specific language can enhance the communication between domain experts and

programmers in the field of heuristic optimization. However, graphical models can get quite complex and difficult to change for complex algorithmic concepts and it is crucial to choose a sufficient level of abstraction.

- **Collaboration:** Using the prototype, top-down and bottom-up modeling approaches are possible which advances the collaboration between the different stakeholders.

- **Abstraction:** The algorithm models are designed independently of the underlying framework and programming language. However, it has yet to be shown that these models can be mapped to frameworks other than HeuristicLab.

- **Generation:** The generated code turned out to be less efficient than the handcrafted code. Furthermore, the generated code is very different from the way a domain expert would model the algorithms in the HeuristicLab environment. This has a negative impact on the maintainability.

- **Model validation:** Data flow validation has been implemented and prevents the user from creating invalid models.

- **Flexibility:** The algorithm model provides full flexibility. This is shown by the fact that several algorithmic concepts have been used in the example models.

In the future, additional code generators could be developed that produce more optimal code or produce code that is closer to the algorithm model of HeuristicLab. Also additional code generators could be developed that produce code for other frameworks such as ParadisEO or HotFrame. This would be especially beneficial for the comparison of different frameworks.

In terms of validation, control flow validation could be implemented in addition to the existing data flow validation.

Concluding, apart from being beneficial as a case-study, the work described in this paper could also have impact on the further development of HeuristicLab. Especially aspects concerning abstraction, generation and model validation could be transfered to the HeuristicLab algorithm model.

ACKNOWLEDGMENTS

The work described in this paper was done within the Josef Ressel Centre for Heuristic Optimization *Heureka!* (http://heureka.heuristiclab.com) sponsored by the Austrian Research Promotion Agency (FFG).

REFERENCES

Blum, C.; Roli, A., 2003. Metaheuristics in combinatorial optimization: Overview and conceptual comparison. In: *ACM Computing Surveys 35(3)*, 268-308.

Collete, P., Luttion, E., Schoenauer, M. And Louchet, J., 2000. Take It EASEA. *PPSN VI: Proceedings of the 6th International Conference on Parallel Problem Solving from Nature*, pp. 891-901. London (UK).

Da Costa, L.; Schoenauer, M., 2009. Bringing Evolutionary Computation to Industrial Applications with GUIDE. *GECCO 2009*. Montreal, Quebec (Canada).

Fink, A; Voss, S.; 2001. *Reusable metaheuristic software componentsand their application via software generators.* In: Proceedings of the 4th Metaheuristics International Conference, Porto,pages 637–642.

Johnson, R.E.; Foote, B., 1988. Designing reusable classes. In: *Journal of object-oriented programming 1(2)*, 22-35.

Jones, M.S., 2000. *An Object-Oriented Framework for the Implementation of Search Techniques*. Thesis (PhD). University of East Anglia.

Talbi, E.-G.., 2009. *Metaheuristics: from design to implementation*. John Wiley & Sons.

Voss, S. And Woodruff, D., 2002. *Optimization Software Class Libraries*. Kluwer Academic Publishers.

Wagner, S.; Winkler, S.; Braune, R.; Kronberger, G.; Beham, A. 2007. Benefits of plugin-bases heuristic optimization software systems. *Computer Aided Systems Theory - EUROCAST Conference*, pp. 747-754.

Wagner, S. 2009. *Heuristic optimization software systems – Modeling of heuristic optimization algorithms in the HeuristicLab software environment*. Thesis (PhD). Johannes Kepler Univiersity, Linz, Austria.

Wolpert, D.H.; Macready, W.G., 1995. *No Free Lunch Theorems for Search*. Santa Fe Institute.

AUTHORS BIOGRAPHY

The web-pages of the authors as well as further information about HeuristicLab and related scientific work can be found at http://heal.heuristiclab.com.

ENHANCED PRIORITY RULE SYNTHESIS WITH WAITING CONDITIONS

Andreas Beham[(a)], Monika Kofler[(b)], Stefan Wagner[(c)] , Michael Affenzeller[(d)], Helga Heiss[(e)] , Markus Vorderwinkler[(f)]

[(a – d)] Upper Austria University of Applied Sciences
School for Informatics, Communications, and Media
Heuristic and Evolutionary Algorithms Laboratory
Softwarepark 11, 4232 Hagenberg, Austria

[(e-f)] PROFACTOR GmbH
Im Stadtgut A2
4407 Steyr-Gleink, Austria

[(a)]andreas.beham@fh-hagenberg.at, [(b)]monika.kofler@fh-hagenberg.at, [(c)]stefan.wagner@fh-hagenberg.at, [(d)]michael.affenzeller@fh-hagenberg.at, [(e)]helga.heiss@profactor.at, [(f)]markus.vorderwinkler@profactor.at

ABSTRACT
This work concerns the automated synthesis of priority rules for schedule optimization. Metaheuristic optimizers, in particular genetic programming (GP), are applied to develop the rule system for several scheduling situations in manufacturing scenarios. In this work, the rules are enhanced with a "no work" decision that leaves the deciding entity in a waiting state. Through simulation experiments it is shown how this enables the rule system to achieve a wider range of solutions.

Keywords: priority-rule, dispatching, scheduling, genetic programming

1. INTRODUCTION

Scheduling is one of the key problems in the manufacturing industry. A bad schedule can result in problems such as low throughput, long lead times, large amounts of work in process (WIP) and failure to meet the shipping deadlines. Given an increasing number of product variety and customizations, naturally, it is difficult not to struggle with any of these. Usually however, companies focus on the last problem of matching the due dates only as they try to create and maintain a positive image in the eyes of their business partners. If there are signs that a deadline cannot be met, extra human effort is added to hold the deadline, sometimes "at all costs". Still, the other problems remain and contribute to the overall situation. For workers this means that they have to work in a more stressful environment with deteriorating motivation.

For a large production site with many jobs, solving a scheduling problem is an arduous task, even for a computer. A scheduling problem such as the job shop scheduling problem (JSSP) is NP-hard which means that there does not exist a polynomial time algorithm that calculates the optimal solution (Pinedo 2001; Garey, Johnson, and Sethi 1976). The complexity of these problems grows exponentially with the problem size, making it especially difficult to provide good solutions for larger and larger problems.

Algorithms that solve such problems can be classified as being either *online* or *offline*, depending on what kind of information is available to them (Albers 1997). Online algorithms schedule immediately while offline algorithms know all jobs to be scheduled in advance.

In this work a priority rule-based scheduler is introduced that is able to delay a certain decision and consider it at a later time. It is not a pure online algorithm as it does not schedule jobs immediately, but is also not offline in that it does not know about all jobs in advance. Rather it aims to bridge the gap between online and offline algorithms. It is trained with several possible scenarios through simulation and thus has some expectations of how the near future may look like. It does not know about all the jobs that are to be scheduled in advance, but it has learned about a possible set of these jobs in the training phase. Thus the rule encodes an expectation of the set of jobs, but does not know the actual set of jobs. Based on this learned knowledge, the algorithm can delay a decision when it looks more promising to make the decision at a later stage.

1.1. Literature Review

Synthesizing priority rules is still a rather young field of research. Existing publications describe the use of machine learning methods such as classifiers to derive new dispatching rules. The training and analysis of such rules is still performed on simple models. In the following a brief overview is given.

(Olafsson and Li 2010) describe a method to learn new scheduling rules from generated schedules by simple rules using data mining techniques. They

combine a decision tree learner and an instance selector to derive high quality decision trees and thus priority rules that describe simple precedence conditions. For any two jobs the decision tree decides which of them should come before the other. A similar approach is described in (Aufenanger, Varnholt, and Dangelmaier 2009), but they learn from the best of a large set of randomly generated schedules with different parameters. Their classifier detects similar situations and applies the same parameters that have led to promising results in the learning phase.

(Mouelhi-Chibani and Pierreval 2010) describe an artificial neural network (ANN) that receives system parameters and states dispatching rules that should be applied as inputs and outputs. They use a simplified flow-shop model on which they run their learning method and compare it with dispatching rules selected by experts. Their approach is able to achieve a similar quality, but without requiring domain expert knowledge.

Another different priority rule base approach is described in (Vázquez-Rodríguez and Petrovic 2009). Similar to (Mouelhi-Chibani and Pierreval 2010) they do not synthesize new rules, but optimize a batch of dispatching rules that are applied in cycles to rank the jobs in the queue. Their dispatching rule based genetic algorithm showed good performance on a number of test problems. However they do not take system or state information into account. This approach is more an example of an offline algorithm. The derived batches are likely not reusable and specific to a certain instance.

The remainder of the paper is organized as follows: We will describe the method in section 2 and describe some of the scenarios that it is applied on in section 3. We will show and analyze the results in section 4 and finally draw conclusions.

2. PRIORITY RULE SYNTHESIS

(Olafsson and Li 2010) mention the interpretability of the learned model that is used as dispatching rule: “The interpretability of the results is also important and this can be directly related to the complexity of the resulting classification algorithm.” The model of a decision tree can be well interpreted, but the question remains how powerful it is to include the necessary information for more complex scenarios. The neural network of (Mouelhi-Chibani and Pierreval 2010) cannot be interpreted as easily and can be seen more as an automated black box method, however, ANN might scale to more complex situations more easily.

It is a challenge to have a model class that is expressive enough to describe complex scenarios, but still remain interpretable. From the point of view of the authors genetic programming might be a good solution to this problem as has been shown in (Beham, Winkler, Wagner, and Affenzeller 2008).

2.1. From Simple to Complex Priority Rules

In the case of online algorithms, such as priority-rule based scheduling, with non-preemptive tasks the question on what to do next needs to be determined at fixed points in time, e.g. when a job is introduced into the system, a machine becomes idle, or another kind of event changes the system state. Priority rules generally determine the next action by ranking each possible action according to predefined criteria and choosing the best ranked action. The rule itself is usually not very complex and can be evaluated in very short time on even a large set of possible actions. When an offline algorithm would probably run from several minutes to hours to react to a change in the system, the online algorithm takes just a few seconds.

Several simple priority rules have already been identified in the literature, among them for example earliest due date first, shortest processing time first, least number of steps to complete first, and many others (Panwalkar and Iskander 1977). These rules usually take just a very small number of attributes into account.

In previous publications it was described how these simple priority rules can be combined to complex priority rules using techniques such as genetic algorithms (GA) or genetic programming (Beham, Winkler, Wagner, and Affenzeller 2008; Kofler, Beham, Wagner, and Affenzeller 2009). By combining simple rules with mathematical functions and constants one can include a multitude of different attributes into the rule, see for example Figure 1.

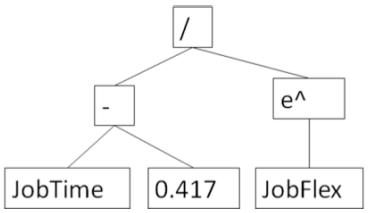

Figure 1 Example of a formula found by GP that combines the simple priority rules JobTime, which is the amount of time spent in the current queue, and JobFlex, the number of alternate machines a job can be processed on.

These complex priority rules are synthesized by combining members of the terminal set and members of the non-terminal set to create a mathematical formula. The terminal set consists of attributes of all entities (jobs, machines, workers, buffers, resources,…) that could possibly be taken into account as well as numerical constants. The non-terminal set consists of mathematical functions and relations.

2.2. Benefit of Waiting Conditions

Even though this optimization procedure can result in quite complex rules that are fit to a certain situation, there is a disadvantage in how these rules are applied. Currently a priority-rule would always rank available actions by the calculated priority and thus take an action at the first possible time. If there is only one job in the queue and the machine becomes idle, an online algorithm generally would schedule that job immediately. This leads to situations where e.g. a job

could be scheduled even though its due date is still far away. Under the presence of sequence dependent setup times this could for example mean that a setup step is introduced.

We thus propose to enhance priority rules by introducing a "wait" decision with the ability to delay a certain decision and reevaluate it at a later time. With this in mind a priority rule will not attempt to take an action at the first possible time, but rather aims to take it at the best possible time given some expectations of the future state.

Naturally, predicting the future is a difficult and error prone task and requires that the priority rule has in some ways learned about it. In the case of genetic programming this ability can be implicitly learned and trained. If the rule is evaluated by simulation in a virtual plant, then those rules that make the best estimation on the future state are able to perform the best decisions at the best time. They will dominate the others during the optimization run. As a result we will obtain an online algorithm in the form of a complex priority rule which has been trained offline. This algorithm is better informed than a pure online algorithm and can thus make better decisions, but of course it is also specific to the scenario or scenarios that it has been trained with. The rule implicitly decides whether the expected future is a more promising time to take a decision than the current time.

To achieve this behavior, we use a threshold level, that is, a certain priority that needs to be surpassed for an action to be considered. Because GP is able to produce any complex priority-rule within any range we can arbitrarily decide on such a threshold, e.g. zero. The action that will finally be selected by the complex priority rule is the one with the highest priority greater than the threshold level. If no action has a priority greater than the threshold, the decision will be delayed until another event occurs that possibly results in a different ranking.

2.3. Genetic Programming

Genetic programming (GP) is a metaheuristic with a formula tree as its solution representation. Unlike the canonical genetic algorithm that uses a binary string to represent a solution of the problem domain, GP uses a mathematical formula which consists of functions (nodes) and terminals (leafs). The set of functions ranges from mathematical operations such as addition, subtraction, multiplication, and division to more complex ones such as cosine or the exponential function. In addition GP is able to make use of logical functions such as IF-THEN-ELSE or the logical connectors AND, OR, and NOT. The terminals in such a function tree are either constant values or variables. In the case of rule synthesis the variables represent the current state of the production system, job characteristics, or the rank that would be obtained with a simple priority rule.

Out of the possible space of function trees genetic programming then creates a random initial population and uses selection, crossover, and mutation to enhance and optimize them over the course of the simulated evolution.

The power to combine these simple priority rules into complex rules and enrich them with even more information on the current state is one of the major advantages of this approach. If GP is given a good set of information on the state of the system and a good set of simple priority rules it is able to combine this information in complex and presumably higher quality rules.

3. MANUFACTURING SCENARIOS

Systems such as the Game of Life show that even simple rules can lead to very complex results in the end. So, to evaluate the behavior of a priority rule it is required to test them in various scenarios. Computer simulation is one technique of evaluating these rules given a model of the production system that it will be applied to.

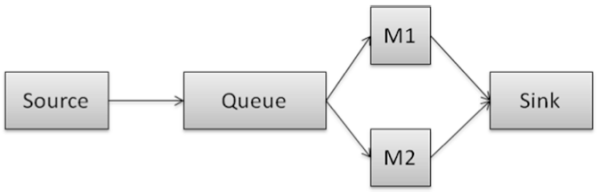

Figure 2 Simplified manufacturing scenario involving two machines, and a shared queue. Products flow along the arrows from source to sink and through either one of the two machines.

To evaluate the enhanced rules we have defined a basic manufacturing scenario which is shown in Figure 2. There is a set of products **P** with two kinds of products p_1 and p_2 and a set of machines **M** with two machines m_1 and m_2. Each product should be painted in shades of gray out of the set **G** at either machine. There are three different shades g_1, g_2, and g_3. There is a processing time matrix **T** with elements t_{ij} that defines the processing times for each p_i **P** on machine m_j **M**, a cost matrix **C** with elements c_{ij} that defines the costs for producing product p_i **P** on machine m_j **M**, and a setup matrix **S** with elements s_{kl} that defines the time required to change from shade k **G** to shade l **G**.

We consider several scenarios where one time the costs should be optimized such that a priority rule is found that assigns each product to the machine with the lowest cost, and another scenario where setup times are taken into account.

3.1. Scenario A

The first scenario is a very simple scenario that primarily exists as a proof of concept. It does not consider setup times, and the only thing that a certain path through the shop has an effect on is costs. Certain products are cheaper to manufacture on certain machines. The optimal rule in this case is known beforehand and selects the appropriate products to be

processed on their cheapest machine. Since no other factors such as due dates are considered in the objective functions the rule is rather simple.

Table 1 Cost matrix of Scenario A

C [€]	p_1	p_2
m_1	1	2
m_2	2	1

The processing time matrix **T** is defined such that $\forall_{i,j} t_{ij} = 5$, the setup time matrix **S** is the zero matrix. The products are generated with equal probability at a rate that is equal to the mean of the processing times of the machines.

There is a difference though in the optimal rule, with regard to total costs, in the case without waiting conditions compared to the case with waiting conditions. Allowing a wait enables the machine to not act on a queue with products that would cost too much to be processed. This rule can achieve a better quality, because it can achieve a perfect split.

However, naturally there are disadvantages. The downside of the rule goes hand in hand with the implication of introducing a decision to not work: Not producing anything would lead to zero costs. This is of course a problem that has to be dealt with and will be discussed in the results section.

3.2. Scenario B

This scenario is slightly more advanced than the previous and also more complex so that an a priori optimal solution is not known. The processing time matrix is given in Table 2 and the setup time matrix is given in Table 3. The cost matrix is the same as in Scenario A and given in Table 1. Note that minimizing the costs as well as the total processing time are in this case conflicting goals. The more expensive process is quicker to complete. As in Scenario A each product has equal probability to enter the queue, and the shade that it should be painted with is also chosen with equal probability among all three choices.

The fitness function has also changed due to the multi-objective nature of the problem. It is a combination of average costs per product and average processing time per product such that both have about equal weight.

Table 2 Matrix of processing times of products on the available machines of Scenario B.

T [min]	p_1	p_2
m_1	6	4
m_2	4	6

Table 3 Matrix of setup times for Scenario B. The value represents the time in minutes to change from the shade in the row header to that in the column header.

S [min]	g_1	g_2	g_3
g_1	0	1	1
g_2	2	0	1
g_3	4	2	0

4. RESULTS

4.1. Software Environment

To test the hypothesis that a waiting condition is beneficial to the synthesis of advanced priority rules a simulation model that describes the simplified manufacturing scenario is created using the simulation framework SiRO (http://www.profactor.at/en/production/produkte/siro.html). It models the flow of products as shown in Figure 2. Products arriving at the *Sink* are evaluated according to the selected performance criteria and after a predefined number of products have been passed through the system the aggregated performance over all finished products is calculated and presented to the GP metaheuristic as fitness value for the priority rule that was used in the simulation.

The GP algorithm was configured and tested in the HeuristicLab open source optimization environment (http://dev.heuristiclab.com). HeuristicLab was first released to the public in 2004. The latest version 3.3 was released in 2010 and aims at providing a unified environment for metaheuristic optimization intended to cover algorithm design, configuration, experimenting, and analysis.

The results were computed using HeuristicLab's genetic programming in version 3.2.0.2683. The full configuration is given in Table 4.

Table 4 Configuration of the genetic programming optimizer

Parameter	**Value**
PopulationSize	100
Selector	TournamentSelector
Tournament Group Size	2
Crossover	Exchange sub trees
Mutators (one of them will be chosen each time it is applied)	OnePointShaker, FullTreeShaker, ChangeNodeTypeManipulation, CutOutNodeManipulation, DeleteSubTreeManipulation, SubstituteSubTreeManipulation
MutationRate	15%
Elites	1
Maximum Generations	1000

4.2. Scenario A

The problem of the "no work" decision appearing very often in certain rules posed a difficulty when evaluating their performance. Some rules exist that did not dispatch any jobs and the machines remained empty during the whole run, meanwhile the queue grew large and the evaluation of several thousand jobs in the queue slowed the simulation down considerably. Also there have been rules that managed to assign only half of the jobs correctly and the other half remained in the queue. These problems required to redesign the fitness function such that it combined two objectives: That of producing at the least cost possible and that of finishing as much jobs as possible. So the fitness function, at the end of a simulation run, assigned each job still in the queue the highest possible production cost. Finally the total costs were divided by the amount of jobs injected into the system. Additionally an early abort criterion was added to the model that detected when a rule would not dispatch any jobs at all. If such an abort occurred, the fitness value was multiplied with the ratio of injected to finished jobs as additional penalty.

For the simple scenario the best result is easy to obtain when **C** is known to the priority rule. The best rule was found quickly and says

$$1.2 * c \leq \frac{2.44}{1.1 * c}$$

where c is substituted by the cost of the currently evaluated product on the currently evaluated machine. This formula can be simplified and interpreted easily: Any product is chosen where the costs are below a certain threshold. In our a priori optimal solution this would be an arbitrary number in the half-open interval]1, 2]. In the concrete rule this is the value 1.36.

4.3. Scenario B

In the more advanced second scenario sequence dependent setup times play an important role as they delay the production process. As has been stated the goal is to find a rule where the machine's utilization can be lowered while maintaining the costs. After several generations, following rule was found to solve this problem best

$$-0.6 * s + 0.8 * e^{1.2*c} * i$$

where again c is the cost, s is the appropriate setup time given the product shade and the current shade of the machine; *i* is the length of the period a machine has remained idle which was an additional system state available to the optimizer. Again with a little work the formula can be easily interpreted: The first job which doesn't require setup should be taken, but if there is setup necessary, wait for a portion of the setup period and then take the job. The term -0.6*s is actually pulling the decision below the threshold line until the factor *i* increases the costs to a level that surpass the setup effort. The synthesized rules are quite elegant to analyze and reveal several things about the underlying system. A rule that has been found to optimize a certain situation can say a lot about that situation also providing important feedback to the human operator. Note that these cases are not free of starvation, because a starving job does not affect the fitness in this case.

A comparison of the actual results reveals that the found rule has slightly higher costs per unit, but a much lower utilization and processing times while having about an equal number of finished units. Table 5 lists the difference between a FIFO rule and the optimized rule broken down to several output values. As can be seen the optimized rule has finished about the same number of units, albeit at a slightly higher cost, but at a much lower utilization that helps to reduce stress in the plant. Certainly the rule could be optimized to favor costs more than processing time by changing the weights in the fitness function since costs and processing time are conflicting goals.

Table 5 Comparison of the FIFO rule with that found by GP

	FIFO	GP
Utilization AP_1/AP_2	96.7%/96.7%	74%/80%
Avg. cost per product	1.51€	1.55€
Processing time	372.75s	297.55s
Produced Units	3135	3129

5. CONCLUSIONS

This work described the synthesis of priority rules using genetic programming and showed the benefit of including a no work decision. When a simulation model of the underlying process is available the rules can be optimized with an expectation of the future implicitly present in the rules themselves. The rules may choose to not perform decisions at the current time, but to delay them if it seems likely that a better choice is soon to arrive.

Naturally a problem with all learning approaches and also with the one described is the characteristics of training data set in comparison to the real situation. If they are very similar the rule has a good chance to make near optimal decisions, however if the real situation differs greatly the decisions will be made under false assumptions. One way to overcome this problem is to continually monitor the process and optimize rules in parallel to the real situation.

ACKNOWLEDGMENTS

The work described in this paper was funded by the Austrian Research Agency (FFG) under grant FdZ-Projekt PROCOMPOSITE: FFG-ProjNr.: 813760 F-WGF.

REFERENCES

Albers, S., 1997. Better bounds for online scheduling. STOC '97: *Proceedings of the 29th annual ACM symposium on Theory of computing*, pp. 130-139.

Aufenanger, M., Varnholt, H., and Dangelmaier, W., 2009. Adaptive Flow Control in Flexible Flow Shop Production Systems - A Knowledge-Based Approach. *Proceedings of the 2009 Winter Simulation Conference*, pp. 2164-2175, Austin, TX, USA.

Beham, A., Winkler, S., Wagner, S., and Affenzeller, M., 2008. A Genetic Programming Approach to Solve Scheduling Problems with Parallel Simulation. *Proceedings of the 22nd IEEE International Parallel & Distributed Processing Symposium (IPDPS08)*, IEEE.

Garey, M.R., Johnson, D.S., and Sethi, R., 1976. The complexity of flowshop and jobshop scheduling. *Mathematics of Operations Research*, 1 (2), pp. 117-129.

Kofler, M., Beham, A., Wagner, S., and Affenzeller, M., 2009. Evaluation of Various Dispatching Strategies for the Optimization of a Real Production Plant. *Proceedings of the 2nd International Symposium on Logistics and Industrial Informatics* (LINDI 2009), pp. 25-30. IEEE Publications.

Mouelhi-Chibani, W., and Pierreval, H., 2010. Training a neural network to select dispatching rules in real time. *Computers & Industrial Engineering*, 58, pp. 249-256.

Olafsson, S., and Li, X., 2010. Learning effective new single machine dispatching rules from optimal scheduling data. *International Journal of Production Economics*, doi:10.1016/j.ijpe.2010.06.004.

Panwalkar, S.S., and Iskander, W., 1977. A Survey of Scheduling Rules. *Operations Research*, 25, pp. 45-61.

Pinedo, M., 2001. Scheduling: Theory, Algorithms and Systems, 2nd edition. Prentice Hall.

Vazquéz-Rodríguez, J.A., and Petrovic, S., 2009. A new dispatching rule based genetic algorithm for the multi-objective job shop problem. *Journal of Heuristics*, doi: 10.1007/s10732-009-9120-8.

AUTHORS BIOGRAPHY

ANDREAS BEHAM received his MSc in computer science in 2007 from Johannes Kepler University (JKU) Linz, Austria. His research interests include heuristic optimization methods in production environments. Currently he is a research associate at the Research Center Hagenberg of the Upper Austria University of Applied Sciences (Campus Hagenberg).

MONIKA KOFLER studied Medical Software Engineering at the Upper Austrian University of Applied Sciences, Campus Hagenberg, Austria, from which she received her diploma's degree in 2006. She is currently employed as a research associate at the Research Center Hagenberg and pursues her PhD in engineering sciences at the Johannes Kepler University Linz, Austria.

STEFAN WAGNER received his MSc in computer science in 2004 and his PhD in engineering sciences in 2009, both from Johannes Kepler University (JKU) Linz, Austria; he is professor at the Upper Austrian University of Applied Sciences (Campus Hagenberg). Dr. Wagner's research interests include evolutionary computation and heuristic optimization, theory and application of genetic algorithms, machine learning and software development.

MICHAEL AFFENZELLER has published several papers, journal articles and books dealing with theoretical and practical aspects of evolutionary computation, genetic algorithms, and meta-heuristics in general. In 2001 he received his PhD in engineering sciences and in 2004 he received his habilitation in applied systems engineering, both from the Johannes Kepler University of Linz, Austria. Michael Affenzeller is professor at the Upper Austria University of Applied Sciences, Campus Hagenberg, and head of the Josef Ressel Center *Heureka!* at Hagenberg.

HELGA HEISS works for PROFACTOR GmbH and received her bachelor degree in hardware software systems engineering in 2008 and currently pursues her master degree in software engineering at the Upper Austria University of Applied Sciences in Hagenberg. Her research interests include computer simulation and software development.

MARKUS VORDERWINKLER received his diploma and doctoral degrees both in electrical engineering from Vienna University of Technology. Dr. Vorderwinkler works for PROFACTOR GmbH where he is head of consulting & solutions for simulation based design & optimisation of logistics systems. He managed more than 50 industrial and international research projects. Mr. Vorderwinkler is lector at the Upper Austrian University of Applied Sciences. His research interests include manufacturing, digital factory and computer simulation.

The Web-pages of the authors as well as further information about HeuristicLab and related scientific work can be found at http://heal.heuristiclab.com/. The Web-page of PROFACTOR GmbH can be found at http://www.profactor.at.

USING ERP-DRIVEN FLOW ANALYSIS TO OPTIMIZE A CONSTRAINED FACILITY LAYOUT PROBLEM

Andreas Beham[(a)], Monika Kofler[(b)], Stefan Wagner[(c)] , Michael Affenzeller[(d)], Walter Puchner[(e)]

[(a – d)] Upper Austria University of Applied Sciences
School for Informatics, Communications, and Media
Heuristic and Evolutionary Algorithms Laboratory
Softwarepark 11, 4232 Hagenberg, Austria

[(e)] ROSENBAUER INTERNATIONAL AG
Paschinger Strasse 90
4060 Leonding, Austria

[(a)]andreas.beham@fh-hagenberg.at, [(b)]monika.kofler@fh-hagenberg.at, [(c)]stefan.wagner@fh-hagenberg.at,
[(d)]michael.affenzeller@fh-hagenberg.at, [(e)]walter.puchner@rosenbauer.com

ABSTRACT
Enterprise Resource Planning (ERP) systems are nowadays widely used in large companies and even starting to appear in small and medium sized businesses. These systems hold many enterprise specific aspects and store them in a machine readable format. In this paper we will show how to use job dependency and demand information extracted from the data of a certain ERP system to simulate the process and material flows in a given production scenario. Material flows are among the most expensive processes in manufacturing businesses since they do not increase the value of the manufactured goods. We will show how to use the simulated flow information to optimize the arrangement of work centers. This problem is defined as a constrained facility layout problem using several real-world constraints in order to find realistic solutions that are close to implementation. The goal is to reduce traffic and increase efficiency on the shop floor.

Keywords: material flow simulation, facility layout problem, constrained optimization

1. INTRODUCTION

The wide availability of ERP systems in manufacturing companies has made it considerably easier to obtain data about manufacturing processes. Data can be easily exported or accessed directly through the database and a number of possibilities have opened regarding the automated analysis and, more importantly, steering of the enterprise. Several ERP systems already come with planning modules and demand for customer specific automated production steering has risen over the years.

Material-handling costs are among the highest cost factors in many manufacturing businesses these days. Their expensiveness simply stems from the fact that material handling increases the cost of the product without increasing the value of the product. Material handling however is a necessity for manufacturing and thus increasing the efficiency of the process is one of the goals successful companies strive for.

There exist a multitude of different material-handling systems from simple conveyors to complex automated guided vehicles with readily available commercial solutions. These systems have their advantages and disadvantages and carefully choosing the right type is certainly advised. But, regardless of the underlying system the simple fact that one unit of material is transported from A to B means that there is cost involved and usually an increasing distance also means increasing costs.

One way to consider this general problem of transportation within an enterprise is to first identify an optimal arrangement of the underlying machines, and then decide on the material handling system. This becomes more and more important the more time has passed after a layout has been implemented, for example when the company has grown over the years, new machines and technologies have replaced older ones and the original assumptions regarding the flow of materials are not up to date with the actual layout. On the other hand if the arrangement cannot be altered easily the problem becomes highly constrained, several facilities need to remain in place, some need to maintain a certain distance between each other or to infrastructure end points and others need to remain separated from each other by a certain distance. The costs of moving the work centers on the shop floor may have to be taken into account when they can be estimated accurately enough.

Because of the dynamic nature and change in production processes as well as in the product portfolio it is important to continuously monitor the layout and plan ahead to be able to make the decisions on time. Ideally, the processes and flows thus should be generated automatically from the company data and

presented to the layout planner to make effective decisions quickly, based on past and present data.

1.1. Literature Review

Existing work on facility layout optimization seems to concentrate more on the problem of solving the layouting scenario with fully parameterized models than treating the question about getting the parameters. In the view of the authors, to gather the right data and configure the models requires a deep understanding of the processes under consideration. The task of obtaining the flow values is not always a trivial one and there are several obstacles present that one has to overcome. The following brief review lists some recent publications on the topic of facility layout optimization.

(Benjafaar 2002) shows the difficulty still present with the "simplified" view on layout optimization as a quadratic assignment problem (QAP). The assumption that shorter connecting paths are beneficial to the underlying plant does not hold in all cases. Several situations are shown in which the work in process (WIP) increases while the formulation of the QAP attributes the layout a better fitness. The paper concludes that even departments without material flows can have a strong relationship e.g. when they share the same material handling resource.

(McKendall, Shang and Kuppusamy 2006) as well as (McKendall and Hakobyan 2009) investigate the case of dynamic facility layouting problems, that is they consider rearrangement costs as well as material handling costs when optimizing over several periods with different flow characteristics. In the 2006 article they describe two simulated annealing metaheuristics with look-ahead/look-back strategies adapted to the dynamic facility layout problem that they test on a problem instance taken from the literature. The problem formulation is still very close to the quadratic assignment problem (QAP). In the 2009 article they use a tabu search heuristic to optimize the layout of rectangles on a continuous floor. Their results are interesting for future work when trying to find those points in time that benefit from a reorganization automatically.

(Scholz, Petrick and Domschke 2009) describe a different approach to optimizing facility layout in that they use a slicing tree representation and a tabu search heuristic for optimization. The slicing tree is a binary tree with the departments as leafs and the nodes specify whether its sub-nodes are vertically aligned or horizontally aligned. While this representation is quite interesting, the problem is that the departments are always packed tightly and that it is difficult to extend the problem into situations with e.g. distinguished locations for placing the departments. The authors have addressed some of these concerns, for example including aisles in a very recent publication (Scholz, Jaehn and Junker 2010). It is however a very interesting approach as the representation automatically locates departments close together. In a coordinate based representation the algorithm needs to find the right layout by manipulating the coordinates, which is a more general abstraction of the problem.

In this paper we will focus a little more on the parameterization of the models and show how to use data from the ERP system to perform a flow simulation and calculate the process and material flows between the work centers of a given shop floor. With these results we will look at how to model the problem of arranging these work centers and show some of the constraints that are considered important. Finally we will apply an optimization method to obtain high quality solutions and show the results given a close to real-world instance of the problem.

2. FLOW SIMULATION

ERP systems hold the relevant data for the operation of manufacturing companies. Common to most implementations is the notion of a *job* that is split into several *operations* which are performed using several *resources*. A job results in a product or material which can be added to the company warehouse or which is finished and shipped to the customer. The operations describe basic tasks that need to be completed to finish such a job and are executed in a given order. Operations are not limited to production tasks; they may also include management tasks such as monitoring or coaching. Operations can be visualized via a connected graph that provides information on the predecessor-successor relationship between them. Any given operation may have multiple successor and multiple predecessor operations.

The resources that are used to perform the operations range from manpower to machines, raw materials and tools. While job and operations are abstract concepts resources are real. For the purpose of layout optimization some of these resources are considered part of the optimization such as manpower, machines. These are assumed to be grouped and available at fixed locations, but there is a *demand* of raw materials and tools that flows between the locations or warehouses. This demand holds information about which materials flow in the production facility.

Given this representation of a manufacturing process consisting of jobs, operations, resources, and demands we simulate the execution of these jobs and obtain the flows in the form of a matrix specifying the strength of the source-destination relationship for the resources that are to be located. To calculate the actual strength value several different ways are identified.

The strengths can be accumulated by the weighted number of transitions between any two operations. If the weights are equal to 1 each transition is considered to be an atomic event, if the weights are set to a different value for each such event different situations emerge. For example if the actual number of resources being transported is used as weight the flow strength denotes the total amount of materials being passed. It depends on the actual shop floor however if such a number is realistic or rather misleading. If the material diversity is high the transportation of a hundred small

screws does not likely represent an effort similar to the transportation of a single big item. Choosing the right weighting factor is an important step in the preparation of the problem data.

Other impacts on the outcome of the flow simulation emerge in 1:N, and N:1 transitions. When a single operation has several possible successors or predecessors, the question arises to which successor the actual flow is moving. Two possible ways that this can be dealt with, without specifying additional data such as process flow charts, are to either split and combine or duplicate the handling events. This does not seem to be an unrealistic assumption per se, given that the successor relationship implicitly encodes dependency information and waiting conditions for those items that leave the machine on which the operation is executed.

Which one of these possibilities to interpret the given data is more appropriate depends largely on the problem situation and can even depend on certain parts of the problem situation. It is necessary to discuss and decide on these possibilities in the preparation stage. Otherwise the strength of the flow is not a valid approximation of the necessity of the two involved departments to be located closer to each other.

Regardless of the actual weighting factor and the ways a flow's trajectory is computed, three different kinds of flows are identified to occur in a manufacturing environment. The importance of these flows to a certain production facility may be different and it is necessary to look at each of them, as well as decide on a proper weighting when combining them into the final flow matrix which can be used to parameterize the problem model. These different kinds are:

- Sequential process flows
- Parallel process flows
- Material flows

2.1. Sequential Process Flows

These flows occur whenever there is a transition from one operation to the next. The dependency in the operations is interpreted as a flow from the current operation to its successor. In the case of multiple successors, there are several possibilities: The flows could be duplicated and thus passed to each of the successor, or split according to some distribution. If the assumption is true that there are indeed materials flowing between the different resources that execute these operations, then this kind of matrix may be very relevant for the problem model.

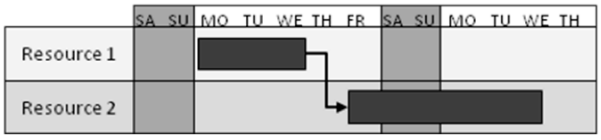

Figure 1 Example of a sequential process flow from Resource 1 to Resource 2

2.2. Parallel Process Flows

In manufacturing scenarios there is also a degree of parallelism in the operations. It happens that when a product is assembled two operations are applied to it in parallel and thus there is a need for coordination and frequently a benefit in efficiency if those resources are located physically closer to each other.

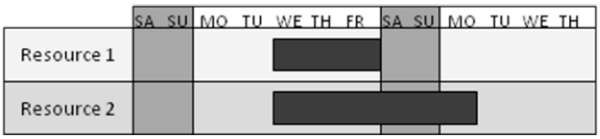

Figure 2 Example of a parallel process flow between Resource 1 and Resource 2

2.3. Material Flows

Material flows occur when an operation needs certain materials from the warehouse or a buffer location and also when the job has finished and produced a number of resources. These resources are then stored again in the warehouse or in the distribution center. In some cases the materials for a sequence of operation are requested together with the first operation and passed through to the others, in some cases these are requested within a sequence. For production environments that are served mostly by warehouses the material flow does not represent inter-facility flows to a very large degree.

Thus for realistic results a combination of these three different flow types has to be considered for optimizing an arrangement.

3. FACILITY LAYOUT PROBLEM

This problem was introduced as the Machine Placement Problem (MPP) in (Beham, Kofler, Wagner, and Affenzeller 2009) and has since changed slightly, as well as it has been extended with more real-world constraints. To describe the problem briefly: It consists of arranging a set of rectangular shapes **R** on a flat surface **G** such that they lie completely within a boundary polygon **P** with p_i being the points of the polygon. The polygon is constructed by connecting each point with the next in sequence and finally the last point with the first. The problem further contains the set **B** of fixed blocks, which are immobile locations in the layout. The set **L** then describes the layout such that **L**=**R**∪**B**. Each shape in **R** represents a machine or work center and is specified by the location of the center coordinates, the dimensions of the rectangle, and a number denoting the rotation in 90° intervals. Each shape in **B** is specified by the lower left and upper right points. Finally the matrix **F** that specifies the flow strength is given as a NxN matrix with N = |**R**|. Elements of this matrix are called f_{ij} and denote the strength of the flow from *i* to *j*.

There are several constraints regarding the distance between shapes: Some shapes must be within a specified distance to other shapes, some must maintain a minimum distance to other shapes, and some may have even both a minimum and a maximum distance. The shapes itself are also constrained with bounds on their aspect ratio, e.g. a shape may not be stretched to the very extreme, or not stretched at all.

A solution to this problem specifies the location as x and y position, dimension as width and area, and rotation of each shape. The solution thus can be encoded in the form of multiple vectors of integer values. Two vectors $\vec{x}, \vec{y}$ encode the location on the plane, one vector $\vec{w}$ denotes the width (the height is automatically calculated given that the area A_i of each rectangle remains constant) and the last vector denotes the rotation state $\vec{\omega}$.

The evaluation function computes the layout from this solution vector and first calculates the distance matrix **D** with elements d_{ij} between all shapes $i, j \in \mathbf{R}$. Each d_{ij} represents the shortest Manhattan-distance between the rectangles' edges. The main fitness characteristic, the flow-distance-fitness Q_{flow} can then be given as

$$Q_{flow} = \sum_{i=1}^{N} \sum_{j=1}^{N} d_{ij} * f_{ij}$$

The second fitness characteristic, the relayouting costs $Q_{relayout}$ represent the cost of transforming the initial layout that can be defined by the user into the optimized layout. For this purpose each shape $i \in \mathbf{R}$ can be attributed with a movement cost mm_i that depends on the distance that the shape is moved as well as a fixed cost ms_i, e.g. for packing and unpacking or calibration. For this purpose a vector of transition distances t_i is calculated that contains the Manhattan-distance between initial and optimized location.

$$Q_{relayout} = \sum_{i=1}^{N} x_i * (ms_i + mm_i * t_i)$$

Where x_i is a decision variable that is 1 if $t_i > 0$ and 0 otherwise. If the shape is in a different rotation state $Q_{relayout}$ is added half the area multiplied by the Manhattan-distance to the new location. To adhere to the constraints during the optimization a soft constrained approach was used and infeasible solutions were penalized, by adding a penalty value that depends on the strength of the constraint violation. This penalty guides the optimization strategy in creating feasible solutions.

The first penalty $C_{overlap}$ deals with the problem of creating layouts with overlapping elements. This can occur frequently as an element's location is modified in a manner that does not consider feasibility, by simply adding a value to the coordinates or swapping the location of two elements. The penalty is computed according to

$$C_{overlap} = \sum_{i \in L} \sum_{j \in L, j \neq i} \frac{A_{ij}}{2}$$

where A_{ij} is the intersecting area between shape $i, j \in \mathbf{L}$ or zero in case there is either no overlap or both $i, j \in \mathbf{B}$. The second penalty $C_{boundary}$ puts a penalty on shapes that lie at least partly outside **P** by summing all areas that fall beyond the boundary. In case the whole shape is outside the bounds, the penalty for that shape is further increased by adding its area times the closest distance to the boundary. Let $\mathbf{O_p} \subset \mathbf{R}$ be the set of all shapes that are partially outside, $\mathbf{O_f} \subset \mathbf{R}$ be the set of all shapes that are fully outside, $A_{outside}(i)$ with $i \in \mathbf{R}$ be the area of the shape minus the intersecting area with **P**, and $d(i,\mathbf{P})$ a distance function specifying the distance between the bounds of shape $i \in \mathbf{R}$ and **P**, the constraint can be formulated as

$$C_{partial} = \sum_{i \in O_p} A_{outside}(i)$$

$$C_{full} = \sum_{i \in O_f} A_i * d(i, P)$$

$$C_{boundary} = C_{partial} + C_{full}$$

There is also a constraint violation when the distance of two shapes is smaller or larger than the bounds specified on their distance. Let $dmax_{ij}$ be the maximum allowed distance and $dmin_{ij}$ be the minimum required distance between shape i and j, the constraint $C_{distance}$ can be formulated as

$$C_{distance} = \frac{1}{2} * \sum_{i \in L} \sum_{j \in L, j \neq i} \max(dmin_{ij} - d_{ij}, 0) + \max(d_{ij} - dmax_{ij}, 0)$$

Finally the last constraint adds a penalty to solutions in which the aspect ratio of the shape is outside the given bounds. Let $amin_i$ be the minimum allowed aspect ratio, $amax_i$ be the maximum allowed aspect ratio of shape i, and a_i be the aspect ratio (width / height) of shape i, the constraint C_{aspect} can be formulated as

$$C_{aspect} = \sum_{i=1}^{N} \max(amin_i - a_i, 0) + \max(a_i - amax_i, 0)$$

The fitness value is then computed as weighted sum of the qualities and constraints as formulated by

$$fitness = \alpha_1 * Q_{flow} + \alpha_2 * Q_{relayout} + \alpha_3 * C_{overlap} + \alpha_4 * C_{boundary} + \alpha_5 * C_{distance} + \alpha_6 * C_{aspect}$$

3.1. Optimization Scenario

In the optimization scenario that we are considering a small part of the facility is examined. Naturally, the data does not show the true situation of the real world scenario, but has been modified, such that the main characteristics are still present, but that the results cannot be traced back to the actual facility. The flows have been calculated through the simulation as described in Section 2.

The optimization scenario can be seen graphically in Figure 3.

4. SIMULATED ANNEALING

In (Beham, Kofler, Wagner, and Affenzeller 2009) it was reported that simulated annealing (SA) was able to perform best when compared with a genetic algorithm and an evolution strategy. In this work the previously described algorithm was applied again.

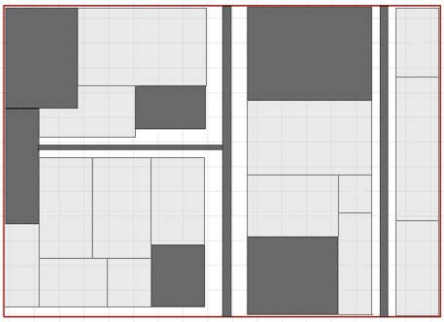

Figure 3 Image of the problem scenario with fixed blocks marked as dark gray and movable shapes in light gray.

Simulated annealing (SA) is among the oldest metaheuristics which offered an explicit strategy to escape from local optima. (Kirkpatrick 1983) was the first to term the algorithm simulated annealing in analogy to the annealing process in metallurgy, and successfully applied the algorithm to optimize computer chip design and the traveling salesman problem. SA employs the temperature as a simple control parameter that guides the search and balances phases of diversification and intensification. As the algorithm proceeds, a step-wise reduction of the temperature focuses the search on a promising region of the solution space, which eventually leads to convergence. The algorithm's performance depends largely on the initial temperature as well as on the cooling scheme. If the temperature drops too quickly the search might get stuck in a worse local optimum; on the other hand, if the cooling is too slow, the algorithm might not have converged when it reaches the stop criterion, which might be for example a maximum number of evaluated solutions. A typical annealing scheme is multiplicative annealing which decreases the temperature in an exponentially shaped curve.

4.1. Problem representation and operators

As has been mentioned in Section 3 the solution representation consists of several vectors. The x and y locations of each facility are given in an array of integer values each, the rotation state is given in another integer array, and finally the width is given in the fourth integer array. The solution thus consists of 4 integer arrays which are modified by several different operations.

- AdditiveNormalManipulation
- AdditiveNormalSingleManipulation
- SwapManipulation
- UniformManipulation

AdditiveNormalManipulation adds a normal distributed random variable with $\mu=0$ and $\sigma=2$ to each value in the vectors. AdditiveNormalSingle-Manipulation is a variant where only one shape is changed. The random value is rounded to the nearest integer before it is added. SwapManipulation swaps the indices of two randomly selected positions in the arrays. UniformManipulation sets the values to randomly selected values within the respective boundaries.

These manipulating operations allow the solution to be modified in small ways by moving the shapes a little bit on the plane, exchange two shapes in their locations, or randomly place the shapes in a given area.

The parameters of the simulated annealing heuristic were set as given in Table 1.

Table 1 Parameters for SA

Parameter	Value
Iterations	50000
Temperature	200000
Annealing Factor	0.9996
Inner Iterations	100
α	(1, 0, 10000000, 10000000, 0, 100000000)

5. RESULTS AND CONCLUSIONS

The optimization of the problem leads to interesting conclusions regarding the rearrangement of the layout as can be seen in Figure 4. The layouts solved by the current model do not lead to immediate practical layouts, there are still a number of factors to consider and extend in the current model so that the practical relevance of the solution becomes higher, nevertheless the relationship between the machines becomes obvious and the optimized placement is a good start for the human planner to begin redesigning the layout.

In this paper a method was introduced to simulate process and material flows between facilities directly from the ERP data which can be computed in automated fashion for any given situation. There is no need to specify flow strengths or calculate them by hand. The problem model was described in more detail with the quality and constraint criteria as well as an optimization procedure to derive improved layouts.

In future work we would further extend the problem model to include pathways as well as define infrastructure endpoints in more details. There is still some work necessary regarding the fitness function, the optimizer frequently violates the aspect ratio constraint as it can reach even better, but infeasible solutions. The penalty regarding the aspect ratio is likely too small in contrast to the others.

ACKNOWLEDGMENTS

The work described in this paper was done within the Josef Ressel Centre for Heuristic Optimization *Heureka!* sponsored by the Austrian Research Promotion Agency (FFG).

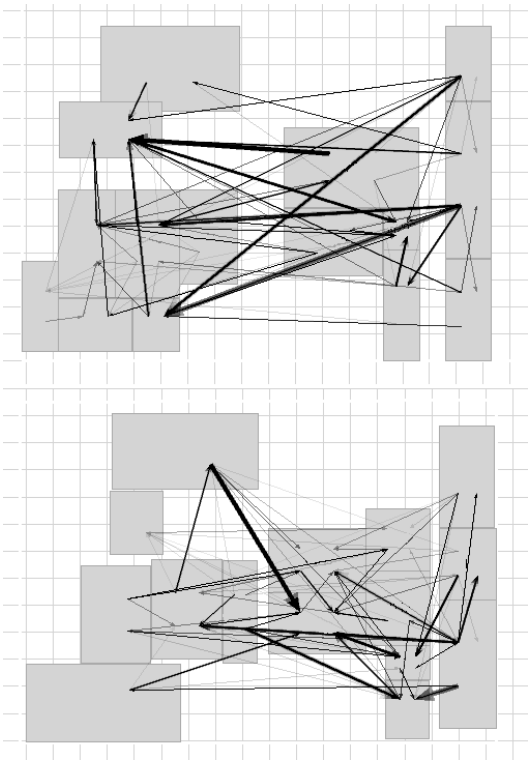

Figure 4 Original (top) and optimized (bottom) layout of the facilities under consideration with arrows marking the flow strength. The thicker and darker an arrow is the stronger the flow. The fixed blocks are not present in this figure.

REFERENCES

Beham A., Kofler M., Wagner S., and Affenzeller M., 2009. Coupling Simulation with HeuristicLab to Solve Facility Layout Problems. *Proceedings of the 2009 Winter Simulation Conference*, pp. 2205-2217. December 13-16, Austin (Texas, USA).

Benjafaar S., 2002. Modeling and Analysis of Congestion in the Design of Facility Layouts. *Management Science*, 48, pp. 679-704.

Kirkpatrick, S., Gelatt, C.D., and Vecchi, M.P., 1983. Optimization by simulated annealing. *Science*, 220, pp. 671–680.

McKendall, A.R., and Hakobyan, A., 2009. Heuristics for the dynamic facility layout problem with unequal-area departments. *European Journal of Operational Research*, 201, pp. 171-182.

McKendall, A.R., Shang, J., and Kuppusamy, S., 2006. Simulated annealing heuristics for the dynamic facility layout problem. *Computers & Operations Research*, 33, pp. 2431-2444.

Scholz, D., Jaehn, F., and Junker, A., 2010. Extensions to STaTS for practical applications of the facility layout problem. *European Journal of Operational Research*, 204 (3), pp. 463-472.

Scholz, D., Petrick, A., and Domschke, W., 2009. STaTS: A Slicing Tree and Tabu Search based heuristic for the unequal area facility layout problem. *European Journal of Operational Research*, 197, pp. 166-178.

AUTHORS BIOGRAPHY

ANDREAS BEHAM received his MSc in computer science in 2007 from Johannes Kepler University (JKU) Linz, Austria. His research interests include heuristic optimization methods and simulation-based as well as combinatorial optimization. Currently he is a research associate at the Research Center Hagenberg of the Upper Austria University of Applied Sciences (Campus Hagenberg).

MONIKA KOFLER studied Medical Software Engineering at the Upper Austrian University of Applied Sciences, Campus Hagenberg, Austria, from which she received her diploma's degree in 2006. She is currently employed as a research associate at the Research Center Hagenberg and pursues her PhD in engineering sciences at the Johannes Kepler University Linz, Austria.

STEFAN WAGNER received his MSc in computer science in 2004 and his PhD in engineering sciences in 2009, both from Johannes Kepler University (JKU) Linz, Austria; he is professor at the Upper Austrian University of Applied Sciences (Campus Hagenberg). Dr. Wagner's research interests include evolutionary computation and heuristic optimization, theory and application of genetic algorithms, machine learning and software development.

MICHAEL AFFENZELLER has published several papers, journal articles and books dealing with theoretical and practical aspects of evolutionary computation, genetic algorithms, and meta-heuristics in general. In 2001 he received his PhD in engineering sciences and in 2004 he received his habilitation in applied systems engineering, both from the Johannes Kepler University of Linz, Austria. Michael Affenzeller is professor at the Upper Austria University of Applied Sciences, Campus Hagenberg, and head of the Josef Ressel Center *Heureka!* at Hagenberg.

WALTER PUCHNER works for ROSENBAUER INTERNATIONAL AG since 1978. He started his career as machinist apprentice, after which he pursued a master and worked in toolmaking and assembly. Since 1989 he coordinates special projects, among them the extension and adaption of the company's infrastructure.

REASSIGNING STORAGE LOCATIONS IN A WAREHOUSE TO OPTIMIZE THE ORDER PICKING PROCESS

Monika Kofler[(a)], Andreas Beham[(b)], Stefan Wagner[(c)] , Michael Affenzeller[(d)], Clemens Reitinger[(e)]

[(a – d)] Upper Austria University of Applied Sciences
School for Informatics, Communications, and Media
Heuristic and Evolutionary Algorithms Laboratory
Softwarepark 11, 4232 Hagenberg, Austria

[(e)] ROSENBAUER INTERNATIONAL AG
Paschinger Strasse 90
4060 Leonding, Austria

[(a)]monika.kofler@fh-hagenberg.at, [(b)]andreas.beham@fh-hagenberg.at, [(c)]stefan.wagner@fh-hagenberg.at,
[(d)]michael.affenzeller@fh-hagenberg.at, [(e)]clemens.reitinger@rosenbauer.com

ABSTRACT

Warehouses are an essential component of the supply chain, used for buffering the material flow, stock consolidation and value-added-processing. Operation managers typically do a good job of filling their warehouse but initially assigned storage locations might become sub-optimal over time, due to seasonal fluctuations in demand, short product life cycles or high inventory levels. Fragmented storage is a particular issue in order picking environments, where the optimal storage location of a product is not only dependent on its turn-over rate but also on the storage locations of items that frequently occur in the same picking job. In practice, operations managers are forced to periodically reorganize the warehouse to keep it operating efficiently. This process is generally done manually without any decision-support tool. In this paper we introduce an optimization approach that automatically reorganized item locations. Results are evaluated using a simulation model that simulates the picking and transport processes in the warehouse.

Keywords: re-warehousing, storage location problem, warehouse simulation

1. THE STORAGE ASSIGNMENT PROBLEM AND PERFORMANCE INDICATORS

The storage assignment problem involves the placement of a set of items or pallets in a warehouse in such a way that one or more performance measures are optimal. In typical distribution centres travel time to retrieve an order has been found to be the largest component of labour, amounting to 50% or more of total order picking time according to (Tompkins et al. 1996). By contrast, only 10% of the total order picking time is invested in the actual retrieval of products from their storage locations. Under the assumption that picking times are not correlated with particular storage locations we may treat them as fixed costs and omit them in the evaluation of warehouse assignments, thereby focusing on travel time.

Directly optimizing the picker travel times is complex, requiring a detailed warehouse layout and resource model (pickers, possible routes, routing strategy, collision detection and avoidance). Most approaches do therefore use an alternative, albeit related, objective measure. Early attempts to reduce travel time were for example based on the idea that fast-moving items should be located in easily accessible forward pick areas. Heskett (1964) extended this simple policy and proposed the cube order index (COI) rule, which ensures that heavy or fast-moving products are stored in more desirable locations close to ground level. Modifications of the COI rule have since been published, which also consider inventory costs or zoning constraints (Malmborg 1996). In general, these turn-over based policies work well if the order sizes are small and pickers return to the shipping deck after each pick.

In order picking environments a picker usually retrieves multiple items per order. Items that are frequently ordered together are said to be *correlated* or *affine* (Garfinkel 2005). Storing affine items close to each other may reduce the total travel time of the order pickers, although this is not guaranteed and depends on the picker routing. As noted by Waescher (2004) the fact that two items appear in the same order does not necessarily mean that a picker will directly proceed from one to the other on his route. In addition, structural conditions, such as narrow aisles that do not allow reverse back out, or large orders might require a full traversal of the warehouse anyway. In this case storing by affinity does not significantly reduce travel time but could on the contrary lead to congestion in certain aisles since it does not enforce balanced storage of fast-moving items.

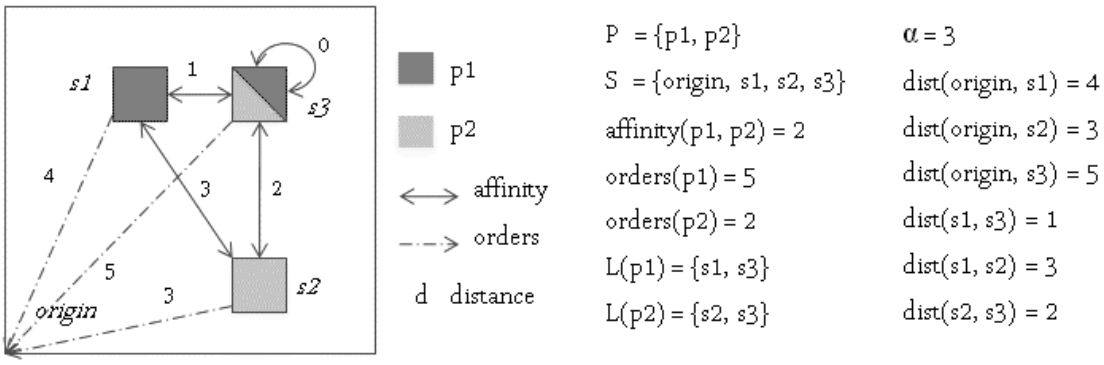

Figure 1: Example for the calculation of the quality of a simple assignment, consisting of a rack where two *products* p_1 and p_2 are stored in three *locations* s_1, s_2 and s_3. In addition, the location *origin* denotes the lower left corner of the rack. The stored *quantity* per location and product is one. All other storage locations are empty. The two quality measures, as defined in Equation 8 and 9, amount to *totalPickFrequencyScore* = 30.5 and *totalPartAffinityScore* = 6.

2. WAREHOUSE ASSIGNMENT EVALUATION

We combine two objectives to evaluate warehouse assignments generated by our optimization approach. Products with strong affinity should be placed together and fast-moving objects should be placed close to the shipping docks.

Prior to defining the objective function, we need to introduce a couple of variables. First of all, the warehouse definition consists of the set of storage locations **S** and a distance matrix denoting the travel distances (or efforts) between pairs of storage locations.

S = set of all storage locations s_k ; $0 < k <= m$ (1)

where $m = |S|$

$dist(s_k, s_l)$ = distance between storage location s_k and s_l (2)

In addition to the storage locations that can hold products, at least one special *origin* locations must be defined that denotes the shipping dock. In our case we employ a return routing strategy, were aisles are always entered and left from the front (cf. *Section 4: Warehouse Simulation Model*). Therefore we have defined an *origin* location in the lower left corner of each warehouse rack, ensuring that fast-moving objects are placed in more favorable locations close to the ground and near the front of an aisle.

The distance is a scalar value that can be assigned in different ways. For a rough estimate one might pick the linear distance between storage locations. For a more realistic approximation one could sum up the total travel distance, taking transport paths and perhaps even height differences into account. For our scenario we used a travel time estimate. First we split the travel distances into sub-movements such as aisle switch, forward/backward movement of the truck and fork up-down/left-right movement. Then we weighted the travel distances with empirically determined average travel velocities for the different movement types and summed up the resulting values to obtain an estimate for the required travel time between locations.

Usually, the storage locations and the distance matrix need to be determined only once for a given warehouse and can later be re-used for different problem instances.

Conversely, the following parameters are likely to change over time and need to be retrieved from the enterprise resource planning or warehouse management system. Most importantly, the set **P** lists all products that are present in a particular assignment.

P = set of all products p_i; $0 < i <= n$ where $n = |P|$ (3)

For each product p_i we need to know the total number of picking orders **orders(p_i)** in which the product occurs. Similarly, the affinity matrix stores how often two products are ordered together. Finally, the current warehouse assignment defines how many products p_i are stored at location $\mathbf{s_k}$. The set of locations **L(p_i)** stores all locations of a particular product.

$orders(p_i)$ = number of orders in which p_i occurs (4)

$affinity(p_i, p_j)$ = number of orders in which products p_i and p_j occur together (5)

$quantity(p_i, s_k)$ = number of packing units of product p_i stored at location s_k (6)

$L(p_i)$ = set of all $s \in S$ where $quantity(p_i, s) > 0$ (7)

The entities defined in 3-7 can be calculated from order picking histories and the current warehouse assignment. We can now define the objective functions in equation 8 and 9.

totalPickFrequencyScore = (8)

$$\sum_{i=1}^{n} \frac{orders(p_i)}{|L(p_i)|} * \sum_{s \in L(p_i)} dist(s, origin)$$

The *totalPickFrequencyScore*, as defined in Equation 8, ensures that frequently picked products are placed in more favorable storage locations near the ground and the aisle entries. For each product it detects all current

storage locations $L(p_i)$, calculates their distance to the origin and weighs each distance with the expected number of picks given the number of previous orders(p_i). The picks are uniformly distributed on all storage locations, independent of the actual stored quantities in the different locations.

totalPartAffinityScore = (9)

$$\sum_{i=1}^{n}\sum_{j=1}^{n}\frac{\text{affinity}(p_i,p_j)}{|L(p_i)|*|L(p_j)|} * \sum_{s_k\in L(p_i)}\sum_{s_l\in L(p_j)}\text{dist}(s_k,s_l)$$

The *totalPartAffinityScore* takes all pairs of products p_i and p_k, and retrieves all respective storage locations $L(p_i)$ and $L(p_j)$ from the current assignment. The distance between each resulting storage location pair is calculated and weighted with the part affinity divided by the number of location pairs $|L(p_i)|* |L(p_k)|$. The term reduces to zero for products with no part affinity, therefore the calculation can be sped up by only looking at products p_k that have an affinity greater than zero with a given product p_i.

The resulting multi-objective evaluation function for assignments is computed as weighted sum of the two objective functions given in Equation 8 and 9 such that

quality = α * totalPickFrequencyScore (10)
+ β * totalPartAffinityScore.

Figure 1 demonstrates how to calculate the quality of a small sample assignment with the given objective function.

As already mentioned the assessment of storage configurations via the proposed objective function alone might - in some cases - lead to solutions that are far from optimal in practice. We believe that a realistic evaluation of routing and storage strategies needs to incorporate dynamic aspects such as fluctuating travel and picking times, floor space utilization in the docking area, resource constraints (e.g. a limited number of pallets) or potential congestion situations when forklifts wish to access the same aisles simultaneously. We therefore employ a complementary simulation model for the evaluation of storage configurations as described in Section 4.

3. HEURISTICLAB

HeuristicLab (http://dev.heuristiclab.com) is a framework for heuristic and evolutionary optimization which is based on the Microsoft .NET framework. One core design goal of HeuristicLab was to shift the application of optimization strategies from an implementation point of view to a modeling point of view. In HeuristicLab algorithms are modeled by combining several generic parts using a graphical user interface. Similarly, problems are abstracted such that they make use of a certain representation and provide a fitness function as well as import parsers and graphical representations. The underlying representation, also called the encoding of a solution, provides manipulation operators such as crossover or mutation. All optimization runs were conducted with HeuristicLab and solutions were evaluated via the objective function given in Section 2. The best solutions were subsequently validated via simulation, to get a more realistic assessment of the quality of the generated assignments.

4. WAREHOUSE SIMULATION MODEL

We developed a simulation model in AnyLogic™ 6 that was based on a real-world high rack warehouse. Our project partner kindly provided enterprise data such as layout information, order picking histories and daily warehouse storage assignments. The warehouse floor plan was built to scale, with two fork-lift trucks for picking. Travel and pick time distributions were obtained empirically and used to parameterize the fork-lifts. Storage assignments can be loaded into the model as well as a set of picking jobs that ought to be simulated. The model employs a return routing strategy for incoming orders, were aisles are always entered and left from the front (de Koster and Roodbergen 2007), and calculates and performs an optimal picking sequence for each order.

The simulation model allows decision makers to parameterize and evaluate different warehouse configurations according to the various performance indicators, such as

- **Total travel distance:** The total distance travelled by all pickers.
- **Fork lift blocking time**: The model puts certain access restraints on the pickers. For instance, only one fork lift trunk can access the aisle per time. The total blocking time sums up the time spent waiting for an aisle to become free again.
- **Average order picking time**: The average time required to complete an order, including travel, waiting and picking times

All generated warehouse assignments were evaluated according to objective function introduced in Section 2 and the three indicators given above.

5. STORAGE LOCATION REASSIGNMENT

The literature about re-warehousing activity is limited. As stated in (Garfinkel 2005) one known approach was introduced by (Sadiq 1993), who periodically revises the assignments in accordance to the variation of item pick frequencies over a longer time period. Similarly, Housseman et al. (2009) used a simulation model to estimate the impacts of re-warehousing in cryo-conservation centers. In this paper we employ

- **first improvement local search** and
- **simulated annealing** (see Kirkpatrick 1983)

to optimize a given initial warehouse configuration. The base of both improvement methods is a set of moves that relocate a given quantity of items to a new location. In particular, we implemented different *move* operators, which swap the whole content of two randomly selected locations.

- **Random Swap 2**: Random swap of two pallets
- **Random Swap 3:** Cyclic swap of three pallets
- **Attraction Move:** Movement of pallets towards a more *attractive* position, meaning closer to affine products or – in case of a high turnover rate – the shipping dock

Table 1: Parameters for SA

Parameter	Value
Iterations	500,000
Temperature	80000
Annealing Factor	0.998
Annealing Scheme	Multiplicative
Inner Iterations	20

6. EXPERIMENTS AND RESULTS

We conducted test runs on data from a high-rack warehouse with more than 7,000 storage locations. As already mentioned, our project partner provided historical order pick data, consisting of information about more than 10,000 products and roughly 300,000 individual picking operations. The affinity matrix was calculated using this historical data set. Moreover, daily snapshots of the current warehouse assignment and planned picking orders for the day were exported from the warehouse management system. We used five such snapshots, optimized each assignment with respect to the objective function and subsequently evaluated the resulting assignments by simulating the scheduled picking orders. All optimization runs were conducted in a high performance computing environment on an 8-core machine with 2x Intel Xeon CPU, 2.5 Ghz and 32GB memory.

To investigate the trade-offs between placement by part affinity and placement by retrieval frequency, we had to find a good setting for the parameters α and β in the objective function (cf. Section 2, Equation 10). We first sampled the Pareto-optimal set with first improving neighborhood search and simulating annealing. We fixed $\beta = 1$ and conducted tests for $\alpha \in \{1, 2, 3, \ldots 20, 30, 40, 50, 60\ 70, 80, 90, 100\}$. We found that setting $\alpha = 2$ achieved a good trade-off between the two objectives for the given warehouse. The parameterization must of course be adapted for other warehouses, but in this paper all test runs were conducted with these settings. The result tables list the individual quality values separately, to better compare the assignments.

We initially employed simulated annealing with fairly long algorithm execution times of thirty minutes to five hours to get a rough estimate of the optimization potential. With the algorithm settings from Table 1 and by stochastically selecting from the three move operators for each move creation with equal probability we were able to generate assignments that improved the total quality, as defined by our objective function, on test set 1 by 32%. The optimized assignment improved the part affinity score by 11% and the pick frequency score by 40%. To illustrate the effects of the optimization, we implemented two visualizations for the inspection of assignments. The front view (cf. Figure 2) depicts the perspective of a worker, standing within an aisle and looking at one set of racks. The top view (cf. Figure 3) shows a bird's eye perspective on the warehouse, clearly showing the different aisles. On the one hand the views can show the quality of the assignment in a heat map like display. On the other hand it is possible to select a particular part in the warehouse and only display all affine parts with their locations and qualities. In this case, the relative lightness or darkness of the locations depicts the weighted part affinity score. Darker locations store parts with higher scores than lighter locations.

As can be seen in Figure 2, the initially scattered affine parts from test set 1 are tightly packed within the rack after optimization. Parts with higher scores (and therefore a probably high individual pick frequency) are positioned in more favorable locations towards the lower left edge of the row. Similarly, Figure 3 shows that affine parts are mostly concentrated within one aisle after the optimization.

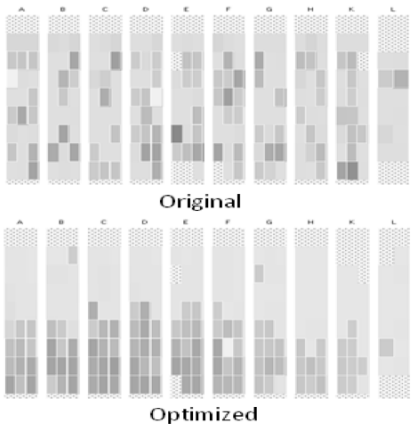

Figure 2: Set of affine parts before and after the optimization within one rack (so-called front view).

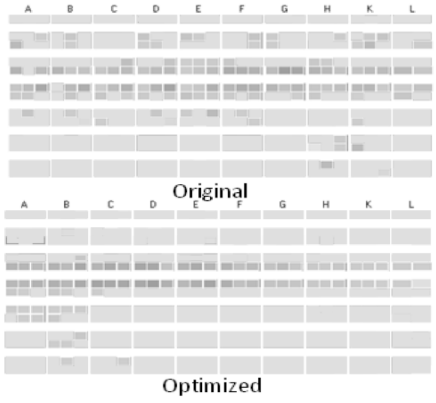

Figure 3: Set of affine parts before and after the optimization visualized in top view.

It should be noted that this is only an example, illustrating the effects of the optimization on the storage locations of one particular part and its affine parts. Also, the displayed result took 3 hours to generate with SA and led to a complete overhaul of the warehouse with more than 95% of the parts changing locations compared to the initial assignment.

For practical purposes, shorter algorithm runtimes would be preferable, in particular if re-assignments should be carried out on demand, when resources are available in the warehouse. We therefore also conducted tests with first-improvement local search and tight optimization time windows of 1-3 minutes. Once again, all three move operators were used with equal probability.

Table 2: Best results for tests with local search and a very tight optimization time window of 1-3 minutes for five test sets

Test Set	Affinity Score	Frequency Score	Computing time
1	-1%	-11%	1-3 min
2	-1%	-13%	
3	-1%	-8%	
4	-3%	-19%	
5	-3%	-18%	

As can be seen in Table 2, improving the placement of parts according to their pick frequency is much easier than grouping affine parts close together. This is not surprising, since the latter requires more moves and products that are picked with a wide variety of other products may experience conflicting "pulls" (e.g. via the attraction move) towards multiple areas in the warehouse.

Finally, to assess the impact on picker travel distance and order picking time, we conducted simulation runs for the test sets to compare the initial and generated assignments. In particular, we wished to investigate if assignments with better qualities would also lead to improved picker travel times and if the ratios were similar. We simulated five replications per assignment to account for stochastic variability. Due to the employed deterministic picker routing algorithm the travelled distance per assignment is the same across replications.

We exemplarily list and discuss the simulation results for test set 1 and the best SA test run in Table 3 and 4. While the generated assignment achieves better results on all three performance indicators, the improvement is not as great as one might hope for, given a 40% improvement on the objective function. The total travel distance of the two forklifts could be reduced by 1.85 km or about 7%. Blocking time, which we knew to be an issue beforehand, could also be improved by 18% and the average order picking time dropped by 8.5 minutes or roughly 35%. It should be noted, though, that results fluctuate a lot between replications, since the underlying distribution from which we estimate the picking times has a large variance. We are currently discussing these results with the warehouse operator and evaluating possible improvements to the simulation model. However, even our initial and very basic tests show that the employment of simulation is crucial for a more realistic estimate of the impacts of different assignments on warehouse logistics.

Table 3: Simulation results for the original warehouse assignment from test set 1.

Replication number	Travel distance [km]	Blocking time [min]	Average order picking time [min]
1	18.91	255.17	24.96
2		239.42	28.92
3		232.08	23.76
4		252.5	24.84
5		210.7	18.3

Table 4: Simulation results for the warehouse assignment from test set 1 after optimization with SA.

Replication number	Travel distance [km]	Blocking time [min]	Average order picking time [min]
1	17.06	208.08	18.54
2		209.08	15.36
3		194	15.66
4		146.83	12.78
5		217.17	15.84

7. CONCLUSIONS AND FUTURE WORK

The optimization approach presented in this paper is still a work in progress. The main innovations of our approach lie in the custom objective function and the employment of simulation for a realistic evaluation of the generated assignments. So far, we have acquired and pre-processed the required data, specified a generic model for the warehouse assignment problem, created and parameterized a simulation model for the evaluation of results, implemented solution manipulation operators and generated preliminary results with two standard algorithms. Our future research will focus on the following aspects:

First of all more exhaustive tests need to be conducted, also employing a more diverse set of heuristic optimization techniques, such as tabu search, evolution strategy and force-driven algorithms. This will be a major research focus in the second stage of our project.

Secondly, even short optimization runs such as those conducted with local search perform a large number of moves and thus re-arrange a multitude of parts. Such extensive rearrangements, an approach that we call *re-warehousing*, can block the fork lift truck for a couple of hours at least, is costly and might therefore

not be possible too frequently. Conversely, it should be easier to conduct a small number of cleanup tasks in idle slots between order picking or at the end of shifts. The idea behind this *healing* approach is that iteratively improving the placement of parts will lead to a good total warehouse assignment. We plan to conduct a study on the relative merits and efforts involved in *re-warehousing* vs. *healing* and derive recommendations for different warehouse types.

Finally, the company data used in this study is copyrighted and proprietary. We do however plan to publish a properly pre-processed and masked data set in the near future to allow other researchers to reproduce our results. In addition, we wish to apply our approach to different warehouses to investigate scaling, applicability and variance.

ACKNOWLEDGEMENTS

The work described in this paper was done within the Josef Ressel Centre for Heuristic Optimization *Heureka!* and sponsored by the Austrian Research Promotion Agency (FFG). For more information about Heureka! please visit http://heureka.heuristiclab.com.

REFERENCES

Garfinkel, M., 2005. *Minimizing Multi-zone Orders in the Correlated Storage Assignment Problem*, PhD thesis, GA Tech.

Heskett, J.L., 1964. Putting the cube-per-order index to work in warehouse layout, *Transportation and Distribution Management*

Housseman, S., Absi, N. Feillet, D. and Dauzère-Pérès, S., 2009. Impacts of Radio-identification on cyro-conservation centers through simulation, *Proceedings of the 2009 Winter Simulation Conference*, 2065–2077.

Kirkpatrick, S., Gelatt,, C. D. and Vecchi, M. P., 1983. Optimization by simulated annealing. *Science* 220, 671–680.

de Koster, R., Le-Duc, T. and Roodbergen, K.J., 2007. Design and Control of Warehouse Order Picking: a literature review, *European Journal of Operational Research*, 182 (2), 481-50.

Malmborg, C.J., 1996. Storage Assignment Policy Tradeoffs, *International Journal or Production Research*, 33, 989–1002

Sadiq, M., 1993. *A hybrid clustering algorithm for reconfiguration of dynamic order picking systems*, Ph.D. Dissertation, University of Arkansas.

Waescher, G., 2004. *Order Picking: A Survey of Planning Problems and Methods*, In: Dyckhoff, H., Lackes, R. and Reese, J., *Supply chain management and reverse logistics*, Springer, 323-347, Heidelberg, Berlin.

Tompkins, J.A., White, J.A., Bozer, Y.A., Frazelle, E.H., Tanchoco, J.M.A. and Trevino, J., 1996. *Facilities planning*. Wiley, New York.

AUTHORS BIOGRAPHY

MONIKA KOFLER studied Medical Software Engineering at the Upper Austrian University of Applied Sciences, Campus Hagenberg, Austria, from which she graduated in 2006. She is currently employed as a research associate at the Research Center Hagenberg and pursues her PhD in engineering sciences at the Johannes Kepler University Linz, Austria.

ANDREAS BEHAM received his MSc in computer science in 2007 from Johannes Kepler University (JKU) Linz, Austria. His research interests include heuristic optimization methods and simulation-based as well as combinatorial optimization. Currently he is a research associate at the Research Center Hagenberg of the Upper Austria University of Applied Sciences (Campus Hagenberg).

STEFAN WAGNER received his MSc in computer science in 2004 and his PhD in engineering sciences in 2009, both from Johannes Kepler University (JKU) Linz, Austria; he is professor at the Upper Austrian University of Applied Sciences (Campus Hagenberg). Dr. Wagner's research interests include evolutionary computation and heuristic optimization, theory and application of genetic algorithms, machine learning and software development.

MICHAEL AFFENZELLER has published several papers, journal articles and books dealing with theoretical and practical aspects of evolutionary computation, genetic algorithms, and meta-heuristics in general. In 2001 he received his PhD in engineering sciences and in 2004 he received his habilitation in applied systems engineering, both from the Johannes Kepler University of Linz, Austria. Michael Affenzeller is professor at the Upper Austria University of Applied Sciences, Campus Hagenberg, and head of the Josef Ressel Center *Heureka!* at Hagenberg.

CLEMENS REITINGER studied Mechanical Engineering - Economics (Industrial Engineering) at Vienna University of Technology, Austria, from which he graduated in 2003. He is currently employed as Head of Logistics at Rosenbauer International AG and also involved in the *Heureka!* project.

PROCESSOR-ORIENTED PERFORMANCE MEASUREMENT TOOL

Martin Schwarzbauer[(a)], Michael Bogner[(b)], Franz Wiesinger[(c)], Andreas Gschwandtner[(d)]

[(a, b, c, d)] Upper Austria University of Applied Sciences, Hagenberg Austria,
Hardware/Software Design & Embedded Systems Design

[(a)]martin.schwarzbauer@fh-hagenberg.at, [(b)]michael.bogner@fh-hagenberg.at,
[(c)]franz.wiesinger@fh-hagenberg.at, [(d)]andreas.gschwandtner@fh-hagenberg.at

ABSTRACT
Nowadays, a lot of powerful and different processors with special techniques for improved performance exist. The clock frequency was doubled within a year in the last decades and the number of cores is increasing continuously. Because commonly available performance measuring tools like Microsoft Windows Task Manager are known not to display the exact load of a processor, it is not possible to compare applications and different implementations regarding to their performance on different processors. A special tool is needed which allows the correct and processor-oriented measuring of the processor's load. This paper describes the technique for measuring the performance of modern processors precisely and shows a sample implementation for an Intel Core 2 Duo processor on the Microsoft Windows operating system. Using the implemented tool it is possible to analyze and compare different applications regarding to their performance. The tests have shown that no application is able to generate a processor load higher than 30%.

Keywords: processor performance, performance measurement tool, performance counter

1. INTRODUCTION

Nowadays, a lot of powerful and different processors with different techniques for improved performance exist. The clock rate has been doubled within a year in the last decades and new multi core processors have been developed and sold by the manufacturer. All these techniques improve the performance of the processor and speed up the execution of instructions. But this doesn't mean that the execution of an application also speeds up with the same ratio like the processors do.

It is not possible to utilize the actual processors. A lot of the available performance gets lost and cannot be used for the execution of instructions. The processor itself would be able to execute more instructions but the biggest problem and the bottleneck in current personal computers is the slow access on peripherals.

Processors with doubled clock rates would be able to process nearly twice the number of instructions at the same time but if, for example, data from the hard disk or other peripherals is fetched the processor has to wait. The peripherals like random access memory (RAM) or the hard disk are connected to the processor via bus systems. These bus systems are not as quick as the processor, so it has to wait until the data arrives.

For performance optimization and comparison of different applications a tool is needed to measure the real performance of the processors. There are a lot of tools which are able to display the load of the processor over the time. The most common and widely-used tool is the Microsoft Windows Task Manager (Microsoft Corporation, 2010b) on Microsoft Windows operating systems (Figure 1). There also exist a lot of other possibilities to measure the performance - for example at the high level programming language C# (Microsoft Corporation, 2010).

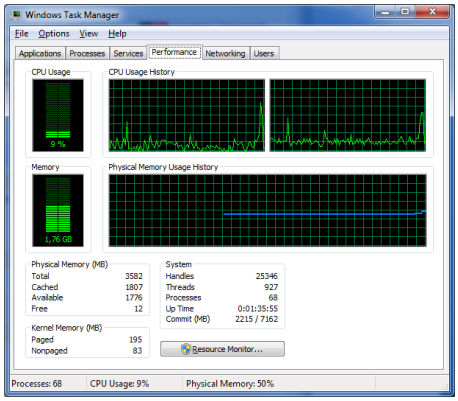

Figure 1: Microsoft Windows Task Manager.

The advantage using these tools is the simplicity in the usage for measuring the performance, but there is a big disadvantage for processor-oriented performance measurements because the measured load is simply incorrect. Available tools show the load of the processor from the point of view of an operating system. This means that wait times – when fetching data from RAM or hard disk – are shown as 100% load of the processor. From this point of view this is correct because without the data from the peripheral the processor couldn't continue its work. But for processor-oriented performance measurements this distores and falsifies the results as the processor is actually idle.

This paper describes a solution to measure the real processor load so that it is possible to evaluate performance optimizations. Using such a measurement tool opens new options for comparing different implementations or compiler options (compile for speed, compile for size) and helps to explore and assemble special performance design pattern for software development to speed up processing simply by design.

2. PERFORMANCE MEASURMENT

The best way to measure the exact load of a processor is to use the processor itself for the performance measurement. The two most common and widely used processors are manufactured by *Intel* and *AMD*. Both implement on their processors options for performance measurement.

Each processor has some specially built in registers in hardware – the so called model specific registers (MSR). The number of available MSRs on Intel processors can be found in (Intel Corporation, 2010, Appendix B). A subset of these MSRs could be used to measure the performance directly in hardware. These registers are called *Performance Counters*. The performance counters could be configured to count specific and processor dependent events in hardware (Dringowski, 2008; Intel Corporation, 2010). Some typical events are *Instructions Retired*, *Instruction per Cycle*, *Level 1 Cache Miss*, and so on. Using the correct event it is possible to calculate the exact load of a processor without the wait times for memory access, stalls and so on.

The advantage of these registers is that they count the configured events in hardware without any overhead in software and impact on the processor's behaviour. To read or write these MSRs the processor uses an assembler instruction (for example on Intel processors: *rdmsr* and *wrmsr*) which has to be executed in real-address mode or at privilege level 0 (Intel Corporation, 2009). The execution of an instruction at privilege level 0 requires on the two most common operating systems - UNIX and Microsoft Windows - a special driver to execute the instructions and access the MSRs. Figure 2 shows an overview of the concept to access the performance counter registers using this driver.

The available events and registers for performance counting are limited and different for each processor – also within a processor family. On newer processors there are more events available than on older ones and the address of the registers also change. So it is necessary to implement the performance measuring for each processor differently.

On multi core processors it is necessary to measure the performance of each core independent from the others. The manufacturer implements for each core a set of registers which could be used to count different events. For the sake of convenience these registers have the same address on each core. To access the register it is necessary to ensure that the application which reads or writes the register is executed at the core the event should be counted.

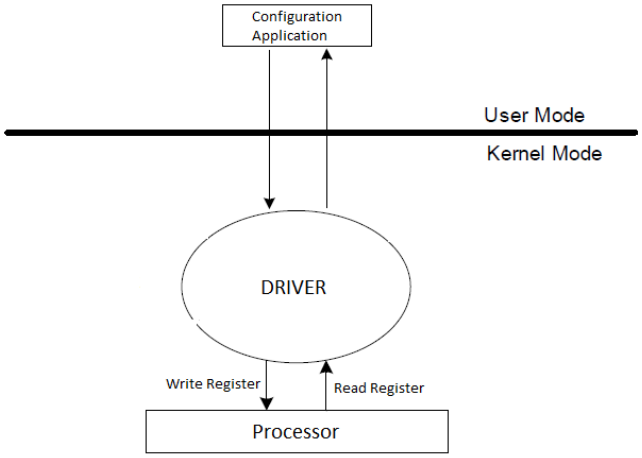

Figure 2: Accessing the performance counter registers using a driver.

The usage of the performance counters always follows the same principle described below:

1. Ensure that execution is running on core X.
2. Set the configuration register to count the specific event.
3. Continue step 1 + 2 for each core and event.
4. Ensure that execution is running on Core X.
5. Read number of counted events from the register.
6. Continue step 4 + 5 for each core.

Intel introduced different MSRs years ago in their processors so it was able to count different processor events in hardware. The configuration and access to these MSRs was processor depended. Since the Pentium 4 processor Intel standardised the access and configuration of the MSRs for performance measurement. This standardisation provides two different versions to configure up to seven defined events (even more on newer processors) for performance measurement. These seven architecture and processor independent events are

1. Unhalted Core Cycles
2. Instructions Retired
3. Unhalted Reference Cycles
4. LLC Reference
5. LLC Misses
6. Branch Instructions Retired
7. Branch Misses Retired

Figure 3 shows the necessary MSRs for configuration and performance measurement in dependency of the two different available versions (Registers marked with * are used for configuration). When any other events except the seven mentioned

above should be used, the configuration and usage is described in the different processor's manuals.

When using the event *Instructions Retired* it is possible to calculate the processors' load in percent using (1). Because of the processors ability to execute more than one instruction per cycle the maximum number of instruction per cycles must be known and used for the load calculation in (1).

$$Load\ [\%] = \frac{Instructions\ \ Retired}{Clock\ \ Cycles * max\ .Instructions\ \ per\ \ Cycle} \qquad (1)$$

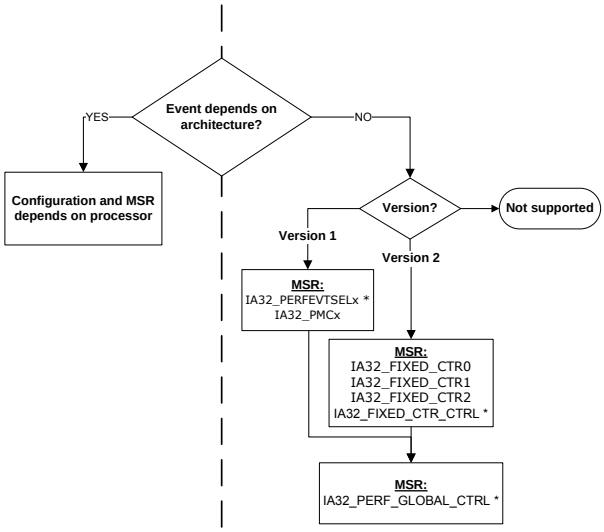

Figure 3: Overview of the available MSRs in dependency of the supported version.

The configuration for counting the *Instructions Retired* event differs by the two supported versions. Using the assembler instruction *cpuid* it is possible to detect which version is supported by the current used processor. Based on the supported version there are different MSRs for configuration and reading the collected performance data. In version 1 each of the seven events mentioned above could be counted – but maximum two events at the same time. Version 2 only supports counting the three following events

1. Instructions Retired (IA32_FIXED_CTR0)
2. Unhalted Core Cycles (IA32_FIXED_CTR1)
3. Unhalted Reference Cycles (IA32_FIXED_CTR2)

Figures 4, 5 and 6 show the different MSRs in detail that are needed for configuration.

MSR IA32_PERFEVTSELx (Figure 4) is used to configure the performance counting mechanism in version 1. The fields Unit Mask and Event Select identify the event which should be counted. USR and OS bit specify if the event should be counted in user mode and/or in operating system mode. Bit EN enables counting the selected event.

The MSR shown in Figure 5 is used to enable each of the three possible events in version 2. Bit PMI defines if an interrupt should be generated when a counter overflow occurs. The bit EN specifies the mode where the events should be counted.

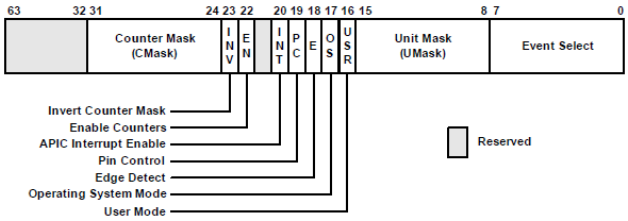

Figure 4: IA32_PERFEVTSELx MSR is used to configure the counting mechanism in version 1 (Intel Corporation, 2010).

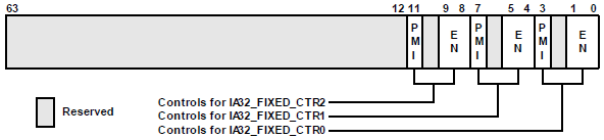

Figure 5: IA32_FIXED_CTR_CTRL MSR is used to configure and enable the event counting mechanism in version 2 (Intel Corporation, 2010).

In Figure 6 the global enable MSR is shown. When bit 32, 33 and/or 34 is set, the event counting for version 2 is enabled. Bit 0 and 1 is used to enable performance measurement in version 1.

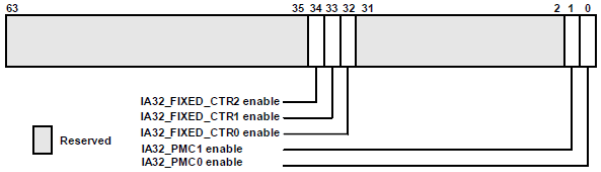

Figure 6: IA32_PERF_GLOBAL_CTRL MSR is used to enable the different events (Intel Corporation, 2010).

To retrieve the number of counted events the MSRs IA32_PMCx in version 1 and IA32_FIXED_CTRx in version 2 must be read.

The following pseudo code shows the usage of the *Instructions Retired* event on an Intel Core 2 Duo processor using version 1.

```
if event supported then
   if version 1 supported then
       switch to core 1;

       // set UMASK and EventSelect to
       // specify the event
       // EN=1: activate counting
       // OS=USR=1: count event in user
       // and kernel mode
       IA32_PERFEVTSEL0= (UMASK=0x00) |
           (EventSelect=0xC0) | (EN=1) |
           (USR=1) | (OS=1);

       switch to core 2;

       // config core 2
       IA32_PERFEVTSEL0= (UMASK=0x00) |
           (EventSelect=0xC0) | (EN=1) |
           (USR=1) | (OS=1);

       //enable counting
       IA32_PERF_GLOBAL_CTRL =
```

```
                    (IA32_PMC_0 enable = 1);

        while not terminate then
            sleep(pollintervall);

            // read events counted on core 1
            Switch to core 1;
            Value1 = IA32_PMC0;

            // read events counted on core 2
            Switch to core 2;
            Value2 = IA32_PMC0;
        end while
    end if
end if
```

With the collected number of occurred events stored in Value1 and Value2 it is possible to calculate the processor's load in percent. When using version 2 the configuration and access to the counted events only differs from version 1 in different MSRs.

Because of the widely-used combination of Intel processor and the operating system *Microsoft Windows* a sample application has been implemented for this platform for the performance measuring on an Intel Core 2 Duo processor.

3. IMPLEMENTATION

In Figure 7 all components required for the realization of a performance analysis tool are shown. The arrows illustrate the interaction between the different components.

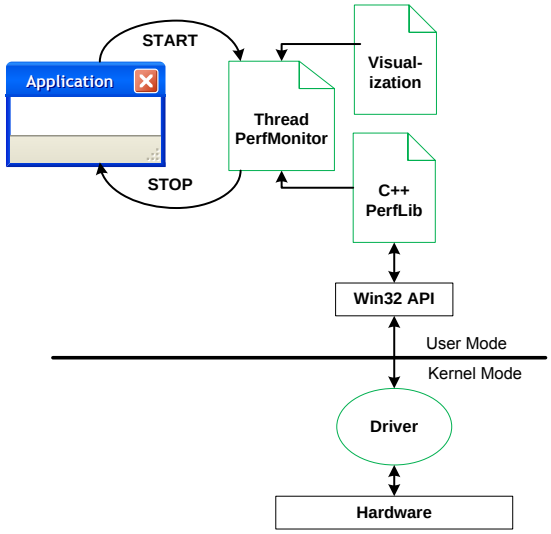

Figure 7: Overview of the implementation.

The C++ class ThreadPerfMonitor configures the performance measurement. Using the methods *start* or *stop* the application can control the time of measurement. The collected performance data will be written into a file in comma-separated-values (CSV) format, so that it is possible to process the values with different applications.

The interaction between the processor's hardware is encapsulated in a C++ class called PerfLib. This class provides methods to write and read the different MSRs using the driver.

As already mentioned a driver is needed to execute the instructions *rdmsr* and *wrmsr* to access the different MSRs. In Figure 8 the usage of the driver is shown for reading a MSR using the *rdmsr* instruction. A Win32 API accesses the driver via Input/Output Controls (IOCTL). Using the IOCTL IOCTL_READMSR the driver dispatches the registered function and executes the *rdmsr* assembler instruction with the given parameters. The read value will be returned to the user mode and could be processed.

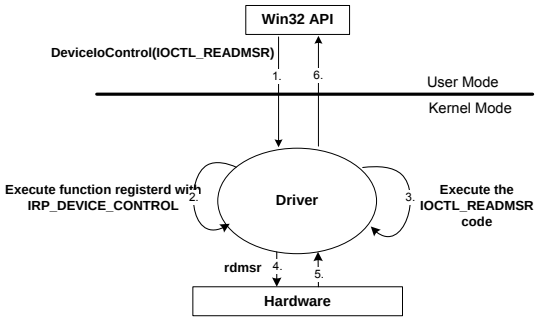

Figure 8: Sequence reading a MSR.

This implementation can easily be extended for different processors on the Microsoft Windows platform. Accessing the registers on UNIX, a different driver must be implemented but the assembler instructions and the configuration sequence of these MSRs will be the same. The application uses the *Instructions Retired* event to collect information of the processor so that it is possible to calculate the load in percent.

4. RESULTS

The implemented measurement application is written in C++ and is able to count different events on an Intel Core 2 Duo processor. Currently only this processor is supported but the software can be easily expanded so that any other processor and event can be used for performance measurement. This could be done by specifying the different processor dependent register addresses for reading and writing the registers and the configuration values that have to written to the MSRs. At the moment the application configures the processor to count the event *Instructions Retired*. Using this event, the number of clock cycles, and the maximum count of instructions (on Intel Core 2 Duo: 4; Intel Corporation, 2008), which could be executed at one clock cycle, it is possible to calculate the processor's load in percent (see (1) on page 3).

To visualize the results the application writes the data into a file in CSV format. Using the written values it is possible to visualize them, use it for calculations or any other application can read the values and process them. One of the most common tools to create a graph based on a CSV file is Microsoft Windows Excel (Figure 4 show a graph created with this application).

The realized performance measurement tool could be used as a standalone application to record the load of the processor's cores independent of any other

application. Another practice is to use the performance tool explicit in the own application for performance measurement. This could be easily done in applications implemented in C++ because the developer only has to call a Start- and Stop-Routine for the performance measurement. The advantage is that only the period of time is recorded the developer wants to measure.

Figure 9 and Figure 10 show the comparison between the Microsoft Windows Task Manager and the values recorded with the implemented processor-oriented performance measurement tool during the execution of a test application. The Microsoft Windows Task Manager shows a load of 100% on core one. In comparison to this we can see in Figure 10 that the processor only uses effectively 25% of its available resources. This example shows the difference in the performance measurement tools. The test application fetches a lot of data from the hard disk so that the processor has to spend most of its time on waiting. Available tools display the processor's load from the point of view of an operating system. This means that while fetching data from peripherals the operating system cannot continue with its work so the load for the operating system is 100%.

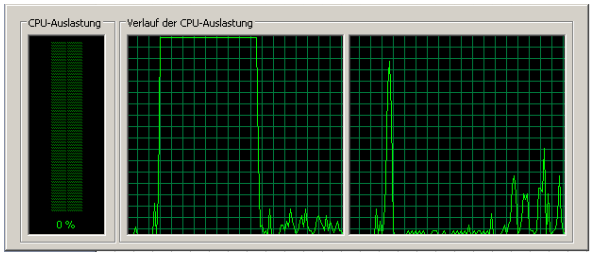

Figure 9: Processor load measured with Microsoft Windows Task Manager.

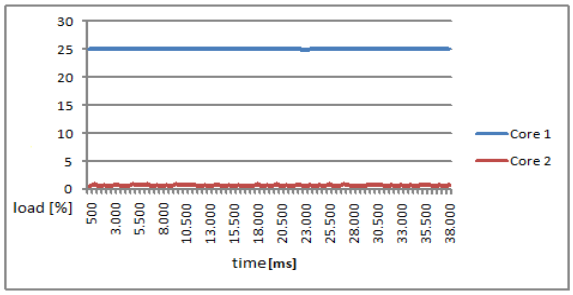

Figure 10: Processor load measured with the processor's performance counters.

The implemented tool shows the exact load of a processor so these results are more significant than the results of common tools. Based on these results it is not advisable to use common tools for performance measurements and testing optimization possibilities.

With the implemented application and their measured results different optimization techniques could be evaluated and compared regarding their performance on the processor's core.

Based on different test applications (e.g. benchmark Prime95, Mersenne Research Inc., 2010) there were nearly always the same results. Modern processors can reach only a maximum load of about 30%. This means that the processor spends about 70% of the available time on waiting for data or simply doing nothing. At this point of view an application has a good performance when it can reach a maximum of about 30% load on common processors – because this is still the maximum reachable load using current computer systems.

To sum up it could be said that the results have shown that modern processors and highly optimized compilers aren't able to create applications that can use the available resource of the processor's core in an adequate way. It is necessary to find different techniques and design pattern for software development to improve application's execution so that the load increases. Using the implemented processor-oriented performance measurement tool it is possible to collect performance data and find software techniques and design pattern and their different impact on the processor's load.

REFERENCES

Dringowski, P.J., 2008. *Basic Performance Measurements for AMD Athlon(TM) 64, AMD Opteron(TM) and AMD Phenom(TM) Processors.* Available from: http://developer.amd.com/Assets/Basic_Performance_Measurements.pdf [accessed 31 March 2010]

Intel Corporation, 2008. *Intel(R) Core(TM)2 Duo Processor. Maximizing Dual-Core Performance Efficiency.* Available from: http://download.intel.com/products/processor/core2duo/mobile_prod_brief.pdf [accessed 5 April 2010]

Intel Corporation, 2009. *Intel(R) 64 and IA-32 Architectures. Software Developer's Manual. Volume 2B: Instruction Set Reference, N-Z.* Available from: http://www.intel.com/design/processor/manuals/253667.pdf [accessed 31 March 2010]

Intel Corporation, 2010. *Intel(R) 64 and IA-32 Architectures Software Developer's Manual. Volume 3B. System Programming Guide, Part2.* Available from: http://developer.intel.com/Assets/PDF/manual/253669.pdf [accessed 17 July 2010]

Mersenne Research Inc., 2010. *Prime95*. Available from: http://mersenne.org/freesoft [accessed 31 March 2010]

Microsoft Corporation, 2010a. *Performance Counters*. Available from: http://msdn.microsoft.com/en-us/library/aa373083(VS.85).aspx [accessed 31 March 2010]

Microsoft Corporation, 2010b. *What is Task Manager?*. Available from: http://windows.microsoft.com/en-US/windows-vista/What-is-Task-Manager [accessed 9 April 2010]

A DECISION SUPPORT SYSTEM FOR DESIGN AND ASSESSMENT OF HYBRID SYSTEMS FOR COGENERATION OF ELECTRICITY AND WATER

A. Kartalidis, G. Arampatzis, D. Assimacopoulos

National Technical University of Athens, School of Chemical Engineering,
9 Heroon Polytechniou st., Zografou Campus, GR-15780, Athens, Greece.
assim@chemeng.ntua.gr

ABSTRACT
A decision support system (OPEN-GAIN DSS) for the design, assessment and implementation of a hybrid energy system is presented. The DSS integrates a number of operational actions that can be accessed to answer all the questions raised during the phases of the decision making process and to assist in making reasonable decisions. A suite of design and modeling tools have been developed and adopted into the DSS environment in order to implement the logic of the DSS actions. The design of the hybrid system is based on a simplified algorithm with minimum data requirements, while the performance assessment of the system is accomplished with the aid of a time-series simulation model. A Monte-Carlo approach has been adopted to quantify the underlying risk and the evaluation action is based on a Multi-Criteria Analysis framework. The operation of the DSS is demonstrated through a case study concerning a medium-size prototype unit in Tunisia.

Keywords: renewable energy sources, hybrid energy system, decision support system

1. INTRODUCTION

The cogeneration of electricity and water through desalination by exploitation of renewable energy sources (RES) is becoming an increasingly promising option, especially in arid and remote areas, where alternative energy supply is either unavailable or too costly to develop (Mathioulakis, Belessiotis, and Delyannis 2007). Various aspects should be taken into account when designing a stand-alone energy production system. The energy sector in Europe is expected to be influenced by two factors: the need to meet Kyoto commitments and the issue of energy supply security (Hemmes, Zaharian-Wolf, Geidl and Anderson 2007). In view of this, the sustainability of the energy supply system must be assessed on the basis of its environmental impacts as well as the need to assure that the system has the capacity to meet the requirements set by the consumers. Renewable energy resources, such as solar and wind power, are inexhaustible and environmentally friendly potential energy options. However, neither a standalone solar nor a wind energy system can provide a continuous supply of energy, due to daily and seasonal variations (Elhadidy and Shaahid 2000). In order to satisfy the load demand, hybrid energy systems are implemented that combine solar and wind energy conversion units with conventional diesel generators and energy storage systems.

The design, assessment and optimization of such a hybrid energy system would require an overall system engineering approach. System analysis emphasizes a holistic approach to problem solving and the use of mathematical models to solve important characteristics of complex systems, which can be further integrated into a Decision Support System (DSS) to address the problem of decision making in a generic way.

Several research groups have presented methods for designing renewable and hybrid energy systems (Bernal-Agustin and Dufo-Lopez 2009). These methods range from simplified algorithms (Siegel, Klein, and Beckman 1981; Celik 2006; Kartalidis, Arampatzis and Assimacopoulos 2008), based on monthly average values of renewable energy potential (solar radiation and wind speed), to more sophisticated time series simulation models (Ekren and Ekren 2009), requiring detailed meteorological and energy demand measurements. Experience has shown that simplified algorithms are best suited to the preliminary design (sizing) of the hybrid system's components while simulation methods are more useful in assessing the performance of the system under realistic operational conditions and various management rules.

Numerous papers have been published on the optimum economic design of PV and/or wind and/or diesel systems with energy storage, such as batteries. Usually, the optimum configuration is selected for minimizing the total cost of the entire system or the levelized cost of energy i.e. total cost divided by the energy supplied by the system (Elhadidy amd Shaahid 2000; Dufo-Lopez, and Bernal-Agustin 2005). However, decision making in real hybrid energy systems is complex, principally due to the inherent existence of trade-offs between economic, environmental and social factors. For the sustainability assessment of a hybrid system, appropriate indicators have been proposed (Afgan and Carvalho 2008) and the use of multi-criteria evaluation methods is essential, in

order to account for the combined effects of all criteria under consideration.

Available software tools to support system designers have the form of specialized hybrid system simulation models, which can be used to evaluate the performance of a system, and generic optimization or multi-criteria assessment applications. There is thus far no integrated decision support system capable of answering all the questions raised during the phases of the decision making process (from the preliminary design to the selection of the most efficient configuration) and helping in making reasonable decisions. The DSS presented in this paper was designed to provide guidance in framing the problem in an integrated way, to assist system designers in making decisions by answering all the questions raised and to help selecting the optimal hybrid system configuration.

The different components of a hybrid energy system for cogeneration of water and electricity and their roles are introduced in section 2. Section 3 presents the conceptual design of the DSS, outlining the role of the DSS actions in the phases of the decision making process. The architectural design of the DSS is presented in section 4, while the functional capabilities of the DSS are demonstrated in section 5.

2. HYBRID ENERGY SYSTEM CONFIGURATION

A hybrid energy system produces power from more than one generating source such as wind-driven turbines, solar panels and conventional diesel engines. The system stores excess power in battery storage units. Such a system should be tailored to the specific energy resources available at the specific site and to meet the power generation needs. A configuration representative of this system is presented in Figure 1.

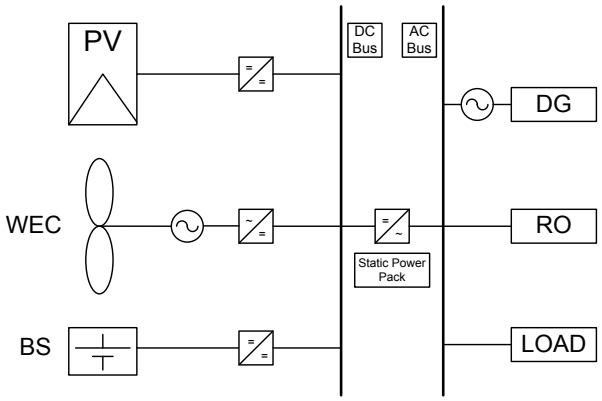

Figure 1: General configuration of the hybrid energy system

The main parts of the system are: the Wind Energy Conversion system (WEC); the Photovoltaic system (PV); the Diesel Generator (DG); the Battery Storage system (BS); the Reverse Osmosis plant (RO); and other power loads (LOAD), if the system is designed to supply energy to additional units at the installation area.

3. CONCEPTUAL DESIGN OF THE DSS

Decision making is the study of identifying and choosing alternatives based on the values of evaluation criteria and on the preferences of the decision maker(s). Making a decision implies that there are alternative choices to be considered, and in such a case it is necessary to identify as many of these alternatives as possible and to select the alternative with the highest probability of success or effectiveness and that best fits with the goals. Decision making is also the process of sufficiently reducing uncertainty and doubt about alternatives to allow a reasonable choice to be made among these. Table 1 presents the phases during a typical decision making process and summarizes the questions that is expected to be answered.

Table 1: Phases in the decision making process

Phase	**Questions**
Feasibility Analysis	- Is it possible to satisfy power and water requirements of a remote area with a RES powered desalination system?
Preliminary Design	- Which are the alternative configurations of the hybrid energy system? - What is the size of each energy component?
System Assessment	- How does each configuration perform under realistic conditions? - What is the investment cost? - What is the operational cost during the life cycle of the project? - What are the environmental costs/benefits?
Screening and Refinement	- Does the configuration satisfy the water and power requirements of the area? - Does the configuration efficiently exploit the RES Potential of the area? - How sensitive are the expected outputs to changes in the component sizes or other input parameters? - Are there dominated configurations?
Risk Assessment	- How do uncertain conditions influence the system performance? - Which are the extreme scenarios and their consequences? - What is the risk of system “failures”?
Evaluation	- Which are the preferences of stakeholders? - Which features and performance indicators are important?
Selection	- Which is the optimal configuration?

The design specification of the DSS is to support the user through the decision making phases of Table 1. This is accomplished through six operational Actions.

The role of each DSS action in the decision making process is depicted in Figure 2.

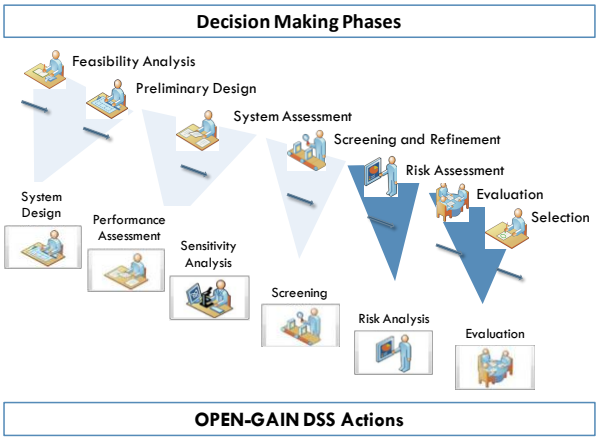

Figure 2: Relation between decision making phases and DSS actions

The six DSS actions are:

System Design Action. The aim of this action is to identify the set of alternative system configurations that satisfy the water and energy requirements of the examined region. The output of this action is a list of alternative configurations, distinguished by the sizes of the various system components and energy management rules.

Performance Assessment Action. The purpose of this action is to assess the performance of each alternative configuration, based on detailed meteorological and demand data. This is accomplished through a time series simulation of the system, producing detailed results on the energy flows, and information on the status of the components and the failures of the system. These results are used to compute the values of a set of performance indicators (presented in Table 2) which is the main output of this action.

Sensitivity Analysis Action. This action serves to examine the importance of each parameter on the performance of each alternative configuration. The information gained by performing this action may guide the user to proceed to minor or major revisions of the system.

Screening Action. This action can be used to highlight the trade-offs that must be made by the decision maker/s and to identify the configurations that do not appear to warrant further attention. The main output is the elimination of dominated configurations from the evaluation step. Dropping dominated configurations is logical because a valid evaluation methodology (like Multi-Criteria Analysis) will never choose a dominated alternative.

Risk Analysis Action. The purpose of this action is to quantify the risk that arises due to the uncertainty associated with the parameters used as input to the assessment step. This is accomplished through a Monte-Carlo simulation. The output of the action is a number of risk indicators, so that risk can be traded off against other indicators when evaluating the alternative configurations.

Evaluation Action. This is the final action on the DSS workflow and serves to evaluate the list of alternative configurations on the basis of the indicators produced in the "Performance Assessment" and "Risk Analysis" actions. The methodology used in this action is a multi criteria analysis using the preferences of the decision maker/s on the importance of the evaluation criteria (indicators). The output of this action is a ranking of the alternative configurations and their overall scores (values).

Table 2: Performance indicators

No	Indicator/Description
1	*Energy Delivered / Energy Demand* Describes the energy balance of the system. For the system to be operating without problems, the indicator should be equal to "1".
2	*Renewable Energy Delivered / Energy Demand* Describes the contribution of the renewable energy to the energy balance of the system. Higher values are preferable, as they indicate high use of RES to meet energy demands.
3	*Renewable Energy Delivered / Energy Collected* Higher values are preferable, indicating maximum exploitation of the WEC and the PV systems to meet energy demands.
4	*Diesel Engine Operation Time (%)* Lower values are preferred as they indicate limited usage of the diesel engine to meet energy demands.
5	*Daily Average Diesel Engine Cycles* Describes the frequency of the use of the diesel engine. Lower values are preferable.
6	*Energy Delivered by the Battery / Demand* The ratio of the energy delivered by the battery to the energy demand for the simulation period.
7	*Battery Time below Critical Depth of Discharge* The percentage of the time that the battery charge level is below a critical threshold. Lower values are preferable.
8	*Capital Cost* The total purchase cost of the system, calculated as the sum of the cost of its components. Lower values are preferable.
9	*Diesel Consumption Cost* The annual cost fuel consumed by the diesel engine. Lower values are preferable.
10	*Green House Gases Emissions* The annual amount of CO_2 released due to diesel engine use. Lower values are preferable, indicating smaller environmental impact.
11	*RO Unit Stable Operation* The ratio of the total time that energy production is not adequate to meet the energy requirements of the RO unit vs. the duration of the simulation period. The indicator should be equal to "1" to ensure that the RO unit is operating without problems.

4. ARCHITECTURE OF THE OPEN-GAIN DSS

The OPEN-GAIN DSS is a software tool, designed to support the decision making process presented in previous section. The software was developed in Microsoft Visual Basic .NET and the database in Microsoft Access. Figure 3 presents the different parts of the tool, and the way they are integrated to provide the decision support functionalities.

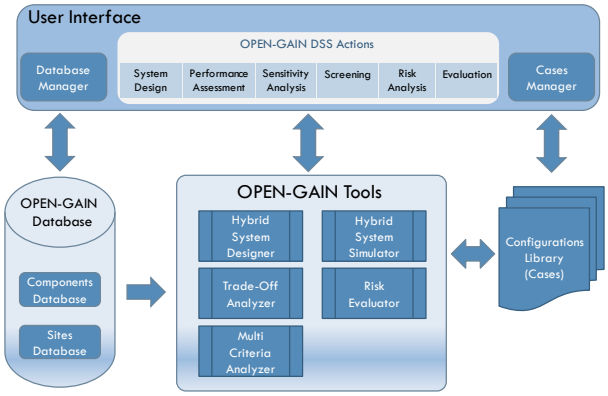

Figure 3: OPEN-GAIN DSS Architecture

4.1. User Interface

The User Interface is the part of the software that the user sees and interacts with the DSS software. The different parts of the User Interface allow the user to:

- Perform the DSS Actions presented in section 3 and to view the results of those actions.
- Manage the OPEN-GAIN Database through the Database Manager.
- Manage the library of alternative system configurations (cases), produced and assessed by the DSS actions, through the Cases Manager.

4.2. Database and Configuration Library

The OPEN-GAIN Database is the central repository for data and findings of the project. It consists of two parts:

- The Components Database contains all the available equipment in the market for the power subsystem in order to adopt the optimum equipment. This equipment consists of wind generators, photovoltaic modules, batteries, diesel engines and power electronics. The components are registered in the database with their operational, economic and environmental characteristics.
- The Sites Database mainly contains meteorological data for the Renewable Energy sources (wind and solar availability). Other data concerning the sites are the quality of the sea and brackish water and demand profiles for potable/desalinated water and electricity.

The Configurations Library is a storage area for the alternative system configurations generated, assessed and evaluated with the aid of the OPEN-GAIN DSS.

4.3. OPEN-GAIN Tools

The heart of the system is the collection of OPEN-GAIN Tools. It's a suite of independent modeling tools, integrated and adopted into the OPEN-GAIN DSS environment in order to implement the logic of the DSS actions. The five tools are:

Hybrid System Designer. Sizes a hybrid energy system based on a minimum set of meteorological data and design parameters. The procedure that is used for the sizing of the installed RES components and their auxiliaries is based on specific goals and constraints. The design goals concern the maximization of RES exploitation, the minimization of the undelivered excess energy, the minimization of costs (capital and operating) and the minimization of environmental impacts. The operational constraints are the constraints and stable operation of the desalination plant. Detailed description of the design procedure can be found in Kartalidis, Arampatzis and Assimacopoulos 2008.

Hybrid System Simulator. Simulates the performance of the hybrid energy system, according to the design, based on detailed meteorological data (time-series) and operational strategies. A one hour time step is used throughout the simulation. The electrical load and the renewable resources are treated as constants within each time step. The mode of operation of the simulator is as follows: Under normal operating conditions (i.e. adequate solar radiation and/or wind speed), the WEC and PV feed the energy demand (RO plant and additional power LOAD). The excess energy (i.e. the energy above this demand) from WEC and PV is stored in the battery system until full storage capacity is reached. If the output from WEC and PV exceeds the load demand and the battery's state of charge is maximized, then excess energy is dumped (undelivered energy) or fed back into a utility grid, in case of grid-connected systems. The diesel generator is used to support the system in meeting the energy demand, when the WEC and PV systems fail to manage it and battery is depleted.

Trade-Off Analyzer. Performs trade-off display and dominance analysis on a set of options.

Risk Evaluator. Quantifies the risk of an option due to uncertainty about long-term future using Monte-Carlo simulation.

Multi Criteria Analyzer. Analyzes complex decision problems by evaluating alternative options on the basis of conflicting criteria following a Multi-Criteria Analysis framework.

Figure 4 depicts the role of OPEN-GAIN tools as building blocks for the implementation of DSS actions

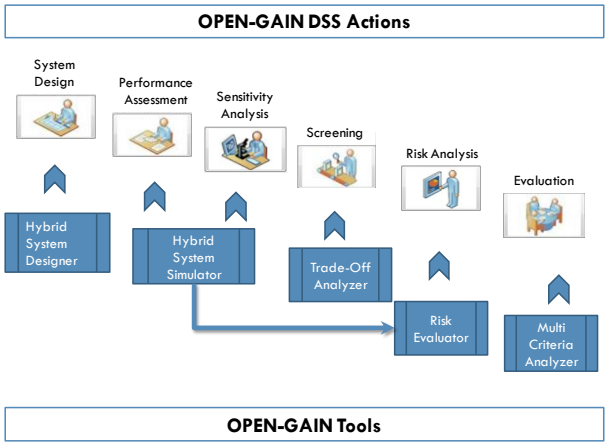

Figure 4: Relation between OPEN-GAIN Tools and DSS actions

5. OPERATIONAL ASPECTS

The operation of the OPEN-GAIN DSS is demonstrated in this section through a case study of the design and implementation of a pilot hybrid power plant. The prototype unit will be installed in the campus of the C.R.T.En research institute in a seaside location 25 km from Tunis, Tunisia. It is designed to meet the water and electricity needs of a small community situated in an arid area not connected to the electricity network. For meeting local water needs, the capacity of the desalination unit is set at 24 m^3/d. Further assumptions include the additional power needed to meet the external electricity load, estimated at 4 kW, and the quality of brackish water to be desalinated (TDS = 16,000 mg/l).

Figure 5 presents a screenshot of the DSS front-end. A friendly GUI allows the user to have access to the six DSS-Actions, either sequentially, during the decision making phases, or separately.

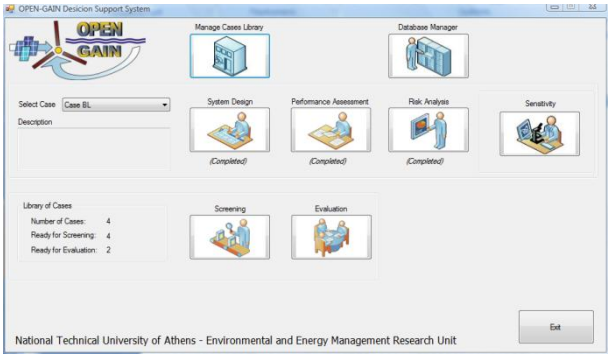

Figure 5: OPEN-GAIN DSS Front-End

The system design action of the DSS has been described in Kartalidis, Arampatzis and Assimacopoulos 2008 and will not be elaborated here. The results from the performance assessment, sensitivity analysis and risk analysis actions refer to a single configuration (Tunis Pilot Plant). The installed power of the system components, as was proposed by the system design action, is presented in Table 3

Table 3: Components sizes for case study

Component	Model	Total Size
PV Panel	Green Solar 185W	15 (kWp)
PV Inverter	Sunny Mini Central 5000	15 (kW)
WEC Turbine	Proven 15	15 (kW)
WEC Inverter	Windy Boy 6000A	18 (kW)
Diesel Engine	Perkins 404C 22-G	22 (kW)
Energy Manager	Sunny Island 5048	15 (kW)
Batteries	Sun Extender Concorde	40.32 (kWh)

The screening and evaluation actions are demonstrated by comparing the base case (Tunis Pilot Plant) to three alternative configurations:

- *Battery to Load*: Corresponds to the same component configuration as in the base case where the battery system can also be used to cover external electricity demand (by default, the battery system provides electricity only for meeting the RO unit energy requirements and not external load). This case is expected to increase the exploitation of the renewable energy through more intensive use of the battery.
- *Diesel to Battery*: Corresponds to the same component configuration as in the base case, where the diesel engine can be used to charge the battery system when the battery charge level falls below a critical point. This case is expected to decrease the period of time that the battery charge is below the critical level, thus increasing its lifetime.
- *No Diesel*: Corresponds to an alternative configuration to the power plant, where all components are of the same size, except for the diesel engine which is not included. This case is used to examine the role of the diesel engine in meeting the energy demand when the renewable components fail to manage it.

Figure 6 is a screenshot of the OPEN-GAIN DSS Cases Manager, which is used to manage the library of alternative system configurations, produced and assessed by the DSS actions.

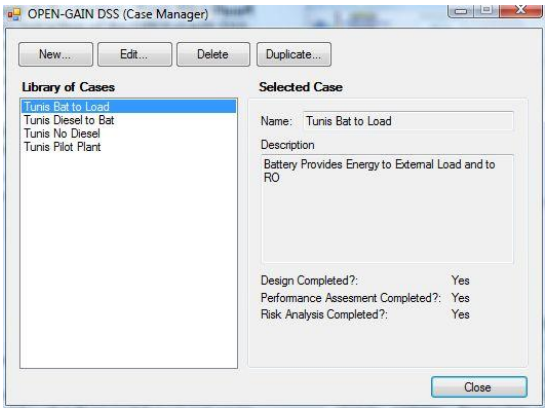

Figure 6: OPEN-GAIN DSS Cases Manager

5.1. Performance Assessment of Tunis Pilot Plant (Base Case)

The output of the performance assessment action, on the basis of 3,000 measured hourly meteorological data, is presented in Figure 7. The left column of the results page contains summary results for energy flows, diesel engine operation, battery status and financial and environmental cost. The right column presents the values of the eleven performance indicators, as described in Table 2. The main conclusions from the presented results are:

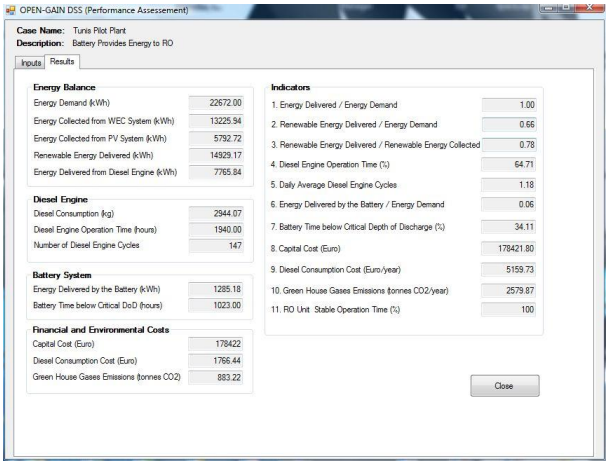

Figure 7: Performance assessment results

- The hybrid system is capable to provide all the power required for the operation of the RO unit as well as the additional power needed to meet the external electricity load (indicators 1 and 11).
- The share of renewable energy to the total energy supplied to the loads is 66% (indicator 2), while the remaining 34% of the energy required to match the loads is supplied by the diesel generator. This results in extensive use of the diesel generator (indicator 4) as well as frequent start/stop cycles (indicator 5) that contribute to wear-off of the diesel engine. The contribution of the renewable energy is expected to increase with increasing PV (or WEC) size. It is thus important to further investigate the influence of PV size on the performance of the system.
- The percentage of the renewable energy collected and delivered to the demand is 78% (Indicator 3). The remaining 22% is excess energy that needs to be dumped. This energy can be better exploited by installing a battery system with higher capacity (Indicator 6 values indicate that the battery system is under-used).
- The results can help the user to quantify the expected energy production, the annual fuel cost, the CO_2 emissions, the expected battery and diesel engine cycles, the installation cost etc.

5.2. Sensitivity analysis on the PV size

The influence of the installed PV size on different aspects of the system is illustrated in Figures 8 to 11. The charts presented in these figures have been produced using the sensitivity analysis action of the OPEN-GAIN DSS, where PV size ranges from 10 kWp to 20 kWp.

As illustrated in Figure 8, the contribution of the renewable energy to the energy balance increases with increasing PV size (from 61% to almost 69% when PV size changes from 10 to 20 kWp). However, as can been seen in Figure 9, the excess renewable energy that must be dumped also increases. This means that a larger battery system is required in order to better exploit the renewable energy potential of the area.

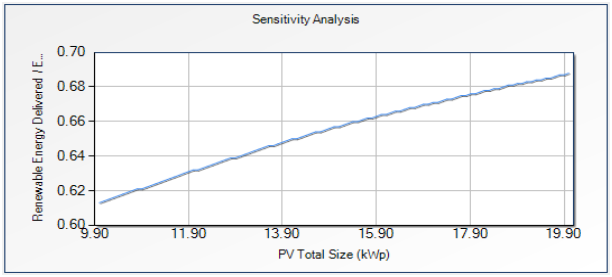

Figure 8: Influence of PV size on the ratio of renewable energy delivered to the total energy demand

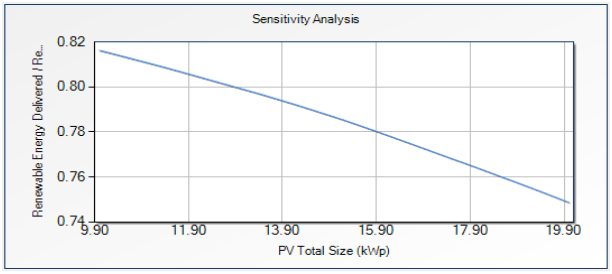

Figure 9: Influence of PV size on the ratio of renewable energy delivered to the renewable energy

The extensive use of PV system makes the diesel generator less important and the diesel consumption decreases with increasing PV size (Figure 10). However, more start/stop cycles of the diesel generator are required if PV size increases (Figure 11). This is due to the fact that the diesel generator is used to meet the shorter but more frequent peaks of the energy demand that is not met by the renewable energy components.

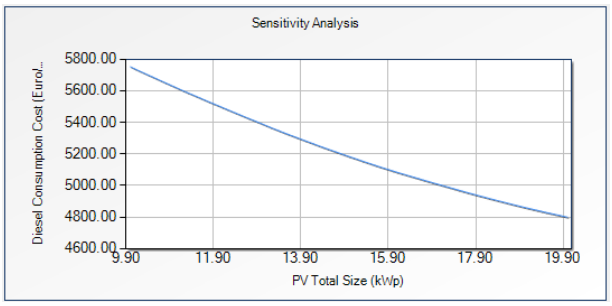

Figure 10: Influence of PV size on the diesel consumption cost

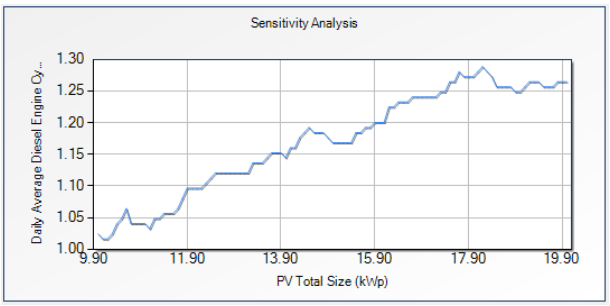

Figure 11: Influence of PV size on the daily average diesel engine cycles

5.3. Comparison of alternative cases

The use of the screening action of the OPEN-GAIN DSS is demonstrated by comparing the performance of the base case to the three alternative cases, all designed to meet the same energy requirements as the base case.

A comparison of the base case (Tunis Pilot Plant) and the battery to load case (Tunis Bat to Load), is presented in Figure 12. From the results presented in the Figure it is evident that:

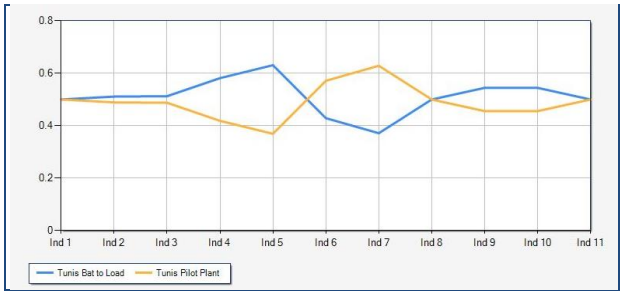

Figure 12: Comparison of base case and the battery to load case

- The "Battery to load" case performs significantly better in Indicators 4 (Diesel Engine Operation Time), 5 (Daily Average Diesel Engine Cycles), 9 (Diesel Consumption Cost) and 10 (Green House Gasses Emissions). The use of the battery system to cover the external load results in less intensive use of the diesel engine. For example, diesel consumption cost drops to 4,317 from 5,160 Euro/year in the base case while the daily diesel engine cycles drops to 0.69 from 1.18 in the base case.
- As expected, the "Battery to load" case also achieves higher exploitation of the renewable energy. The contribution of renewable energy to the energy balance (indicator 2) rises to 69% from 66% in the base case. The percentage of renewable energy collected and delivered to demand (indicator 3) also increases (from 78% to 82%).
- However, because of the intensive use of the battery, the "Battery to load" case performs lower in indicators 6 (Energy Delivered by the Battery / Energy Demand) and 7 (Battery Time Bellow Critical DoD).

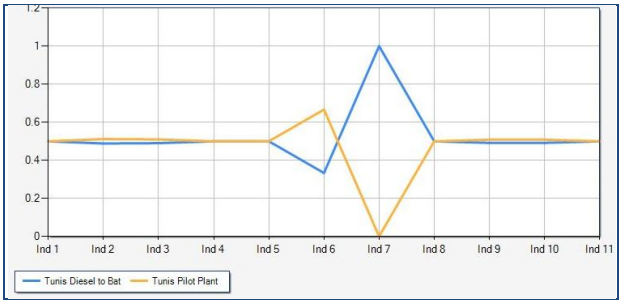

Figure 13: Comparison of base case and the engine to battery case

A comparison of the base case (Tunis Pilot Plant) and the engine to battery case (Tunis Diesel to Bat), is presented in Figure 13. The applied energy management rule significantly decreases the percentage of time that the battery is below the critical charge level (indicator 7). In fact, this percentage drops to 0%, from 34% in the base case. However, the use of the battery becomes more intensive (indicator 6), because part of the energy generated by the diesel engine must first be stored in the battery before it is delivered to the demand.

A comparison of the base case (Tunis Pilot Plant) and the case without a diesel engine (Tunis No Diesel) is presented in Figure 14. This is an extreme case that results in zero diesel consumption, also affecting the relevant indicators (indicator 4 - diesel engine operation time, indicator 5 – diesel engine cycles, indicator 9 – diesel consumption cost and indicator 10 – GHG emissions). However, the main drawback of the configuration is that it is unable to fully meet the energy demand (both the demand of RO unit and the external load). The ratio of the energy delivered to energy demand drops to 0.68 while the RO unit stable operation time is reduced to 87%. This means that 13% of the time, the produced energy is not sufficient to operate the RO unit. This percentage would decrease if the size of the renewable energy components is increased.

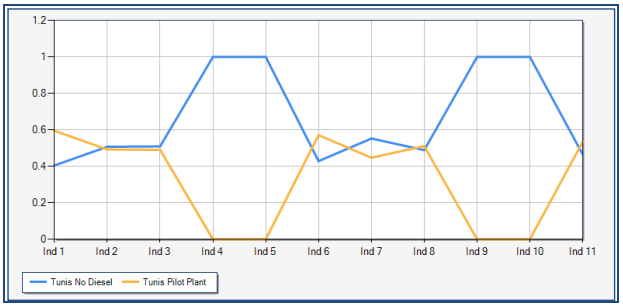

Figure 14: Comparison of base case and the case without a diesel engine

5.4. Sensitivity analysis of the No Diesel case

Figures 15 and 16 present the variation of the RO unit stable operation time with the size of the PV and battery system, respectively. It is obvious that, even when increasing the size of each component by 300%, fully stable operation of the RO unit (100%) is not achieved. The indictor reaches a maximum value of 96% when

increasing the size of the PV system and rises almost linearly when increasing the battery size.

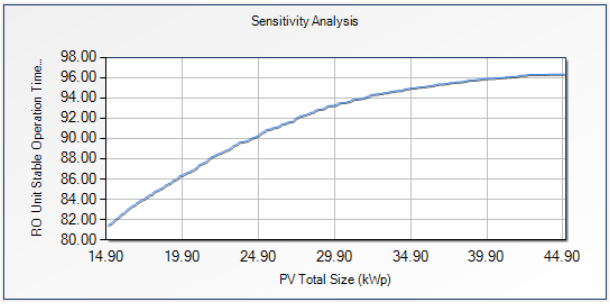

Figure 15: The RO unit stable operation time, as the PV total size rises from 15 kWp to 45 kWp

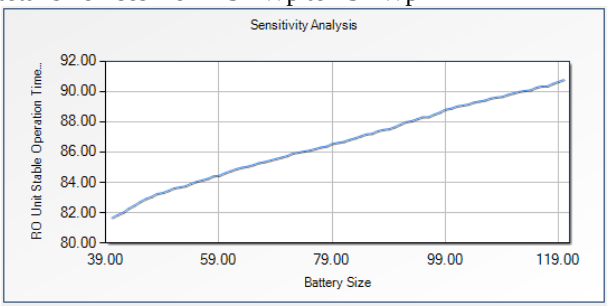

Figure 16: The RO unit stable operation time, as the battery size rises from 40 kWh to 120 kWh

5.5. Risk Analysis

The Risk analysis tool action provides information about the distribution of the performance indicators if the risk parameters of the system are taken into account. These parameters are:

- Diesel Price
- Mean Wind Speed
- Solar Radiation
- Daily Water Demand
- Daily Power Demand

The user provides the distribution and the specific values governing the parameters (e.g. mean value, deviation etc.). The results are given as histograms of the distribution of the performance indicators. Figure 17 illustrates the distribution of the diesel consumption cost indicator.

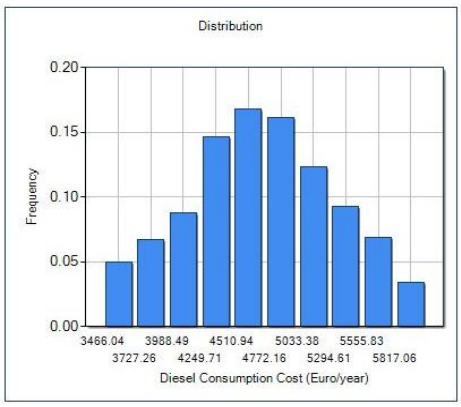

Figure 17: Diesel consumption distribution

5.6. Evaluation

Evaluation is the last action of the OPEN-GAIN DSS. The user selects cases from the cases library in order to evaluate them using a multi criteria analysis and obtain a ranking. The user defines weight factors for the multi criteria analysis according to their experience and priorities. A typical ranking for the 4 alternative cases is illustrated in Figure 18.

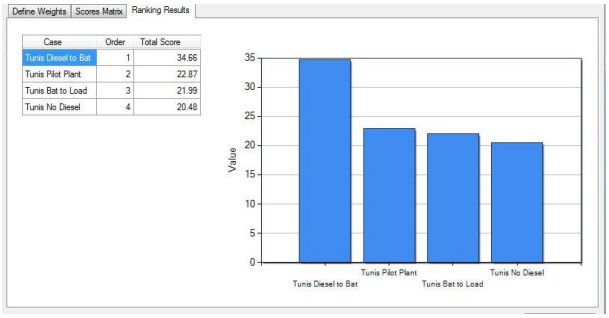

Figure 18: Cases ranking histogram

The "Tunis Base Case – Diesel to Battery" has the best performance, while the other three cases all have lower scores.

6. CONCLUSIONS

The OPEN-GAIN DSS is a software tool that can help the user/designer to design and evaluate the performance of renewable energy hybrid power plants for producing water and electricity. The software's interface is user friendly with an integrated meteorological and components database. The outputs of the software provide practical results for the user/designer. The system design provides accurate design results but also expected operational results. The performance assessment is a simulation tool that can evaluate different operational strategies of the hybrid system. The sensitivity analysis tool gives the variation of the indicators as a function by defining a size range for different components, and risk analysis can provide information for probability distribution of some indicators. The screening and the evaluation indicates the best alternative according to the specific needs.

ACKNOWLEDGMENTS

The work described in this paper was inspired and carried out as Work Package 4 in the Open Gain Project funded by the EC under FP6 (Contract No. 32535).

REFERENCES

Afgan, N.H., Carvalho, M.G., 2008. Sustainability assessment of a hybrid energy system. *Energy Policy*, 36, 2903– 2910.

Bernal-Agustin. J.L., Dufo-Lopez, R., 2009. Simulation and optimization of stand-alone hybrid renewable energy systems. *Renewable and Sustainable Energy Reviews*, 13, 2111–2118.

Celik, A.N., 2006. A simplified model for estimating yearly wind fraction in hybrid-wind energy systems. *Renewable Energy*, 31, 105–118.

Dufo-Lopez, R., Bernal-Agustin, J.L., 2005. Design and control strategies of PV–diesel systems using genetic algorithms. *Solar Energy*, 79, 33–46.

Ekren, B.Y., Ekren, O., 2009. Simulation based size optimization of a PV/wind hybrid energy conversion system with battery storage under various load and auxiliary energy conditions. *Applied Energy*, 86, 1387–1394.

Elhadidy, M.A., Shaahid, S.M., 2000. Parametric study of hybrid (wind + solar +diesel) power generating systems. *Renewable Energy*, 21, 129–139.

Hemmes, K., Zaharian-Wolf, J.L., Geidl, M. and Anderson, G., 2007. Toward multi-source and multi-product energy systems. *International Journal of Hydrogen Energy*, 33, 1322-1338.

Kartalidis, A., Arampatzis, G., Assimacopoulos, D., 2008. Rapid Sizing of Renewable Energy Power Components in Hybrid Power Plants for Reverse Osmosis Desalination Proceedings of iEMSs 2008: International Congress on Environmental Modelling and Software, pp. 1264-1271.

Mathioulakis, E, Belessiotis V. and Delyannis, E., 2007. Desalination by using alternative energy: Review and state-of-the-art. *Desalination*, 203, 346–365.

Siegel, M.D., Klein S.A. and Beckman, W.A., 1081. A simplified method for estimating the monthly-average performance of photovoltaic systems. *Solar Energy*, 26, 413-418.

Modelling and control of a wind turbine equipped with a permanent magnet synchronous generator (PMSG)

J. Salazar[(a)], F. Tadeo[(b)], C. de Prada[(c)], L. Palacin[(d)]

[(a) (b) (c)]Dpt of System Engineering and automatic control, Faculty of Science, University of Valladolid, Spain
[(d)] Sugar Technology Center (CTA), Valladolid, Spain

[(a)] johanna@autom.uva.es, [(b)] fernando@autom.uva.es, [(c)] prada@autom.uva.es, [(d)] palacin@cta.uva.es

ABSTRACT
This paper describes the dynamic models for a wind turbine system equipped with a permanent magnet synchronous generator (PMSG) and a back-to-back Voltage Source Converter, which is operated with the Space Vector Modulation Technique using a symmetric switching sequence. The generator side converter works as a three-phase rectifier and the grid side converter works as an inverter, which is used to interface the wind turbine system with the stand-alone hybrid system. All the components of the wind turbine system, including a typical generator side controller and except the DC-link and the grid side converter were analyzed. These dynamic models can be used for dynamic simulation in order to test different configurations, as well as control strategies and fault detection and accommodation algorithms.

Keywords - wind turbines, pitch angle control, Permanent magnet generator, three-phase PWM rectifiers, Space Vector Modulation, Symmetric Switching Sequence.

I. INTRODUCTION

The objective of this paper is to develop computer models for a variable speed Wind Turbine System (WTS) equipped with PMSG that can be used for dynamic simulation to test different configurations, as well as control strategies and fault detection and accommodation algorithms.
One of the problems associated with variable-speed wind turbine systems is the presence of the gearbox coupling the wind turbine to the generator. This mechanical element suffers from considerable faults and increases maintenance expenses. In order to improve reliability of the wind turbine and reduce maintenance expenses, the gearbox is frequently eliminated. Hence, a variable speed wind turbines equipped with Permanent Magnet Synchronous Generators (PSMG) and power converters are being used more frequently in wind turbine application [1,2].
The conventional power converter for a small power wind turbine system (WTS) is shown in Fig. 1, which consists of the diode rectifier, boost circuit, and a grid side converter[3]. Since the uncontrolled diode rectifier is connected to the PMSG, it is not possible to control the generator speed for output power control. Moreover, high harmonic distortion currents are obtained in the generator that might reduce efficiency and produce torque oscillations.

Figure 2 shows the scheme for a variable speed wind turbine system based on a permanent magnet synchronous generator, which is analyzed in this paper. This wind turbine system is connected to the AC side of a stand-alone hybrid system which includes a battery storage system, a diesel generator and a photovoltaic system as a renewable source. This hybrid system combines with a reverse osmosis desalinization unit will be used to supply fresh water and electricity to rural remote communities not connected to the public grid. The whole designed plant is installed in the site of Bordj Cedria in Tunisia in CRTEn (Centre de Recherche et des Technologies de l'Enegie) [4].
This wind turbine system consists of a Permanent Magnet Synchronous Generator (PMSG) connected to a power electronic system, which is composed of a back-to-back Voltage Source Converter (VSC), where the generator side converter works as a three-phase rectifier and the grid side converter works as an inverter [5] This paper is focused mainly on the generator side, only the wind turbine components and generator side controller until the DC-link.

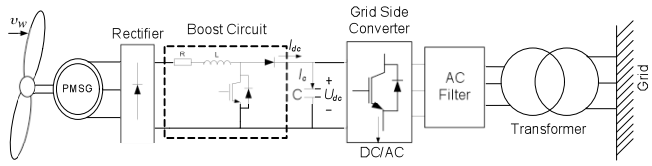

Figure 1.- Conventional block diagram of a wind turbine with PMSG

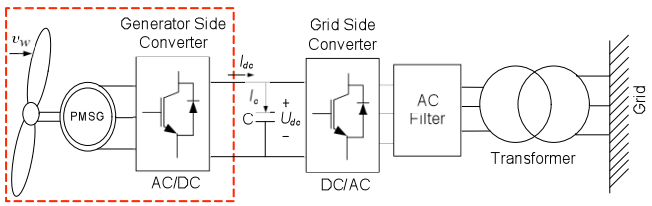

Figure 2.- Block diagram of a wind turbine with PMSG

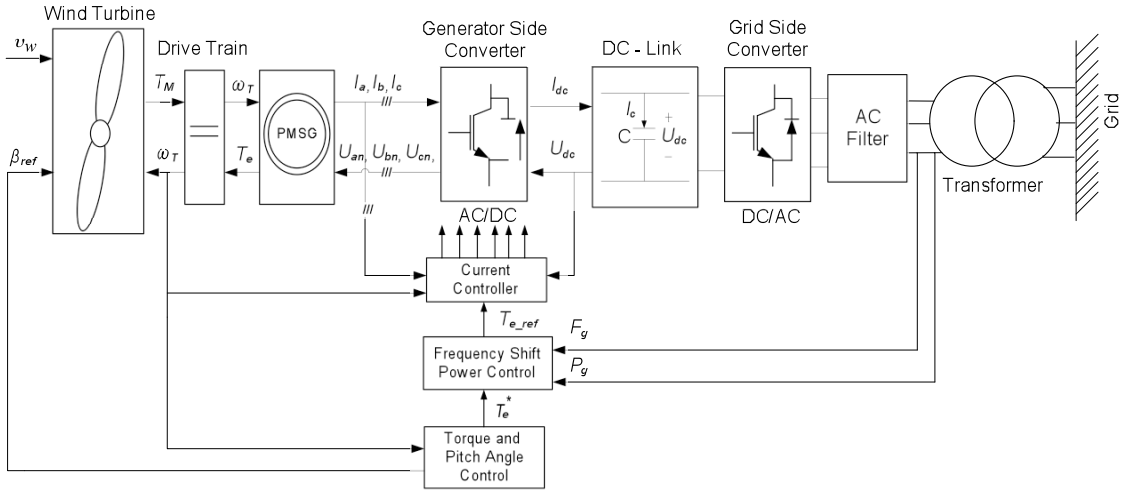

Figure 3.- PMSG driven wind turbine connected to the utility grid

Figure 3 shown a wind turbine system with its control scheme. Generator side controller is divided into a current controller, a frequency shift power control (FSPC) and Torque and Pitch Angle control. Theses controller will be briefly presented in section III. The input signals to the Generator side controller are: Grid Frequency (F_g), Grid Power (P_g), turbine rotor speed (ω_T), three phase sinusoidal current from PMSG (I_a, I_b, I_c) and the voltage of the dc bus capacitors (U_{dc}). The output signals are reference pitch angle (β_{ref}) and Generator Side Converter control

II. SYSTEM DESCRIPTION AND MODELING

The description and the modeling of a wind turbine with PMSG are described throughout this section. The mechanical components of the Wind Turbine System (the wind turbine rotor and the drive train) as well as the electrical components (the synchronous generator and the generator side converter) will be briefly presented.

A. Wind Turbine Model

The power in the wind is known to be proportional to the cube of the wind speed and may be expressed as

$$P = \frac{1}{2}\rho A v_w^3, \tag{1}$$

where ρ is the air density, A is the area swept by the blades and v_w is the wind speed. However, a wind turbine can only extract a fraction of the power, which is limited by the Betz limit (maximum 59%). This fraction is described by a power coefficient, C_p, which is a function of the blade pitch angle β and the tip speed ratio λ. Therefore the mechanical power of the wind turbine extracted from the wind by the turbine is

$$P_{mec} = \frac{1}{2}C_p(\beta,\lambda)\rho A v_w^3, \tag{2}$$

where the tip speed ratio λ is defined as the ratio between the blade tip speed and the wind speed v_w:

$$\lambda = \frac{\omega_T R}{v_w}, \tag{3}$$

ω_T is the turbine rotor speed and R is the radius of the blades. A hydraulic actuator model of pitch angle β control wind turbine is shown in Figure 4. The actuator is modeled in closed loop with saturation of the pitch rated limitation [6]. The maximum rate of change of the pitch angle is in the order of 3 to 10 degrees per second, depending on the size of the wind turbine. The signal β_{ref} is taken from *Torque and Pitch Angle Control*

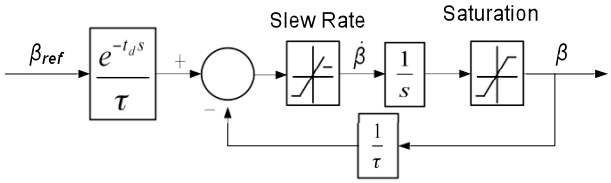

Figure 4.- Hydraulic Actuator Model

In this paper, the power coefficient is given by [7]

$$C_p(\lambda,\beta) = 0.5\left(\frac{114}{\lambda_i} - 0.4\beta - 3\right)\exp\left(\frac{-25}{\lambda_i}\right) + 0.000571\lambda, \tag{4}$$

Where

$$\lambda_i = \left[\frac{1}{\lambda + 0.08\beta} - \frac{0.035}{\beta^3 + 1}\right]^{-1} \tag{5}$$

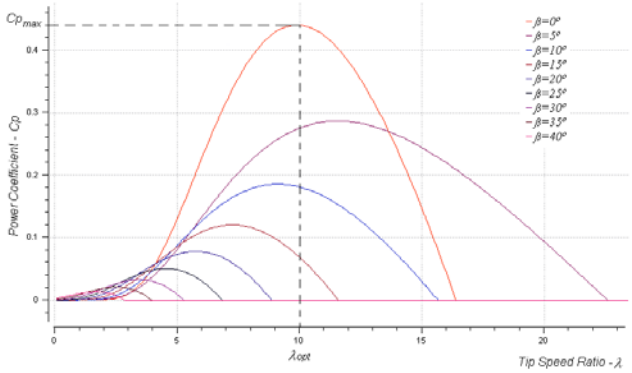

Figure 5.- Power coefficient versus tip-speed ratio

Thus, any changes in the rotor or wind speeds induce changes in the tip speed ratio, leading to power coefficient

variation. In this way, the generated power is affected. Figure 5 shows a typical C_P-λ curve for a wind turbine that follows (4). The wind turbine power coefficient is maximized (C_{p_max}=0.44) for a tip-speed ratio of λ_{opt}=6.9 when the blades pitch angle is β=0°.

The wind turbine is said to have a yaw error, if the rotor is not perpendicular to the wind. Considering θ_w as the wind direction and θ_t the yaw turbine angle, then the yaw error angle θ_c is defined as the difference between θ_w and θ_t.

$$\theta_c = \left| \theta_w - \theta_t \right| \tag{6}$$

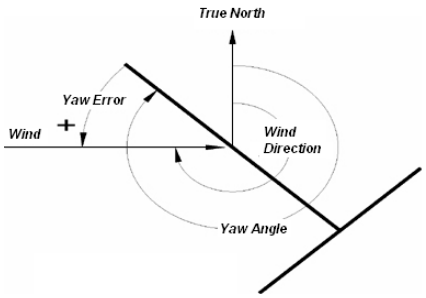

Figure 6.- Yaw angle convention

θ_c implies that a small wind energy share is going to be converted. The turbine generated power follows a cosine function of θ_c.

$$P_{mec} = P_{mec}(\theta_w)\cos(\theta_c) \tag{7}$$

B. Drive Train Model

The mechanical system of the wind turbine can be simply modeled with the one-mass model given by [8]:

$$J_{total}\frac{\partial \omega_T}{\partial t} = T_M - T_e, \tag{8}$$

where $J_{total}=J_T+J_g$ is the inertia constant of the whole drive train, with J_T and J_g the inertia constants of the turbine and the generator, respectively; n_p is the number of pole pairs; T_e is the generator electromagnetic torque and the mechanical torque of the turbine T_M is given by

$$T_M = \frac{P_{mec}}{\omega_T} = \frac{1}{2}\frac{C_p(\beta,\lambda)\rho A v_w^3}{\omega_T}, \tag{9}$$

C. Permanent Magnet Synchronous Generator Model

The rotor excitation of the Permanent Magnet Synchronous Generator (PMSG) is assumed to be constant, so its electrical model in the synchronous reference frame is given by [9, 10]:

$$L_S\frac{\partial i_{ds}}{\partial t} = u_{ds} - R_S i_{ds} + L_S\omega_e i_{qs}, \tag{10}$$

$$L_S\frac{\partial i_{qs}}{\partial t} = u_{qs} - R_S i_{qs} - L_S\omega_e i_{ds} + \omega_e\psi_f, \tag{11}$$

where subscripts'd' and 'q' refer to the physical quantities that have been transformed into the dq synchronous rotating reference frame; R_s is the stator resistance; L_s is the inductances of the stator; u_{ds} and u_{qs} are, respectively, the d- and q- axis components of stator voltage; i_{ds} and i_{qs} are, respectively, the d- and q- axis components of stator current; ψ_f is the permanent magnetic flux and the electrical rotating speed ω_e is given by:

$$\omega_e = n_p\omega_T, \tag{12}$$

Considering Inverse Park and Clarke Transformation a two co-ordinate time invariant (i_{qs}, i_{ds}) is transformed into a three phase sinusoidal system (I_a, I_b, I_c), where are the inputs to the generator side converter model.

$$\begin{bmatrix} I_a \\ I_b \\ I_c \end{bmatrix} = \begin{bmatrix} \cos(\omega_e t) & -\sin(\omega_e t) \\ \cos\left(\omega_e t - \frac{2\pi}{3}\right) & -\sin\left(\omega_e t - \frac{2\pi}{3}\right) \\ \cos\left(\omega_e t + \frac{2\pi}{3}\right) & -\sin\left(\omega_e t + \frac{2\pi}{3}\right) \end{bmatrix} \begin{bmatrix} i_{ds} \\ i_{qs} \end{bmatrix} \tag{13}$$

The power equations are given by

$$P_s = \frac{3}{2}\left(u_{ds}i_{ds} + u_{qs}i_{qs}\right), \tag{14}$$

$$Q_s = \frac{3}{2}\left(u_{qs}i_{ds} - u_{ds}i_{qs}\right), \tag{15}$$

where P_s and Q_s are the output active and reactive powers, respectively.

The electromagnetic torque T_e can be derived from

$$T_e = -\frac{3}{2}n_p\psi_f i_{qs}, \tag{16}$$

D. Generator Side Converter Model

Nowadays the back-to-back Voltage Source Converter (VSC) is the most used converter topology in the wind turbine industry as depicted in Figure 7. This converter can operate in rectifier or inverter mode, thus a bi-directional power flow can be achieved. In the present paper, the generator side converter works as a rectifier, being able to control the torque and speed, while the grid side converter works as an inverter keeping constant the voltage in the DC-link [11].

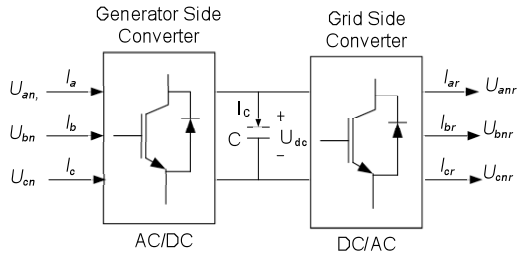

Figure 7.- Structure of the back-to-back voltage source converter

A VSC can be implemented in several ways: six-step, Pulse Amplitude Modulated (PAM) or Pulse Width Modulated (PWM). The paper is focused on the implementation of a PWM VSC, but the idea can be easily extended to other configurations.

A three-phase rectifier is shown in Figure 8: U_{dc} is the voltage of the dc bus capacitors; U_{an}, U_{bn} and U_{cn} are the phase voltage and each switch is identified with the letter S. It is assumed

that S_a and S_a^*, S_b and S_b^* as well as S_c and S_c^* are switched in a complementary way to avoid a short circuit in the voltage source. Thus, the analysis of the switches turn-ons/offs is simplified as we only consider the switches of the three upper transistors S_a, S_b and S_c. If S_a is equal to 1, the switch of the transistors is on and vice verse. As we have three variables, there are (2^3=8) possible switching vectors; as shown in Table I.

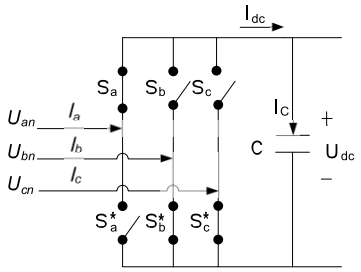

Figure 8.- Structure of the back-to-back voltage source converter

The applied voltages at the Permanent Magnet Synchronous Generator terminals as a function of the DC-link voltage and the switching functions are:

$$\begin{bmatrix} U_{an} \\ U_{bn} \\ U_{cn} \end{bmatrix} = \frac{U_{dc}}{3} \begin{bmatrix} 2 & -1 & -1 \\ -1 & 2 & -1 \\ -1 & -1 & 2 \end{bmatrix} \begin{bmatrix} S_a \\ S_b \\ S_c \end{bmatrix} \quad (17)$$

Considering Park and Clarke Transformation a three phase sinusoidal system (U_{an}, U_{bn}, U_{cn}) is transformed into a two co-ordinate time invariant (u_{ds} ,u_{qs}, u_o), where are the inputs to the Permanent Magnet Synchronous Generator (PMSG) Model. The angle used to make the transformation is given by:

$$\theta = \omega_e t \quad (18)$$

Considering this angle, the transformation gives:

$$\begin{bmatrix} u_{ds} \\ u_{qs} \\ u_o \end{bmatrix} = \frac{2}{3} \begin{bmatrix} \cos(\theta) & \cos\left(\theta - \frac{2\pi}{3}\right) & \cos\left(\theta + \frac{2\pi}{3}\right) \\ -\sin(\theta) & -\sin\left(\theta - \frac{2\pi}{3}\right) & -\sin\left(\theta + \frac{2\pi}{3}\right) \\ \frac{1}{2} & \frac{1}{2} & \frac{1}{2} \end{bmatrix} \begin{bmatrix} U_{an} \\ U_{bn} \\ U_{cn} \end{bmatrix} \quad (19)$$

The DC-link current can be expressed as a function of the input currents and the switching functions by:

$$I_{dc} = \begin{bmatrix} S_a & S_b & S_c \end{bmatrix} \begin{bmatrix} I_a \\ I_b \\ I_c \end{bmatrix} \quad (20)$$

III. MODEL OF CONTROLLERS

A. Current controller Model

The current control scheme of the generator side converter is show in Figure 9. This control is based on projections which transform a three phase time and speed dependent system into a two co-ordinate (d and q co-ordinates) time invariant system. These projections lead to a structure similar to that of a DC control that make easier AC control [12]. In order to design independent controllers for the two coordinates, the influences of the q-axis on the d-axis component, and vice versa, must be eliminated [13]. For this the decoupling voltages u_{ddec} and u_{qdec} are given by

$$u_{ddec} = u'_{ds} - L_s \omega_e i_{qs} \quad (21)$$

$$u_{qdec} = u'_{qs} + L_s \omega_e i_{ds} - \omega_e \psi_f \quad (22)$$

These decoupling voltages are added to the current controller outputs, resulting in the control signal for the PWM-rectifier. In order to combine a fast response of the controlled variable to a change of the set point with zero steady state deviation, proporcional integral (PI) current controllers are chosen. Control equations are given by:

$$\frac{\partial x_1}{\partial t} = i_{ds\_ef} - i_{ds} \quad (23)$$

$$\frac{\partial x_2}{\partial t} = i_{qs\_ef} - i_{qs} \quad (24)$$

$$u'_{ds} = K_{p1} \Delta i_{ds} + K_{i1} x_1 \quad (25)$$

$$u'_{qs} = K_{p2} \Delta i_{qs} + K_{i2} x_2 \quad (26)$$

The required d-q components of the rectifier voltage vector are given by:

$$u_{ds\_ref} = K_{p1} \Delta i_{ds} + K_{i1} x_1 - L_s \omega_e i_{qs} \quad (27)$$

$$u_{qs\_ref} = K_{p2} \Delta i_{qs} + K_{i2} x_2 + L_s \omega_e i_{ds} - \omega_e \psi_f \quad (28)$$

The control requires the measurement of the stator currents, dc voltage and rotor position. Space Vector Modulation (SVM) is used to generate the switching signals for the power converter semiconductors.

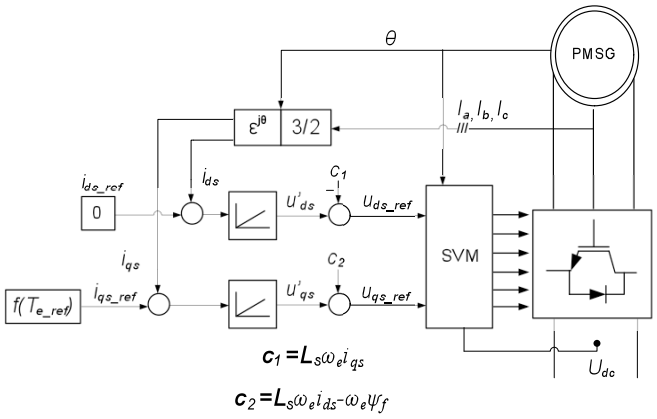

Figure 9.- Current controller Model

The stator current reference in d-axis $i_{ds\text{-}ref}$ is maintained at zero, for producing maximum torque, due to the non-saliency of the generator. The stator current reference in q-axis $i_{qs\text{-}ref}$ is calculated from the reference torque $T_{e\text{-}ref}$ as follows.

$$i_{qs\_ref} = -\left(\frac{2}{3 n_p \psi_f}\right) T_{e\_ref} \quad (29)$$

B. *Frequency Shift Power Control Model*

If Wind Turbine System (WTS) is connected to the AC side of the stand-alone hybrid system, as depicted in Figure 10, battery inverter must be able to inform to the WTS when it must limit its output power in order to prevent the excess energy from overcharging the battery. The communication language is frequency. In other words, the battery inverter recognizes this situation and changes the frequency at the AC output. This frequency is analyses by Wind Turbine System which limits its output power according to the frequency previously defined by battery inverter. The operating principle used by WTS is called Frequency Shift Power Control (FSPC) [14]. This function is shown in the Figure 11, for more information read Sunny Island 5048 Manual

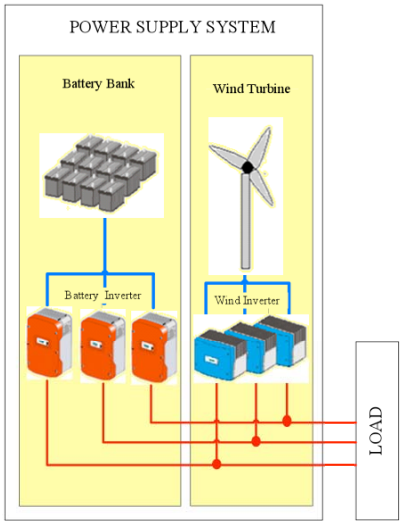

Figure 10.- Block diagram of a stand-alone grid

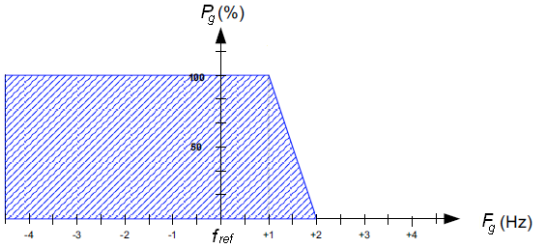

Figure 11.- Frequency Shift Power Control

f_{ref} refers to the base frequency of the stand- alone grid, in our case, it is equal to 50Hz. When the grid frequency deviation is less than 1 Hz and higher than -5Hz, $\%P_g$ is equal to 100%; when a grid frequency deviation occurs between 1 and 2 Hz, $\%P_g$ is different from 100% and when the grid frequency deviation is higher than 2 Hz, $\%P_g$ is equal to 0%.

The control scheme is depicted in Figure 12. When a grid frequency deviation Δf occurs a bias power set point, ΔP, is generated follows function shown in Figure 11. Then, the bias power set point is divided into the turbine rotor speed ω_T to obtain a bias electric torque set point, ΔT_e, which is added to the electric torque set point T_e^* from *Torque and Pitch Angle Control* to calculate a reference electric torque, $T_{e\text{-}ref}$, which is used to calculate $i_{qs\text{-}ref.}$ in *Current Controller*.

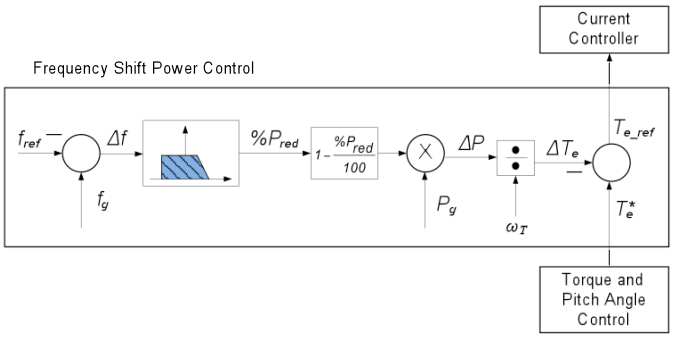

Figure 12.- Frequency Shift Power Control

C. *Torque and Pitch Angle Control*

From Figure 13, you can see that the power curve is split into three distinct regions. Region I consists of low wind speeds and is below the rated turbine power, the turbine is run at the maximum efficiency to extract all power. In other words, the turbine controls with optimization in mind. On the other hand, Region III consists of high wind speeds and is at the rated turbine power. The turbine then controls with limitation of the generated power in mind when operating in this region. Finally, Region II is a transition region mainly concerned with keeping rotor torque and noise low [15].

When the wind speed is lower than cut-in wind speed or higher than cut-out wind speed, the wind turbine could not generate power, and the pitch angle is usually set to 90°.

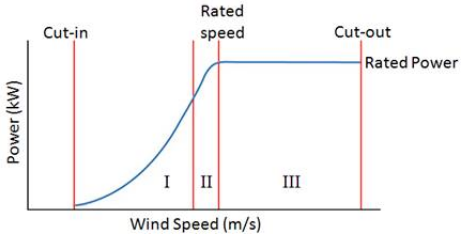

Figure 13.- Operating region of wind turbines

1.- Low Wind Speed Operation (Region I)

The main objective is to capture as much power as possible from the wind. All three control strategies (yaw drive, generator torque, and blade pitch) may be used in this region; however, it is common to use only generator torque and yaw control for most of the time in region 2, keeping the blade pitch constant at an optimal value β_{ref}=0°. To ensure maximal energy yield, the reference speed is set such that the tip speed ratio, λ is maintained at its optimal value, λ_{opt} according to equation X

$$\omega_T^* = \frac{\lambda_{opt}\, v_w}{R} \tag{30}$$

The control scheme is shown in Figure 14

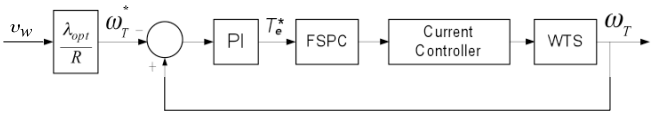

Figure 14.- Control scheme in low wind Speed

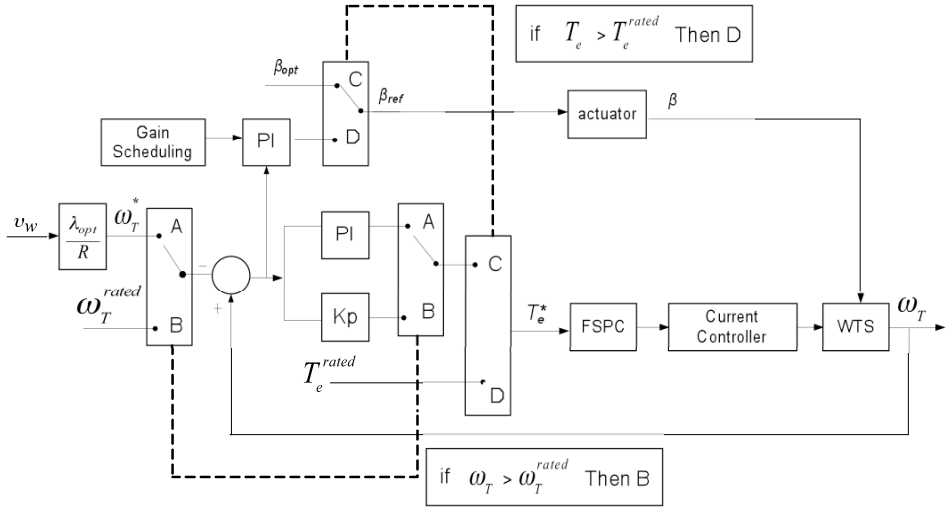

Figure 17.- Overview of the complete control scheme

2.- Middle Wind Speed Operation (Region II)

The main objective is to keep the rotor speed in a certain spam, described as a speed band around the maximum rotor speed. The rotor speed, torque and energy capture are determined similarly as in the case of a classic fixed speed wind turbine approach. Usually this interval ends when nominal generator power is reach so in this region turbine operate below rated power. The basic scheme is shown in Figure 15.

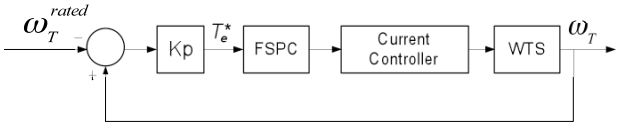

Figure 15.- Control scheme in middle wind Speed

3.- High Wind Speed Operation (Region III)

The main objective is to keep the rotor speed and especially the generated power as close as possible to the nominal. Yaw control, generator torque, and blade pitch strategies can all be used to shed excess power and limit the turbine's energy capture as well as to achieve other control objectives. The electric torque control objective is defined as production of constant rated electric power ($T_e^* = T_e^{rated}$), while the pitch control objective is defined as follows: Rotor speed regulation at rated rotor speed and yield of rated power, by controlling the blade pitch angle according to scheme shown in Figure 16.

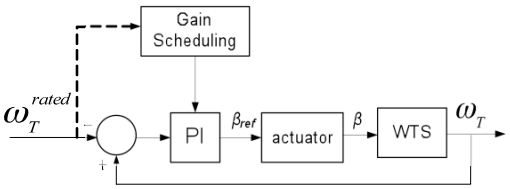

Figure 16.- Control scheme in high wind Speed

To cope with nonlinear turbine behavior caused by aerodynamics, the controller gains have been scheduled dependent on reference rotor speed. Adaptation of the rotor speed set point is a possibility that makes it possible to use the allowed rotor speed fluctuation for maintaining rated power at sudden negative wind gusts.

The control overview scheme is shown in Figure 17. It is not possible to operate in the whole speed area using only one controller and due to this the final controller is a combination of the controllers from the various wind speed intervals. Finally, after modelling and analyzing those three different controllers, the whole control scheme is obtained [16].

D. Yaw Mechanism

Horizontal axis wind turbines (HAWT) need extra devices to orientate their rotors against the wind. Yaw control would be an excellent way of controlling the power input to the wind turbine rotor. The main problem with yaw control is that the part of rotor which is closest to the source direction of the wind, however, will be subject to a large force (bending torque) than the rest of the rotor.

The yaw mechanism can be divided into two types: passive (free yaw) and active (forced yaw). Passive yaws have large application in small wind turbines. The turbine freely aligns itself to the wind direction by using a tail vane, with no need of wind measurement. Rotors with downwind configuration are another example of use of passive yaws.

IV. SPACE VECTOR MODULATION

Space Vector Modulation (SVM) became a standard for the switching power converters. The block diagram of (SVM) is shown in Figure 18. The reference output voltage vector is sampled at a fixed frequency, equal to the inverter switching period T_s. Then, the position of reference vector and the times of application of each vector generators involved are calculated. After that, a switching sequence system takes these application times to define the switches control signal. Thus, the reference vector will be really reflected in the output of the inverter during the switching period next to the reference voltage sampled time [17].

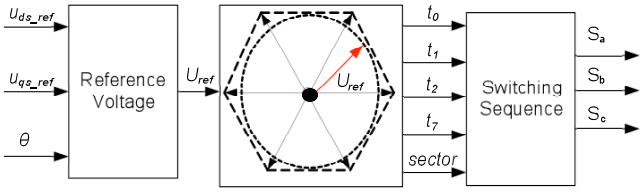

Figure 18.- Block diagram of Space Vector Modulation (SVM)

The reference voltage components in the dq reference frame ($u_{ds\text{-}ref}$, $u_{qs\text{-}ref}$) are transformed to a stationary $\alpha\beta$ reference frame using the rotor position θ as given by

$$\omega_T = \frac{\partial\theta}{\partial t}, \tag{31}$$

$$\begin{bmatrix} u_{\alpha ref} \\ u_{\beta ref} \end{bmatrix} = \begin{bmatrix} cos\theta & -sin\theta \\ sin\theta & cos\theta \end{bmatrix} \begin{bmatrix} u_{ds\_ref} \\ u_{qs\_ref} \end{bmatrix}, \tag{32}$$

where ($u_{\alpha ref}$, $u_{\beta ref}$) form an orthogonal 2-phase system. A rotating vector can be uniquely defined in the complex plane by these components as follows:

$$U_{ref} = u_{\alpha ref} + j\,u_{\beta ref} \tag{33}$$

The magnitude and angle of the output reference vector are

$$\left|U_{ref}\right| = \sqrt{u_{\alpha ref}^2 + u_{\beta ref}^2} \tag{34}$$

$$\varphi = Tan^{-1}\left(\frac{U_{\beta ref}}{U_{\alpha ref}}\right) \tag{35}$$

As shown in the Table I, the eight inverter states give eight vectors called *vector generators* (**U0, U1, ..., U7**), which are divided into 6 active switching vectors **U1, U2, ..., U6** plus 2 vectors corresponding to the zero states **U0** and **U7,** where the magnitude of the active vectors is $(2/3)U_{dc}$. Since the output voltages are at $2\pi/3$ out of phase from each other, the Space Vectors system can occupy a number of positions with an order multiple of three.

The vector generators on the αβ plane are shown in Figure 19. The tips of these vectors form a regular hexagon. We define the area enclosed by two adjacent vectors, within the hexagon, as a *sector*. Thus there are six sectors numbered 1 to 6 [18].

The reference vector, U_{ref}, placed on the αβ plane, is decomposed using any subset of the eight space vectors. Nonetheless, decomposition is done typically using only the two adjacent active vectors, by averaging the two adjacent vectors and the zero state vectors. In other words, the switching pattern is obtained by selecting the nearest two active vectors of the six available and filling the rest of the switching period with zero space vectors **U0** and **U7**.

Voltage Vector	S_a	S_b	S_c
U0 = 0	0	0	0
U1 = $\left(\frac{2}{3}\right)U_{dc}$	1	0	0
U2 = $\left(\frac{1}{3}\right)U_{dc} + j\left(\frac{\sqrt{3}}{3}\right)U_{dc}$	1	1	0
U3 = $-\left(\frac{1}{3}\right)U_{dc} + j\left(\frac{\sqrt{3}}{3}\right)U_{dc}$	0	1	0
U4 = $-\left(\frac{2}{3}\right)U_{dc}$	0	1	1
U5 = $-\left(\frac{1}{3}\right)U_{dc} - j\left(\frac{\sqrt{3}}{3}\right)U_{dc}$	0	0	1
U6 = $\left(\frac{1}{3}\right)U_{dc} - j\left(\frac{\sqrt{3}}{3}\right)U_{dc}$	1	0	1
U7 = 0	1	1	1

Table I.- Inverter Voltage Vectors

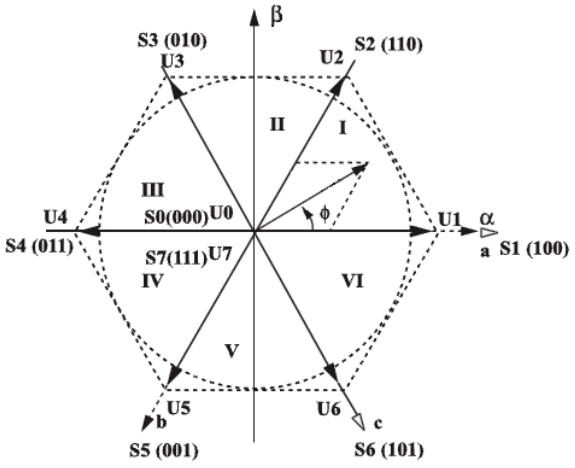

Figure 19.- Voltage space vectors on the αβ plane

In the particular example of Figure 20, the reference vector is represented by an vector U_{ref} rotating in the counter

clock wise direction, located between 0° and 60° degree, the two adjacent active vectors are **U1** and **U2**.

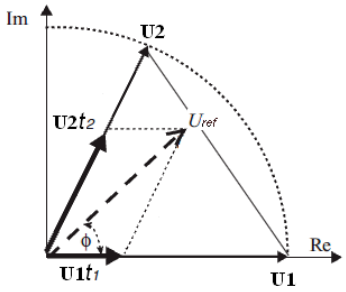

Figure 20.- Reference Vector placed on the αβ plane

The time spent on each of the active space vectors (denoted t_0, t_1, t_2 and t_7) are determinated by

$$U_{ref} = \frac{t_1}{T_s}\mathbf{U1} + \frac{t_2}{T_s}\mathbf{U2} + \frac{t_0}{T_s}\mathbf{U0} + \frac{t_7}{T_s}\mathbf{U7}, \quad (36)$$

Considering that the magnitudes of zero space vectors **U0** and **U7** are 0, we obtain

$$T_s U_{ref} = \mathbf{U1}t_1 + \mathbf{U2}t_2, \quad (37)$$

where T_s is the switching period; t_1 and t_2 are the time spent respectively on the two active vectors **U1** and **U2** adjacent to the reference vector. Decomposition along the Real and Imag axes yields

$$T_s\left|U_{ref}\right|\cos\varphi = \frac{2}{3}U_{dc}t_1 + \frac{1}{3}U_{dc}t_2 \quad (38)$$

$$T_s\left|U_{ref}\right|\sin\varphi = 0t_1 + \frac{\sqrt{3}}{3}U_{dc}t_2 \quad (39)$$

with the solution:

$$t_1 = \frac{3\left|U_{ref}\right|T_s}{2U_{dc}}\left[\cos\varphi - \frac{\sin\varphi}{\sqrt{3}}\right] = \frac{\sqrt{3}\left|U_{ref}\right|}{U_{dc}}T_s\sin\left(\frac{\pi}{3} - \varphi\right) \quad (40)$$

$$t_2 = \frac{\sqrt{3}\left|U_{ref}\right|}{U_{dc}}T_s\sin\varphi \quad (41)$$

Zero state vectors are used to fill-up the gap to a constant sampling interval. t_0 and t_7 is the time spent on the zero space vectors **U0** and **U7**, respectively.

$$t_0 + t_7 = \frac{T_s - t_1 - t_2}{2} \quad (42)$$

The angle of reference vector, φ, identifies one of the six sectors on αβ plane. An relative angle, ε_r ($0 \le \varepsilon_r \le \pi/3$), is defined according to a specific sector, such as

$$\varepsilon_r = \varphi - (r-1)\frac{\pi}{3}, \qquad r = 1,2,\ldots,6 \quad (43)$$

The application times are given by

$$t_a = \frac{\sqrt{3}\left|U_{ref}\right|}{U_{dc}}T_s\sin\left(\frac{\pi}{3} - \varepsilon_r\right) \quad (44)$$

$$t_b = \frac{\sqrt{3}\left|U_{ref}\right|}{U_{dc}}T_s\sin\varepsilon_r \quad (45)$$

Switching Sequence Schemes

The active space vectors generate the same average output voltage regardless of the order in which they are applied within the current sampling period. SVM does not recommend any specific order. These degrees of freedom make the difference between Space Vector methods.

Space vector modulation also offers flexibility with zero vectors. They can be used in any order within the switching period and relative to active vectors. The order of individual zero vectors during the inactive time is another degree of freedom.

In this paper we have chosen the switching sequence called Symmetric Sequence: each switching period starts and ends with a zero vector and active vectors are exchanged. The reference voltage can be constructed by the switching pattern shown in Figure 21. **Ux** can be **U1**, **U3**, **U5**. **Uy** can be **U2**, **U4**, **U6**. This pattern satisfies the condition that only one transistor is switched during a change interval. This scheme is expected to have low THD (***T**otal* ***H**armonic* ***D**istortion*) because of the symmetry in the waveforms [19].

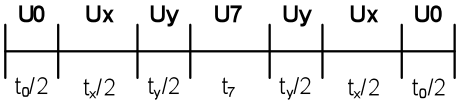

Figure 21.- Switching pattern for Symmetric Sequence

The switching pattern for different sectors is shown in the Figure 22.

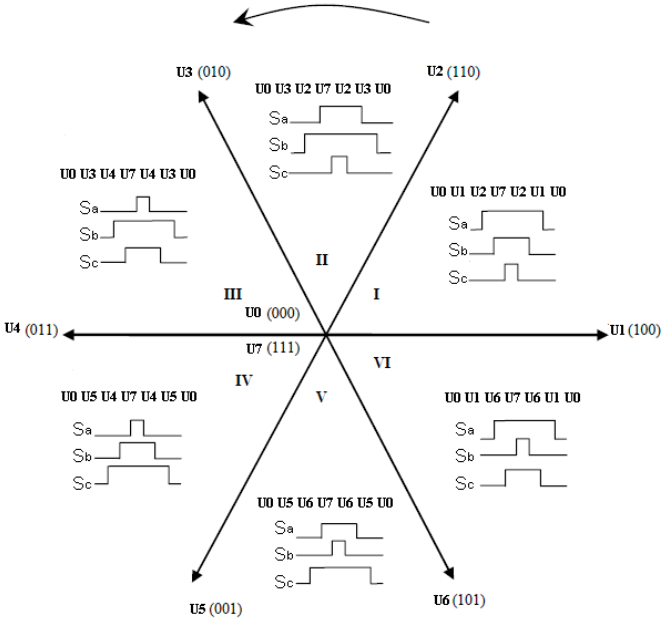

Figure 22.- Switching pattern for different sectors

In the example of Figure 23, the sequence of vectors applied in this scheme is shown in Figure 11 for sector 1. The number of commutations in one switching period is six with three turn-ons and three turn-offs.

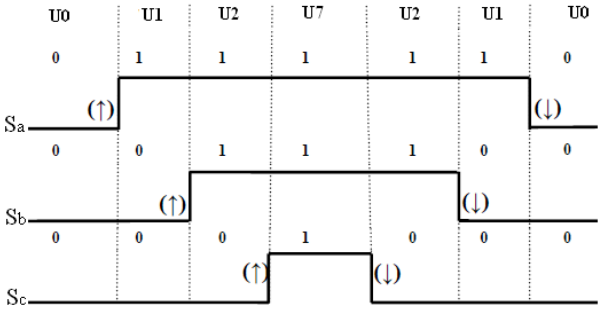

Figure 23.- Switching pattern for vector reference located in the sector 1

V. CONCLUSION

This work has presented the modelling of a wind turbine system equipped with a Permanent Magnet Synchronous Generator (PMSG) for dynamical simulation and controller design. PMSG generated voltage is converted into DC voltage though a Voltage Source Converter (VSC) that works as rectifier. The generator side converter is used to control power; the grid side converter is used to control dc-link voltage. The DC-link capacitor voltage is maintained at a constant value by ensuring the balance of the input and output energies at both sides of the capacitor. The future work will be to complete the scheme wind turbine system, simulate the whole system and compare this result with typical configurations for controller design.

REFERENCE

[1] H. Polinder, F. F. A. Van De Pijil, G. J. De Vilder and P. J. Tavner, "*Comparison of direct drive and geared generator concepts for wind turbine*", IEEE Trans. Energy Conver. 21(3) (2006) 725-733

[2] J.G. Slootweg, S.W.H. de Haan, H. Polinder, and W.L. Kling, "*Modeling wind turbines in power system dynamics simulations"* IEEE Power Engineering Society Summer Meeting, vol. 1, July 2001,pp. 22 – 26.

[3] Fujin Deng and Zhe Chen, "*Power Control of Permanent Magnet Generator Based Variable Speed Wind Turbines"*, IEEE Trans Energy Conver. (2006).

[4] J. Salazar, F. Tadeo, C. Prada. "*Renewable Energy for Desalinization using Reverse Osmosis*" International Conference on Renewable Energies and Power Quality (ICREPQ'10) Granada (Spain), 23th to 25th March, 2010

[5] DENG Qiu-ling, LIU Gou-rong and XIAO Feng. "*Control of Variable-speed Permanent Magnet Synchronous Generators Wind Generation System*". IEEE Trans Energy Conver (2008).

[6] Fernando D. Bianchi, Hernan De Battista, and Ricardo J. Mantz. "*Wind Turbine Control Systems*". British Library Cataloguing, 2007.

[7] Raiambal K. y Chellamuthu C. "*Modelling and simulation of grid connected wind electric generating system*". Anales de IEEE TENCON, 1847-1852. 2002

[8] F. Mei, B. C. Pal, "*Modelling and small-signal analysis of a grid connected doubly-fed induction generator*" presented at Proceeding of IEEE PES General Meeting 2005, San Francisco, USA, 2005.

[9] F. Wua, X.-P. Zhangb, P. Jua; "*Small signal stability analysis and control of the wind turbine with the direct-drive permanent magnet generator integrated to the grid*"; 2009

[10] Dmitry Svechkarenko, "*Simulations and Control of Direct Driven Permanent Magnet Synchronous Generator*", Proyect Work, Royal Institute of Technology, Department of Electrical Engineering, Electrical Machines and Power Electronics, December, 2005.

[11] Cristian Busca, Ana-Irina Stan, Tiberiu Stanciu and Daniel Ioan Stroe. "*Control of Permanent Magnet Synchronous Generator for Large Wind Turbines*". IEEE (2008).

[12]. A.J. Mahdi, W.H. Tang, L. Jiang and Q.H. Wu. "*A Comparative Study on Variable-Speed Operations of a Wind Generation System Using Vector Control*". International Conference on Renewable Energy (ICREPQ'10). (Granada, Spain). 23rd to 25th March, 2010.

[13] Mónica Chinchilla, Santiago Arnaltes and Juan Carlos Burgos; "*Control of Permanent-Magnet Generators Applied to Variable-Speed Wind-Energy Systems Connected to the Grid*"; March 2006

[14] *Sunny island 5048, Installation and Instruction Manual.* www.sma.de/en/products/off-grid-inverters/sunny-island-5048-5048u.html. Last View: June 28, 2010

[15] Mika Rasila. "*Torque- and Speed Control of a Pitch Regulated Wind Turbine*". Department of Electric Power Engineering Chalmers University of Technology. Goteborg, Sweden 2003

[16] Arkadiusz Kulka. "*Pitch and Torque Control of Variable Speed Wind Turbines*". Department of Electric Power Engineering. Chalmers University of Technology. Goteborg, Sweden 2004.

[17] YANG Yong, RUAN Yi, SHEN Huan-qing, TANG Yan-yan and YANG Ying. "*Grid-connected inverter for wind power generation system*" J Shanghai Univ (Engl Ed), 2009, 13(1): 51–56

[18] D.C. Aliprantis S.A. Papathanassiou M.P. Papadopoulos A.G. Kladas; "*Modeling and control of a variable-speed wind turbine equipped with permanent magnet synchronous generator*"; March 2008

[19] V.Himamshu Prasad, Dushan Boroyevich and Richard Zhang; "*Analysis and Comparison of Space Vector Modulation Schemes for a Four-Leg Voltage Source Inverter*"; 2006

SIMULATION OF AN HYBRID POWER SYSTEM TO PRODUCE WATER AND ELECTRICITY FOR REMOTE COMMUNITIES IN TUNISIA

K. Ben Youssef[(a)], K. Makhlouf[(a)], S. Chehaibi[(a)], L. Khemissi[(b)], R. Landolsi[(b)], H. El Fil[(c)], A. Guizani[(a)]

[(a)] Thermal process Laboratory, CRTEn, BP 95, Hammam Lif, 2050, Tunisia
[(b)]Photovoltaic Laboratory, CRTEn, Tunisia
[(c)] Water Researches and Technologies Centre, CRTE, Tunisia

[(a)] kamilia.ben-youssef@laposte.net

[(a)] amenallah.guizani@crten.rnrt.tn

ABSTRACT
OPEN-GAIN project's aim is to supply fresh water and electricity to rural remote communities not connected to the public grid, using the renewable energies and the reverse osmosis desalination technique. In this paper, the system used is described and several scenarios were investigated in the simulation to compare the PV only and Wind only systems with the hybrid system. The simulations were carried out using HOMER tool provided by NREL (National Renewable Energy Laboratory). The results show that the combination of PV and WT power generators, with batteries, allows obtaining a better renewable energy fraction of 95%.

Keywords: renewable energies, hybrid system, water desalination, open gain

1. INTRODUCTION

Fresh water and electrical energy are the two elements that absolutely must be available to guarantee a better quality of life. Unfortunately, a significant number of the world population lives in extremely arid or semi-arid areas. Those areas have usually an important solar radiation causing a lack of water, and their connection to the public grid of electricity is subject of heavy technical and financial constraints. The OPEN-GAIN project (OPtimal ENgineering design for dependable water and power Generation in remote Areas using renewable energies and INtelligent automation) (www.open-gain.org) deals with these facts and its global objective is to develop a new model-based optimal system design approach to economically improve the overall performance, dependability, reliability and availability of co-generating water-electricity plants powered by renewable energy for remote arid areas using a high level of automation to meet specific cost requirements and to disseminate the new technology MENA wide (Middle East and Northern Africa).

The OPEN-GAIN technological challenge consists on supplying fresh water using reverse osmosis as a desalination technique of brackish water, and to feed the Reverse Osmosis plant with electricity via renewable energies sources, backed up by a conventional one (diesel generator), the whole designed plant is installed in the site of Borj Cedria in Tunisia in CRTEn (Centre de Recherche et des Technologies de l'Energie).

2. DATA REQUIREMENTS FOR THE SYSTEM DESIGN

To identify the adequate solution of fresh water supply from water desalination with autonomous powered RO plant in the site of Borj Cedria, several studies were realized in order to obtain the required database essential for the components design(Ulrike Seibert & al, 2004). The collected data concerns the following parameters:

Water:

- Collection and assessment of data on water resources, availability, and type of water (lake, river, rain, ground water, sea water, brackish water…)
- Density of rural homes not connected to water pipelines
- Analysis of fresh water demand and capacity needed for domestic use, agriculture use…

Energy:

- Collection, and assessment of data on energy resources and availability
- Density of rural homes not connected to the grid
- Type of alternative energy available in the site
- Analysis of energy demand and capacity needed for domestic use and others (Reverse Osmosis plant)

In Tunisia, a typical rural site contains about 480 inhabitants. The average water consumption is around

60 liters per day per person, when is it around 100 liters per day per person in the urban areas, these data are necessary to estimate the water production needed for the concerned remote area and to know consequently the electrical power required for the reverse osmosis unit. In the case of OPEN-GAIN project, the typical water user profile lead to the design of 24m^3 per day RO plant, which needs 5kW/m^3 as power supply. The estimation of power demand should include electrification of both RO plant and households. According to national electricity authority, one household in rural areas in Tunisia have a daily power consumption of 1.9kWh in winter and 3.03kWh in summer, the annual average consumption is estimated to 966kWh.

A database of the specific weather data of CRTEn's site was collected, as the whole prototype is going to be installed there. In CRTEn, a meteorological station is installed to collect regular values of the following parameters:

- Wind speed, and direction
- Solar radiation and temperature

For 2009, the wind speed varied from 4.33m/s to 6.54 m/s, which means that the target site is rather windy all over the year. The average speed is 5.45m/s. Concerning the solar radiation, the worst value was registered in January: 0.108kW/m^2, and the best one was in July: 0.3kW/m^2.

3. THE OPEN-GAIN'S HYBRID SYSTEM

The data described in the previous part allowed the estimation of the required installed power of the renewable energies components: the Photovoltaic generator (PV) and the Wind Turbine (WT). In the case of OPEN-GAIN project, the total installed power of each component is 15kW.

The optimal design is when the renewable energy sources provide a quantity of power equal to the power required by the loads (RO plant and households) in a same period of time (day, year or month). This sort of equilibrium point can't always be reached, especially in a continuous way, that's why a diesel generator of 20kVA was foreseen, to compensate an eventual lack of energy. A storage system of 12 batteries, 12V, 210 Ah each, was also foreseen to stock potential energy excess.

OPEN-GAIN is a cooperation of several participants; the figure below shows a block diagram of the physical decomposition of the plant and the localization of the work packages (Adrian Gambier & al, 2009):

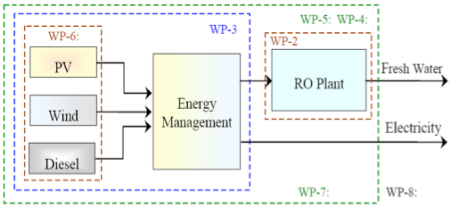

Figure 1: Physical Decomposition Of The Plant And Localization Of The Work Packages

CRTEn, as a leader of the WP-7, is responsible of the complete integration of all other work packages and the final ensemble of the whole prototype. The first activities were the selection of the site and the construction of the data base of the weather characteristics and user profile. The design of the renewable sources and the diesel engine and the batteries and the convertors, as well as the RO plant, was a result of a fruitful cooperation between all the participants. CRTEn received all the components and brought each one safely to the place where it should be installed.

CRTEn team is responsible of the PV generator installation, so, according to electrical requirements, the total installed PV power were divided in 3 rows of 5kW each. Each row is composed of 3 strings in parallel, and each string contains 9 panels in series, delivering 15.3A as a maximum current. The PV panels were divided in 3 rows to obtain a three phase system.

The PV generator, which can deliver 15.3A as a maximum current, was installed and tested to confirm its electrical specifications. The tests were performed in a typical sunny day of January to establish the curve of the current I as a function of the voltage V (I(V) characteristic) of the PV modules:

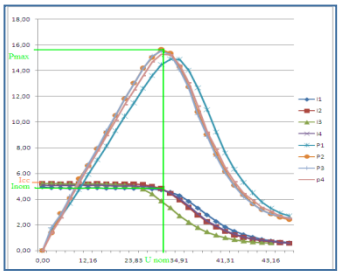

Figure 2: Test Of The PV Modules In The CRTEn's Site

According to the standard test conditions, (1000W/m^2 of solar radiation), the maximum power of the module is P_{max}=185W. During the tests performed in CRTEn, and as the solar radiation was lower than the standard value, the maximum power obtained was P_{max}=155W.

The PV generator, as well as the rest of the components (Wind turbine, diesel generator and batteries), are connected to the loads (RO Plant and electrification) via inverters and electrical boxes to adapt the energy and to insure the necessary protections.

The first set of inverters allows converting the direct current delivered by the PV generator into alternative current to be injected in the AC bus. The alternative current delivered by the wind turbine crosses first a rectifier to obtain direct current and then, an inverter converts it into alternative current and injects it in the AC bus. The batteries and the diesel generator are connected to bidirectional invertors that manage the

charge and discharge cycles of the batteries and start/off cycles of the diesel engine. The inverters will be connected to a web box that will allow the Ethernet connection to a monitoring system.

4. INVESTIGATION AND OPTIMIZATION OF THE HYBRID SYSTEM

A feasibility study of such a hybrid system was carried out using the software HOMER which is a sizing and optimization tool provided by NREL (National Renewable Energy Laboratory) (www.nrel.gov).
For the given site, with water and power demand specified, we simulate the behavior of the hybrid system under various scenarios of running with the aim of satisfying the demand using mainly the renewable sources.

As main entries, we have to specify the meteorological characteristics of the site of Borj Cedria, of the load and of the power sources. The installed power of the diesel generator must be sufficient to feed the load in the worst meteorological conditions and the capacity of the battery system must be able to store a potential energy excess and insure the system's autonomy. Obviously, the diesel engine must intervene as a last resort in order to minimize the fuel consumption and the CO_2 emissions. The unmet energy demand is fully satisfied first by the excess energy stored in the batteries and then by the energy supplied from diesel generator.

4.1 PV generator alone

The simulation of a system with only PV as renewable energy, without battery storage system, gives a renewable fraction of only 0.4. The 15kW of installed PV power are insufficient to feed the load, this leads the diesel engine to work at 60%, in terms of yearly production (kWh/yr).

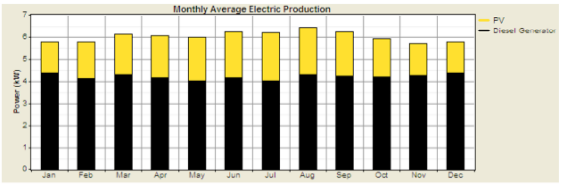

Figure 3: Monthly Average Electric Production Of The System PV + Diesel Generator Without Batteries

4.2 WT Generator alone

The simulation with only the Wind turbine as renewable source, and without battery storage system, gives a renewable fraction of 0.56. The diesel generator works at 44% in this case.

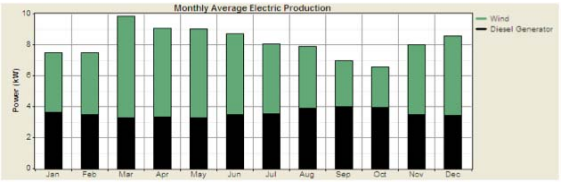

Figure 4: Monthly Average Electric Production Of The System Wind + Diesel Generator Without Batteries

This difference between the PV only and Wind only systems, without batteries, is due to the weather resources: the site of Borj Cedria is windy all over the year, while there is a difference in the solar radiation between months of winter and summer. In addition, the wind potential can be available along the 24 hours of a day, when the solar radiation is available only during few hours around midday.

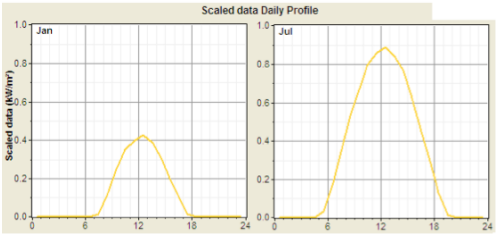

Figure 5: Example Of Solar Radiation Distribution Along A Day Of Winter And A Day Of Summer

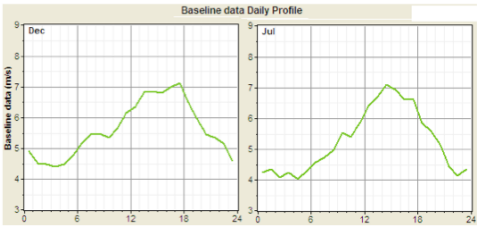

Figure 6: Example Of Wind Potential Distribution Along A Day Of Winter And A Day Of Summer

4.3 Combination WT and PV Generators

We simulate first the combination of the two renewable sources to obtain a hybrid system, without storage. The results give a renewable fraction of 0.73.

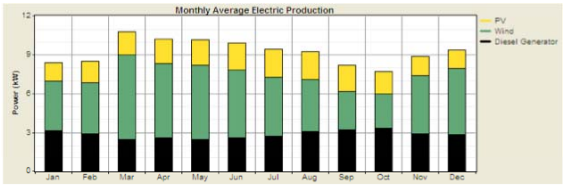

Figure 7: Monthly Average Electric Production Of The System Wind + PV + Diesel Generator Without Batteries

When we add to the previous hybrid system, a battery storage system, the renewable fraction is enhanced to 0.95 (95%). The diesel engine works for only 5%.

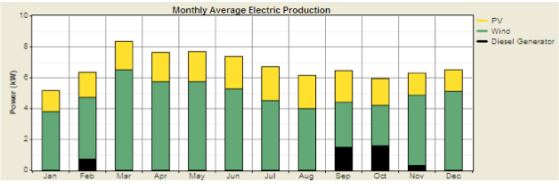

Figure 8: Monthly Average Electric Production Of The System Wind + PV + Diesel Generator + Batteries

5. CONCLUSION AND PERSPECTIVES

We presented a simulation of a hybrid energy system devoted to satisfy the needs in water and electricity of a rural community using the software HOMER. First results show that a combination of PV and WT power generators allows the renewable energy fraction to reach 95%.

At the present time, activities in progress are the finalization of subsystems installation and then the global wiring of the components. After the prototype assemblage, it will be started-up subsystem by subsystem by using an iterative procedure to solve malfunctions once a failure is detected before the next subsystem is started up until the correct operation is finally verified (www.open-gain.org). Finally, last activities of other work packages may be concluded. Once the model has been tuned to the real plant, the control system will be adjusted to the real model and finally implemented in real time. The control system first have to be tested and evaluated by simulation on the adjusted model and at last, the overall hybrid control system including all control levels has to be assembled and implemented in real-time. Here, it is necessary to choose proper hardware and software for real-time applications and the algorithms have to be tuned for real application conditions.

It is expected in the end of the project period that the integrated system engineering design works properly and that it will be able to be transferred for industrial development (Adrian Gambier & al, 2009).

REFERENCES

Dahmouni. A.W. & al. May 2010. Wind energy in the Gulf of Tunis, Tunisia. *Renewable and Sustainable Energy Reviews* volume 14, Issue 4, Pages 1303-1311.

Gambier. A & al, September 2009. Optimal systems engineering and control co-design for water and energy production: A european project. *Desalination and water treatment* volume 10, pages 192-199.

Gambier. A and Badreddin. E. Application of hybrid modelling and control techniques to desalination plants. *Desalination* volume 152, pages 175-184.

Houcine. I & al, November 1999. Renewable energy sources for water desalting in Tunisia. *Desalination* volume 125, Issue 1-3, Pages 123-132.

Kartalidis. A, Arampatzis. G, Assimacopoulos. D, 2008. Rapid Sizing of Renewable Energy Power Components in Hybrid Power Plant for Reverse Osmosis Desalination Process. *International Congress on Environment Modelling and Software*, Barcelona.

Mohammedi. K, Sadi. A, Cheradi. T, Belaidi. I, Bouziane. A, 2009. OPEN-GAIN Project: Simulation and Analysis of an Autonomous RO Desalination and Energy Production Systems Integrating Renewable Energies. *The 2nd Maghreb Conference on Water Treatmentand Desalination (CMTDE 2009)*, December 19-22, Hammamet, Tunisia.

Ribeiro. J & al, 2002. Potential use of PV for water desalination, PV in Europe. *From PV Technology to Energy Solutions*, October 7-11, Rome, Italy.

Seibert. U & al, March 2004. Autonomous desalination system concepts for seawater and brackish water in rural areas with renewable energies-Potential, technologies, field experience, socio-technical and socio-economic impacts-ADIRA, *Desalination*.

www.open-gain.org

www.nrel.gov

Estimation of the energy production of a 15kW wind turbine in the site of BORJ-CEDRIA

A.W. DAHMOUNI [a], M.M. OUESLATI [a], M. BEN SALAH [b], F. ASKRI [c], C. KERKINI [a], A. GUIZANI [b], S. BEN NASRALLAH [c]

[a] Laboratoire de Maîtrise de l'Energie Eolienne et de Valorisation Energétique des Déchets, Centre de Recherche et des Technologies de l'Energie, Technopôle de Borj-Cedria, BP 95 Hammam Lif 2050, Tunisia.
[b] Laboratoire des Procédées Thermiques, Centre de Recherche et technologies de l'Energie, Technopôle de Borj-Cedria, BP 95 Hammam Lif 2050, Tunisia.
[c] Laboratoire d'Etudes des Systèmes Thermiques et Energétiques, Ecole Nationale d'Ingénieurs de Monastir, avenue Ibn El Jazzar 5019, Monastir, Tunisia.

Email: dahmouni_anouar_wajdi@yahoo.fr

ABSTRACT

To satisfy increases in the world energy requirement it is necessary to find solutions and to diversify them. Renewable energy like wind, solar and hydraulic energy seems to be the suitable solution in the future. In fact many developments have been made in these domains and especially in the wind energy technologies. In this paper we present a study of the electrical wind energy production in the site of Borj-Cedria. The data collected at 20 and 30 m height during 2008 and 2009, have been used to estimate the monthly net energy output of the a 15 kW wind turbine. Results show a promising performance and affirm that Borj-Cedria is one of the best sites for wind project in Tunisia.

Keywords: Wind speed distribution, Wind Turbine, Wind energy, Net energy output.

1. INTRODUCTION

In the last report of Intergovernmental Panel on Climate Change, observations carried out on all the continents and in the majority of the oceans show that a multitude of natural systems are affected by the climate changes, in particular by the increase of temperature IPCC (2008). The scientists affirm that these ecological problems are directly related to the rise of fossil fuel uses. Furthermore, Oil price fluctuations are one of the major sources of disturbance for the economy of oil importing countries. To cure these problems, governments have already adopted programs aiming to increase the contribution of renewable sources in their energy balance. According to last statistics, wind energy seems to be most reliable solution with the highest growth rate.

Recently, many researchers are interested to the evaluation of wind resource and wind turbine production. In fact, Shata and Hannitch (2008), have presented a data bank of electricity generation and wind potential assessment of Hargada i.n Egypt. Moreover, the study of Omer (2008), showed the estimation of the wind energy resources of Sudan using the data collected over the country and propose a study of wind pump profitability in the Soba site. Gökçek and Genç (2009) have evaluated the electricity generation and energy cost of eight wind energy conversion systems in many locations at Central Turkey. A comparative simulation of wind park design and siting in five locations in Algeria has been presented by Ettoumi et al. (2008). They have compared nine commercialized wind turbine with different power output. In the United States of America, Wichser and Klink (2008) have used the data collected in four sites in Minnesota during three years at the altitude of 70-75m to estimate the wind resources in this location. They have also conducted a comparative simulation of three configurations of the GE 1.5 MW series wind turbine to evaluate the potential gain in power production that may be realized with low wind speed technology. In Tunisia, Ben Amar, Elamouri and Dhifaoui (2008), have presented the energy assessment of the first wind farm section of Sidi Daoud. The energetic and aerodynamic characteristics of aerogenerator Made AE-32 installed on site were also studied over 4 years. Dahmouni et al. (2009) have presented the wind potential in the Gulf of Tunis as well as the net energy production of the Enercon E82 wind turbine.

In this general context our study is devoted to the simulation of the electrical production of the a 15kW wind turbine. Using over then 105 264 observations collected during 2008-2009, we estimate the annual Weibull distribution functions, the monthly and the annual net energy production in the site of the Centre of Research and Technologies of Energy (CRTEn) in Borj-Cedria area.

2. THEORETICAL MODEL

2.1. Weibull Distribution

Wind velocity distribution can be modeled by several functions. According to Gumbel (1958), the best one is Weibull distribution. This function can be described by two or three parameters.

The advantages of the use of the function of Weibull with two parameters were highlighted by Justus, Hargraves and Yalcin (1976); Justus, Hargraves, Mikhail and Graber (1976). A model of Weibull with three parameters was proposed by Van Der Auwera, De Meyer and Malet (1980). This model is a generalization of the Weibull function with two parameters.

In wind industry, the use of the Weibull function with two parameters is frequent. It is expressed by

$$f(V) = \frac{k}{c}\left(\frac{V}{c}\right)^{k-1} \exp\left(-\left(\frac{V}{c}\right)^{k}\right) \quad (1)$$

Where $f(V)$ is the probability density function, c and k are respectively the scale and the shape parameters which can be calculated using Eqs. 2 and 3

$$k = \left(\left(\frac{\sum_{i=1}^{n} V_i^k \ln(V_i)}{\sum_i V_i^k}\right) - \left(\frac{\sum_{i=1}^{n} \ln(V_i)}{n}\right)\right)^{-1} \quad (2)$$

$$c = \left(\frac{\sum_{i=1}^{n} V_i^k}{n}\right)^{\frac{1}{k}} \quad (3)$$

Where n is the observation number and V_i the wind speed.

2.2. Wind Power Density And Net Energy Production

For a series of measurements, the mean wind power density in the site is given by the following expression

$$\overline{P} = \frac{1}{2}\rho\overline{V^3} \quad (4)$$

Eq. 4 depends on the frequency of each velocity, therefore the mean wind power density is given by

$$\overline{P} = \int_0^{\infty} \frac{1}{2}\rho V^3 f(V) dV \quad (5)$$

Thus, the Eq. 5 has the advantage of making it possible to quickly determine the average of annual production of a given wind turbine if its characteristics and the Weibull distribution on the site are known.

For any wind turbine the electrical power output for each wind speed is given by

$$P_{out}(V) = C_p(V) S \frac{1}{2}\rho V^3 \quad (6)$$

Where $C_p(V)$is the performance coefficient of the wind turbine at the wind speed V and S is the rotor area of the wind turbine.

Eqs. 5 and 6 give the mean power output:

$$\overline{P}_{out} = \int_{V_{min}}^{V_{max}} C_p(V) S \frac{1}{2}\rho V^3 f(V) dV$$

$$\overline{P}_{out} = \int_{V_{min}}^{V_{max}} P_{out}(V) f(V) dV \quad (7)$$

V_{min} and V_{max} are respectively the minimal and the maximal wind speed in the site.

2.3. Wind speed extrapolation

The wind speed measurements are collected in the site at 20 and 30m above ground level. For wind turbine simulation, it is necessary to estimate the wind speed at the turbine hub height. According to the literature, the most commonly used method to adjust the wind velocity at one level to another is the power law method expressed by

$$V = V_{mes}\left(\frac{h}{h_{mes}}\right)^{\beta} \quad (8)$$

Where V_{mes} is the wind speed recorded at anemometer height h_{mes}, V is the wind speed to be determined for the desired height h and β is the power law exponent.

3. SIMULATION AND RESULTS

Using the data collected in the site, we estimate the wind speed at the wind turbine hub height (25m) using values of power low exponent equal to 0.185 and 0.155 respectively in 2008 and 2009. Figs. 1 and 2 show the wind speed distribution function in the two years at the altitude of 25m.

The annual Weibull distribution functions at 25m are expressed by

$$f_{2008}(V) = \frac{1.81}{6.14}\left(\frac{V}{6.14}\right)^{0.81} \exp\left(-\left(\frac{V}{6.14}\right)^{1.81}\right) \quad (9)$$

$$f_{2009}(V) = \frac{1.82}{6.62}\left(\frac{V}{6.62}\right)^{0.82} \exp\left(-\left(\frac{V}{6.62}\right)^{1.82}\right) \quad (10)$$

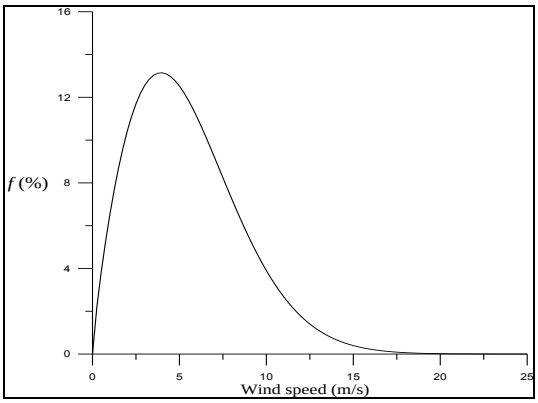

Figure 1: Annual Weibull distribution in the site (2008)

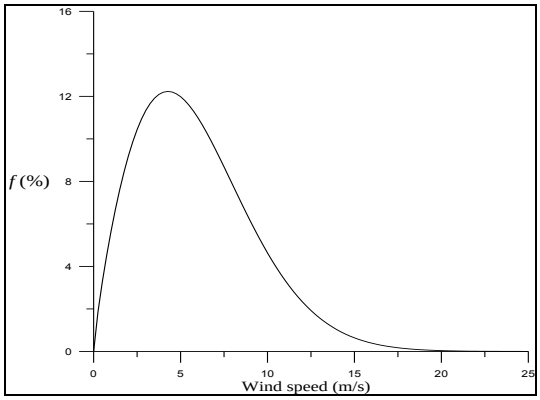

Figure 2: annual Weibull distribution in the site (2009)

To estimate the power output in each month, a procedure was developed according to the International Electrotechnical Commission recommendations (IEC standard 61400-12-1 (2005)) and using the linear interpolation, the characteristic of the wind turbine and the Eq.7.

Fig. 3 presents the power curve of the studied aerogenerator which is the "Proven 15" wind turbine manufactured by "Proven Energy" Scottish company. As shown, this wind turbine represents the advantage of a lower cut-in wind speed.

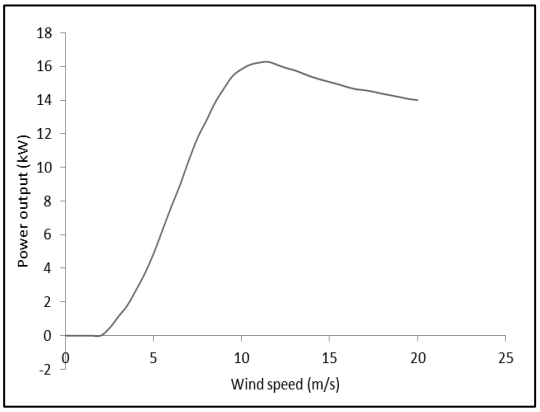

Figure 3: Characteristic of the "Proven 15" wind turbine

Fig. 4 and 5 show the variation of the mean net energy output of the studied wind turbine respectively in 2008 and 2009. We can clearly observe that the production undergoes a monthly basis according to the existing wind resource in the site. So, the highest mean energy output is observed during March with a value of 5445 kWh in 2008 and 5485 kWh in 2009. However lowest values are obtained in October during 2008 and in August during 2009. We can note again that a large production difference was recorded in October, December and February between the two years.

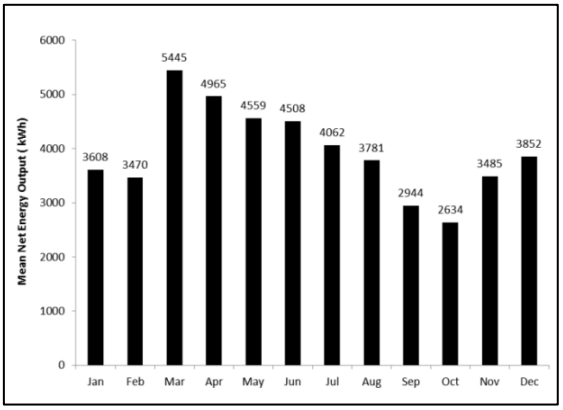

Figure 4: Net energy output during 2008

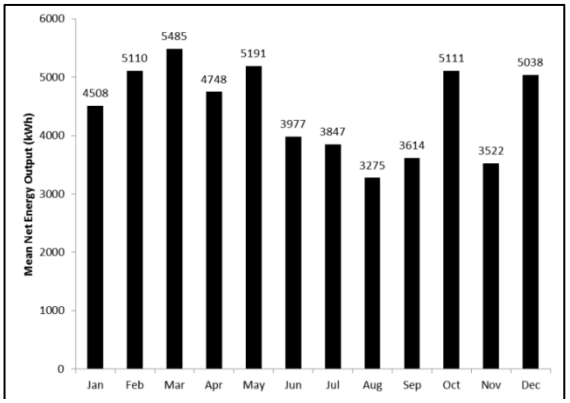

Figure 5: Net Energy output during 2009

So with these results we can confirm that:

- The site of Borj-Cedria presents a good wind energy potential in camper with many other sites presented in various paper.
- The "Proven 15" wind turbine seems to have a good performance in the site of Borj-Cedria with over than 38% of capacity factor.

4. CONCLUSION

In this study, the electrical generation of a 15kW Wind turbine was discussed. Using the estimated Wiebull distributions in the site of Borj-Cedria and the data provided by manufacture, a procedure given the mean net energy output in each

month has been developed. Results for 2008 and 2009 years show that Borj-Cedria is a good site for wind project implantation. Furthermore, with a total energy output of about 50 325 kWh/year we can affirm that the "Proven 15" wind turbine is one of the best commercialized wind turbine adapted to the site conditions. The obtained results will be compared to experiment for validation and optimization of the used method.

ACKNOWLEDGMENTS

This paper presents a contribution in the European project Optimal Engineering Design for Dependable Water and Power Generation in Remote Areas Using Renewable Energies and Intelligent Automation (OPEN-GAIN).

REFERENCES

Dahmouni A.W., Ben Salah M., Askri F., Kerkeni C., Ben Nasrallah S., 2010, Wind energy in the Gulf of Tunis, Tunisia, Renewable and Sustainable Energy Reviews 14;1303–1311.

Ben Amar F., Elamouri M., Dhifaoui R., 2008, Energy assessment of the first wind farm section of SidiDaoud, Tunisia, Renewable Energy 33; 2311–2321.

Ettoumi F.Y. , Adane A.H., Benzaoui M.L., Bouzergui N., Comparative simulation of wind park design and siting in Algeria,2008, Renewable Energy 33; 2333–2338.

Gumbel E. J., 1958, Statistics of extremes, Columbia University Press.

Gökçek M. , Genç M.S. , 2009, Evaluation of electricity generation and energy cost of wind energy conversion systems (WECSs) in Central Turkey, Applied Energy 86; 2731–2739.

Intergovernmental Panel on Climate Change, Climate Change 2007: Synthesis Report, 2008, GIEC publication, Suisse.

Justus C. G., Hargraves W. R., Yalcin A., 1976, Nationwide assessment of potential output from wind-powered generators, Journal of Applied Meteorology 15; pp 673-678.

Justus C. G., Hargraves W. R., Mikhail A., Graber D., 1978, Methods for estimating wind speed frequency distribution, Journal of Applied Meteorology 17; pp350-353.

Omer A.M., 2008, On the wind energy resources of Sudan, Renewable and Sustainable Energy Reviews 12; 2117–2139.

Shata A.S.A., Hanitsch R. , 2008, Electricity generation and wind potential assessment at Hurghada, Egypt, Renewable Energy 33; 141–148.

Van Der Auwera L., De Meyer F., Malet L. M., 1980, The use of the Weibull three parameter model for estimating mean wind power density, Journal of Applied Meteorology 7; pp 819-825.

Wichser C., Klink K., 2008, Low wind speed turbines and wind power potential in Minnesota, USA, Renewable Energy 33; 1749–1758.

DIAGNOSIS OF THE OPEN-GAIN REVERSE OSMOSIS DESALINATION UNIT

K. Maklouf[(a)], K. Ben Youssef[(a)], A. Guizani[(a)] H. Elfil[(b)]

[(a)]Laboratoire des Procédés Thermiques, Centre de Recherche et des Technologies de l'Energie, BP 95, Hammam-Lif, 2050, Tunisia
[(b)]LabTEN, Water Researches and Technologies Centre; Borj-Cedria Technopole; Tunisia

[(a)]amenallah.guizani@crten.rnrt.tn, [(b)]h_elfil@yahoo.com

Abstract
In the framework of the OPEN-GAIN project (OPtimal ENgineering design for dependable water and power Generation in remote Areas using renewable energies and INtelligent automation) a Reverse Osmosis unit was installed at CRTEn (Tunisia) by the end of 2008. This prototype, which needs 5kW/m^3 as power demand, was designed to desalinate well water with about 15 g.L^{-1} TDS (Total Dissolved Salts). It provides 1 m^3/h permeate flux with approximately 600 mg.L^{-1} TDS with 60% recovery rate. The RO unit was running in both closed and open circuit to desalinate well water. Theirs performances are registered and analyzed. The different desalinate waters (Feed, produced, reject) are characterized to prevent scaling and aggressiveness. Comparing to TDS values, the inlet water conductivity sensor is suspected to present some defaults. The reliability of the conductivity sensor is tested by a model based on a semi-empiric formula, function of water conductivity, of the produced water flux.

Keywords: desalination, reverse osmosis, scaling, conductivity

1. INTRODUCTION

In the last few years, the use of small scale Reverse Osmosis (RO) water desalination unit has sharply increased. Their use covers several economical sectors: industry, agriculture, hostelry and small isolated communities in arid or semi-arid areas **(**Ayoub and Alward 1996; El-Zanati and Eissa E. 2004**).** A great number of RO plants installed in arid or semi-arid areas are functioning with renewable energies. To have longevity, the RO membranes need pretreated feed water to avoid matter deposit on its surfaces such as suspended matter, inorganic precipitation and biological matter. The deposit matter causes membrane fooling resulting in permeate flux decrease and quality production drop of in the RO unit.

Calcium carbonate is the major contributor of the fooling build up in RO units for desalination process. This phenomenon has to be prevented at all expenses. During membrane separation, calcium and bicarbonate elements are retained by the membrane in one hand and CO_2 passes with the produced water in another hand. As consequence, the rejected water will be highly scaling and the produced one will be highly aggressive. The acid use, to adjust feed water pH, reduces the scaling power of the rejected water and increases the aggressiveness of the osmosis water.

In many cases, the chemical products use, and specially acids, presents a real problem. Acid conservation and manipulation need a lot of care which often doesn't exist in the absence of qualified technician. In other cases as mobile or tap water RO units, the avoiding chemical treatment is looked for (Hannachi, Chernie and Elfil 2009).

The RO plants are usually equipped by several sensors in order to follow the performances and evaluate any malfunction. However, some of these sensors, which are very sensitive such as conductivity and pH meters, can easily present false values after a short running period. The detection of the sensor default is not obvious. It will be interesting to develop models which can detect earlier the sensor default. In this work we are interested to the inlet water conductivity sensor. It was suspected to present some defaults. Its reliability will be tested by comparing the experimental permeate flux value to the calculated one using a semi-empiric formula function of water conductivity

2. DESALINATION UNIT DESCRIPTION

The reverse osmosis desalination unit was commissioned in December 2008 in the framework of a European research project OPtimal ENgineering Design for Dependable Water and Power Generation in Remote Areas Using Renewable Energies and INtelligent Automation (Open-Gain 2007). This prototype was designed to work with different renewable energy sources and supplementary conventional energy sources such as diesel power generator (Gambier, Wolf and Badreddin 2008; Mohammedi et al. 2009). The research prototype is equipped with different sensors to follow its performances. It is used to desalinate well water with about 15 g.L^{-1} TDS. It provides 1 m^3/h permeate flux with approximately 600 mg.L^{-1} TDS with 60% of recovery rate.

In this unit (figure1), water undergoes a pretreatment before passing through the RO modules arranged in one stage. Before exciting the unit, a post treatment is performed. The unit is also equipped with membrane washing circuit.

The pretreatment is carried out in three steps:

- Sand filtration to retain suspended matter and colloids;
- Chemical pretreatment with many injection stations, such as chlorination, dechlorination, pH adjustment and scaling inhibition.
- A 5µm cartridge filter to trap micro-particles

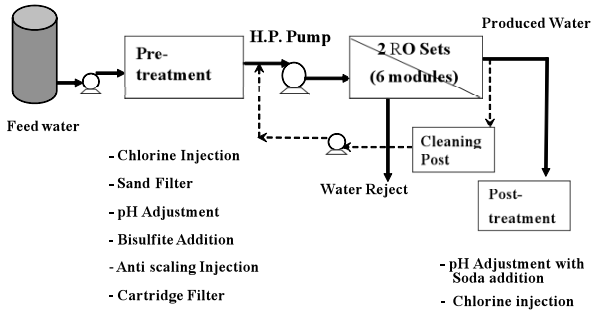

Figure 1: Schema of the Open-gain RO unit

Six RO modules are arranged in 2 sets. They are CPA2-4040 type, Spiral wound configuration and composite polyamide membrane with a nominal area of 85 ft^2.

The maximum applied pressure is 41 bars.

The permeate goes through a post-treatment operation where the pH is adjusted and the water is disinfected by chlorination.

The membranes are automatically washed for 2 minutes with osmosis water at the stop running of the RO unit.

3. EVALUATION OF THE RO UNIT OPERATION

3.1. Physical chemical analysis of water fluxes

The well water quality and temperature are varying along the seasons. Upper and lower values for the important features of the well water are given in Table 1. For example, the water TDS and temperature have ranged between 14 and 17 mg/L; and 12 and 29 °C respectively. The water hardness is very high and the iron concentration reaches 0.5 ppm which can be rapidly oxidized and transformed to a precipitate of iron hydroxide

The Open-Gain RO unit, which is running in closed and open circuit, has a fixed recovery rate (Permeate flux/Feed flux) of around 60 % as shown in figure 1. For open circuit, the produced waters present a TDS lower than 1 $g.L^{-1}$and conductivity between 1.2 and 0.6 mS. cm^{-1}. This TDS is in accordance with Tunisian standards for potable water.

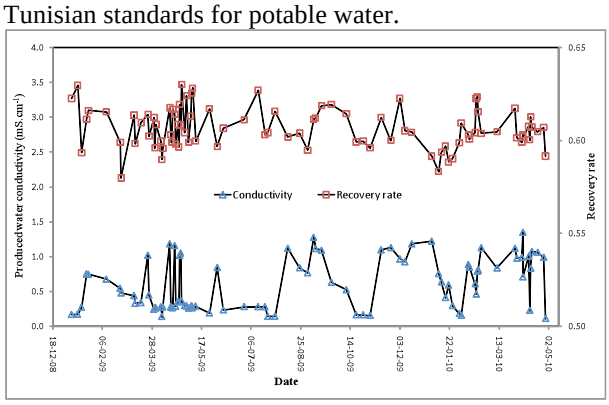

Figure 2: Evolution of the RO unit recovery rate and the water produced conductivity

The water fluxes within the desalination unit have been chemically analyzed. The data for the date of 10-02-2010, which are reported in Table 2, give relevant physical properties and chemical composition of the feed, permeate and reject fluxes. The membrane salt retention is about 95%. The rejection rate of divalent ions is between 97 and 98%. For monovalent ions, it is between 93 and 96%. The reject water is under-saturated with respect to gypsum ($\Omega_{Gypsum} < 1$) and then there is no risk of membrane scaling with gypsum.

3.2 Scaling/equilibrium/aggressive behavior of water fluxes

The $CaCO_3$ membrane scaling depends on chemical composition, temperature and pH of the water and the recovery rate of the RO unit. The phenomena can be predicted by using the best available knowledge of the behavior of what is been commonly known as the calco-carbonic system (Elfil and Roques 2004). Behaviors in terms of scaling, equilibrium and aggressive of the RO desalinate waters can be forecasted by using the MLSI index defined as follows (Elfil and Roques 2006; Hannachi et al. 2007):

$$MLSI = pH - pH_{S/MCC} \quad (1)$$

$$pH_{S/CCM} = pK_2 - pK_{S/CCM} - \log([Ca].\gamma_{Ca}) - \log([Alc].\gamma_{HCO3}) \quad (2)$$

Where

$pH_{S/MCC}$ and $pK_{S/MCC}$ are respectively saturation pH and solubility product of the Monohydrate calcium carbonate.

Table 1: Upper and lower limits for some physical-chemical characteristics of CRTEn well water.

	TDS	Cond.	pH	T	Turb.	Ca^{2+}	Mg^{2+}	HCO_3	SO_4^{2-}	Na^+	Cl^-	K^+	Fe^{2+}
	$g.L^{-1}$	mS/cm		°C	FTU	$g.L^{-1}$	$g.L^{-1}$	$g.L^{-1}$	$g.L^{-1}$	$g.L^{-1}$	$g.L^{-1}$	$g.L^{-1}$	ppm
Min	14	18	6.5	11	0.2	0.56	0.19	0.53	1.0	3.9	7.4	0.090	0.2
Max	17	30	7.3	30	1.4	0.83	0.45	1.10	1.2	4.4	7.9	0.014	0.5

γ_i : activity coefficient calculated by a simplified Pitzer model (Pitzer 1973)
pK_2 : 2nd dissociation constant of carbonic acid
Alc : Alkalinity, it is equal to bicarbonate concentration at pH under 8.3

Table 2: Chemical and physical analyses of the desalination unit water fluxes (10-02-1010)

	Feed	reject	permeate	Salt Retention (%)
pH	7.4	7,75	6,3	
T (°C)	18.2	19.0	18.4	
Cd ($mS.cm^{-1}$)	26.1	-	0.8	
TDS (g/L)	15.3	30.8	0.72	95.4
Ca^{2+} ($mg.L^{-1}$)	812.6	1740.0	25.2	96.9
Mg^{2+} (mg/L)	400.0	815.2	14.0	96.7
Na^{+} ($mg.L^{-1}$)	4114.1	8660.3	222.0	94.6
K^{+} ($mg.L^{-1}$)	107.9	202.9	7.0	93.5
Cl^{-} ($mg.L^{-1}$)	7633.1	15794.0	396.4	94.8
$SO_4^{=}$ ($mg.L^{-1}$)	989.9	2182.6	21.9	97.8
HCO_3($mg.L^{-1}$)	1260.1	2600.2	44.2	96.4
MLSI	-0.1	0.5	-3.6	
Gypsum supersaturation	0.2	0.3	<0.1	

The scaling/equilibrium/aggressive behaviors, with respect to the $CaCO_3$, are presented by the calco-carbonic diagram (figure 3). The well water used to feed the RO unit has MLSI values in the range (-1.33 – 0), then it is considered at calco-carbonic equilibrium and there is no risk of scaling. The rejected water presents a high risk of scaling (MLSI > 0.5), when there is no acidification as shown in the calco-carbonic diagram (Figure 2). The pH adjustment of the feed water eliminates membrane scaling risk with calcium carbonate. Acid dosing should be optimized by considering the presence of chemical inhibitors. The produced water by RO process is slightly acid and very aggressive (MLSI < -3, see Table2). It needs a post treatment.

To avoid osmosis water pH adjustment with NaOH, The degassing of the solution with atmospheric air (with a flow rate equal to 2 $L.mn^{-1}$ per Liter of water) is tested. The pH is neutralized Within 8 min. After half an hour the pH riches the value of 7.7, but the produced water remains under saturated in relation to calcium carbonate as shown in figure 4. Even at maximum theoretical pH value (≈ 8) that can be obtained by degassing, the osmosis water remains aggressive ($\Omega_{Calcite} \approx 0.35$).

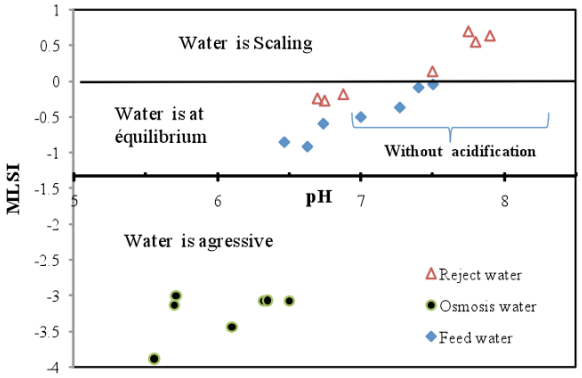

Figure 3: Scaling/Equilibrium/aggressive behavior of the RO desalinate waters

Then pH adjustment as post treatment is not sufficient to provide calco-carbonic equilibrium to produced water.

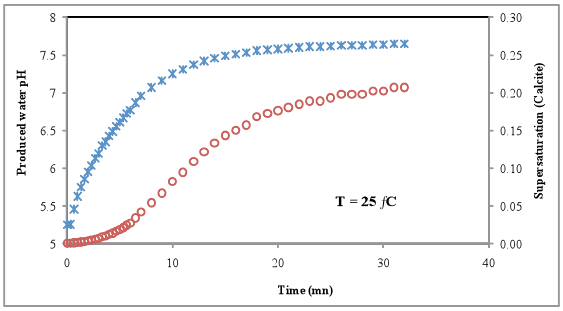

Figure 4 : Effect of degassing with atmospheric air on osmosis water pH -∗- and supersaturation -o- relative to calcite

3.3. Reliability test of the inlet water conductivity

Compared to salinity values determined experimentally, the inlet water conductivity seems to be presenting some defaults and its values are sometimes incorrect. The evolution of RO applied pressure versus the inlet water conductivity, as shown in figure 5, confirms the finding especially at values superior to 20 $mS.cm^{-1}$. All the running experimental sets, even when those tested by tap and mixed water, are presented. The recovery rate is fixed to around 0.61, and then the applied pressure should be closely depending on the feed water salinity which is function of the conductivity. Indeed, the permeate flux is proportional to the Net Driving Pressure (Equation 3) equal to the difference between trans-membrane pressure and osmotic pressure gradient on both sides of the membrane. As shown by equation 8, the osmotic pressure is proportional to the water conductivity. Then to keep a constant permeate flux, the applied pressure should be regularly increased with inlet water conductivity. The increase of the pressure versus conductivity is revealed on figure 5, but with high fluctuation at values superior to 20 $mS.cm^{-1}$. These fluctuations cannot be due to temperature's variations between 15 and 21 °C.

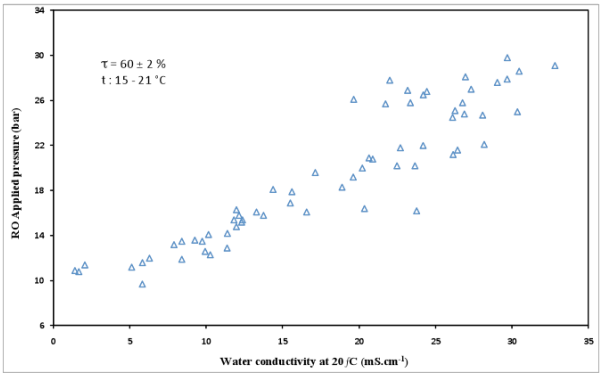

Figure 5: Evolution of the RO applied pressure versus feed water conductivity

It is important to develop a model which can detect non negligible default of the inlet water conductivity sensor in RO process. This model is based on the calculation of a semi-empiric value of the produced water flux.

The permeate flux across a reverse osmosis membrane is given by modified Darcy equation (Maurel 2006).

$$Q_P = L_m.A_m\,(\Delta P - \Delta\pi) \qquad (3)$$

L_p : hydraulic permeability of the RO membrane
A_m : membrane area
ΔP : pressure gradient on both sides of the membrane
$\Delta\pi$: osmotic pressure gradient on both sides of the membrane

$$\Delta P = ½.(P_F + P_R) - P_P \qquad (4)$$

$$\Delta\pi = \pi_{av} - \pi_P = K_\pi.S_{Av} - K_\pi.S_P \qquad (5)$$

F, P, R, Av,: indexes relative to Feed, Produced, Reject and Average value between feed and reject
S: Salinity of water
K_π: osmotic pressure constant

Using the mass balance on the RO modules and neglecting S_P comparing to S_R (in our case $S_P < 0.02\ S_R$), S_{Av} can be determined by:

$$S_{Av} = \frac{Q_F S_F + Q_R S_R}{Q_A + Q_R} = \frac{S_F + (1-\tau)S_R}{1+(1-\tau)} \approx \frac{2S_F}{1+(1-\tau)} \qquad (6)$$

where τ (Q_P/Q_F) is the recovery rate.

In desalination field, water Salinity (S) is often estimated from the conductivity value at 20°C ($Cd_{20°C}$) by using empirical constant (K_S) as shown by equation 7 (Maurel 2006).

$$S = K_S.Cd_{20°C} \qquad (7)$$

The conductivity value at 20°C is calculated from the value measured at the water temperature (t) via a temperature correction factor (Fc)

$$S_{20°C} = Fc.C_t \qquad (8)$$

Then

$$S_{Av} \approx \frac{2K_S.Fc.Cd_{tF}}{1+(1-\tau)} \qquad (9)$$

The average osmotic pressure will be

$$\pi_{Av} \approx \frac{2K_\pi K_S.Fc}{2-\tau} Cd_{tF} \qquad (10)$$

Combining the precedent equations, the semi-empirical one of permeate flux can be considered as follows:

$$Q_P = L_m.S_m\,[\frac{(P_F + P_R)}{2} - P_P - k_\pi.Fc.(\frac{2K_S Cd_{tF}}{1+(1-\tau)} - K'_S Cd_{tP})] \qquad (11)$$

The calculated values of the permeate flux are compared to the experimental ones on figure 6.

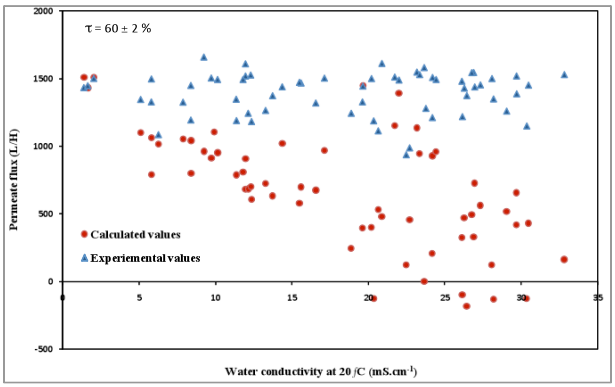

Figure 6: Comparison between experimental and calculated values of the permeate flux

The differences between the experimental permeate flux values and the calculated ones are very important. The difference amplitude increases with the water conductivity and often exceeds 100%. Some negative values are observed, they are due to a negative value of the Net driving pressure ($\Delta P - \Delta\pi$). Indeed, the calculated osmotic pressure ($\pi = K_\pi.\ K_S.Cd_{20°C}$) is closely dependent on the feed water conductivity. Any non negligible default in conductivity sensor will considerably affect the calculated net driving pressure and permeate water flux.

This proposed model confirms the existence of suspected values of the inlet water conductivities. Thereby, it can be developed to test directly the reliability of the RO water conductivity sensors for non negligible default.

4. CONCLUSION

Reverse Osmosis unit designed, to desalinate well water with about 15 $g.L^{-1}$ TDS, in the framework of the European OPEN-GAIN project is diagnosed. The physical and chemical analysis of water fluxes has shown that the feed water is found in equilibrium state, the produced water is very aggressive and the rejected one present a high risk of calcium carbonate scaling especially when there is no pH adjustment. Acidification needs to be optimized by taking into account of the anti-scaling dosing.

The developed model, based on the calculation of the semi-empiric value of the produced water flux, confirms the suspected defaults of inlet water conductivity sensor. In this model, the salinity, used to calculate the osmotic pressure, is replaced by a formula function of the water conductivity. The reliability of the feed water conductivity sensor can be tested by comparing the experimental permeate flux values to the calculated ones. The sensor default can be detected earlier and then avoid any malfunction consequence on the RO unit.

REFERENCES

Ayoub, J. Alward, R., 1996. Water requirements and remote arid area: the need for small scale desalination. *Desalination,* 107: 131-139.

Gambier, A., Wolf, M., Badreddin, E., 2008. Open Gain: A European project for optimal water and energy production based on high level of automation. *Euromed*, November 9-13, Jordan.

Elfil, H., Roques H. 2004. Prediction of the metastable zone in "$CaCO_3$-CO_2-H_2O" system. *AIChE Journal* 50(8): 1908-1916.

Elfil, H., Hannachi, A., 2006. Reconsidering water scaling tendency assessment. *AIChE Journal* 52(10): 3583-3591.

ElZanati, E., Eissa, E., 2004. Development of a locally designed and manufactured small scale reverse osmosis desalination system. *Desalination,* 165: 133-142.

Hannachi, A., Chernie, S., Elfil, H., 2009. Operating a RO desalination plant without an inlet water pH adjustment". *IDA World Congress on Desalination and Water Reuse*. Dubai - UAE.

Hannachi; A., Dridi, I., Zinoubi, R., Elfil, H., 2007. A New Index MLSI for Scaling Assessment. *IDA Word Congress on desalination and water reuse*, October 21-26, Grand Canaria- Spain.

Open-gain, 2007 Available from: http://www.open-gain.org

Maurel A., 2006. *Dessalement de l'eau de mer et des eaux saumâtres*, 2nd ed. Paris: Tec & Doc Lavoisier.

Mohammedi, K., Sadi, A., Cheradi, T., Belaidi, I., Bouziane, A., 2009. OPEN-GAIN Project: Simulation and Analysis of an Autonomous RO Desalination and Energy Production Systems Integrating Renewable Energies. *The 2nd Maghreb Conf. on Water Treatment and Desalination*. December 19-22, Hammamet, Tunisia.

Pitzer; K. S., 1973. Thermodynamics of electrolytes: Theoretical Basis and general equations. *Phys. Chem. J*., 77(2): 268-277.

ACKNOWLEDGMENTS

The authors acknowledge all the team members for their hard effort to succeed the Open-gain project funded by EC under Contract no.: 032535

.

OPTIMAL SCHEDULING OF HYBRID ENERGY SYSTEMS USING LOAD AND RENEWABLE RESOURCES FORECAST

Sami H. Karaki, Ayman Bou Ghannam, Fuad Mrad, Riad Chedid

American University of Beirut, P.O. Box: 110236, Beirut, Lebanon
skaraki@aub.edu.lb

ABSTRACT

In this paper, the integration of an optimizer and a forecaster into the energy management system (EMS) of a hybrid renewable energy system is studied. The role of the optimal EMS is to select the best decision set for the operation of the system based on a 24-hour forecast, reducing power conversion losses and unnecessary battery charge discharge cycles. Different forecast methods have been chosen for the 24-hour forecast of load, wind speed, and solar irradiance. A Genetic Algorithm is used for the optimizer. The cost function for evaluating system performance accounts for the fuel consumed, battery degradation, the amount of load shed, and the startups of the diesel engine. The results of the simulation have shown about 50% reduction in the number of battery cycles while preserving the same level of diesel engine fuel consumption as compared to classical EMS.

***Keywords*:** Energy management systems, renewable energy, hybrid energy system, load forecast, wind speed forecast, solar irradiance forecast, and genetic algorithms

1. INTRODUCTION

The basic components found in a typical hybrid renewable energy system include: a photovoltaic (PV) generator, a wind turbine (WT), a diesel engine, a storage battery, an electric load, and a dump load. The EMS controls the energy required from the sources to balance the connected loads. Thus, it turns on or off the diesel engine, charges or discharges the battery, connects or disconnects the dump load, or even sheds some load. For optimal performance, it should maximize the power utilized from renewable energy resources, minimize fuel consumption, minimize load shed, while operating the system safely within its operational constraints. Authors have investigated and discussed EMS of hybrid systems.

Soni and Ozveren (2006) proposed a model that gives the PV array and wind turbine the highest priority to supply the load. The battery supply balances the deficiency in RE resources. When the battery state of charge level falls below 20% of its rated value, the diesel generator is turned on. Wichert et al (2001) described an EMS for a system consisting of PV cells, batteries and a diesel engine. The diesel generator is operated at 80% of its rated output to maximize its efficiency. A predictive three hour distribution of the net load minus the PV is used. Seeling-Hochmuth (1998) proposed optimized fixed system control strategies that consist of certain predetermined control settings from offline optimization by running a genetic algorithm on a simulator of the system. Scrivani (2005) proposed an energy management technique for sea water reverse osmosis (RO) desalination plant, PV cells, batteries, and a diesel engine. To reduce fuel consumption, the proposed algorithm forecasts the expected levels of solar irradiance for the next 12 hours to determine whether to start the RO plant or not. The hourly average of the irradiance for the last 5 days is used as a forecast for the future values.

In this paper, we investigate the integration of a load and resource forecast and an optimizing algorithm into the EMS to increase the life of battery storage and reduce the switching of supplies and loads, and energy wasted in dump loads. Load is forecasted using established short term load forecast methods that divide the load into weather sensitive and base load (Karaki, 1999). The wind forecast uses weighted least squares to fit past observed data and expected weather stations' forecast to a polynomial. The solar irradiance forecast uses the statistical model of Perez et al. (2007) relating it to clear solar irradiance and sky cover parameter available from weather forecasts. The optimal decisions in the EMS are obtained by a Genetic Algorithm (GA) that evaluates system performance using a cost function accounting for the fuel consumed, the battery degradation, the amount of load shed, and the number of starts of the diesel engine.

2. SYSTEM COMPONENTS

The different components of the system are shown in Fig. 1, and the EMS coordinates their operation by calculating the power output levels to be supplied based on data recorded and the expected forecast of weather and load. Power is then dispatched among loads and supplies.

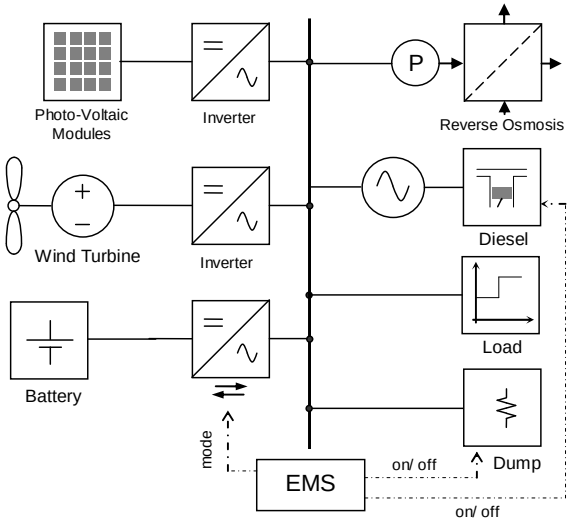

Figure 1: Hybrid renewable energy system

Renewable energy (RE), delivered by the solar modules and the wind turbine, is non-dispatchable and must be supplied at its available power level. Dispatchable units have a slack capability to maintain power balance at the busbar. These units may be the diesel engine (DE) when it is on, or alternatively, the battery and dump load when the DE is off. Load shedding may also used as a form of slack in the balance of power but only in extreme cases, e.g. the diesel fuel has run out. So, the classical EMS strategy to match RE and load is:

- If power from RE resources exceeds demand, then charge the battery until it is full, and supply the dump load with the excess; the DE is off.
- Else if RE power and battery discharge power exceed demand, then discharge the batteries, and turn off the dump load; the DE is off
- Else if RE power and DE power exceed demand then turn on the DE (if not already on); charge batteries if SOC is less than 80%.
- Else we have to shed load, since all available resources are not enough.

Based on this logic, the EMS can turn on and off the diesel engine, specify the battery charge/ discharge level, and connect and disconnect loads (load shed) or dump loads. The grid forming unit is specified at a lower control level; thus, if the DE is on then it is the grid forming unit, else it is the battery inverter. This logic is, however myopic and cannot tell if the sun will be up in two hours, for example, or that the wind resource is likely to be lost.

An optimizing EMS should contain a resource and load forecast and integrate their result in the decision making process, as shown in Figure 2. The optimal EMS bases its decision on forecasted values of load and renewable energy resources. But since forecasting and analyzing data is a slow and computationally demanding process, the EMS will be divided into three independent parts: a forecaster, an optimizer, and a dispatcher, each running at a different rate.

3. LOAD AND RESOURCE FORECASTS

Short-term forecasts of load and renewable energy resources for the next 24 hours are provided by a process that runs once per half-hour. Different forecast mechanisms are used for wind speed, solar irradiance, and load. The method used for short term forecast splits the load into a base load, a weather sensitive component, and special events (Karaki 1999).

On the other hand, the estimate of the net power flow (renewable energy power minus load power) in the system for the next hour is highly dependent on the most recently observed values, and it will vary each time the forecaster runs. Thus another very short term forecaster function is run each time the optimizer or dispatcher runs. Its inputs are the short term forecast, and the most recent readings of the net power flow; and its output is a forecast over a 1 hour horizon of the net power flow at intervals of 6 minutes.

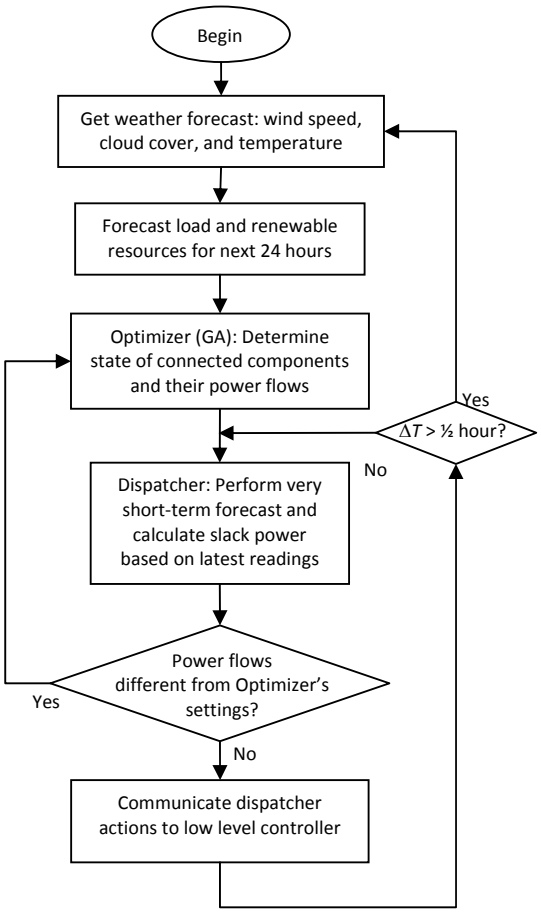

Figure 2: The optimal EMS algorithm

3.1 Wind Forecast

The method consists of finding a polynomial that fits the past data points and future wind speeds available from weather forecast data using the least squares method. Suppose that the current value of measured wind speed is y_0, the previous ones are y_{-1}, y_{-2} ..., and future values are y_4, y_8 ..., then y as a polynomial function of time is:

$$y_i = a_0 + a_1 t_i + a_2 t_i^2 \qquad (1)$$

By considering equally spaced samples y_i at times $t_i = i\,dt$ the equations (1) in matrix form become:

$$\begin{bmatrix} y_4 \\ y_0 \\ y_{-1} \\ y_{-2} \\ y_{-3} \\ y_{-4} \\ y_{-5} \end{bmatrix} = \begin{bmatrix} 1 & 4dt & (4dt)^2 \\ 1 & 0 & 0 \\ 1 & -dt & (-dt)^2 \\ 1 & -2dt & (-2dt)^2 \\ 1 & -3dt & (-3dt)^2 \\ 1 & -4dt & (-4dt)^2 \\ 1 & -5dt & (-5dt)^2 \end{bmatrix} \begin{bmatrix} a_0 \\ a_1 \\ a_2 \end{bmatrix}$$

$$\boldsymbol{y = Ha}$$

Since older data points are less relevant than more recent ones, the weighted least square method is used to take this factor into consideration. The coefficients $\boldsymbol{a}$ are given by: $\boldsymbol{a = (H^T W H)^{-1} H^T W\, y = X\, y}$, where $\boldsymbol{W}$ is a diagonal matrix of measurement weights. Exponential

smoothing is used on the weights starting from a value of 1 for the current reading and decreasing by 25% at -5. As we can see $\boldsymbol{X}$ is a constant matrix, and it needs to be calculated only once. Thus all the forecast algorithm has to calculate is the matrix product $\boldsymbol{X}\,\boldsymbol{y}$.

3.2 Solar Irradiance Forecast

It uses the empirical model of Perez et al (2007) relating solar irradiance to that of a clear sky using the sky cover parameter available from the weather forecast. The ratio of irradiance to that of clear sky irradiance is given by:

$$\frac{GHI}{GHI_{clear}} = 1 - 0.87SK^{1.9}$$

Where GHI is the average hourly irradiance, GHI_{clear} is the hourly clear sky irradiance, and SK is the forecasted sky cover parameter, which is a nine-level number between 0/8 and 8/8 with 0 corresponds to clear sky and 1 corresponds to total overcast.

The hourly average clear sky irradiance is obtained from historical data assuming that it is reached at least once in a week. So for any hour, the clear sky irradiance is equal to the maximum irradiance of the previous 7 days at the same hour. Here the variation in the maximal solar irradiance level throughout a week is assumed negligible. This method of estimation of clear sky irradiance level doesn't need any pre-setting and adapts to the location in which it is installed.

3.3 Very Short Term Forecast

The very short term net power forecast is carried out by a least squares method based on past five data points and future data points (forecasted by the short term forecaster). A second order polynomial is used to forecast the net power at the next step, i.e., 6 minutes ahead, by fitting past data points at -6, -12, -30 and -60 minutes together with the 60 minutes ahead obtained earlier from short term forecast.

4. THE OPTIMIZER

The optimizing methodology is based on a genetic algorithm with an appropriate representation of the possible solutions and has a method to calculate the fitness of these solutions. The input of this function is the short term forecast of load and resources, and its outputs are the diesel engine state (on/off), the battery power level, and load shed levels. In the operation of the system the following rules are considered:

- The dump load is not connected if the batteries are discharging or if the diesel engine is running,
- Supplying the load has a higher priority than charging the battery and fuel consumption considerations.

With these rules, we are left with two parameters to control: the power of the diesel engine and the power of the batteries. But due to power flow balance constraints, only one of these needs to be determined. We have chosen the diesel engine power since this variable is a composite of a discrete variable stating whether the engine is on or off and a continuous one specifying its power when running.

So the diesel engine (DE) power is divided into discrete levels to reduce the computational complexity without major degradation of performance. A reasonable approach is to divide the operation range of the DE power into eight levels within the permitted zone of operation. The selected levels are: 0, 60%, 65%, 70%, 80%, 90%, 95%, and 100%. A higher level of accuracy has been chosen near the limits to allow for smoother behavior of the system. Thus the DE generator power levels are represented as a string of 24 bits corresponding to 8 hours with 3 bits each representing the 8 levels of the diesel engine.

The heuristic used to speed up the solution process was to divide the 24 hour horizon into 3 periods of 8 hours each. This was found to be sufficient since he optimizing process is being repeated progressively at half-hour intervals. Increasing the horizon to 24 hours simply increased the computations without any noticeable improvement in the quality of decisions reached. The Cost function defined below is used as a fitness measure of the represented solutions. Reproduction was based on a single crossover point, and selection is based on tournament stochastic polling with an elite count of 5 in a generation population of 50. The mutation rate had a uniform distribution from 0 to 0.3.

4.1 Cost Function

The GA algorithm uses the system cost function as an individual fitness evaluation. The system cost function has the following form:

$$L = \sum_{i=1}^{N} u_i F_{DE}(P_{DEi}) + S_{DE}(u_i, u_{i-1}) + F_{LS}(LS_i) + F_{BT1}(SOC_i, \Delta T) + F_{BT2}(\Delta W)$$

Where:

- u_i is a Boolean defining the state of generator (on/off)
- $F_{DE}(P_{DEi}) = C_{DE}\,P_{DEi}$ is the cost of operating the diesel engine in \$/h, with P_{DEi} being the power delivered in kW in time interval i, C_{DE} is the cost of energy obtained from the diesel generator in \$/kWh; a typical value is 0.17 \$/kWh for the selected 20kW diesel generator.
- $S_{DE}(u_i,\, u_{i-1}) = 5C_{DE}\,u_i(\,u_i - u_{i-1})$ is the cost of starting the diesel engine, which is essentially a penalty factor selected heuristically to limit the number of start-ups to 8 per day as a maximum. In addition to that, the minimal time to run the diesel engine is 18 minutes. Violating this limit is penalized by a large cost of $10C_{DE}$.
- $F_{BT1}(SOC_i, \Delta T) = C_{BT}Q_{BT}(1 - SOC)k\Delta T$ is the cost of prolonged discharge of the battery, which is proportional to the depth of discharge of the battery and its duration; where C_{BT} is the cost of replacing the battery, ΔT is the discharge time in days, and k is a constant calculated considering that a battery should

be recharged to its full capacity once every 4 days (Mattera et al, 2003) to avoid sulfation. For a battery of 10 years lifetime when kept at full charge, and 50% reduction if kept at 40%, *k* would be equal to 0.022.

- $F_{LS}(P_{LSi}) = 50\ C_{DE}\ P_{LSi}$ is the cost of load shedding, which represents the social cost of not serving the load arbitrarily set at 50 times the cost of supplying it from the diesel engine.
- $F_{BT2}(\Delta W)$ is the cost of battery degradation (ΔW) that accounts for the limited number of charge/ discharge cycles. This item is further explained below.

4.2 Battery Degradation

The number of discharge cycles that a battery can undergo over its lifetime is specified by manufacturer's curves for different discharge levels. Scrivani (2005) suggested that the total power a battery can supply over its life is nearly constant irrespective of the depth of discharge if the SOC of a battery is kept above 40%. A somewhat related approach is used here. The degradation in battery life for each cycle is calculated as the inverse of the number of cycles the battery can undergo at a given discharge level. Thus, if ΔW is the degradation of the battery due to one cycle from full charge to a depth DOD and back to full charge, then

$$\Delta W = \frac{1}{N_{DOD}}$$

Where N_{DOD} is the number of cycles the battery can undergo for the given discharge level, read from the manufacturer's curve. For a partial discharge from SOC_1 to SOC_2 , ΔW is then taken as:

$$\Delta W = \frac{1}{N_{DOD_2}} - \frac{1}{N_{DOD_1}}$$

Thus, the lifetime *W* of the battery is started at 1 and is updated as $W = W_{old} - \Delta W$; total degradation of the battery occurs when *W* becomes zero. Thus the cost of the battery degradation is simply:

$$F_{BT2}(\Delta W) = \Delta W\ \ C_{BT}$$

4.3 Constraints

The diesel engine operation levels are confined to 8 discrete levels, the diesel engine will always operate within its permissible limits, and thus there are no additional constraints on the optimization variable. As for the batteries, the power that can be delivered (P_{BT}) and the state-of-charge (*SOC*) have upper and lower bounds:

$$-P_{BT}^{\max} < P_{BT} < P_{BT}^{\max}$$

$$0.4 < SOC < 1$$

The other variables are computed from the power balance equation:

$$P_{LS} - P_{DL} = P_{load} - P_{RE} - P_{DE} - P_{BT}$$

Where $P_{LS} \geq 0$ and $P_{DL} \geq 0$

Thus any solution produced by the optimizer would be feasible.

5. THE DISPATCHER

The role of the Dispatcher is to check if the profile assigned by the optimizer is valid for the current data readings. In case it is consistent with observed data, the assigned values will be applied; else, the optimizer will be called to recalculate the optimal profile using the latest readings. The Optimizer having specified the state of the DE and the power flow into the different components, the Dispatcher operates as follows:

- If the diesel engine is on then it is the grid forming unit; if DE power is much different than the one specified by the optimizer, or bus frequency has deviated from its reference value (power mismatch), then run the optimizer again; else set battery, load shed, and dump load to their assigned values.
- Else if the DE is off, the battery (BT) is the grid forming unit; if BT power is much different than the one specified by the optimizer, or bus frequency has deviated from its reference value (power mismatch), then run the optimizer again; else set load shed, and dump load to their assigned values.

6. SIMULATION AND RESULTS

The methodology was applied to the system being installed at Bourj Cedria, Tunis, with the sizes of the different subsystems given as: wind turbine size is 15 KW, the PV generator size is 15 kW, the battery size is 3.6 kWh, the reverse osmosis plant is 4 kW, and the general electrical load has a peak of 11 kW. Wind speed and solar irradiance data for one year starting on 12/12/2007 was used in the evaluation.

Data from a weather station at Bourj Cedria in Tunis has been used in testing the methods. Forecasts from weather stations were not available, and were simulated from average values over 4 hours with the addition of 25% perturbation. The solar irradiane forecast error is about 8% and is almost constant over the 24 hours forecast range.

A second order polynomial has been used for the very short term forecast of net load. Past data points corresponding past 6, 12, 30 and 60 minutes have been chosen together with the 1 hour ahead short term forecast. The error in the six minutes forecast is about 8% and increases to about 10% for the 1 hour forecast.

A typical week in winter and another in spring have been selected for the simulation. The winter week has insufficient renewable energy resources contributing to about 50% of load demand. Spring days on the other hand have more abundant renewable energy resources of about 94%.

The EMS has been tested in two different configurations. In the first case, a classical if-then-else static EMS similar to the one used in commercial controllers has been used (Chedid et al, 2008), which is considered as a reference for comparison. In the second case, the performance of the forecaster and the optimizer are tested together.

Figure 3 shows the power flow of diesel engine and that of the battery. We can see that the diesel engine is always running near its rated power, and thus at its highest efficiency. Nevertheless, the efficiency gained from running diesel engine at a high load factor is wasted in the unnecessary charge discharge cycles of the battery (Figure 4) and reducing the life of the batteries due to a relatively high frequency of cycling. This could be seen clearly in the interval from 60 to 140 hours. The net load is always positive all over this zone meaning that there is no surplus of resources to be stored, and thus the battery need not be discharged.

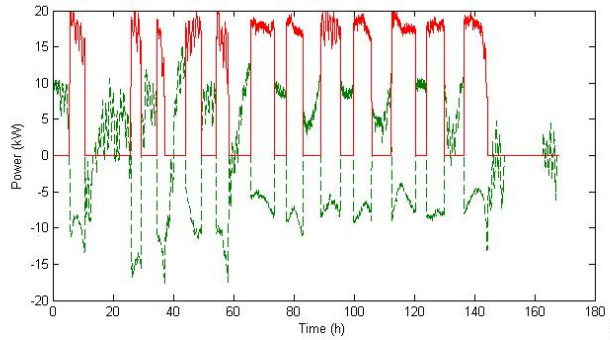

Figure 3: Diesel engine (continuous) and battery (dashed) power flows for the winter week: classical EMS

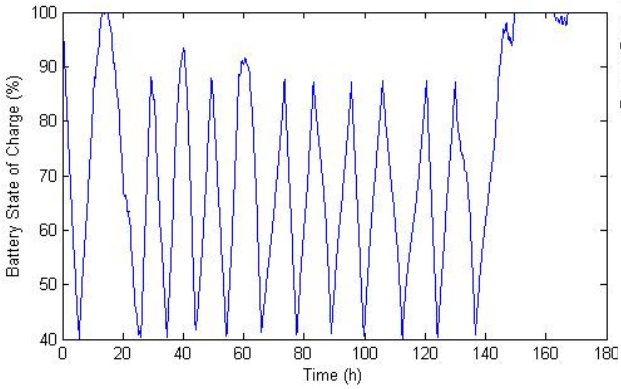

Figure 4: Battery State of Charge in the winter week: classical EMS

For the optimal EMS, the diesel and battery power flows are shown in Figure 5. In this case, the diesel engine runs for prolonged intervals at a lower load factor, and the power supplied to the battery is small. The latter takes the form of discrete steps set by the optimizer as a compromise between diesel engine efficiency and battery charging efficiency. As a result the battery is cycled less often (Figure 6), thus prolonging its useful life. There are some spikes in the diesel engine operation due to high perturbations in the wind power or load, but within the imposed limits (t_{on} >18 minutes).

The results of the simulation of the system using the Classical EMS and the proposed optimal EMS are given in Table 1 for typical weeks in winter and in spring. The number of runs per hour of the optimizer for the 7 winter days was monitored and the mean was found to be one call every about half an hour and its decision set remains valid for that period. As can be seen in the table below, there is a considerable reduction of in the number of charge discharge cycles of the batteries is reduced by more than 50%, which indicates that the battery life would be more than doubled.

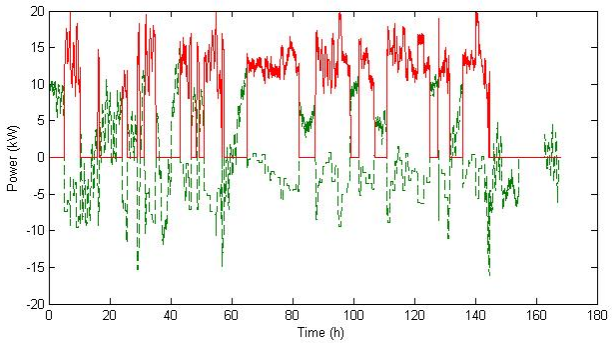

Figure 5: Diesel engine (continuous) and battery (dashed) power flows for the winter week: optimal EMS

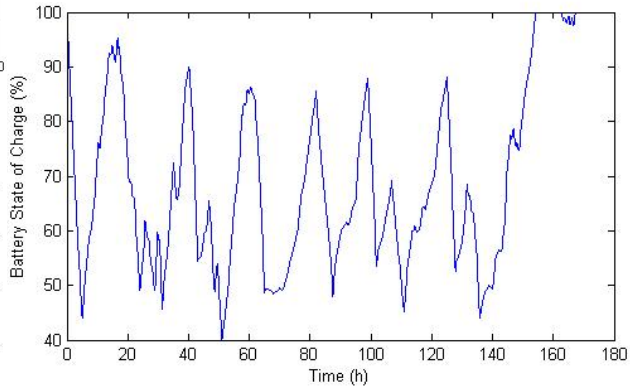

Figure 6: Battery State of Charge in the winter week: optimal EMS

Table 1: Simulation Results for a Winter and Spring Week

	Winter Week		Spring Week	
EMS Type	Classical	Optimal	Classical	Optimal
Demand (kWh)	1959	1959	1959	1959
RE Supply (kWh)	1032	1032	2085	2085
Dumped (kWh)	89	62	462	463
Diesel (kWh)	1181	1105	391	389
Fuel (liters)	384	368	127	130
DE Starts	12	16	5	15
Battery Cycles	12	7	5	1

There is a reduction in the required power from the diesel engine (about 6%) and in the fuel consumption (about 4%) for the winter week, whereas the diesel engine power is almost the same in spring with a slight increase in fuel consumption. This is due to the fact that the optimal EMS doesn't always run the diesel engine at its peak load, which would introduce some losses. Using two diesel engines would however solve this problem. The number of diesel engine starts is limited to about 2 per day, which is less than the permissible value. Overall, the optimal EMS has achieved almost the same level of fuel consumption but with a major decrease in the number of cycles of the batteries.

The response of the system in different configurations has been simulated to analyze the effect of variations in system size on the EMS performance. For a battery size reduced by 10%, the results are shown in Table 2, cols. 1 and 2. The classical EMS shows a slight reduction in fuel cost but an increase in the number of battery cycles (from 12 to 15), when compared to cols. 1 and 2 in Table 1. On the other hand, the optimal EMS has produced a slight increase in fuel consumption (1%) but a lower increase in the number of cycles (7 to 8).

Since the battery is needed to store excess energy, its size reduction should lead to an increase in the dump load power. The results show that this is true for the optimal EMS, but not for the classical one, which is an indication of the bad management of battery storage by the classical EMS that has more dump load energy and more fuel consumption in base case. On the other hand, the optimal EMS performance has degraded a little with the decrease in the battery size indicating that the system is capable of handling the extra storage. However, it remains better in terms of fuel consumption and battery life taken together.

Table 2: Winter Week Reductions: Battery Capacity (10%), PV generator (10%), and Diesel Engine (25%)

	Battery		PV		DE	
EMS Type	C[1]	O	C	O	C	O
Demand (kWh)	1959	1959	1959	1959	1959	1959
RE Supply (kWh)	1032	1032	993	993	1032	1032
Dumped (kWh)	81	85	77	60	57	59
Diesel (kWh)	1177	1117	1200	1131	1102	1056
Fuel (liters)	382	371	390	376	360	350
DE Starts	13	14	12	18	9	14
Battery Cycles	15	8	12	4	8	1

Note 1: C for classical and O for optimal

When the PV generator size is reduced by 10% results are shown in Table 2, cols 4 and 5. The fuel consumption with the classical EMS has increased by 1.5%, whereas the number of battery cycles is the same. In the optimal system the fuel consumption is increased by 2.2% but the number of battery cycles is reduced from 7 to 4. This is expected since battery storage is less useful in systems with low renewable energy resources. Here also overall system performance with the optimal EMS remains significantly better than that of a classical EMS.

The performance of the system with a 25% reduction in the Diesel engine rated power has also been analyzed (Table 2, cols 6 and 7). Here we note a 3% reduction in the fuel consumption with a large drop in the number of battery cycles. System efficiency has improved for both the Classical and Optimal EMS which indicates that there is a need for a smaller diesel engine.

The performance of the system is dependent on both, the component sizes and the EMS logic, by using an "optimal" EMS logic the dependence of system performance on the EMS is thus ideally eliminated but practically reduced. Thus the performance is more dependent on the component sizes when using an "optimal" EMS as compared to a classical if-then-else EMS logic.

7. CONCLUSIONS

This paper has investigated the integration of a reconfigurable optimizer and a forecaster into the Energy Management System (EMS) as compared to a classical EMS of a hybrid energy system. The results of the simulation have shown about 50% reduction in the number of battery cycles while preserving the same level of diesel engine fuel consumption as compared to a classical EMS. This reduction should elongate the life of the batteries up to 100%, thus introducing a major reduction in the operation cost of the system. The effect of the optimal EMS on the size of system components has been studied. Sensitivity analysis has shown that the system operating with an optimal EMS is more sensitive to changes in system component sizes, because it is operating near its peak efficiency boundary.

ACKNOWLEDGEMENTS

The work described in this paper was inspired and partly carried out as Work Package 3 in the Open Gain Project funded by the EC under FP6 (Contract No. 32535). The Open Gain project is carried out by a consortium of MENA institutions led by Prof. Essam Badreddin, head of the Automation Lab at the University of Heidelberg, Germany.

REFERENCES

Chedid R, S. Karaki, D. Fares, E. Azar, K. Kabalan, 2008, Open Gain Integrated Energy Management System Design, *AUB Progress Report Document (WP3)*.

Karaki S., 1999, Weather Sensitive Short Term Load Forecasting using Artificial Neural Networks and Time Series, *International Journal of Power and Energy Systems*, Vol. 19, No. 3, pp. 251-256.

Mattera F., D. Benchetrite, D. Desmettre, J. Martin, E. Potteau, 2003, Irreversible Sulfation in Photovoltaic Batteries, *Journal of Power Sources* 116, 248–256.

Perez R. et al, 2007, Forecasting solar radiation–Preliminary evaluation of an approach based upon the national forecast database, *Solar Energy* 81, 809–812.

Scrivani A., 2005, Energy management and DSM techniques for a PV-diesel powered sea water reverse osmosis desalination plant in Ginostra, Sicily, *Desalination* 183, 63–72.

Seeling-Hochmuth G., 1998, *Optimization of Hybrid Energy Systems Sizing and Operational Control*, PhD Dissertation, University of Kassel.

Soni A., Ozveren C., 2006, Improved Control of Isolated Power System by the Use of Feeding Technique, *Proceedings of the 41st International Universities Power Engineering Conference* (UPEC '06), September 2006.

Wichert B., M. Dymond, W. Lawrance, and T. Friese, 2001, Development of a Test Facility for Photovoltaic-Diesel Hybrid Energy Systems, *Renewable Energy* 22, 311-319.

FAULT-TOLERANT SUPERVISORY CONTROL OF A REVERSE OSMOSIS DESALINATION PLANT POWERED BY RENEWABLE ENERGIES

A. Gambier, T. Miksch, E. Badreddin

Automation Laboratory, Heidelberg University

gambier@uni-heidelberg.de, {tobias.misch, badreddin}@ziti.uni-heidelberg.de

ABSTRACT

Many applications of Reverse Osmosis desalination plants (RO plants) require a fault tolerant system, in particular when human life depends on the availability of the plant for producing fresh water. However, they have been little studied in the literature from this point of view, in particular, when the plant is powered by renewable energies. In this case, the availability of the power supply is limited and depending on weather conditions. Therefore, the plant has to be able to work at different operating point and hence, fault tolerance becomes essential.

The present work reports a study, in the framework of the European project Open Gain, on Fault-Tolerant Control (FTC) of a RO plant powered by renewable energies. The approach is based on optimized PID control loops in the lowest control level and a Model Predictive Control (MPC) as supervisory controller. The MPC provides fault tolerance by using a prioritized lexicographic algorithm.

Keywords: fault tolerant control, reverse osmosis desalination

1. INTRODUCTION

Reverse osmosis desalination plants use sensible components, which are also prone to parameter changes because membranes are sensitive to temperature of feed water, fouling, scaling and pressure variations. RO plants are normally controlled by using PID control laws, which are tuned but not optimized.

Although such plants are difficult to control and control is a very important aspect for the safety and economical plant operation, this subject is not much researched and only some contributions can be found in the literature. For example, the first multi-loop control system for a RO plant was proposed in Alatiqi, Ghabris, and Ebrahim (1989). It includes one pressure controller and two pH controllers. For desalination plants in general and RO in particular, only few contributions regarding model based control have been reported. A simplified dynamic model for an industrial plant is reported in Al-Bastaki and Abbas (1999). In Alatiqi, Ettouney, and El-Dessouky (1999), an overview about process control of desalination plants is given and Assef et al. (1995) presents some advanced control techniques for RO plants. DMC (Dynamic Matrix Control) is compared with standard PID control in Robertson et al. (1996). Decoupled control is proposed in Riverol and Pilipovik (2005). Some ideas of using hybrid control in desalination plants are proposed in Gambier and Bareddin (2002) and the simultaneous design of two PI controllers for a RO plant by using multi-objective optimization is the subject of Gambier, Wellenreuther, and Badreddin (2006). A nonlinear control approach for a high recovery RO system is proposed in McFall, et al. (2008). FTC (Fault Tolerant Control) approaches are presented in McFall et al. (2007) with simulation results and in Gambier,. Blümlein and Badreddin (2009) for a real-time application. Dynamic models for the control of RO plants are reviewed in Soltanieh and Gill (1981) and in Gambier, Krasnik and Badreddin (2007). Finally, different configurations for the control system are analyzed in Gambier, Wellenreuther, and Badreddin (2009), and a laboratory plant for experimenting with the real-time control of a RO process is described in Gambier, Miksch, and Badreddin (2009).

Until now, no work has proposed a fault tolerant control system, which is optimized in order to operate with renewable energies. In the present study, a supervisory control system based on a fault tolerant MPC, which optimize the set points according to the available energy is presented. The low level control is implemented by using parameter optimized PID controllers. In Section 2, the RO process is described from the control viewpoint. Section 3 is devoted to introduce the problem of fault-tolerant control. In Section 4, the proposed approach is described. Simulation results are shown and analyzed is Section 5. Finally, conclusions are drawn in Section 6.

2. PROCESS DESCRIPTION

A basic RO system consists in general of a pretreatment stage, a high-pressure pump, a membrane assembly (RO unit) and a post-treatment unit (see Figure 1). Salty feed water is first pretreated to avoid membrane fouling. Afterward, it passes through filter cartridges (a safety device) and is sent through the membrane modules (permeators) by a high-pressure pump. Because of the high pressure, pure water permeates through the membranes and the salty water becomes concentrated (retentate or brine). The water product flows directly from the permeators into the post treatment unit, and the retentate (at high pressure) is discharged, usually, after

passing through an energy recovery system (see Buros (2000) and Wilf et al. (2007) for a review of membrane processes).

Pretreatment is important in RO plants because suspended particles must be removed in order to maintain the membrane surfaces continuously clean. Thus, pretreatment consists of fine filtration and the addition of chemicals to inhibit precipitation and the growth of microorganisms. The pH value of the feed water is also adjusted in this unit. The high-pressure pump supplies the pressure that is needed to allow water to pass through the membrane in order to reject salts. The pressure range is from 15 to 25 bars for drink and brackish water and from 54 to 80 bars for seawater.

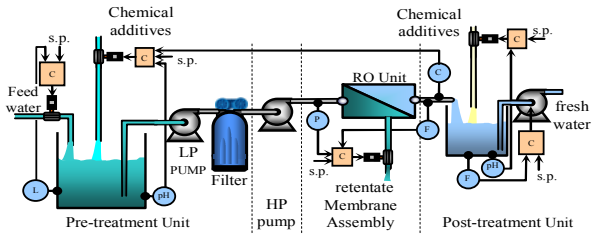

Figure 1: Schematic Diagram of a RO Plant and Its Control Loops

The membrane assembly consists of a pressure vessel and several membrane units such that feed water is pressurized against the membrane. The membrane must be able to resist the entire pressure drop across it. The semi-permeable membranes vary in their ability to pass fresh water and reject the passage of salts. Finally, the post-treatment consists of stabilizing the water and preparing it for distribution. This post-treatment might consist of removing gases such as hydrogen sulfide, adding minerals and adjusting the pH value.

Two valves are used for the control of permeate flow rate and its conductivity, which are carried out by manipulating the flow rate of retentate and the chemicals at the pretreatment unit, respectively, as it is shown in Figure 2.

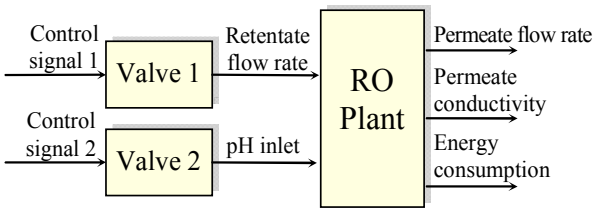

Figure 2: I/O Representation of the RO Plant

Notice that changes in the retentate flow rate also affect the permeate conductivity. However, changes in the pH of feed water do not modify the permeate flow rate. This leads to a triangular system as given in Figure 3.

3. FAULT-TOLERANT CONTROL

3.1. Overview and Definitions

There are several definitions and classifications of FTC systems (FTCS). In the following, the definitions given in Mahmoud, Jiang, and Zhang (2003) are adopted, where a FTCS is a control system that can work stably with an acceptable degree of performance even though in the presence of component faults. FTCS should detect and accommodate faults avoiding the occurrence of failures, i.e. irrecoverable damages at the system level.

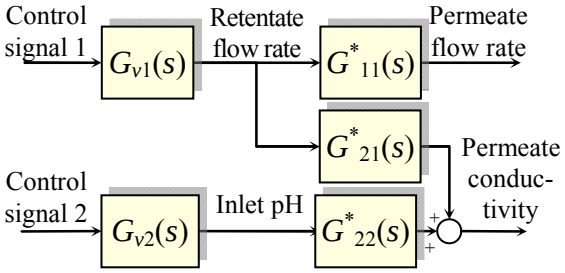

Figure 3: Block Diagram of a RO plant

Fault tolerance can be reached by means of different mechanisms. For example, it is possible to obtain a limited fault tolerance by using a robust control system design. This approach is sometimes named Passive Fault-Tolerant Control System (PFTCS). Contrarily, Active Fault-Tolerant Control Systems (AFTCS) require a new controller either by using adaptive control or switching control. Adaptive control leads to the faults accommodation, whereas switching control makes possible a reconfiguration of the control system. Notice that reconfiguration can take place at different levels depending on the severity of the fault and on the available system infrastructure. The most simply case of reconfiguration is given by controller switching. However, there could be other kind of reconfigurations if some redundancy is available: changes on the control system topology by using functional redundancy (redesign of the control system by using other actuators or/and other sensors) or plant reconfiguration if physical redundancy (i.e. standby backup of sensible components) is foreseen in the plant. AFTCS need a priori knowledge of the expected faults or a mechanism for the detection and isolation of unanticipated faults, namely a FDI scheme. A simplified classification of FTCS is summarized in Figure 4.

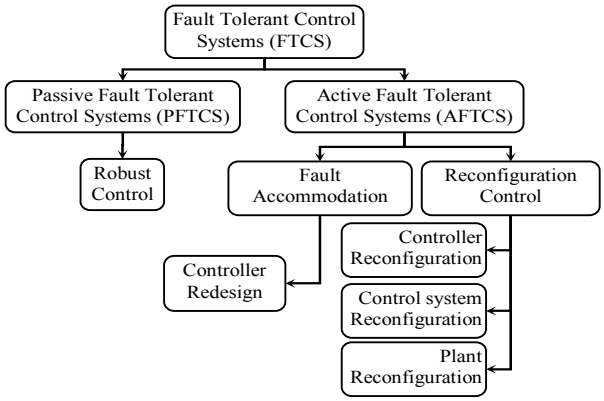

Figure 4: Classification of FTCS

3.2. Control Laws for FTSC

The above mentioned mechanisms for providing fault tolerance have different degree of complexity. PFTCS is the simplest case, followed by fault accommodation and finally the system reconfiguration in its different stages.

Hence, the design of FTC systems should be undertaken including this sequence, i.e. first the controller should be robust, then it has to provide facilities for a fault accommodation and if all these mechanisms are insufficient in order to solve the problem a reconfiguration should be attempted.

Some control laws have been modified as well as developed to manage fault accommodation: For example in Abdel-Geliel, Badreddin and Gambier (2006), the Dynamic Safety Margin (DSF) is proposed to provide fault accommodation for controllers that cannot manage constraints as for example PID (Proportional, Integral and Derivative) control, LQ (Linear Quadratic) optimal control and unconstrained MPC (Model Predictive Control); another approach for LQ controllers can be found in Staroswiecki (2006); fault tolerance based on controllers designed by using Eigenstructure Assignment (EA) has been proposed in Jiang (1994). A different approach, the Pseudo Inverse Method (PIM), is proposed in Staroswiecki (2005). It tries to obtain a controller for the faulty closed loop system by minimizing the distance to the nominal control system. The constrained MPC has also been studied for fault-tolerant behavior. It was first proposed in Maciejowski (1997) and later implemented in Ocampo-Martinez (2007). A real-time study of MPC is presented in Miksch, Gambier and Badreddin (2008a). Results of a comparison between LQ, PIM and MPC from a real-time point of view are presented in Miksch, Gambier and Badreddin (2008b), where it is shown that MPC has several advantages regarding the other ones.

4. FTC APPROACH FOR THE RO PROCESS

The proposed approach includes a low level control system based on parameter optimized PID controllers and a MPC, which provides supervisory control and fault tolerance.

4.1. Lowest Control Loops

Standard control systems of RO plants are normally based on PID controllers. A method for the join optimazation of two coupled control loops of a RO plant has been proposed in Gambier, Wellenreuther, and Badreddin (2007). Later the authors investigate in Gambier, Wellenreuther, and Badreddin (2009) other control system topologies. They found that a better topology for such kind of systems is such one as given in Figure 5. Therefore, this is the control system used in the current approach for the lowest control loops.

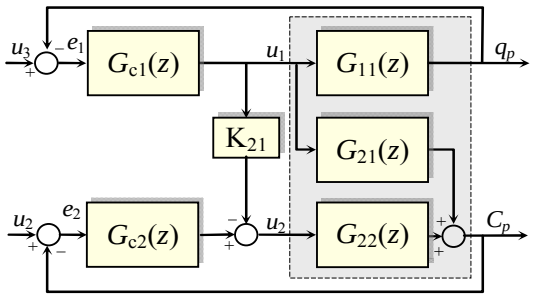

Figure 5: Control system topology for the low level control system

The transfer function for the first control loop is given by

$$e_1(z) = \frac{A_{11}\, r_{10}}{A_{11}^*}\,, \tag{1}$$

and the transfer function of the second control loop is in this case

$$e_2(z) = \frac{A_{21}A_{22}A_{11}^* r_{20} - A_{11}Q_{11}T_1^* r_{10}}{A_{21}A_{11}^*A_{22}^*}\,. \tag{2}$$

Polynomials A_{ij} and B_{ij} are denominator and nominator of the transfer function $G_{ij}(z)$, where the variable z has been eliminated for simplicity in the notation. Constants r_{10} and r_{20} are the amplitude of the set points. Transfer functions for the control signals are:

$$\Delta u(z) = \frac{A_{11}Q_{11}r_{10}}{P_{11}A_{11} + Q_{11}B_{11}} = \frac{A_{11}Q_{11}r_{10}}{A_{11}^*} \text{ and} \tag{3}$$

$$\Delta u(z) = \frac{Q_{22}(A_{21}A_{22}A_{11}^* r_{20} - A_{11}Q_{11}T_1^* r_{10})}{A_{21}A_{11}^*A_{22}^*}\,. \tag{4}$$

where $A_{11}^* = P_{11}A_{11} + Q_{11}B_{11}$, $A_{22}^* = P_{22}A_{22} + Q_{22}B_{22}$ and $T_1^* = B_{21}A_{22} + B_{22}A_{21}K_{21}$.

PID controllers are obtained taking

$$u_i(z) = \frac{Q_{ij}(z)}{P_{ij}(z)} e_j(z)\,. \tag{5}$$

$$P_{ij}(z) = z(z-1) \text{ and } Q_{ij}(z) = q_{ij,0}z^2 + q_{ij,1}z + q_{ij,2}\,, \tag{6}$$

respectively. Moreover, parameters have to satisfy the constraints

$$\begin{bmatrix} -1 & 0 & 0 \\ 1 & 1 & 0 \\ -1 & -1 & -1 \\ -1 & 0 & 1 \end{bmatrix} \begin{bmatrix} q_{ij,0} \\ q_{ij,1} \\ q_{ij,2} \end{bmatrix} < \mathbf{0} \tag{7}$$

in order to show PID behavior.

The parameter optimization is carried out following Gambier, Wellenreuther, and Badreddin (2009) by using an Multi-objective Optimization method (MOO). This is not presented here in order to save space.

4.2. Improving the Lowest Level Controller Design

A particular control problem with RO plants consists in that plant parameters change fast because of fouling and membrane cleaning has to be carried out often (e.g. once a week). Thus, process parameters obtained after cleaning are very different from the parameters obtained one week later before cleaning. Therefore, the control performance deteriorates fast in the course of the week, when the controller was adjusted by using parametric optimization. Hence, a robust control approach should be used. The method given in Gambier (2009) extended the parameter optimization of PID controllers by using MOO when

the parameter uncertainties are given in the form of intervals polynomials. Thus, it is possible to design robust control loops in the lowest level satisfying the first level of fault tolerance.

An additional problem is given by the fact that MOO optimization requires a predefined parameter space in which the controller parameters should be searched. This problem has been solved by Bajcinca and Hulin (2004). The toolbox presented in that work allows obtaining all stabilizing PID controllers in the parameter space for a given plant. This is used here in order to initialize the MOO algorithm.

4.3. Supervisory Control Loop

The supervisory control is implemented according to Figure **6** by using model predictive control. The MPC has two main functions. On the one hand, it provides the optimal set points for the low level control loops, such that the system works at the optimal operating point according to the energy availability. On the other hand, the MPC is responsible for providing fault tolerance.

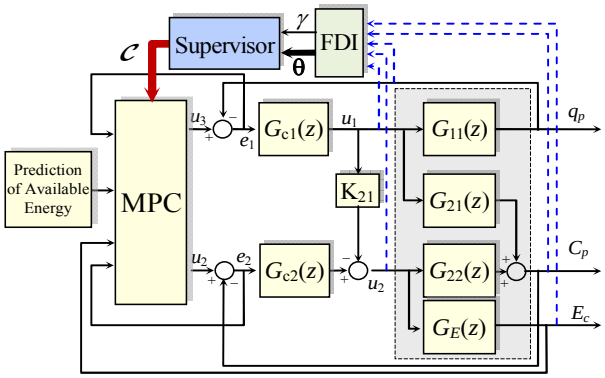

Figure 6: FT-MPC as Supervisory Controller

The MPC design for fault tolerance follows the work of Miksch, Gambier, and Badreddin (2010). It is based on the lexicographic multi-objective optimization of an l_1 norm by using a linear program. Constraints are given in the way of prioritized objectives, whose priorities are defined in order to satisfy the definition of performance regions as given in the example of Figure **7**.

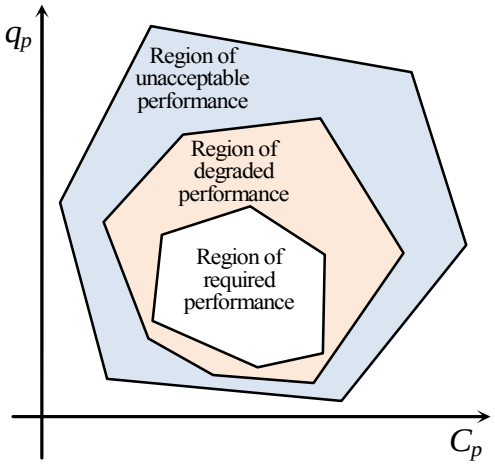

Figure 7: Example of performance regions for the outputs (C_p, q_p)

Constraints are adjusted according to the information supplied by a FDI unit (Fault Detection and Identification). However, the FDI block of Figure 6 is for the current work only simple logic that gives as output the corresponding value for γ, according to a predefined known fault. A general FDI unit has still to be implemented. The supervisor implements a logic that builds the constraints set $\mathcal{C}$ depending on $\gamma=\{0, 1, \ldots, n_\gamma\}$ and the fault parameters $\boldsymbol{\theta}$, i.e.

$$\mathcal{C} = \vartheta(\gamma, \boldsymbol{\theta}) . \qquad (8)$$

For example, if the valve opening of valve 1 is limited now until a maximum value of 70%, the FDI unit yields $\gamma = 3$ and $\theta(\gamma) = 0.7$. Thus, the supervisor will deliver at the output $\mathcal{C}(\gamma) = 0.7$ (this is the new constraint for u_1).

4.4. Predictor for the Available Energy

An experimental model of the energy consumption and a prediction of the available energy from the PV and wind subsystems are used to determine the set points for the PID controllers.

The predictor of the available energy is carried out according a simple charging model for the lead-acid battery pack. This model is obtained from Huang et al. (2010) as a linear perturbed model. Model parameters are experimentally obtained for satisfy a real laboratory system.

5. STUDIES AND RESULTS

The control system proposed in this work is being implemented at the present time. Some results of the low level control system can be found in Gambier, Wellenreuther, and Badreddin (2009). Some results about using the MPC as a fault tolerant controller are presented in the following.

For the studies, the plant is set to a permeate flow rate of 250 l/h and a valve openings of 50%. Permeate flow rate and the conductivity are the controlled variables. Then, the reference signal for the permeate flow rate is changed first to 350 l/h and afterward to 300 l/h. The conductivity is set at the operating point of 425 µS/cm. This conductivity is assumed to be an index for the water quality, which in most applications of such plants is a very important property and normally also the reason for using this kind of equipments. Therefore, this variable is considered of highest priority in the fault-tolerant control system. This means that in case of faults, the permeate flow rate can freely change within a defined range in order to maintain the conductivity as close as possible to its set point.

The conductivity is normally controlled by Valve 2. However, the conductivity can be modified by both control signals. This provides some redundancy that can be used for obtaining fault tolerance. The performed studies are summarized in Table 1.

Table 1: Studies of Fault-tolerance for the Water Conductivity

	Description	*u*min,1	*u*max,1	*u*min,2	*u*max,2
Nominal		0	100	0	100
Case 1	Valve 2 limited to 0-50%	0	50	0	100
Case 2	Valve 2 stuck at 100%	50	50	0	100
Case 3	Valve 1 stuck at 30%	0	100	30	30

The design parameters for the MPC are given in Table 2. The sampling time and the prediction horizon are optimally chosen according to Gambier and Badreddin (2009).

Table 2: Design Parameters for the MPC

PARAMETERS	NUMERICAL VALUES
R	*diag*(1.0, 0.01)
$\mathbf{Q}_1$ ($\mathbf{Q} = \mathbf{C}^T\mathbf{Q}_1\mathbf{C}$)	*diag*(100, 0.1)
$\mathbf{S}_1$ ($\mathbf{S} = \mathbf{C}^T\mathbf{S}_1\mathbf{C}$)	$\mathbf{Q}_1$
ρ	0
T_0	0.15 s
Horizons	$N = 14$ $N_u = 14$

The delay of the FDI to find the fault has been assumed to be 5s and the adaption of the fault-tolerant MPC for accommodating faults has been supposed to take 1s. Results are presented in Figure 8, 9 and 10, respectively. For all figures, results for nominal MPC are presented with solid red lines and results for the fault-tolerant MPC are shown with dashed black lines. The first fault case is presented in Figure 8. It consists of limiting the range of valve two between 0 and 50%. After the fault, the nominal MPC tries the continue maintaining the outputs at the set points but the conductivity cannot be controlled any more. The fault-tolerant MPC abandon the set-point control of the flow rate (but maintained it in a pre-defined band) in order to improve the conductivity control, since this is the most important variable.

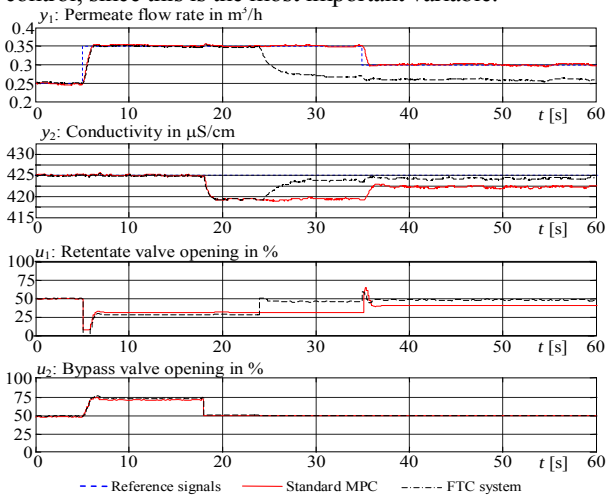

Figure 8: Control system behavior for Case 1 ($0 \leq u_2 \leq 50$ % for $t \geq 18$ s)

In the second fault case, Valve 2 goes to an opening of 100% and it stays permanently at this value. The standard MPC shows a similar behavior as the first case. The fault-tolerant MPC recovers the fault returning the conductivity to its set point at the expense of an acceptable steady-state error. This is shown in Figure 9.

Finally, Case 3 (Valve 1 is maintained fix at 30%) is the most difficult because it is not possible control the flow rate only with Valve 2 (Figure **10**). The standard MPC introduces a major deviation from the set point for the conductivity, whereas the fault-tolerant MPC recover the fault without steady-state error.

Notice that the concurring nature of the two outputs in the fault case, i.e. producing as much water as possible but keeping the right range of salinity, is a multi-objective optimization problem. This will be undertaken in a future work.

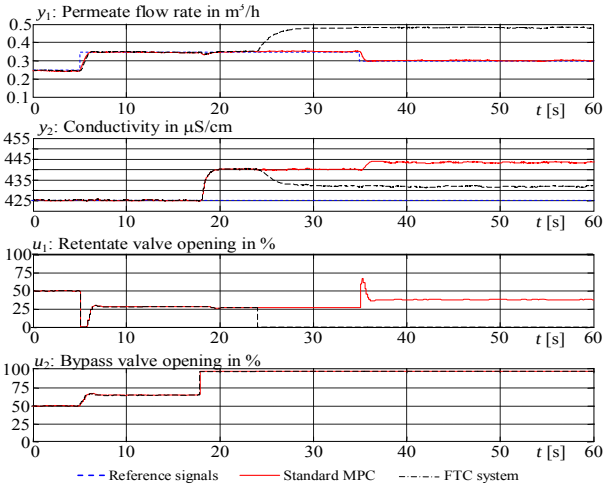

Figure 9: Control system behavior for Case 2 ($u_2 = 100$ % for $t \geq 18$ s)

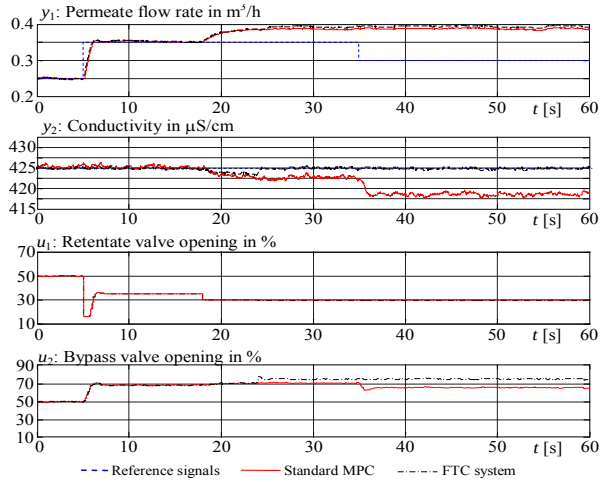

Figure 10: Control system behavior for Case 3 ($u_1 = 30$ % for $t \geq 18$ s)

6. CONCLUSIONS AND FUTURE WORK

In this contribution, the control problem of a reverse osmosis desalination plant is studied. In order to guarantee an acceptable water quality along the complete operation time even in case of faults, a fault-tolerant MPC based on adjusting its constraints in the supervisory level is proposed. In this first study, only actuators constraints are considered. Obtained results are very satisfactory and this motivates the extension of the work in order to include other faults, additional fault-tolerant mechanisms. Moreover, the whole control system of Figure 6 has still to be implemented since it has only been tested partially. Finally, the approach has to be combined with a robust fault-detection approach.

ACKNOWLEDGMENTS

This work has been supported by the European Commission by means of the project Open-Gain (contract No. 032535).

REFERENCES

Abbas, A., Model-predictive control of a reverse osmosis desalination unit. Desalination, **194**, 268-280, 2006.

Abdel-Geliel, M., E. Badreddin and A. Gambier. Application of dynamic safety margin in robust fault detection and

fault tolerant control. Proceeding of the *2006 IEEE Conference on Control Applications*, 337-342, Munich, October 4-6, 2006.

Alatiqi I., H. Ettouney, H. El-Dessouky, 'Process control in water desalination industry: an overview'. *Desalination*, 126, 15-32, 1999.

Alatiqi, I., A. Ghabris, and S. Ebrahim, "Measurement and control in reverse osmosis desalination," Desalination, 75, 119–140, 1989.

Al-Bastaki, N. M. and A. Abbas, Modeling an industrial reverse osmosis unit. *Desalination*, 126, 33-39, 1999.

Assef, J. Z., J. C. Watters, P. B. Desphande and I. M. Alatiqi, Advanced control of a reverse osmosis desalination unit. *Proc. Int. Desalination Association World Congress*, Vol. V, 174-188, Abu Dhabi, 1995.

Bajcinca, N. Hulin, T., 2004. RobSin: a new tool for robust design of PID and three-term controllers based on singular frequencies. *Proceedings of the 2004 IEEE Conference on Control Applications*, pp. 1546-1551, September 2-4, Taipei.

Buros, O., K. 2000. The ABCs of desalting. Topsfield: *International Desalination Association*.

Gambier A. and E. Badreddin, Application of hybrid modeling and control techniques to desalination plants. *Desalination*, 152, 175-184, 2002.

Gambier, A., A. Krasnik, and E. Badreddin, Dynamic modelling of a simple reverse osmosis desalination plant for advanced control purposes. Proc. of the 2007 American Control Conference, 4854-4859, New York, July 11-13, 2007.

Gambier, A., A. Wellenreuther and E. Badreddin, Optimal operation of reverse osmosis plants based on advanced control. *Desalinat. and Water Treat.*, **10**, 200-209, 2009.

Gambier, A., A. Wellenreuther, and E. Badreddin. Optimal control of a reverse osmosis desalination plant using multi-objective optimization. Proceedings of the *2006 IEEE Conference on Control Applications*, 1368-1373, Munich, October 4-6, 2006.

Gambier, A., and E. Badreddin, Control of small reverse osmosis desalination plants with feed water bypass. Proc. of the *2009 IEEE Conference on Control Applications*, 800-805, Saint Petersburg, July 8-10, 2009.

Gambier, A., N. Blümlein and E. Badreddin, Real-Time fault-tolerant control of a reverse osmosis desalination plant based on a hybrid system approach. Proc. of the 2009 ACC, Saint Louis, June 10-12, 2009.

Gambier, A., 2009. Optimal PID controller design using multiobjective Normal Boundary Intersection technique. Proc. of the *7th Asian Control Conference 2009*, 1369-1374, Hong Kong, August 27-29.

Gambier, A., T. Miksch and E. Badreddin, A reverse osmosis laboratory plant for experimenting with fault-tolerant control. Proc. of the *2009 American Control Conference*, 3775-3780, Saint Louis, June 10-12, 2009.

Huang, B. J., Hsua, P. C., Wua, M. S. and P.Y. Ho, 2010. System dynamic model and charging control of lead-acid battery for stand-alone solar PV system. *Solar Energy*, **84** (5), 822-830.

Jiang, J., Design of reconfigurable control system using eigenstructure assignments. *International Journal of Control*, **59**, 395-410, 1994.

Maciejowski, J., Modelling and predictive control: Enabling technologies for reconfiguration. Proc. of the *IFAC Conf. on Systems Structure and Control,* Bucharest, October 23-25, 1997.

Mahmoud, M., J. Jiang and Y. Zhang, Active Fault Tolerant Control Systems: Stochastic Analysis and Synthesis. Springer, Lecture Notes In Control And Information Sciences, Berlin-Heildelberg, 2003.

McFall, C., A. Bartman P. D. Christofides and Y. Cohen, Control of reverse osmosis desalination at high recovery. Proceedings of the *2008 American Control Conference*, 2241-2247, Seattle, June 11-13, 2008.

McFall, C., P. D. Christofides, Y. Cohen and J. F. Davis, Fault-tolerant control of a reverse osmosis desalination process. Proceedings of *8th IFAC Symposium on Dynamics and Control of Process Systems,* 3, 163-168, Cancun, June 6-8, 2007.

Miksch, T., A. Gambier and E. Badreddin, Realtime performance evaluation of fault tolerant control using MPC on the three-tank system. Proc. of the *17th IFAC World Congress*, Seoul, 11136-11141, July 6-11, 2008.

Miksch, T., A. Gambier und E. Badreddin: Realtime performance comparison of fault-tolerant controllers. Proc. of the *2008 IEEE Multi-conference on Systems and Control*, San Antonio, 492-497, 3-5 September 2008.

Miksch, T., A. Gambier und E. Badreddin: Fault-tolerant control of a reverse osmosis plant based on MPC with lexicographic multiobjective optimization. To be presented in the *2010 IEEE Multi-conference on Systems and Control*.

Ocampo-Martinez, C., Model predictive control of complex systems including fault tolerance capabilities: Application to Sewer Networks. Doctoral thesis. Technical University of Catalonia, Automatic Control Dep., 2007.

Riverol, C., and V. Pilipovik. Mathematical modeling of perfect decoupled control system and its application: A reverse osmosis desalination industrial-scale unit. *Journal of Automated Methods and Management in Chemistry*, 2005, 50-54, 2005.

Robertson, M.W., J. C. Watters, P. B. Desphande, J. Z. Assef and I. M. Alatiqi, Model based control for reverse osmosis desalination processes. *Desalination*, 104, 59-68, 1996.

Soltanieh, M. and W. N. Gill, Review of reverse osmosis membranes and transport models. *Chemical Engineering Communications*, 12, 279-, 1981.

Staroswiecki, M. *Robust fault tolerant linear quadratic control based on admissible model matching*. Proc. of the *45th IEEE Conference on Decision and Control*, 2006.

Staroswiecki, M., Fault tolerant control: The pseudo-inverse method revisited. Proceedings of the *16th IFAC World Congress*, Prague, July 4-8, 2005.

Wilf, M., L. Awerbuch; C. Bartels; M. Mickley, G. Pearce and N. Voutchkov, The guidebook to membrane desalination technology. Balaban Pub., 2007.

VALIDATION OF A REVERSE OSMOSIS DYNAMIC SIMULATOR

Luis Palacín[(a)], Fernando Tadeo[(b)], Johanna Salazar[(c)], César de Prada[(d)]

University of Valladolid, Dpt. of Systems Engineering and Automatic Control, 47011, Valladolid, Spain

[(a)]palacin@cta.uva.es, {[(b)]fernando, [(c)]johanna, [(d)]prada}@autom.uva.es

ABSTRACT

Reverse Osmosis (RO) is the most common technique to produce drinkable water in arid and semi arid regions, from brackish and sea water. However, these plants are usually not optimally designed and operated, because only a short number of constant operation points is considered and not a changeable control strategy. Dynamic tools of design and simulation of RO plants will help to improve the design and operation of this kind of desalination plants. In order to do this, a new dynamic simulation library of RO plants was previously presented and a hydraulic validation shown elsewhere. Now, the present paper deals with the chemical validation of that library, using experimental data from a real RO plant.

Keywords: desalination plants, reverse osmosis, dynamic simulator, validation, parameter estimation.

1. INTRODUCTION

Reverse Osmosis (RO) is known to be an effective technique to produce drinkable water from brackish and sea water, (Fritzmann et al. 2007). This is because RO plants need less energy, investment cost, space and maintenance than other alternative desalination processes, (Gambier et al. 2007), hence, it is the preferred desalination technique worldwide, (Baker 2004; Wilf 2007). In the particular case of water supply of villages and small settlements, small to medium-size RO plants are successfully used. In this case, energy consumption is commonly fulfilled by renewable energy sources, such as solar or wind, while diesel generators are needed in order to keep it operating when no renewable sources are available, (Tadeo et al. 2009).

ROSA© and TorayDS© are perhaps the most common software for design of RO plants. They have been developed by two important membrane manufactures (Dow Chemical and Toray respectively) and are very powerful tools for static simulation of RO membranes. First, the user defines the characteristic of the feed water (solutes concentration, pH, temperature, etc.) and the required characteristic of the permeate (flow, TDS, Boron concentration, etc.). Next, the software helps to choose the best membrane model and configuration for the plant: number of pressure vessels, number of membranes per pressure vessel, possibility of a second pass, feed pressure, etc.

This software responds to the typical methodology of operation of RO plants. These plants, specially the high productions ones (50,000 - 200,000 m3/day of permeate), operate usually at a constant operation point, (Palacin et al. 2009a). However, this operation method looks incoherent if it is taken into account that consumed water varies along a day and along a year. Figure 1 shows a typical water demand curve of a population of 300 inhabitants over two days. It can be seen that during the night, the water consumption reaches its minimum value. Water demand curves are slightly different for each day of the week, and especially, for each month of the year.

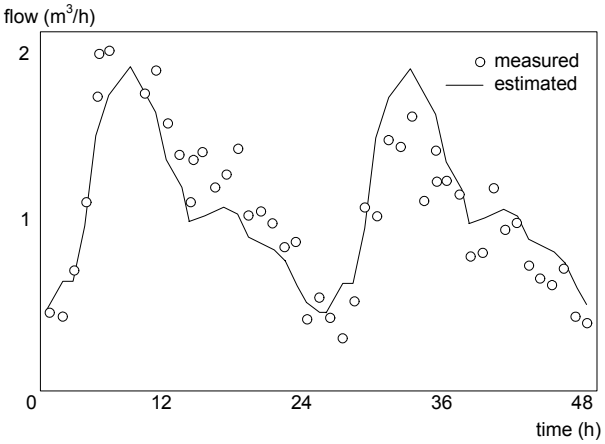

Figure 1: Typical water demand curve along two days.

Typical RO plants solve the daily variation of water demand by using big freshwater tanks at the end of the production line, and the annual variation by switching on/off membrane banks. It is easily understood that a priori this operation methodology is not optimal. On the other hand, using a variable operation point, producing more potable water when more is consumed, it will be possible to decrease the size of supply tanks, reducing the evaporation and minimizing the consumption of chemical products and the cost of equipments, (Palacin et al. 2009b). From an energy consumption point of view, a variable operation point looks more adequate too. It is very common that the availability and cost of electric energy varies along a day. This looks that producing more permeate water when energy cost is cheaper, the water total prize will

decrease, (Salazar et al. 2010). In order to find the better operation point curve, both effects must be taken into account: the variation of the water demand and the energy cost. Advanced control design techniques, which take into account a changeable operation point, improve efficiency of the RO plant, extend the life of the components and reduce installation and operation costs, (Palacin et al. 2010a). Several interesting and advantageous applications of advanced control techniques in desalination plants can be seen in (Bacelli et al. 2009; Bartman et al. 2009a; Bartman et al. 2009b; McFall et al. 2008; Palacin et al. 2009c; Zafra-Cabeza et al. 2009).

Unfortunately, using static simulation tools, as ROSA© or TorayDS©, it is not possible to design a RO plant with a variable operation point and better performance, (Gambier et al. 2004). In order to solve this, a complete tool for the dynamic simulation of RO plants was developed and presented elsewhere (Palacin et al. 2008), and upgraded in (Palacin et al. 2009a). This software is a dynamic and modular library, which is developed in EcosimPro© simulation environment, and it is based on using first-principles and correlations from the literature and requires the typical system parameters in a RO plant (quality of feed water, salinity, scale concentration, pH, temperature, pump characteristic curves, type of the filters, characteristic of the membranes, etc.). A description of the math model can be consulted in (Syafiie et al. 2008). An initial validation of the hydraulic part of this dynamic library (pressures and flows) was shown previously (Palacin et al. 2010b). Now, the present paper deals with the chemical validation (salinity, feed water quality...) of the library. Initially, the values of the different parameters of the math models of the library had been taken from the specialized bibliography. It is now shown how these parameters can be directly estimated from simple experiments on real RO plants.

This paper is organized as follows: Section 2 shows the pilot plant used for validation and section 3 presents a brief description of the dynamic library. Finally, methodology and results of the validation are shown in section 4, followed by Conclusions and References.

2. REVERSE OSMOSIS PILOT PLANT

The RO pilot plant used for validation of the library is shown in Fig. 2, and a simplified diagram of the plant is shown in Fig. 3. First, a pump (B1) pumps brackish water from a well to the supply tank (T1). From this tank, water is pumped to a set of filters and chemical additions. The high pressure pump (B2) increases its pressure to a value above the osmotic pressure so that the pressurized water can pass then through the RO membrane rack. The difference in pressure between each side of the membranes produces a flow of clean water through the membranes. Finally, this clean water is stored in other tank (T2), which supplies water to the consumers.

Figure 2: RO plant for testing.

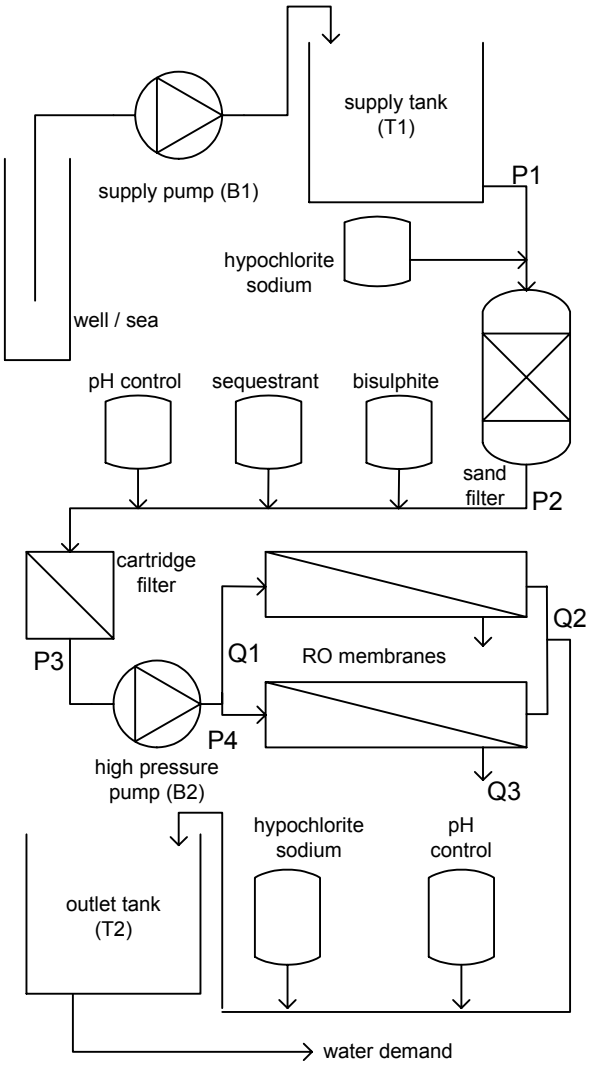

Figure 3: Diagram of the pilot plant.

Reverse osmosis is a separation process that uses high pressure to force a solvent (water) through a semi permeable membrane that retains the solute (salt) on one side. The clean water flow is called “permeate” and needs a remineralization before consumed, and the

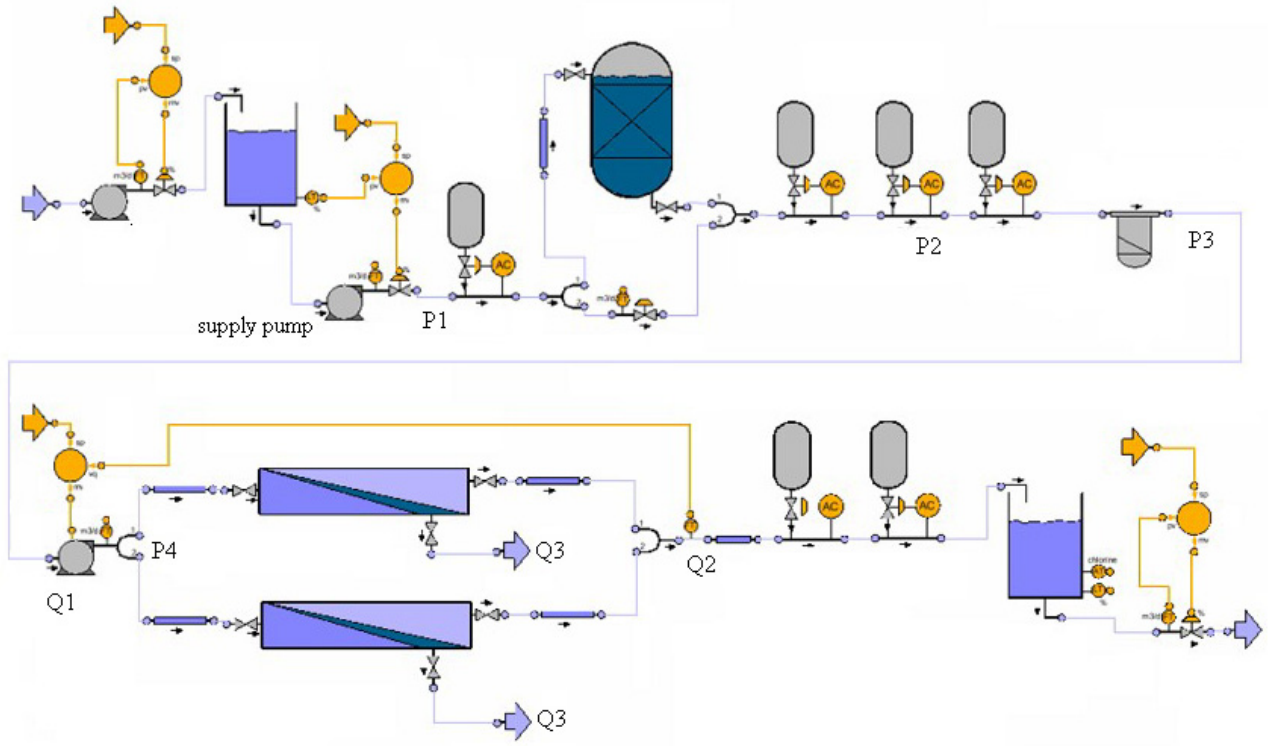

Figure 4: Graphical simulator of the pilot plant, made with the dynamic library.

rejected water flow is called "retentate" or "concentrate". The ratio between retentate and feed is called recovery. Typical values of recovery are 45% for sea water and until 80% for brackish water. An in-depth description of the components of an RO plant could be seen in (Al-Bastaki et al. 1999).

The RO plant which is utilized in this paper has been design to produce 800 L/h of permeate water from a flow of 2000 L/h of brackish water. A central problem during operation is the decrease in performance of the membranes, due to deposits (silt, scale, organic components, etc). Thus, in order to prevent precipitation and eliminate microorganisms, a pretreatment is needed. It normally consists of filtration and the addition of chemical products. In addition, periodic cleanings are scheduled to reduce the amount of deposits. The final part of the process is a post-treatment, to make the water drinkable, by the addition of chlorine and a remineralization.

The RO process requires a high pressure on the feed side of the membrane: close to 30bar bar for the plant utilized in this validation (and up to 80 bar for extreme cases with very salty seawater). This pressure is generated by the high pressure pump (B2), (that, in this case, it is a positive displacement pump), that consumes most of the electrical energy needed by the plant.

The permeate flow is controlled by a PID, which manipulates the velocity of the high pressure pump, using a variable-frequency drive. The recovery of the system is controlled manually by a back pressure valve in the outlet the concentrate.

3. DYNAMIC LIBRARY OF RO PLANTS

The dynamic library of RO plants has been developed in the simulation environment EcosimPro©. EcosimPro© is a powerful modeling and simulation tool that follows advanced methodology for modeling and dynamic simulation. It provides an object oriented and non causal approach that allows creating new simulations interconnecting reusable component libraries. EcosimPro© is based on very powerful symbolic and numerical methods capable of processing complex systems represented by DAE equations and discrete events. Moreover, free versions are available for research and teaching (http://www.ecosimpro.com).

The dynamic library of RO plants is based on a set of components representing the different units of a RO plant. As sand filters, cartridge filters, different types of pumps, RO membranes, storage tanks, exchanger energy recoveries, valves, control systems (such as PIDs or PLCs), etc.Every component has been modeled using first principles and correlations from literature: Mass balances, energy balances, and physic-chemist equations are in the core of the models. Complex elements, such as sand filters or RO membranes, have been discretized by using the finite volume method. Fig. 4 corresponds to the graphical simulator of the real plant (shown in Fig. 1.), than is validated in the present paper. The simulator consists of two parallel membranes, one high pressure positive displacement pump, one sand filter, one cartridge filter, the addition of several chemical components (hypochlorite, bisulphite, sequestrant, chloride acid, etc.), supply centrifugal pumps and storage tanks.

4. VALIDATION

The evolution of all important variables in RO plants (flows, pressure, salt concentration, solids concentration, pH, temperature, etc.) is calculated by the dynamic library. However, the present paper only deals with the validation of the chemical part (salinity and quality of the feed water). The hydraulic part (pressure and flow) of the validation was shown elsewhere (Palacin et al. 2010b). The pilot plant was specially designed for testing and experimentation and has a huge number of sensors, bigger than in a typical RO plant. All the main parameters in the RO plant can be measured in different points of the plant. Sensors are managed from an OMRON PLC, and the data loading is carried out by the use of OPC protocol. In order to realize correctly the parameter estimation, several experiments were carried out changing the quality of the feed water and covering all the range of pressures and flows allowed in the plant. Once enough experiments have been done and data have been filtered and treated, it is possible to do the parameter estimation and the validation of the library. This is done by the minimization of a certain objective function that penalizes the different between the value of the measured variables, y, and the value of the calculated, by the math model, variables, $\hat{y}$, for each sample time and for each variable, and modifying the value of the parameters to be identified.

$$objective\ function = \sum_{variable}\sum_{sample\ time}(y - \hat{y})^2 \qquad (1)$$

The minimization of the single objective function can be solved by any non linear optimization algorithm, such as Sequential Quadratic Programming (SQP). This algorithm is available directly in the own EcosimPro©. For the calculation of the variables of the system, the simulator of the pilot plant needs to know the value of some variables, or boundary conditions. The typical boundary conditions are the input and output conditions of the system. In particularly, the simulator requires to know the value of the inlet pressure of the system (P1), the outlet pressure of the system (atmospheric pressure in this case), the quality of the feed flow and the setpoint of the different PID controllers. Figure 5 and 6 show the profile of the setpoint of the permeate flow realized in experimentation. Measured data from the pilot plant obtained with the profile of the figure 5 are used for parameter estimation, and data from the profile of the figure 6 are used for validation. The setpoints profiles are repeated three times, with different values of the salinity of the feed water (15, 17 and 19 g/L). Figure 7 shows the velocity of the high pressure pump, automatically manipulated in order to get the permeate flow fixed in the setpoints profile of the figure 6. The relation between velocity of the pump and flow is calculated by the simulator using the characteristic curve of the pump, which, in this case, is a positive displacement pump. Figure 8 shows the estimated values of the curve of the pump, as well as the measured data. Notice how both curves coincide in the most part of cases. The coefficient of determination, R^2, for the characteristic curve of the pump gets the 0.92, which is reasonably good.

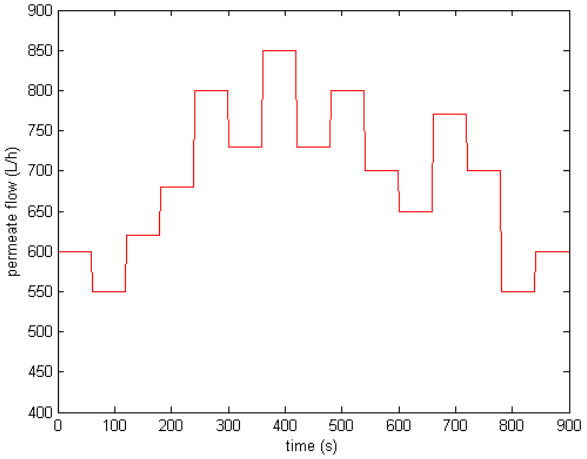

Figure 5: Profile of setpoint of permeate flow, used for parameter estimation.

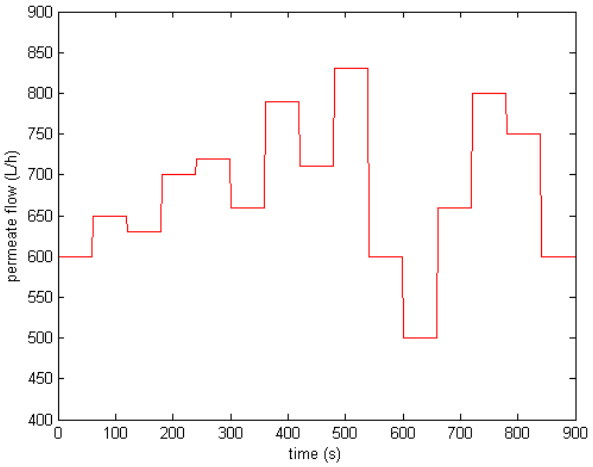

Figure 6: Profile of setpoint of permeate flow, used for validation.

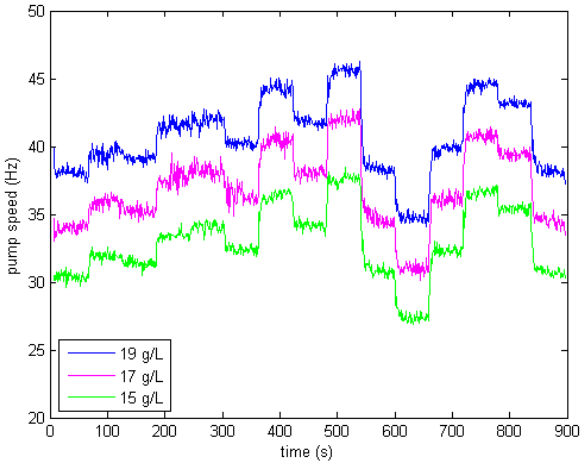

Figure 7: Velocity of the high pressure pump, the manipulated variable of the control of permeate flow.

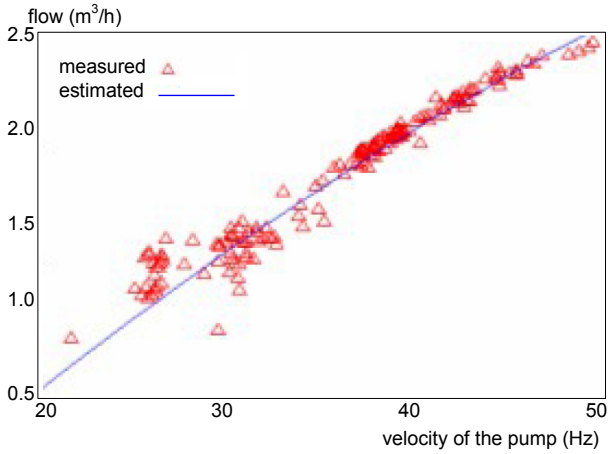

Figure 8: High pressure pump curve.

The permeate flow, which is the critical variable in the system, is typically calculated depending of the difference between the drop pressure (ΔP) and the osmotic pressure ($\Delta\Pi$) through the membrane. As it can be seen in equation 2, where A is the area of the membrane and L is the permeability. A and L are two parameters fulfilled by the membrane manufacturer.

$$permeate\ flow = L \cdot A \cdot (\Delta P - \Delta\Pi) = L^* \cdot (\Delta P - \Delta\Pi) \quad (2)$$

However, permeability is not a constant value, and depends dynamically on the inevitable and unwanted fouling. As it was mentioned before, in order to avoid this, different types of cleanings should be periodically realized. Figure 9 shows the evolution of the permeability during one experiment. The permeability was correctly estimated using the equation 3. Data from experimentation in the pilot plant were used to estimate the parameters of this equation for this particular case: $L_o \sim 230$ L/(h·bar) and $\Psi \sim 1100$ s.

$$L^* = L_o \cdot exp(-t/\Psi) \quad (3)$$

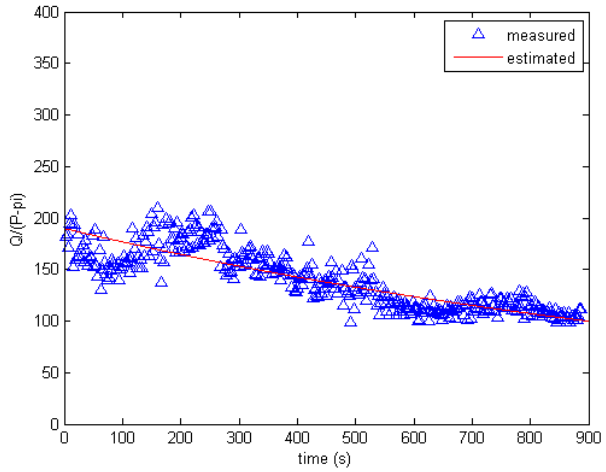

Figure 9: Fouling affecting the permeability.

On the other hand, the salt flow that is able to cross along the membrane is typically calculated depending on the difference of concentration through the membrane (ΔC). As is can be seen in the following equation, where L_s is the salt permeability:

$$salt\ flow = L_s \cdot A \cdot (\Delta C) = L_s^* \cdot (\Delta C) \quad (4)$$

Salt flow is not a measured variable in a typical RO system. The important variable is the salt concentration of the permeate flow, which is easily calculated dividing equations 4 and 2:

$$salt\ concentration = L_s^*/L^* \cdot (\Delta C)/(\Delta P - \Delta\Pi) \quad (5)$$

Figure 10 shows the salt concentration of the permeate vs. the term $(\Delta C)/(\Delta P - \Delta\Pi)$ for different experiments. This curve corresponds to a straight line, whose slope is L_s^*/L^*. Data from experimentation in the pilot plant were used to estimate this slope, and then, the salt permeability of the membrane, $L_s^* \sim 360$ L/h.

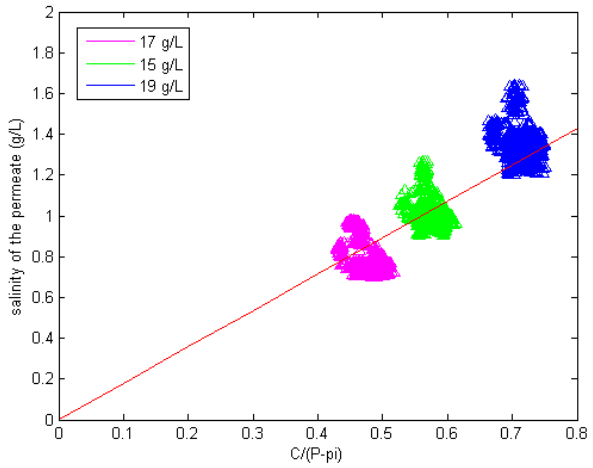

Figure 10: Salinity of the permeate vs. $(\Delta C)/(\Delta P - \Delta\Pi)$.

Once the parameter estimation has been completed, it is possible to do the validation of the library. Figures 11-13 show the estimated profile of the permeate flow and the real one, which has been measured in the pilot plant. Notice how both curves roughly coincide, which validate this part of the library. The average error between the estimated curve and the real one is around 3%. Figures 11, 12 and 13 correspond to the permeate flow with a salinity of the feed flow of 15, 17 and 19 g/L respectively.

CONCLUSIONS

The importance of dynamic simulation tools for the design of RO plants has been discussed. In order to improve the design and control of this kind of plants, a dynamic library of RO plants previously developed, has been checked, and initial results for a preliminary validation based on experiments carried out on the real plant are presented here. More precisely, tests of the chemical part of the simulator are presented, confirming the validity of this part of the dynamic library.

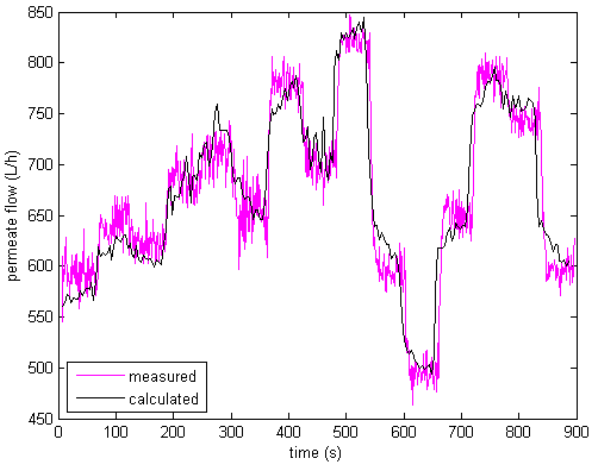

Figure 11: Permeate flow, estimated and measured, with a feed salinity of 15 g/L.

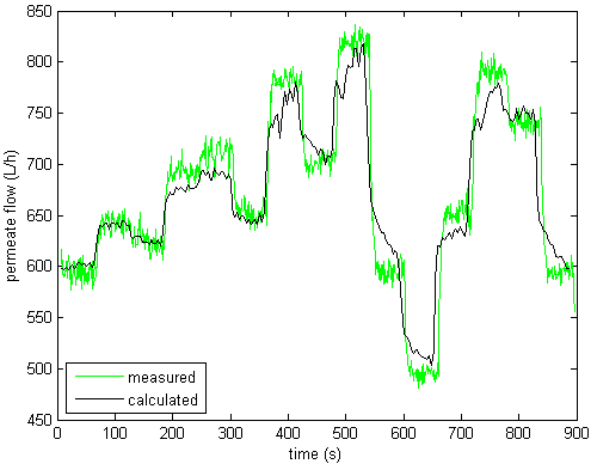

Figure 12: Permeate flow, estimated and measured, with a feed salinity of 17 g/L.

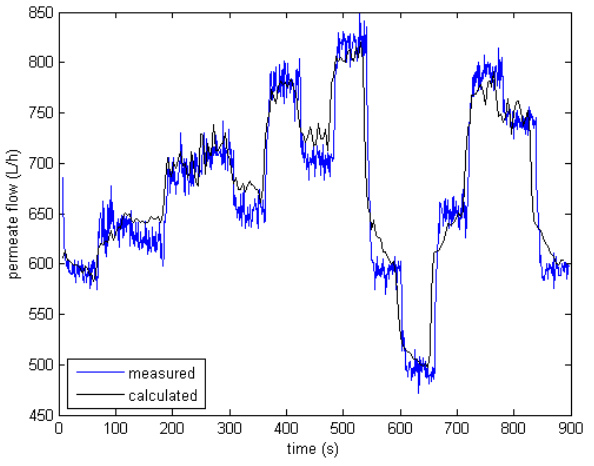

Figure 13: Permeate flow, estimated and measured, with a feed salinity of 19 g/L.

ACKNOWLEDGMENTS

The authors wish to express their gratitude to the Spanish MICINN for its support through project DPI2006-13593, as well as the EU for its support through 6FP, OPEN-GAIN contract 032535.

REFERENCES

Al-Bastaki, N. M., and Abbas, A., 1999. Modeling an Industrial Reverse Osmosis Unit. *Desalination*, (126), 33-39.

Baker, R., 2004. Membrane technology and applications. *Wiley, West Sussex*, England, UK.

Bartman, A., Christofides, P. D., and Cohen, Y., 2009. Nonlinear model-based control of an experimental reverse osmosis water desalination system. *Ind. & Eng.Chem*, (48), 6126-6136.

Bartman, A., McFall, C., Christofides, P. D., and Cohen, Y., 2009. Model predictive control of feed flow reversal in a reverse osmosis desalination process. *J. Proc. Contr*., (19), 433-442.

Bacelli, G., Gilloteaux, J. C., and Ringwood, J., 2009. A predictive controller for a heaving buoy producing potable water. *Proc. of the European Control Conference*, Budapest, Hungary.

Fritzmann, C., Löwenberg, J., Wintgens, T., and Melin, T., 2007. State-of-the-art of reverse osmosis desalination. *Desalination*, (216), 1-76.

Gambier, A., Krasnik, A., and Badreddin, E., 2007. Modeling of a simple reverse osmosis desalination plant for advanced control purposes. *Proc of the American control conference,* New York, USA.

Gambier, A., and Badreddin., E., 2004. Dynamic modelling of MSF plants for automatic control and simulation purposes: a survey. *Desalination*, (166), 191-204.

McFall, C., Bartman, A., Christofides, P. D., and Cohen, Y., 2008. Control and monitoring of a high-recovery reverse-osmosis desalination process. *Ind. & Eng. Chem. Res*., (47), 6698-6710.

Palacin, L., de Prada, C., Syafiie, S., and Tadeo, F., 2008. Library for dynamic simulation of reverse osmosis plants. *Proc. of 20th European modeling and simulation symposium*, Briatico, Italy.

Palacin, L., Tadeo, F., Elfil, H., and de Prada, C., 2009. New dynamic library of reverse osmosis plants with fault simulation. *Proc. of the 2nd Maghreb conference on desalination and water treatment*, Hammamet, Tunisia.

Palacin, L., Tadeo, F., and de Prada, C., 2009. Operation of desalination plants using hybrid control. *Proc. of the 2nd Maghreb conference on desalination and water treatment*, Hammamet, Tunisia.

Palacin, L., Tadeo, F., and de Prada, C., 2009. Integrated design using dynamic simulation of reverse osmosis plants. *Proc. of the international conference on industrial engineering and engineering management*, IEEE 2009. Hong Kong, China.

Palacin, L., Tadeo, F., Salazar, J., and de Prada, C., 2010. Operation of medium-size reverse osmosis plants with optimal energy consumption. *Proc. of IFAC International Symposium on Dynamics and Control of Process Systems*, DYCOPS 2010, Leuven, Belgium.

Palacin, L., Tadeo, F., Salazar, J., and de Prada, C., 2010. Initial Validation of a Reverse Osmosis Simulator. *Proc. of the 15th IEEE International Conference on Emerging Technologies and Factory Automation*, ETFA 2010, Bilbao, Spain.

Salazar, J., Tadeo, F., and de Prada, C., 2010. Control system for reverse osmosis plant (RO) and renewable energy generation. *Proc of the international conference on renewable energies and power quality 2010*, Granada, Spain.

Syafiie, S., Palacin, L., de Prada, C., and Tadeo, F., 2008. Membrane modeling for simulation and control of reverse osmosis in desalination plants. *Proc. of control 2008,* Manchester, UK.

Tadeo, F. Val, R., Palacin, L., Salazar, J., and de Prada, C., 2009. Control of reverse osmosis plants using renewable energies. *Proc. of control and applications 2009*, Cambridge, UK.

Wilf, M., 2007. The guidebook to membrane desalination technology. *Balaban desalination publication*, L'Aquila, Italy.

Zafra-Cabeza, A., Ridao, M. A., and Camacho, E. F., 2009. Optimization in reverse osmosis plants through risk mitigation, *Proc. of the European Control Conference*, Budapest, Hungary.

EMPIRICAL AND SIMPLIFIED MODELS FOR AN INDUSTRIAL BATCH PROCESS

A. Rodríguez, L.F. Acebes, C. de Prada
Department of Systems Engineering and Automatic Control
University of Valladolid
47011 Valladolid (Spain)
e-mail: {alexander.rodriguez; felipe; prada}@autom.uva.es

ABSTRACT
In this paper, a dynamic model of the first stage of the crystallization section of a sugar factory is developed In the model is assumed that the sugar room has continuous and batch units. Therefore, it comprehends variables and phenomena relevant to the process and combines the global mass balance; as partial mass balances of solids and sucrose in continuous units, the melter and mulling equip; with empirical and simplified event models for discrete units (such as the batch crystallizer and centrifuges).

Keywords: Empirical models, simplified hybrid models, industrial process.

1. INTRODUCTION

In this work is developed a dynamic model of the first stage of the crystallization section of a sugar factory. The model will be used to make dynamic data reconciliation and to run simulation scenarios in an optimization software tool to manage the process efficiently.

In the sugar industry is used a well-known modelling tool Sugars™ (Weisser 2010), other significant tool is SIMFAD (ICIDCA, 2010). But both of them are based on stationary models and they are not suitable for our purpose. The Center of Sugar Technology of the University of Valladolid (CTA) has developed complex dynamic models of the main process units of the sugar production process (Mazaeda et al. 2010). However, their complexity implies that are difficult to parameterize and its execution has a large computational load. So, neither they are appropriate to our purpose

Nowadays, it is possible to implement dynamic mathematical models in an easy way using a tool of the family of the object oriented modelling and simulation language (OOMSL). Modelica represents an effort to standardize them (Modelica 2010). In our case we use EcosimPro (EcosimPro 2010), because though it does not implement Modelica, it has a complete and simple language for describing hybrid models, a suitable environment for the definition of libraries and models, a good DAE solvers and it allows to use the simulation code as a C++ class.

We propose to develop a hybrid model of the first stage of the sugar room. This model is based on a continuous and dynamic first principles models for the elements responsible for the accumulation of product (melter and mulling unit) and an empirical and event based model for the batch elements (batch vacuum pans and centrifuges), that slow the simulation execution.

Due to the lack of real data, we have used the realistic simulators of the sugar process units of the crystallization section developed by the CTA to obtain a set data to adjust the empirical models.

The paper is organized in this way. In the first section the problem is introduced. In the second the crystallization section of a sugar factory is described. The third part is dedicated to the empirical mathematical model of the batch process units. In the fourth section the validation of the model is outlined. Finally some conclusions and further research is given

2. CRYSTALLIZATION SECTION

The crystallization section is the last department of the sugar factory, in which the sugar is obtained by a crystallization process using the concentrate juice that arrives from the evaporation section.

In modern factories the crystallization section is divided in three stages. The first stage, called stage A, produce commercial sugar and a by-product to fed the second stage. The second stage (B) is a stage of exhaustion, in which sugar B, to feedback to stage A, and a by-product, to feed the third stage, are obtained. Finally, in the stage C, that is other phase of exhaustion, sugar C is obtained and recycled to stage A. Besides the stage C produce a by-product called molasses (Mazaeda 2010, Sarabia 2007).

As the crystallization section, that is also called "sugar room", contains a great amount of process units, the stage A has been selected as study case (see Figure 1). It can be observed that the melter receives sugar juice from the evaporation section and high purity syrup from the A centrifuges. The melter feeds three batch vacuum crystallizers. The molasses produced by the vacuum pans, each time that a batch has finished, are added to a mulling tank. This tank feds to the batch centrifuges that produce commercial sugar, high purity syrup and low purity syrup that is used to fed the stage B of the crystallization section.

The basic physical principles of the process are the next ones. The syrup from the evaporation stage is sent to the melter, and it dissolves the higher purity syrup from the centrifuges, obtaining a solution that is called *standard syrup*, after a filtering process, it is sent to the vacuum crystallizers. When a vacuum crystallizer is full, it contains a product called massecuite or cooked mass that is a high concentrate water solution formed by crystallized sucrose, sucrose and impurities dissolved. Using steam, as heating way, the massecuite reaches the super-saturation conditions, then small sugar crystals

are added and they begin to grow. New syrup must be added to maintain the super-saturation condition. When a suitable size of the crystals has been reached and the vacuum pan is completely full of a product called *mother honey*, vacuum crystallizer is discharge and cleaned. The mother honey is stored in a mulling equipment to feed the batch centrifuges.

Finally, the battery of batch centrifuges are used to separate the sugar crystals from the mother honey. The centrifuges discharged three products: first, the lower purity syrup, second, the higher purity syrup, and, third, the commercial sugar.

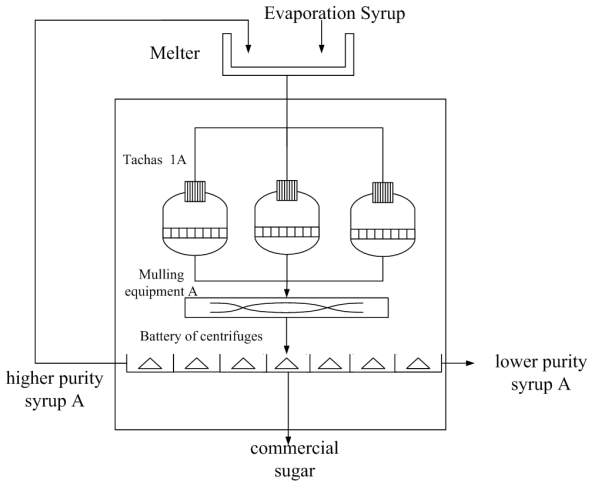

Figure 1. Diagram of stage A of the crystallization section.

The optimal management of the sugar room depends on many criteria that actually must be managed by the operators. Some of them are:

- The steam demand of the sugar room must be homogeneous to not disturb the operation of the steam producer (the evaporation section). Because, the flow rate and sucrose concentration of the syrup that arrives to the crystallization section depends on the operation of the evaporating section. So, each vacuum crystallizer must be turn on in a suitable time to avoid peaks in the steam demand.
- Besides, each sugar crystallizer only must be turn on if there is enough syrup in the melter.
- The discharge of each crystallizer must happen when there is enough space in the mulling equipment. If it is not possible to unload the crystallizer, this one waits until the mulling equipment has enough space to store the mother honey contained in the crystallizer.
- The amount of rich and poor honey separated in the centrifuges affects the quantity of sucrose that must be re-processed with the consequent power consumption and problems of storage. It is possible decide the time in which the centrifugals switch from producing rich honey to poor honey.

3. MATHEMATIC MODELS

It is necessary to develop a mathematical model to simulate the behaviour of the sugar room to calculate the steam demands, the level of the storage units and the properties of the obtained products. As a function of the boundary conditions of the syrup that goes into the crystallization, the pressure of the supplied steam, the start time of production of each crystallizer, the number of batch centrifugals operating and the time to switch from produce the two types of honeys in the batch centrifugals.

For process units in charge of store products (melter and mulling equipment) we use dynamic first principle models based on mass balances of global product, sucrose, sugar crystals and impurities.

As it was shown in the introduction, it is possible for batch crystallizers and centrifugals to develop complete dynamic models based on first principles (Mazaeda 2010), several reasons discourage their use in our case:

- They are too complex to parameterize.
- They are hybrid models, with a lot of events related to state variables. It implies a high computational cost in their resolution. So they are not suitable to decision making based on optimization techniques, because in this case the simulation program must be run a lot of times.

For this reason we propose to develop empirical and simple models of the batch units suitable to our purpose. In particular the model of the batch crystallizer will be detailed and the next assumptions were made:

- There is no interest in the thermodynamic aspects.
- As it can be seen in Figure 2, the flow profiles of steam demand, syrup consumption, and obtained mother honey are always the same ones. Only change the magnitude of the flows in each stage and theirs time events that both of them are calculated using empiric tables.
- As it was impossible to make experiments in the real process, the values to fill the tables were obtained using the realistic vacuum pan simulator developed in the CTA.
- The experiments consist on simulate a complete batch maintaining some boundary conditions.
- The empiric flow profiles must satisfy the mass balances in each batch.

The method used to calculate the flow profiles is the next one:

- First, the supply steam pressure and the properties of standard liquor syrup (brix and purity) are selected as boundary conditions and theirs ranges are specified.

- Second, the execution of each model is made varying only one boundary condition. Thus, the variation of the response can be attributed to the change factor, and therefore it reveals the effect of that factor. The procedure is repeated using next boundary condition. The results of each model execution are the loading and cooking mass, the unloading mass and its properties, the global steam consumption and the loading, cooking and unloading stage times. The Tables 2, 3, and 4 shows some results taken from a more detailed table.

Table 1. Mass of the standard liquor in the load stage and the cooking stage

Pressure 0.9 bar				
Purity\Brix	Mass standard liquor in the load stage .[kg] ($Mass_{load\ stage}$)			
	70	72	74	76
90	58645	58730	58868	58969
92	58655	58736	58871	58971
94	58653	58736	58872	58970
96	58659	58772	58872	58970
Pressure 0.9 bar				
Purity\Brix	Mass Standard liquor in the cooking stage.[kg] ($Masa_{stage\_cooking}$)			
	70	72	74	76
90	626	626	626	636
92	636	636	636	653
94	653	653	653	681
96	681	681	681	523

Table 2. Mass of the mother honey in the discharge stage**.**

Pressure 0.9 bar				
Pureza\Brix	Mass cooking in the unloading stage.[kg] ($Mass_{unloading}$)			
	70	72	74	76
90	7500	6625	5783	5003
92	9065	8078	7135	6248
94	8264	7344	6457	5620
96	7543	6673	5838	5051

Table 3. Time events of the loading, cooking and unloading stage.

Pressure 0.9 bar				
Purity\Brix	Duration of the loading stage [s] ($time_{loading}$)			
	70	72	74	76
90	91	90	92	92
92	92	91	92	93
94	92	92	92	93
96	92	92	92	93
Pressure 0.9 bar				
Purity\Brix	Duration of the cooking stage ($time_{cooking}$)			
	70	72	74	76
90	9907	8839	7841	6895
92	9047	8047	7107	6216
94	8250	7329	6440	5607
96	7500	6625	5783	5004
Presseure 0.9 bar				
Purity\Brix	($time_{unloading}$)			
	70	72	74	76
90	686	686	686	686
92	696	696	697	696
94	713	713	713	713
96	742	741	742	741

- Then, linear adjustments are made of the table experiment values for incorporate into the model. The linear fit is given by equations 1 to 6 and it depends on the boundary conditions.

$$Mass_{loading} = f_n(Brix, Purity, \Pr essure) \quad (1)$$

$$Mass_{cooking} = f_n(Brix, Purity, \Pr essure) \quad (2)$$

$$Mass_{unloading} = f_n(Brix, Purity, \Pr essure) \quad (3)$$

$$time_{loading} = f_n(Brix, Purity, \Pr essure) \quad (4)$$

$$time_{coking} = f_n(Brix, Purity, \Pr essure) \quad (5)$$

$$time_{unloading} = f_n(Brix, Purity, \Pr essure) \quad (6)$$

- Finally, profiles (Figure 2) are estimated using the equations 7, 8 and 9, which satisfy the mass balances and allow interaction with the melter and mulling equip.

$$Win\_loading = \frac{Mass_{loading}}{time_{loading}} \quad (7)$$

$$Win\_cooking = \frac{Mass_{cooking}}{time_{cooking}} \quad (8)$$

$$Woutput = \frac{Mass_{unloading}}{time_{unloading}} \quad (9)$$

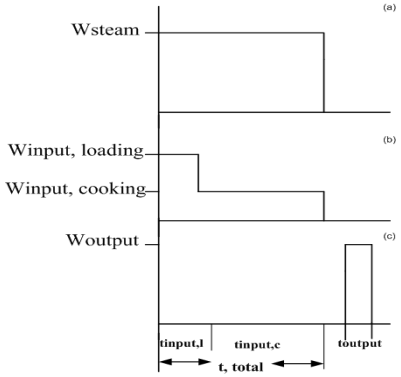

Figure 2. Flow profiles. a) Supply steam. b) Supply syrup. c) Output mother honey.

The batch centrifugal was modelled using the same procedure that for the vacuum crystallizer.

The model of each process unit has been implemented in an object oriented modelling language for hybrid systems named EcosimPro. Later, the model of the first stage of the sugar room has been made selecting, parametrizing and connecting each of the process units that contains.

5. VALIDATION

A qualitative analysis is carried out to validate the resulting model of each process unit in an independent way.

For the vacuum crystallizer, the qualitative analysis consisted in varying some of the boundary conditions such as brix and steam pressure. As an example in the figures 3 and 4 are illustrated the effect of increased and decreased steam pressure supply. An increase in supply pressure causes a decrease in time at the cooking stage, while a decrease of supply pressure causes the opposite effect, due to the fact that the steam pressure falls on the rate of evaporation water contained in the mass within vacuum crystallizer.

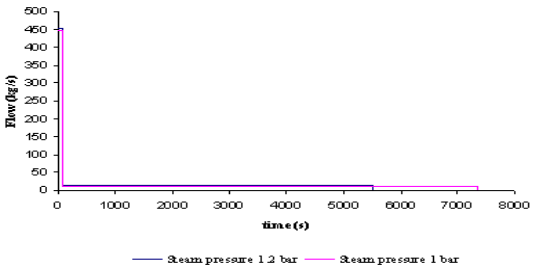

Figure 3. Increased of the steam supply pressure.

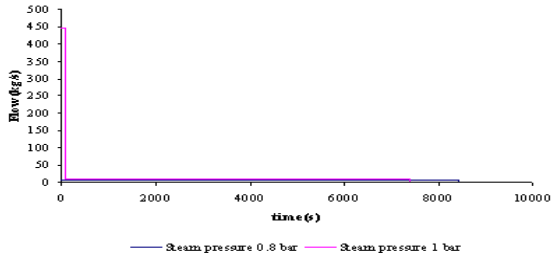

Figure 4. Decrease of the steam supply pressure.

On the other hand, the qualitative analysis in the centrifuge consisted in modifying the time of commutation of honey and varying brix, leaving a fixed value of 12 kg/s of standard syrup received at the melter, with a purity value of 93% size of the crystals 45%. The effect of modifying the time of commutation of honey in the centrifuges is showed next.

The separation between lower purity syrup and the higher purity syrup can be established freely by the operator within certain limits. Must occur at a time after the introduction of water, but can not establish a "best" time for change fits-all operating situations of the plant. If the switching is delayed produce a higher purity of both honeys, which increases the amount of sucrose that is sent to the stages of exhaustion, a change instead of honey in advance will ensure the purity of the honey less poor, but also harm the purity of the rich increased the amount of impurities is recycled to the first stage.

Figures 5 and 6 show the implications of the change of honey. In Figures 5.a and b are plotted the purity and brix of lower purity syrup and higher purity honey, for a switching time of 28 seconds, while in Figure 6.a and b, equivalent information is provided for the case a switching time of 12 seconds. It is noted that an increase of switching time of honey causes increased both the purity of honey, while in the brix this effect is less significant because it does not influence much on the operational level.

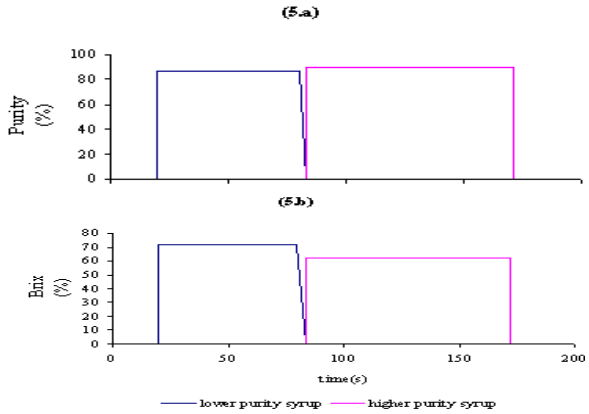

Figure 5. Purity and brix of lower purity syrup and higher purity honey, for a switching time of 28 seconds.

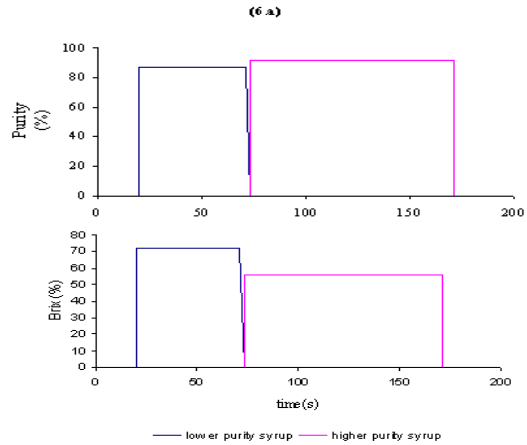

Figure 6. Purity and brix of lower purity syrup and higher purity honey, for a switching time of 12 seconds.

The objectives in this project were to simulate each process unit as an independent element. Further work could be focused in model validation of the whole stage A of the crystallization section. However, this would be a challenge that will require real process data and a full simulation of the process as a whole.

4. CONCLUSION

In this work, a dynamic model of the first stage of the crystallization section of a sugar factory has been

developed. The model has hybrid formulation, because use ODEs and events and besides it is a mixture between first principles and empiric formulations.

The next step is to validate the model and complete with the second and third stage of the sugar room. Later, the global model must be used to manage the sugar room in an efficient way.

ACKNOWLEDGEMENT

The authors thank to the Spanish firms ACOR and Azucarera Ebro for their support to carry out this research.

REFERENCES

Acebes L. F.,Merino A., Alves R., de Prada., (2009). *Análisis en línea del estado energético de plantas azucareras.* Revista de Informática y Automática Industrial. Vol. 6, num. 3, 2009, pp: 68-75.

Dynasim (2010), Available from: http:// www.dynasim.es, [accessed in April 2010]

EcosimPro by EA *Internacional, Dynamic Modeling & Simulation Tool*, Available from: http://www.ecosimpro.com, [accessed in April 2010].

ICIDCA (2010). *Cuban research institute of derivates of sugar cane*. Available from: http://www.icidca.cu, [accessed in April 2010].

Mazaeda, R., (2010). *Librería Orientada a Objetos para el Modelado y Simulación del Cuarto de Azúcar de Fábricas de Azúcar para el Entrenamiento de Operarios.* Thesis (PhD). Supervisor: Prada, de C., Universidad de Valladolid, Spain.

Mc Ginnis R. A., (1982). *Beet sugar technology*. 3d Edition. Beet Sugar Development Foundation. Colorado, USA.

Merino A., Acebes L.F., Mazeda R., de Prada C., (2009) *Modelado y Simulación del proceso de producción de azucar*. Revista Iberoamerica de Automática e Informática Industrial.

Merino A., (2008), *Librería de Modelos del Cuarto de Remolacha de una Industria Azucarera para un Simulador de Entrenamiento de Operarios.* Thesis (PhD). Supervisor: Acebes, L.F., Universidad de Valladolid, Spain.

Modelica Association (2005) Available from: http// www.modelica.org. [Accessed in April 2010].

Sarabia D, (2007), *Modelado, Simulación y Control Predictivo de Sistemas Hibrídos*, Thesis (PhD). Supervisor: Prada, de C., Universidad de Valladolid, Spain.

Van der Poel P. W., Schiweck H., Schwartz T., (1998). *Sugar Techonology: Beet and Cane Sugar Manufacture*. Ed. Bartens. Berlín.

Sugar International (2010). *Software for modelling and simulation sugar factories.* Available from: http// www.sugarsonline.com. [Accessed in April 2010].

OBJECT ORIENTED MODELING AND SIMULATION OF BATCH SUGAR CENTRIFUGES

Rogelio Mazaeda[(a)], César de Prada[(b)]

(a) System Engineering and Automation Department, University of Valladolid. Real de Burgos S/N, CP 47011 Valladolid, Spain.
(b) System Engineering and Automation Department, University of Valladolid. Real de Burgos S/N, CP 47011 Valladolid, Spain.

[(a)]rogelio@cta.uva.es, [(b)]prada@autom.uva.es,

ABSTRACT
Sugar crystallizers deliver a slurry where the sugar grains are suspended in the so called mother liquor. The centrifuges are the units in charge of mechanically separating the former form the latter guaranteeing the quality of the final product and the efficiency of the process. In the typical Sugar House there are batch and continuous types of centrifuges. Batch centrifuges are deployed in the stage directly concerned with the production of the commercial product. In what follows the hybrid character models of batch sugar centrifuges are described as part of a reusable Sugar House library specially designed for the training of control room personnel.

Keywords: process modeling, simulators, simulation languages, process equipment

1. INTRODUCTION

The conduction of sugar factories has experimented over the years a significant improvement by putting in place automatic control procedures wherever possible. But the role of control room operators remains decisive due mainly to the lack of measurements regarding the main quality related variables but also to the intrinsic complexity of the process.

In this context, the correct training of technical personnel is critical, and even more so due to the seasonal character of the industry which imply long periods of inactivity along the year.

An object oriented hybrid library specifically dedicated to the purpose of building simulators for operators training which features the main units to be found in the last department of sugar factories, the Sugar House, has been developed (Mazaeda, 2010) as part of larger effort to model the whole factory (Merino, Mazaeda, Alves, Acebes, Prada, 2006).

The present paper will describe the model of batch sugar centrifuges and will present some simulation results.

2. THE SUGAR HOUSE

The sugar fabrication process involves the extraction of the sucrose from the beets by diffusion, the ulterior conditioning, in a purification stage, of the obtained juice in order to remove the maximum possible amount of the impurities that where inevitably pulled out along with the sucrose and also the elimination of water in a cascade of industrial evaporators. The resulting concentrated syrup is fed to the last department of the factory, the Sugar House, where the crystallization of the solute is carried out to deliver the sugar crystals with the average size, uniformity, and purity which are commercially appreciated.

Crystallization is conducted in batteries of semi-batch operated vacuum pans (Georgieva, Meireles, and Feyo de Azevedo 2003, Mazaeda y Prada 2007). In each one of the crystallizers, the migration of the sucrose molecules in the solution to the faces of the population of crystals which are suspended in the contained magma or slurry is made to happen by keeping the concentration of the dissolved substance at the right value, carefully controlling the rate of water evaporation and the input of syrup to the equipment. The supersaturation of sucrose, that is the ratio of its actual concentration to the one defining the solubility at the current temperature and purity, should be higher than unity for the crystallization to be possible but it must be prevented to exceed the so called metastable limit if the uncontrolled apparition of new crystals with its negative impact on the uniformity of the grains, is to be avoided.

The resulting magma should be processed by centrifuges where the *mother liquor* (the remains of the original impure solution containing the non crystallized sucrose) gets expelled out of a rotating basket through conveniently sized holes while the sugar crystals are retained.

Sugar Houses are typically organized in three stages of similar structure (fig.1), with the first one dedicated to the production of the commercial white sugar and the remaining two, to the exhaustion of the syrups delivered by the previous stages in the flowsheet. A scheme of this type allows a technologically convenient separation of concerns: the first “A” stage is devoted to guaranteeing the quality of the marketable crystals, while the “B” and “C” exhausting stages should recover as much sucrose as possible by recurring to the same mechanism of crystallization. The sugar obtained in the “B” and “C” stages gets finally recycled

to conform the fed liquor of the "A" stage while the unrecoverable syrup separated at the end of the "C" stage, the so called molasses, is a by-product of the factory, still useful for alcohol production (Azucarera Ebro. S.A 2002-2008, Van der Poel, Schiweck and Schwartz 1998).

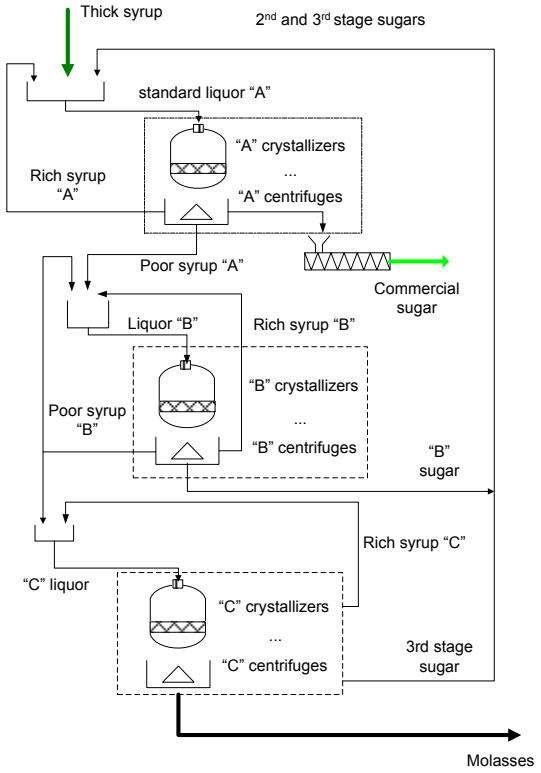

Figure 1: Sugar House three stages scheme.

The fact that the sucrose solution to be processed is contaminated with an assortment of other inorganic and organic substances which are termed collectively as impurities is the single most important quality and technological hurdle that should be sorted out. The purity of the syrups, for example, steadily decreases from the "A" to the "C" stage and this is the intended effect achieved as the dissolved sucrose is progressively crystallized. But the solubility of sucrose in water increases with the presence of impurities and this fact implies the need for a greater concentration of the syrups to achieve a similar degree of supersaturation and consequently the presence of, harder to handle, more viscous flows. The sugar production logic then favors the use of batch type of units in the "A" stage: the batch crystallizers for delivering an slurry containing a sugar crystals population with the right average size and spread and of batch centrifuges for performing a sharp separation of the grains and the syrup so as to offer a high purity commercial product. In the exhausting stages, however, the use of simpler, more robust continuous processing units is stipulated, since their smooth operation around a slowly varying reference, is more appropriate for the handling of viscous streams. The quality requirements of continuous equipment is relaxed in the "B" and "C" stages even though they shouldn't be neglected completely: a bad functioning of the continuous centrifuges, for instance, could easily compromise the quality of first product by inducing the recycling of a too impure recovered sugar.

3. SUGAR CENTRIFUGES

In what follows, batch sugar centrifuges will be described along with their mathematical models.

The developed model needs to be in tune with the declared purpose of the Sugar House Library of being instrumental in the creation of operators training simulators. The mathematical and logical description attempted should be complete in the sense that all the elements over which the trainee has access in the real equipment and the main phenomena taking place there, are to be represented. The generic model should capture the correct behavior when deployed in different conditions of the simulated factory and so the right relations between the properties of the manipulated masses and the performing abilities of the equipment should be adequately accounted for.

The intention is for the components of the library to be put to use as part of higher hierarchy larger models representing the flowsheet of a complete beet sugar factory, because only in this broader context the operators under training can get the full implication of the different operation policies. So, the need to keep the complexity of the individual unit models under check as a means of controlling the numerical integration effort for the final aggregated simulation job, has been an important conscious aim in the design of the library.

3.1. Batch sugar centrifuge description.

The main constructive elements of a regular sugar batch centrifuge are depicted in figure 2.a. There is a electric motor driven rotating basket with perforated walls whose angular velocity profile can be specified by programmable speed controller. The drum is housed in an exterior case intended for receiving the filtrate expelled from the former. The basket bottom is provided with gates which should be opened at the end of the cycle to discharge the wet mass of sugar crystals on the appropriate conveyor to be transported to the factory sugar dryer.

In batch centrifuges, the basket is charged, at the beginning of every cycle, with the designated amount of magma. From the very beginning, the mother liquor starts to be expelled out of the drum through the holes in the basket's wall, while the crystals, trapped inside the case, rapidly build a solid porous sugar cake. In a first moment, when there is still mass on top of the sugar bed, in the so called filtering mode, the outgoing syrup must overcome the resistance represented by the cake. The existence of the two separated phases, the sugar cake and the supernatant slurry, which are ideally here considered as perfect concentric cylindrical rings of radii r_c and r_l respectively, is represented in figure 2.b.

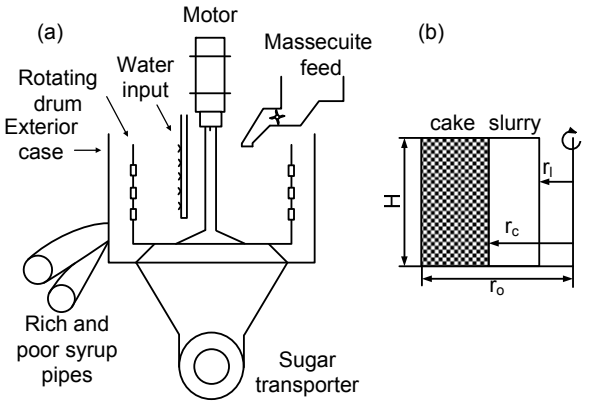

Figure 2. Batch centrifuge.

Eventually, since there is a finite amount of magma to be processed at each cycle, the supernatant slurry disappears, and a so called draining mode is entered. Centrifuging is, nevertheless, prolonged with the purpose of eliminating the maximum possible amount of the syrup which remains trapped in the space represented by the pores of the bed. Not all the liquid can be drained off the cake by centrifugal force alone, so it is important, at a certain moment of the cycle, to introduce water to reduce the amount of impurities of the final product below the maximum established by the quality requirements for the first product. But the injection of water provokes the dissolution of part of the already crystallized sugar and so, the increasing of the purity of the syrup which is pushed out after the introduction of water. So the need to meet the demanded purity of sugar implies that the efficiency of the equipment is compromised. As a result, the batch centrifuges delivers not only the mass of sugar grains but two additional streams of syrups differing in purity: the so called *poor syrup*, of relatively low concentration of sucrose and then the *rich syrup*, of a higher purity, since it contains the contribution of the dissolved crystals. Poor syrup is processed in the following stages but the rich syrup of higher purity gets recycled to the same "A" stage.

Critical to the performance of the centrifuge is the resistance offered by the sugar bed which depends on the characteristics of the grain grown in the crystallizers (Bruhns, 2004). A uniform population of crystals with the right average size implies a more permeable bed and consequently the possibility of obtaining the desired level of purity with less water and thus a much better conservation of crystals. There would be also a less amount of rich syrup and, therefore, less recycling with a greater efficiency in the use of the installed base.

4. BATCH SUGAR CENTRIFUGE MODEL.

The model to be developed for the batch centrifuge not only need to state the dynamical mathematical equations describing the physicochemical phenomena taking place in the unit. It is also important to the describe the sequencing program that drives the stage by stage evolution for each cycle.

4.1.1. Modeling the batch program.

Each working cycle of the batch centrifuge consists of a number of stages including the loading of the drum with the nominal amount of magma, the administration of two water washing phases, the discharge of the sugar obtained and finally the cleaning of the basket.

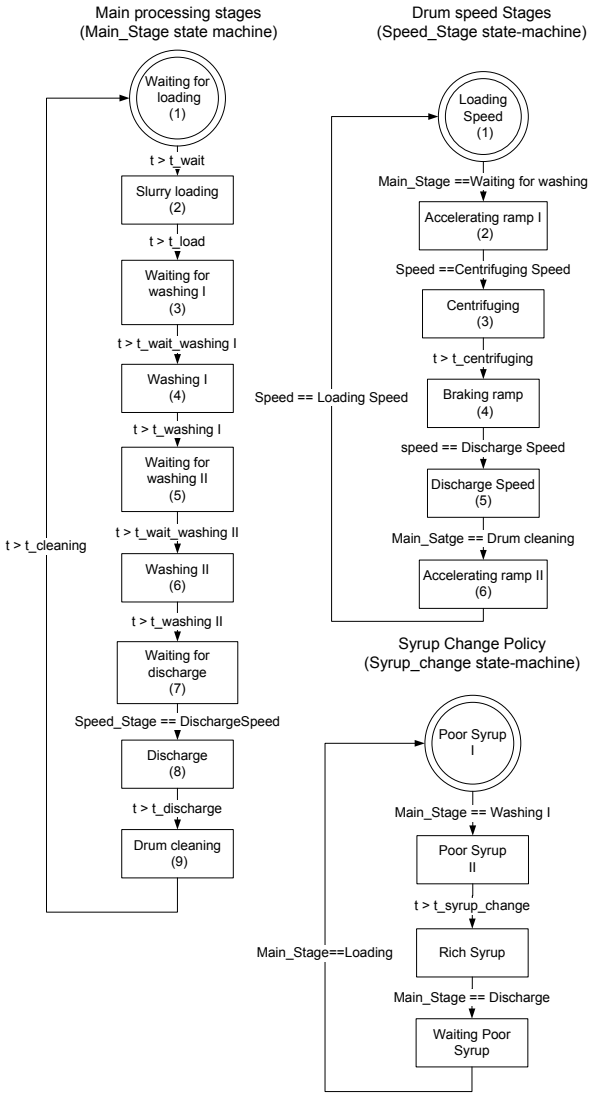

Figure 3: The batch centrifuge program.

The transition from one stage to the next under the control of the centrifuge program is decided mostly based on the time elapsed since the beginning of the phase as shown in the state machine of fig. 3a. There are two concurrent extra threads of execution of the control program: one is in charge of establishing the adequate angular velocity profile for the basket (fig. 3.b) and the other decides the position of the syrup output gate used to redirect the expelled filtrate from the circuit of poor syrup at the beginning of the cycle to the pipes transporting rich syrup at some instant after the application of the first washing (fig. 3.c). The exact switching time is defined by a parameter of the program, t_{sw}, which decides the relative purities of poor and rich syrups.

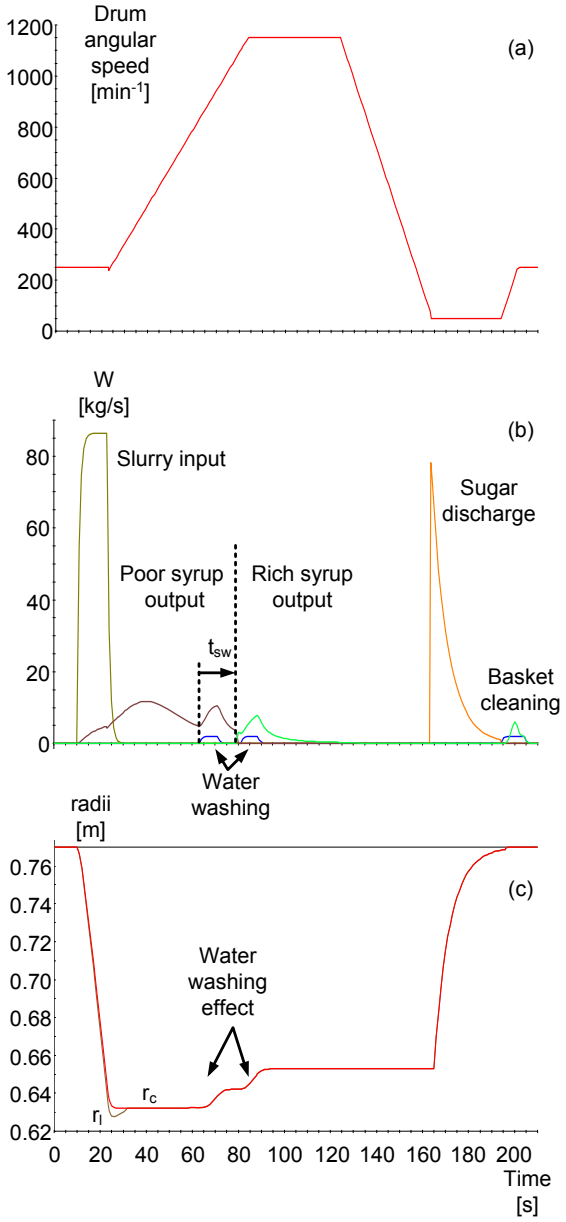

Figure 4. A batch centrifuge cycle.

There are a few points of synchronization between the three state machines, for example: the discharge state is not entered in fig. 3.a until the basket speed doesn't reach a predefined low angular velocity in fig.3.b. Whereas the accelerating ramp from a low angular speed, adequate to avoid the abrasion of sugar crystals while the basket is being filled with slurry, to the high centrifuging velocity appropriate for getting rid of as much syrup as possible, isn´t entered till the moment the loading stage is finished.

Figure 4 gives, at a glimpse, the main activities which are carried out in a cycle of the centrifuge. It shows the rotating drum angular speed profile in fig. 4.a, the material flows into and out of the unit at different points in the evolution of the program in fig 4.b and the evolution of the radii of the bed (r_c) and of the slurry on top (r_l) of the first in fig. 4.c.

4.1.2. Mass balances

In the filtering mode, the dynamic mass balances to each of the species concerned must be carried out for the supernatant space and for the cake. But when the state event triggered by the disappearance of the slurry on top of the bed marks the beginning of the draining mode ($r_l = r_c$), the balances which describes the evolution of each of the species in the bed are the only ones needed. In the model here described, both mentioned volumes are considered as perfectly mixed. This last requirement, in the case of particle systems, include not only the assumption of homogeneous composition and temperature in the continuous, liquid phase but the more stringent **MSMPR** (*Mixed-Solids Mixed-Products Removal Reactor*) condition stipulating that the properties of the discrete, crystal phase, that is, its size distribution, is the same everywhere in the considered volume and that the output flow contains a representative sample of grains. The real situation is, of course, more complex (Barr, White 2006). There is a continuous slip of the particles with respect to the solution, describable on time and on the radial dimension and whose degree depends on their density difference. So that the boundary between what is considered slurry and cake are not well defined and it is more like a convenient convention. The **MSMPR** supposition is specially severe in the description of the cake. In this space there isn´t even a suspension but a network of sugar grains in physical contact with the solution flowing through the tortuous conductions formed by the empty spaces between the crystals. In any case, the assumption here adopted is compatible with the numerical simplicity requirement previously stated.

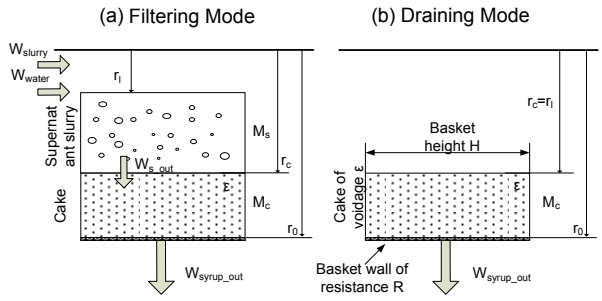

Figure 5: The batch centrifuge.

$$\begin{bmatrix} M_s' \\ M_{s\_suc}' \\ M_{s\_imp}' \\ M_{s\_cris}' \end{bmatrix} = \begin{bmatrix} W_{in} + W_{water} - W_{s\_out} \\ W_{in\_suc} - W_{s\_out\_suc} \\ W_{in\_imp} - W_{s\_out\_imp} \\ W_{in\_cris} - W_{s\_out\_cris} \end{bmatrix} \quad r_l < r_c \qquad (1)$$

In (1) M_s (kg) stands for the total mass of slurry in top of the cake, while M_{s_suc}, M_{s_imp} and M_{s_cris} are the masses of sucrose, impurities and crystals. The mass flow rates prefixed with *in* correspond to the input of slurry to the centrifuges, W_{water} (kg/s) is the flow rate of water, while W_{s_out} (and the similar terms corresponding

to each of the mentioned species) are the flows than abandons the supernatant space to be incorporated to the bed.

Similar mass balances are carried out in the cake space (2), where now W_{s_out} terms are input flow rates to the volume considered, W_{s_water} the flow rate of water that enters the bed. The terms prefixed with *un* are the flow rates leaving the basket with its final discharge, while the ones with the *filt* prefix are the mother liquor components that are filtered out. The term W_{dis} (kg/s) is the mass flow rate of sucrose representing the partial dissolution of the sugar crystals which is mostly important during both water washing stages.

$$\begin{bmatrix} M'_{c} \\ M'_{c\_suc} \\ M'_{c\_imp} \\ M'_{c\_cris} \end{bmatrix} = \begin{bmatrix} W_{s\_out} + W_{s\_water} - W_{filt} - W_{un} \\ W_{s\_out\_suc} + W_{dis} - W_{filt\_suc} - W_{un\_suc} \\ W_{s\_out\_imp} - W_{filt\_imp} + W_{un\_imp} \\ W_{s\_out\_cris} - W_{dis} - W_{un\_cris} \end{bmatrix} \quad \textbf{(2)}$$

In the filtering mode (Wakeman and Tarleton 1999), the mass flow of syrup out of the unit can be described by the Darcy law according to (3.a), where η_{ml} (kg/ms) and ρ_{ml} (kg/m^3) are the dynamic viscosity and the density of the syrup, H (m) is the height of the drum, R (m^{-1}) the resistance of the basket perforated wall. The resistance to the flow of the latter is represented by the inverse of the permeability k (m^2).

$$W_{filt} = \begin{cases} \dfrac{\rho_{ml}^2 \omega^2 \left(r_0^2 - r_l^2\right)}{2 \cdot \left(\dfrac{\eta_{ml}}{2\pi H} \dfrac{1}{k} \ln\left(\dfrac{r_0}{r_c}\right) + \dfrac{\eta_{ml} R}{2\pi r_0 H} \right)} & (a) \\ \dfrac{\rho_{ml}^2 \omega^2 \left(r_0^2 - r_c^2\right)}{2 \cdot \left(\dfrac{\eta_{ml}}{2\pi H} \dfrac{1}{k_{rl} k} \ln\left(\dfrac{r_0}{r_c}\right) + \dfrac{\eta_{ml} R}{2\pi r_0 H} \right)} & (b) \end{cases} \quad \textbf{(3)}$$

In the draining mode, the situation changes, however. Now the movement of the syrup out of the bed is governed by the relation between the hydrostatic pressure of the liquid and the surface tension in the capillaries formed by the pores. The description of this process could be quite involved, but here the model suggested in Ambler, (1988) is adopted. The flow of each phase, liquid and air, is thought to individually follow Darcy law (3.b). The applicable permeability for the draining of syrup will now be affected by a factor krl which will decrease as the relative volume (S_R) occupied by the syrup in the pores diminishes (4).

$$k_{rl} = S_R^{\frac{(2+3\lambda)}{\lambda}} \quad \textbf{(4)}$$

In (4) λ is a so called pores distribution index to be adjusted and S_R is defined as in (5). The pores saturation term S_{sat} gives how much of their volume (V_{pores}) is occupied by the liquid. The volume taken by the latter (V_{ml}) can be easily determined form the mass balance (2).

$$S_R = \frac{S_{sat} - S_\infty}{1 - S_\infty} \quad \textbf{(5)}$$

$$S_{sat} = \frac{V_{ml}}{V_{pores}} \quad \textbf{(6)}$$

$$S_\infty = k_\infty L_{mm}^{-0.5} \left(\frac{\omega^2 r_0}{g} \right)^{-0.5} \rho_{ml}^{-0.25} \quad \textbf{(7)}$$

The draining will never be complete, since there always remains a residual saturation S_∞ which had been here characterized by equation (7) as function of the crystal average size L_{mm}, the angular speed and the density of the liquor.

The characterization of the permeability as a function of the characteristics of the grains in the suspension can be attempted with the following expression due Carman-Kozeny:

$$k = \frac{\varepsilon^3}{5 S_0^2 (1-\varepsilon)^2} \quad \textbf{(8)}$$

Where S_0 (m^{-1}) is the specific surface of the bed, which is defined as the relation of the area to the volume of the particles, and ε (m^3/m^3) its voidage: the relation between the volume of the pores to the bulk volume of the cake.

4.2. Dissolution of sugar crystals

Dissolution will mainly occur when the application of water makes that the concentration of sucrose in the solution (C_{suc} in kg/m^3) that goes through the pores of the bed fall below the solubility (C_{suc_sat}) of that substance in water calculated at the existing temperature (Bubnik, Kadlec, Urban and Bruhns, 1995). For simplicity, the dissolution is not considered in the supernatant space and this can be justified because in the normal functioning of the centrifuge the two washing stages are performed when the mentioned phase has already disappeared. So the mass rate of dissolving sucrose (W_{dis}) in the bed is to be described as:

$$W_{dis} = J_{cris} A_{cris} = \beta \left(C_{suc\_sat} - C_{suc} \right) A_{cris} \quad \textbf{(9)}$$

In (9) A_{cris} is the aggregate area of sugar crystals and β the mass transfer coefficient (m/s) that could be estimated by the following Frössling correlation that relates the Sherwood (Sh), Schmidt (Sc) and particle referred Reynolds (R_{ep}) non dimensional numbers, enhanced by factor f_ε which depends on the voidage ε:

$$Sh = f_\varepsilon\left(2 + 0.664 R_{ep}^{1/2} Sc^{1/3}\right) \Rightarrow$$

$$\beta = \frac{D_{ml}}{L_e} f_\varepsilon \left[2 + 0.664\left(\frac{uL_e\rho_{ml}}{\eta_{ml}}\right)^{\frac{1}{2}}\left(\frac{\eta_{ml}}{D_{ml}\rho_{ml}}\right)^{\frac{1}{3}}\right] \quad \textbf{(10)}$$

$$f_\varepsilon = \left[1 + 1.5(1-\varepsilon)\right] \quad \textbf{(11)}$$

In the above expressions $\boldsymbol{L_e}$ is the crystals average size equivalent to the sphere of same volume, $\boldsymbol{D_{ml}}$ the coefficient of diffusion (m^2/s) and $\boldsymbol{u}$ is slip velocity between the grains and the liquid. An estimation of the diffusion coefficient for sucrose solution have been compiled in Bubnik, Kadlec, Urban and Bruhns (1995). The slip velocity $\boldsymbol{u}$ applicable can be obtained readily from superficial filtrate velocity $\boldsymbol{v}$ and the voidage of bed by using (12).

$$u = \frac{v}{\varepsilon} = {W_{filt}}\Big/{\varepsilon \cdot 2\pi \cdot r_0 \cdot H \cdot \rho_{ml}} \quad \textbf{(12)}$$

4.3. Energy balances.

Energy balances are likewise performed for each of the considered volumes. In the case of the slurry on top of the cake, the rate of change of the specific enthalpy, $\boldsymbol{h_s}$ (J/kg), can be determined form:

$$\frac{dh_s}{dt} = \frac{W_{in}\cdot h_{in} + W_{water}\cdot h_{water} - W_{s\_out}\cdot h_s - h_s\cdot\frac{dM_s}{dt}}{M_s} \quad \textbf{(13)}$$

The value of temperature can be recovered from the specific enthalpy applying known relations depending of massecuite composition (Bubnik, Kadlec, Urban and Bruhns, 1995).

For the cake, the energy balances are stated independently for the crystal (14) and mother liquor (15) phases.

$$\frac{h_{cris}}{dt} = \frac{\left[\begin{array}{l} W_{s\_out\_cris}h_{s\_out\_cris} - W_{dis}h_{mm\_c} + Q \\ -W_{un\_cris}h_{cris} - h_{cris}\dfrac{dM_{c\_cris}}{dt}\end{array}\right]}{M_{c\_cris}} \quad \textbf{(14)}$$

$$\frac{h_{ml}}{dt} = \frac{\left[\begin{array}{l} W_{s\_mm}h_{s\_ml} + W_{dis}h_{mm\_c} - W_{un\_ml}h_{ml} \\ -Q - W_{filt\_ml}h_{mm} - h_{ml}\dfrac{dM_{mm}}{dt}\end{array}\right]}{M_{ml}} \quad \textbf{(15)}$$

In the preceding expressions, $\boldsymbol{h_{mm\_c}}$ accounts for the specific enthalpy of the dissolved sucrose, while $\boldsymbol{Q}$ (W) stands for the heat energy exchange between the crystals forming the bed and the filtrate which could be expressed according to (16).

$$Q = \alpha_T \cdot A_{cris} \cdot (T_{mm} - T_{cris}) \quad \textbf{(16)}$$

Where $\boldsymbol{T_{mm}}$ and $\boldsymbol{T_{cris}}$ are the temperatures of the filtrate and of the crystals in the bed, obtained from the respective specific enthalpy values given by (15) and (14) through known relations. The term $\boldsymbol{\alpha_T}$ ($W/m^{2o}C$) represents the heat transfer coefficient, a parameter that could be estimated by the non dimensional expression (17) relating the Nusselt, Prandtl and Reynolds particle numbers and which is the exact analogous to the one used in the mass transfer coefficient determination for dissolution (Baehr and Stephan, 2006).

$$Nu = f_\varepsilon\left(2 + 0.664\, R_{ep}^{1/2} P_r^{1/3}\right) \quad \textbf{(17)}$$

4.4. Population balance

Terms related to the crystal size distribution (CSD) are described appealing to a population balance equation. The interest here is on following the evolution of the first moments of the number density function describing the characteristic size of particles which can be described by the following set of ODEs (Ramkrishna, 2000).

$$\frac{d}{dt}\mu_k = \frac{Q_{s\_ml}\mu_k^{in} - Q_{un\_ml}\mu_k - \frac{dV_{ml}}{dt}\mu_k}{V_{ml}} + kG\mu_{k-1} \quad \textbf{(18)}$$

Where $\boldsymbol{\mu_k}$ and $\boldsymbol{\mu_k^{in}}$ are the moments of order $\boldsymbol{k}$ in the bed and of the incoming mass, the latter suspended in the syrup flow represented by $\boldsymbol{Q_{s\_ml}}$. The term $\boldsymbol{Q_{un\_ml}}$ stands for the discharge volumetric flow rate while $\boldsymbol{V_{ml}}$ is the volume occupied by the syrup in the pores. The linear growing velocity of crystals, $\boldsymbol{G}$ (m/s), which can be obtained as function of the already known mass transfer flux $\boldsymbol{J_{cris}}$ (9) using (19), will be negative, representing dissolution. The terms $\boldsymbol{f_a}$ and $\boldsymbol{f_v}$ are form factors expressing, respectively, the relation between the square and the cube of the crystal characteristic dimension and its surface and volume.

$$G = \frac{f_a \cdot J_{cris}}{3 \cdot f_v \cdot \rho_{cris}} \quad \textbf{(19)}$$

From the moments of the CSD it is possible to obtain the total crystal surface of bed (20), its specific surface (21), the mass average size (22) which corresponds to the magnitude which is usually measured in the sugar industry by performing sieve analysis, the sphere equivalent average size (23) needed in the Frössling correlation (10) and a quantity that evaluates the spread of the population sizes, the coefficient of variation ($\boldsymbol{CV}$), defined as the ratio between the standard deviation and the average size, which is determined as in (24) .

$$A_{cris} = f_a \mu_2 V_{ml} \quad \textbf{(20)}$$

$$S_0 = \frac{A_{cris}}{V_{cris}} = \frac{f_a \mu_2}{f_v \mu_3} \quad \textbf{(21)}$$

$$L_{mm} = \frac{\sum L_i mass_i}{\sum mass_i} = \frac{\mu_4}{\mu_3} \quad \textbf{(22)}$$

$$L_e = \sqrt[3]{\frac{6}{\pi} f_v \frac{\mu_3}{\mu_0}} \quad \textbf{(23)}$$

$$CV = \frac{\sigma}{L_{mm}} = \sqrt{\frac{\mu_5 \mu_3}{(\mu_2)^2} - 1} \quad \textbf{(24)}$$

A key element of the model is the determination of the voidage $\boldsymbol{\varepsilon}$ and the description of its dependence on the crystal size distribution on the incoming suspension. It is known that grains with a smaller average size ($\boldsymbol{L_{mm}}$) or with a too great dispersion (***CV***), would create a more compact bed with a smaller voidage and, consequently, with a reduced permeability. The impact on the increase of the degree of bed packaging due to the presence of a substantial mass of too small crystals, the so called false grain or fines (***FG***), is also very important. The threshold for classifying crystals as fines is arbitrary. A reasonable value for the present case, where the nominal average size of crystals is about 550 µm, could be established around 135 µm.

So, in accordance with the previous discussion, the effect of CSD characteristic on voidage will be modeled with a the power law of the kind shown in (25). The parameters ***c***, ***eMa***, ***eCV***, ***eGF*** should be adjusted with experimental data.

$$\varepsilon = f\left(c L_{mm}{}^{eMA} CV^{eCV} FG^{eFG}\right) \quad \textbf{(25)}$$

4.5. Calibration and Validation

Calibration and validation of the batch centrifuge model has had to be performed appealing to historical data and in a context of lack of enough measurements.

The batch centrifuge used as reference has been a FIVES-CAIL's COMPACT, C41 unit.

Calibration has been conducted fixing the known physical dimensions, drum speed profile and typical stage timing.

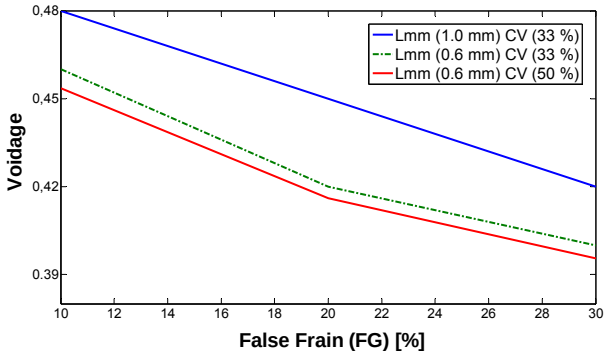

Figure 6. Data to determine voidage of bed.

The important functional dependence between the voidage of the bed and the characteristics of the grain has been fixed at the values shown in table 1, that were obtained by adjusting the free parameters in expression (25) to reproduce the data shown in figure 6. The data in the latter graphic has been extracted from the experimental results obtained by Bruhns (2004) which establishes the relation between voidage, average size and the presence of false grain. Information regarding the possible influence of the coefficient of variation has been assumed, reflecting the known tendency (Heffels 1986).

Table 1. Assumed parameters.

c	***eL***	***eCV***	***eFG***
0.7114	0.1037	-0.0283	-0.1244

Other model parameters (***R***, $\boldsymbol{k_\infty}$) of difficult identifiability due to scarcity of measurements have been fixed to reasonable values extracted from the literature. The final average measured humidity of 0.805 %, corresponding to the discharged sugar has been reproduced by adjusting the pores distribution index parameter, $\boldsymbol{\lambda}$, to a value of 15.

Table 2. A massecuite characteristics.

$\boldsymbol{B_{mm}}$ ***(%)***	$\boldsymbol{P_{mm}}$ ***(%)***	***cc (%)***	***FG (%)***	$\boldsymbol{L_{mm}}$ ***(µm)***	***Cv (%)***
79	84.6	55	10	55	35

Table 3. "A" poor syrup characteristics.

"A" poor syrup			
$\boldsymbol{B_{mm}}$ (%)		$\boldsymbol{P_{mm}}$ (%)	
Measured	Simulated	Measured	Simulated
77.1	77.91	85.0	85.3
78.0		86.8	

Table 4. "A" rich syrup characteristics.

"A" rich syrup			
$\boldsymbol{B_{mm}}$ (%)		$\boldsymbol{P_{mm}}$ (%)	
Measured	Simulated	Measured	Simulated
67.9	71.6	94.6	94.8
71.8		95.3	

Table 2 offers average data describing the characteristics of the "A" stage massecuite which is fed to the centrifuges and that have been used in the calibration-validation exercise. The variables recorded are the mass fraction (or Brix) of dissolved substances in the mother liquor ($\boldsymbol{B_{mm}}$) and its purity ($\boldsymbol{P_{mm}}$), the mass fraction of crystals referred to the whole suspension (***cc***), the amount of fines which has been assumed and the average size ($\boldsymbol{L_{mm}}$) and ***CV*** of CSD.

On the other hand, tables 3 and 4 presents measured and simulated data regarding the poor and rich syrups, respectively. The measured data

corresponds to various laboratory analysis performed during the period here considered. Rather than stating a single value, the interval where the true average value for each variable would reside with a 95% confidence, is recorded. Static simulated final values for the Brix and purity of both types of syrups, and which corresponds to variables not specifically adjusted during calibration, are well within the correct range, so contributing to increase the trust on the model.

It had been not viable to conduct a conventional dynamic validation, but the fact that the model is able to reproduce the workings of the represented unit in its evolution through strictly timed stages adds to credit of the former. For example, it is known that the supernatant slurry had disappeared by the time the first washing arrives, since otherwise it would be pointless. It is also common knowledge in industrial sugar practice, that the rate of crystal dissolution is swift enough so as to guarantee the maximum possible degree of dissolution according to the amount of water introduced meaning that at each wash stage, the mother liquor is able to return to the equilibrium state defined by the solubility. The above type of behaviors, with a marked a dynamic character, and whose gross violation would have cast severe doubts on the validity of the model, have been dutifully verified.

5. SOME SIMULATION RESULTS

A wise conduction of the batch centrifuges is key in guaranteeing the quality and economical objectives of the factory. The operator must pay attention to the measured variables and to the reports periodically arriving from the factory laboratory to make the required adjustments. A prejudicial decrease in the purity of white sugar is probably an indication that the amount of water introduced in the unit is not enough given the characteristics of the processed grain and so should be increased.

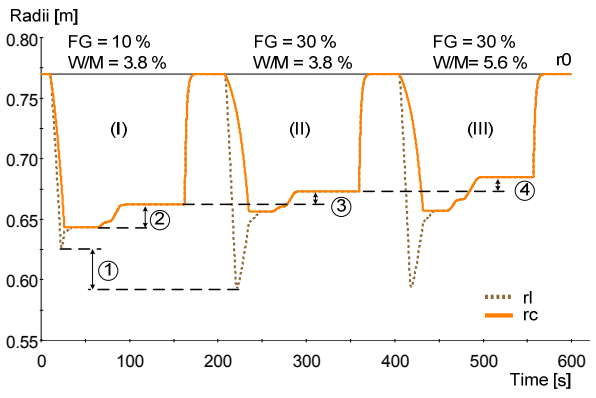

Figure 7. Three simulation experiments illustrating effects of false grain presence.

In fig. 7, the evolution of the radii of the supernatant slurry (r_l) and of the bed (r_c) are shown for three experiments. In the cycle labeled as (I), the grain delivered by the first stage crystallizers is good, in particular the presence of false grain is a moderate 10%. The following cycle (II), the same variable has risen to a high value of 30% and this fact, that can be indirectly appreciated as a more closely packed bed (label 3) implies a worse filtering capability. This effect is evidenced in the higher peak reached by the mass of slurry (1) and, more importantly, by the increased presence of mother liquor which remains saturating the pores of the bed at the end of the draining phase (fig. 8). The extra amount of residual traces of mother liquor, if the purity of the massecuite and the amount of water applied are kept constants, implies a lower total purity (P_{mc}) of the commercial product as reflected in table 5.

The preferred solution to the above situation implies the improvement of the uniformity of the crystals delivered by the crystallizers. An immediate remedy, however, would be the increase of the amount of water introduced in the unit. In the processing of the batch (III) (fig. 7), the water to mass ratio has been increased from the original 3.5 % to a value of 5.6%. A greater relative presence of water implies a correspondingly higher mass of dissolved sugar crystals as can be observed in the reduction of the radii of the bed which is obtained after washing (label 4 if fig. 7). Thus, the purity of the residual syrup, and consequently of the total humid sugar mass, is higher, an effect not only due to the above mentioned greater dissolution but to the fact that its composition is more favorable: the amount of syrup finally remaining is relatively insensitive to the increase on water but the presence of impurities is lower since it is more diluted.

Table 5. Simulated experiments.

	W/M (%)	FG (%)	P_{mc} (%)	C_{con} (%)	ε
(I)	3.7	10	99.94	86.2	0.45
(II)	3.7	10	99.93	86.2	0.45
(III)	5.6	30	99.97	77.0	0.39

Table 6. Simulated experiment syrup characteristics.

	Poor syrup			Rich syrup		
	P_{mm} (%)	B_{mm} (%)	M (kg)	P_{mm} (%)	B_{mm} (%)	M (kg)
(I)	86.4	81.5	373	92.7	77.0	184
(II)	86.4	81.5	368	92.5	77.0	188
(III)	86.4	81.4	371	94.5	76.0	261

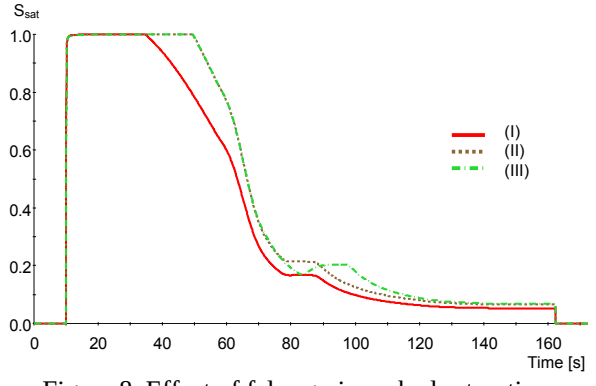

Figure 8. Effect of false grain on bed saturation.

So the increase of the water to mass ratio implies the reduction of the efficiency associated to a lesser conservation of crystals which is also evidenced as an increase of the purity of the expelled syrups (table 6). The extra mass of water also ends up increasing the amount of rich syrup (M) which needs to be recycled, meaning a consequent reduction of the capacity of the installed base to process the incoming fresh concentrated juice. The operator can counterbalance this latter effect by acting on the parameter which determines the poor to rich syrup switching time (t_{sw}). An increase of t_{sw} from the nominal situation labeled in fig. 9 as (i) to the value represented in (ii) implies the simultaneous increase of the purities of both syrups. The extra time allotted to the syrup classified as poor means a corresponding reduction of the amount of rich juice to be recycled as evidenced in the results shown in table 7. The operator should weigh the relative importance of the benefit so obtained, with the risk of finally losing too much sucrose in the molasses due to the increase in purity of the poor syrup which gets sent to the "B" and "C" exhausting stages (see also table 7).

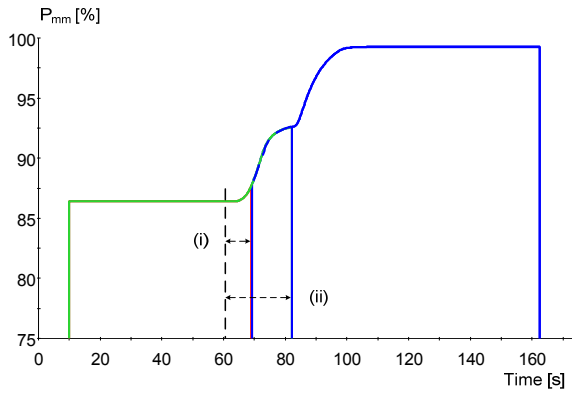

Figure 9. Implication of poor to rich syrup switch policy.

Table 7. Simulated experiment modifying syrups switching time.

	Poor syrup			Rich syrup		
	P_{mm} (%)	B_{mm} (%)	M (kg)	P_{mm} (%)	B_{mm} (%)	M (kg)
(i)	86.4	81.4	371	94.5	76.0	261
(ii)	87.5	80.5	477	97.5	75.5	154

6. THE OPERATORS TRAINING LIBRARY AND TRAINING SIMULATION TOOL

The centrifuges model, along with those corresponding to the other main units to be found in a typical Sugar House, are offered as part of an object oriented library. In the current state of the art of the modeling and simulation discipline for dynamical continuous or hybrid systems, the OO paradigm (Cellier, and Kofman 2006) is the one that offers the best adapted tools for dealing with the complexity posed by the need of representing large plants. Furthermore, in the case here addressed, the very nature of a project aiming at creating a general library of reusable components, practically claims for the use of the OO paradigm with its provision for allowing the hierarchical creation of models and its ability for closely mimicking the plant to be represented by connecting the individual components reflecting the real life processing units. In figure 10, this kind of *physical modeling* is used to represent a battery of three batch centrifuges which has been carried out by deploying a matching number of instances of the corresponding model class and by connecting them, trough compatibles ports, to objects modeling other typical process industry equipment such as tanks and conveyors.

The modeling and simulation software chosen for implementing the Sugar House Library project has been **EcosimPro** (EA International 1999). This state of the art tool features **EL**, its own full-fledged OO language, able to deal with dynamical continuous processes but that also has the ability of managing hybrid type of systems.

This last capability is badly needed for implementing batch kind of models, like the one here described. The existence, for example, of a controlling program that defines a recipe whose stages are mostly specified in terms of the their duration, implies the need for the simulation to respond to time defined discrete events.

Moreover, the fact that a finite amount of material is to be process each cycle, means that the model must represent widely different situations, probably requiring a discrete type of logic for switching between different sub-models. Occurs, for instance, that the need for the equations which describes mass balances in the supernatant space, eventually disappears. The discrete event which requires attention in this latter case, is different than the first, and more difficult to handle, since it is triggered, not by time, but by the state of the simulation.

EcosimPro (**EL**) offers the language constructs that can adequately deal with both type of events, and this is useful for alerting the numerical integration machinery of their occurrence since otherwise the simulation could be severely slowed down or even disrupted.

Another advantage of the simulation concerns more specifically the particular project here reported. **EcosimPro** is an open tool in the sense it offers the final model, ready to be numerically simulated, as C++ class that could be driven from third party systems. This characteristic is relevant for the purpose of creating stand-alone simulation application software. A deed which is imperative if the purpose is that of providing an effective training experience by reproducing an interface similar to the one to be found in the control room of the factory.

The simulation code delivered by **EcosimPro** is wrapped (Alves, Normey-Rico, Merino, Acebes and Prada 2005) as an **OPC** (Ole for Process Control) server, so that the values of simulated variables can be transparently accessed from any client implementing the

mentioned standard communication protocol, the one currently preferred in process industries.

But the job of training demands the use of specific features such as the need of controlling the pace of the numerical integration for allowing real time or accelerated performance, or the provision for the role of the instructor, an actor which is authorized to change model parameters or introduce a simulated failure mode, to challenge the trainee and so conduct her learning process, among others. This special tasks have been specifically addressed in the development of the HMI/SCADA tool, EDUSCA, (Alves, Normey-Rico, Merino, Acebes y Prada 2006) used in the present project.

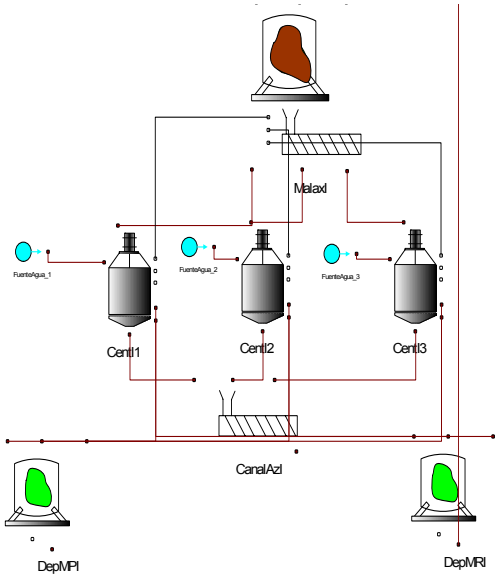

Figure 10. EcosimPro connection diagram for "A" stage centrifuges battery.

Figure 11, shows, for example, the interacting panel for dealing with one of the batch centrifuges of the simulated factory.

Figure 11. Training interface for one batch centrifuge.

REFERENCES

Alves, R., J.E. Normey-Rico, A. Merino, L.F. Acebes, C. Prada, (2005), OPC based distributed real time simulation of complex continuous processes. *Simulation Modelling Practice and Theory*, 13 (7), 525-549.

Alves, R., J.E. Normey-Rico, A. Merino, L.F. Acebes, C. Prada, (2006), EDUSCA (EDUCATIONAL SCADA): Features and Applications. ACE 2006. 7th IFAC Symposium in Advances in Control Education, Madrid, Spain.

Ambler, C.M., (1988), Centrifugation. Handbook of Separation Techniques. New York: McGraw Hill.

Azucarera Ebro. S.A, 2002-2008. *Internal Technical Reports*. Spain.

Baehr, H.D., Stephan, K., 2006. *Heat and Mass Transfer*. Germany: Springer Verlag.

Barr, J.D., L.R. White, (2006), Centrifugal drum filtration II: A compression rheology model of cake draining,52, 557–564. *AIChE Journal*.

Bubnik, Z., Kadlec, P., Urban, D., M. Bruhns (1995), Sugar Technologist Manual. Chemical and Physical Data Manufacterers and Users. Germany: Verlag Dr. Albert Bartens.

Bruhns, M., 2004. The viscosity of massecuite and its suitability for centrifuging. *Zuckerindustrie*. Vol. 129. No. 12 pp: 853-863. Germany: Verlag Dr. Albert Bartens.

Cellier, F.E., E. Kofman (2006), Continuous System Simulation. New York: Springer-Verlag,

EA International and ESA, 1999. EcosimPro User Manual, EL Modeling Guide.

Georgieva, P., Meireles, M.J., Feyo de Azevedo, S. (2003), Knowledge-based hybrid modelling of a batch crystallization when accounting for nucleation, growth and agglomeration phenomena. *Chemical Enginnering Science*, 58, 3699-3713.

Heffels, S. K., (1986), Product size distributions in continuous and batch sucrose crystallizers. PhD Thesis. Delft Technical University.

Mazaeda, R., Prada, de C., 2007. Dynamic Simulation of a Sucrose Batch Evaporative Crystallizer for Operators Training, *19th European Modeling and Simulation Symposium (Simulation in Industry), EMSS 2007*, Bergeggi, Italia.

Mazaeda, R., 2010. Librería de Modelos del Cuarto de Azúcar de la Industria Azucarera para Entrenamiento de Operarios. Thesis (PhD), University of Valladolid.

Merino, A., Mazaeda, R., Alves, R., Acebes, L.F., Prada, C., 2006. Sugar factory simulator for operators training. *ACE 2006 7th. IFAC Symposium in Advances in Control Education*, Madrid, Spain.

Ramkrishna, D. (2000), Population Balances: Theory and Applications to Particulate Systems in Engineering, NewYork, USA: Academic Press..

Van der Poel, P.W., Schiweck, H., Schwartz, T., 1998. Sugar Technology. Beet and Cane Sugar Manufacture. Germany: Verlag Dr. Albert Bartens.

Wakeman, R.,J., Tarleton, E.,S., (1999), Filtration. Equipment selection, modelling and Process Simulation. 1st Edition Netherlands: Elsevier.

DYNAMIC SIMULATION OF A COLLECTOR OF H_2 USING A DYNAMIC LIBRARY

M. Valbuena[(a)], D. Sarabia[(b)], C. de Prada[(c)]

[(a)]Department of Systems engineering and Automatic, C/Rel de Burgos s/n, Valladolid, University of Valladolid
[(b)] Department of Systems engineering and Automatic, C/Rel de Burgos s/n, Valladolid, University of Valladolid
[(c)] Department of Systems engineering and Automatic, C/Rel de Burgos s/n, Valladolid, University of Valladolid

[(a)] mvalbuena@autom.uva.es, [(b)] dsarabia@autom.uva.es, [(c)] prada@autom.uva.es

ABSTRACT
This work treats the problem of dynamic simulation of a collector of H_2 in a refinery, as the first step for the development of a dynamic simulation of the complete network of H_2. There try to be studied the phenomena of transport of matter and energy of the collectors of H_2 from the point of view of the pressure, temperature, molecular weight, etc., having in it counts the spatial distribution of the same ones. For it, we use a graphical library developed in EcosimPro® that allows the study of different structures.

Keywords: dynamic simulation, networks of hydrogen, numerical methods, dynamic library of components in EcosimPro®.

1. INTRODUCTION

The present work allows to a wider project of investigation. Its aim is of developing new knowledge in the field of the control and systems optimization of large scale in the process industry and demonstrating his applicability on an industrial scale.

The interest for this type of systems has been growing progressively for his impact in the global functioning of a system or factory, so much economically as technician, as for the strategic paper that often they recover (Prada 2004). Between them they find the distribution networks: of water, of electricity, of gas, of telecommunications, etc., of whose effective management there can depending both the satisfaction of the demands of the users and the profitability of his operation. Especially, the networks of steam distribution, gas, water treatment, etc. of many industries of processes they connect the centers of production or storage with the plants where the above mentioned resources are consumed across a distribution system which habitual characteristics are his large scale, the interaction between the different elements, the variability of the demands, the presence of diverse restrictions of operation and the control of his functioning across decisions of different nature. The production of hydrogen in large quantities today is only feasible from hydrocarbons in plants where the principal element are the ovens of reformed. From them it is distributed to the different consuming plants across a complex system of pipelines (collectors) of several kilometers of length, different diameters and working to different pressures and purities.

Though the networks have several kilometers along a refinery, his capacity of storage is very limited, for what to guarantee the fulfillment of the changeable demands of the consuming plants an excess of hydrogen is kept in the distribution network that ends up by being sent to the gas network to fuel consumption in ovens and other equipments mixed with other fuels or, eventually, to the torch of the refinery. However, to the being the hydrogen an expensive gas of producing, is not desirable an overproduction though this one assures the supply of the consuming plants. On the other hand a fault of hydrogen can limit the production or the life of the catalysts of the reactors. For it, the management of the network must attend simultaneously to a level of control of pressures and flows of the system and to a level of optimization of the global decisions. The topic of the optimization has been approached by means of an approach based on the determination of the condition of the network and on the next optimization of the decisions, on the frame of a system of help to the capture of decisions (Gómez et al. 2008) and (Sarabia et al. 2009). The above mentioned approach is based in addition on stationary models of the network of H_2, supposing that the flow is a ideal gas mixtures and without bearing in mind the spatial distribution of the own network. However, since normally the control system of the network is decentralized, with classical control structures, may not be easy to implement the global recommendations of the optimizer for whole network both the interactions between its components as dynamics constraints of low level of flows and pressures that have not been taken into account explicitly to level of optimization.

2. DESCRIPTION OF THE COLLECTOR OF H_2

To know the dynamics of the variables (density, pressure and temperature) in function so much time as of the longitudinal coordinate of the conduction, appear the corresponding balance sheets of mass, quantity of movement and energy based on a macroscopic description. In addition it is supposed that in the direction of the radial coordinate there is no variation of

density, pressure and temperature, that is to say, the model goes global with regard to this coordinate. Next there appear the equations of the model distributed of the collector. The equation (1) describes the global mass balance when the phenomenon of transport is only due to the convention (Ames 1977):

$$\frac{\partial m}{\partial t}+\frac{1}{r}\frac{\partial}{\partial r}(rv_r m)+\frac{1}{r}\frac{\partial}{\partial \theta}(v_\theta m)+\frac{\partial}{\partial z}(v_z m) = \frac{1}{r}\frac{\partial}{\partial r}\left[\rho \widetilde{D}_R r\frac{\partial}{\partial r}\left(\frac{m}{\rho}\right)\right]+\frac{1}{r^2}\frac{\partial}{\partial \theta}\left[\rho \widetilde{D}_\theta \frac{\partial}{\partial \theta}\left(\frac{m}{\rho}\right)\right] + \frac{\partial}{\partial z}\left[\rho \widetilde{D}_z \frac{\partial}{\partial z}\left(\frac{m}{\rho}\right)\right]+R \quad (1)$$

Being variables m, v_r, v_θ, v_z, ρ, $\widetilde{D}_R$, $\widetilde{D}_\theta$, $\widetilde{D}_z$, r, θ, z y t are the mass, component of the speed in direction *r*, component of the speed in direction θ, component of the speed in direction *z*, density of the fluid, component of the coefficient of dispersion in direction *r*, component of the coefficient of dispersion in directionθ, component of the coefficient of dispersion in direction *z*, radial coordinate, angular coordinate, longitudinal coordinate and time, respectively. The equations (2) and (3) show the individual mass balance being C_k is the composition of the component k (hydrogen and impurities):

$$\frac{\partial(mC_k)}{\partial t}+\frac{1}{r}\frac{\partial}{\partial r}(rv_r mC_k)+\frac{1}{r}\frac{\partial}{\partial \theta}(v_\theta mC_k)+\frac{\partial}{\partial z}(v_z mC_k) = \frac{1}{r}\frac{\partial}{\partial r}\left[\rho \widetilde{D}_R r\frac{\partial}{\partial r}\left(\frac{mC_k}{\rho}\right)\right]+\frac{1}{r^2}\frac{\partial}{\partial \theta}\left[\rho \widetilde{D}_\theta \frac{\partial}{\partial \theta}\left(\frac{mC_k}{\rho}\right)\right] + \frac{\partial}{\partial z}\left[\rho \widetilde{D}_z \frac{\partial}{\partial z}\left(\frac{mC_k}{\rho}\right)\right]+R \quad (2)$$

$$\sum C_k = 1 \quad (3)$$

The equation (4) shows the quantity of movement balance:

$$m\left(\frac{\partial v_z}{\partial t}+v_r\frac{\partial v_z}{\partial r}+\frac{v_\theta}{r}\frac{\partial v_z}{\partial \theta}+v_z\frac{\partial v_z}{\partial z}\right) = -\frac{\partial P}{\partial z}Vol + \left[\frac{1}{r}\frac{\partial}{\partial r}\left(\tilde{\mu}_{zr} r\frac{\partial v_z}{\partial r}\right)+\frac{1}{r^2}\frac{\partial}{\partial \theta}\left(\tilde{\mu}_{z\theta}\frac{\partial v_z}{\partial \theta}\right) + \frac{\partial}{\partial z}\left(\tilde{\mu}_{zz}\frac{\partial v_z}{\partial z}\right)\right]+mg_z \quad (4)$$

Being P, $\tilde{\mu}_{zr}$, $\tilde{\mu}_{z\theta}$ y $\tilde{\mu}_{zz}$ correspond with the pressure of the fluid and with the effective viscosity in coordinate *r*, θ y *z*, respectively. It thinks that the fluid that circulates along the interior of the pipeline suffers loss of quantity of movement due to the friction. Then, this term is added in the second member of the equation (4): $P_{roz} = -\rho\frac{\emptyset}{2d}v\|v\|$. Equation (5) shows the corresponding energy balance, where there has not been included the phenomenon of the viscous dissipation that is the conversion of the kinetic energy in heat owed to the internal friction to the fluid since it is possible to consider it despicable.

$$mC_p\left(\frac{\partial T}{\partial t}+v_r\frac{\partial T}{\partial r}+\frac{v_\theta}{r}\frac{\partial T}{\partial \theta}+v_z\frac{\partial T}{\partial z}\right) = \frac{1}{r}\frac{\partial}{\partial r}\left(\tilde{k}_R r\frac{\partial T}{\partial r}\right)+\frac{1}{r^2}\frac{\partial}{\partial \theta}\left(\tilde{k}_\theta\frac{\partial T}{\partial \theta}\right)+\frac{\partial}{\partial z}\left(\tilde{k}_z\frac{\partial T}{\partial z}\right) + S_R \quad (5)$$

Being C_p, T, $\tilde{k}_R$, $\tilde{k}_\theta$ y $\tilde{k}_z$, are it respectively the calorific capacity, the temperature and the component of the conduction in the coordinates *r*, θ y *z*. It thinks that along the pipeline heat losses exist towards the exterior. This term gets in the second member of the equation (5): $Q_{pérdidas} = -U(T-T_{ext})$, being U the global coefficient of heat transmission. Finally, there is had the equation of the ideal gases since the gas that circulates along the interior of the collectors is not to very high pressures and temperatures:

$$PV = nRT \quad (6)$$

Being V the volume, n the number of masses and R the constant of the ideal gases.

3. MODELLING IF THE COLLECTOR OF H_2

The analytical approximation methods of the solution of an equation in partial derivatives, provide frequently useful information over of the behavior of the solution in critical values of the dependent variable, but they tend to be more difficult to apply that the numerical methods (González 2008). The numerical methods are technical by means of which it is possible to formulate mathematical problems in such a way that they could be solved using arithmetical operations. The use of distributed models for (1) - (6) exclude the utilization of conventional integrators to integrate the model. The collocation orthogonal method and finite differences method are widely used to solve numerically equations in derivatives partial (PDEs), transforming the partial derivatives into a set of differential ordinary equations (ODEs) doing a discretization the spatial domain.

3.1. Finite Differences

The finite differences method is widely used to solve numerically equations in derivatives partial (PDEs), transforming the partial derivatives for an approximation into a set of differential ordinary equations (ODEs) doing a discretization the spatial domain. In this method, a derivative equation in a discreet point, x_j, is evaluated using the information about the variables in this point x_j (local information). One of the big advantages of the finite differences method is the wealth of existing theory to help solve different problems. Topics like the numerical consistency, convergence and stability have been deeply studied. In addition it offers a considerable flexibility

when one works in discretización of meshes since there can be chosen the dimensions of time and space and it is a question of a method intuitive and easy to help. There are several variations on the finite differences method and they are function of how to perform the approach of the partial differential equation (Ramírez et al. 2006). However, the finite central difference is often the most exact and it is the used one in this work.

3.2. Collocation orthogonal

The collocation orthogonal method is a variant of the method of weighted residues, where the nodes of approximation are given by the roots of orthogonal polynomials as those of Jacobi, Legendre and Hermite, between others. The polynomial approximation is done in the whole domain. This methodology offers major precision those other methods, since the equation of discretización for a node involves to all the nodes of the domain. The choice of these collocation points remains of some arbitrary form until there appears the work (Villadsen and Stewart 1967), those who establish the choice of the collocation points as the roots of orthogonal appropriate polynomials. There exist some variants that depend in the form of the function of test and in the form of selecting the location of the nodes, as: simple collocation with function Dirac's Delta, Sub-domains, Moments, Galerkin, Square Minimums, etc. (Finlayson 1980), (Ames 1977).

3.3. Collocation orthogonal on finite elements

In the finite elements method, the domain is subdivided into a set number of small regions, where each is unique. On each finite element, the dependent variables (temperature, speed, concentration, etc.), are approximated by using known functions. These functions can be linear or nonlinear (polynomials generally), depending on the nodes used to define finite elements. Next, the model equations are integrated in each finite element and the set of individual solutions that are obtained are assembled on the total domain. As consequence of these operations, one obtains a set of algebraic equations which is solved for know the value of the dependent variables in the nodes (Finlayson 1980). This method is suitable for problems with irregular geometries. Next, the finite elements are coupled following the principle of continuity. This methodology is adapted for problems in those who are known that abrupt changes exist in the values of the dependent variables (Carey and Finlayson 1975).

3.4. Finite Volumes

It is considered to be a discretization mesh of the fluid space. Around each point of this grid is built a control volume that does not overlap with those of neighboring points. Of this form, the total volume of fluid will have to be equal to the sum of the considered control volumes. The set of differential equations for a model is integrated over each control volume, which translates as a discretization of the set of equations. The finite volume methods are narrowly related to the finite differences methods (Leveque 2004). It is intuitive to think that the accuracy will be greater the lower the volume size; by what is interesting divide the domain into as many pieces as possible. The price to pay is that the coefficient matrix of the system to be solved is large, so the computational cost of resolution can be increased greatly if the number of nodes is too high. The point of commitment is reached when it find the mesh with the minor possible number of nodes that there provides a solution independent from this one, that is to say, a mesh in which the solution does not change significantly if the space reduces.

4. LIBRARY OF COMPONENTS IN ECOSIMPRO FOR DISTRIBUTED SYSTEMS

Creating a dynamic library of components (Figure 2) in EcosimPro® allows constructing of simple form different models. The components of "*Entrada*", "*Salida*", "*Aporte*", "*Consumo*" and "*Tubería*" contain the described equations of (1) - (6) discrete using the numerical methods. The components "*Nodo_1a2*" and "*Nodo_2a1*" contain equations of continuity.

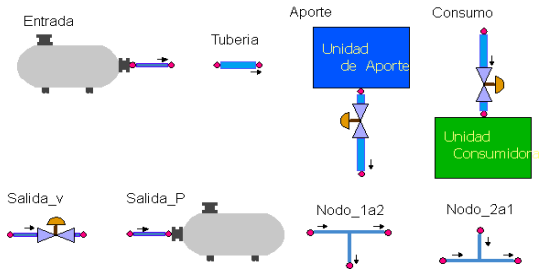

Figure 1: Librería de componentes en EcosimPro®

The component of "*Entrada*" comes from a warehouse, so the contour conditions in this point will be the pressure, the temperature and the concentration of the fluid. The component "*Aporte*" has a valve in the beginning of the pipeline, for what the velocity, the temperature and the concentration of the fluid is boundary conditions. On the other hand, the component "*Consumo*" finishes with a valve that will be at the entry of the consuming units and, for this reason, in this point the velocity is a boundary condition. Finally, analyzing the component "*Salida*", it is possible to have at the end of the pipeline a valve or a warehouse. Then, the boundaries are the velocity or the pressure, respectively. Depending of the bounds of boundaries that are chosen, the problem to resolving is different. To bear it in mind different components have been included. With this library of components can be realized precise analyses of transitory. In addition, he presents the advantage of which it is possible to extend of rapid and simple form with new components that could turn out to be necessary for the simulation of the most complex systems, for example, components of type of control as regulators PID, etc.

5. EXAMPLE AND RESULTS

The example consists into considered the system of the Figure 2, which it has a collector formed by two units of

contribution and three consuming units. The Table 1 shows the number of equations, the number of variables and the time that is late the simulation in executing 600 seconds. In the Table 2 there appears the number of nodes in which every component has been divided. The difference in simulation time is due to the type and number of equations that are used. The collocation orthogonal method in finite elements has the greatest number of equations and variables (since it has more nodes) and it has the bigger simulation time.

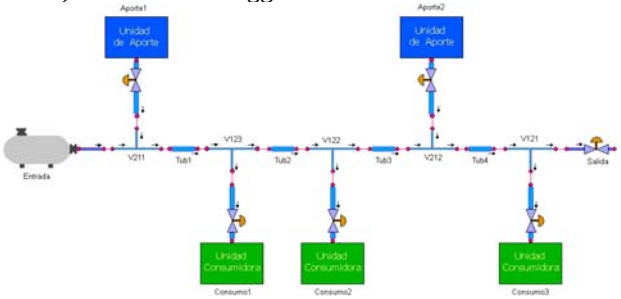

Figure 2: Example of a collector with two units of contribution and three consuming units

Table 1: Number of equations and variables

	CO	CO in EF	DF	VF
Nº eq.	929	1406	1397	807
Nº var.	1369	1720	1864	1101
Simulation time (s)	2.953	4.828	3.640	2.578

Table 2: Number of nodes of every component

	CO	CO in EF	DF	VF
Nº Nodes Interiors	2	2	5	5
Nº Nodes Total	N_{tot}=4	Nº EF: 2 N_{tot} = 7	N_{tot}=7	N_{tot}=7

It has been realized a jump in the composition of the fluid of entry to the collector that proceeded from the component "*Entrada*" to see the evolution of the composition of the fluid along the collector. At first, all the compositions of contribution are equal (purity of the hydrogen of the 99.9 %). Next, the composition of "*Entrada*" happens to be 99.85 % in purity of the hydrogen. To see clearly the results, it is represented in the graphs the first node of every component of the principal collector (it is to say, the first nodes of the components "*Entrada*", "*Tubería*" y "*Salida*").

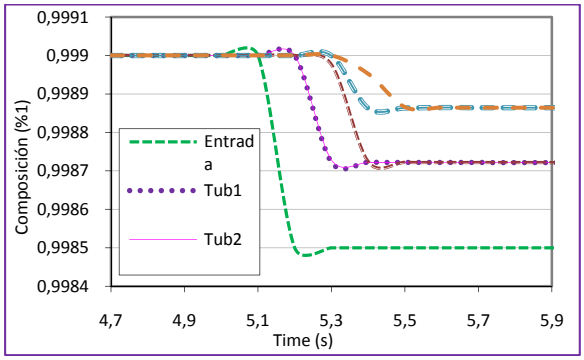

Figure 3: Composition of the collector using CO on having changed the composition of "*Entrada*"

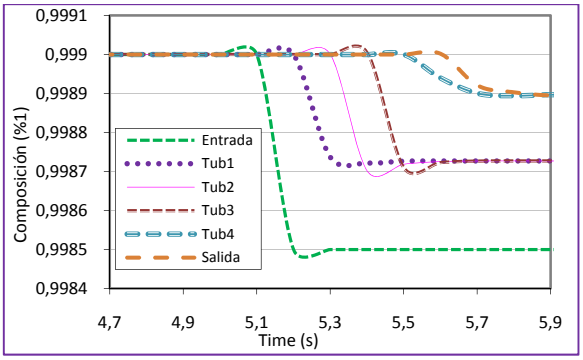

Figure 4: Composition of the collector using CO in EF on having changed the composition of " *Entrada*"

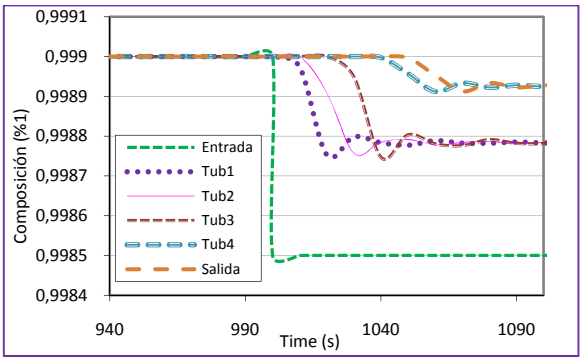

Figure 5: Composition of the collector using DF on having changed the composition of " *Entrada*"

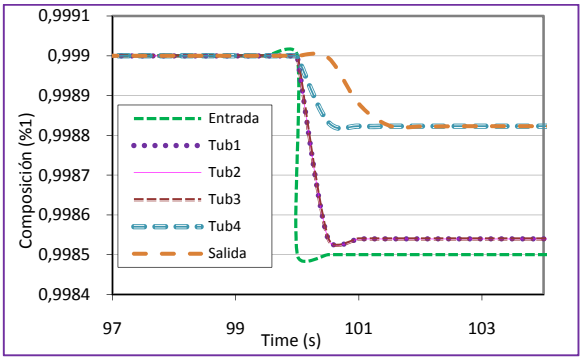

Figure 6: Composition of the collector using VF on having changed the composition of " *Entrada*"

As show the figures 4 - 7, on having diminished the composition of the fluid of entry to the principal collector, it diminishes the composition along the collector since this variation is transmitted from a component to other one. It is necessary to emphasize that the composition of the components "*Tubería1*", "*Tubería2*" and "*Tubería3*" is same, but different from the composition of "*Entry*" since in the middle exists a current of contribution, "*Aporte1*" whose fluid possesses a composition of 99.9 % in purity of H_2. The same thing happens with the composition of the components "*Tubería2*" and "*Exit*", that though between them they have the same composition, this one is different from the rest of the components of the principal collector since in this point appears a new current: "*Aporte2*" with a 99.9 % in purity of H_2. Also it is possible to observe that the response of the model before these changes is soft, of the second order,

underdamped and with a small time of stabilization (except for the case of finite differences). As expected, there is a delay in the response of the fluid as it moves through the collector. Next a jump is done in the composition of entry to the principal collector from the component *Aporte1*" happening from 99.9 % to 99.86 % and after 99.86 % to 99.91 %.

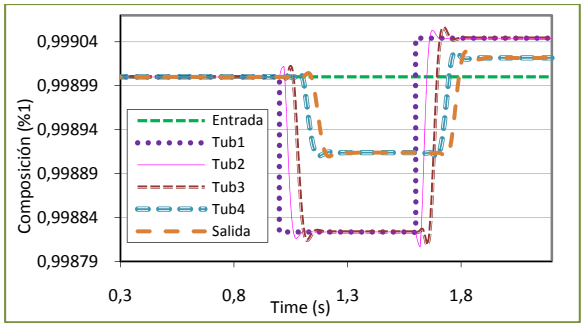

Figure 7: Composition of the collector using CO on having changed the composition of "*Aporte1*"

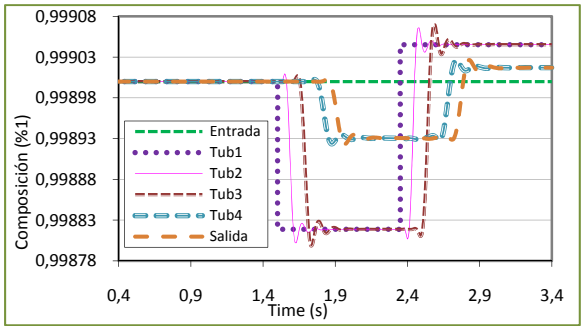

Figure 8: Composition of the collector using CO in EF on having changed the composition of "*Aporte1*"

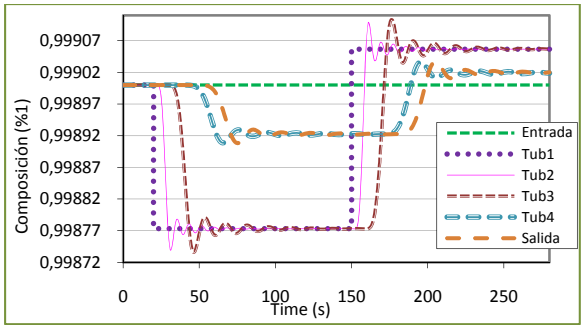

Figure 9: Composition of the collector using DF on having changed the composition of "*Aporte1*"

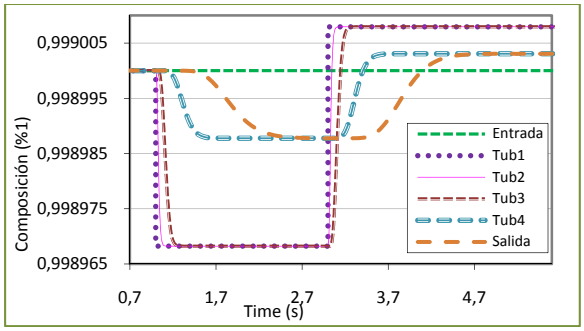

Figure 10: Composition of the collector using VF on having changed the composition of "*Aporte1*"

In this case, the composition of the fluid in the component "Entrada" does not intervene since the component "Aporte1" appears in a place later, so this composition always will have the same value. The conclusions obtained are equivalent to those of the previous case as for the type of response that is obtained and to the value of the composition along the collector. Another type of jump that has been realized is the change in the pressure of entry to the collector from the component "Entrada". Initially, the pressure of entry to the collector is of 1.8982 • 106 Pa (18.7 atm.) and later there happens to cost 1.8907 • 106 Pa (18.6 atm.).

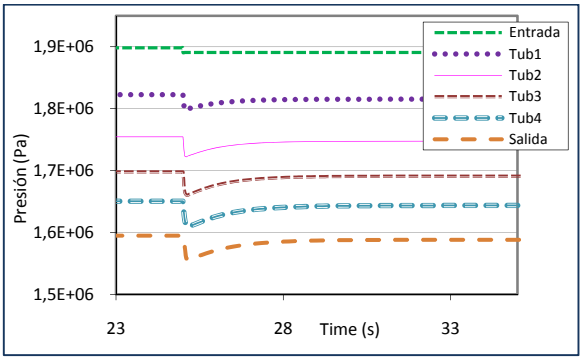

Figure 11: Pressure of the collector using CO on having changed the pressure of "*Entrada*"

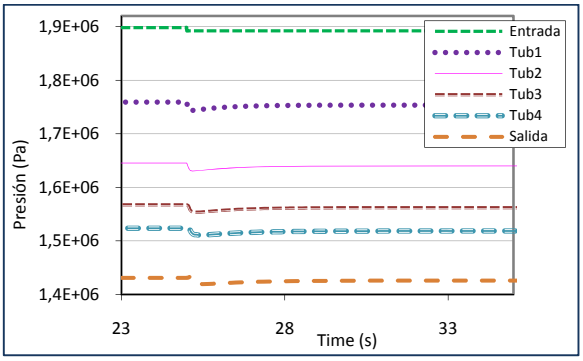

Figure 12: Pressure of the collector using CO in EF on having changed the pressure of " *Entrada*"

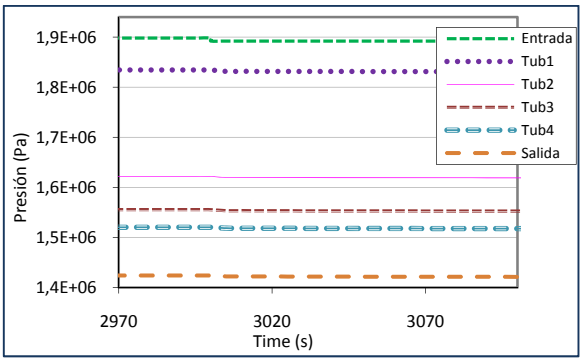

Figure 13: Pressure of the collector using DF on having changed the pressure of " *Entrada*"

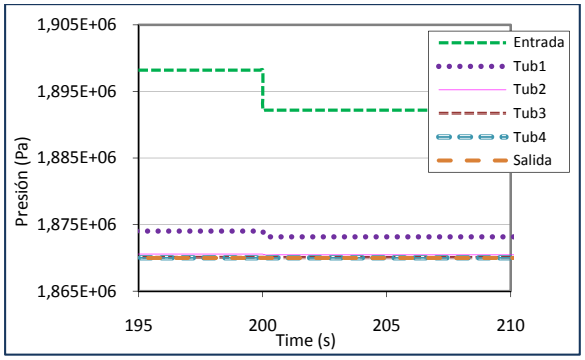

Figure 14: Pressure of the collector using VF on having changed the pressure of " *Entrada*"

As shown in Figures 12-15, a decrease in inlet pressure causes a decrease of the pressure along the collector. In the case of orthogonal collocation and orthogonal collocation on finite elements, the kind of response you get is underdamped, the response in every case has a small stabilization time. Also we can found significant changes in the density of the fluid since that increasing pressure increases the mass and, for a constant volume, density increases, and vice versa. The other variables also change, but its effect is not so obvious.

6 CONCLUSIONS

There has been created a graphical library of dynamic components that allows to constructing of easy form complex systems of pipelines. Of this form, it is possible to study the dynamics of a fluid that circulates in different systems. It is a question of a very useful tool that in a future work will be extended with components of control.

The results obtained in the simulations are coherent with the physical and chemical laws formulated.

In the simulation, obstacles were encountered at the moment of the initialization of the problem, but these are resolved of satisfactory form. However, one is working in order that the resolution of these problems of initialization is realized of automatic form.

Finally, we have found many bibliographical references that explain the fundaments of the methods of integration. Generally they use the example of a bar that warms up in an end and they apply these methods to solve the equation of heat conduction. Others use the equation of movement in examples like porous beds, catalytic beds, etc. However, we have not found enough references that combine the equations of conservation of mass, conservation of movement and heat conduction, which are those who are used in this work.

ACKNOWLEDGMENTS

The authors wish to thank Repsol-YPF and Petronor refinery in Bilbao for their help and collaboration as well as to the Ministry of Science and Technology and to the Junta of Castilla and Leon for funding through of the projects of Optimal Operation of Plant Process, CICYT (ref. DPI2006-13593) and Management Optima of Complex Plants (ref. GR85) respectively.

REFERENCES

Ames, W. F., 1977. Numerical Methods for Partial Differential Equations. Second Edition. Orlando, Florida. Academic Press, Inc.

Carey, G. F., Finlayson, B. A., 1975. Orthogonal collocation on finite elements. Chemical Engineering Science, 30, 587-596.

Finlayson, B. A., 1980. Nonlinear Analysis in Chemical Engineering. New York, McGraw Hill.

Gómez, E. Sarabia, D., Méndez, C.A., Prada, C., Cerdá, J., Sola, J.M., Unzueta., E., 2008. Optimal management of hydrogen supply and consumption networks of refinery operations. *European Symposium on Computer Aided Process Engineering*, ESCAPE 18, Lyon, France.

González A. H., 2008. Comparación de métodos analíticos y numéricos para la solución del lanzamiento vertical de una bola en el aire. *Lat. Am. J. Phys. Educ*, 2 (2).

Leveque, R.J., 2004. Finite-Volume Methods for Hyperbolic Problems. Cambridge Texts in Applied Mathematics. Cambridge University Press. New York. Cambridge University Press.

Prada, C., 2004. El futuro del control de procesos. *Revista Iberoamericana de automática e informática industrial*, 4 (1), 5-20.

Ramírez, J. J. R., Vanegas, C. A. G., Villegas, A. M. R., 2006 Método de Diferencias Finitas para la Solución de Ecuaciones en Derivadas Parciales. *Universidad Eafit, Medellín*, Colombia.

Sarabia, D., Cristea, S., Gómez, E., Gutierrez, G., Méndez, C.A., Sola, J.M., Prada, C., 2009. Data reconciliation and optimal management of hydrogen networks of a real refinery. ADCHEM, Istanbul, Turkey.

Villadsen, J. V., Stewart, W. E., 1967. Solution of boundary-value problems by orthogonal collocation. *Chemical Engineering Department, University of Wisconsin, Madison*, 22, 1483-1501.

OPTIMAL DESIGN FOR WATER AND POWER CO-GENERATION IN REMOTE AREAS USING RENEWABLE ENERGY SOURCES AND INTELLIGENT AUTOMATION

Amr A. Kandil[(a)], Adrian Gambier[(b)], Essam Badreddin[(c)]

[(a),(b),(c)]Automation Laboratory (PROAUT)
Institute of Computer Engineering
University of Heidelberg, 68131 Mannheim, Germany

[(a)]Kandil@uni-heidelberg.de, [(b)]Gambier@uni-heidelberg.de, [(c)] badreddin@ziti.uni-heidelberg.de

ABSTRACT
In this paper a reverse osmosis desalination plant for brackish water powered by renewable energy sources, and a diesel generator as back-up will be described. The whole system serves as a laboratory prototype for testing new automatic control methods to increase the plant reliability, which is crucial in remote arid areas. The necessary steps for the design of an optimal co-generation of both water and electricity such as the decision support system, modelling and simulation of the system and developing a fault tolerant control system will be depicted. The overall goal is to provide a cost optimal way to produce water and energy under the regional and technical boundary conditions.

Keywords: reverse-osmosis desalination, hybrid energy, decision support, fault tolerant control, energy management.

1. INTRODUCTION

The use of reverse osmosis (RO) plants for water desalination is becoming more popular especially in remote arid areas, where grid electricity might be unavailable. In this case hybrid energy sources, such as wind and solar energy, are used to generate the necessary electricity for running the RO-plant and for the domestic use of the living community.

Reverse Osmosis (RO) desalination plants powered by renewable energies and electricity co-generation have been intensively studied in the past ten years (Seeling-Hochmuth 1998). They seem to be a very convenient solution for de-central small communities in remote arid regions. Nevertheless, the state of the art indicates that the current product development does not include optimal systems engineering and that plants are not thought to be tolerant in the presence of faults, malfunctioning or operator mistakes. This is however of crucial importance in remote areas where skilled personnel are normally absent in such areas. When the plant fails, severe difficulties can be caused to people, who depend on it.

To tackle this problem a consortium was built within the framework of the European co-funded project OPEN-GAIN (2007) with the main goal to develop a new model-based optimal system design approach to economically improve the overall performance, dependability, reliability and availability of co-generating water-electricity plants powered by renewable energy sources for remote arid areas using a high level of automation to meet specific cost requirement (Gambier, Wolf, Badreddin, 2008).

Based on this goal a desalination plant powered by renewable energy sources was built and installed in Borj-Cedria in Tunisia. A decision system was developed to support the designer by choosing and sizing the different components of the plant. A library for the design and simulation of reverse-osmosis desalination processes was also built. A fault tolerant control concept which allows running the reverse osmosis plant in case of faults based on hybrid control was introduced. An energy management system that coordinates the usage of the different energy sources according to weather forecast, battery charge levels and user's consumption profile of water and electricity was designed. As a brackish water source, a 30 meter deep water well was digged. In the following the plant and the individual steps towards the optimal cogeneration of water and electricity system will be handled.

2. PLANT DESCRIPTION

A reverse-osmosis desalination plant that produces 24 m^3/day was installed in Borj-Cedria (figure 1). The plant has been constructed and equipped with additional sensors to cope with the control algorithm and system monitoring. The RO-plant and the community are supplied by electricity from a bank of batteries, that are charged by the wind turbine and the photovoltaic modules, which present the renewable energy sources. The batteries are arranged in serial and parallel configuration to give 630Ah at 48V. The PV-modules are arranged in 3 parallel strings with 9 PV-modules in series for each string to give a total power of 15kWp (figure 2). The wind turbine is of 15kW and installed on a 25m tower. If the available charge level of the batteries is low and at the same time wind and solar irradiation are not sufficient to start the RO-plant, the diesel generator is switched on to supply the RO-plant and community with electricity and to load the batteries.

This is actually the role of the energy management system, which will be described later.

For the connection of the plant components an AC-bus architecture was chosen (figure 3), where the power delivered by all the energy conversion systems and the battery is fed to the standalone grid. The AC-bus architecture allows building up of larger power systems with multiple energy units distributed along the grid. This offers a theoretically unlimited expandability and reduction of distribution line costs and decentralized location of renewable energy generators.

Figure 1: Reverse-Osmosis Desalination Plant

Figure 2: Photovoltaic modules

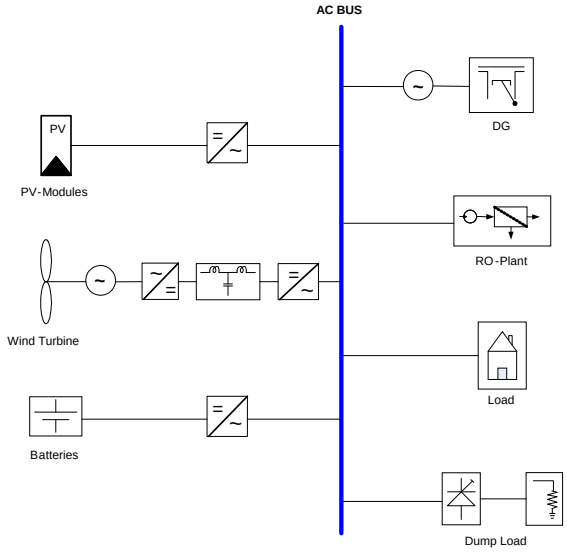

Figure 3: Structure of the AC-Bus System

3. DECISION SUPPORT SYSTEM

The Decision Support System (DSS) is a tool for the system implementation under site conditions taking into account energy efficiency, cost effectiveness, socio-economic impact and environment protection. A decision support tool is necessary to solve the problem of decision-making for engineering design.

The DSS integrates a database that hosts relevant meteorological, technical and market data for the design and evaluation of the hybrid energy system. The solar irradiation data, and wind speeds and directions were recorded, as well as the user's demand for water and electricity for more than one year, and integrated into the DSS database. The technical data and prices of several types of plant components from market leading manufacturers are also considered in the database. The database can be extended to included greater number of component types and manufacturers.

A multi-criteria optimization algorithm is implemented to adequately size the system components under the given site and market conditions. The DSS tool was developed by the group of Prof. Dionysis Assimacopoulos at the National Technical University of Athens in Greece (Kartalidis, Arampatzis, Assimacopoulos, 2008).

4. LIBRARY FOR MODELING RO-PLANT

The objective of modeling the RO-plant is to develop computer models that can be used for dynamic simulation of RO-plant to test different configurations, as well as control strategies (Palacin, Tadeo, Salazar, de Prada, 2009) and fault detection and accommodation algorithms. The models are provided as a library of components that can be interconnected in order to simulate different configurations of the plant, which can be used for sizing, component specifications and controller design. The group of Prof. Cesar de Prada at the University of Valladolid in Spain has developed the library OSMOSIS that runs under the professional simulation software package EcoSimPro (Palacin, Tadeo, de Prada, Syafiie, 2008). The tool enables modeling and simulation of pre- and post-treatment processes as well as the desalination membranes. The bacterial growth and scaling of the membranes can also be modeled and simulated. This allows also for planning cleaning strategies of the membranes.

5. FAULT TOLERANT CONTROL

In case faults of the RO-plant take place due to scaling, faulty pumps, leakage, etc., it is required that the RO-plant keeps on producing water even it has to work at reduced capacity. This due to the fact that a total failure of the plant can not be afforded, especially in remote arid areas, where the skilled personnel to repair the plant, are not available. The group of Prof. Essam Badreddin at the Automation Laboratory of the University of Heidelberg has developed the fault tolerant control (FTC) system. A model-based fault tolerant control strategy was utilized to design a control strategy on the supervisor level that allows the plant to

keep produce water when subject to faults. The idea to introduce the supervisor is because of the necessity to design a dependable system. The design of the supervisor was carried out applying hybrid control and discrete events supervision strategies. The supervisor includes a diagnosis unit, which is responsible for the detection and identification of faults, and a recovery unit that adjusts the control to the faulty system by carrying out a controller switching. For modeling of the hybrid system, a hybrid automaton was used (Gambier, Blümlein, Badreddin, 2009).

6. ENERGY MANAGEMENT SYSTEM

As different energy sources are used to run the RO-plant, an energy management system (EMS) is necessary for the optimal administration of the energy sources, which appear in hybrid form (wind, PV, diesel and batteries). The main duty of the manager is to decide in an optimal way, how the different energy sources have to be combined according to forecasting information of weather and demand of both energy and water, and the current conditions of subcomponents and loads, etc. In other words, the EMS should maximize the power utilization from renewable energy resources and the minimize fuel consumption of the diesel generator by reducing the number of switching on the diesel generator taking into account the system safely within its constraints. The group of Prof. Sami Karaki at the American University of Beirut in Lebanon has developed the architecture for the EMS and its real time implementation using genetic algorithm as an optimizer (Karaki, Bou Ghannam, Mrad, Chedid, 2010).

7. CONCLUSION

This project OPEN-GAIN offers a solution to cost optimal co-production of energy and water using renewable energy sources (PV, wind) besides diesel generators as a conventional energy source in remote arid areas. Cost optimization is achieved through a high level of automation, which is necessary to adapt the working conditions to the strongly varying renewable energy supply, and remote maintenance. The approach is based on thorough modeling of the processes and offers a large degree of flexibility in the design to meet different production requirements.

ACKNOWLEDGMENTS

This work was carried out by European and Mediterranean research institutes in cooperation with industrial partners. The work is co-funded by the Commission of the European Union within the sixth framework programme FP6, Project OPEN-GAIN, INCO-CT-2006-032535, www.open-gain.org.

REFERENCES

Gambier, A., Blümlein, N., Badreddin, E., 2009. Real-Time fault-tolerant control of a reverse osmosis desalination plant based on a hybrid system approach. *Proceeding of the 2009 American Control Conference*, pp. 1598-1603, June 10-12, Saint Louis, USA.

Gambier, A., Wolf, M., Badreddin, E., 2008. Open Gain: A European project for optimal water and energy production based on high level of automation. *Euromed 2008*, November 9-13, Jordan.

Kartalidis, A., Arampatzis, G., Assimacopoulos, D., 2008. Rapid Sizing of Renewable Energy Power Components in Hybrid Power Plant for Reverse Osmosis Desalination Process. *IEMSS 2008, International Congress on Environment Modeling and Software*, Barcelona, Spain.

Karaki, S., Bou Ghannam, A., Mrad, F., Chedid, R., 2010. Optimal Scheduling of Hybrid Energy Systems Using Load and Renewable Resources Forecast. *The 20th International Symposium on Power Electronics, Electrical Drives, Automation and Motion Speedam 2010*, accepted for presentation. 14-16 June, Pisa, Italy.

Mohammedi, K., Sadi, S., Cheradi, T., Belaidi, I., Bouziane, A., 2009. OPEN-GAIN Project: Simulation and Analysis of an Autonomous RO Desalination and Energy Production Systems Integrating Renewable Energies. *The 2nd Maghreb Conference on Water Treatment and Desalination (CMTDE 2009)*, 19-22 December, Hammamet, Tunisia.

OPEN-GAIN, 2007. Optimal Engineering Design for Dependable Water and Power Generation in Remote Areas Using Renewable Energy Sources and Intelligent Automation, INCO-CT-2006-032535, www.open-gain.org.

Palacin, L., Tadeo, F., de Prada, C., Syafiie, S., 2008. Library for Dynamic Simulation of Reverse Osmosis Plants. *EMSS2008 (20th European Modeling and Simulation Symposium*. 17-19 September, Campora San Giovanni, Amantea (CS), Italy.

Palacin, L., Tadeo, F., Salazar, J., de Prada, C., 2009. Control of Reverse Osmosis Plants using Renewable Energies. *International Conference on Control and Applications CA 2009*. 13-15 July, Cambridge, United Kingdom.

Palacin, L., Tadeo, F., de Prada, C., 2009. Operation of Desalination Plants Using Hybrid Control. *The 2nd Maghreb Conference on Water Treatment and Desalination, (CMTDE 2009)*. 19-22 December, Hammamet, Tunisia.

Seeling-Hochmuth, G., 1998. *Optimization of Hybrid Energy Systems Sizing and Operational Control*. Thesis (PhD). University of Kassel, Germany.

SIMULATION OF BOILERS FOR HEATING AND HOT WATER SERVICES

R. Tosato

Department of Mechanical Engineering
University of Padua. Italy

renzo.tosato@unipd.it

ABSTRACT

The combination of boilers of high efficiency is presented which contribute to energy saving in domestic heating plants and solve the problems of delivery of hot water in the favourable terms. They present the following features: conventional or condensing instantaneous boiler, flame modulating, and with electric ignition.

A natural gas-fired high efficiency conventional boiler is considered: maximum output 35kW; combined instantaneous boiler to produce heating and hot water; with a hermetically sealed gas combustion chamber, fan assisted, ready to be connected to flue-gas and external air ducts.

Experimental efficiencies and cyclic values, calculated by simulation at partial load, are compared with those of other three different high efficiency boilers, for heating and tap water services:

- ON-OFF, conventional boiler with tank;
- ON-OFF, conventional instantaneous boiler;
- flame modulating, conventional instantaneous boiler;

Keywords: combination boilers, plant efficiency, hot water supply

1. INTRODUCTION

Cyclical efficiency of a gas boiler can be defined by its experimental efficiency at full load, for a given return water temperature and by its experimental stand-by losses, considering its actual regulation system (Tosato R. 2008).

A relationship of the cyclic efficiency of the boiler to the regulation system can be calculated using two experimental curves: the efficiency at full load and the stand-by losses. This relationship can be used for condensing boilers, other kinds of boilers, and also for the usual regulation systems provided the appropriate values of the constants have been experimentally defined. The evaluation of the seasonal efficiency of boiler requires the knowledge of the estimated efficiency at the defined loads (Tosato R. 2009, Defu C., Yanhua L., Chunyang G., 2004).

Sinusoidal loads from zero to maximum load depending on season variations seems to be suitable in the apartment with heating plants. The relationship between energy consumption end energy demand in cyclical operation can be used with a sufficient degree of precision to calculate the seasonal consumption as a function of the sinusoidal load.

The efficiency of a condensing boiler is very high and it can exceed by 25% the efficiency of traditional boilers.

The energy problem of boilers lies in the unfavourable decrease in cyclic efficiency when boilers deliver hot water.

One way to maximize efficiency is to integrate space and water heating in a single appliance.

While improvements in the building envelope reduce the space of heating load it is somehow difficult to justify the expenses of a condensing boiler solely to provide the heating load. To take the advantage of the efficiency potential of condensing gas-fired systems, it makes sense to combine space heating with other functions, in particular, domestic water heating. Domestic hot water loads have remained fairly constant during season variations making it logical to put more effort into improving the efficiency of the hot water generator.

An integrated, high-efficiency space and water condensing gas-fired heating system, using water from municipal mains as the driving mechanism to condense the flue gas, maximizes efficient operation and it can achieve efficiencies of over 90 percent for both, space and water heating. This combination also eliminates the need for multiple exhaust systems.

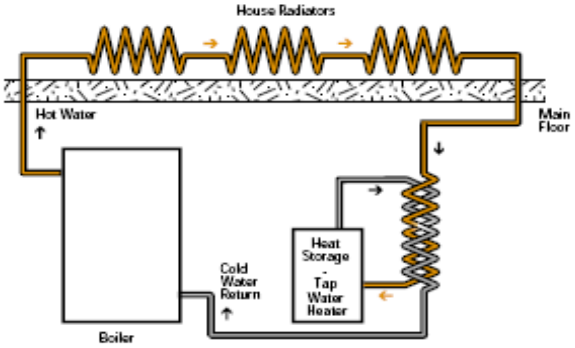

Figure 1: Scheme of high-efficiency combined space and water heating system (Heating With Gas *ISBN 0-662-34205-4, Cat N. M91-3/3-2003E*)

The gas-fired boilers can have problems in condensing when the return water temperature is above the dew point of the fluid gases. By installing a water-to-water heat exchanger and storage tank for tap hot water upstream of the boiler, the return water temperature can be brought below the dew point, fluid gases will condense and the efficiencies will be improved. Such a high-efficiency combined system is shown in Figure 1.

Standard-efficiency gas-fired combined systems also exist, but their efficiency is lower than those of condensing units. A standard-efficiency boiler coupled with an external storage tank is another efficient solution.

Combi boilers are highly popular in Europe, where in some countries market share is 70%.

There are certain advantages to tankless water heaters :

- a tankless water heater may result in both energy and cost savings in the long term. As water is heated only when it is needed, there is no storage of hot water kept warm all day even if it never get used and heat loss through the tank walls will result in a continual energy drain.

- As water is heated while passing through the tankless water heater - an unlimited supply of hot water is available constantly.

- less physical space has to be dedicated to heating water.

Tankless heaters also have some disadvantages:

- there is a longer wait to obtain hot water, since heater starts only upon demand, which is one of its chief advantages, so all idle water in the piping starts at room temperature.

- for intermittent use applications (for example when a hot water faucet is turned on and off repeatedly at a sink) this can result in periods of hot water, followed by some small amount of cold water.

The word combi is a short term for combination. Combi boilers are the most energy efficient boilers in the actual market since they are above 90% energy efficient. As term suggests, combi boiler is both high-efficient water heater and a central heating boiler combined within a single unit presented in Figure 2. These type of boilers don't require any hot water cylinder, hence saving a lot of space in the storage area of a house. Combination boilers produce hot water immediately whenever it is required. It has a built-in water heater which boils the water instantly and produces hot water. They have internal heat exchanger which enables the boiler to heat and cool the water rapidly.

A combi-instantaneous boiler is the most widely used combi boiler type and directly heats incoming mains cold water to supply the taps of the house, showers and other hot water demanding appliances.

A combi-instantaneous-condensing boiler operates as an 'instantaneous' boiler but at somewhat higher efficiencies than the standard combi boiler.

A combi-storage boiler is a variant of the instantaneous combi boiler type and is designed to give better performance through the internal storage of heated water. The stored water also can give better initial water supply from cold water mains at the first tap turning. Once the stored heat has been used, this boiler will tend to operate as an 'instantaneous' type. In the various manufactures and models, the improvement in heated water delivery will depend upon the size of water store, and this can vary widely.

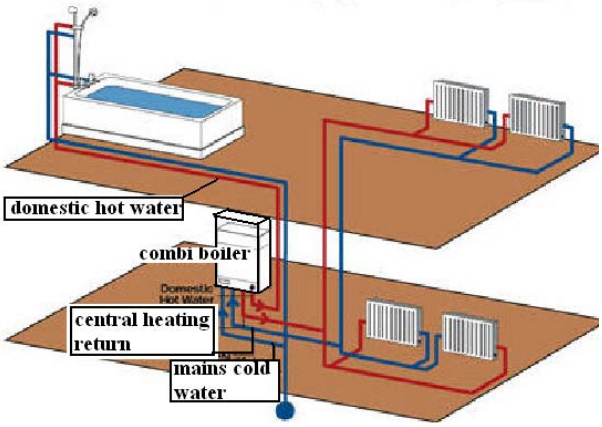

Figure 2 - Combination boiler

High costs often prevent the market diffusion of novel and efficient boilers. Monitoring cost and price decline for these technologies is thus important in order to establish effective energy policy. Experience curves and cost-benefit analyses for condensing gas **boilers** produced and sold in the Netherlands between 1981 and 2006 are important (Weiss M., Dittmar L., 2009). For the most dominant boiler type on the Dutch market, i.e., condensing gas combi boilers, the authors identify learning rates of 14±1% for the average price and 16±8% for the additional price relative to non-condensing devices. The net present value of condensing gas combi boilers shows an overall increasing trend. Purchasing in 2006 a gas boiler of this type instead of a non-condensing device generates a net present value of 970 EUR (Euro) and realizes CO_2 (carbon dioxide) emission savings at negative costs of −120 EUR per tonne CO_2. Tfey attribute two-thirds of the improvements in the cost-benefit performance of condensing gas combi boilers to technological learning and one-third to a combination of external effects and governmental policies.

2. DESCRIPTION OF THE BOILER

The main features of the boiler prototype are summarized in the abstract. Other particular functional and energy characteristics, tested with a laboratory test rig, are:

a) it is relatively cheap because it doesn't require the expensive exchanger of condensing boilers. The flue-gas temperatures are higher than 80°C and so they are very far from the dew point, throughout the entire range of operation conditions;

b) it is provided by a modulating combustion device, able to cover a wide range of loads. It attains an output of 35 kW to produce tap water and a very low level of output (lower than 6 kW) for heating and hot water services;

c) it is also provided with an ON-OFF combustion device, to control the output at partial loads (less than 6 kW during the heating operation);

Figure 3: The prototype of high efficiency domestic combined boiler.

d) the boiler is fan assisted, with an automatic variation in the 2-speed revolution, to provide the control of dew point of flue gases and the air excess, when the output decreases below 15 kW:

e) it has been designed to be connected to the plant without any mixing valve in the most efficient way (direct-connection), and is provided with an electronic power regulation depending on the external air temperature.

Tests have been performed at full and partial loads, by directly connecting the boiler to an experimental rig, and they show the actual possibilities of comfort and energy saving of this system:

a) constant tap water temperature (between 30 and 60°C) and a flow of up to 1200 kg/h to ensure a high degree of comfort for the whole family;

b) high efficiencies (H.E. 0.73-0.81 on High Heat Value) at an output higher than 6 kW, on heating or tap water production in cyclic operation modes. The same acceptable mean seasonal efficiency may be reached in comparison with other H.E. boilers providing only heating services.

3. SIMULATION OF TAP WATER AND HEATING SYSTEM

By means of a control system, two pumps transfer hot water from the boiler to the central heating system or to the tap water heater. A three-way valve permits the use of only one pump.

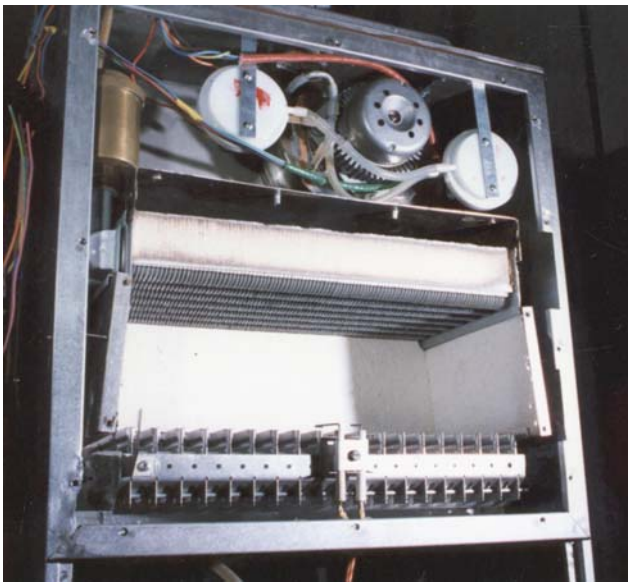

Figure 4: Dry combustion chamber: atmospheric burner, igniter, flame sensor and compact heat exchanger mounted at the ceiling.

Generally, the outputs required for heating systems in small apartments (0-15 kW) are always lower than the output for hot water (10-35 kW).

Usually this problem is solved by an ON-OFF boiler with low nominal output and a storage tank for hot water. But this device decreases the thermal seasonal efficiency of the system in comparison with the seasonal efficiency of the boiler, even if the boiler is a condensing one**.** Only the instantaneous production of hot water can ensure a high level of seasonal efficiency.

A domestic heating system, which has the same kind of boiler as the prototype, can be reduced as in Fig. 3**.** Even though there is one fluid-gas water heat exchanger and one natural gas burner inside the boiler, the energy flow has been separated in order to better specify the heat input QSR for heating service and QST for tap water with QUR and QUT corresponding to the outputs. In every combined boiler and in the prototype as well, there is an automatic device which stops any heat being transferred to the heating plant at the moment when hot water is required.

During the summer and winter seasons these operational loads vary greatly and energy flow is transferred with different efficiencies to the tap water and central heating device. Especially, the energy amounts are not constant throughout the days and months.

Slow variations in heating loads permit the transient effects on thermal balance in every heating system to be neglected. In the case of tap water device each ignition causes an additional loss of PA energy .

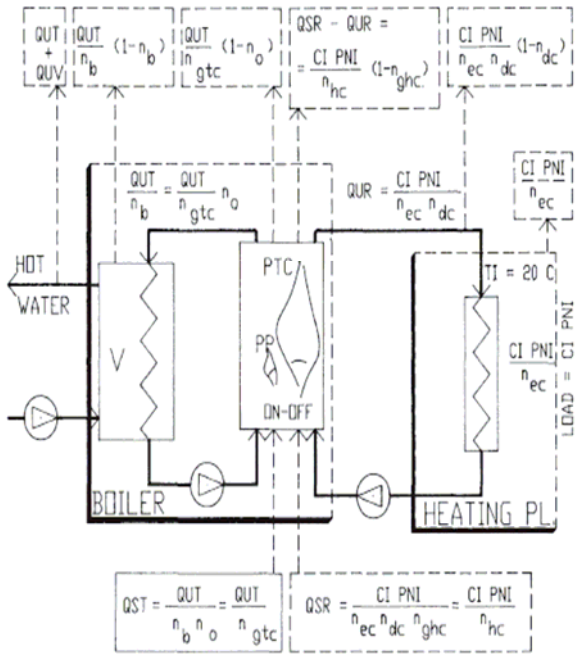

Figure 5: Thermal balance of the plant for the time step

The well known cyclic efficiencies, usually considered to forecast mean efficiency, have to be thought as being constant over each time interval of the entire season ***:***

ηghc = cyclic efficiency of heating device at partial load;

ηtc = cyclic efficiency of tap water at partial load.

3.1. Energy Balance of Tap Water Service

The heating system in a closed circuit is composed of three elements:

a) the heat generator, characterized by a nominal thermal input PTCMAX and the output PP of the possible pilot burner. The nominal efficiency η* is defined by means of PNC=η**PTCMAX. PTC is the nominal input PTCMAX if the regulation system is ON-OFF, otherwise PTC is the thermal input as fixed by the flame modulation device. Cyclic efficiencies, at partial loads C=QUR/PNC, are ηghc=QUR/QSR;

b) the hot water circuit, without any loss (ηdc=l).

c) the utilization, composed of heating bodies and an internal distribution circuit, is taken as ideal (ηec=l).

By applying the conservation law of mean energy transferred in a time interval **t**, to maintain the rooms at a comfortable temperature **TI**, the following formula may be used:

$$CI \cdot PNI \cdot t = \eta ghc \cdot QSR \cdot t = \eta hc \cdot QSR \cdot t \qquad (1)$$

A curve of cyclic efficiency of the boiler only can be expressed very simply, as function of the load C, by:

$$\eta ghc = \eta o / \left[1 + (1/I1 - 1) \cdot PR1/PTC\right] \qquad (2)$$

The boiler load is:

$$C = I1 \cdot \eta o \cdot PTC / (\eta^* \cdot PTCMAX \qquad (3)$$

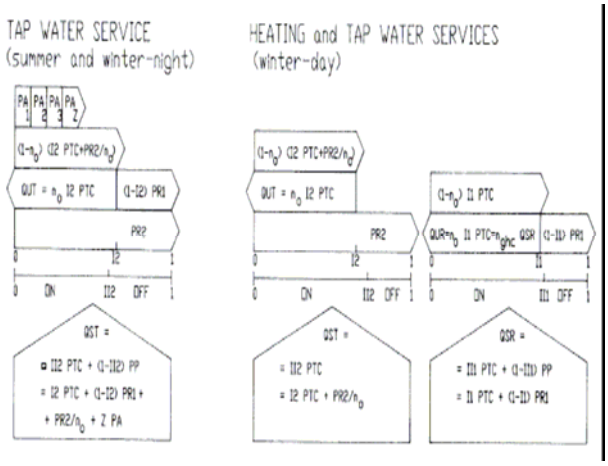

Figure 6: Simulation of boilers at partial loads.

This mathematical equation results from an operational model of boilers at partial loads based on the following assumptions (Fig. 6):

- if the boiler is ON-OFF**,** PTC=PTCMAX and ηoMAX is the efficiency of the boiler at full load, PR1 is the power lost at null load to maintain the boiler at a mean temperature (PRl* to maintain the water at 70°C inside the heat exchanger). During the time I1 the efficiency is the same ηo = ηoMAX as during the full load operation. In the model, the energy consumption QSR in the time unit is composed of [Il*PTC + (1-Il)*PRl] which is the same as that used in the actual boiler, composed of (III*PTCMAX), burnt during the ON time II1, and (l-III)*PP, burnt during the OFF time. The energy losses during the OFF period are (l-Il)*PRl and the load is C=I1*ηo/η*

- if the boiler is flame modulating, IIl=Il=l and the input QSR=PTC, stand-by losses are nil and the boiler load is C=(ηo*PTC)/(η**PTCMAX).

The cyclic efficiency is ηghc=ηo. The following equation accounts for the PREA losses due to flame modulation:

ηo = ηoMAX/(l+(l-PTC/PTCMAX)*PREA/PTC) (4)

PREA losses can be attributed to the increases in excess air at partial loads.

3.2. Energy Balance of Tap Water Service

The energy balance of the rig used for the tap water production can be written imagining the rig inside the boiler, even if this is true only for instantaneous boilers. This open circuit is composed of:

a) the heat generator, characterized by the same nominal parameters already considered.

b) a water to water compact heat exchanger, characterized by a low boiler water content and by little inertia;

c) the volume V of a possible tank is characterized by a continuous power loss PR2. The efficiency of the tank and exchanger is ηb.

Everybody knows that the tank is used only to ensure comfort, disregarding cost and size of boiler and its extra energy consumption. The loss PR2 increases

the seasonal fuel consumption because stand-by periods are over 10 times longer than tap using periods. Comfort is ensured by the very high available flow (QUT+QW) of hot water, 2-10 times greater than those corresponding to the boiler output.

When the volume V is nil, the boiler is regarded "instantaneous" and the efficiency ηb=l. The available flow is limited to the nominal output of the boiler (QUT=PNC).

In comparison to the previous energy balance, some different aspects now have to be considered:

a) for instantaneous boilers, the tap water causes great load increments and corresponding transient losses have to be accounted for in energy terms PA, spent at every time the tap is turned on. In the time unit, z*PA is the amount of this energy loss. The value **z** changes with loads and depends on how tap water is drawn;

b) during the cyclic operation, the boiler is affected by PR2 losses, when a tank is installed.

Stand-by losses PR1 are again present, so the cyclic efficiency ηtc is generally lower than **ηghc** .

c) during winter days, when heating service is also supplied, it is not realistic to consider PR1 and PA in the energy balance of tap water.

Mean seasonal load of boiler on heating service assumes that stand-by losses PR1 and transient losses PA are negligible. Therefore the cyclic efficiency **ηgtc** of the boiler only is not too different from **ηo.**

Referring to Fig. 6 **,** during the summer season and the winter nights, to produce a useful power QUT the input has to be:

$$QST = II2 \cdot PTC + (1 - II2) \cdot PP = \\ = II2 \cdot PTC + (1 - I2) \cdot PR1 + PR2 / \eta o + z \cdot PA \quad (5)$$

and the cyclic efficiency is:

$$\eta tc = QUT / QST = \eta o \cdot [1 + (1 / I2 - 1) \cdot PR1 / PTC + \\ + 1 / I2 \cdot (PR2 / \eta o / PTC + z \cdot PA / PTC)] \quad (6)$$

where all three kind of losses are considered.

On winter days PR1 and PA are supposed to be negligible in the tap water energy balance and the cyclic efficiency is reduced to the following equation:

$$\eta tc = \eta o \cdot [1 + (PR2 / (\eta o \cdot I2 \cdot PTC)] = \\ = \eta o / [1 + \eta * / [CA \cdot (1 - PR2 \cdot \eta * / (PNC \cdot \eta o)] \cdot PR2 / PNC] \quad (7)$$

where the load CA when tap water is being used

$$CA = QUT / (\eta o \cdot PTCMAX - PR2) \quad (8)$$

The comparison between Eqns. (5) and (7) shows very clearly that PR1 and PA losses affect efficiency only when, on summer and winter nights, tap water only is being used, especially if boilers are poorly insulated and heavily constructed. Seasonal efficiency is always very low when a tank is installed because the extra losses PR2 are continuously present and its mean load is very low.

4. RESULTS OF SIMULATION

To compare performances of the prototype, especially its cyclic efficiency measured on laboratory test rig, three other high efficiency boilers (tab. I) have been chosen and all of them have been simulated by the model already described. The boilers were:

(1) high efficiency, ON-OFF, conventional boiler with tank: permanent pilot;

(2) high efficiency, ON-OFF, conventional instantaneous boiler: permanent pilot;

(3) high efficiency, flame modulating, conventional instantaneous boiler: permanent pilot;

(4) prototype: high efficiency, flame modulating, conventional instantaneous boiler: electric ignition.

The losses PR1 become proportional to the boiler load following the simple equation:

PR1 = (PP + PRl*).C (9)

and PR2 is proportional to the mean temperature of the tank (PR2* at 50°C).

tab. I. Experimental parameters to forcast ∩ghc and ∩tc of the four combined boilers.

boiler	1	2	3	4	
∩*	0.81	0.81	0.81	0.81	
PNC	14.0	23.0	23.0	35.0	kW
PTCMAX	17.3	28.4	28.4	43.2	kW
PR1*	0.7	1.15	1.15	1.75	kW
PP	0.25	0.25	0.25	0.	kW
I1	0÷1	0÷1	1	1	
PR2*	0.7	0.	0.	0.	kW
PA	0.	0.7	0.7	0.7	kW
I2	0÷1	0÷1	1	1	

The curves in Fig.7 represent the simulation results of the prototype and of three combined boilers as functions of outputs of heating and tap water.

Values obtained by tests on the prototype are also indicated. The main energy results can be analysed as follows:

a) the efficiency ηghc of the prototype is high when the heating service operates at a nominal output of 35 kW and at outputs usually required by a domestic heating plant, at partial load during the winter season. The seasonal efficiency is almost the same as high efficiency boilers having the 14 kW nominal output usually adopted:

b) for tap water, the cyclic efficiency ηgtc is at the same levels of ηghc values without any unacceptable decrease at partial outputs.

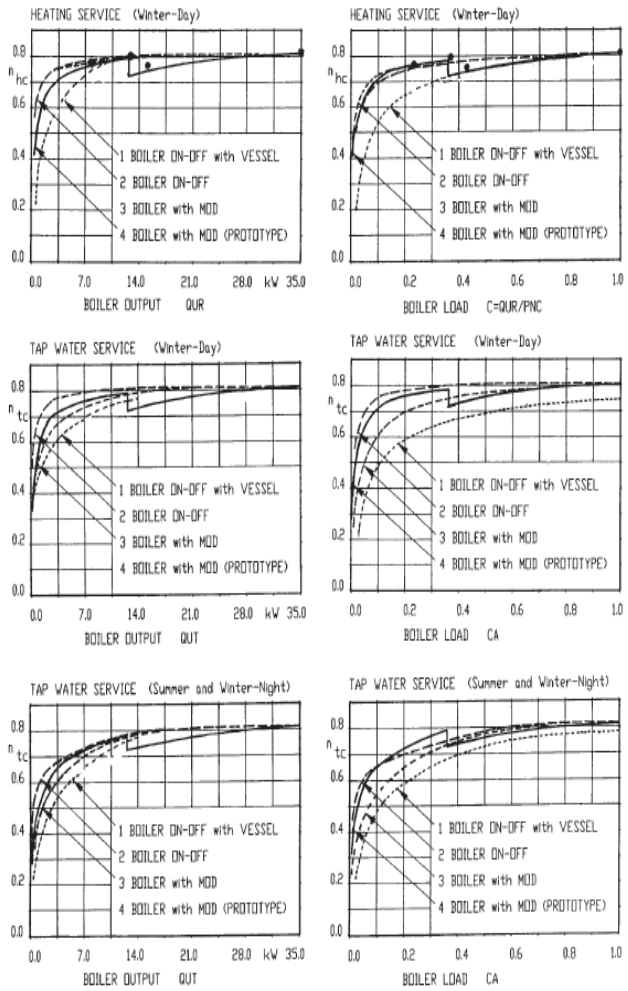

Figure 7: Cyclic efficiency of four combined boilers calculated from the operating model on heating service during the winter season and on tap water service, as functions of the output and the load.

5. CONCLUSION

A model of energy losses of gas-fired domestic boilers at partial loads providing heating and tap water enables to calculate using experimental parameters of boilers, of their cyclic efficiencies including the effects of tank losses.

These results are in agreement with experimental values obtained by testing a prototype combined boiler, characterized by a high nominal output (35 kW) and, capable of maintaining high efficiency when it operates at loads required by heating installation (below 14 kW). This system gives high efficiency values on both services because:

- permanent pilot and vessel volume are not used,
- inertia losses and stand-by losses are very low in comparison with the nominal output of the boiler,
- an automatic device with the varying revolution speed of the combustion air fan is used to reduce excess air losses and to control the dew point of flue-gases at low loads.

ACKNOWLEDGMENTS

This work has been supported by Italian Ministero Istruzione Università Ricerca MIUR funds. Their contribution is gratefully acknowledged.

5.1. REFERENCES

Defu C., Yanhua L., Chunyang G., 2004. Evaluation of retrofitting a conventional natural gas fired boiler into a condensing boiler *Energy Conversion and Management, Volume 45, Issue 20, December 2004, Pages 3251-3266*

Weiss M., Dittmar L., 2009. Market diffusion, technological learning, and cost-benefit dynamics of condensing gas boilers in the Netherlands, *Energy Policy, Volume 37, Issue 8, August 2009, Pages 2962-2976*

Heating With Gas (Home Heating and Cooling Series), *ISBN 0-662-34205-4, Cat N. M91-3/3-2003E*

Tosato R., 2008. Mathematical models of gas fired boilers, *20th EMSS, 2008 European Modeling and Simulation Symposium (Simulation in Industry) September, 17-19, 2008, Campora San Giovanni, Amantea (CS) Italy*

Tosato R., 2009. Tests and simulation of gas boilers in domestic heating plants. *21th EMSS International Mediterranean Modelling Multiconference, 23-25 September 2009 Tenerife (SP)*

AUTHOR BIOGRAPHY

MSc in Mechanical Engineering, 1968; 1968-1980 Assistant Professor at the Dept. of Mechanical Engineering, and lecturer in the undergraduate course "Fluid Machines" at the University of Padova Teacher in undergraduate course of "Fluid Machines" at the University of Trento. Present position: since 1980, Associate Professor of "Fluid Machines" at the Dept. of Mechanical Engineering, University of Padova. Research activity:
experimental analysis and simulation of efficiency of gas boilers;
experimental and numerical analysis of alternative compressors;
experimental and numerical analysis of unsteady gas flow.

A COMPUTERIZED METHODOLOGY AND AN ADVANCED APPROACH FOR THE EFFECTIVE DESIGN AND PRODUCTIVITY ENHANCEMENT OF AN INDUSTRIAL WORKSTATION

[(a)]Antonio Cimino, [(b)]Francesco Longo, [(c)]Giovanni Mirabelli, [(d)]Rafael Diaz

[(a)(b)(c)]MSC-LES, University of Calabria, Mechanical Department, Ponte P. Bucci, 87036, Rende (CS), Italy
[(d)]VMASC, Virginia Modeling, Analysis, & Simulation Center, Old Dominium University, VA, USA

[(a)]acimino@unical.it, [(b)]f.longo@unical.it, [(c)]g.mirabelli@unical.it, [(d)]RDiaz@odu.edu

ABSTRACT

It is the intent of the research work to propose a methodology for achieving the ergonomic effective design of a real industrial workstation and an advanced approach for enhancing its productivity. In particular the design methodology is based on multiple design parameters, Design of Experiments (DOE) and multiple performance measures. The Design of Experiments supports the comparison of the actual configuration of the workstation with alternative operative scenarios (different workstation configurations). The advanced approach for workstation productivity enhancement aims at comparing different work methods in order to reduce the workstation process time. The evaluation of the process time as well as of the best work method is achieved by contemporaneously using the Methods and Tine Measurement and the Maynard Operation Sequence Techniques. Simulation, 3D Visualization and human modelling are used as support tool for recreating workstation operations, executing experiments (ergonomics effective design) and apply work measurement methodologies (selection of the best work method).

Keywords: Industrial plants, Industrial Workstation, Modeling & Simulation, Ergonomic analysis, Work measurement

1. INTRODUCTION

An overview of the state of the art, starting from the second half of the 1990s, reveals that industrial plants continuously provide challenging problems in terms of both workstations ergonomic design and workstations productivity enhancement. The ergonomic effective design of an industrial workstation attempts to achieve an appropriate balance between the worker's capabilities and worker's requirements as well as provide the worker with physical and mental well-being, job satisfaction and safety (Das and Sengupta, 1996). The industrial workstations productivity enhancement attemps to achieve a reduction of workstations process time obtaining higher productivity levels (Cimino et al., 2008a). According to Zandin (2001) the study of workstations process times is indicated as work measurement and aims at evaluating and improving the times standard for performing workstations operations.

Let us consider the workstations ergonomic effective design within industrial plants. Most of the works developed in the late '90s consider single ergonomic performance measures (based upon a specific ergonomic standard) for the ergonomic redesign of workstations belonging to industrial plants. Among ergonomic standards, the following are the most widely used: (i) the NISOH 81 and the NIOSH 91 equations for lifting tasks (NIOSH stands for *National Institute for Occupational Safety and Health*); (ii) the OWAS for working postures analysis (OWAS stands for *Ovako Working Analysis System*); (iii) the Burandt Schultetus analysis for lifting tasks involving a large number of body muscles; (iv) the Garg analysis for assessing the energy expenditure for performing an operation. Further information about the cited ergonomic standards can be found in the Niosh Technical Report 81-122 (1981), the Scientific Support Documentation for the Revised 1991 NIOSH Lifting Equation (1991), Waters et al. (1994), Kharu et al. (1981), Schultetus (1980) and Garg (1976). Examples of research works that propose the ergonomic redesign of industrial workstations based on single ergonomic performance measure are reported in Temple and Adams (2000), Waters et al. (2007).

The integration of two or more ergonomic standards was the successive step carried out by the researchers working in this specific area for achieving multiple and simultaneous ergonomic improvements. Examples of ergonomic standards integration can be found in Russell et al. (2007) and Cimino and Mirabelli (2009).

Consider now the workstations productivity enhancement within industrial environments. Among different solutions for improving workstations productivity, the work measurement plays a critical role supporting the definition and design of alternative and more efficient work methods. In this regards, work measurement as part of Methods Engineering is a systematic technique for the design and the improvement of work methods as well as for their adoption within industrial workstations (Zandin, 2001). Motion and time study are the heart of work measurement (Ben-Gal and Bukchin, 2002). As reported in Lawrence (2000) the motion study determines the best work method to perform an

operation and the time study measures the time required to complete the operation by using the best method. The following time study tools (also known as work measurement tools) have to be regarded as the most important: MTM (Methods and Time Measurement) and MOST (Maynard Operation Sequence Techniques). Further information about the cited work measurement tools can be found in Maynard et al. (1948), Karger and Bayha (1987) and Zandin (2001).

Another important issue to take into consideration in the industrial workstations ergonomic design and productivity enhancement is the relation between the ergonomics and work measurement. Laring et al. (2002) and Udosen (2006) take into consideration in their research works both ergonomics and work measurement aspects. Finally the last important issue is whether the workstation ergonomic effective design and/or the productivity enhancement are carried out directly in the real industrial workstation or by using simulation models. Researchers and practitioners very often use simulation as problem solving methodology for creating an artificial history of the system, analyzing its behaviour, choosing correctly, understanding why, diagnosing problems and exploring possibilities (Banks, 1998). Moreover, simulation can be jointly used with virtual three-dimensional environments in which observe the system evolution over the time and detect ergonomic and work measurement problems that otherwise could be difficult to detect (an overview on attributes and capabilities of virtual environments can be found in Wilson, 1997). Feyen et al. (2000) propose a PC-based software program for studying ergonomic issues during the industrial workstation design process. Longo and Mirabelli (2009) use Modeling&Simulation in combination with ergonomic standards and work measurement (multi- measures based approach) for the effective design of an assembly line still not in existence (note that in this last case the authors take simultaneously into consideration ergonomic aspects and work measurement).

The main contribution of this paper to the state of the art is to propose a methodology for achieving the ergonomic effective design of a real industrial workstation and an advanced approach for enhancing its productivity. In particular the design methodology is based on multiple design parameters, Design of Experiments (DOE) and multiple performance measures. The advanced approach for workstation productivity enhancement aims at comparing different work methods in order to reduce the workstation processes time. The design methodology and the advanced approach are proposed to the reader contextually to their application to the most critical workstation (the Seal Press workstation) belonging to an industrial plant that manufactures high pressure hydraulic hoses. As support tool for applying both the design methodology and the advanced approch the authors use a 3D simulation model of the industrial workstation for investigating different ergonomic configurations of the workstation as well as comparing alternative work methods. Each workstation ergonomic configuration comes out from a design of experiments based on multiple design parameters and the choice of the final configuration (the ergonomic effective design of the workstation) is made according to multiple ergonomic performance measures. As concerns the work methods comparison, the choice of the best work method is made according to a single time performance measure (the process time evaluated by using the simulation model).

Before getting into details of the study let us give a brief overview of each section of the paper. Section 2 provides a brief description of the industrial plant as well as the Seal Press Workstation. Section 3 proposes the methodology for the industrial workstation ergonomic effective design. Section 4 presents the simulation model of the Seal Press Workstation. Section 5 presents the simulation results analysis and the Seal Press effective design. Section 6 presents the advanced approach for productivity enhancement within the Seal Press workstation. The last section reports the conclusions (that summarize the scientific contribution of the work) and the research activities still on going.

2. THE INDUSTRIAL PLANT AND THE SEAL PRESS WORKSTATION

The industrial plant, AlfaTechnology s. r. l., manufactures high pressure hydraulic hoses and is located in the South of Italy (Calabria). The authors already carried out research activities (in cooperation with AlfaTechnology s. r. l.) on workstation ergonomic effective design (Cimino et al., 2009) and production planning and control (Cimino et al., 2008b). However in order to provide the reader with enough information for understanding the research work proposed in this paper, a brief description of the operations performed in each workstation in reported below.

1) *Preparation workstation*: the operator takes the main components from the raw materials warehouse shelves and defines the length of the rubber hose.
2) *Seal Press workstation*: the operator prints on ring-nuts and fittings the quality and traceability identifying numbers by using the seal press machine and places the components inside apposite boxes.
3) *Cutting workstation*: the operators take rubber hose rolls from the raw materials warehouse shelves and cut the rolls according to the Shop Orders (S. Os) requirements (by using an automated or manual cutting machine).
4) *Skinning workstation*: the operators eliminate a part of rubber at the ends of each hose in order to guarantee a good junction with the fittings.

5) *Assembly workstation*: the operators manually assemble the rubber hoses with fittings and ring-nuts.
6) *Stapling workstation*: the operators tighten the ring-nuts on the hoses by using the stapling machine.
7) *Pressure Test workstation*: the operators test the hydraulic hoses by using a pressure machine (setting a pressure value higher than the nominal value).
8) *Check and packaging workstation*: the operators compare the S.Os requirements and the hoses characteristics (quality controls), they also put the hydraulic hoses in the shipping cases.

Figure 1 shows the final products (the high-pressure hydraulic hoses). Each hydraulic hose is made up of a rubber hose, two fittings and two ring nuts.

Figure 1: The final products of the manufacturing plant

A preliminary analysis carried out by production managers shows that the productivity of the Seal Press workstation (evaluated on monthly basis) always falls below target levels causing delays in S.Os completion. The operator of the Seal Press workstation performs the following operations: (1) seal press machine set up and preparation; (2) components positioning (ring nuts or fittings) within the machine; (3) printing operations (quality and traceability identifying numbers on the component); (4) components removal from the machine (components are then placed in a box); (5) update of the operation status on the company informative system (end of the operation); (6) transportation of the components to the successive workstation by using a manually operated dolly. Moreover, note that the worker can perform the above mentioned operations by using 4 different work methods each one characterized by a different number of ring nut/fitting to be simultaneously positioned into the seal press machine (operation 2). By using the first work method the operator inserts one ring nut/fitting into the seal press machine, by using the second work method, the operator inserts two ring nuts/fittings into the seal press machine, by using the third and the fourth work methods, three and four ring nuts/fittings, respectively.

3. THE DESIGN METHODOLOGY FOR WORKSTATION ERGONOMIC EFFECTIVE DESIGN

The first goal of the paper is to propose a methodology for the ergonomic effective design of the most critical workstation of a manufacturing plant (the Seal Press workstation) by simultaneously considering multiple design parameters and multiple performance measures based on ergonomic standards. To this end, the methodology being advanced in this paper uses a well-planned Design of Experiments (DOE) for supporting the comparison of the actual configuration of the Seal Press workstation with alternative operative scenarios (different workstation configurations). The generation of alternative configurations comes out from the variation of multiple design parameters that affect multiple performance measures (ergonomic performance measures). The quantitative evaluation of the effects of the multiple design parameters on the multiple performance measures is achieved by using the Design of Experiments (DOE). Such evaluation allows to choose the final configuration of the workstation. The design methodology consists of the following steps: design parameters definition (section 3.1), performance measures definition (section 3.2), workstation simulation model development (section 4), workstation effective design (section 5). Finally after the ergonomic effective design, the workstation will be tested under the 4 different work methods with the aim of enhancing productivity and select the optimal work method.

3.1. Definition of the design parameters

A preliminary analysis has detected the design parameters (factors) that could have an impact on the workstation performance (in terms ergonomic risks and work methods). The analysis reveals that some distances and angles (associated to objects and tools position) could be significant factors for the Seal Press workstation. The investigation and comparison of all possible workstation configurations require a correct design of experiments. We take into consideration the following factors:

- *Support table angle*: let us indicate this angle with α, it defines the orientation of the support table respect to the actual position (see figure 2);
- *Raw materials bin height*: let us indicate this height with *rmh*, it defines the height of the bin containing the raw materials (see figure 2);
- *Ring nuts bin height*: let us indicate this height with *rnh*, it defines the height of the bin containing ring nuts exiting from the seal press machine (see figure 2).

Table 1 reports factors and levels.

Table 1: Design parameters and levels

Seal Press Workstation				
Factors	**Factor ID**	**Level 1**	**Level 2**	
Support Table Angle	α	0	π/2	rad
Raw Materials bin height	rmh	17	86	cm
Rings nuts bin height	rnh	30	65	cm

The factors levels combination generates 8 different configurations, so the design of experiments will investigate 8 different workstation configurations.

3.2. Definition of the performance measures

As reported into the introduction, the effective ergonomic design of a workstation should consider a multi-measures based approach. Let introduce now the performance measures used for evaluating each workstation configuration. We propose a multi-measures approach based on ergonomic indexes. The ergonomic performance measures, based on ergonomic standards, are the lift index (evaluated by using the Burandt Schultetus analysis), the stress level associated to each working posture (evaluated by using the OWAS analysis) and the energy expenditure associated to each activity (evaluated by using the Garg analysis). Further information concerning these ergonomic standards can be found in Schultetus (1980), Kharu et al. (1977), Kharu et al. (1981), Garg (1976).

4. THE SIMULATION MODEL OF THE SEAL PRESS WORKSTATION

The design of experiments requires to test 8 different workstation configurations, involves different design parameters and ergonomic performance measures. Similarly the approach proposed for workstation productivity enhancement requires to test four different work methods. Any investigation or analysis directly carried out within the real systems disturbs the normal workstation operations, causing as consequence efficiency losses and additional costs. Therefore the authors decide to support experiments execution and work methods analysis by using a simulation model of the Seal Press workstation. The simulation model recreates, within a 3 D virtual environment, all the workstation operations including human model (worker), kinematics and activities.

The Modelling & Simulation tools, used for developing the Seal Press workstation simulation model, are the CAD software Pro-Engineer by PTC (further information can be found at http://www.ptc.com/products/proengineer/) and the simulation software eM-Workplace by Tecnomatix Technologies (further information can be found at http://www.plm.automation.siemens.com/en_us/products/tecnomatix/assembly_planning/process_simulate_human/index.shtml). Before getting into the details, let us summarize the most important steps of the simulation model development. The first phase is the creation of the three-dimensional geometric models representing the workstation and tools being used during the production process (*workstation virtual layout development*). The completion of this phase requires to import the geometric models into the virtual environment provided by the simulation software. The second phase is the *insertion and training of the human model* (the human model has to be inserted into the virtual environment and trained to perform workstation operations). The last phase is the *simulation model validation* in order to check the simulation model accuracy in recreating the real workstation.

4.1 Workstation virtual layout development

The implementation of the geometric models of the Seal Press workstation follows three different approaches: (i) geometric models implementation by using the CAD software Pro-Engineer; (ii) geometric models implementation by using the eM-Workplace internal CAD software; (iii) geometric models imported from eM-Workplace libraries.

The geometric models implementation requires an accurate data collection on objects types, dimensions and weights. The data collection includes the following elements of the Seal Press workstation: machine, equipment and tools, worktables, manual operated dollies, raw materials, containers and bins. Table 2 reports the objects description, dimensions and weights.

Table 2: Data collection for geometric models implementation

Object Description	Object Type	Weight (Kg)	Dimensions (cm) L x W x H
Ring nut	Component	0.168	Depending on S.O.
Fitting	Component	0.336	Depending on S.O.
Marking die	Component	1.800	Depending on S.O.
Workstation stamp	Component	0.100	Depending on S.O.
Scanner	Component	0.400	12 x 7 x 18
Empty bin	Component	0.300	30 x 20 x 15
Rubber hose	Component	1.020	Depending on S.O.
Manual operated Dolly	Equipment	35.300	100 x 120 x 76
Rings bin	Equipment	0.300	30 x 20 x 15
Work table	Equipment	52.700	150 x 70 x 86
Support table	Equipment	50.120	106 x 76 x 94
Seal Press machine	Machine	131.250	65 x 65 x 160
Pallet	Equipment	25.000	80 x 120 x 15

The figure 2 shows the real hands operated dolly (left side) and the geometric model (right side).

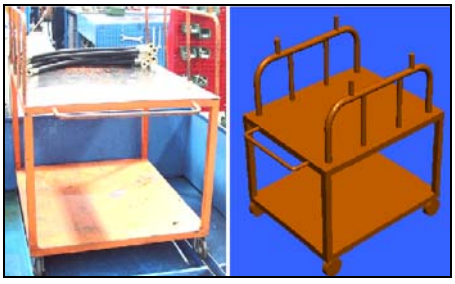

Figure 2: Real and virtual hand operated dolly

The geometric models, created by using the CAD software Pro-Engineer, have to be imported and positioned into the eM-Workplace virtual environment (geometric models created by using the eM-Workplace internal CAD software or imported from the software libraries are directly created and positioned into the virtual environment). Figure 3 shows the real Seal Press workstation and figure 4 shows the workstation geometric models imported into the eM-Workplace virtual environment and the human model (refer to the next section for human model insertion and training procedure).

Figure 3: Real Seal Press workstation

Figure 4: Simulation model of the Seal Press workstation

4.2 Human models insertion and training

The selection of the human models type is based upon an accurate analysis of operators' characteristics (age, gender, height, weight and health conditions). The objective is to select and import, from eM-Workplace libraries, human models representing as much as possible the real workers. After the insertion into the virtual environment, the human model is only able to stand in the waiting position; the model has to be trained to perform workstation operations. eM-Workplace provides the user with a programming language for teaching different types of activities and recreating correctly each type of operation.

The human model training requires an accurate analysis of the operations (performed in the Seal Press workstation) in terms of basic motions. In effect, the programming language provides the user with specific commands for teaching basic motions (i.e. reach, grasp, release, move, etc.). Consequently, each operation has to be subdivided in basic motions.

4.3 Simulation model validation

To increase significantly the probability of success of a simulation study, one of the most important phases is the simulation model validation. The main goal of the validation is to verify if the simulation model is capable of recreating the real system evolution over the time with satisfactory accuracy.

The validation phase has been carried out by using the debugging technique. As reported in Banks (1998) the debugging is an iterative process whose purpose is to discover errors and misconceptions that cause the model failure and to define and carry out the model changes that correct the errors. Such tecnique has been applied with the help of the workstation operators and production engineers: some wrong working postures, wrong motions and redundant motions were corrected or deleted and the simulation model was correctly validated.

5. SIMULATION RESULTS ANALYSIS AND WORKSTATION EFFECTIVE DESIGN

In this section the authors propose the application of the methodology and achieve the ergonomic effective design of the Seal Press workstation. In particular the authors use the simulation model for comparing the 8 workstation configurations obtained by considering all the factors levels combinations (see section 3.1). The analysis of the multiple performance measures defined in section 3.2 will determine the workstations final configuration. Table 3 reports the results of the simulation experiments. First, let us consider separately the effect of each design parameter on the performance measures. The variation of the support table angle α ($0 < \alpha < \pi/2$, keeping fixed the remaining factors levels) does not affect the Burandt Schultetus and the OWAS performance measure. In effect, in both cases ($\alpha = 0$ and $\alpha = \pi/2$) the *Permissible Force* (PF) and the *Stress Level* (SL) remain unchanged (PF = 121.3 N and SL = 3). The variation of the support table angle does not affect lifting tasks and working postures. However, the support table rotation causes an ergonomic improvement: the higher is the angle α the lower is the Energy Expenditure (EE). Note that for $\alpha = 0$ the EE = 1480.0 Kcal, for $\alpha = \pi/2$ the EE = 1439.4 Kcal (the reduction is about 2.7%). As additional information, table 3 reports the *Actual Force* (AF); the AF is the same for each scenario and it is the weight of the objects being handled during the operations. For each scenario, the Burandt Schultetus analysis compares PF and AF: if PF > AF than the ergonomic risk can be accepted otherwise a corrective intervention is required for increasing the PF (or reducing the AF). For both $\alpha = 0$ and $\alpha = \pi/2$ it results PF < AF, it means that the ergonomic risk cannot be accepted.

The variation of the raw material bin height, *rmh* (17 < *rmh* < 86 cm, keeping fixed the remaining factors levels) affects all the performance measures. The

greater is the *rmh* the higher is the PF, the lower are the SL and the EE. By increasing the *rmh*, the operator can easily reach and grasp the bin of the raw materials without torso and legs bending (see figure 5). The stand up position during grasping operations guarantees greater PF values (PF = 137.7 N, note that PF is still lower than AF) as well as more comfortable working postures (SL = 2, however such stress level could create ergonomic problems in the near future). Furthermore by avoiding torso and legs bending, smaller amount of energy is required for performing the same operations (EE = 1403.6 Kcal). In this workstation configuration (see the right part of figure 6), the increase of the PF is about 13.5 %, the SL falls now into the second category, the reduction of the EE is 5.2%.

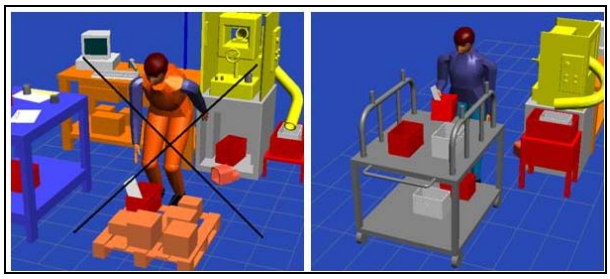

Figure 5: Alternative workstation configuration (raw material bin height)

Let us consider now the variation of the ring nuts bin height *rnh* (30 < *rnh* < 65 cm, keeping fixed the remaining factors levels). As in the previous case, the greater is the *rnh* the higher is the PF, the lower are the SL and the EE. By increasing the *rnh*, the operator reaches and grasps the bin of the ring nuts (exiting from the seal press machine) without torso and legs bending (see figure 6). Consequently, he can exert a greater permissible force (PF = 135.0 N), he works in a more comfortable position (SL = 2) and performs the operations with a smaller amount of energy (EE = 1438.8 Kcal). The increase of the PF is about 11.3 %, the SL falls now into the second category (as before mentioned) and the reduction of the EE is about 2.8%. Figure 6 shows the modified configuration of the workstation in case of *rnh* = 65 cm.

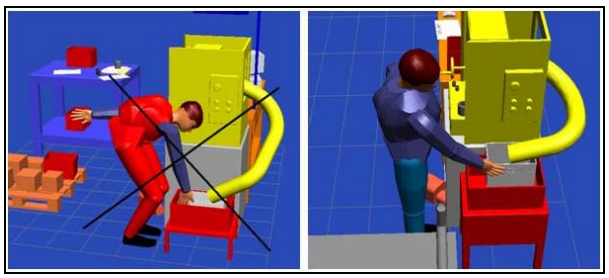

Figure 6: Alternative workstation configuration (ring nuts bin height)

Let us consider now the factors levels interactions. Table 3 reports the following results:

- The interaction between and *rmh* gives, as result, a greater PF (PF = 137.7 N, increase 13.5%), the second category stress level for the working postures and a smaller EE (EE = 1363.0 Kcal, reduction 7.9%). Note that the PF is still lower than the AF and the SL associated to the working postures still falls in the second category.
- The interaction between and *rnh* gives as result a greater PF (PF = 135 N, increase 11.3%), the second category stress level for the working postures and a smaller EE (EE = 1398.3 Kcal, reduction 5.5%). As in the previous case, the PF is still lower than the AF and the SL still falls in the second category.
- The interaction between *rmh*and *rnh* gives as result a greater PF (PF = 151.4 N, increase 24.8%), the first category stress level for the working postures and a smaller EE (EE = 1362.4 N, reduction 7.9%). Note that the PF is now greater than the AF (it means no ergonomic risks during lifting activities) and the SL falls in the first category (it means the SL associated to working postures is optimum).
- The interaction among all the factors levels guarantees the best workstation ergonomic performances. In effect, table 3 reports the following results: the PF = 151.4 N (the highest value, the increase is 24.8%), the SL for the working postures falls into the first category and the EE = 1321.9 Kcal (the lowest value, the reduction is 10.7%). Note that by choosing this workstation configuration the PF > AF (the ergonomic risks related to lifting activities can be accepted), the working postures are characterized by the first category stress level (no further ergonomic interventions are required).

Figure 7 shows the real Seal Press Workstation, the simulation model actual configuration and the effective ergonomic design (final design) respectively on the left, middle and right part. Note that the support table has been completely removed and the length of the main worktable has been slightly increased. In addition, the raw materials are now placed on a hand-operated dolly and the height of the bin containing the ring nuts exiting from the Seal Press machine is greater than the initial height in the actual workstation configuration.

Figure 7: Effective ergonomic redesign of the Seal Press workstation

6. SEAL PRESS PRODUCTIVITY ENHANCEMENT: AN ADVANCED APPROACH

The second goal of the paper is to propose an advanced approach for the productivity enhancement of the Seal Press workstation by comparing four different work methods in terms of process time. To this end, the approach advanced in this research work uses the simulation model of the Seal Press workstation for supporting the comparison of the different work methods. The evaluation of the process time is achieved by using the most widely used work measurement tools: the Methods and Time Measurement (MTM) and the Maynard Operation Sequence Techniques (MOST). In the section 6.1 the authors apply the MTM and MOST to the Seal Press workstation.

6.1 Seal Press workstation productivity enhancement

In this section the authors propose the application of MTM and MOST to the Seal Press workstation.

As already stated in section 2, each work method is characterized by a different number of ring nuts/fittings to be simultaneously inserted into the seal press machine: one single ring nut/fitting (scenario 1) two, three and four ring nuts/fittings simultaneously inserted (respectively scenario 2, scenario 3 and scenario 4) by taking into consideration a typical Shop Order made by 12 ring nuts/fittings.

The operations performed in the Seal Press workstation have been subdivided in 4 different groups (each group has to be regarded as a macro-activity), described as follows.

- *Macro-activity 1* – the operator sets the workstation for starting printing operations.
- *Macro-activity 2* – the operator moves the component (ring nut/fitting) into the Seal Press machine and starts the printing phase.
- *Macro-activity 3* – after the printing phase the operator performs visual checks and place the components into a bin;
- *Macro-activity 4* – the operator completes the Shop Order (setting the status of "end of the operation" on the informative system, moving all the components to the successive workstation.

The authors suppose to subdivide the macro-activities in two different categories: preparation operations (performed just once for the entire Shop Order) and cyclic operations. The macro-activities 1 and 4 (workstation set-up and Shop Order completion) belong to the first category. The macro-activities 2 and 3 belong to the second category. Note that the number of the ring nuts/fittings being simultaneously inserted into the seal press machine does not affect the time of the preparation operations. On the contrary, the work method used by the operator affects both frequency and time of cyclic operations. In effects, higher number of ring nuts/fittings inserted into the seal press machine, correspond to: (1) lower frequency of the cyclic operations, (2) higher time for inserting components into the machine, (3) higher time for the printing phase, (4) higher time for removing the components from the machine. On the contrary, lower number of ring nuts/fittings inserted into the seal press machine, correspond to: (1) higher frequency of the cyclic operations, (2) lower time for inserting components into the machine, (3) lower time for printing phase, (4) lower time for removing the components from the machine. Table 4 and table 5 consist of process times for each macro-activity (expressed in seconds and evaluated respectively by using MTM and MOST).

Table 6 and table 7 consists of process times for each scenario expressed in seconds and evaluated respectively by using MTM and MOST (a scenario includes a Shop Order made by 12 ring nuts/fittings).

The third scenario (three ring nuts/fittings simultaneously inserted into the Seal Press machine) is characterized by the minimum Shop Order process time (according to both MTM and MOST). As concerns the

MTM, the total process time is 201.92 s (about 3 min and 22 s). Note that the process time improvement is about 41% respect to the first scenario, 9.6% respect to the second scenario and 13.9% respect to the fourth scenario. As concerns the MOST, the total process time is 208.82 s (about 3 min and 28 s).

Note that the process time improvement is about 38,8% respect to the first scenario, 7% respect to the second scenario and 11.6% respect to the fourth scenario. Figure 9 shows the scenarios comparison in terms of process times evaluated by means of MTM (left side) and MOST (right side). Let us focus on the Seal Press

Table 3: Simulation results for the Seal Press workstation

Seal Press Workstation						
α	**rmh**	**rnh**	**Burandt Schultetus**		**OWAS**	**Garg**
			Permissible Force (N)	**Actual Force (N)**	**Stress Level**	**Energy Expenditure (Kcal)**
0	17	30	121.3	147.2	3	1480.0
0	17	65	135.0	147.2	2	1438.8
0	86	30	137.7	147.2	2	1403.6
0	86	65	151.4	147.2	1	1362.4
π/2	17	30	121.3	147.2	3	1439.4
π/2	17	65	135.0	147.2	2	1398.3
π/2	86	30	137.7	147.2	2	1363.0
π/2	86	65	151.4	147.2	1	1321.9

Table 4: MTM results for each macro-activiy in the Seal Press Workstation

MTM				
Seal Press Workstation	***1ring nut/fitting***	***2ring nuts/fittings***	***3ring nuts/fittings***	***4ring nuts/fittings***
Macro-activity 1	3.19	3.19	3.19	3.19
Macro-activity 2	9.42	11.23	15.48	23.84
Macro-activity 3	17.76	23.44	31.21	49.24
Macro-activity 4	11.97	11.97	11.97	11.97
Total (s)	42.34	49.83	61.85	88.24

Table 5: MOST results for each macro-activiy in the Seal Press Workstation

MOST				
Seal Press Workstation	***1ring nut/fitting***	***2ring nuts/fittings***	***3ring nuts/fittings***	***4ring nuts/fittings***
Macro-activity 1	3.41	3.41	3.41	3.41
Macro-activity 2	9.54	11.48	16.01	23.78
Macro-activity 3	17.54	23.22	32.14	49.51
Macro-activity 4	12.81	12.81	12.81	12.81
Total (s)	43.30	50.92	64.37	89.51

Table 6: MTM results for each scenario of the Seal Press Workstation

MTM				
Preparation	***Macro-activity 1***	***Macro-activity 4***	***Total Preparation Time (s)***	
Scenario 1	3.19	11.97	15.16	
Scenario 2	3.19	11.97	15.16	
Scenario 3	3.19	11.97	15.16	
Scenario 4	3.19	11.97	15.16	
Cyclic	***Macro-activity 2***	***Macro-activity 3***	***Total Cyclic Time (s)***	
Scenario 1	113.04	213.12	326.16	
Scenario 2	67.38	140.65	208.03	
Scenario 3	61.92	124.84	186.76	
Scenario 4	71.52	147.72	219.24	
	Scenario 1	Scenario 2	Scenario 3	Scenario 4
Total time (s)	341.32	223.19	201.92	234.4

workstation productivity and let us consider the total time required for completing a Shop Order (process time), the 8 hours shift time and the operators' allowance for physiological needs, fatigue and delay (calculated as 20% of the process time).

Regardless of the work measurement tools (MTM or MOST), the workstation productivity (in the third scenario) is about 118 Shop Orders per day. The productivity enhancement is about 69% respect to the first scenario, 11% respect to the second scenario and 16 % respect to the fourth scenario.

Table 7: MOST results for each scenario of the Seal Press Workstation

MOST				
Preparation	***Macro-activity 1***	***Macro-activity 4***	***Total Preparation Time (s)***	
Scenario 1	3.41	12.81	16.22	
Scenario 2	3.41	12.81	16.22	
Scenario 3	3.41	12.81	16.22	
Scenario 4	3.41	12.81	16.22	
Cyclic	***Macro-activity 2***	***Macro-activity 3***	***Total Cyclic Time (s)***	
Scenario 1	114.48	210.48	324.96	
Scenario 2	68.88	139.32	208.2	
Scenario 3	64.04	128.56	192.6	
Scenario 4	71.34	148.53	219.87	
	Scenario 1	**Scenario 2**	**Scenario 3**	**Scenario 4**
Total time (s)	341.18	224.42	208.82	236.09

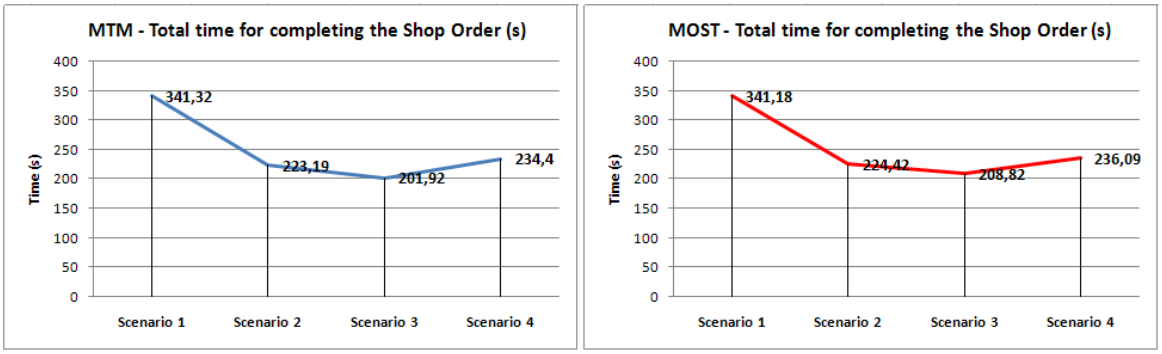

Figure 9: Scenarios comparison

CONCLUSIONS

The paper advances the ergonomic redesign and the productivity enhancement of a real workstation (the Seal Press workstation) within an industrial plant. In the first part of the paper, the authors propose a methodology based on the investigation of multiple workstation configurations by using three different ergonomic standards: the Burandt Schultetus, the OWAS and the Garg analysis. Each workstation configuration is characterized by different levels of three critical design factors: the evaluation of all the factors levels combination required a factorial experimental design executed by using a 3D simulation model of the Seal Press workstation (the simulation model includes a human model able to recreate all the worker's operations). For each workstation configuration the impact of the design parameters has been determined and discussed in terms of permissible force for lifting activities, stress levels for working postures and energy expenditure. As concerns workstation productivity enhancement, the authors use the simulation model of the Seal Press Workstation for supporting the comparison of the four work methods. Each work method is characterized by a different number of ring nuts/fittings to be simultaneously inserted into the seal press machine. The simulation model calculates the process time related to each work method by means of the most widely used work measurement tools (MTM and MOST). Such evaluation allows to choose the best work method in terms of ring nuts/fittings to be simultaneously inserted into the seal press machine.

REFERENCES

Banks, J. (1998). Principles of Simulation. In: J. Banks, Handbook of Simulation, vol. 1 (1st ed., pp. 3-30). New York: Wiley Interscience.

Bell, P.C., O'Keefe, R.M. (1994). Visual interactive simulation: a methodological perspective. Annals of Operations Research, 53 (1), 321-342.

Cimino, A., Curcio, D., Longo, F., Papoff, E. (2008a). Workstation productivity enhancement within hydraulic hoses manufacturing process. Proceedings of the 7th International Workshop on Modeling & Applied Simulation, Amantea (CS), Italy, 268-274.

Cimino, A. , Longo, F. , Mirabelli, G. (2008b). Shop orders scheduling: dispatching rules and genetic algorithms based approaches. Proceedings of the 20th European Modeling & Simulation Symposium, Amantea (CS), Italy, 817-823.

Cimino, A., Longo, F., Mirabelli, G. (2009). Multi-Measures Based Approach for the Ergonomic Effective Design of Manufacturing System Workstations. International Journal of Industrial Ergonomics, 39 (2), 447-455.

Cimino, A., Mirabelli, G. (2008). Modeling, simulation and ergonomic standards as support tools for a workstation design in manufacturing system.

International Journal of Simulation and Process Modeling, 5 (2), 138-148
Das, B., Sengupta, A. K. (1996). Industrial workstation design: a systematic ergonomics approach. Applied Ergonomics, 27 (3), 157-163.
Garg A. (1976). A metabolic rate prediction for manual materials handling jobs. Dissertation, University of Michigan.
Karger, O., Bayh, F. (1987). Engineered Work Measurement. New York: Industrial Press.
Kharu, O., Kansi, P., Kuorinka, I. (1977). Correcting working postures in industry: a practical method for analysis. Applied Ergonomics, 8 (4), 199-201.
Laring, J., Forsman, M., Kadefors, R., Örtengren, R. (2002). MTM-based ergonomic workload analysis. International Journal of Industrial Ergonomics, 30 (3), 135-148.
Lawrence, S.A. (2000). Work Measurement & Methods Improvement. New York: John Wiley & Sons.
Longo, F., Mirabelli, G. (2009). Effective Design of an Assembly Line using Modeling & Simulation, International Journal of Simulation, 3 (1), 50-60.
Maynard, H.B., Stegemerten, G.J., Schwab, J.L. (1948). Methods-time measurement. New York: McGraw Hill book company.
Niosh Technical Report 81-122. National Institute for Occupational Safety and Health (Hrsg.). Work practices guide for manual lifting. Center for Disease Control, U.S. Department of health and human services, Cincinnati, OH, USA: NTIS 1981.
Russell, S. J., Winnemuller, L., Camp, J. E., Johnson P. W. (2007). Comparing the results of five lifting analysis tools. Applied Ergonomics, 38 (1), 91-97.
Scientific Support Documentation for the Revised 1991 NIOSH Lifting Equation: Technical Contract Reports, May 8, 1991, NTIS No. PB-91-226-274.
Udosen, U.J. (2006). Ergonomic workplace construction, evaluation and improvement by CADWORK. International Journal of Industrial Ergonomics, 36 (3), 219-228.
Waters, T.R., Lu, M.L., Occhipinti, E. (2007). New procedure for assessing sequential manual lifting jobs using the revised NIOSH lifting equation. Ergonomics, 50 (11), 1761–1770.
Wilson, J. R., (1997). Virtual environments and ergonomics: needs and opportunities. Ergonomics, 40 (10), 1057-1077.
Zandin, K.B. (2001). Maynard's Industrial Engineering Handbook. New York: McGraw-Hill.
eM-Workplace by UGS. Available from: <http://www.plm.automation.siemens.com/en_us/products/tecnomatix/assembly_planning/process_simulate_human/index.shtml>.
Pro-Engineer by PTC. Available from: <http://www.ptc.com/products/proengineer>.

AUTHOR BIOGRAPHIES

Antonio Cimino took his degree in Management Engineering, summa cum Laude, in September 2007 from the University of Calabria. He is currently PhD student at the Mechanical Department of University of Calabria. He has published more than 20 papers on international journals and conferences. His research activities concern the integration of ergonomic standards, work measurement techniques and Modeling & Simulation tools for the effective workplace design. His e-mail address is: acimino@unical.it and his Web-page can be found at http://www.ingegneria.unical.it/impiantiindustriali/index_file/Cimino.htm

Francesco Longo received his Ph.D. in Mechanical Engineering from University of Calabria in January 2006. He is currently Assistant Professor at the Mechanical Department of University of Calabria and Director of the Modelling & Simulation Center – Laboratory of Enterprise Solutions (MSC-LES). He has published more than 80 papers on international journals and conferences. He is Associate Editor of the "Simulation: Transaction of the society for Modeling & Simulation International". For the same journal he is Guest Editor of the special issue on Advances of Modeling & Simulation in Supply Chain and Industry. He is Guest Editor of the "International Journal of Simulation and Process Modelling", special issue on Industry and Supply Chain: Technical, Economic and Environmental Sustainability. His e-mail address is: f.longo@unical.it.

Giovanni Mirabelli is currently Assistant Professor at the Mechanical Department of University of Calabria. He has published more than 60 papers on international journals and conferences. His research interests include ergonomics, methods and time measurement in manufacturing systems, production systems maintenance and reliability, quality. His e-mail address is: g.mirabelli@unical.it

Rafael Diaz graduated from the Old Dominion University with a Ph.D. in Modeling and Simulation in 2007, and became a Research Assistant Professor of Modeling and Simulation at Old Dominion University's Virginia Modeling, Analysis, and Simulation Center (VMASC). He holds an M.B.A degree in financial analysis and information technology from Old Dominion University and a B.S. in Industrial Engineering from Jose Maria Vargas University, Venezuela. His research interests include operations research, operations management, production and logistic systems, reverse logistics, dependence modeling for stochastic simulation, and simulation-based optimization methods. He worked for six years as a process engineer and management consultant prior to his academic career.

A SIMULATION ANALYSIS OF PALLET MANAGEMENT SCENARIO BASED ON EPAL-SYSTEM

Maria Grazia Gnoni[(a)], Gianni Lettera[(b)], Alessandra Rollo[(c)]

[(a), (b), (c)]Department of Engineering for Innovation, University of Salento, Lecce, Italy

[(a)]mariagrazia.gnoni@unisalento.it, [(b)]gianni.lettera@cerpi.it, [(c)]alessandrarollo@unisalento.it

ABSTRACT

Pallet management usually involves direct and reverse logistic models as it represents a critical activity in supply chain management. Pallets are needed in order to ship products from the producers/distributors to the retailers. The ”EPAL-System“ is a cross-sector open pallet exchange pool based on standardized quality-assured EURO pallets. The whole performance of a pallet management system could be improved by an appropriate strategy which aims both to increase pallet availability in the direct logistics and to reduce total cost of the reverse logistics. A simulation model has been applied to compare alternative pallet management scenarios based on EPAL-System aiming to assess more effective policies.

Keywords: pallet management, simulation model , scenario analysis

1. INTRODUCTION

In logistics activities, producers, distributors and retailers share a common objective, such as optimizing logistic costs and performances. Logistic activities are mainly based on a standardized equipment: the pallet. Several researches are focalized on pallet loading problem; few attention has been assigned to the overall pallet management process. The reverse logistic of empty pallet represents usually a valuable activity; a recent survey (Dallari and Marchet 2008) has evaluated the annual volume of palletized load units in Italian logistic market about 600.000 units. These issues contribute to confirm that pallets represents an important company asset; therefore, enterprises have to face with new organizational, economic and managerial issue regarding pallet management.

The most widespread pallet type is the wooden pallet which are characterized by unified features; this is the so called *EURO pallet* which specific features have been defined by the European Pallet Association (EPAL) aiming to asses a shared level for quality assurance and inspection standards. Others pallet types are mainly made by plastic and aluminum. In the last years, pallets with a RFID tag are spreading throughout the market, but they currently represent a low quantity in the whole market.

The purpose of the paper is to propose a simulation model of a pallet management scenario in which direct and postponed interchange are implemented simultaneously to analyze the flows of incoming and outgoing pallets. The simulation analysis can provide an effective tool to manage both direct and reverse flow involved in pallet management. The software AnyLogic ®6.0 has been applied to develop a discrete event simulation model for evaluating most effective pallet management system. The virtual prototype of the pallet management scenario is made up by system state variables, entities and attributes, lists processing, activities and delays. Moreover AnyLogic has animation functions allow the development of visually rich, interactive simulation environments (Borshchev 2010). The pallet flows can be analyzed under certain conditions like pallet storage capacity, the frequency of incoming shipment or orders processing, the quantity of new pallet annually purchased, the percentage of pallet repaired or disposed, etc.. Through a dynamical setting of operative conditions in the simulation model, the quantity of pallets exchanged in direct or postponed way can be evaluated.

At first, an analysis on main issues concerning organizational procedures and factors which affect pallet reverse logistic has been carried out. Next, a brief description on discrete event simulation model and related tool are reported. Finally, the simulation model of pallet management based on the well know “EPAL-System” is described. The developed scenario could represent a baseline in order to compare economical and technical performances of different organizational alternatives in pallet management such as pallet pooling or outsourcing.

2. THE PALLET MANAGEMENT: MAIN ISSUES AND ORGANIZATIONAL SCENARIOS

2.1. Organizational scenarios

Traditionally, one of the main cost added activity in pallet management is the reverse logistic: pallets have to be collected downstream in the supply chain where products are delivered to final customer. Pallet management activities are analyzed considering a

supply chain configuration where a producer or a distributor ships products to a wholesaler or a retailer. Two organizational procedures are mainly applied for reverse logistics of pallets: the direct and the postponed interchange. In the *direct interchange*, all pallets have been collected by the final logistic provider at the final customer (such as the wholesaler or the retailer) during delivery activities; therefore, the total delivery time increases due to required pallet interchange activities, such as quality and integrity check. The logistics provider picks up the same pallet number delivered; usually, this activity usually does not require additional waiting time until pallets have to be unloaded because they could be collected in following deliveries. By an organizational point of view, an identification pallet activity will be carried out by logistic provider.

In the *postponed interchange*, the final customer supplies during delivery activities a pallet voucher to the logistics provider according to pallet number delivered in each trip. This order allows to collect – usually within three months in EPAL interchange system – such a pallet (ECR 2006). Therefore, tracking and tracing pallets may be represent a complex activity in this procedure. Moreover, quality check carried out on delivered pallets and the administration of pallet voucher may require time and effort were not acceptable. These activities affects the overall logistic cost.

Different organizational options could be implemented to manage pallets aiming to reduce its costs. The main organizational scenarios identified are direct management, outsourcing management and pallet pooling which are analyzed following.

- Direct Management scenario: all activities regarding pallet management - such as purchase, tracking and shipping, collection, maintenance, washing and sanitizing disposal, and, finally, recovery activities - has been carried out internally by the firm. The firm has to evaluate investment costs both in pallet park purchase and in management activities. Pallet interchange could be immediate or postponed.
- Outsourcing Management scenario: the firm has to carry on investment in pallet park purchase; pallet management activities are carried out by an external logistic company(e.g. a third-party provider). The logistics provider retrieves the pallets downstream in the supply chain and it tracks them via customer dispatch data. Pallet interchange requires only postponed type. Services supplied by external logistic company usually are pallet maintenance, disposal, monitoring, handling, and final collection. The global leader firm in pallet management is *CHEP- Commonwealth Handling Equipment Pool*, which manages the so called "blue pallet" in several sizes all over the world. Other European companies are *PGS Groupe* (France), *iPallet* (Italy), *Palletpol Ltd* (United Kingdom).
- Pallet Pooling scenario: a third-party logistics provider rents its own pallets to customers (i.e. producers and/or distributors) according to a service contract. The company ships pallets to his customers and usually supplies tracking service about time and location of customer shipments. One of the most important pallet pooling operators is *CHEP*.

2.2 Critical activities

Each process consists of one or more activities defined by their outputs. Then, main activities involved in pallet management are detailed following in order to highlight critical areas of interventions.

Pallet Replenishment: this activity refers to the annual cost supported for annual pallet park renewal due to breakage or loss. The unitary cost varies according to pallet type; the total purchase cost incurred has been evaluated based on a specific renewal level defined by the firm management.

Pallet Disposal: wooden and plastic pallets represent a source for recycling; otherwise, if recycling option is not suitable, pallets have to be disposed as a waste. Wooden pallets have a shorter life cycle than plastic pallets; they are easily disassembled due to their simple designs and standardized part sizes (Bejune et al. 2002).

Maintenance: the activity involves all repairing actions – e.g. adding new nails, metal brackets or replacing a broken board - carried out periodically on pallets aiming to maintain their full functionality as defined by the European Pallet Association (2009). Maintenance activity affects mainly wooden pallets; usually, plastic pallets could not be repaired, because they are a one-piece design.

Cleaning: the specific activity depends on pallet type. It mainly consists of the sterilization activity carried out by a specific heat treatment for wooden pallets; Cleaning activities are required by an international Standard for Phytosanitary Measure – the standard ISPM-15 (FAO 2002) – aiming to disinfect wooden pallets. The ISPM-15 is being progressively implemented throughout the world; this treatment is obligatory when exporting to several industrial countries. Similarly, a cleaning activity has to be carried out periodically for plastic pallet.

Storage: a percentage of empty pallets needs continuously a dedicated storage areas inside and/or outside the plant. The percentage level depends on organizational procedures for pallet management (i.e. the direct and the postponed interchange).

Reverse logistics: a closed loop system affects pallet management at the wholesaler/retailer level. The time spent for reverse logistic activities mainly depends on organizational scenarios applied by the firm for managing the reverse flow of pallets from retailer: if direct interchange is working, pallet quality has to be

verified among retailer and pallet carriers. Otherwise, in postponed interchange, usually pallets are stored by the retailer in a dedicated area; thus quality control is reduced because carrier retires its own pallets.

Pallet tracking and tracing: pallets, like other industrial assets, require an effective control during all their lifecycles; thus, tracking and tracing refer mainly to monitor load and empty pallet trips along the distribution chain. In traditional pallet management systems, the main cost is due to accounting activities required for evaluating the actual number of pallets available in the systems; usually it represents a high operational cost.

Pallet information management: data about pallet availability (both in terms of quantity in the storage areas and at each destination) have to be placed in the Warehouse Management System (WMS); in traditional systems, this represents a high time-requiring activity. This activity supplies an information reporting system about pallet utilization.

Inspection activities: it regards control carried out by the carrier during both pallet loading and empty pallets returned from end users. These activities are carried out manually by an operator or semi-automatically by optical barcode readers.

Accounting. This activity is closely linked to tracking and tracing systems and specific organizational procedures for pallet management applied in the firm. It also includes administrative activities involved in pallet vouchers management if postponed interchange is applied. In the proposed model, the management of legal disputes between actors involved has been neglected.

3. THE SIMULATION MODEL

A simulation model has been developed aiming to compare performance of two different management scenarios for pallet reverse logistics: **direct interchange scenario** where the logistics provider returns an equivalent number of pallets delivered, and **postponed interchange scenario** where vouchers can be returned for pallets. The model simulates major processes (previously described) which characterize traditional pallet management system; a brief description is proposed as follows:

- *Warehouse of empty pallets*: empty pallets are stored in a dedicated warehouse. Here, quality control activities are performed to select pallets compatible to EPAL requirements; a selection activity highlights pallets requiring maintenance or disposal as they cannot be reconditioned. In direct interchange scenario, a stock level below the safety stock results in a purchase order for new pallets.
- *Entry Pallets:* two main inputs for the pallet warehouse have been evaluated in the simulation model. The first type refers to by purchased orders: the company has decided to define an average level of its pallet park, thus, order have been carried out periodically to maintain this level. The second input derives from empty pallets from received goods: the goods are delivered as palletized loads; therefore, a pallets entry in warehouse with goods. The activity of separation of pallet from its contained goods has not been evaluated in the simulation model.
- *Returning empty pallets or voucher*: when entry goods are handled in the warehouse, the logistics provider has to supply to the carrier an equivalent pallet number. In the postponed interchange scenario, if the company has a stock of empty pallets which are under the minimum stock level, vouchers are issued.
- *Internal Operations*: received goods could be quickly delivered or stocked by the logistics provider; a certain number of empty pallet are needed for the picking activity.
- *Empty pallet reverse logistics*: empty pallets that are shipped with the goods, have to came back to the warehouse. The return may occur under immediate or postponed interchange. Some pallets pull off the whole system as they were lost or broken.
- *Repair and disposal*: pallets that are failed the quality control are sent to maintenance center; if they could not be repaired according to EPAL standards, they are disposed or recycled as secondary materials.

3.1. The model hypothesis

The simulation model is based on a set of parameters which characterize quantitatively the dynamic of the problem. A brief description is proposed as follows.

Pallet input by purchased order: the P_1 represents the maximum number of pallets purchased in a year by the firm and P_2 represents number of pallet units for each purchase order. The order lead time is defined by parameter P_3.

Pallet input by receiving goods: I_1 represents is incoming pallets per delivery; $I_{2\ is}$ the interarrival time of deliveries (expressed in minutes) and I_3 the required time for unloading of goods delivered in entrance.

The Returning activity of empty pallets or voucher is defined by F_1, i.e. the percentage of pallets or vouchers that are not returned to the carrier because it arrived broken or heavily being damaged and therefore not interchangeable according to the standards EPAL.

Empty pallets warehouse is characterized firstly by W_1 which represents the Safety stock level of empty pallets. The W_2 is the required time for pallets quality control: this parameter defines the effort applied for pallet sorting pallets. Activity results determine number of "good" pallets and those not usable or interchangeable according to the EPAL standards; thus, a parameter (W_6) defines the average rate of pallets which fail the quality control. Required manpower is defined by W_3 and W_4 is the average lead time for pallet handling. Finally, W_5 defines the Number of empty pallets simultaneously drop off from the warehouse;

Internal Operations. Picking activity is characterized by several parameters: O_1 is the Picking rate, that is percentage of palletized loads affected by picking activities; the lead time required for delivering

palletized load without picking is defined by O_2. *Lead time* before picking is defined by O_3; O_4 is utilization rate of empty pallets in picking activities defined as the ratio between empty pallets and palletized load processed. The time required for picking activities *is* O_5; O_6 is the picking capacity. O_7 represents the percentage of pallet not shipped after picking activities and O_8 pallets per shipment, i.e. the number of palletized loads for each shipment.

Reverse Logistics of empty pallets. R_1 represents the failure rate, that is the percentage of pallets lost or not interchangeable due to a poor quality over the palletized loads delivered. In this rate, passive franchise is included. R_2 is the estimated time for quality control of pallets, and R_3 the manpower required by this activity. Three scenario parameters are R_4 which represents the Postponed interchange rate, R_5 is the Direct interchange time, which is the time needed for returning of shipped pallets when direct interchange is implemented and R_6 the Postponed interchange time, that is the time required for returning shipped pallets when postponed interchange is implemented.

Repair and disposal of pallet. This activity is characterized by D_1 the pallet disposal rate and D_2 – which represents the average time required to repair pallets.

4. THE MODEL APPLICATION

The case study analyzed regards a small distribution center: its pallet park is about 11.500 units; the simulation period is one years, i.e. 300 work-days. Two different management scenarios were simulated as defined previously:

- **Scenario 1 – Direct interchange**: to the carrier making the delivery of palletized loads is returned immediately an equivalent number of empty pallets. The number of pallets to be returned is agreed with the carrier following the quality control of pallets delivered. Incoming deliveries are processed individually, and the single process ends with the return of empty pallets to the carrier. Therefore the following carrier waits that the previous carrier releases the unloading platform.
- **Scenario 2 – Postponed interchange**: to the carrier has made delivery of the goods can be returned an equivalent number of empty pallets or vouchers. In particular, if the company has a stock of empty pallets which are under the minimum stock level, vouchers are issued.

Each year an average value of 5.000 pallets were purchased due to replenishment policies in both scenarios. Moreover, in the direct interchange scenario, up to 7.000 units of new pallets can be purchased during the year to overcome the temporary unavailability of pallets to be returned to transporters. In the postponed interchange scenario, in the absence of pallets to be returned, vouchers are issued and they are accounted at year end. The parameters used in the case study are presented in table 1.

Table 1: Estimated values in the case study

Model Flows	Parameter	Value
Pallet input by purchase order	P_1	7.000 pallets
	P_2	100 pallets
	P_3	1 day
Pallet input by receiving goods	I_1	30 pallets
	I_2	60 minutes
	I_3	60 minutes
Returning empty pallets or voucher	F_1	5% of pallets received
Warehouse of empty pallets	W_1	300 pallets
	$W_2 – R_2$	20 seconds
	$W_3 – R_3$	1 person
	W_4	4 minutes
	W_5	10 pallets
	W_6	1 over 300 pallets controlled
Internal Operations	O_1	20% of pallets received
	O_2	2 days
	O_3	20 days
	O_4	2/3
	O_5	20 minutes
	O_6	1.500 pallets
	O_7	20% of pallets picked
	O_8	25 pallets
Reverse Logistics of empty pallets	R_1	1 over 200 of shipped pallets
	R_4	20% of shipped pallets
	R_5	1 day
	R_6	30 days
Repair and disposal of pallets at the repairer	D_1	10% of pallets sent at the repairer
	D_2	3 days

4.1. Results analysis

First results obtained by the simulation outline that palettized loads received and shipped are 215.970 and 249.332 in scenario 1 and 2 respectively, with a ratio between the flow of incoming and outgoing pallets equal to 1,15. Moreover, the average value of empty pallets in stock is equal to 413 pallets in the scenario 1, and 394 empty pallets in the scenario 2. Therefore, scenario 2 is characterized by a slight increase in the average level of empty pallet warehouse; the comparison in the two scenarios of the level of stock is shown in Figure 1.

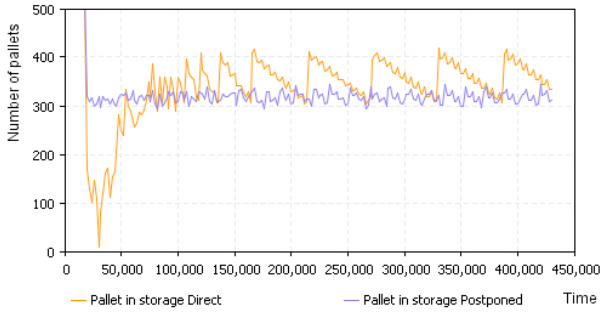

Figure 1: Comparison between warehouse level of empty pallets in the two scenarios.

As reported in Figure 1, safety stock level of empty pallets is guaranteed by issuing vouchers in the postponed interchange scenario; otherwise, stock levels below the safety threshold will generate a purchase order of new empty pallets in the direct interchange scenario. This scenario is the critical one as the lack of empty pallets determines a slowdown in deliveries to final customers. Therefore, Out of stocks occurs in scenario 1, determining a delay in unloading of goods. This determines a domino effect by inducing a delay in the empty pallet return, in internal material handling and picking activities (see Figure 2).

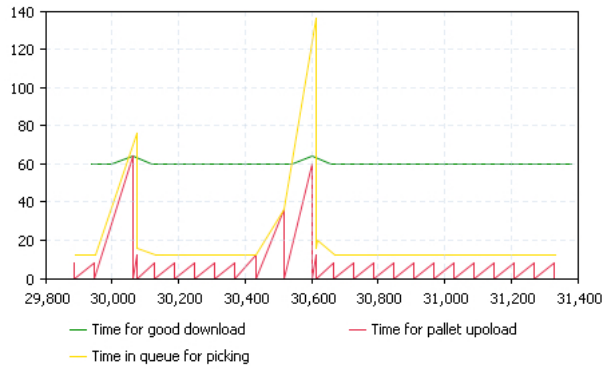

Figure 2: Estimated firm service level in scenario 1

The time trend of purchase orders of new pallet for the restoration of the level of stock in direct interchange scenario is reported in figure 3, compared with total pallet voucher in the postponed interchange scenario.

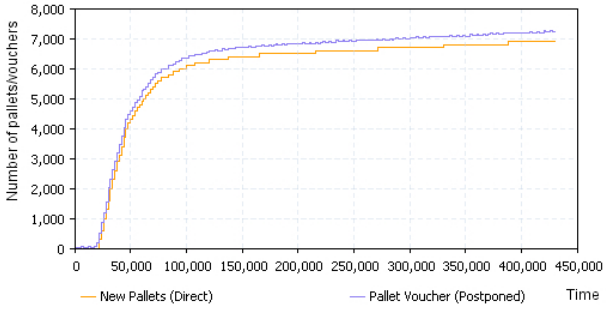

Figure 3: New pallets purchased in scenario 1 and pallet vouchers emitted in the scenario 2.

Overall in a year of activity (i.e. in the simulion period) 7.230 vouchers are issued in the postponed interchange scenario, while the new pallets purchased in scenario 1 are 6.900. This means that the direct interchange scenario in which new pallets are purchased according to fixed order quantity method is characterized by lower cost of assets purchase.

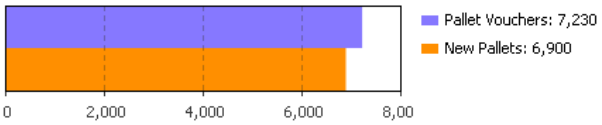

Figure 4: New pallets purchased level (scenario 1) versus pallet vouchers emitted (scenario 2).

Other types of delay occur in the picking activities in both scenarios. These delays of less importance, are related to normal operation and occur in association with certain goods deliveries: if the pallets are picked from the warehouse for returning the carrier, they could not be taken for picking activities. Thus, delays are generated for picking activities.

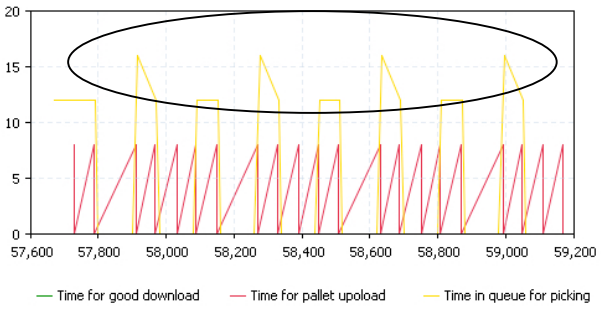

Figure 5: Estimated delays in picking activities

On the contrary, if empty pallets are loaded from the warehouse for picking activities, an incoming delivery is processed, the activity of the return of empty pallets suffers minor delays as outlined by the Figure 6.

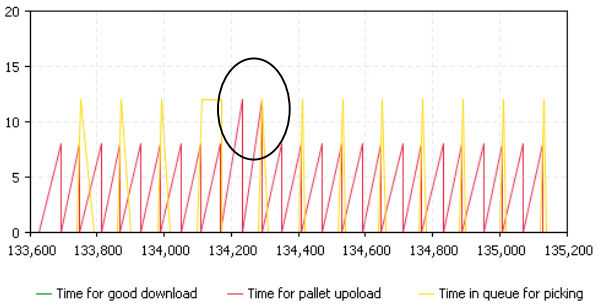

Figure 6: Example of delay in empty pallet restitution to carrier when empty pallets are needed both for picking activity and interchange.

Finally, Table 2 shows the minimum, maximum, average, the confidence interval for the mean and standard deviation of service level characterizing the logistics provider.

Table 2: Statistics for analyzed scenarios.

	Scenario	min	max	mean	mean confidence	deviation
Good unload Time	1	60	64	60,001	$2,812*10^{-4}$	0,067
	2	60	60	60	0	0
Empty pallet upload Time	1	0	64	4,07	0,014	3,418
	2	0	12	4,046	0,014	3,294
Picking Queue Time	1	0	136	3,301	0,078	5,535
	2	0	16	2,888	0,072	5,132

REFERENCES

Borshchev, A, 2010. *Simulation Modeling with AnyLogic: Agent Based, Discrete Event and System Dynamics Methods*. Available from: http://www.xjtek.com/anylogic/resources/book/ [accessed 29 July 2010]

Dallari,F., Marchet G., 2007. *Il ruolo dei pallet nei morderni sistemi distributive*, Lampi di Stampa.

Dallari,F., Marchet G., 2008. *La Gestione dei pallet. Indagine presso gli operatori di logistica integrata*. Available from: http://www.liuc.it/ricerca/clog/cm/upload/OPAL3PL_EXE2.pdf [Accessed 10 April 2010].

ECR, 2006. *Interscambio Pallets EPAL. Raccomandazione ECR*, ECR Italia. Available from: http://indicod-ecr.it/ecr_italia/download_documenti/Raccomandazione_ECR_Interscambio_Pallet.pdf [accessed 29 July 2010]

FAO, 2002. *International standards for phytosanitary measures. Guidelines for regulating wood packaging material in international trade*. FAO Corporate Document Repository. Available from: http://www.fao.org/docrep/006/y4838e/y4838e00.htm [accessed 10 April 2010]

AUTHORS BIOGRAPHY

Maria Grazia Gnoni is Assistant Professor at the Engineering Faculty of the University of Salento. Her research interests are focused on the design and the management of sustainable supply chains and logistics.

Gianni Lettera is a contractor researcher at the Department for Innovation of the University of Salento. His research activities are focused on environmental and safety management.

Alessandra Rollo, Phd student, master degree cum lodem in Management Engineering at the University of Salento (Italy) in 2007. Her research interests are in the fields of operations management with the attention on IT utilization (in particular RFID technology).

A SIMULATION-BASED ERGONOMIC EVALUATION FOR THE OPERATIONAL IMPROVEMENT OF THE SLATE SPLITTERS WORK

Nadia Rego Monteil[(a)], David del Rio Vilas[(b)], Diego Crespo Pereira[(c)] Rosa Rios Prado[(d)]

[(a) (b) (c) (d)] Grupo Integrado de Ingenieria (GII), University of A Coruna, Spain

[(a)]nadia.rego@udc.es, [(b)]daviddelrio@udc.es, [(c)]dcrespo@udc.es, [(c)]rrios@udc.es

ABSTRACT

The natural roofing slates manufacturing process relies on highly labour-intensive activities and more specifically on the mastery of a specialized group of workers known as splitters. The splitting of slate blocks is a complex manual and demanding work that involves both important physical exertions and quick and accurate decision making processes. Since a lot of repetitive and potentially hazardous movements have to be made there is a substantial risk of developing musculoskeletal disorders (MSDs). Besides, plant's costs and productivity depend largely on their individual performance. In this paper we present a quantitative approach to a combined ergonomic and operational assessment of the slates splitters tasks. A RULA analysis is carried out by means of a Digital Human Model (DHM) aiming at quantifying the level of ergonomic risk in several scenarios and leading to a set of simple improving workplace proposals in terms of ergonomics and productivity.

Keywords: ergonomics, DHM, slate splitters, workplace design.

1. INTRODUCTION

Spain is the first slate producing country in the world, with an export volume that exceeds 80% of slate mined and produced. On its part, Galician slate production accounts for around 70% of the national production.

Europizarras is a Galician medium company mainly devoted to the production of the highest value added roofing slates, that is to say, the thinnest commercial tiles. The thinner a tile is the harder and more wasteful the manufacturing process becomes. Europizarras exports more than 90% of its production to the French market which presents a quite constant demand (AGP 2010).

Despite this constant demand, the slates price evolution shows a downward trend when expressed in terms of constant Euros, i.e., discounting the effect of inflation, as depicted in Figure 1.

Figure 1: Exportations to France (up) and Spanish Slate Aggregated Prices Evolution between 1970 and 2006 (down). In red, Prices in Constant Euros.

Attending to the production costs set up, whilst the quarry costs present the typical even distribution in mining activities, the costs distribution regarding the slates manufacturing plant is very characteristic, mainly depending on personnel expenses (Table 1). This is due to the artisanal nature of the processes involved. As a matter of fact, an average slate manufacturing plant employs six workers for every dedicated worker in the quarry. (BIC-Galicia 1997).

Table 1: Costs Distribution in Slate Production Centres

Concept	Personnel	Maint.	Supplies	Amort.
Quarry	27%	26%	25%	22%
Plant	78%	13%	5%	1%

It is also known that 55% on average of the total production costs are incurred in the manufacturing plant. Therefore, the weight of personnel costs involved in manufacturing operations in the plant accounts for almost 43% of the total company costs. Splitters salaries play a fundamental role in this matter, especially in the case of our company. Because of their relative geographic isolation from the main production areas they

have to offer a surplus income to attract specialized splitters.

The splitting of slate blocks is a manual work involving a lot of repetitive movements, lifting, pushing and pulling, twisting, and hitting actions so that there is a substantial risk of developing Musculoskeletal Disorders (MSDs). From an ergonomic point of view many factors can contribute, either individually or in combination, to the development of MSDs at work (OSHA EU 2005):

1. Physical: including using force, repetition of movements, awkward and static posture, vibration and cold working environments.
2. Organizational: including high work demand, lack of control over work, low job satisfaction, repetitive work, high pace of work, time pressure.
3. Individual: including prior medical history, physical capacity and age.

All of these factors are present in the everyday working activities of the slate splitters. Besides, as slate needs to be wet to allow a proper exfoliation, it is carried out in a cold and wet environment. The inhalation of silica dust is also a well acknowledged problem (Fundacion 2008)

Whereas there are many other previous studies that have focused on other different ergonomic risks assessment (Walsh 2000, Guiver 2002) the approaches to the study of MSDs in slate splitters are scarce and traditionally conducted (Weber 1996). But above all, all these studies are conducted under an epidemiologic prism so they do not pretend to link ergonomics and productivity.

On the other hand, there are numerous and important references of simulation-based conducted experimentation for the operational assessment of different workplaces (Cimino 2010). Digital Human Models (DHM) applications in the automotive sector (Shao 2007) as well as in the aeronautical sector (Boeing 2010) are common, but its role as an usual workplace design tool in Small and Medium Enterprises is still rare (Santos 2006).

The splitting operation is at the core of the whole manufacturing process. It is the task where product, resources and process circumstances converge in a less controllable way from a variability point of view (del Rio 2009). So far, attempts on the splitting process automation have not succeeded, especially when the nominal thickness is 3.5 millimetres as is our case.

For all the above described reasons, we propose a quantitative approach to the slates splitting process risk assessment regarding MSDs for the operational improvement of the slate splitters work. To do so, we first determine the set of tasks and postures a splitter normally performs. Then, a virtual model of the splitter and its workplace is built so that the RULA analysis can be conducted by means of the DHM software DELMIA Human. Finally, attending to the obtained results, a set of simple improving workplace proposals in terms of ergonomics and productivity is presented.

2. THE SPLITTING PROCESS

After the extraction of slate blocks from the quarry and its transportation to the manufacturing plant, the slate is cut in slabs by means of circular saws. Later on, they are taken by the splitters one by one and cut in several pieces by means of a special type of chisel so they can handle them better and also determine the presence of flaws. Then, they change to a smaller chisel for cutting these parts into plates. The chisel, placed in position against the edge of the block, is lightly tapped with a mallet. The natural structure of slate allows its exfoliation; a crack appears in the direction of cleavage, and slight leverage with the chisel serves to split the block into two pieces with smooth and even surfaces. This is repeated until the original block is converted into a variable number of pieces. The resulting number of plates depends mostly on the quality of the slate rock from quarry as well as the splitters experience and skill. Splitters classify slates into two groups. One is the target format of tiles of 32x22x3.5 mm –the 80% of the total, that we named L32 (Slates Lots of 32) – and the other one gathers all other formats in a category named LN32 (Lots of Not 32).The splitting working cycle is divided in four main subtasks:

1. Previous Operations (grey blocks in Figure 2)
2. Rough Splitting (blue blocks): it happens a non constant number of times depending on the size of the slate block.
3. Splitting (orange blocks): it happens as many times as final plates are obtained.
4. Sorting (green blocks).

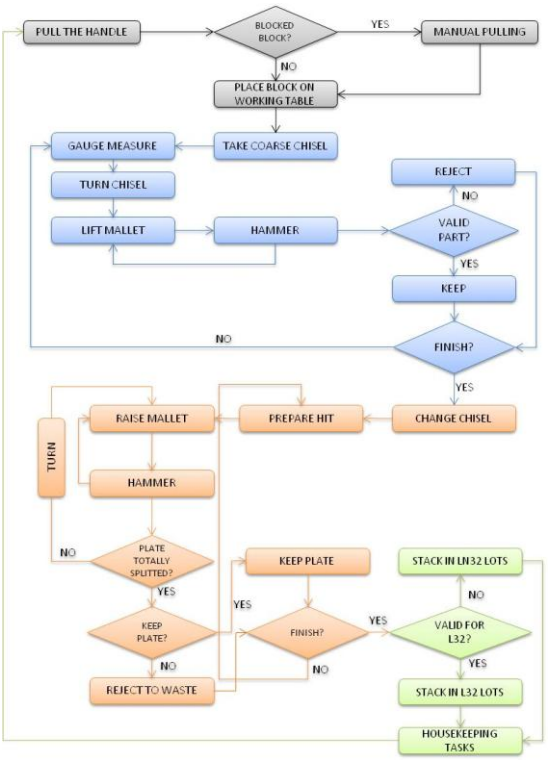

Figure 2: Splitting Process Diagram.

These tasks have been statistically characterized for the simulation model. Data have been collected from digital video recordings taken in situ. Data collection based on commercial video-recorder technology is portable, familiar to many people, does not encumber the worker and is relatively inexpensive (Neumann 2001). Once a workplace recording is made, it must then be processed to extract the desired information. In Table 2 we present the standard times for the set of activities of which a normal working cycle is made up.

Table 2: Standard Times

Activity			Standard Time (s)
Previous Operations			8.00
Rough Splitting			2.94
Splitting	To waste	Turning	9.45
		No turning	6.60
	To keep	Turning	7.02
		No turning	4.17
Sorting			27.90

THE ERGONOMIC METHOD: RULA

RULA (Rapid Upper Limb Assessment) is a classic ergonomic risk assessment method proposed in 1993 (McAtamney 1993). Originally it is thought to be applied on those postures which seem to be critic along the task. It separately analyzes left and right sides of the body by dividing the human body into two groups. Group A comprises arms, forearms and wrists, and group B is composed by legs, trunk and neck. After a series of evaluations it scores the potential risks associated to the postures under analysis according to a grand score from which derive a risk level and a resultant set of recommendations (Table 3).

RULA is a well known and widely used ergonomic assessment method (Cimino 2008) and it is commonly employed among the commercial DHM simulators. It is especially thought for the assessment of tasks that mainly imply the upper limbs as is the splitters case. Besides, as it is implemented into DELMIA, it allows its continuous application to every single modelled posture of which a task is made up. On the contrary, were the same method applied in a traditional manner it would be limited only to those tasks a priori considered as the most dangerous.

Table 3: RULA Action Levels

Level	Action levels from RULA
1	When grand score is 1 or 2, posture is acceptable.
2	When grand score is 3 or 4, further investigation is required; changes may be necessary
3	When grand score is 5 or 6, investigation and changes are required soon.
4	When grand score is 7, investigation and changes are required immediately.

3. THE SIMULATION TOOL: DELMIA

Human modelling systems are considered a basic element for a more efficient design process. In this sense, virtual ergonomic simulation can be used for taking decisions concerning worker postures or sequence of movements, workplace layout and other features which have consequences both in cost and risk of injures. Thus, DHM's not only need to be realistic but their results must be reproducible and verifiable in order to be useful tools for design and evaluation purposes. Some studies regarding this issue have been made. One of them was conducted jointly by the U.S. Air Force and TNO Human Factors and showed that a DELMIA virtual manikin provides 94% fidelity compared to a real subject, in contrast to 64% to 80% fidelity for other competitors in this field (Oudenhuijzen 2008).

The simulator allows the generation of human postures using either direct or inverse kinematics. DELMIA proposes a predetermined set of angular joint speeds corresponding to the average performance of the considered segment of population. Although these times do not directly imply an ergonomically safe movement, they are a reasonable basis to this end. Accordingly, comparative analyses of deviations between actual and simulated times have been conducted as a means of identifying plausible sources of ergonomic exposures.

A typical splitter has centred the tasks analysis although data were also collected and analyzed from other two different splitters for validating purposes. This worker is a well trained and experienced middle-aged man. A right-handed virtual manikin corresponding to the 50th percentile (P50) of the French male population anthropometric distribution was adopted for the simulation model as it fits the splitter's profile. Also, all data related to the geometric and operational workplace characterization were obtained and the corresponding elements were built.

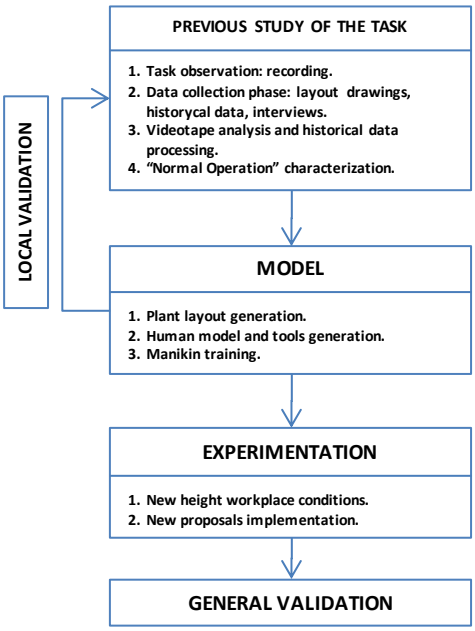

Figure 3: The General M&S Sequence

The overall M&S development process is depicted in Figure 3. The tasks have been characterized and analyzed by means of video recordings, technical layout drawings, historical data and interviews. Then the modelling process may start by reproducing a virtual environment assuring the geometric similarity (Figure 4). Defining the precise and complete set of tasks and MTPs –Moves to Posture- is a delicate and exact process. Once the model is verified and validated, the experimentation phase may begin. After this phase, a general validation is considered. It will imply to fit the new proposal in a simulation model of the whole plant in order to ensure their feasibility and productivity.

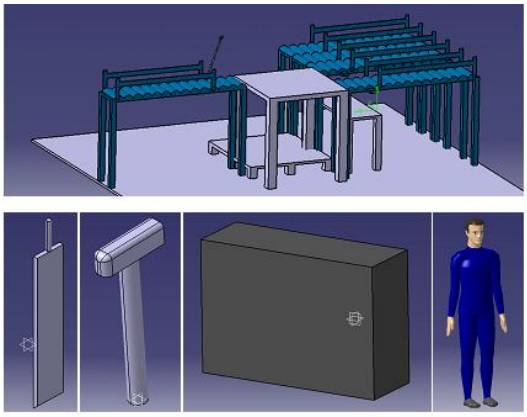

Figure 4: The elements of the Virtual Model.

4. SIMULATION MODEL VERIFICATION AND VALIDATION

The valid recreation of a real system in a simulation environment demands the accomplishment of both verification and validation phases. To do so, we based on a combination of visual and operational assessment of the simulation model.

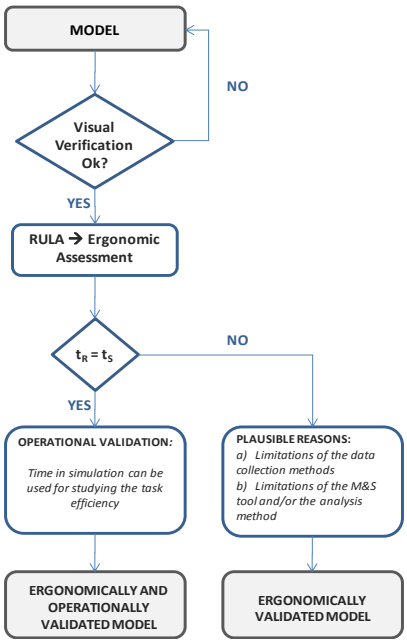

Figure 5: The Validation Model Scheme.

The exhaustive visualization of the model as it is simulated allows the identification of discrepancies and inaccuracies between the virtual and the real process. At this point the experience and opinions of the actual workers and company engineers have been necessarily considered. At the same time, we compared real and virtual tasks times and then we analyzed their fitness. Deviations between simulation times (tS) and their equivalent real times (tR) were then studied until finding out their origin. The followed procedure is shown in Figure 5.

This process leads to an ergonomic and operational validation in most cases. However, in some tasks only the ergonomic validation has been reached as the operational accuracy has not been good enough. We took this decision whenever the gap between simulation and real times was more than 20%. We have identified two main reasons that explain these differences.

The first one is that despite the easiness and quickness of our video tape approach, its limitations as a data acquisition method are important when compared with other motion capture systems. As a consequence, it was difficult to model some complex, quick and simultaneous body movements. The second cause of these deviations is that DELMIA does not consider accelerations as such but to assimilate percussions to sweeping movements. However, it is important to point out that our model has provided valuable, quick and fit for purpose results, according to the company expectations and also to our budget, time and scope restrictions.

5. EXPERIMENTATION

The National Institute for Occupational and Safety Health (NIOSH) proposes general ranges of optimal workbench heights depending on the required effort level of the task. Working activities are generally classified in three categories, namely, precision work, light work and heavy work. In addition, as workers heights are evidently different, it is also generally accepted to take not the workbench height as a reference but the elbow height. As a result, workbench height should be above elbow height for precision work, just below elbow height for light work, and between 10 and 16 centimetres below elbow height for heavy work (NIOSH 1997).

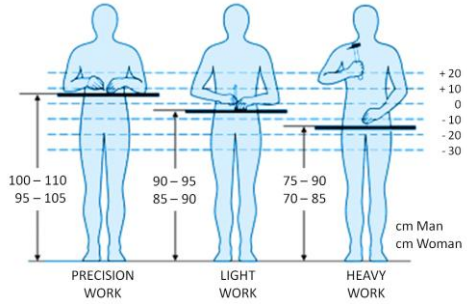

Figure 6: Recommended Workbench Heights depending on the Task Effort Level.

While performing their tasks, splitters combine heavy, light and precision work in a continuous series of quick and repetitive movements so that it is very difficult to identify their corresponding shares and so determining a kind of ergonomically workbench height. Besides, as most of them use a pallet to separate from the wet floor, the effect of height on the ergonomic characterization of the actual operation is far from immediate.

Our manikin is 1.74 metres height but considering the extra pallet height, the effective worker height is ten centimetres higher. Another consideration is that the workbench surface is not actually where the splitter is engaging his tasks, but the upper surface of the slate block.

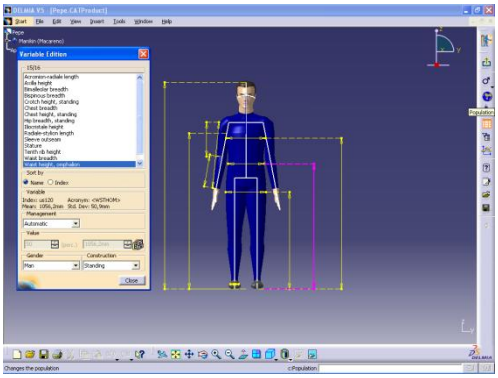

Figure 7: Virtual Manikin Anthropometric Characteristics

To assess the influence of working height on the task performance, two simulation scenarios have been proposed. The first one is analyzed in the so called H1 simulation. It implies that the splitter's elbow is 16 centimetres above the upper surface of the slate block, so this arrangement is in line with a heavy work approach. In the H2 simulation, we do not consider the presence of the pallet so the worker's elbows are 6 centimetres above the working surface. This scenario fits with a light work level. In both cases, the whole range of tasks a splitter has to accomplish has been simulated.

5.1. H1 Previous Operations

Previous Operations include receiving and placing the block on the working table. Not seldom it requires the worker to laterally push it until is properly placed. The worker holds the hammer with his right hand and is forced to bend his back to grasp the rough splitting chisel which is on the working table.

Previous Operations modelling has involved the definition of more than 80 postures that happen in a sequence of 8 seconds. Every posture is assessed using RULA. There is little difference between the actual total operation time and the simulated, which means that it represents quite enough the operation.

As shown in Figure 9, the risk level reaches 4 at the beginning, corresponding with the initial block positioning that requires waist twisting and pushing. It maintains level 3 until the final back bending when it rises to level 4.

Figure 8: Previous Operations.

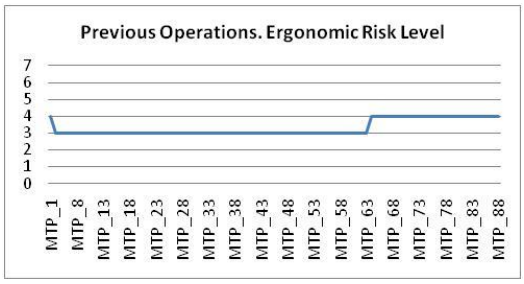

Figure 9: Previous Operations Ergonomic Assessment.

5.2. H1 Rough Splitting

This is the task where physical strength requirements are higher. The block is initially divided into several slabs depending on its length and on the presence of flaws so it may present different durations. If the worker notices the existence of flaws that affect either to the whole block or a part of it, he will throw it to the waste conveyor belt next to him. In this sense, splitting has also a deal of responsibility regarding inspection tasks. The early flaws detection saves time and costs as it reduces reprocessing tasks.

The Rough Splitting simulation shows a significant deviation of -65% between the simulated and the actual hamming time. The cause of this deviation is that the simulator does not consider accelerations as such but to assimilate percussions to sweeping movements, so is underestimating the level of effort. Moreover, two factors have to be accounted. On the one hand, percussions imply noise and vibrations that are transmitted to the body through the hand and arm. On the other hand, inspection time is not being considered in this simple model. As a result, the time of the simulation is not realistic. However, ergonomic results are still acceptable.

Figure 10: Rough Splitting

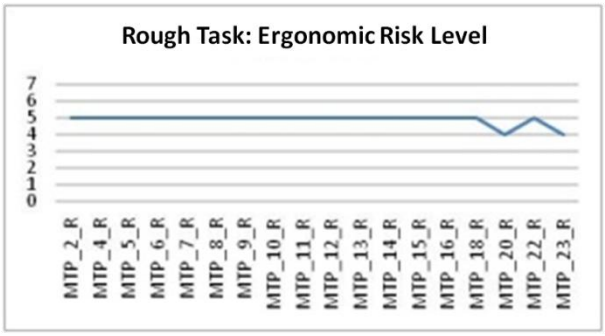

Figure 11: Rough Splitting Grand Score

Figure 11 depicts the associated risk for every posture. Risk levels range between 4 and 5. These levels indicate the convenience of changes to preventing from injuries in the mid and long term.

5.3. H1 Splitting

Splitting is a very skilful activity that determines the final commercial thickness of the slate tiles. Splitting with turning refers to the fact that the worker eventually needs to totally turn the part and hit it from the opposite side in order to effectively split it up.

In the splitting with turning case, the difference between real and virtual times is one of 54%. We probably commit this deviation due to the complexity of the positions being modelled. A set of complex positions -hand grasping, wrist turning, forearm approaching and the assistance of the left arm, among others- has to be built in a very quick sequence. A better biomechanical data input system should be preferable rather than an estimation of trajectories from recorded video frames.

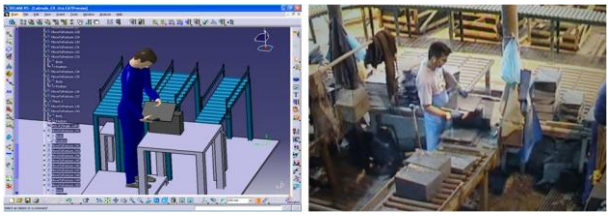
Figure 12: Splitting with Turning. The part is lifted and turned to be split again.

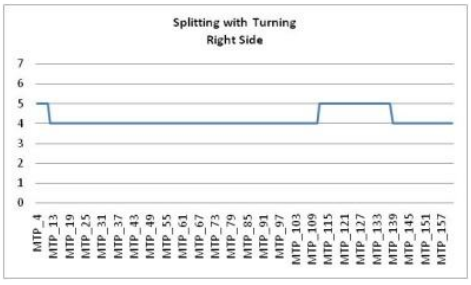

Figure 13: Right Side Analysis.

When the splitting task is simulated without turning, virtual times are similar to the real ones, but ergonomic risk level does not change compared with the turning case.

5.4. H1 Sorting

Sorting may result in many different situations. For the sake of simplicity, we model the two main sub-operations which happen more often. The first one is to reject the slate plate which implies that the worker needs to throw the slate over the waste conveyor belt which is located on his left side. The second one is to put a lot of slates on its corresponding rolling table, usually between 12 and 15 plates that involve a lifting load – about 10 kilograms– and a consequent exertion.

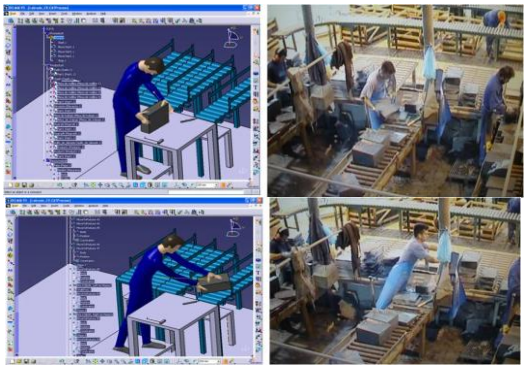
Figure 14: Sorting Task. Grasping and Placing a Lot of Target Size Plates.

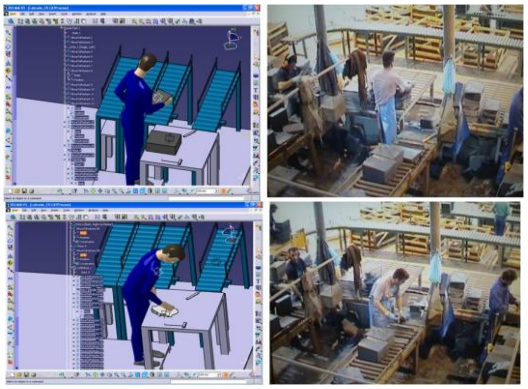
Figure 15: Sorting Task. Placing a Lot of Secondary Size Plates and Housekeeping.

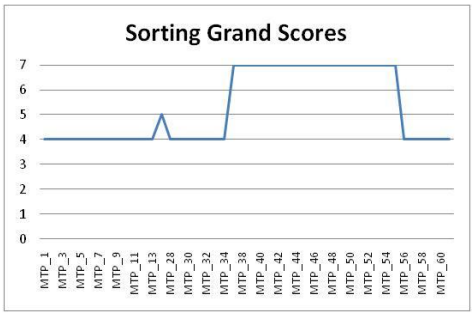

Figure 16: Sorting Task. Grand Scores according to the set of Moves To Posture (MTPs).

We have also modelled the workplace housekeeping tasks. The manikin bends, take a cloth, and cleans his workbench. Although this is not a truly productive task it plays an essential role in maintaining a safe and right production rate.

5.5. H1 Tasks Ergonomic Characterization

In Figure 17, a summary of the H1 case results is given. As it was expected, the overall ergonomic valuation of the splitter tasks is negative. The level of intervention is urgent in the sorting set of tasks and necessary or suggested for the rest.

TASK	PREVIOUS OPERATIONS	ROUGH SPLITTING	SPLITTING				SORTING
			NO TURNING		TURNING		
			KEEP	REJECT	KEEP	REJECT	
RISK LEVEL	3 and 4	4 and 5	4 and 5	4 and 5	4 and 5	4 and 5	4 to 7
LEVEL OF INTERVENTION	Suggested	Necessary	Necessary	Necessary	Necessary	Necessary	Urgent
PROPOSAL	Use of a Tool Belt			Layout Change		Layout Change	Layout Change

Figure 17: Summary of Results. Risk, Level of Intervention and Proposals for every Task are shown.

Some tasks are inevitable. Unless effective technological changes happen in the way the splitting operation is at present being done, splitting necessarily would require impacts and awkward movements and postures. So the chances of feasible and improving changes must focus on those tasks were unnecessary or unproductive movements have been identified. As a result, a set of three proposals that will be commented later on have been suggested.

5.6. H2 Simulation

To consider the influence of height we have also simulated all the previous working activities without the presence of the elevating pallet. We have named this experimentation scenario as H2. To summarize, in Figure 18, we present a results comparison between the H1 and the H2 scenarios

TASK	Previous Operations	Rough Splitting	Splitting		Sorting
			Keep	Reject	
Case H1	3 and 4	4 and 5	5	4	4 to 7
Case H2	3 and 4	5 and 6	4 and 5	3 and 4	3 to 6
Assessment H2 vs H1	Better	Worse	Better	Better	Much Better
Comments	Less duration in level 4 in H2	Higher grand scores in H2	Lower grand scores in H2	Lower grand scores in H2	Lower grand scores in H2

Figure 18: H2 and H1 Grand Scores by Task

For a 1.74 meters height splitter it is ergonomically better not to use the pallet, except in the case of rough splitting, where the grand score is then higher. It is more convenient for the splitter to work between 5 and 10 centimetres below his elbow rather than working as they currently do, i.e. between 15 and 20 centimetres. To do so, we suggest the employment of stackable drainage anti-fatigue floor mats so that the splitter can adjust exactly his working height and keep his feet dry. This would also help in absorbing vibrations and impacts so alleviating stress and fatigue in the feet, legs and back. These mats also have a non slip surface reducing the risk of slips and falls (CCOSH 2006).

6. IMPROVING PROPOSALS

The modelling process requires a thorough observation of the tasks under study. That is why the designer systematically questions the reasons behind every task and subtask. This is a very productive attitude as it eventually ends in improvement proposals to be simulated before their effective implementation. As a consequence, we propose a set of three actuations in order to improve the ergonomic and productive performance.

The first one consists of the employment of a tool belt by the splitters. The second proposal implies a feasible and almost immediate change in the workplace layout. The third proposal suggests a total change in the traditional layout scheme

6.1. The Use of a Tool Belt

The proposal of using a tool belt came up after the observation that the splitter needs to use his both hands so he is in many occasions forced to bend his back to put his tools –hammer and two chisels- on the table and pick them again later. These are unnecessary movements that should be avoided.

Although this may sound as a platitude, it is a remarkable fact that the employment of tool belts among the splitters, unlike other artisanal professionals, would be a brand new action, not only in this particular company, but in the whole sector. This simple accessory facilitates the work as it ensures comfortable reaching out to take the chisels without the need to bend forward or sideways.

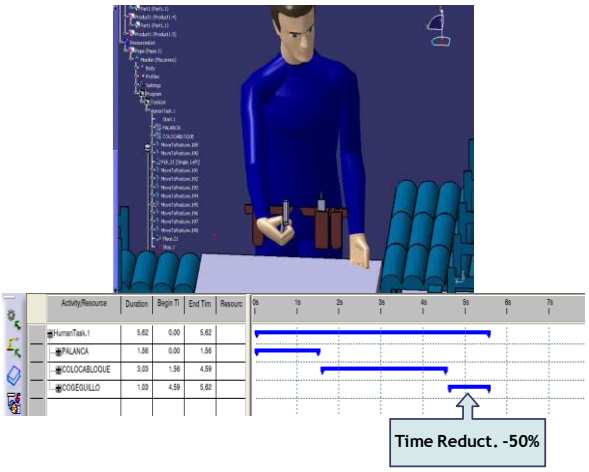

Figure 19: The Splitter wearing a Tool Belt. On the right, the Gantt Chart corresponding to the Previous Operations Task.

As shown in the Gantt chart in Figure 19, a 50% time reduction in the grasping chisel subtask is obtained. Besides, the operation is ergonomically better as risk reduces from level 4 to level 3.

6.2. Simple Layout Modification

We have simulated a simple low investment modified workplace layout. At present, the waste conveyor belt is located on the left side of the splitter so he is frequently obliged to twist and bend his trunk at the same time he is grasping and holding a variable number of plates or

even a whole block. So the aim is at avoiding these lateral movements required every time a block or a lot of plates are rejected which suppose a 25% of the total sorting movements.

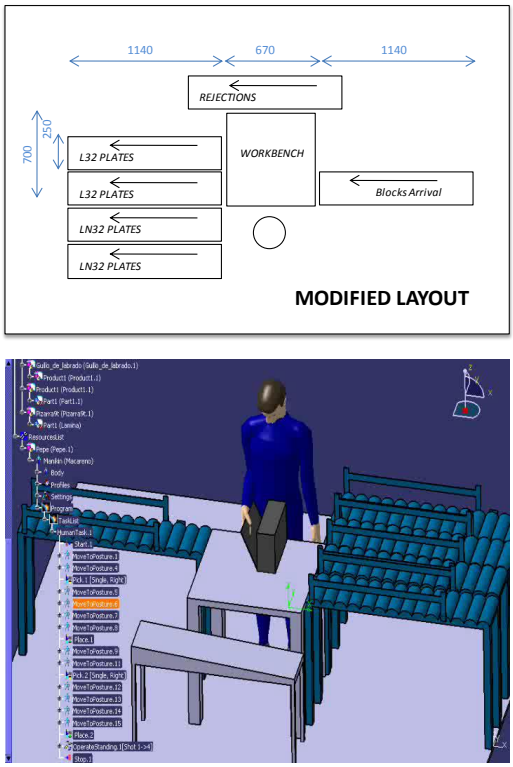

Figure 20: The Proposed Workplace Design.

The use of a front slide ramp connecting the working table with the waste conveyor belt would help reducing ergonomic risk from original level 4 to level 3. Besides, it is also a 15% faster, resulting in a more productive task.

6.3. Brand New Design: Circular Distribution

Whilst the two before mentioned proposals came up as a result of the information gathered during the modelling process, this initiative is the outcome of a specific design effort aimed at reducing the ergonomic impact and improving productivity of the sorting tasks, which show the highest grand scores.

A radial distribution scheme is then presented as an innovative conceptual design in this sector. It would imply a moderate investment since changes in layout and in production and transportation means would be required both upstream and downstream from this point.

The distribution belts have been located accordingly to their frequency of use in order to minimize the ergonomic impact and to maximize productivity. Thus, blocks arrive from the right side of the splitter. Then, the L32 plates belt is located, followed by the To Waste belt. The rejected materials are this way frontally pushed away, which is a much safer and faster operation. Finally, the less frequent movements correspond to the stacking of the two general sorts of LN32 plates.

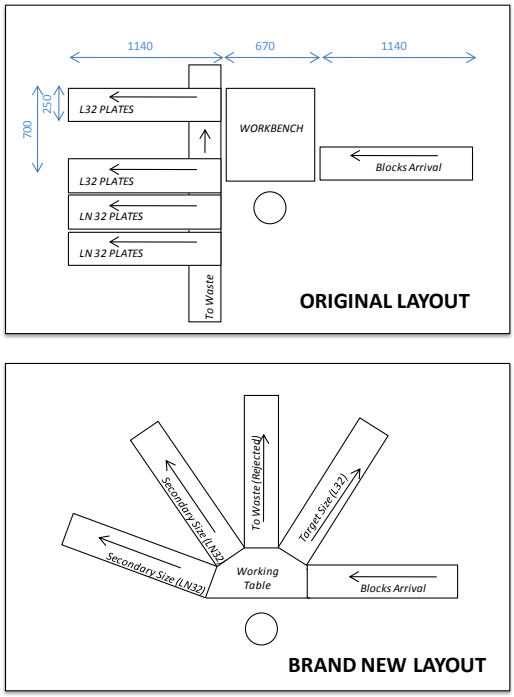

Figure 21: The Original Layout versus the The Proposed Radial Workplace Design.

This layout dramatically improves the time spent in sorting tasks. A 75% reduction in placing target size lots on its delivery rolling table is found. This also involves a less ergonomic risk as it never rises over level 3.

Table 4: Comparison in Sorting Times for several Scenarios

Time (s)	H1	H2	Radial Layout
Rejection	2,36	2,55	3,14
Target Lots	7,46	5,11	1,23
Total	11,15	8,29	4,37

CONCLUSION

A quantitative approach to a combined ergonomic and operational assessment of the slates splitters tasks has been presented. This is a brand new initiative in the slate roofing manufacturing sector. A RULA analysis has been carried out by means of a Digital Human Model (DHM) implemented in DELMIA aiming at the characterization, analysis and improvement of the whole set of tasks involved. The use of a DHM allows a systematic approach to the problem and provides a reproducible and modifiable model. After their implementation in the simulation environment, the model was then validated. The main conclusion is that this is an ergonomically hard work, especially during the sorting tasks. In addition, it is more convenient to work between 5 and 10 centimetres below the elbow rather than working between 15 and 20 centimetres. To do so we suggest avoiding the use of elevating pallets and substituting them by modular and stackable flooring mats for a good height adjustment.

A set of three improving changes was proposed and analyzed. The employment of tool belts would avoid unnecessary back bending and increase productivity. A simple ramp would change the sequence of movements required every time a rejection has to be done to a better ergonomically and faster operation. Finally, a specific new design aimed at optimizing simultaneously ergonomics and productivity was investigated, achieving these goals more than satisfactorily.

This paper summarizes the ergonomic assessment of the splitters work in the context of a broader process optimization project. So, it is not meant to be a rigorous and deep ergonomic analysis, but a means for the global improvement of the manufacturing process. Further research is still being carried out in cooperation with the company for the actual implementation of the results found.

ACKNOWLEDGMENTS

We wish to express our gratitude to the Xunta de Galicia, which has funded this work through the research project "Análise mediante simulación para a optimización do proceso de fabricación de lousas" (IN841C-2008/108).

REFERENCES

A.G.P. Asociacion Gallega de Pizarristas, 2010. *Slate, A Sector in Expansion*. Available from: http://www.agp.es/es/slate/ [accessed 11 April 2010]

BIC-Galicia, Escuela Técnica Superior de Ingenieros de Minas de Vigo, 1997. *La Industria de la Pizarra en Galicia*. Consellería de Industria e Comercio de la Xunta de Galicia.

Boeing Human Modelling System, 2010. Available from: http://www.boeing.com/assocproducts/hms/index.html/ [accessed 11 April 2010]

Campbell, M., Thomas, H., Hodges, N., Paul, A., Williams, J., 2005. A 24 year cohort study of mortality in slate workers in North Wales. *Occupational Medicine*, vol. 55,nº 6,pp.448 – 453

CCOHS Canadian Center for Occupational Health and Safety, 2006. *Anti-fatigue Mats*. Available from: http://www.ccohs.ca/oshanswers/ergonomics/mats.html [accessed 30 July 2010]

Cimino, A., Curcio, D., Longo, F., Mirabelli, G., 2008. Workplaces Effective Ergonomic Design: A Literature Review. *Proceedings of the European Modelling and Simulation Symposium*. September 17-19, Campora San Giovani (Amantea, Italy).

Cimino, A., Mirabelli, G., 2010. Modelling and Simulation and Ergonomic Standards as a Support Tools for a Workstation Design in Manufacturing System. *International Journal of Simulation and Process Modelling*, Vol. 6, Number 11, pp. 78-88.

del Rio Vilas, D., Crespo Pereira, D., Crespo Mariño, J.L., Garcia del Valle, A., 2009. Modelling and Simulation of a Natural Roofing Slates Manufacturing Plant. *Proceedings of The International Workshop on Modelling and Applied Simulation*, pp. 232-239.September 23-25, Puerto de la Cruz (Tenerife, Spain).

Fundación para la Prevención de Riesgos Laborales, CIG, 2008. *Identificación de riesgos laborales y guía de buenas prácticas en la extracción de piedra natural*. Report. CIG Gabinete Técnico de Saúde Laboral.

Guiver R, Clark R., 2002. *Visualization of occupational exposure to respirable crystalline silica dust during slate splitting activities*. HSL Report FMS/02/03.

McAtamney, L., Corlett, E.N., 1993. RULA: A survey method for the investigation of work-related upper limb disorders. *Applied Ergonomics*, 24 (2), 91-99.

NIOSH National Institute for Occupational Safety and Health, 1997. *Elements of Ergonomics Programs. A Primer Based on Workplace Evaluations of Musculoskeletal Disorders.* U.S. Department of Health and Human Services. Public Health Service, USA.

Neumann, W.P., Wells, R.P., Norman, R.W., Kerr, M.S., Frank, J., Shannon, H.S., OUBPS Working Group, 2001. Trunk posture: reliability, accuracy, and risk estimates for low back pain from a video based assessment method. *International Journal of Industrial Ergonomics*, 28, 355-365.

Oudenhuijzen A., Zeltner G.F., Hudson J.A., *Verification and Validation of Human Modeling Sytems*, Cap.23, Handbook of Digital Human Modelling: research for applied ergonomics and human factors engineering. Edited by Vincent G. Duffy, CRC Press, 2008.

OSHA European Agency for Safety and Health at Work, Risk Observatory, 2005. *Expert forecast on emerging physical risks related to occupational safety and health.* European Communities, Belgium.

Santos, J., Sarriegi, J. M., Serrano, N., Torres, J. M., 2007. Using ergonomic software in non-repetitive manufacturing processes: A case study. *International Journal of Industrial Ergonomics*, 37, 267-275.

Shao-Wen, C., Mao-Jiun J. W., 2007. Digital human modeling and workplace evaluation: Using an automobile assembly task as an example. *Human Factors and Ergonomics in Manufacturing & Service Industries*, Volume 17, Issue 5, 445 – 455.

Weber, M., Capron, J. L., Schwartz, P., 1996. Lombalgies chez les mineurs des ardoisières d'Angers: analyse de 299 cas vus au contrôle médical. Archives des maladies professionnelles et de médecine du travail, vol. 57, No. 4, pages 294-296.

AUTHORS BIOGRAPHY

Nadia Rego Monteil obtained her MSc in Industrial Engineering in 2010. She works as a research engineer at the Engineering Research Group (GII) of the University of A Coruna (UDC). Her areas of major interest are in the fields of Ergonomics and Process Optimization.

David del Rio Vilas holds an MSc in Industrial Engineering and has been studying for a PhD since 2007. He is Adjunct Professor of the Department of Economic Analysis and Company Management of the UDC. He has been working in the GII of the UDC as a research engineer since 2007. He is involved in R&D projects development related to industrial and logistical processes optimization.

Diego Crespo Pereira holds an MSc in Industrial Engineering and he is currently studying for a PhD. He is Assistant Professor of the Department of Economic Analysis and Company Management of the UDC. He also works in the GII of the UDC as a research engineer since 2008. He is mainly involved in the development of R&D projects related to industrial and logistical processes optimization.

Rosa Rios Prado works as a research engineer in the GII of the UDC since 2009. She holds an MSc in Industrial Engineering. She is especially dedicated to the development of transportation and logistical models for the assessment of multimodal networks and infrastructures.

ENHANCING QUALITY OF SUPPLY CHAIN NODES SIMULATION STUDIES BY FAILURE AVOIDANCE

Francesco Longo[(a)], Tuncer Ören[(b)]

[(a)]M&SNet (McLeod Modeling & Simulation Network)
Modeling & Simulation Center Laboratory of Enterprise Solutions (MSC-LES)
University of Calabria, Italy

[(b)]M&SNet (McLeod Modeling & Simulation Network)
SITE, University of Ottawa, Ottawa, ON, Canada

[(a)]f.longo@unical.it, [(b)]oren@site.ottawa.ca

ABSTRACT

An example for simulation studies of a supply chain node is developed. Highlights of failure avoidance (FA) – as a paradigm to enhance simulation studies– is given. Some cases of the application of FA to enhance supply chain node simulation studies are enumerated. It is worth exploring the potential of FA as explained in detail by Ören and Yilmaz (2009) to extend ways to avoid failures in simulation studies and to enhance their usefulness.

INTRODUCTION

According to Simchi-Levi et al. (2007), a Supply Chain is a network of different entities or nodes (i.e. industrial plants, contractors, distribution centers, warehouses, retailers, marine ports, etc.) that provide materials, transform them in intermediate or finished products and deliver them to customers to satisfy market requests (including information and finance flows). The business globalization has transformed the modern companies from independent entities to extended enterprises that strongly cooperate with all supply chain actors/nodes. Each supply chain manager aims to reach the key objective of an efficient supply chain: 'the right quantity at the right time and in the right place'.

To this end, each supply chain node carries out various processes and activities for guarantying goods and services to the final customers. The competitiveness of each supply chain actor depends by its capability to activate and manage change processes, in correspondence of optimistic and pessimistic scenarios as well as to quickly capitalize the chances given by market. Such capability is a critical issue for improving the performance of the 'extended enterprise' and it must take into account the complex interactions among the various nodes of the supply chain. The evaluation of correct trades-off between conflicting factors, i.e. inventory reduction (control policies) and fill rates, customers' satisfaction (service levels) and transportation cost (lead times), sales loss and inventory costs, is the complex task of an efficient supply chain manager (De Sensi et al., 2008).

The behaviour of real-world supply chains is usually affected by a wide range of factors. The ways in which such factors interact and the stochastic nature of their evolution over the time increase their complexity up to critical levels, where the use of ad-hoc methodologies, techniques, applications and tools is the only way to tackle problems and succeed in identifying proper and optimal solutions. Modelling & Simulation (M&S) has been widely recognised as one of the best and most suitable methodologies for investigation and problem-solving in real-world supply chains in order to choose correctly, understand why, explore possibilities, diagnose problems, find optimal solutions, train personnel and managers, and transfer R&D results to real systems (Banks, 1998). Therefore it is worth exploring new paradigms to enhance simulation studies. In the first half the article proposes, as example, a detailed simulation study for Genoa-Voltri container terminal (*Voltri Terminal Europa*). The second part of the article is devoted to Failure Avoidance (FA). Along with Verification & Validation (V&V) and Quality Assurance (QA), Failure Avoidance provides a third layer of possibilities to enhance simulation studies where the capabilities of the first two layers are exhausted.

MARINE TERMINALS AS CRITICAL SUPPLY CHAIN NODES

Marine terminals and, above all, container terminals are critical nodes of the global supply chain. Genoa-Voltri container terminal (*Voltri Terminal Europa*) is one of the most important container terminals of the Mediterranean area (see figure 1). The port capacity is about 1.0 million of equivalent containers (TEU) per year. The total berth length is 1,400 meters, the deep-water berth is about 15 meters and the yard covers more than 900,000 square ~~s~~ meters. The technical equipment in the docking area includes 10 portainers post-panamax for ships loading and

unloading operations (from 40 to 50 tonnages). Connections between docking area and yard are performed by using 22 forklifts (with variable tonnages) and 60 yard tractors. Yard area equipment includes 23 Rubber Tired Gantry (RTG) for container movements (from 35 to 45 tonnages). In addition, located opposite to the berth, the container terminal is equipped with the rail service: 8 different tracks (700 meters in length) for loading/unloading operations) and 4 lead tracks. In the rail area, loading and unloading operations are performed by using 3 Rail Mounted Gantry (RMG) up to 45 tonnages. The Genoa-Voltri container terminal scenario is subdivided in 4 different parts:

- Berth Operations;
- Yard Operations
- Rail Service and Trucks Operations;
- Security Operations and Containers Inspection.

Figure 1: A view of Voltri Terminal Europe

An accurate description of the container terminal main operations (and related simulation models) is reported in the sequel. Note that one of the most important steps of a simulation study is data collections. Some of the data used in the simulation model are gathered from the website of the Voltri Terminal Europe; other data are based on subject estimation based on authors' experience (Longo and Bruzzone, 2005; Longo et al. 2005; Bruzzone et al. 2005; Curcio et al. 2007;; Longo 2010). Input data analysis follows the classic approach based on distribution fitting (Montgomery, 2003; Nist/Sematech, 2007).

Berth Operations

The ships entering the port are about 280 meters in length with capacity between 2000 and 4000 TEUs. The exact number of containers transported by each ship is inferred from uniform distribution with minimum value 2000 and maximum value 4000. Docking and undocking operations are performed by using tugboats. The amount of time for docking and sailing operations is inferred from a triangular distribution with average value 2 hours. The portainers mean productivity is 30 TEUs per hour, the mean operating time is 2 min/TEU and the standard deviation, expressed as percentage of the mean operating time, is 12-20%. After ship docking operations, unloading/loading operations begins: in both the cases containers wait in small buffers located in correspondence of each portainer.

The simulation model is developed by using Anylogic, by XjTech as seen in Figure 2. The first part of the simulation model flow chart recreates the berth operations. The arrivals process of the vessels is managed by source objects. Each *vessel* entity has specific attributes as, for instance, the number of containers to unload, the logistic company, the type of materials inside the containers. Once the *vessel* entity has been created, it is moved to the object *traffic Manager* Object that decides whether the vessel can enter the port or not (it must wait outside because of vessels traffic conditions). Each vessel entity moves then into the *Docking Operations* Object to check berth availability and select berth position. A tugboat resource (that support docking operations) is seized by the vessel entity; after seizing a *tugboat* resource and completing docking oeprations the *vessel* entity moves into the *Berth Operation* to start loading/unloading operations. Note that both the *Docking Operation* Object and the *Berth Operation* Object have multiple in/out ports used to allows the allow the flow-in and flow-out of vessels and containers in the berth area.

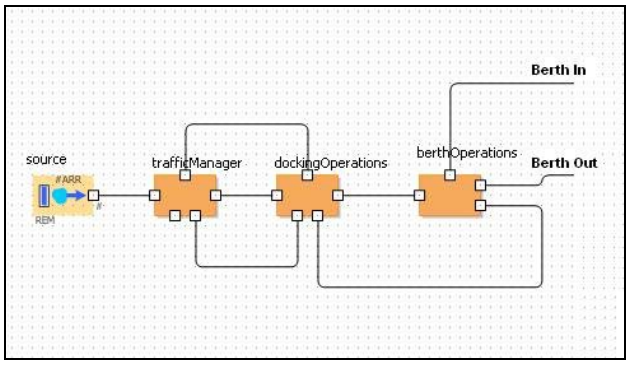

Figure 2: First part of the flow chart: vessel docking operations and berth operations

Yard Operations

Let us consider only the containers unloaded from a vessel after docking operations; in other word let us consider the modelling aspects related to the containers flow-in (the modelling aspects of containers flow-out are very similar).

At this stage, the containers have been unloaded from the vessel and wait to be moved to some destinations in the yard. Connections between buffers of portainers and yard are performed using tractors. Tractors mean productivity is 4 min/TEU and the standard deviation, expressed as percentage of the tractor mean productivity, is 35%-45%.

Tractors leave the containers in the yard; containers handling within the yard is performed by using RTGs and forklifts. RTGs and forklifts mean productivities are quite similar to tractors productivity (RTGs are characterized by smaller standard deviations, about 20%-30%). The figure 3 shows the remaining part of the simulation model.

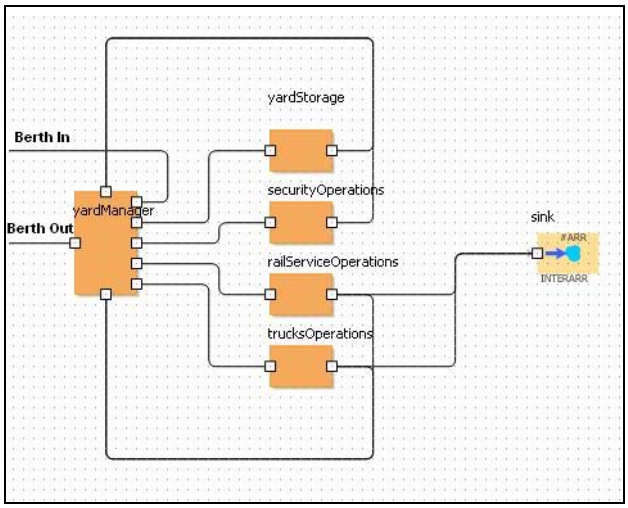

Figure 3: Second part of the flow chart: yard operations, security operations, rail service and trucks operations

Containers entities enter the *Yard Manager* object which task is to recreate yard management operations according to logic and rules used in real container terminals. Containers entities can be stored in the yard or follow another path toward *Security Operations* (discussed in the next section), *Rail Service Operations* or *Trucks Oeprations* (in the last two cases the containers leave the port respectively by train or truck). In each case the *container* entity waits for a tractors to be moved to its final destination. If the *container* entity is moved into the *Yard Storage* Object or into the *Security Operation* Object then it does not leave the port. When the *container* leaves the *Yard Storage* Object there are three possible alternatives:

- the container is moved into the *Trucks Operations* Object then a truck picks up the container and leaves the port by road transportation.
- the container is moved into the *Rail Service Operations* Object then a tractor picks up the container and moves it in the rail area (to be loaded on a train).
- The container is moved into the *Security Operations* Object then a truck picks up the container and moves it into the security area for inspection operations.

Please note that similar alternatives are available when the *container* leaves the *Security Operations* Object (in this case the *container* can move into the yard, rail service or trucks). Furthermore as previously stated, the modeling aspects related to container flow-out are pretty similar to those already described in this section, therefore they are not reported in the article.

Security Operations and Container Inspection

A *container* is moved into the *Security Operations* Object according to the value of its risk index defined as entity attribute and randomly generated before the unloading operations. Security in the container terminal is mostly related to the containers inspection operations that include different activities. First, by using a scanning equipment a digital image of the container is created (i.e., by using gamma ray). The image analysis aims at discovering container anomalies. In addition, security officers carry out container physical and visual checks and radiation inspections. In case of detection of anomalies, the officers perform additional inspection operations. If no anomalies are detected the entity is sent back to its final destination

THE ANIMATION AND THE FINAL SIMULATION MODEL

The simulation model animation is based on a previous simulation model developed by authors (Longo, 2007) and use *network* objects. Network objects include

- rectangles to recreate entry/exit points, idle positions for resources, or destination points in the port;
- Lines to recreate trajectories followed by entities moving among rectangles;
- Resources to provide entities flowing in the network (i.e. containers, tractors, trucks, etc.) with different types service while moving within the network (i.e. a *container* entity seizes a *tractor* resource to move from the berth into the yard).

The *network* objects combined with the images of the terminal layout, containers, vessels, tractors, trucks, RTG, RMG, form the simulation model animation. Among others, one of the difficulties in implementing the animation was to set correctly the scale. This is required to set appropriately resources speeds and distances in the port area.. The animation is finally completed reporting information about port operations and simulated time in a display (see figure 4).

Note that in the simulation model the most important system variables are defined as parameters.

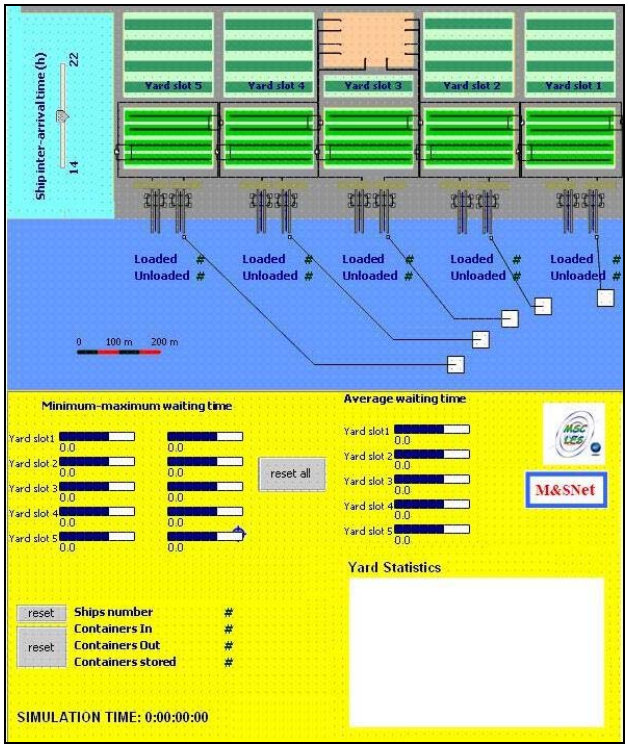

Figuure 4 – Animation and Final Simulation Model

All the parameters can be controlled from a graphic user interface (not depicted in figure 4). The graphic user interface of the simulation model allows changing the following parameters:

- Number of containers to load/unload (both from ships and from trains);
- Ships and trains mean inter-arrival times;
- Tugboats number and average speed;
- Forklifts numbers and average speed;
- Tractors number and average speed;
- RTGs number and average speed;
- RMGs number and average speed;
- Trucks number and average speed;
- Loading and unloading time for each yard, berth and rail equipment;
- Containers percentage to inspection;
- Manpower for inspection procedures;
- Tractors for inspection procedures;

Statistics and performances measures defined in the simulation models can be plotted on graphics, diagrams, histograms as well as can be exported on excel or text files. Statistics and performance measures regard number of inspected containers, inspection service time, inspection waiting time, containers daily flow entering the port, containers daily flow exiting the port, total number of containers entered, total number of containers exited, actual number of stored containers, berth cranes utilization, moved TEUs per structural unit (indicating the container terminal total efficiency).

Note that a container terminal is a non-terminating system, in other words the duration of a simulation run is not a-priori fixed. The first objective in this type of simulation model is to understand the optimal length of a simulation run. To this purpose we used the *Mean Square Pure Error* Analysis (MSpE) on different performance measures. In most of the cases the Mean Square pure Error becomes negligible after 290 days, so, such value has been chosen as optimal simulation run length.

Some preliminary analysis has been made to validate the simulation model. The results obtained show that the virtual container terminal moves, on the average 90.000 TEUs per month. Such value is similar to the statistics recorded in 2008 in the Genoa-Voltri container terminal.

FAILURE AVOIDANCE

The supply chain nodes simulation study presented in the first part of this article is a realistic study in an important logistic problem. In this second part, we elaborate on an important novel paradigm to avoid errors in modeling and simulation studies.

Similar to real systems, errors can occur in modeling and simulation. Appendix A is a list of 175 types of errors. Some relevant concepts are failure, mistake, error, fault, defect, deficiency, flaw, shortcoming, sophism, and paralogism. Brief definitions follow:

"Failure – "An event that does not accomplish its intended purpose."
"1. The condition or fact of not achieving the desired end or ends.
2. Nonperformance of what is requested or expected." (AHD)

Mistake – "1. An error or fault resulting from defective judgment, deficient knowledge, or carelessness.
2. A misconception or misunderstanding." (AHD)

Error – "1. An act, assertion, or belief that unintentionally deviates from what is correct, right, or true.
2. The condition of having incorrect or false knowledge.
3. The act or an instance of deviating from an accepted code of behavior.
4. A mistake.
5. *Mathematics* The difference between a computed or measured value and a true or theoretically correct value." (AHD)

Fault – "Something that impairs or detracts from physical perfection; a defect." (AHD)

Defect – "A serious functional or structural shortcoming." (AHD)
*Deficien*cy– "The quality or condition of being deficient; incompleteness or inadequacy." (AHD)
Flaw – "An often small but always fundamental weakness." (AHD)
Shortcoming – "A deficiency; a flaw." (AHD)
Sophism – "A deliberately invalid argument displaying ingenuity in reasoning in the hope of deceiving someone."
Paralogism – "Mistakenly invalid argument: in logic, an invalid argument that is unintentional or that has gone unnoticed" (Ören and Yilmaz, 2009).

There are three paradigms to reduce errors in simulation studies. They are: (1) V&V (validation and verification, (2) QA (quality assurance), and (3) FA (failure avoidance).

V&V (validation and verification) and QA paradigms

It is out of the scope of the article to present on overview of V&V and QA paradigms; however the most important references are provided below. V&V paradigm consists of a large number of techniques (Balci and Sargent, 1984; Balci, 1987, 1998). The focus is to develop a correct and appropriate model of the system of interest and computerize it correctly. Some early references on QA of simulation studies are developed by Ören (1981, 1984). Later, Ören (1986, 1987) developed quality assurance paradigms for Artificial Intelligence in modeling and simulation. Quality assurance paradigm is more comprehensive than verification and validation paradigm. (Balci 2004, Balci et al. 2009).

FA (failure avoidance) paradigm

"Two relationships exist between failure avoidance and simulation. Simulation can be used successfully for failure avoidance in several fields and failure should be avoided in simulation" (Ören and Yilmaz 2009). Many examples of failures in simulation studies are referred to in Ören and Yilmaz (2009). Failure avoidance paradigm benefits from systems approach and systems engineering paradigms and considers all aspects of failure. Table 1 lists categories of sources of errors that can occur.

Table 1. Categories of sources of errors
(adopted from Ören and Yilmaz, 2009)

In M&S, sources of failures can be:
Project management
Goal of the study
Scope of the study
Instrumentation
Data collection
Assumptions (explicit and/or implicit) in specifications of problem, models, experiments
- (scenarios, experimental frames) and
- (model, experimental frame) pairs
Modeling (conceptual models)
Scenarios (experimental conditions)
- realism and applicability of scenarios
- consistency of joint scenarios in federations and federations of federations
Design of experiments
Experimentation (behavior generation)
Computerization (of models, experiments, run-time libraries, and infrastructure)
Computation
- numerical computation
- soft computing
Logic and fallacies in logic (paralogism, sophism)
Artificial intelligence
- rule-based –expert– systems
- software agents (trustworthy agents, moral agents)
M&S infrastructure (including run-time facilities)
Documentation (inconsistent, erroneous, non-existent)
Communication (between stakeholders)
Recommendation of the simulation study
Implementation of the recommendations
- not implementing (ignoring the study)
- late implementing
- improper implementation

A successful M&S study can benefit from a multi-paradigm approach; i.e., from application of V&V, QA, as well as FA approach.

Some concerns to enhance the supply chain nodes simulation studies

Each simulation study has a goal and associated scope of applicability. However, most simulation studies can be enhanced either (1) by failure avoidance or (2) by extending its scope. To *enhance* the operations of the supply chain nodes operation, the study can be extended by systematically asking "what can go wrong?" type of questions. For example, the supply chain nodes operation study can be enhanced in the following dimensions:

- *Role of terrorist activities*. Impact of two types of activities can be studied; to eliminate them or to alleviate their impact: (1) Using containers to smuggle material to be later used in terrorist activities within a country. (2) Impact of terrorist activities on the equipment of a supply chain node.
- *Global supply chain risk management simulations.* In effect, the authors already used simulation for

supply chain risk and resilience enhancement (see Longo and Ören, 2008).

- *Container scanning risk management simulation.* As in the previous case the authors are well aware of the importance of simulation in container scanning/inspection operations (Longo, 2010).
- *Role of maintenance of several types of equipment*. Similar to the simulation studies of a job shop, several types of equipment in a supply chain node would require maintenance. The existing study can be extended for this purpose. Otherwise, the existing study may not be sufficient to analyze the need and allocation of resources for maintenance purposes.
- *Trend analyses of the usage of the capacity of supply chain node*. Under different past conditions the capacity utilizations and associated usage trends can be established. This information can be used in marketing the unused capacity; or coupled with simulation studies with anticipated demands can be used to perform investment analyses.

CONCLUSION

An example for supply chain node simulation studies is developed (the simulation model of a container terminal is presented). Highlights of failure avoidance (FA) – as a paradigm to enhance simulation studies – is given. And some cases of the application of FA to enhance supply chain node simulation studies are enumerated. In is worth exploring the potential of FA as explained in detail by Ören and Yilmaz (2009) to extend ways to avoid failures in simulation studies and to enhance their usefulness.

REFERENCES

(AHD) – American Heritage Dictionary. http://www.bartleby.com/61/27/F0012700.html

Balci, O. (1987). Credibility and Assessment of Simulation Results: The State of the Art. Methodology and Validation Proceedings of the Conference on Methodology and Validation, pages 6–9, 1987.

Balci, O. (1998). Verification, Validation, and Testing. In: J. Banks, Editor, Handbook of Simulation, Engineering & Management Press (1998), pp. 335–393.

Balci, O. (2004). Quality Assessment, Verification, and Validation of Modeling and Simulation Applications. Winter Simulation Conference 2004, 122-129. http://www.informs-cs.org/wsc04papers/015.pdf

Balci, O and R.G. Sargent (1984). A Bibliography on the Credibility Assessment and Validation of Simulation and Mathematical Models," Simuletter 15:3, 15-27.

Balci, O., Ormsby, W.F., and L. Yilmaz (2009). Quality Assurance of Simulation Studies of Complex Networked Agent Systems. In Yilmaz, L. and T.I. Ören (eds.) (2009). Agent-Directed Simulation and Systems Engineering. Wiley Series in Systems Engineering and Management, Wiley-Berlin, Germany.

Banks, J., 1998. Handbook of Simulation, Wiley Interscience Publication.

Bruzzone A.G., Longo F., Papoff E., 2005. Metrics for global logistics and transportation facility information assurance, security, and overall protection. Proceedings of 17th European Simulation Symposium, October 20th – 22nd, Marseille, France.

Curcio D., Longo F., Mirabelli G., Papoff E. 2007. Analysis of Security Issues in Airport Terminals using Modeling & Simulation , Proceedings of European Conference on Modeling and Simulation, June 4-6, Prague, Checz Republic.

De Sensi G., Longo F., Mirabelli G. (2008). Inventory policies analysis under demand patterns and lead times constraints in a real supply chain. International Journal of Production Research, vol. 46(24); p. 6997-7016.

Longo F., Bruzzone A.G., 2005. Modeling & Simulation applied to Security Systems. Proceedings of Summer Computer Simulation Conference, July 24th – 28th, Philadelphia, Pennsylvania, USA.

Longo F., Mirabelli G., Viazzo S., 2005. Simulation and Design of Experiment for analyzing security issues in container terminals. Proceedings of the International Workshop on Modeling and Applied Simulation, October 16th – 18th, Bergeggi (SV), Italy.

Longo F., T. Ören (2008). Supply Chain Vulnerability and Resilience: A state of the Art Overview. In: Proceedings of the European Modeling & Simulation Symposium. Campora S.Giovanni (CS), Italy, 17-19 September, vol. I, pp. 527-533.

Longo F. (2010). Design and Integration of the Containers Inspection Activities in the Container Terminal Operations. International Journal of Production Economics, Vol. 125(2); p. 272-283, ISSN: 0925-5273.

Montgomery D.C. 2003. Applied Statistics and Probability for Engineers, John Wiley & Sons, Inc.

Nist/Sematech, 2007. eHandbook of Statistical Method, http://www.itl.nist.gov/div898/handbook/

Ören, T.I. (1981). Concepts and Criteria to Assess Acceptability of Simulation Studies: A Frame of Reference. CACM, 24:4, 180-189.

Ören, T.I. (1984). Quality Assurance in Modelling and Simulation: A Taxonomy. In: Simulation and Model-Based Methodologies: An Integrative View, T.I.

Ören, B.P. Zeigler, M.S. Elzas (eds.). Springer-Verlag, Heidelberg, Germany, pp. 477-517.
Ören, T.I. (1986). Artificial Intelligence in Quality Assurance of Simulation Studies. In: Modelling and Simulation Methodology in the Artificial Intelligence Era, M.S. Elzas, T.I. Ören, B.P. Zeigler (eds.), North-Holland, Amsterdam, pp. 267-278.
Ören, T.I. (1987). Quality Assurance Paradigms for Artificial Intelligence in Modelling and Simulation. Simulation, 48:4 (April), 149-151.
Ören, T.I. and L. Yilmaz (2009). Failure Avoidance in Agent-Directed Simulation: Beyond Conventional V&V and QA. In L. Yilmaz and T.I. Ören (eds.). Agent-Directed Simulation and Systems Engineering. Systems Engineering Series, Wiley-Berlin, Germany, pp.189-217.
Simchi-Levi, D., Kaminsky, P., Simchi-Levi, E., 2007. Managing the Supply Chain: the definitive guide for the business professional. McGraw-Hill College.

BIOGRAPHIES

FRANCESCO LONGO took the degree in Mechanical Engineering from University of Calabria (2002) and the PhD in Industrial Engineering (2005). He is currently researcher at the Mechanical Department (Industrial Engineering Section) of University of Calabria. His research interests regard modeling & simulation of manufacturing systems and supply chain management, vulnerability and resilience, DOE, ANOVA. He is Responsible of the Modeling & Simulation Center – Laboratory of Enterprise Solutions (MSC-LES), member organization of the MS&Net (McLeod Modeling & Simulation Network) He is also member of the Society for Computer Simulation International and Liophant Simulation.

TUNCER ÖREN is a professor emeritus of Computer Science at the University of Ottawa. His current research activities include (1) advanced M&S methodologies such as: multimodels (to encapsulate several aspects of models), multisimulation (to allow simultaneous simulation of several aspects of systems), and emergence; (2) agent-directed simulation; (3) cognitive and emotive simulations (including simulation of human behavior by fuzzy agents, agents with dynamic personality and emotions, agents with perception, anticipation, and understanding abilities); and (4) failure avoidance in M&S and user/system interfaces. He has also contributed in Ethics in simulation as the lead author of the Code of Professional Ethics for Simulationists, M&S Body of Knowledge, and multilingual M&S dictionaries. He has over 430 publications (some translated in Chinese, German and Turkish) and has been active in over 370 conferences and seminars held in 30 countries. He received "Information Age Award" from the Turkish Ministry of Culture (1991), Distinguished Service Award from SCS (2006) and plaques and certificates of appreciation from organizations including ACM, AECL, AFCEA, and NATO; and is recognized by IBM Canada as a Pioneer of Computing in Canada (2005). His home page is: http://www.site.uottawa.ca/~oren/ .

Appendix A. A List of 175 Types of Errors (adapted from Ören and Yilmaz, 2009)

absolute error	decision error	latent error	requirement error
acceptance error	deductive error	linearization error	residual error
accidental error	definition error	loading error	resolution error
accumulation error	description error	local error	rounding error
acknowledged error	design error	local integration error	round-off error
activation error	detected error	logical error	sampling error
active error	detection error	loss-of-activation error	scientific error
adjustment error	diagnostic error	machine error	semantic error
algorithm error	digitization error	measurement error	sensitivity error
algorithmic error	discretization error	measuring instrument error	sensor error
ambiguity error	disk error	mechanical error	sequence error
analysis error	dumping error	method error	simplification error
angular error	dynamic error	mode error	simulation error
approximation error	environment error	model error	single error
ascertainment error	error of rejecting valid model	modeling error	software design error
assumption error	estimation error	moral error	software error
attribution error	ethical error	non-sampling error	solution error
balance error	experimental error	observation error	specification error
balanced error	experimentation error	observational error	stable error
bearing error	extrapolation error	offset error	standard error
bias error	fatal error	omission error	static error
biased error	fixed error	overestimation error	substitution error
bit error	fractional error	parameter error	syntactic error
calculation error	frequency error	parameterization error	syntactical error
calibration error	gain error	parity error	syntax error
capture error	global error	perception error	system error
chaotic error	global integration error	persistent error	systematic error
classification error	global relative error	phenomenological error	transcription error
clerical error	hardware error	prediction error	transmission error
computational error	heuristic error	process error	truncation error
computer error	human error	processing error	type I error
computerization error	hypothesis error	program error	type II error
conceptual error	identification error	program-sensitive error	type III error
consistency error	inadvertent error	programming error	typical error
constraint error	inherited error	projection error	unacknowledged error
convergence error	input quantization error	propagated error	unbiased error
copying error	inscription error	proportional error	uncorrelated error
correlated error	instrument error	quadratic error	undetected error
cultural bias error	instrumentation error	random error	unification error
cultural perception error	integration error	read error	unstable
cumulative error	interpolation error	reasoning error	usage error
damping error	irrecoverable error	rejection error	user error
data error	judgment error	relative error	willful error
data-driven error	language error	representation error	

A STOCHASTIC APPROACH FOR THE DESIGN OF END-OF-LINE STORAGE AREA

Sara Dallari[(a)], Elisa Gebennini[(b)], Andrea Grassi[(c)], Magnus Johansson[(d)]

[(a, b, c)] Dipartimento di Scienze e Metodi dell'Ingegneria, Università degli Studi di Modena e Reggio Emilia
Via Amendola 2 – Pad. Morselli, 42122 Reggio Emilia, Italy

[(d)] Elettric 80 S.p.A.
Via G. Marconi 23, 42030 Viano (RE), Italy

[(a)]sara.dallari@unimore.it, [(b)]elisa.gebennini@unimore.it, [(c)]andrea.grassi@unimore.it, [(d)]johansson.m@elettric80.it

ABSTRACT
Nowadays, many companies tend to minimize inventories throughout the entire logistic process by adopting a cross-docking policy, i.e. preferring direct shipping rather than to store products.

In these systems the objective is to maintain synchronization between production and shipping processes, but storage areas are still necessary in practice to work as buffers able to compensate short period mismatches.

The paper proposes a stochastic approach to design such storage areas. In particular, the case in which a good trade-off between the number of storage zones (called *bins* in the following) and their size is addressed. The simulation is adopted to determine storage requirements from a stochastic point of view, and an analytic formulae is derived to evaluate an approximate coverage probability.

Keywords: cross-docking, storage requirements, stochastic aspects, block-stacking , lane depths

1. INTRODUCTION

The situation addressed in this paper is representative of many industrial companies, especially companies producing final goods with a shelf life quickly absorbed by market (e.g. beverage, foods). In this case, cross-docking policies are generally preferred (see Apte and Viswanathan 2000; Baker 2007).

In this paper it is assumed that Stock-Keeping Units (SKUs) are placed in specific zones of the storage area called *bins*. Such bins are limited zones where a number of pallets of the same SKU type can be stored. We assume that each bin has a single access point. Usually, bins are positioned on the ground or by gravity shelves.

Bins are not dedicated to a particular SKU type, but once just one pallet of a certain type of SKU is placed into a bin, that bin must hold that specific SKU type only. Once a bin gets empty again, it could be assigned to another SKU type as needed.

Configurations with an high number of low-capacity bins allow to hold different SKU types contemporaneously but the space available for storing products is reduced as a consequence of an high number of aisles needed to access the bins. On the other hand configurations with few high-capacity bins makes it possible to have an increased total storage space but it can hold only few SKU types. A trade off should be found to determine a good configuration.

This paper deals with the design and management of such storage areas. Thus, *tactical decisions*, i.e. medium term decisions regarding the dimensioning of the system and the layout determination (see the classification by Rouwenhorst et al. 2000) are addressed.

Even if various frameworks about warehouse design are available in the literature (refer as exemples to Baker and Canessa 2009; Ashayeri and Gelders 1985), the problem addressed in this paper is quite innovative and it is related to the pallet block-stacking problem. Block-stacking refers to unit loads stacked on top of each other and stored on the warehouse floor in lanes.

Gu et al. (2010) provided a comprehensive review of existing research results about warehouse design and performance evaluation, in particular for what concerns the pallet block-stacking problem.

This specific problem was treated by several authors and in particular the decision about the selection of lane depths was addressed.

Moder and Thornton (1965) developed mathematical models to evaluate ways of stacking pallets. Berry (1968) proposed an analytic model to evaluate a tradeoff between the material handling costs and the space utilization. Marsh (1979) provided a simulation model to estimate the space utilization of different lane depths. Marsh (1983) compared the layout design found using these two aforementioned approaches. A dynamic algorithm to maximize the space utilization by selecting lane depths was developed by Goetschalckx and Radliff (1991). Larson et al. (1997) proposed a heuristic approach to this problem,

having the purpose to maximize the utilization of the storage space minimizing material handling costs.

Thus, the specific problem is of interest but it was mainly approached in a deterministic way and, as Gu et al. (2010) pointed out, it was addressed usually with restrictive assumptions. Thus, further improvement is needed taking into account the uncertainty of storage and retrieval requirements.

The aim of this paper is the development of an approach and a methodology to define a good configuration of bins in the storage area. The goodness of a specific configuration is evaluated in terms of capacity of meeting storage requirements, under a stochastic point of view. Space constraints, SKUs' storage requirements and the contemporary presence of different SKUs in the storage area are taken into account.

2. THE METHODOLOGY

The methodological approach proposed in this paper aims to compare different bin configurations by taking into account stochastic aspects (e.g. production and shipping patterns).

In particular the methodology provides:

- a framework to model input data so that a stochastic representation of the space requirements in the storage area is given. This phase is carried out by using a simulation approach;
- the individuation of a performance function able to evaluate the satisfaction of the storage requirements.

The methodology, applied to a significant case study in Section 3, is organized in the following steps:

- Step 1: data collection;
- Step 2: analysis of production and shipping;
- Step 3: simulation model for each SKU type;
- Step 4: simulation campaign;
- Step 5: simulation output analysis;
- Step 6: bin configuration evaluation.

Each of the above steps is described in more detail in the following.

Step 1: Data collection. Production and shipping data referring to a specific period of time can be collected from the Enterprise Resource Planning (ERP) of the system under study.

The focus is on those SKU types that are frequently produced but not in a continuous manner, i.e. when the risk of temporary mismatches between production and shipping is significant. In this case, a proper storage area decoupling the two processes is needed.

Step 2: Analysis of production and shipping. Production and shipping are stochastic processes. We assume that the processes under study behave according to the conceptual model reported in Figure 1.

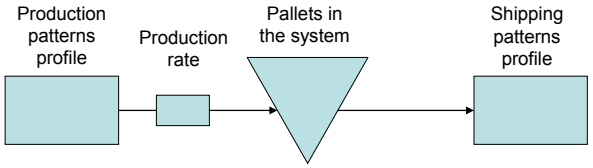

Figure 1: Conceptual model.

On-field production and shipping data can be grouped according to the SKU type so that both order sizes and interarrival times can be derived.

Then, these sequences of interarrival times and sizes of both production and shipping orders are fitted to achieve characteristic mass probability distributions. The probability distributions are the key input data of Step 3 where a simulation model of the system is developed according to the above conceptual model.

Therefore, in order to model realistic operative conditions, the conservation of the mean flow across the system must be guaranteed by the following equation:

$$\textit{Mean production flow} = \textit{Mean shipping flow} \qquad (1)$$

Moreover, any unrealistic values that can derive from the above distributions (e.g. too much large order sizes) are neglected.

Step 3: Simulation model for each SKU type. A simulation model is developed for each SKU type using the discrete-events simulator Flexsim™, in which production and shipping processes are represented by the mass probability distributions obtained in previous steps (Figure 2). The production orders can be satisfied on different production lines, even at the same time. Pallets processed by production lines enter endless queues waiting to be shipped. Thus, the queues between production and shipping provide the storage requirements over time for each SKU type.

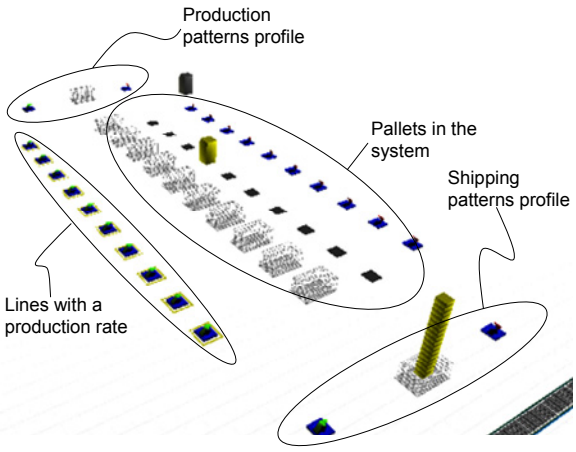

Figure 2: Simulation model.

Step 4: Simulation campaign. The simulation campaign consist in a long simulation run for each SKU type. Periodically, during the run, storage requirements

are logged to obtain a representative sample for each SKU type.

Step 5: Simulation output analysis. The simulation output is the trend of storage requirements for each SKU type. Note that the values of interest are those related to the steady state and do not include the warm-up period. As shown in Figure 3 the warm-up period can be easily identified.

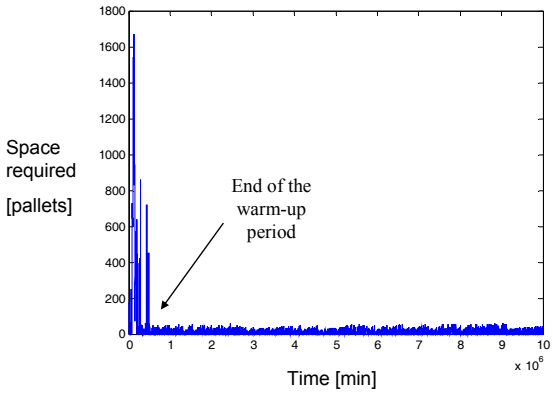

Figure 3: Example of the identification of the warm-up period.

Similarly as input data, output data are fitted as well, so as to achieve the probabilistic representation of the required storage space for each SKU type of interest. Thus, probability distributions of such space requirements are obtained and denoted as $f^i(x)$, $i=1,...,N$, where N is the number of SKU types. An example is shown in Figure 4.

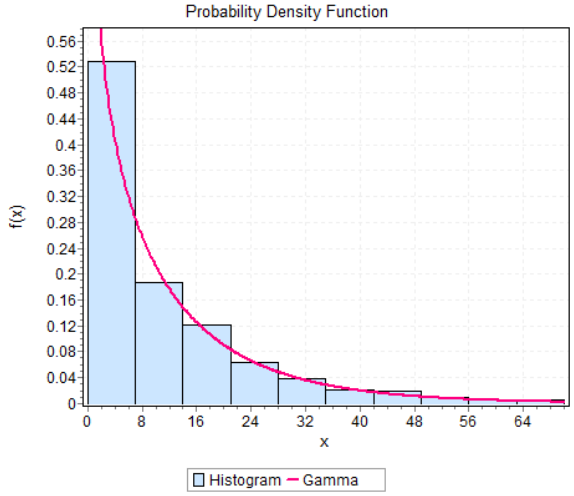

Figure 4: Example of mass probability distribution of storage requirements.

Note that the contemporary presence of different SKU types in the storage area must be taken into account. As an example, if some SKU types are very rarely present at the same time in the storage are (e.g. they are produced in different periods of time), the actual required storage space may be less than the sum of the single space requirements.

Step 6: Bin configuration evaluation. Given the probability distributions related to all the SKU types under study, this step provides a method to evaluate the goodness (or badness) of a certain bin configuration.

Specifically, let k be the number of bins in the storage area and y be the capacity of each bin, the objective is to compute the service level of the possible storage requirements that may occur at the storage area according to a certain probability. Note that the probability of any storage requirement depends on the SKUs' probability distributions.

By varying the parameters k and y, a set of bin configurations, denoted as the BC set, is generated. Among the bin configurations belonging to BC, the feasible ones are that satisfying the following constraint: the space occupied by a certain bin configuration (k,y) (considering both the zones for storing pallets and the aisles) must be at most equal to the space available in the storage area. Thus, a set of feasible bin configurations BC' is obtained.

Each bin configuration (k,y) belonging to BC' can be evaluated considering the mass probability distributions of storage requirements for all the SKU types and the contemporary presence of different SKU types in the storage area.

For the sake of clarity, we focus on the approximate probability of not satisfying the storage requirements (i.e. of exceeding the required storage space) related to a certain bin configuration (k,y), i.e. a badness function $BF(k,y)$ is formulated. The lower the obtained BF value, the better the bin configuration is.

The following notation is adopted:

$i=1,...,N$	SKU type;
k	number of bins;
y	bin capacity;
$f^i(x)$	probability distribution of SKU i, for $i=1,...,N$;
$z_i=0,1,\ldots,k$	variable identifying the number of bins assigned to SKU i, for $i=1,...,N$.

The proposed method consists in selecting all the possible combinations $\{z_i\}_{i=1,...,N}$ so that $\sum z_i = k$. As an example, a possible combination consists in assigning all the k bins to the first SKU and none of them to the other SKUs, i.e. $z_1 = k$ and $z_i = 0$ for $i=2,...,N$.

Then, the badness function can be formulated for a certain bin configuration (k,y) as follows:

$$BF(k,y) = \sum_{\forall\{z_i\}_{i=1,...,N}} \left(\prod_{i=1}^{N} \int_{y \cdot z_i}^{\infty} f^i(x)dx \right). \quad (2)$$

Among all the bin configurations belonging to BC', the one with the lowest BF value is selected.

3. CASE STUDY

In the case study, we apply the methodology for designing bin configurations proposed in the previous section to the actual storage area of a company operating in the beverage field.

The company under study produces different SKU types (e.g. 1 l still water bottle, 1.5 l still water bottle, 1 l sparkling water bottle, etc.). They can be divided into three SKU classes.

The SKU class I includes all the SKU types produced in high and constant volumes. Such SKUs present a continuous flow from the production process to the shipment area so that they are not significant for the specific problem addressed in this paper, i.e. it is possible to manage both the processes so that the synchronization between them is guarantee.

The SKU class II involves SKU types with a less regular demand. In this case the difficulty in maintaining synchronization between the production process and the shipping process leads to the necessity of an intermediate storage area.

The SKU class III includes SKU types occasionally produced, i.e. only when a specific order is coming.

The methodology proposed in this paper is suitable for the SKU class II. Specifically, seven SKU types are identified in the proposed case study and denoted as *SKU A*, *SKU B*, …., *SKU G*.

The application of all the methodology steps introduced in Section 2 is described in the following.

Step 1: Data collection. Data on a 6 months period are collected from the Enterprise Resource Planning (ERP) of the system. Data are arranged so that production and shipment orders of each SKU type are available over time.

Step 2: Analysis of production and shipping. Data from the previous step are fitted by using a statistical software tool so that the mass probability distributions of both size and interarrival times of production and shipping orders are obtained for each SKU type. In this case, Gamma distributions (location equal to zero) are selected to represent these processes.

The parameters of the Gamma distributions representing the production process are reported in Table 1 as regards the interarrival times and in Table 2 as regards the order sizes. The corresponding Gamma distribution parameters for the shipping process are given in Table 3 and 4.

Table 1: Gamma distribution parameters of the production process – Interarrival times [min]

SKU Type	Shape	Scale	Mean
SKU A	0.743	3001	2229
SKU B	0.104	22878	2372
SKU C	0.140	19061	2667
SKU D	0.380	9376	3567
SKU E	0.290	15845	4593
SKU F	0.155	26365	4089
SKU G	0.228	28561	6521

Table 2: Gamma distribution parameters of the production process – Order sizes [pallets]

SKU Type	Shape	Scale	Mean
SKU A	1.360	87	119
SKU B	1.421	78	111
SKU C	1.404	96	135
SKU D	1.690	77	130
SKU E	1.546	68	105
SKU F	2.161	41	88
SKU G	1.672	69	116

Table 3: Gamma distribution parameters of shipping process – Interarrival times [min]

SKU Type	Shape	Scale	Mean
SKU A	0.133	2050	273
SKU B	0.040	13012	520
SKU C	0.052	13497	698
SKU D	0.133	6447	859
SKU E	0.116	12317	1424
SKU F	0.139	6950	969
SKU G	0.067	19378	1305

Table 4: Gamma distribution parameters of shipping process – Order sizes [pallets]

SKU Type	Shape	Scale	Mean
SKU A	0.642	23	15
SKU B	1.021	24	24
SKU C	3.947	9	35
SKU D	2.117	15	31
SKU E	1.647	20	33
SKU F	1.365	15239	21
SKU G	1.085	21	23

The obtained probability distributions are used to choose, in a probabilistic way, appropriate and realistic input data for the simulation model explained in the next step.

Thus, it is important to assure that the balancing equation (1) is satisfied. Moreover, to avoid unrealistic values for the order size and the interarrival times, proper limits are adopted for the probability distributions describing both the production process (see Table 5) and the shipping process (see Table 6).

Table 5: Distribution limits for the production process

SKU type	Max interarrivaltime [min]	Max size [pallets]
SKU A	11963	470
SKU B	36997	430
SKU C	35619	525
SKU D	27504	465
SKU E	41186	391
SKU F	51697	282
SKU G	66753	418

Table 6: Distribution limits for the shipping process

SKU type	Max interarrivaltime [min]	Max size [pallets]
SKU A	3745	84
SKU B	12286	111
SKU C	14976	89
SKU D	11775	101
SKU E	21012	118
SKU F	12964	82
SKU G	25028	103

Step 3: Simulation model for each SKU type. The simulation model consists in parallel production lines processing pallets of a certain SKU type at a predefined production rate and according to the order size and interarrival times obtained from the previous step. Similarly, shipment orders are generated according to the related probability distributions.

Pallets from the production lines enter a queue waiting for the shipment. When a new shipping order arrives and the number of waiting pallets matches the order size, the queue is reduced of this amount.

Step 4: Simulation campaign. The simulation run, for each SKU type, corresponds to a period of 10.000.000 minutes. During the run, space requirements (i.e. the length of pallets queues) are logged every 100 minutes to obtain a representative sample for each SKU type.

Step 5: Simulation output analysis. Once the warm-up period have been identified and cut-off, data about space requirements of each SKU type are fitted in order to find a representative mass probability distribution.

Figure 5 shows the probability distributions for all the SKU types of interest. Note that Gamma distributions are chosen and the corresponding parameters are reported in Table7.

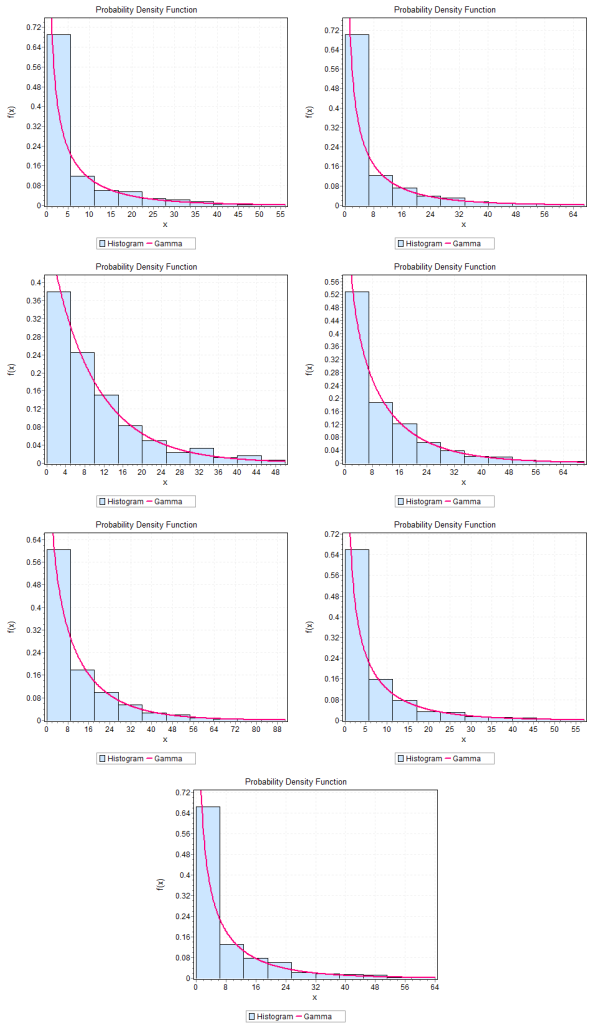

Figure 5: Mass probability distributions of storage requirements for the SKU types of interest

Table 7: Gamma distribution parameters – Storage requirements

SKU types	Shape	Scale	Mean
SKU A	0.392	15	6
SKU B	0.379	18	7
SKU C	0.964	10	10
SKU D	0.728	15	11
SKU E	0.701	17	12
SKU F	0.446	14	6
SKU G	0.461	16	7

Step 6: Bin configuration evaluation. Given the probability distribution $f^i(x)$ for *i*=A,…,G by Step 5, it is possible to apply equation (2) for any couple (k,y) so that the badness value is compute for a specific number of bins *k* having capacity *y* each.

Since functions $f^i(x)$ are continuous functions while the number of pallets to store into the bins is an integer, a further observation is needed: the x-axis can be divided into intervals centered on any integer value so that if $x<0.5$ we consider not to have any pallet to

store, if $x<1.5$ we consider to have at most 1 pallet to store, and so on.

Then, various possible solutions (k,y) belonging to the set of feasible bin configurations BC' can be examined.

Specifically, Table 8 shows the *BF* values for $k=7$ bins of different capacities, i.e. $y=9,10,...,21$

Table 8: *BF* solutions for *k*=7 and different capacities *y*

Solution #	*y*	*BF*
1	9	0.705
2	10	0.400
3	11	0.229
4	12	0.132
5	13	0.077
6	14	0.045
7	15	0.026
8	16	0.015
9	17	0.009
10	18	0.005
11	19	0.003
12	20	0.002
13	21	0.001

We notice from Table 8 that if a *BF* value less than 0.01 is considered to be acceptable, Solution #9 ($y=17$) is the first feasible solution. Note that from Solution #9 to Solution #13 the *BF* values are low and closed to each other so that it may be convenient to avoid occupying too much space by choosing the Solution #9, i.e. the one with the less capacity *y* associated.

Similarly, Table 9 reports the *BF* value for a different *k*, i.e. 8 bins in the storage area.

Table 9: *BF* solutions for *k*=8 and different capacities *y*

Solution #	*y*	*BF*
1	9	0.557
2	10	0.294
3	11	0.156
4	12	0.084
5	13	0.045
6	14	0.025
7	15	0.014
8	16	0.007
9	17	0.004
10	18	0.002
11	19	0.001
12	20	0.001
13	21	0.000

In this case, having one more bin, assuming the same *BF* limit of acceptance 0.01, Solution #8 ($y=16$) is the more convenient.

Therefore, solutions (*k*=7,*y*=17) and (*k*=8,*y*=16) are both able to assure an acceptable *BF* value.

The same procedure can be applied to other bin configurations.

4. CONCLUSIONS

The paper proposes a methodological approach to design storage areas in cross-docking systems. Stochastic aspects of the production and shipping processes are taken into account. The approach consists in identifying storage requirements from a statistical point of view, and then in formalizing a function to compare different bin configurations.

ACKNOWLEDGMENTS

The authors wish to thank Elettric80 company (Viano, Reggio Emilia, Italy), and in particular Vittorio Cavirani and Marco Casarini for their support to the present work.

REFERENCES

Apte, U.M., Viswanathan, S., 2000. Effective Cross Docking for Improving Distribution Efficiencies. *International Journal of Logistics Research and Applications*, 3 (3), 291-302.

Ashayeri, J., Gelders, L.F., 1985. Warehouse design optimization. *European Journal of Operational Research*, 21, 285-294.

Baker, P., 2007. An exploratory framework of the role of inventory and warehousing in international supply chains. *International Journal of Logistics Management*. 18 (1), 64–80.

Baker, P., Canessa, M., 2009. Warehouse design: A structured approach. *European Journal of Operational Research*. 193, 425–436.

Berry, J.R., 1968. Elements of warehouse layout. *International Journal of Production Research*, 7 (2), 105-121.

Goetschalckx, M., Radliff, H.D., 1991. Optimal lane depths for single and multiple products in block stacking storage systems. *IIE Transactions*, 23 (3), 245-258.

Gu, J., Goetschalckx, M., McGinnis, L.F., 2010. Research on warehouse design and performance evaluation: A comprehensive review. *European Journal of Operational Research*, 203, 539-549.

Larson, N., March, H., Kusiak, A., 1997. A heuristic approach to warehouse layout with class-based storage. *IIE* Transactions, 29, 337-348.

Marsh, W.H., 1979. Elements of block storage design. *International Journal of Production Research*, 17 (4), 377-394.

Marsh, W.H., 1983. A comparison with Berry. *International Journal of Production Research*, 21 (2), 163-172.

Moder, J.J., Thornton, H.M., 1965. Quantitative analysis of the factors affecting floor space utilization of palletized storage. *The journal of Industrial Engineering*, 16 (1), 8-18.

Rouwenhorst, B., Reuter, B., Stockrahm, V., van Houtum, G.J., Mantel, R.J., Zijm, W.H.M., 2000. Warehouse design and control: Framework and literature review. *European Journal of Operational Research*, 122, 515-533.

A new approach to describe DEVS models using both UML State Machine Diagrams and Fuzzy Logic

Stéphane Garredu **P.-A. Bisgambiglia** **Evelyne Vittori** **Jean-François Santucci**
University of Corsica – UMR CNRS 6132 - Dept. of Computer Science
Quartier Grossetti Batiment 018 - 20250 Corte FRANCE
garredu@univ-corse.fr **bisgambiglia@univ-corse.fr** **vittori@univ-corse.fr** **santucci@univ-corse.fr**

Keywords: Discrete event simulation, DEVS, UML, MDA, decision support systems.

Abstract

This paper deals with a method which enables to describe a system using both UML State Machine Diagrams and Fuzzy-DEVS (to describe uncertain data) then to perform its simulation using DEVS formalism. The goal of the paper is to simplify the modeling of DEVS models, and also to take into account possible uncertainties on the transitions between states, by using a language based on UML State Machine Diagrams . This language is a part of a larger approach which final purpose is to create a high level intuitive language to enable non-computer scientists to describe DEVS models.

1. INTRODUCTION

In some research fields, the importance of modeling and simulation to describe complex systems has strongly increased. The purpose of modeling is to make a system study be more simple by considering only some of its properties. Simulation makes the model evolve with time, in order to get results.

Our research lab (CNRS SPE) has been working for several years on DEVS formalism defined by Pr. Zeigler during the 70's [1] .

DEVS is a low-level formalism based on the general systems theory; it was introduced by Pr. Zeigler. It allows to describe a system in a modular and hierarchical way, and to consider a global system as a set of other more simple systems, in order to reduce the system's complexity. The simulation is "automatically" performed; the user does not have to focus on the conception of the simulator [1].

DEVS also has great genericity properties, it can be used in many study domains, always considering the fact that a system evolves with events; moreover, DEVS has a good evolutivity, and has often been extended to be able to take into account various systems: dynamic systems (i.e. which structure evolves with time) with DSDE [2] and DynDEVS [3] , systems with uncertain parameters with Fuzzy-DEVS [4] and min-max-DEVS [5], systems with evolutions in their interfaces with Cell-DEVS (cellular approach) [6] and Vector-DEVS (vectorial approach) [7].

Our goal is to create a high level and intuitive specification language for DEVS models, in order to enable non-computer scientists to create their own models. This language will take place in a Model Driven Architecture, it means that mappings between it and DEVS will be performed using a MDA approach.

The purpose of this paper is to simplify the modeling phasis by defining an intermediate language (based on UML State Machine Diagrams and fuzzy logic) which will take place between the intuitive language which is being developed and DEVS models. This intermediate language will be based on UML State Machine Diagrams (used to describe states and transitions) and fuzzy logic (used to describe uncertain transitions with a set of fuzzy words).

In the first part, we will present the DEVS formalism; we briefly describe Unified Modeling Language and Approximate Reasoning. Those three formalisms can be seen as a basis for this work. DEVS is the core of our approach, and the main purpose of our work is to create a different reasoning (included in our intermediate language) to create DEVS models, using both UML State Machine Diagrams and Fuzzy reasoning.

The second part deals with the description of our approach: we discuss about the importance of the modeling phasis.

The third part will show, through a simple example, how our approach can be applied.

Before giving a conclusion, we discuss in the last part about our results and make some comments

2. BACKGROUND

In this part we present some formalisms and theories which will be used later to explain our approach. We begin with DEVS formalism, the core of our works, then we briefly introduce UML formalism and the State Machine Diagrams included in UML 2.0.

After that, we present the fuzzy reasoning and explain its interest when it is needed to introduce uncertainties when modeling a system. Fuzzy sets theory and possibilities theory are described, and we present Fuzzy-DEVS

formalism which is an extension of DEVS formalism able to take into account uncertainties.

2.1. DEVS formalism

The basic concepts of DEVS approach are intended to control the difficulty of the studied problem, by reducing the analysis of the system to a study composed of a sum of simpler subsystems. Our environment, based on the concept of hierarchy, makes it possible to apprehend the complexity of a problem in a completely gradual way.

The representation of complex systems is generally hard to implement. Indeed, it implies to take into account a multitude of elements, linked themselves by many connections. To reduce the impact of this problem, we use the hierarchical approach of modeling introduced by B.P. Zeigler [1], which aims at the gradual introduction of the successive components of the system by successive masking of under components.

This approach uses the concepts of Atomic Model and Coupled Model.

An atomic model (black box see Figures 1) makes it possible to account for the behaviours of inputs/outputs and the changes of states of the studied system. The coupled model describes how to connect in a hierarchical way several components (atomic model and/or coupled model) to get a higher level coupled model.

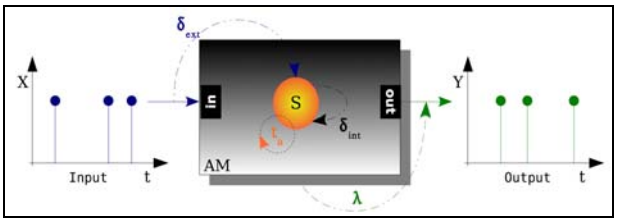

Figure 1: Atomic Model DEVS.

After receiving an input event, the external transition function is executed. This function updates the state of the system. If there was no entry, after the expiration of the lifespan of the state (t_a), the internal transition functions and the output function are executed. The internal transition function updates the state of the model.

The atomic model (see Figure 1) is defined by:

$AM = < X, Y, S, t_a, \delta_{int}, \delta_{ext}, \lambda >$ (1) (1)

With:

X, the input ports set, through which external events are received;

Y, the output ports set, through which external events are sent;

S, the states set of the system;

t_a, the time advance function (or lifespan of a state);

δ_{int}, the internal transition function;

δ_{ext}, the external transition function;

λ, the output function;

The simulation is carried out by associating to each component a simulator making it possible to implement the corresponding simulation algorithms.

Thus, DEVS enables the specialist to be completely abstracted from the simulators implementation. Once the model is built and whatever its form is, B.P. Zeigler defined a simulator able to take into account any model described according to DEVS formalism, and developed the concept of abstract simulator [1]. The architecture of such a simulator represents an algorithmic description making it possible to implement the implicit instructions of the models resulting from formalism DEVS, in order to generate their behaviour. The major advantage of such a simulator is the fact that its construction is independent from the model.

DEVS is a very good tool for the modeling and the simulation of complex systems but it does not allow a lambda user, who is not a computer scientist, to specify his models.

A specification language establishing the link between knowledge of an expert and a DEVS environment would make it possible to extend the advantages of DEVS.

2.2. UML

Unified Modeling Language is a graphical modeling language and provides a toolkit which enables to model the structural aspects of a system as well as its behaviour [8].

Its developpement is driven by the Object Management Group, and its current version is UML 2.0.

One of the main interests of UML is that it is a part of the Model Driven Architecture approach.

MDA[1] (Model Driven Architecture) is a software design approach initiated by the OMG (Object Management Group) in 2001 to introduce a new way of development based upon models rather than code. It defines a set of guidelines for defining models at different abstraction levels, from platform independent models (PIMs) to platform specific models (PSMs) tied to a particular implementation technology. The translation between a PIM and one or more PSMs is to be performed automatically by using transformation tools.

Another interest of UML is a language which is provided to model behavior, and can be used in software engineering (for instance, to model the behavior of class instances) as well as in modeling and simulation (to model states and transitions): this language is named Statecharts (State Machine Diagrams in UML 2.0).

Statecharts are a high-level graphical-oriented formalism used to describe complex reactive systems. They were developped by D. Harel [9] and are an extension of state-transition diagrams (the diagrams representing a Finite State

[1] http://www.omg.org/mda/

Machine or Automaton) [10]. They were added three concepts: orthogonality (the way parallel activities are achieved), composition hierarchy (depth nesting of states) and broadcast communication (events sent from one to many elements).
Statecharts are composed of eight basic elements: Labels, Transitions, States, Actions, Conditions, Events, Expressions and Variables.
Statecharts formalism has been evolving for years now. The most popular derived formalisms are the Classical UML, and those implemented by Rhapsody [11, 12]. Moreover, several other semantics provide them a pretty good evolutivity.
We chose as an intermediate language UML State Machine Diagrams, because they provide a set of graphical elements to specify models. Of course we modified some aspects of this formalism to take into account fuzzy logic.
A state is represented by a rounded rectangle named *blob*.
A transition is an arrow which joins two states. It is triggered by an event.

The general syntax for a transition is *m*[*c*]/*a* where:
m is the event which triggers the transition;
c is the guard, that is to say the condition (or set of conditions) which guards the transition;
a is the action (or the set of actions) which must be executed when the transition fires.
The values in square brackets are guards, and we use them in our approach to express possibilities on transitions.
An initial state is shown as a black filled circle, it cannot have any incoming transitions i.e. once this state left, it is not possible to re-enter it.
A final state is shown as a circle surrounding a small solid filled circle. Once entered in this state, it is not possible to go back (i.e. it can only have incoming transitions, and it cannot have any outgoing transitions). In other words, it is the end of the simulation.
A state can be associated to an action, or several actions: they are written under the name of the state.

2.3. Fuzzy Reasoning

Fuzzy logic was introduced by Goguen (1968-1969) and presented by Zadeh [13,14] as a framework for approximate reasoning, and in particular to handle knowledge expressed using the natural language. Thus, fuzzy logic can be seen as an approach of human reasoning.

Fuzzy logic is a set of mathematical theories which allow representing and handling inaccurate or uncertain data.

2.3.1. Fuzzy Sets Theory

Zadeh introduced in 1965 the fuzzy sets theory [13,14], the first theory of fuzzy logic, which gives to an element the possibility to belong to a set, according to a membership degree. This membership degree belongs to the [0...1] interval, where 0 is the case where the condition can not be fulfilled, and where 1 is the case where the condition is always fulfilled. Classical logic handles Boolean variables, which possible values are 0 or 1.

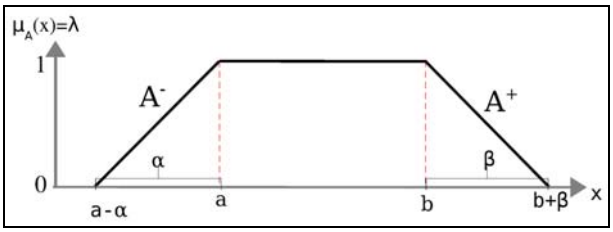

Figure 2: Membership function example. This representation allows us to define the membership degree of an element in a set.

As the purpose of fuzzy logic is to reason with partial knowledge, it replaces Boolean variables by Fuzzy variables. A fuzzy variable can be represented by an interval described as follows:
a = value, expresses the membership degree = 1;
b = value, expresses the membership degree = 1;
alpha = confidence interval;
beta = confidence interval.

Thanks to this representation mode, we are able to represent a real value by fixing a=b=constant and alpha=beta=0.

2.3.2. Possibilities Theory

As we said before, fuzzy sets theory was the first theory of fuzzy logic, it extends the classical set theory in order to take into account inaccuracy, it is based on membership functions.

Possibilities theory is a part of fuzzy logic which enables to take into account uncertainties which are impossible to describe with probabilistic theory. It is based on possibility functions.
Reasoning using probabilities implies to be able to define, for each event, its probability.

Hence, events must be well known. If this knowledge is not totally available, another possible solution is to reason in terms of possibilities.

Let X be a reference set, P(X) the set of parts. Each element of P(X) is given a possibility coefficient between 0 (impossible) and 1 (always possible).

2.3.3. Fuzzy-DEVS

In this subsection we focus on Fuzzy-DEVS, an initial extension of DEVS which takes into account the fuzzy transitions between states.
The Fuzzy-DEVS formalism was introduced by Kwon in [4], drifts DEVS formalism while keeping its semantics, some of its concepts and its modularity. It is based on fuzzy

logic, the "Max-Min" rules shown in [4] and the methods of fuzzification and defuzzification.

To allow the simulation, imprecise parameters must be transformed into crisp parameters (defuzzification) ; to be exploited, the output data is again transformed into fuzzy data (fuzzification).

A Fuzzy-DEVS model takes into account the different possibilities of transitions (δ_{ext} and δ_{int}) between states. The various possibilities of input, output and state update are represented by matrices and the evolution of the model by possibilities trees [4,15]. Fuzzy-DEVS does not address the fuzzy values of a model, but proposes a methodology that provides a tree of options describing various transitions between the states of the system. Fuzzy-DEVS is a theoretical formalism still in research phasis. This approach does not appear fully consistent with the DEVS formalism, but it provides avenues for good work, like the ability to define the lifespan of a state (t_a) with a linguistic label.

In the following part we describe our modeling approach. DEVS can be seen as a multi formalism: it is the core of our works.

There are often several uncertainties when a natural system is being modeled using a state/transitions method. We chose to simplify the problem by taking into account only uncertainties linked to transitions. Fuzzy-DEVS, as a DEVS extension, is a part of the DEVS multi formalism and offers the possibility to include such uncertainties during the modeling and simulation process.

As we want to work at an higher level than DEVS, we use State Machine Diagrams which, thanks to its properties (it is graphical and located at an higher level than DEVS), is a good modeling tool which fulfills many criteria as shown in [16].

3. OUR APPROCH

We chose to focus on the modeling phasis, because once the system is described, the simulator is provided (cf. DEVS properties).

Our approach tries to use both Fuzzy-DEVS and State Machine Diagrams to help a scientist to describe models. It is an intermediate approach, because the final purpose is to use a high-level language [17]. State Machine Diagrams, such as DEVS, is a formalism based on states and transitions. Moreover, it is graphical : hence, it is easier to represent a system with State Machine Diagrams than DEVS. It could be a good intermediate language to specify DEVS models.

We thought it was interesting to add to the description of the model the possibility for the scientist to express inaccurate data using linguistic terms.

We consider that once the states known, the only differences will be on the way they will connect to each other, in other terms inaccuracies will be expressed only in the transitions between those states.

That is why Fuzzy-DEVS will help to specify for the transitions: the possible date before a transition fires, using linguistically terms; an execution coefficient.

3.1. Goals

In this section we give a graphical representation of the goals of this paper, shown in figure 3. The main part of our approach is to give a method to model a system using both State Machine Diagrams and a linguistic description. Moreover, uncertainties on transitions are taken into account.

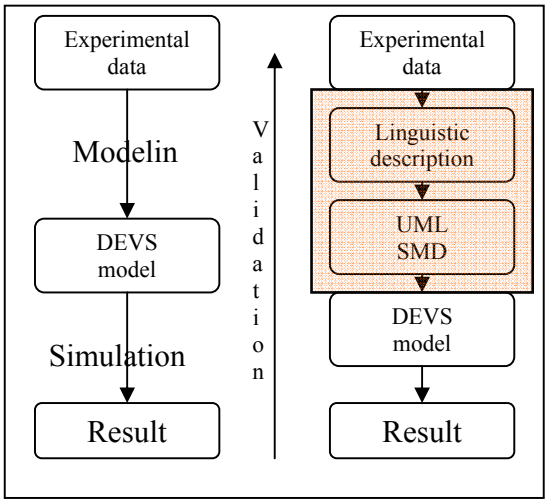

Figure 3: Linguistic description to specify UML State Machine Diagrams models

3.2. General Reasoning

Before starting the modeling phasis, some steps have to be followed.

The first step for the scientist is to identify all the states of the model, and among them the one which will be the initial state. The second one is to define how those states will behave with each other, i.e. he will have to define the transitions.

The last step is to define both the inputs and the outputs of the system, and how the simulation can be started or stopped.

Once those steps finished, we are able to begin the modeling phasis.

The states become *blobs* : for every different state, there is a different blob.

In order to take into account the lambda function, we chose to represent it with actions on transitions and the variable *out*.

The *delta int* and *delta ext* functions are always defined on transitions, because *delta* functions describe how to change from one state to another (i.e. a transition).

The *delta int* function can be translated using the keyword *after* (followed by a duration).
Some times, the expert who wants to model the system does not know exactly the lifetime of a state, represented by *ta* function.
Thanks to fuzzy logic, we can represent *ta* using a membership function, composed of several typical durations expressed with fuzzy words.
So, instead of giving a numerical duration after the keyword *after*, the scientist will be given the possibility to give a fuzzy word.
Fuzzy logic also provides the ability to put a possibility on a transition. Using state machine diagrams, such a possibility can be expressed with a guard. A high possibility will have a value close to 1, and a possibility which value is 1 is certain to happen.

4. EXAMPLE

In this part we apply our method on a simple two-state example. The studied system is a reset-set system, with uncertainties on transition durations.

In the first part, we textually describe the system, as a non-computer scientist could have described it. We provide a list of fuzzy words (to describe durations) to help him during the description process.

In the second part, we create the model using the method explained in chapter III.

In the last part, we translate our model into a DEVS atomic model.

4.1. System

This system is a simple Reset-Set system. It can be described by an expert as follows : the system remains in the reset state (which is the initial state), until it receives an external event which sends a 1 to the input port (for instance, an event from another model). When this external event is received, the *set* state is activated.

The system waits into this state for an unknown duration and then and goes back to the *reset* state. This duration is not exactly known but can be described with a word. Moreover, the transitions between the two states are not certain, even if their possibility is very high.

4.2. Modeling the system

With the expert's textual description given in A there are two states (*reset* and *set*) when we model the system with State Machine Diagrams.

In this example, there is an unknown duration on the transition from *set* to *reset*. The duration is defined by a membership function and linked to a keyword chosen from the list {null; short; medium; long}.

The membership function is described as follows (Figure 4):
- Null = [0,1]
- Short = [2,4,1]
- Medium = [6,8,1]
- Long = [10, ,1]

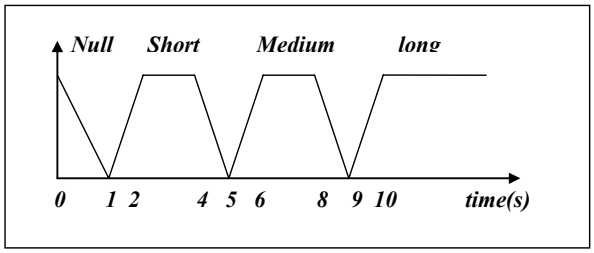

Figure 4: Time membership function

This unknown duration will be translated and applied to the transition from *set* to *reset* as a time event, using the keyword after. Moreover, the two transitions between *reset* and *set*, are not certain.

They are given a probability degree, expressed with a guard. When an external event arrives on the input port of the system, the transition from *reset* to *set* is triggered. The probability degree of this transition is high but not certain. The final model is given in Figure 5.

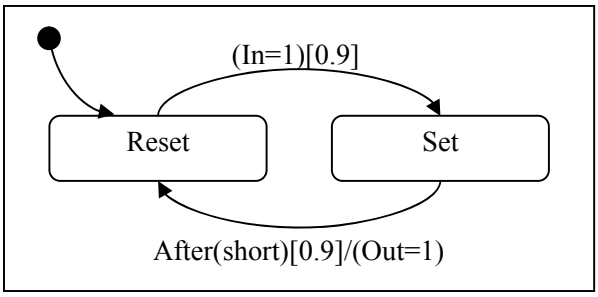

Figure 5: Representation of the system using State Machine Diagrams and Fuzzy-DEVS for the transitions.

4.3. DEVS model

$Atomic_{RS} = < X, Y, S, t_a, \delta_{int}, \delta_{ext}, \lambda >$
$X = \{In\}$
$Y = \{Out\}$
$S = \{Reset, Set\}$
$\delta_{ext}(Reset, In=1) = \{Set\}$
$\delta_{int}(Set) = \{Reset\}$
$\lambda(Set) = \{Out=1\}$

The following diagram is a possibilities tree which gives us an idea of the most possible path followed by the model (Figure 6).

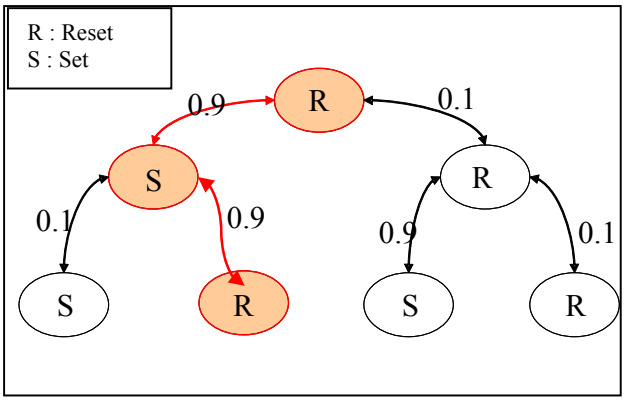

Figure 6: The possibilities tree for the simulation of the model defined by Min-Max Rules Fuzzy-DEVS

5. REMARKS AND DISCUSSIONS

This example was chosen as simple as possible: it represents an atomic model. The number of states is finite and not too high.

Increasing the number of states would increase the size of the possibilities tree, and of course the computation time to create it.

The "classical" transitions are modified because we use possibilities as guards, and fuzzy words instead of absolute (or relative) numerical values to specify the lifespan of a state. So we think it would be useful to create a specific profile, or make an extension of State Machine Diagrams meta model.

We only treated possibilities on transitions, and we will try in a near future to include imprecise data on inputs/outputs using iDEVS method [18].

We also plan to implement an automatic code generation between this intermediate language and DEVS formalism.

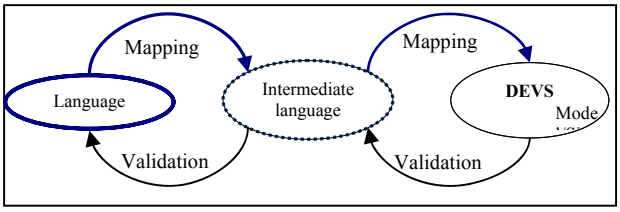

Figure 7: Our global approach.

6. CONCLUSION

DEVS is an interesting tool for M&S. A community of scientists works all around the world in order to add DEVS other modules which can fit several applications fields.

We think it is important to enable the largest part of the scientists to use DEVS formalism that is why we follow an approach which purpose is to offer the possibility to model systems using a more intuitive way.

In this paper, we proposed a new idea, using both the possibility theory and a high level specification language.

The ultimate goal of this idea is to enable a non-computer scientist to create a model using a simple and intuitive specification language.

To reach this goal, we use several tools:

UML which allows the definition of models using a graphical way based on diagrams, because a graphical description is often easier than code writing.

The possibilities theory, which enables the description of a system with pre-defined terms. Those pre-defined terms are useful to describe a system and its inaccuracies using a suitable language.

Those tools are linked to the M&S DEVS formalism, because the simulation of the models is easy to perform with DEVS.

This approach has to be replaced in a larger project, which is the definition of a high-level and intuitive language. UML State Machine Diagrams will only be used to create a link between this language and DEVS, as an intermediate formalism. We will probably define a UML profile for our intermediate language; this will be helpful to reuse some interesting parts of State Machine Diagrams , and to specialize them. This new language is being developed, and will be defined in order to be used by the largest part of the scientists. For instance, it will be possible to define models in a graphical way, or/and using a formal language.

References

[1] - Zeigler, B., H. Praehofer, and T. Kim. 2000. Theory of Modeling and Simulation, Second Edition. Academic Press.

[2] - Barros, F. 1995. Dynamic structure discrete event system specification : a new formalism for dynamic structure modelling and simulation. In *Proceeding of the 1994 Winter Simulation Conference.*

[3] - Uhrmarcher, A. 2001. Dynamic Structures in Modeling and Simulation : A Reflective Approach. *ACM Transactions on Modeling and Computer Simulation vol. 11 2001*, 206-232.

[4] - Kwon, Y., H. Park, S. Jung, and T. Kim. 1996. Fuzzy-DEVS Formalism : Concepts, Realization and Application. Proceedings AIS 1996, 227-234.

[5] - Hamri, A., N. Giambiasi, and C. Frydman. 2006. Min-Max-DEVS modelling and simulation. Simulation Modelling Practice and Theory (SIMPAT), vol. 14, pp. 909–929. Ed. Elsevier, ISSN 1569–190X.

[6] - Ameghino, J., E. Glinsky, and G. Wainer. 2003. Applying cell-devs in models of complex systems. In *Summer Computer Simulation Conference*, Montreal QC, Canada.

[7] - Filippi, J. 2003. *Une architecture logicielle pour la multi-modélisation et la simulation à évènement discrets de systèmes naturels complexes*. PhD Thesis, University of Corsica.

[8] - Booch, G., J. Rumbaugh, and I. Jacobson. 1998. The Unified Modeling Language User Guide. Addison-Wesley.
[9] - Harel, D. 1987. Statecharts : A visual formalism for complex systems. S*cience of Computer Programming*, 8(3):231-274.
[10] - Hopcroft, J.E., R. Motwani, and J.D. Ullman. 2001. Introduction to Automata Theory, Languages, and Computation, 2nd edition. Addison Wesley.
[11] - Crane M.L. and J. Dingel. 2005. UML vs. Classical vs. Rhapsody Statecharts: Not All Models are Created Equal. Model Driven Engineering Languages and Systems: 8th.
[12] - Harel, D., and H.Kugler. 2004. The Rhapsody Semantics of Statecharts. Integration Of Software Specification Techniques for Applications in Engineering.
[13] - Zadeh, L. A. 1975. Fuzzy logic and approximate reasoning. *Synthese* 30 : 407-428.
[14] - Zadeh, L. A. 1965. Fuzzy sets. *Information and Control* 8: 338-353.
[15] - Anglani, A., P. Caricato, A. Grieco, F. Nucci, A. Matta, G. Semeraro, and T. Tolio. 2000. Evaluation of capacity expansion by means of fuzzy-devs. (citeseer.ist.psu.edu/499458.html), 14th European Simulation MultiConference. Ghent, Belgium.
[16] - Garredu, S., V. Evelyne, J.F. Santucci, A. Muzy. 2006. Specification languages as front-ends towards the DEVS formalism. In Proceeding of the Environment Identities and Mediterranean Area, ISEIMA '06. 104-109.
[17] - Garredu, S., P.A. Bisgambiglia, E. Vittori and J.F. Santucci. 2007. Towards the definition of an intuitive specification language. In Proceeding of the Simulation and Planning in High Autonomy Systems (AIS) & Conceptual Modeling and Simulation (CMS).
[18] - Bisgambiglia, P.A., E. De Gentili, J.F. Santucci, and P. Bisgambiglia. 2006. DEVS-Flou: a discrete events and fuzzy sets theory-based modeling environment. International Symposium on Systems and Control in Aeronautics and Astronautics – Harbin (China). 95-100.

Biography

Stéphane Garredu born in 1981. Graduates from the University of Corsica - Research Master of Computer Science option Integrated Information Systems 2006, phd. student since 2006. SCS member's since 2008. His main research interests are modelling and simulation of complex systems and modeling high level of abstraction. He makes his researches in the laboratory of the UMR CNRS 6134.

Paul-Antoine Bisgambiglia born on 14 September 1981 at Peri in Southern Corsica. Graduates from the University of Corsica – Research Master of Computer Science option Integrated Information Systems 2005, phd degree in 2008. IEEE member's since 2007. His main research interests are modelling and simulation of complex systems and fuzzy systems. He makes his researches in the laboratory of the UMR CNRS 6134.

Evelyne Vittori is Associate Professor in Computer Sciences at the University of Corsica. She holds a PhD in computer science. Her research activities concern the techniques of modelling and simulation of complex systems and the Unified Modeling Language. She makes his researches in the laboratory of the UMR CNRS 6134.

Jean-François Santucci is Professor in Computer Sciences at the University of Corsica since 1996. His main research interests are modelling and simulation of complex systems. He has been author or co-author of more than 100 papers published in international journals or conference proceedings. He has been the scientific manager of several research projects corresponding to European or industrial contracts. Furthermore he has been the advisor or co advisor of more than 20 PhD students and since 1998 he has been involved in the organization of more than 10 international conferences.

PERFORMANCE COMPARISON BETWEEN COLORED AND STOCHASTIC PETRI NET MODELS: APPLICATION TO A FLEXIBLE MANUFACTURING SYSTEM

Diego R. Rodríguez[(a)], **Emilio Jiménez**[(b)], **Eduardo Martínez-Cámara**[(c)], **Julio Blanco**[(c)]

[(a)] Fundación LEIA CDT
[(b)]Universidad de la Rioja. Electrical Engineering Department
[(c)]Universidad de la Rioja. Mechanical Engineering Department

[(a)]diegor@leia.es; [(b)]emilio.jimenez@unirioja.es, [(c)]eduardo.martinezc@unirioja.es, [(c)]julio.blanco@unirioja.es

ABSTRACT
Modeling of Flexible Manufacturing Systems has been one of the main research topics dealt with by researchers in the last years. The modeling paradigm chosen can be in many cases a key decision that can improve or give an added value to the example modeling task. Here, two different modeling manners are presented both based in the Petri Net paradigm, Stochastic and Colored Petri Net models. These two models will be compared in terms of the performance measures that could be interesting for the production systems. The production indicators used here are related with the productivity of the systems. These productivity measures could be included in a later stage into an optimization process by changing a certain number of parameters into the model. A comparison between the performance measures and also other computational effort measures will be depicted in order to check whether one model is more appropriate or the other.

Keywords: Colored Petri Nets, stochastic Petri nets, flexible manufacturing, modeling and simulation, performance measures

1. INTRODUCTION

Flexible Manufacturing Systems and their representation in an adequate model that expresses their behavior the more accurately possible is a typical topic treated by many researchers. Here, a comparison between two models based on the same modeling paradigm is presented, namely colored Petri nets and stochastic Petri nets.

Petri nets have shown their capacity to represent the behaviors that Flexible Manufacturing Systems presents, and specially concurrency and resources representation that are typical features of Manufacturing Systems.

Stochastic Petri nets have been used largely to represent systems where a stochastic behavior is associated to tasks. This modeling method has some lacks when dealing with complex models where the state space is clearly untreatable and even simulation can be a great time consuming task.

Table 1: Productive processes involved in the different production systems, and Operators

Task	Description	Performed By
Task1	Selection of materials	Operator 1
Task2	cutting of the PVC profiles	Operator 1
Task3	Introduction of the reinforcements	Operator 1
Task4	Numerical Control Machine 6 Operations	NCM
Task5	Reinforcements material selection	Operator 11
Task6	Reinforcements Cutting	Operator 11
Task7	Reinforcement distribution	Operator 11
Task8	Screwing of reinforcements	Operator 1 and Machining Center
Task9	Leaf cutting	Operator 2
Task10	Inverse Leafs distribution	Operator 2
Task11	Wagon distribution	Operator 2
Task12	Retest the strip/post	Operator 2
Task13	Crossbar distribution	Operator 4
Task14	Soldering and cleaning	Operator 3
Task15	Frame distribution	Operator 6
Task16	Crossbar Mounting	Operator 5
Task17	Locks and hinges fixing	Operator 7
Task18	Window hanging	Operator 7
Task19	Inverse leaf mounting	Operator 6
Task20	Box assembly (with all options)	Operator 9
Task21	Glazing	Operator 10
Task22	Insert the reeds	Operator 10
Task23	Glass selection and distribution	Operator 13
Task24	Reeds cut and distribution	Operator 14
Task25	Disassemble leaf/frame	Operator 12
Task26	Pack finished window	Operator 12

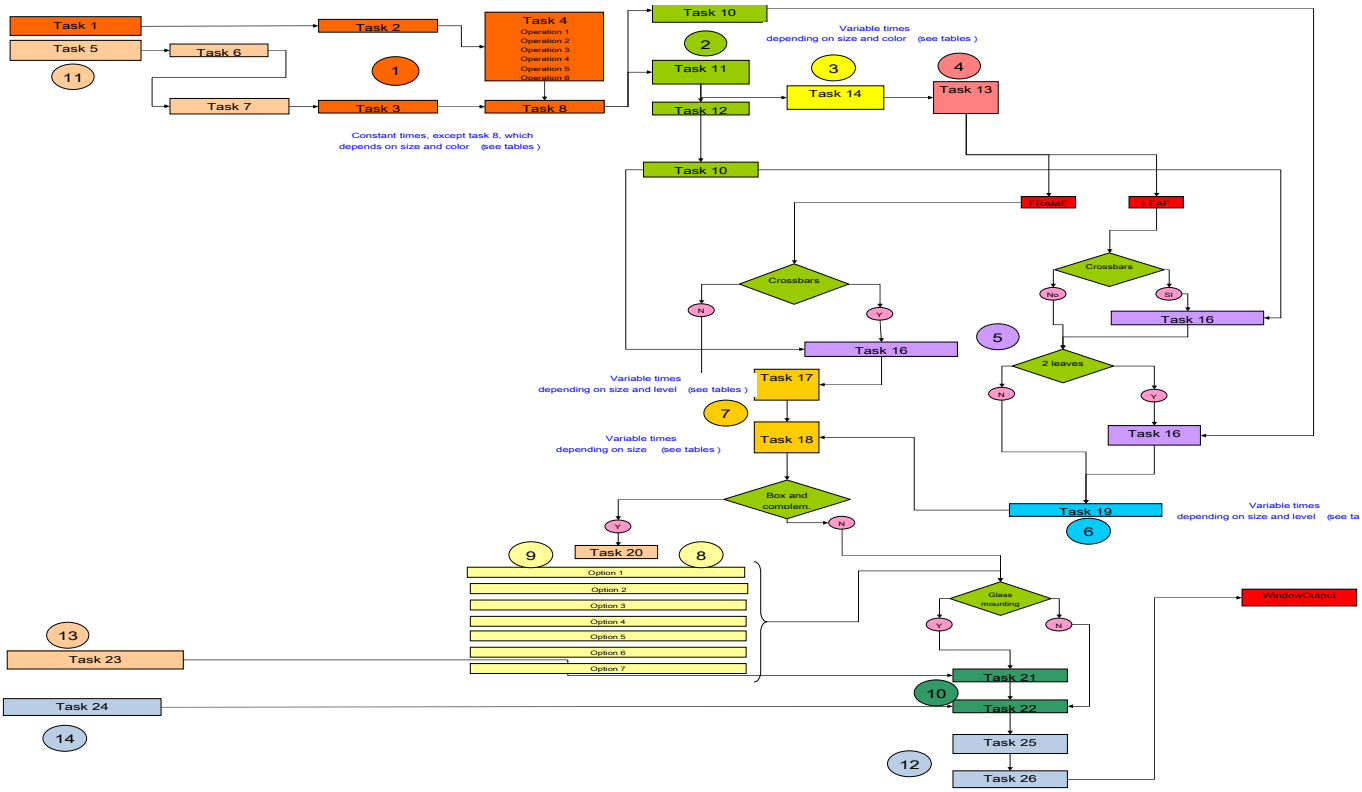

Figure 1. FMS Layout. Productive processes (Tasks, in squares) involved in the different production systems, and Operators (in circles).

To cope with the previous problems that appear when considering complex models mainly related with multi-product manufacturing systems, colored Petri nets have shown their capacity to solve these problems. Here, a colored model that will represent the initial FMS will be depicted, but, in order to be completely sure of the quality of the colored approach, by comparing with the previous stochastic PN model.

The rest of the paper is as follows, in section 2 the FMS that will be used along this paper will be explained and all the elements that will be interesting to be represented in our models will be enumerated. Later on, in sections 3 and 4 the two Petri net models will be depicted. Finally, the results we are interested in are represented associated to the models in section 5 where a comparison of the simulation results is shown. Finally some conclusions are presented in section 6.

2. DESCRIPTION OF THE FMS

The Manufacturing system initially considered is able to perform window frames with the following different features:

Feature 1

The first feature to be considered when modeling the system is the type of window where the frame will be included:

- Accessible window,
- tilt and turn window,
- Slide window
- Frames without any other element.

Feature 2

This feature is related with the presence of a crosspiece that goes horizontally from one extreme to the other of the window frame.

- With crosspiece
- Without crosspiece

Feature 3

The number of leafs that compose the window is the next differentiation element.

- One leaf
- Two leafs

It was considered a third leaf in the initial modeling constraints but finally it was decided that the third leaf could be added as a future improvement of the manufacturing system.

Feature 4

The last feature is related with the size of the window that will change the treatment or steps that must be followed in case of considering one size or the other.

- Big size
- Little size

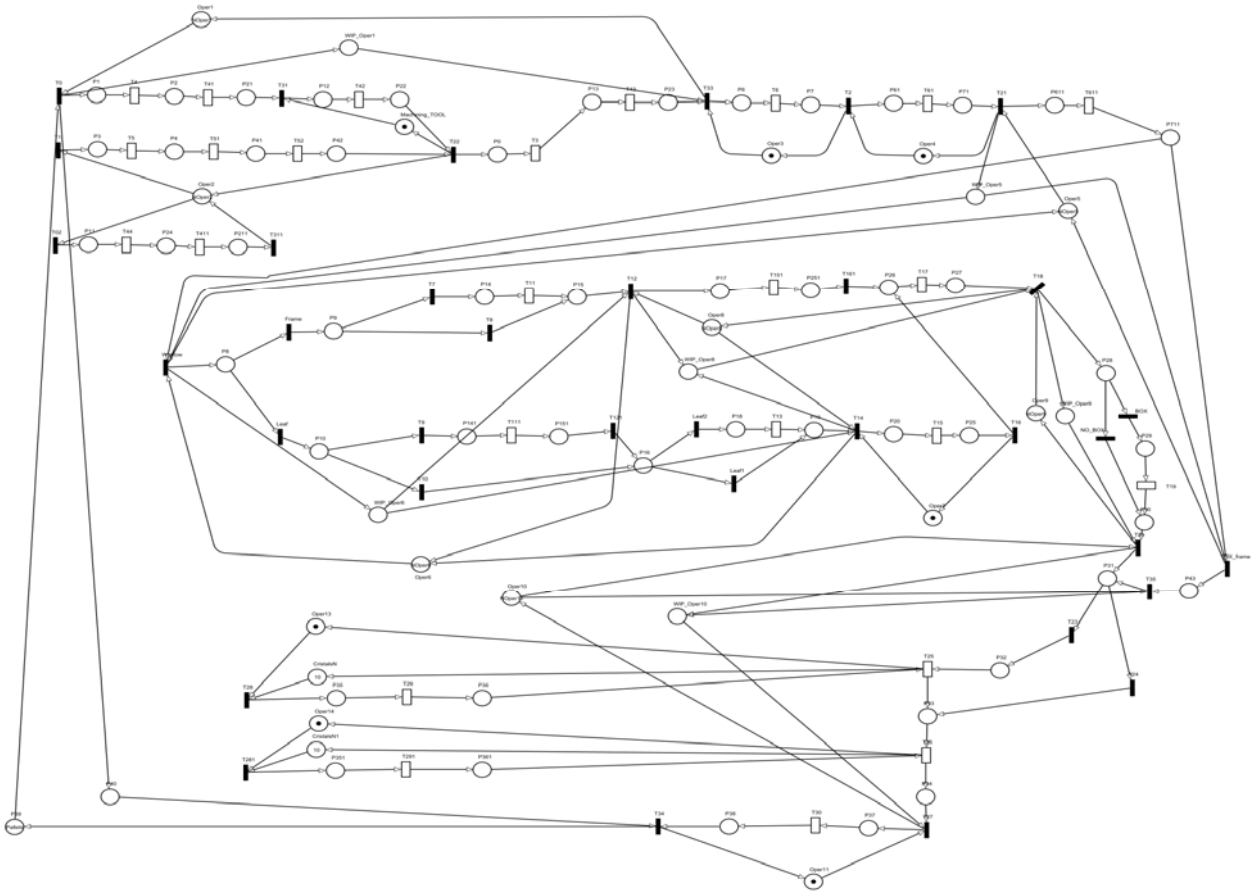

Figure 2. Petri Net model of the FMS defined in Table 1 and Figure 1

Considering all the features depicted here, there are finally 32 different types of products that our manufacturing cell will be able to produce.

Apart from these types of windows, a set of accessories can be added to the different products. These accessories are:

- Box and Guide to include into this device the blind that can be integrated into the window.
- Drip edge to get all the water that can slide through the window

Once considered all the parts that can be produced in our factory, we will concentrate now in the productive processes that have to be fulfilled during the whole production (Table 1). Figure 1 represents the different ways that any window can follow, and which of these productive processes will receive, depending on the type of window.

3. STOCHASTIC PETRI NET MODEL

In this section the Petri net that has been modeled using stochastic PN is presented. The complete model is represented in Figure 2.

This complete Petri net model shown before will be more clearly presented in the next figures where it will be divided in substructures that will help understanding the modeling issues.

Figure 3 presents the operations where operators 1, 2 and the numerical control machine are involved. Places Oper1 and Oper2 represent the availability of the operators when marked. Transitions T45, T412, T32 and T431 represent the 4 operations that can be performed or supervised by Operator 1,while T53, T511, T521, T441 and T4111 represent the five operations that the second operator can perform. Finally, the machining tool availability is represented by place Machining_TOOL1 and the operation is shown under transition T421.

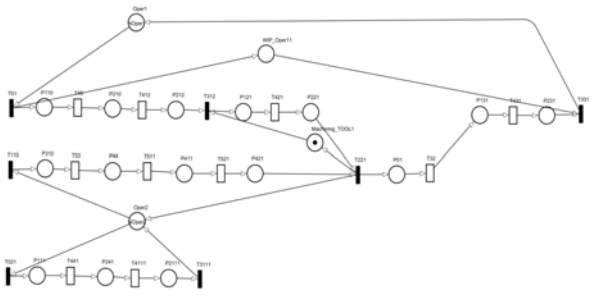

Figure 3. Petri Net model Operator 1, Operator 2, and NCM of the system.

Figure 4, represents the operators 3 and 4, and due to their simplicity, because they are only performing an operation, we have considered that a simple operator can cover each one of the tasks associated. There is no competition for the operators tasks.

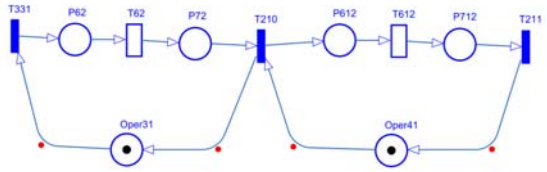

Figure 4. Petri Net model Operator 3 and 4 from example

Figure 5 represents the tasks where operators from 5 to 9 are involved. This Petri net model represents most of the decisions that must be taken (depending on the type of final product that the FMS is generating).After operator 5 performs its task (transition T611) then the raw parts will take one way or another depending on the type of final product (window or frame). If window, it will continue through transition window and then a second decision should be taken depending on what has to be built is a leaf of this window or a frame of it (transitions Leaf or Frame). All these operations will be supervised by operator 6. Then operators 7 and 8 will perform their tasks associated to them (transitions T15, T151 and T17). Finally, operator 9 will perform its operation represented by transition T19, but before that a decision should be taken regarding the presence of a BOX in the window structure represented by immediate transitions BOX and NO_BOX.

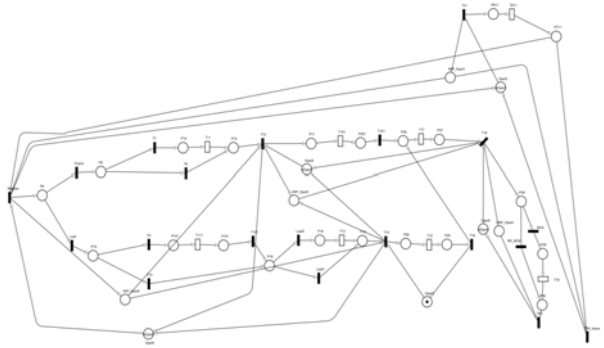

Figure 5. Petri Net model Operators 5 to 9 from example.

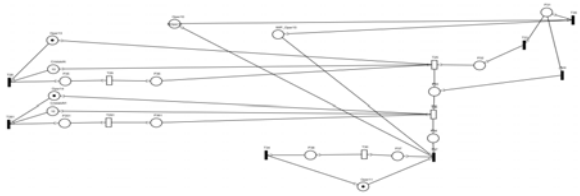

Figure 6.Petri Net model Operators 11 to14 from example

The last Petri net submodel is represented in Figure 6, where operators from 10 to 14 are modeled. These operators generally are performing simpler operations than the previous ones and their model representation is simpler also.

4. COLORED PETRI NET MODEL

The colored Petri Net of the previous model can be simulated and analysed by using the TimeNET software.

The main properties we are interested in with respect to the models are: check that all the places included in the model are at least included in a P-invariant (set of places that conserve a constant number of tokens during the Petri net token evolution). The P-invariants can be computed solving a linear programming problem and the TimeNET package has implemented this algorithm so that it can be computed in a reasonable time. The application calculate that the net contains 87 P-invariants, and that all the places are covered by p-invariants. Also the decisions that should be taken referring to the features of the windows to be produced compose the conflicting situations that the application calculates (Window/FIX_frame, Frame/Leaf, BOX/NO_BOX, and Leaf2/Leaf1).

5. RESULTS AND COMPARISON

The results we are interested to compare between the two models previously shown are related with productivity measures. It will be considered the number of pieces produced per time unit (throughput) for each type of product (32 different types can be produced in the FMS), that is, the optimization that we can carry out based on each one of the models.

Another performance measure we will consider will be the utilization of the different operators that are present into the system.

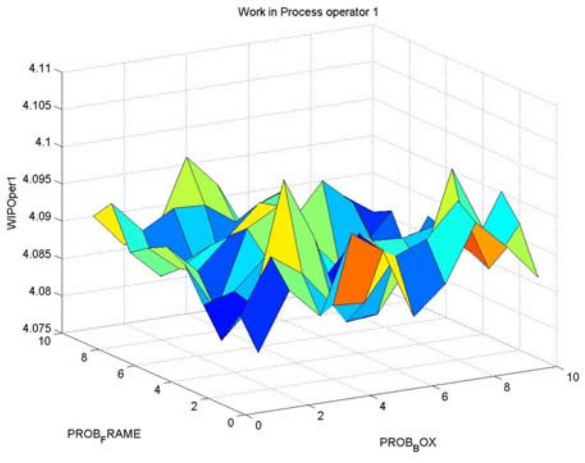

Figure 7. Work in progress of Operator 1 depending on the probability of frame and the probability of Box

Another important comparison measure will be how efficient is the convergence process for the two models and the accuracy they can reach.

Also the computational time that the computer will be calculating the measures will be another measure of how good the simulation process is with respect to the colored and the stochastic models.

The search space corresponding to the optimization problem is composed by the variables of Table 2.

6. CONCLUSIONS

Two different modeling formalism, both of them under the umbrella of Petri nets paradigm, Stochastic and Colored Petri Nets, have been used to model and optimize a real complex production factory. These two models have been compared in terms of the performance measures that could be interesting for the production system, using indicators related with the productivity of the system as well as with the computational effort.

The results shown that in complex production systems, in which an exhaustive analysis is not possible, the best solution is to deal with both formalisms in a combined way, since both of them presents advantages depending on the parameter (production, computational effort) and on the available time.

Table 2. Variables used to compose the search space of the optimization and their values (minimum, maximum, initial, delta, temp)

NOper i	integer variable that represents the number of operators that will perform the operations initially assigned to operator i. (1, 10, 1, 0.9, 1)
Mach_Delay	real variable that represents the time that in average takes to the Numerical Control Machine to perform the different tasks. (1, 140, 1, 0.1, 1)
PROB_BOX	real variable that represents the percentage of windows that has a box inside its structure. (0.05, 0.95, 0.5, 0.1, 1)
PROB_FRAME	real variable that represents the percentage of windows that will be a fixed frame window without any leaf (or with a unique one). (0.05, 0.95, 0.5, 0.1, 1)
PROB_WINDOW	real variable that represents the percentage of products that will have a window struc-ture instead of a frame one. (0.05, 0.95, 0.5, 0.1, 1)

The results of the comparison can be seen represented in Figures 7 to 9.

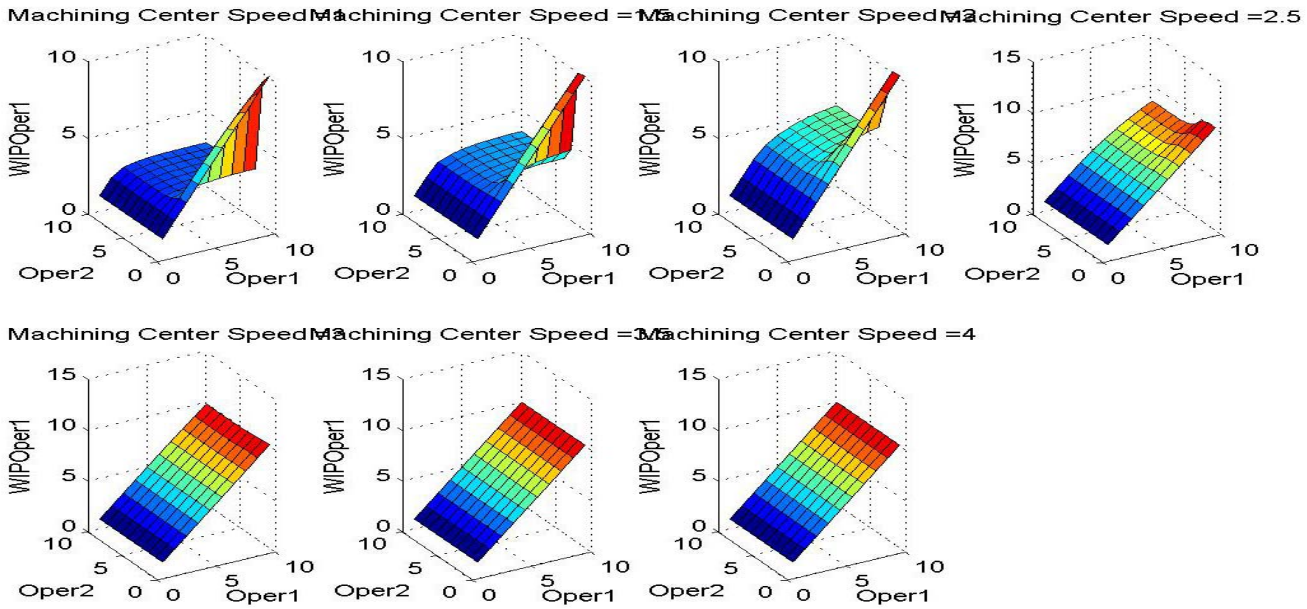

Figure 8. Work in progress of Operator 1 depending on Operator 1 and Operator 2 for different machining center speed (1, 1.5, 2, 2.5, 3, 3.5, and 4)

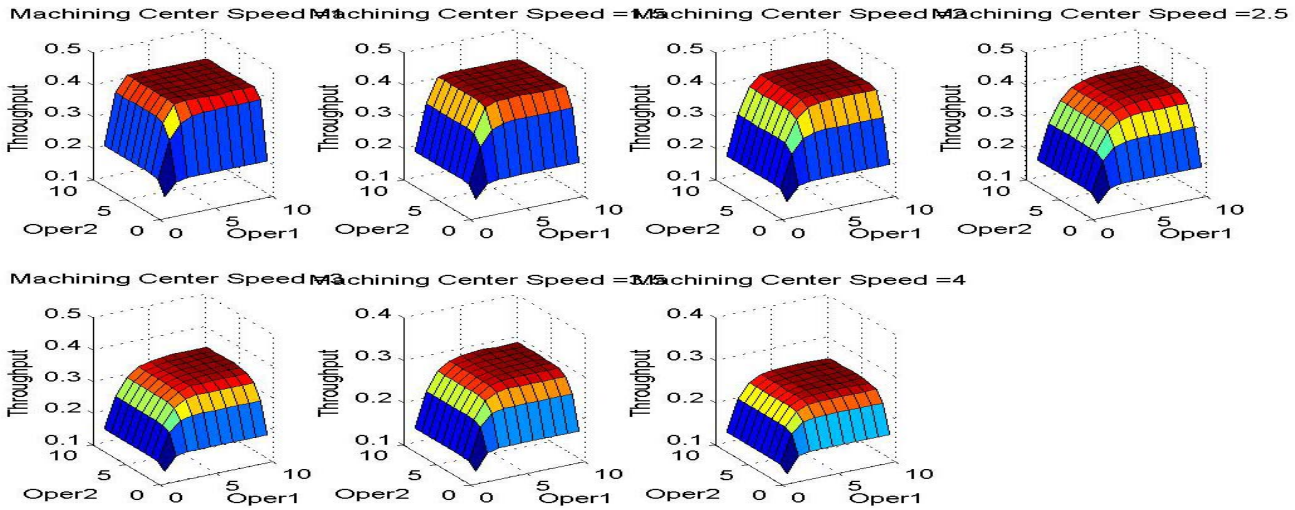

Figure 9. Throughput depending on Operator 1 and Operator 2 for different machining center speed (1, 1.5, 2, 2.5, 3, 3.5, and 4)

REFERENCES

Ajmone Marsan, M., Balbo, G., Conte, G., Do-natelli, S., Francheschinis, G. "Modelling with Generalized Stochastic Petri Nets", *Wiley* (1995)

Balbo, G., Silva, M.(ed.), "Performance Models for Discrete Events Systems with Synchronisations: Formalism and Analysis Techniques" (Vols. I and II), *MATCH Summer School, Jaca* (1998)

DiCesare, F., Harhalakis, G., Proth, J.M., Silva, M., Vernadat, F.B. "Practice of Petri Nets in Manufacturing", *Chapman-Hall* (1993)

Ingber, L. "Adaptive simulated annealing (ASA): Lessons learned", *Journal of Control and Cybernetics*, 25 (1), pp. 33–54 (1996)

Rodriguez, D. "An Optimization Method for Continuous Petri net models: Application to Manufacturing Systems". European Modeling and Simulation Symposium 2006 (EMSS 2006). Barcelona, October 2006

M. Silva. "Introducing Petri nets, In Practice of Petri Nets in Manufacturing" 1-62. Ed. Chapman&Hall. 1993

Zimmermann A., Rodríguez D., and Silva M. Ein effizientes optimierungsver-fahren fr petri netz modelle von fertigungssystemen. In Engineering kom-plexer Automatisierungssysteme EKA01, Braunschweig, Germany, April 2001.

Zimmermann A., Rodríguez D., and Silva M. A two phase optimization method for petri net models of manufacturing systems. Journal of Intelligent Manufacturing, 12(5):421–432, October 2001.

Zimmermann, A., Freiheit, J., German, R., Hommel, G. "Petri Net Modelling and Performability Evaluation with TimeNET 3.0", 11th Int. Conf. on Modelling Techniques and Tools for Computer Performance Evaluation, LNCS 1786, pp. 188-202 (2000).

ON THE DEVELOPMENT OF A RISK BASED VERIFICATION PROTOCOL FOR PROCESS MODELLING AND SIMULATION

Tore Myhrvold[(a)], Arjun Singh[(b)]

[(a, b)]Det Norske Veritas AS
Veritasveien 1, 1363 Høvik, Norway

[(a)]Tore. Myhrvold@dnv.com

ABSTRACT

A risk based procedure for verification of process modelling and simulation (PMS) is presented. The procedure is based on Det Norske Veritas offshore service specification for risk based verification, state-of-the-art methodologies within simulation verification, validation & accreditation, and recognized methods for PMS. The motivation for developing the procedure is the increasing challenges posed by the growing energy demand and climate change which creates an accelerating need for new energy technologies. The procedure is therefore directed towards physical and chemical processes and application with new emerging energy technologies, such as CO_2 capture and CO_2 conversion. Based upon various levels for verification involvement, the procedure describes how to verify subsequent steps in a proposed generalized framework for PMS.

Keywords: verification protocol, risk based, process modelling and simulation

1. INTRODUCTION

To cater the growing energy demand of the world and address the challenges posed by climate change and energy security, new energy processes are being explored and developed. There are several new technical, financial, safety and environmental challenges and risks related to the development of these energy processes.

One of the critical aspects in the development of these new processes is to demonstrate technological feasibility of the concept. To predict and demonstrate technological feasibility, methods such as modelling & simulation and experimental techniques are used. Simulating these new processes often require development of new models and tools. It is important to judge and address the uncertainty and risks associated with their development.

One major uncertainty in the development of models and simulations is the ability to develop them as desired. The objective of the current work is to develop a procedure that addresses this uncertainty and that increases confidence and creates trust for the end user of the simulation results.

1.1. Previous work

Several defence establishments across countries have realized the need for verification, validation and accreditation (VV&A) of simulation of their operation, organization and interests (Australian Department of Defence 2005; Defence Research & Development Canada 2003; United States Department of Defence 2006a). They have published instructions and recommended practices guides for such VV&A's. These guidelines recommend VV&A as a part of modelling and simulation. Use of VV&A is not only considered beneficial but necessary in some cases when use of simulation is critical in decision making.

The US Department of Defence (DoD) published a Recommended Practices Guide for VV&A of modelling and simulation (United States Department of Defence 2001, 2006b). In this Guide, *Verification* means the process of determining that a model implementation and its associated data accurately represent the developer's conceptual description and specifications. Further, *Validation* means the process of determining the degree to which a model and its associated data provide an accurate representation of the real world from the perspective of the intended use of the model. Finally, *Accreditation* is the official certification that a model, a simulation or a federation of models and simulations, and its associated data is acceptable for use for a specific purpose.

The US DoD and the military services have recognized the growing significance of modelling and simulation for many aspects of their operations. The DoD guide describes the interrelated processes that make up VV&A from a number of perspectives. Further, it explains what VV&A is, why it is important to perform, what the key considerations for scoping VV&A are, when it is performed, who the key players are and what are the costs and benefits of such work. The guide by the US DoD is a key document that is referenced and used as a starting point for many others in the literature.

Balci (1997) presented guidelines for conducting VV&A of simulation models. Fifteen guiding principles were introduced to help researcher practitioners and managers better comprehend what VV&A is about. The

VV&A activities were described in the modelling and simulation life cycle. An important principle presented by Balci is that *'VV&A require independence to prevent developer's bias"*.

Preece (2001) provided a critical assessment of the state of the practice in knowledge based V&V. It included a survey of available evidence as to the effectiveness of various V&V techniques in real world knowledge based development projects. For knowledge management practitioners, this paper offers guidance and recommendations for the use of V&V techniques. For researchers in knowledge management, the paper points to the areas where further work needs to be done in developing more effective V&V techniques.

Sargent (2007) discussed the different approaches to deciding model validity. Further, various validation techniques were defined and a recommended procedure for model validation was presented. V&V of simulation was also briefly discussed by Shannon (1998). Sokolowski and Banks (2009) discussed how to perform V&V of simulation including several relevant examples.

The general theory of mathematical modelling and simulation is established, although various descriptions on how to develop and operate a simulation model exist in the literature. Banks (1998) described the steps to guide a model builder in a thorough and sound simulation study. Maria (1997) gave an introduction to modelling and simulation and presented 11 general steps to develop simulation models, designing simulation experiments and performing simulation analyses. Zeigler et al. (2000) described a framework for modelling and simulation by using a different terminology. Hangos and Cameron (2001) described a seven step procedure for process modelling and modelling analysis, directed at the field of process engineering.

The general procedures by Hangos and Cameron (2001) and those described by Banks (1998) have served as the starting point and simulation framework for the verification protocol in the present work.

1.2. Present work

As the previous section shows, VV&A as well as general techniques for process modelling and simulation (PMS) are developed and established by others. The present work extends on these techniques and suggests a risk based verification procedure for PMS that is based on Det Norske Veritas offshore service specification for risk-based verification, state-of-the-art methodologies within V&V, and recognized methods for PMS. The risk based verification concept is described in DNV-OSS-300 (Det Norske Veritas 2004) and is visualized in Fig. 1.

In the present work the definition of *Verification* is: *Confirmation by examination and provision of objective evidence that the specified requirements have been fulfilled. The examination shall be based on information which can be proved true, based on facts obtained through observation, measurement, test or other means.*

Thus, the overall general steps for PMS provide the framework for the verification. The following is addressed in the protocol:

- A generalized procedure for PMS constitutes the framework in which the verification is performed. This framework is based on recognized methods for PMS.
- Description of detailed topics in the verification procedure such as simulation specification, risk assessment and definition of verification involvement by three risk-based verification levels.
- Development and execution of the verification plan that includes a description of how the different steps in the general framework for PMS will be verified for the different levels of verification.

Figure 1: The DNV Risk Based Verification Chain

2. METHODOLOGY

This verification protocol is developed for verification of PMS of physical and chemical processes. The methodology is based on the general principles in the DNV Offshore Service Specification Risk Based Verification (Det Norske Veritas 2004).

The risk based verification process is described in relation to generally accepted methods for PMS, such as the ones described by Hangos and Cameron (2001) and by Banks (1998). These general methods for PMS have been extended to form a generalized modelling and

simulation framework that is used to develop the verification plan as shown in Fig. 2.

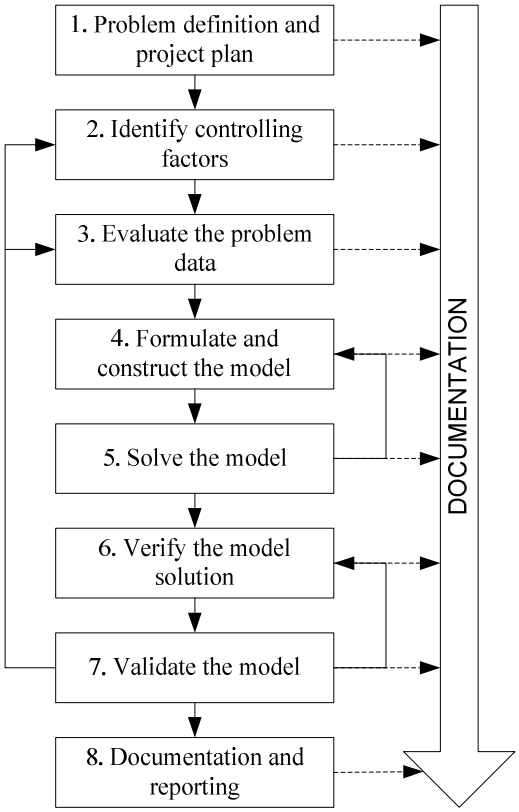

Figure 2: General Steps in Process Modelling and Simulation (PMS)

In this framework, an additional step called '*Documentation*' has been introduced which importance should be emphasized in verification. For detailed description of the key steps in Fig. 2, please refer to Hangos and Cameron (2001) and Banks (1998). A few points regarding the procedure importance are highlighted below.

If the validation results show that the developed model is not suitable for the modelling goal then one has to return to step 2 and perform the sequence again, i.e. it is an iterative procedure. Generally, validation results indicate how to improve the model.

It is recommended to document every action taken in each step of the development of the process model and simulation. This is particularly useful when the process being modelled and simulated is large and complex, and when there are several sub models which constitute the main model.

At the end, a report summarizing all the necessary details about the PMS should be prepared.

3. VERIFICATION OF PROCESS MODELLING AND SIMULATION

This section describes important and detailed aspects related to the verification procedure. This includes planning, simulation specification, risk assessment, determination of verification level and the verification plan of the DNV risk based verification concepts for PMS.

3.1. Simulation planned

This is the starting point for the simulation project and is the decision of the owner. It comprises a general description of the project.

3.2. Simulation specification

At least the following need to be specified at this step:

- Process system description: A process system is a system in which physical and chemical processes that are of interest to a modeller, take place. To define a process system, we need to specify its boundaries, its inputs and outputs and the physio-chemical processes taking place within the system. Process systems are conventionally specified in terms of a flow sheet which defines the boundaries together with inputs and outputs.
- A modelling goal: Specifies what one wants to achieve with the model. The modelling goal has a major impact on the level of detail and on the mathematical form of the model which will be built.
- Acceptance criteria and performance requirements to the simulation.
- Determination of overall verification plan.

3.3. Risk assessment

The risk assessment is a means to determine the required level of verification. The risk assessment includes the identification of hazards, frequencies of occurrence, consequences and risk drivers. It also includes ranking of hazards based on risk evaluation.

The risk can be defined on a general level, for different phases or for detailed elements of the simulation. Risks with PMS are that it fails to give expected results because of aspects such as:

- The model was not built as intended
- The process to be simulated has a degree of novelty and therefore may lead to simplifications in the development of models for the process. These simplifications may distort the results to an extent that these become neither meaningful nor useful in the decision making process.

Consequences of such failure can be the following:

- Incorrect decisions
- Delay in making decisions
- Loss of time, resource and money

3.4. Definition of verification involvement

The level of verification involvement should be differentiated according to the risk to the asset or elements or phases thereof. If the risk to the asset is

higher, the level of verification involvement is higher. Conversely, if the risk to the asset is lower, the level of verification activities can be reduced, without any reduction in their effectiveness.

There are three levels of verification of assets, categorized as *low, medium and high*.

Low is the level of verification applied where the risks to the asset are lower than average. For example it has benign contents, it is located in congenial environment conditions, or the contractors are well experienced in the design and construction of similar assets. The level may also be appropriate when the owner (or other parties) performs a large degree of verification or quality assurance work.

With regard to process simulation verification, it is proposed to use the *Low* category of verification in the following situations:

- The process which is simulated is well known and understood, it has no new technical novelty
- The process simulation is carried out as part of the customary design practice, using well known simulation tools by experienced designer/parties.
- The verification of the process simulation is done as part of the modelling and simulation steps described above by the designer. No independent verification is required.

Medium is the level of verification applied where the risks to the asset are average. This is the level of verification which is customary and is applied to the majority of assets. For process simulation verification, it is proposed to use this category of verification in the following situations:

- The process which is simulated has moderate level of technical novelty (technological or application or both) and the process simulation is carried out to predict the performance.
- The process simulation is carried out with well known tools by less experienced users or by well experienced users with relatively new simulation tools.
- The verification of process simulation may require independent verification.

High is the level of verification applied where the risks to the asset is higher than average. For example, it has a highly corrosive content, it is in adverse environmental conditions, it is technically innovative or the contractors are not well experienced in the design and construction of similar assets. This level may also be appropriate when the owner chooses to have a small technical involvement or perform little own verification.

For PMS verification, it is proposed to use the *High* category of verification in the following situations:

- The process which is simulated has high level of technical novelty (application or technological or both) and process simulation is carried out to predict the performance of the process.
- The PMS is carried out by less experienced users with less known simulation tools.
- The owner of the asset (process) is not involved in the process simulation and uses contractors for simulation work.

Independent verification is strongly recommended for High level verification.

3.5. Develop verification plan

This section describes how to develop the *verification plan* including a list of verification activities. The verification plan is developed based on compliance with the general framework for PMS shown in Fig. 2 and the determined verification level for the simulation.

A questionnaire based approach is proposed for the verification in each step. Each question indicates the levels of verification, i.e. the question is addressed. 'L', 'M' and 'H' to denote low level, medium level and high level verification, respectively. Thus, the development of the verification plan should follow procedures as shown in Table 1 to Table 6. For simplicity, only selected parts of the verification plan development are shown in these tables.

3.6. Verification execution

Verification execution is document review, independent analyses, inspection, monitoring, site visits, process audits, technical audits, testing, etc. according to the verification plan.

Information arising from execution should be used to identify continuous improvements to the verification plan.

The purpose of the verification activities is to confirm compliance or non-compliance with the simulation specification.

3.7. Simulation completed

Simulation completed is the end point of any lifecycle phase or phases, which complies with the relevant planned simulation and the simulation specification.

4. APPLICATION OF THE PROTOCOL

The verification protocol described above is applicable to modelling and simulation of physical and chemical processes. The protocol is currently being tested on specific cases that are particularly relevant for the development of environmentally friendly energy processes.

One such process is the electrochemical conversion of CO_2 into a useful product such as formic acid.

Another process is the separation of CO_2 from combustion flue gases by chemical absorption, followed by compression and injection into an underground storage site.

Table 1: Excerpt from Verification of Problem Definition and Project Plan.

Verification activity	*Level*		
	L	*M*	*H*
Problem statement – purpose of simulation, scope of simulation is well defined and documented			
• What is the process to be simulated and why is it being simulated?	x	x	x
• Has the process been described to a sufficient degree of detail and accuracy?	x	x	x
• What are the model characteristics (spatial or lumped, steady-state or dynamic, etc.)?	x	x	x
How was the problem statement formulated?			
• Was it defined by the technology owner?			x
• Has the problem definition been communicated to all relevant parties?			x
• How was the problem definition communication done?			x

Table 2: Excerpt from Verification of Identification of Controlling Factors or Mechanism.

Verification activity	*Level*		
	L	*M*	*H*
Have the processes or phenomena taking place in the system been identified and documented?	x	x	x
Are these processes or phenomena well known and have they been simulated before?		x	x
What are the new aspects of the processes or phenomena taking place in the system, if any?		x	x
Did new aspects of the processes or phenomena require simplifications and assumptions in the development of the simulation?		x	x
Have accuracy and tolerance of the simulation been discussed and agreed?			x

Table 3: Excerpt from Verification of the Data for the Simulation.

Verification activity	*Level*		
	L	*M*	*H*
What is the data used in the simulation?	x	x	x
How reliable is the data?		x	x
What is the precision and uncertainties with the data and what will be the impact of these on the simulation results?			x

Table 4: Excerpt from Verification of Model Solution.

Verification activity	*Level*		
	L	*M*	*H*
Are the outputs from the model as expected?	x	x	x
Has a sensitivity analysis of the output been done?		x	x
In case of high level verification, it may be necessary to perform simulations using two different simulation tools and compare the results.			x
Have the results been discussed with the client and with experts, and agreed and documented?	x	x	x

Table 5: Excerpt from Validation of the Model.

Verification activity	*Level*		
	L	*M*	*H*
Has the model been validated?	x	x	x
How is the model validated?			
• By verifying experimentally the simplifying assumptions		x	x
• By comparing the model behaviour with process behaviour		x	x
• By developing an analytical model for simplified cases and comparing behaviour		x	x
• By comparing with other models using a common problem		x	x
• By comparing the model with available process data		x	x

Table 6: Excerpt from Verification of Documentation.

Verification activity	*Level*		
	L	*M*	*H*
Has all the work been properly documented?	x	x	x
Has the owner reviewed the report and agreed with the report's findings?		x	x

5. DISCUSSION

No specific document on VV&A directed towards process engineering modelling and simulation has so far been identified by the authors. However, the basic steps and procedures for VV&A found in the literature can also be used for VV&A of PMS.

For instance, the principles explained in the VV&A Recommended Practices Guide by the US DoD are generic and can be applied to the verification of PMS to an extent. This guideline also states that 'risk' determines the detail or level of verification along with technical and resource constraints. The DNV risk based verification as described in DNV-OSS-300 (Det Norske Veritas AS 2004) is more explicit on risk classification

and associated verification activities than what is presented and discussed by the US DoD and others.

Furthermore, the terminology and steps used in PMS, such as those presented by Hangos and Cameron (2001), are not entirely the same as those discussed in literature in general for modelling and simulation.

Thus, the guidelines by DoD alone will not suffice as a guiding and complete document for the verification of PMS. However, the work by the US DoD has served as a starting point for the present work on writing such a guideline. The various verification and validation techniques described in the US DoD documents are the same as those that are typically employed by DNV during verification, such as audit, review, inspection, walkthrough, HAZID etc.

6. CONCLUSIONS

This work has shown the development of a protocol for risk based verification of process modelling and simulation (PMS). Application of the protocol will address uncertainty and risks associated with the development of PMS and thus provide confidence and trust to the stakeholders.

REFERENCES

Australian Department of Defence, 2005. *Simulation Verification, Validation and Accreditation Guide*. Australian Defence Simulation Office, Department of Defence, Canberra, Australia.

Balci, O., 1997. Verification, validation and accreditation of simulation models. *Proceedings of the Winter Simulation Conference*, 135-141. 7-10 December, Atlanta, Georgia.

Banks, J., 1998. *Handbook of Simulation: Principles, Methodology, Advances, Applications, and Practice*. New York:John Wiley & Sons.

Defence Research & Development Canada, 2003. *Review of Verification and Validation Methods in Simulation*. Technical Memorandum 2003-055.

Det Norske Veritas AS, 2004. *Risk Based Verification*. DNV-OSS-300.

Hangos, K. and Cameron, I., 2001. *Process Modelling and Model Analysis*. San Diego:Academic Press.

Maria, A., 1997. Introduction to Modelling and Simulation. *Proceedings of the Winter Simulation Conference*, 7-13. 7-10 December, Atlanta, Georgia.

Preece, A., 2001. Evaluating verification and validation methods in knowledge engineering. In: R. Roy, Ed., *Micro-level knowledge management* Morgan-Kaufman, 123-145.

Sargent, R. G., 2007. Verification and validation of simulation models. *Proceedings of the Winter Simulation Conference*, 124-137. 9-12 December, Washington D.C.

Shannon, R. E., 1998. Introduction to the art and science of simulation. *Proceedings of the Winter Simulation Conference*, 7-14. 13-16 December, Washington D.C.

Sokolowski, J. A. and Banks, C. M., 2009. *Principles of Modelling and Simulation: A Multidisciplinary Approach*. Hoboken:John Wiley & Sons.

United States Department of Defence, 2001. *V&V Techniques*. Available from: http://vva.msco.mil/ [accessed 23 July 2010].

United States Department of Defence, 2006a. *VV&A Recommended Practices Guide*. *RPG BUILD 3.0*. Available from: http://vva.msco.mil/ [accessed 23 July 2010].

United States Department of Defence, 2006b. Key Concepts of *VV&A*. Available from: http://vva.msco.mil/ [accessed 23 July 2010].

Zeigler, B. P., Praehofer, H. and Kim, T.G., 2000. *Theory of Modelling and Simulation* 2nd Ed. San Diego:Academic Press.

AUTHORS BIOGRAPHY

Det Norske Veritas (DNV) is an autonomous and independent foundation with the objectives of safeguarding life, property and the environment, at sea and onshore. DNV undertakes classification, certification and other verification and consultancy services relating to quality of ships, offshore units and installations, and onshore industries worldwide, and carries out research in relation to these functions. http://www.dnv.com/.

Tore Myhrvold is a Principal Researcher at DNV Research & Innovation and is currently working with energy research and process engineering modelling and simulation. His main focus is topics related to CO_2 capture processes and technology verification and qualification. He was the main author of a new DNV Recommended Practise, DNV-RP-J201 "Qualification Procedures for CO_2 Capture Technology", published in April 2010. Myhrvold received a M.Sc within mechanics, thermodynamics, and fluid dynamics in 1997 and a PhD within heat and combustion engineering in 2003 at the Norwegian University of Science and Technology. His main field of competence is turbulent flow and combustion modelling, such as gas turbine combustor flow and emissions, emissions from boilers, pipe flow, etc.

Arjun Singh participated in this work as a Senior Researcher at DNV Research & Innovation. He has a background from Technology Risk Management Consulting in DNV with focus on verification and qualification projects in the oil & gas value chain, specifically towards Liquefied Natural Gas (LNG) processes. Singh received a M. Tech. in mechanical engineering from the Indian Institute of Technology, Kanpur in 2000. He is currently a MBA (PGPX) Student at IIM Ahmedabad, India.

OPTIMIZATION OF FLEXIBLE MANUFACTURING SYSTEMS: COMPARISON BETWEEN STOCHASTIC AND DETERMINISTIC TIMING AASOCIATED TO TASKS

Diego R. Rodríguez[(a)], Daniela Ándor[(b)] , Mercedes Pérez[(c)], Julio Blanco[(d)]

[(a)] Fundación LEIA CDT
[(c,d)]Universidad de La Rioja. Dpto. Ingeniería Mecánica
[(b)]Universidad de la Rioja. Dpto. Ingeniería Eléctrica

[(a)] diegor@leia.es; [(b)] daniela.andoz@alum.unirioja.es ;
[(c)] mercedes.perez@unirioja.es ; [(d)] julio.blanco@unirioja.es

ABSTRACT
Modeling of Flexible Manufacturing Systems has been one of the main research topics dealt with by researchers in the last years. The modeling paradigm chosen can be in many cases a key decision that can improve or give an added value to the example modeling task. Here, two different modeling manners are presented both based in the Petri Net paradigm, Stochastic and Colored Petri Net models. These two models will be compared in terms of the performance measures that could be interesting for the production systems. The production indicators used here are related with the productivity of the systems. These productivity measures could be included in a later stage into an optimization process by changing a certain number of parameters into the model. A comparison between the performance measures and also other computational effort measures will be depicted to check whether one model is more appropriate or the other.

Keywords: Petri nets, flexible manufacturing, deterministic timing, stochastic timing, simulation, optimization

1. INTRODUCTION

The process of optimizing a Production System can be divided clearly into three tasks that will be the modeling, analysis and optimization. The first part applied to the different production systems examples will be the modeling issue. The modeling paradigm used in our case are Petri Nets but other different modeling paradigms can be used to model the FMS. The second part is dedicated to the obtaining of Performance Measures for these models. These results can be exact or approximated depending or even bounds (upper or lower) of the performance measures needed to compute the final cost function. Here, we will consider for the models two possibilities, one where the time associated to the tasks performed can be considered deterministic or a second one where the time is considered stochastic. This timing constraint difference will allow us to consider later on some comparisons int the optimization process at different levels. Finally, the optimization in the design of the Manufacturing System is considered.
The rest of the paper is as follows, in section 2 the FMS that will be used along this paper will be explained and all the elements that will be interesting to be represented in our models will be enumerated. Later on, in sections3 the two Petri net models will be depicted. Section 4 is devoted to the presentation of the optimization problem that will be considered in this paper. Finally, the results we are interested in are represented associated to the models in section 5 where a comparison of the simulation results is shown. Finally some conclusions are presented in section 6.

2. DESCRIPTION OF THE FMS

The example that will be used in the development of this thesis will be a Flexible Manufacturing Cell of the Flexlink. The layout of the cell corresponds with Figure 1.

The Flexible Manufacturing Cell under study is formed by two different lifters (left and right one) that perform the operation of raising/descending of the pallets that are being produced.. The left lifter will perform the operation of taking the pallets from the lower level central line (that has 6 possible positions) to the higher one, while the right lifter is in charge of the opposite operation. The next element that appears in the FMC is the starting GWS, This is in charge of moving the material to the three possible positions (upper layer, middle layer, low layer). This decision will be taken from the moment that a pallet arrives to initial position of the station (middle layer) coming from the left lifter (GWS lifter).The decision whether to go one way or the other two will be taken randomly with equal probabilities for the three options (immediate transitions will be used for this decision). The higher line and the lower one are exactly equal while the intermediate line is a by-pass to the second part of the cell. When the pallets are arriving to the upper/lower line they are process in the GWS main station.

The SpecOpen Line is divided in six parts, each part is controlled by one Controller and the layout is shown in Figure 1.
The shaded part is used to show the part below the line, where the pallet go from left to right, from JOT_Lifter to GWS_Lifter. The conveyors below are controlled by the same PTC as the upper parts.

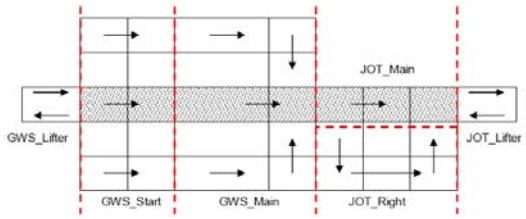

Figure 1: FMS Layout

The following times show how long does a pallet takes to go from one part of the line to the next.

Table 1. Processing times

START	END	TIME (ms)
GWS_Start (Down)	GWS_Lifter(Down)	1800
GWS_Lifter (Out, Down)	GWS_Lifter(In, Down)	2150
GWS_Lifter(In, Down)	GWS_Lifter(In, Up)	1950
GWS_Lifter(In, Up)	GWS_Lifter(In, Down)	1290
GWS_Lifter(In, Up)	GWS_Lifter(Out, Up)	1800
GWS_Lifter(Out, Up)	GWS_Start(Center Cross)	2200
GWS_Start(Center Cross)	GWS_Start(Right Cross)	3820
GWS_Start(Center Cross)	GWS_Start(Left Cross)	3820
GWS_Start(Center Cross)	GWS_Main(Middle Conveyor)	2500
GWS_Start(Left Cross)	GWS_Main(Left Conveyor)	3730
GWS_Start(Right Cross)	GWS_Main(Right Conveyor)	3730
GWS_Main(Middle Conveyor, 1st)	GWS_Main(Middle Conveyor, 2nd)	1640
GWS_Main(Left Conveyor, 1st)	GWS_Main(Left Conveyor, 2nd)	1580
GWS_Main(Right Conveyor, 1st)	GWS_Main(Right conveyor, 2nd)	1580
GWS_Main(Middle Conveyor, 2nd)	GWS_Main(Center Cross)	2300
GWS_Main(Left Conveyor, 2nd)	GWS_Main(Left Cross)	1450
GWS_Main(Right Conveyor, 2nd)	GWS_Main(Right Cross)	1450
GWS_Main(Left Cross)	GWS_Main(Center Cross)	4270
GWS_Main(Right Cross)	GWS_Main(Center Cross)	4270
GWS_Main(Center Cross)	JOT_Main(Start)	1850
JOT_Main(Start)	JOT_Main(Conveyor)	1500
JOT_Main(Conveyor)	JOT_Main(End)	1800
JOT_Main(Start)	JOT_Right(Start)	2100
JOT_Right(Start)	JOT_Right(Conveyor)	1450
JOT_Right(Conveyor)	JOT_Right(End)	1500
JOT_Right(End)	JOT_Main(End)	1900
JOT_Main(End)	JOT_Lifter(Up)	1200
JOT_Lifter(Up)	JOT_Lifter(Down)	7600
JOT_Lifter(Down)	JOT_Lifter(Up)	8500
JOT_Lifter(Down)	JOT_Main(Down, 1st)	1500
JOT_Main(Down, 1st)	JOT_Main(Down, 2nd)	1000
JOT_Main(Down, 2nd)	JOT_Main(Down, 3rd)	1480
JOT_Main(Down, 3rd)	GWS_Main(Down, 1st)	2000
GWS_Main(Down, 1st)	GWS_Main(Down, 2nd)	1900
GWS_Main(Down, 2nd)	GWS_Main(Down, 3rd)	1700
GWS_Main(Down, 3rd)	GWS_Start(Down)	2800

3. STOCHASTIC PETRI NET MODEL

Here we present the Petri net it has been modeled using stochastic PNs.

The complete model is represented in the following figure 2.

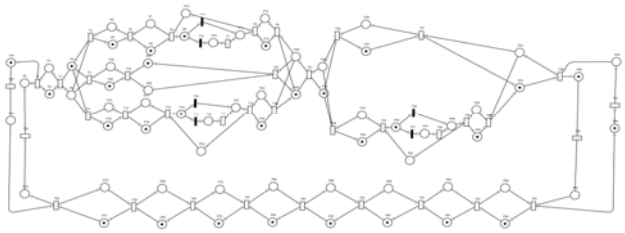
Figure 2: Sample Figure Caption

Now, the different parts/machines that compose this model will be depicted and explained individually and finally these models will be merged reaching finally the model of figure 3.4.

The left lifter model is represented in Figure 3.

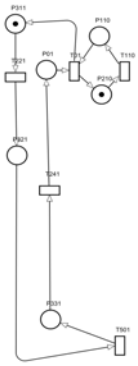
Figure 3: Left lifter Petri net model

Here places P311 and P331 when marked represent the state that the lifter is ready for receiving pallets, from the upper or from the lower level. Transitions T221 and T241 represent the time that takes to the lifter to ascend or descend with the pallet containing the material to be assembled. Transitions

T01 and T501 represent the time that takes to the pallet to get out/enter into the lifter to be ready to go to the corresponding level. Because this lifter is thought to transfer pallets from the lower level to the upper one, the transition T221 is automatically fired when the lifter is free of pallets.

The second lifter is represented in Figure 4. The process is quite similar to the one explained for the first one with the only difference that the process is the opposite, this lifter will carry pallets from the upper level to the lower one. Here transitions T401 and T411 represent the operation times associated to the down and up movement of the lifter respectively.

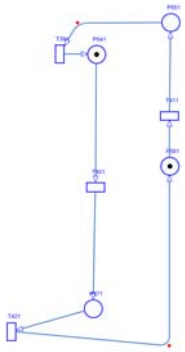

Figure 4: Right lifter Petri net model

The lower level pallet transfer system is represented in figure 5. and the 8 possible positions that the pallet can adopt are shown there.

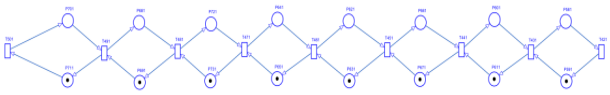

Figure 5: Lower level Petri net model

Finally, the upper level that contains the robot center the JOT Main and Right, the GWS center and all the by-pass parts is represented in figure 6.

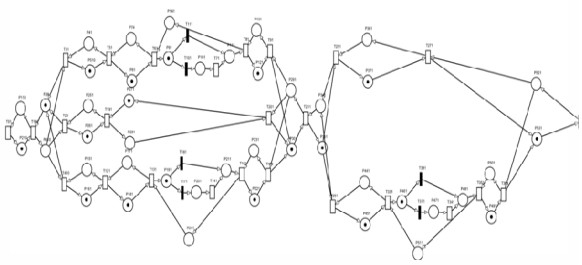

Figure 6: Upper level Petri net model

The deterministic Petri net considered here is represented by the following figure. It can be seen that this model is quite similar to the original stochastic one.

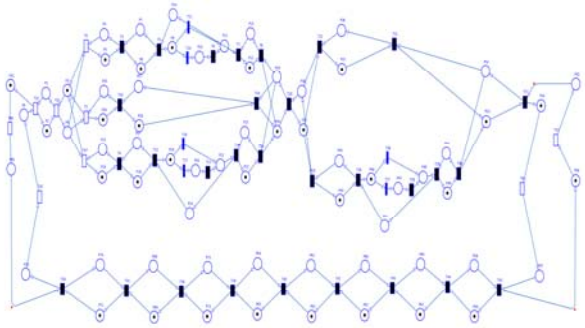

Figure 7: Deterministic FMS Petri net model

It has been considered a deterministic behavior only in the machining part and in the conveyors that compose the system. It has been conserved the stochastic behavior in the lifters due to their possible parameter change associated to their movements. For the transitions that have been changed to deterministic it has been considered the value of the mean associated to the corresponding exponential transition.

4. OPTIMIZATION OF THE FMS MODEL

The search space corresponding to the optimization problem that it is solved during this thesis is composed by the following variables:

Variable ➔ **LiftUP** that controls the time spent by the first lifter to go from the lower level to the upper one

Variable ➔ **Lift2UP** that controls the time spent by the second lifter to go from the lower level to the upper one

Variable ➔ **LiftDown** that controls the time spent by the first lifter to go from the upper level to the lower one

Variable ➔ **Lift2Down** that controls the time spent by the second lifter to go from the upper level to the lower one

Variable ➔ **Prob1** value corresponds to the percentage of situations where the GWS Main Left part is available to operate

Variable ➔ **Prob2** value corresponds to the percentage of situations where the GWS Main Right part is available to operate

Variable ➔ **Prob3** value corresponds to the percentage of situations where the JOT Right station is available to operate
The search space where the optimization process will look for the solution of the problem will be in this particular case the one depicted in the following.

Parameter definitions:

#	name	type	minimum	maximum	initial	delta	temp
0	LiftUP	REAL	2.00	4.00	3.00	0.01	1.000000
1	Lift2Up	REAL	2.00	4.00	3.00	0.01	1.000000
2	LiftDown	REAL	1.00	3.00	2.00	0.01	1.000000
3	Lift2Down	REAL	1.00	3.00	3.00	0.01	1.000000
4	Prob1	REAL	5.00	95.00	50.00	0.10	1.000000
5	Prob2	REAL	1.00	100.00	50.00	0.10	1.000000
6	Prob3	REAL	1.00	100.00	50.00	0.10	1.000000

The Profit function used in this example is a simple combination of the utilizations of the different stations/machines that are available in the FMS (Lifters, JOT, GWS). The objective is to maximize this amount, so that our system is used at the maximum level. This maximal utilization will revert in a maximal throughput of the system, taking into consideration that with the maximum utilization of the devices we are ensuring that the by-pass are used at their minimum value but using them as an option to avoid deadlock or material stopping situations.

Final result of optimization:

LiftUP=3.330168,
Lift2Up=3.501725,
LiftDown=1.330764,
Lift2Down=2.107886,
Prob1=27.838387,
Prob2=76.333992,
Prob3=36.824970
Profit=1.128963

Queue information:

Queue length: 10000
Queue entries: 1006
Cost function calls: 1140
Queue hit rate: 11% (this run only)

Final result of optimization:

LiftUP=3.571091,
Lift2Up=3.948040,
LiftDown=2.404728,
Lift2Down=2.937917,
Prob1=28.740118,
Prob2=11.330377,
Prob3=70.051277
Profit=0.882584

Queue information:

Queue length: 10000
Queue entries: 1010
Cost function calls: 1140
Queue hit rate: 11% (this run only)

For optimizing the problem here shown, it has been considered a Simulated Annealing algorithm based on the Adaptive Simulated Annealing package (Ingber 1996)

5. COMPARISON OF RESULTS

Here the results obtained for the optimization using the two representations are shown.

This first table shows the result obtained with the stochastic model while the second textbox shows the results obtained with the deterministic one.

Table 2 shows in a summarized manner the results obtained for the two experiments. It is clear that the profit obtained with the stochastic model is a bit greater than with the deterministic one and also the computational effort associated to the deterministic experiment is greater than the one obtained with the stochastic one.

Table 2: Experiments results

Example 1

Exp.	Time (Minutes)	Simul.	Profit
STOCH.	2,612.62	1006	1.128963
DET.	2,792.75	1010	0.882584

Once we have obtained these results, it will be interesting to characterize the evolution of the profit function according to the changes in the different variables and also compare the results obtained for the two models here depicted.

In order to check the real difference between the stochastic and the deterministic model we have evaluated a couple of search spaces varying some variables that are included into the original search space.

SEARCH SPACE1:

Parameter definitions:

#	name	type	minimum	maximum
0	LiftUP	REAL	2.00	4.00
1	Lift2Up	REAL	2.00	4.00
2	LiftDown	REAL	1.00	3.00
3	Lift2Down	REAL	1.00	3.00
4	Prob1	REAL	5.00	FIXED
5	Prob2	REAL	5.00	FIXED
6	Prob3	REAL	5.00	FIXED

The following figure 8, represents the results obtained for this experiment. The upper level of the figure corresponds to the stochastic experiment while the lower one corresponds to the deterministic behavior. It

can be observed that the variation in the stochastic version of the model is higher; a clear reasoning is associated to this behavior taking into consideration the stochastic nature of most of the variables included in the model. With respect to the deterministic model it is clear that the variation of certain speed variable has a direct relationship with the utilization of the different devices included, not observing some paradoxical situations that can be clearly identified in the stochastic model.

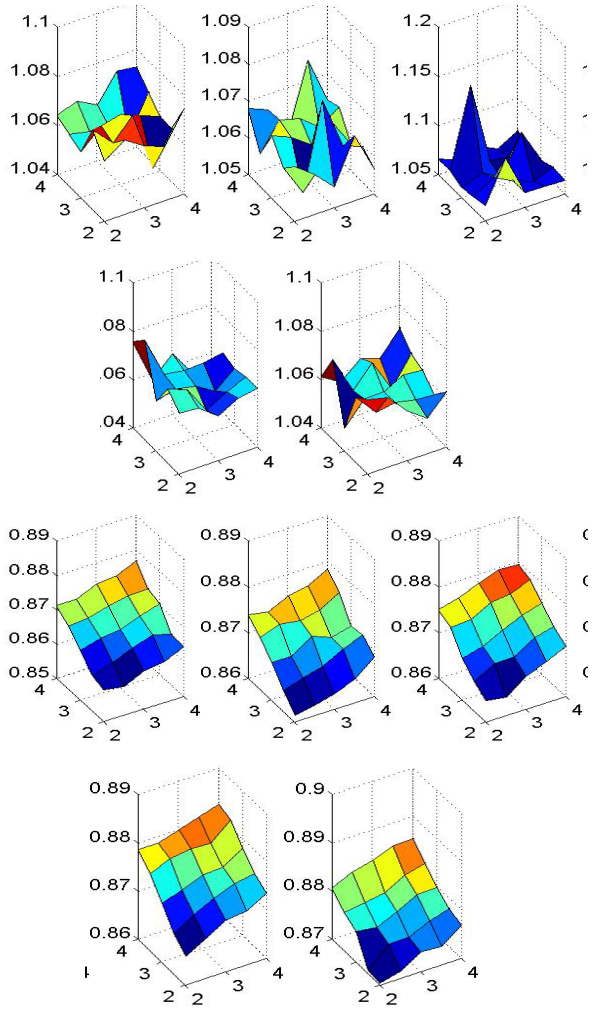

Figure 8: Stochastic vs. Deterministic behavior

Table 2: First Exhaustive Search Experiment results

	Mean	Max	Min	Nº Exps.
Comparison	82.01%	84.18%	73.11%	2500
Stochastic	1.06424	1.2043	1.0448	2500
Deterministic	0.87268	0.8874	0.8874	2500

The comparison between the two representations gives us the following results. The deterministic experiment is in mean an 82% less than the stochastic experiment for this first set of solutions where the machine/operations speeds are varied.

The second search space considered to compare the two approaches is shown below and the change in the parameters in this particular case is more concentrated on the probabilities of utilization of the different machining centers or workstations (variables Prob1 and Prob2).

SEARCH SPACE2:

Parameter definitions:

#	name	type	minimum	maximum
0	LiftUP	REAL	3.00	FIXED
1	Lift2Up	REAL	3.00	FIXED
2	LiftDown	REAL	2.00	FIXED
3	Lift2Down	REAL	2.00	FIXED
4	Prob1	REAL	5.00	95.00
5	Prob2	REAL	5.00	95.00
6	Prob3	REAL	5.00	FIXED

Figure 9 shows the results obtained for these experiments. The left part of the figure corresponds to the deterministic model while the right part corresponds to the stochastic one. As mentioned before, the variation in the results is higher for the stochastic model due to the nature of the variables involved in the process.

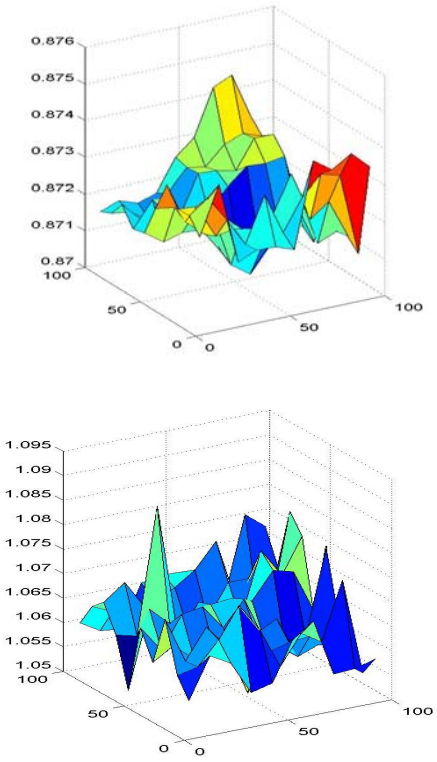

Figure 9: Stochastic vs. Deterministic behavior

Table 3: Second Exhaustive Search Experiment results

	Mean	Max	Min	Nº Exps.
Comparison	82.00%	82.86%	80.22%	100
Stochastic	1.06361	1.0866	1.0520	100
Deterministic	0.87214	0.8745	0.8745	100

Table 3 shows global results obtained for the second experiment comparing the behaviors of the two models (stochastic and deterministic). The results are quite similar to the ones shown in table 2 in terms of comparison of results, showing that there is a clear relationship between the results that can be measured around 82%, independently of the variables that we want to vary.

6. CONCLUSIONS

An approach to the optimization of Flexible Manufacturing Systems modeled using stochastic or deterministic timing associated to the operations is presented in this paper. The paper shows that there is a clear difference between the results obtained with the two approaches in terms of the utilization of the resources present in the system. It has also been shown that the stochastic model has more chaotic behavior with respect to changes in certain parameters.

REFERENCES

Aarts, E., Korst, J. "Simulated Annealing and Bolz-mann Machines", *Wiley* (1989)

Ajmone Marsan, M., Balbo, G., Conte, G., Do-natelli, S., Francheschinis, G. "Modelling with Generalized Stochastic Petri Nets", *Wiley* (1995)

Balbo, G., Silva, M.(ed.), "Performance Models for Discrete Events Systems with Synchronisations: Formalism and Analysis Techniques" (Vols. I and II), *MATCH Summer School, Jaca* (1998)

DiCesare, F., Harhalakis, G., Proth, J.M., Silva, M., Vernadat, F.B. "Practice of Petri Nets in Manufacturing", *Chapman-Hall* (1993)

Ingber, L. "Adaptive simulated annealing (ASA): Lessons learned", *Journal of Control and Cybernetics*, 25 (1), pp. 33–54 (1996)

Rodriguez, D. "An Optimization Method for Continuous Petri net models: Application to Manufacturing Systems". European Modeling and Simulation Symposium 2006 (EMSS 2006). Barcelona, October 2006

M. Silva. "Introducing Petri nets, In Practice of Petri Nets in Manufacturing" 1-62. Ed. Chapman&Hall. 1993

Zimmermann A., Rodríguez D., and Silva M. Ein effizientes optimierungsver-fahren fr petri netz modelle von fertigungssystemen. In Engineering kom-plexer Automatisierungssysteme EKA01, Braunschweig, Germany, April 2001.

Zimmermann A., Rodríguez D., and Silva M. A two phase optimization method for petri net models of manufacturing systems. Journal of Intelligent Manufacturing, 12(5):421–432, October 2001.

Zimmermann, A., Freiheit, J., German, R., Hommel, G. "Petri Net Modelling and Performability Evaluation with TimeNET 3.0", 11th Int. Conf. on Modelling Techniques and Tools for Computer Performance Evaluation, LNCS 1786, pp. 188-202 (2000).

Testing Discrete Event Systems: Synchronizing Sequences using Petri Nets

Marco Pocci[(a)], Isabel Demongodin[(b)], Norbert Giambiasi[(c)], Alessandro Giua[(d)]

[(a)−(c)]Laboratoire des Sciences de l'Information et des Systèmes, Campus de Saint Jérôme, Marseille, France
[(d)]Department of Electrical and Electronic Engineering, University of Cagliari, Cagliari, Italy

{[(a)]marco.pocci, [(b)]isabel.demongodin, [(c)]norbert.giambiasi}@lsis.org, [(d)]giua@diee.unica.it

Abstract

In the field of Discrete Event Systems, an important class of testing problems consists in determining a final state after the execution of a test. This problem was completely solved in the 60's using homing and synchronizing sequences for finite state machines with inputs/outputs. In a synchronizing problem, we want to drive an implementation of a given model, seen as a black-box, to a known state regardless of its initial state and the outputs. In this paper, we propose a first approach to solve the synchronizing problem on systems represented by a class of synchronised Petri nets. We show that, regardless of the number of tokens that the net contains, a synchronizing sequence may be computed in terms of the net structure, thus avoiding the state explosion problem.

Keywords: testing problems, finite state machines, Petri nets, synchronizing sequences

1. Introduction

This paper deals with the problem of determining a final state of an implementation of a Discrete Event Systems (DES), extending the existing approaches for *Finite State Machines* (FSM) to a class of *Petri nets* (PN).

The fundamental problems in testing FSM and the techniques for solving these problems have been pioneered in the seminal paper of Moore (Moore, 1956) and have been reviewed extensively by Lee and Yannakakis (Lee and Yannakakis, 1996). They stated five fundamental problems of testing: i) determining a final state after a test; ii) state identification; iii) state verification; iv) conformance testing; v) machine identification. Among these, we consider the problem of determining a final state after a test. This problem was addressed and essentially completely solved around 1960 using *homing* (HS) and *synchronizing sequences* (SS). An homing sequence is an input sequence that brings a FSM from an initial state —supposed unknown— to a state that can be determined by the observed output event sequence. A synchronizing sequence is an input sequence that brings a FSM from any initial unknown state to a known state regardless of the output sequences.

Several approaches are used to obtain a synchronizing sequence for an FSM. The synchronizing tree method (Kohavi, 1978; Hennie, 1968); since memory required to build up the tree is high, this method is suitable only for small FSM. Simulation-based method, binary decision diagram method (BDD) (Pixley et al., 1994; Rho et al., 1993);the drawback of this method is that the length of the synchronizing sequence may be far away from the lower bound. Homing sequence method (Pomeranz and Reddy, 1994); the method alleviates the need for a machine to have synchronizing sequence but its main disadvantage is that the final state is different for each power-on and we must observe the output responses to determine the final state. Finally Eppstein (Eppstein, 1990) gave an algorithm, based on Natarajan's work (Natarajan, 1986), for *reset sequences*. This algorithm, that in polynomial time either finds such sequences or proves that none exists, has been described by Lee *et al.* (Lee and Yannakakis, 1996) and adapted for synchronizing sequences.

Little has been done in the area of testing of systems specified as Petri Nets. For example Jourdan and Bochmann (G.-V. Jourdan and G.v. Bochmann, 2009) investigated the question of automatically testing Petri Nets, to ensure the conformance and so that an implementation of a specification provided as a Petri Net is correct. Zhu and He gave an interesting classification of testing criteria (Zhu and He, 2002) — without testing algorithm — and presented a theory of testing high-level Petri nets (H. Zhu and X. He, 2000) by adapting some of their general results in testing concurrent software systems. In the Petri net modelling framework, one of the main supervisory control tasks is to guide the system from a given initial marking to a desired one similarly to the synchronisation problem. Yamalidou *et al.* presented a formulation based on linear optimisation (Yamalidou and Kantor, 1991; Yamalidou et al., 1992). Giua and Seatzu (Giua and Seatzu, 2002) defined several observability properties and dealt with the problem of estimating the marking of a place/transition net based on event observation.

The main idea of this paper is to apply the existing techniques developed for FSM to Petri nets. We consider *synchronised nets*, i.e., a net where a label is associated to each transition. The label represents an external input event whose occurrence causes the transition firing, assuming the transition is enabled at the current marking. Note that since we are not considering outputs, we will only be concerned with synchronizing sequences.

It is well known that a bounded PN — that is a PN where the number of tokens in each place does not exceed a finite number k for any marking reachable from the initial one — can be represented by a finite *reachability graph*, i.e., a FSM whose behaviour is equivalent to that of the PN (Murata, 1989). Thus the existence of synchronizing sequences for these models can be studied using the classical approach for FSM with just minor changes to take into account that while a FSM is assumed to be *completely specified* — any event can occur from any state — in the case of the PN's reachability graph it is not usually true.

Then we consider a special class of Petri nets called *state machines* (Murata, 1989), characterised by the fact that each transition has a single input and a single output arc. These nets are similar to automata, in the sense that the reachability graph of a state machine with a single token is isomorph — assuming all places can be marked — to the net itself. However, as the number of tokens k in the net increases the reachability graph grows as

k^{m-1} where m is the number of places in the net. We show that for strongly connected state machines even in the case of multiple tokens, the existence of synchronizing sequences can be efficiently determined by just looking at the net structure, thus avoiding the state explosion problem. We also present some extensions of our results to state machines that are not strongly connected.

This paper is organised as follows: Section 2. presents the FSM and PN model together with the analyse of synchronizing sequences for FSM. In Section 3. is shown how the FSM method can be straightforwardly adapted to PN. Afterwards in Section 4. is reviewed the problem and proposed other techniques for the case of State Machine. Finally conclusion are drawn in Section 5.

2. Background

2.1. Mealy Machine

Mealy machines are the class of FSM concerned in this work. A Mealy machine M is a structure

$$M = (I, O, S, \delta, \lambda)$$

where: I, O and S are finite and nonempty sets of input events, output events and states respectively; $\delta : S \times I \to S$ is the state transition function and $\lambda : S \times I \to O$ is the output function.

When the machine is in the current state $s \in S$ and receives an event $i \in I$, it moves to the next state specified by $\delta(s, i)$ producing an output given by $\lambda(s, i)$. Note that functions δ and λ are assumed to be *total functions*, i.e., functions defined on each element (s, i) of their domain. Such a machine is called *completely specified* to denote that for any state and upon any event a transition occurs producing the corresponding output event.

We denote the number of states, input and output events by $n = |S|$, $p = |I|$ and $q = |O|$. We extend the transitions function δ from input events to strings of input events as follows: for an initial state s_1, an input sequence $x = a_1, \dots a_k$ takes the machine successively to the states $s_{i+1} = \delta(s_i, a_i), i = 1, \dots, k$ with the final state $\delta(s_1, x) = s_{k+1}$. We also extend transition function δ from being defined for a specified state to a set of state as follows: for a set of states $S' \subseteq S$, an input event $i \in I$ takes the machine to the set of states $S'' = \bigcup_{s \in S'} \delta(s, i)$.

A Mealy machine is said *strongly connected* if there exists a directed path from any vertex to any other vertex.

2.2. Synchronizing Sequences on Mealy Machines

A SS takes a machine to the same final state regardless of the initial state and the outputs. That is, an input sequence x is synchronizing to a state s_r iff $\delta(s_i, x) = \delta(s_j, x) = s_r$ for all pairs of states $s_i, s_j \in S$.

The information about the current state of M after applying an input x is defined by the set $\sigma(x) = \delta(S, x)$, called the *current state uncertainty of x*. In other words x is a SS that takes the machine to the final state s_r iff $\sigma(x) = s_r$.

Given a Mealy machine M with n states, we construct an *auxiliary directed graph* $\mathcal{A}(M)$ with $n(n+1)/2$ nodes, one for every unordered pair (s_i, s_j) of nodes of M, including pairs (s_i, s_i) of identical nodes. There is an edge from (s_i, s_j) to (s_p, s_q) labeled with an input event $a \in I$ iff in M there is a transition from s_i to s_p and a transition from s_j to s_q, and both are labeled by a.

M_0	$[2\,0\,0]^T$
M_1	$[0\,1\,0]^T$
M_2	$[1\,0\,1]^T$

Table 1. Markings of the PN in Fig. 1.(a).

The following algorithm, due to Natarajan (Natarajan, 1986), has been introduced by Eppstein (Eppstein, 1990) for the case of *reset sequences* and re-interpreted and described by Lee *et al.* in (Lee and Yannakakis, 1996). We propose a possible implementation of this work in order to construct a synchronizing sequence x which is not necessarily the shortest possible.

***Algorithm** 1.* (Computing SS leading to s_f). Let $M = (I, O, S, \delta, \lambda)$ be the considered Mealy machine.

1. Let s_r be the desired final state.
2. Let $x = \varepsilon$, the empty initial input string.
3. Let $\sigma(x) = \{S\}$, the initial current state uncertainty.
4. Pick two states $s_i, s_j \in \sigma(x)$ such that $s_i \neq s_j$.
5. Find a shortest path in $\mathcal{A}(M)$ from node (s_i, s_j) to (s_r, s_r).
  5.1. If no such a path exists, stop the computation, there exists no SS for s_r.
  5.2. Else, let x' be the input sequence along this path, do
    5.2.1. $\sigma(x) = \delta(\sigma(x), x')$ and
    5.2.2. $x = xx'$,
6. If $\sigma(x) \neq \{s_r\}$ go to step 4.
7. x is the desired SS. ■

To analyse the Algorithm 1 leads us to the following theorem, which provides a reachability condition on the auxiliary graph necessary and sufficient for the existence of a synchronizing sequence for a desired final state.

***Theorem** 2. A FSM M has a synchronizing sequence for a desired final state s_r iff there is a path in its $\mathcal{A}(M)$ from every node (s_i, s_j), $1 \leq i < j \leq n$, to the node (s_r, s_r), with equal first and second components.*

Proof: There is an input sequence that takes the machine from state s_i and s_j, $i \neq j$, to the same state s_r iff there is a path x' in $\mathcal{A}(M)$ from (s_i, s_j) to (s_r, s_r). If such a path does not exist, none of the possible sequences will take the two states to s_r. In that case, when at step 5.2.1. the Algorithm updates the current state uncertainty it always holds that $s_i, s_j \in \sigma(x)$. In no more than n iteration, the Algorithm will be forced to pick the couple (s_i, s_j), then stating that no synchronizing sequence for the state s_r exists. □

We can also propose this theorem to prove the existence of any SSs.

***Theorem** 3. A FSM M has a synchronizing sequence iff there exists a path in its $\mathcal{A}(M)$ from every node (s_i, s_j), $1 \leq i < j \leq n$, to some node with equal first and second components (s_r, s_r), $1 \leq r \leq n$.* ■

The proof is trivial and not reported.

We will use this condition to prove the existence of a synchronizing sequence.

2.3. Synchronised Petri nets

In this section we recall the PN formalism used in the paper. For more details on PN we refer to (David and Alla, 2004).

A *Place/Transition net* (P/T net) is a structure

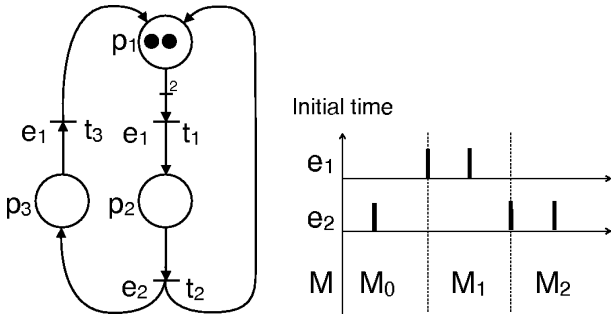

Fig. 1. A synchronised PN (a) and a possible behavior (b).

$$N = (P, T, Pre, Post)\,,$$

where P is the set of m places, T is the set of q transitions, $Pre: P \times T \to \mathbb{N}$ and $Post: P \times T \to \mathbb{N}$ are the pre and post incidence functions that specify the arcs.

A *marking* is a vector $M: P \to \mathbb{N}$ that assigns to each place a nonnegative integer number of tokens; the marking of a place p is denoted with $M(p)$. A *net system* $\langle N, M_0\rangle$ is a net N with initial marking M_0.

A transition t is enabled at M iff $M \geq Pre(\cdot, t)$ and may fire yielding the marking $M' = M - Post(\cdot, t) + Pre(\cdot, t)$. The set of transitions enabled at M is denoted $\mathcal{E}(M)$.

The notation $M[\sigma\rangle$ is used to denote that the sequence of transitions $\sigma = t_1 \dots t_k$ is enabled at M; moreover we write $M[\sigma\rangle M'$ to denote the fact that the firing of σ from M yields to M'. The set of all sequences that are enabled at the initial marking M_0 is denoted with $L(N, M_0)$.

A marking M is said to be *reachable* in $\langle N, M_0\rangle$ iff there exists a firing sequence $\sigma \in L(N, M_0)$ such that $M_0[\sigma\rangle M$. The set of all markings reachable from M_0 defines the *reachability set* of $\langle N, M_0\rangle$ and is denoted with $R(N, M_0)$.

A Petri net is said *strongly connected* if there exists a directed path from any vertex (place or transition) to any other vertex (place or transition). The strongly connected components of a directed graph G are its maximal strongly connected subgraphs.

Let us recall two structural notions. A strongly connected component is said *transient* if its set of input transitions is included in its set of the output transitions. It is said *ergodic* if its set of output transitions is included in the set of its input transitions. We denote Tr and Er as the subset of places and transitions determining respectively a transient and an ergodic component.

A *synchronised PN* (David and Alla, 2004) is a structure $\langle N, M_0, E, f\rangle$ such that: i) $\langle N, M_0\rangle$ is a net system; ii) E is an alphabet of external events; iii) $f: T \to E$ is a labeling function that associates to each transition t an input event $f(t)$. This type of labelling function is called *λ-free* in the literature (Gaubert and Giua, 1999).

The set T_e of transitions associated to the input event e is defined as follows: $T_e = \{t \mid\ t \in T, f(t) = e\}$.

The previous syntactic definition is also common to the so-called *labeled PN* (Gaubert and Giua, 1999). However, while in the case of labelled PN the evolution is autonomous and the events are usually interpreted as outputs, in the case of synchronised nets the events are inputs that drive the net evolution as explained in the following. Furthermore as showed later, in a synchronised nets two or more transitions can simultaneously fire, while this is not possible for labelled nets.

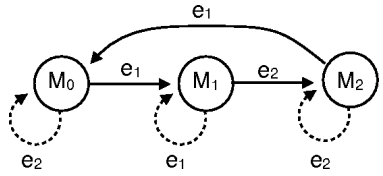

Fig. 2. The completely specified reachability graph of the PN in Fig. 1(a)

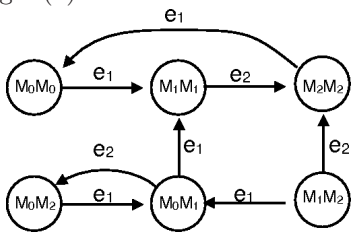

Fig. 3. The auxiliary graph of the PN in Fig. 1.(a).

Let M be the current marking and τ be the current time. A transition $t \in T$ fires at τ only if:
(1) it is enabled, i.e., $t \in \mathcal{E}(M)$;
(2) the event $e = f(t)$ occurs at time τ.
On the contrary, the occurrence of an event associated to a transition $t \notin \mathcal{E}(M)$ does not produce any firing.

In Fig. 1 is shown an example of synchronised PN. The label next to each transition denotes the transition name and the corresponding input event at once.

It can be possible to have two enabled transitions receptive to the same event. When this event occurs, both transitions are fireable and either both fire simultaneously, if there is no conflict between them, or have a non-determinism otherwise.

***Example** 4.* Consider the PN of Fig. 1(a) and let $M = [1\,0\,1]^T$ be the current marking. It is trivial to see that t_1 and t_3 are enabled and the occurrence of the event E_1 will make them fire leading to the marking $M' = [1\,1\,0]^T$. ■

As a consequence, the reachability set of a synchronised PN could be either a subset or equal to the reachable marking set of the underlying net, depending on the labelling function.

***Definition** 1. A synchronised PN system $\langle N, M_0\rangle$ is said to be deterministic if the following relation holds:*

$$\forall M \in R(N, M_0), \forall e \in E:\ M \geq \sum_{t \in T_e \bigcap \mathcal{E}(M)} Pre(\cdot, t). \quad \blacksquare$$

In others words, a synchronised PN is said to be deterministic if for all reachable markings there is no conflict between two or more enabled transitions that share the same label.

A net system $\langle N, M_0\rangle$ is said to be bounded if there exists a positive constant k such that for all $M \in R(N, M_0)$, $M(p) \leq k\ \forall p \in P$. A bounded net has a finite reachability set. In such a case, the behavior of the net can be represented by the *reachability graph*, a directed graph whose vertices correspond to reachable marking and whose edges correspond to the transitions that cause a change of marking. In the case of synchronised PN it is common to show the event next to the arc.

In Fig. 2, paying no attention to the dashed edges, it is shown the reachability graph of to the PN in Fig. 1(a).

In the rest of the paper, we only deal with the class of bounded PN.

3. Synchronizing Sequences for Bounded PN

The use of Petri nets offers significant advantages because of their intrinsically distributed nature where the notions of state (i.e., marking) and action (i.e., transition) are local. In this section, we will be concerned with synchronised and deterministic PN. Given a PN system $\langle N, M_0\rangle$, a straightforward approach to determine a SS consists in adapting the existing FSM approach to the reachability graph. This could be summarised it in the following steps:

- computation of the reachability graph G;
- computation of the auxiliary graph $\mathcal{A}(G)$;
- verification of the reachability condition.

It's easy to verify that this straightforward approach presents one shortcoming that makes it not always applicable: FSM approach requires the graph to be completely specified, while in a PN this condition is not usually true. In fact, the reachability graph of the PN is partially specified because from many marking not all the transitions are enabled. In order to use the mentioned approach it is consequently necessary to make its reachability graph G completely specified, obtaining $\tilde{G}$.

We obtain the graph $\tilde{G}$ by adding a self loop labelled $e = f(t)$, for every marking $M \in G$ and for every transition not enabled $t \notin \mathcal{E}(M)$.

We can summarise in the following algorithm the modified approach for PN:

***Algorithm** 5.* (Computing a SS leading to M_r). Let $\langle N, M_0\rangle$ be a deterministic bounded synchronised PN system and let $M_r \in R(N, M_0)$ be a desired final marking.

1. Let G be the reachability graph of $\langle N, M_0\rangle$
2. Let $\tilde{G}$ be the modified reachability graph obtained by completing G.
3. Construct the corresponding auxiliary graph $\mathcal{A}(\tilde{G})$.
4. A SS for the marking M_r, if such a sequence exists, is given by the direct application of Algorithm 1 to $\mathcal{A}(\tilde{G})$. ■

***Example** 6.* Consider the PN in Fig. 1.(a). The initial marking $M_0 = [2\ 0\ 0]^T$ enables only the transition t_1. Then for that marking we add a self loop labelled e_2 and so on. We obtain the completely specified reachability graph — taking into account also dashed edges — in Fig. 2, whose auxiliary graph is shown in Fig. 3. ■

In Fig. 2 and Fig. 3 are shown the reachability graph and the corresponding auxiliary graph of the PN in Fig. 1.(a). Note that dashed edges are added in order to make it completely specified.

We can now state the following theorem.

***Theorem** 7. A deterministic bounded synchronised PN $\langle N, M_0\rangle$ has a synchronizing sequence leading to a marking $M_r \in R(N, M_0)$ iff the reachability condition on its auxiliary graph $\mathcal{A}(G)$ is verified, i.e., there is a path from every node (M_i, M_j), with $M_i, M_j \in R(N, M_0)$, to node (M_r, M_r).*

Proof: **(only if)** If no path exists in the auxiliary graph from (M_i, M_j) to node (M_r, M_r), then by Theorem 2 no input sequences w exists such that $\exists \sigma_i, \sigma_j \in f^{-1}(w)|\ M_i[\sigma_i > M_r,\ M_j[\sigma_j > M_r$.

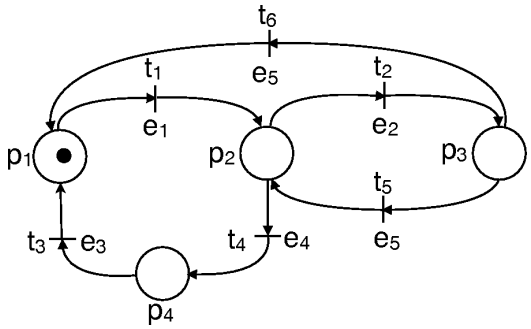

Fig. 4. A synchronised strongly connected PN.

(if) If in the auxiliary graph for each couple (M_i, M_j) there exists a path with input sequence w to some node (M_r, M_r), then by Theorem 2 in the completely specified reachability graph $\tilde{G}$ there exist a path labeled w from any mode M to M_r and this path is unique being the graph deterministic. Thus if the net is in any marking M, the input sequence w drives it to M_r. □

4. Synchronizing Sequences for State Machines

We now discuss the synchronizing sequences problem with reference to a class of PN, called *state machines* (SMs). The approach we propose does not require an exhaustive enumeration of the states in which the system may be. We will initially consider strongly connected PN; later we will relax this constraint to address the general case.

***Definition** 2. A* state machine *is a PN where each transition has exactly one input and one output place.* ■

In Fig.4 is shown an example of a synchronised SM. Note also that such a net is strongly connected.

When the initial marking assigns to this net a single token, it will move from place to place and the corresponding reachability graph will have as many marking as there are places. However, if the number of tokens in the initial marking is greater that one, the cardinality of the reachability graph may significantly increase. It can be shown in fact that for a strongly connected SM with m places and k tokens the cardinality of the reachability set is given by:

$$|R(N, M_0)| = \binom{m+k-1}{m-1} \leq \frac{1}{(m-1)!} k^{m-1}$$

In Table 2 — consider only the first three columns — it is shown the number of states of the reachability graph $|G|$ and of the modified auxiliary graph $|\mathcal{A}(\tilde{G})|$ of the net in Fig. 4 with $m = 4$ places, for different values of the total number of tokens k.

The forth and fifth columns show the computational times necessary to construct the reachability graph $|G|$ and the modified auxiliary graph $|\mathcal{A}(\tilde{G})|$ of the same net. The used functions, together with other MATLAB ones for observability and determination of synchronizing sequences on PN, can be downloaded at the web address in reference (Pocci, 2010).

We now define the concept of a path leading from a set of places $\hat{P}$ to a place p_r.

***Definition** 3. Given a SM $N = (P, T, Pre, Post)$, let $\gamma = p_{i_1} t_{i_1} p_{i_2} t_{i_2} \cdots p_{i_k} t_{i_k} p_{i_1}$ with $\hat{P} = \{p_{i_1}, p_{i_2}, \ldots, p_{i_k}\} \subseteq P$ be a directed cycle that touches all places in $\hat{P}$. Assume*

k	$\lvert G\rvert$	$\lvert\mathcal{A}(\tilde{G})\rvert$	t_G [s]	$t_{\mathcal{A}(\tilde{G})}$ [s]
1	4	10	0.001	0.002
2	10	55	0.002	0.059
3	20	210	0.006	0.285
4	35	630	0.021	1.087
5	56	1596	0.047	3.730
6	84	3570	0.108	11.41
7	120	7260	0.215	32.24
8	165	13695	0.418	79.96
9	220	24310	0.724	186.7
10	286	41041	1.233	411.1

Table 2. Cardinality and computational time of G and $\mathcal{A}(\tilde{G})$ of the PN in Fig. 4.

$p_{i_k} = p_r$ and let $\sigma = t_{i_1} \cdots t_{i_{k-1}}$ be the firing sequence obtained by opening this cycle in p_r and removing its output transition t_{i_k}. We define σ a synchronizing path *leading from $\hat{P}$ to p_r if the following two conditions are verified:*

C1) there do not exist two transitions $t, t' \in T$ such that $t \in \sigma$, $t' \notin \sigma$, and $f(t) = f(t')$;

C2) for all indices $j, h \in \{1, \ldots, k-1\}$, if $p_{i_j} = p_{i_h}$ then $f(t_{i_j}) \neq f(t_{i_h})$. ■

Condition C1 implies that there do not exist any pair of transitions sharing the same event such that the first one belongs to the synchronizing path but not the second one.

Condition C2 states that if the synchronizing path is touching more than once the same place, then the output transitions will not have associated the same event.

***Proposition** 8. Let us consider a strongly connected synchronised SM $N = (P, T, Pre, Post)$ containing a single token. Let σ be a synchronizing path leading from P to a place p_r. It holds that $w = f(\sigma)$ is a SS for the PN that brings the token to place p_r.*

Proof: Let $\sigma = t_{i_1} \cdots t_{i_{k-1}}$ be the corresponding synchronizing path and $\gamma = p_{i_1} t_{i_1} p_{i_2} t_{i_2} \cdots p_{i_k} t_{i_k} p_{i_1}$ the corresponding cycle, that does not need to be elementary. It is assumed that $p_{i_k} = p_r$. Let w be the corresponding input event sequence such that $w = f(\sigma) = e_{i_1} \cdots e_{i_{k-1}}$. At the beginning, the event e_{i_1} drives the token to either p_{i_2} — if p_{i_1} was marked — or from p_{i_j} to $p_{i_{j+1}}$ — if p_{i_j} was marked and $f(t_{i_j}) = e_{i_1}$. At any rate, the token could only be in a place p_{i_k} such that $k > 1$. Afterwards, if p_{i_2} is marked, e_{i_2} drives the token to p_{i_3}. That is because, if p_{i_2} is not repeated in γ — it belongs to more than one elementary cycle —, C1) assures only transition belonging to the cycle to be receptive to e_{i_j}; thus the token can only be driven to p_{i_3}. Otherwise, C1) assures as previously the token to remain in γ whereas C2) assures the token not to come back in the previously marked places. If the tokens is in some of the other places p_{i_j} — $j > 2$ — , for the same reasoning it can only be driven to $p_{i_{j+1}}$. Thus, after the application of the event e_{i_j}, the token could only be in a place p_{i_k} such that $k > j$. □

Note that Condition C1) is sufficient to assure the sequence to be a synchronizing one if γ is an elementary cycle.

***Example** 9.* Let consider the PN in Fig. 4. We want to find a SS that leads the system to the marking $[0\,0\,1\,0]^T$. Let $\gamma = p_2 t_4 p_4 t_3 p_1 t_1 p_2 t_2 p_3 t_5 p_2$ be the direct cycle that touches all the places and $\sigma = t_4 t_3 t_1 t_2$ the synchronizing path for p_3, having ${}^\bullet t_5 = p_3$. It holds that $w = f(\sigma) = e_4 e_3 e_1 e_2$ is the searched SS. ■

We now give a method to obtain a SS in the case of multiple tokens.

***Proposition** 10. Let us consider a synchronised strongly connected SM $\langle N, M_0 \rangle$ with k tokens. A SS for the PN, such that brings all the tokens to the place p_r, can be determined as follows. Let w be the SS leading to the place p_r determined for the case with only one token as in Proposition 8. It holds that w^k is a SS.*

Proof: Let w be a SS leading to the place p_r. By applying this sequence for the same reasoning of Proposition 8 at least one of the tokens will be driven to p_r. Any further application of w does not move the token from p_r as C1) assures every output transition for this place to be not receptive to any of the event $e_i \in w$. Thus w^k takes the k tokens at least one at time to the place p_r. □

***Example** 11.* Let consider the PN in Fig. 4. Let the PN have 2 tokens. We want to find a SS that leads the system to the marking $[0\,0\,2\,0]^T$. Let $w = e_4 e_3 e_1 e_2$ be the SS founded in Example 9 with one token. It holds that $w^2 = e_4 e_3 e_1 e_2 e_4 e_3 e_1 e_2$ is a SS for the desired final marking. ■

In the following, we extend our analyse by relaxing the assumption that a SM has to be strongly connected and we show how the computation of SS is possible by considering the same net with only one token using Proposition 10.

***Proposition** 12. Let us consider a synchronised SM $\langle N, M_0 \rangle$ with two or more ergodic components. This net has a SS iff there is no marked transient component from where two paths leading to two different ergodic components can be determined.*

Proof: By definition of transient component, is known that if for a marking M none of the output transitions are fireable, then none of these transitions will ever be fireable form any marking obtained from M. Thus it is proved that the existence of such two paths implies that none of the possible sequences can synchronise tokens from one ergodic components to another one. Consecutively there does not exist any sequence able to synchronise the net to a final marking regardless of the initial one. □

It is possible to find a SS for a synchronised PN not strongly connected, depending on the initial marking.

***Proposition** 13. Let us consider a totally synchronised SM $\langle N, M_0 \rangle$ with two or more ergodic components. It holds that if the only one initially marked component is an ergodic one then it exists a SS for all the markings M such that $M(p) = 0\ \forall p$ is not belonging to such a component.*

Proof: It is easy to verify that for $M_0(p) = 0\ \forall p$ not belonging to one ergodic component the set $R(N, M_0)$ determines a unique strongly connected component for whose markings a SS can be trivially determined by applying Proposition 8 to the subnet induced by that component. □

We now give a method to obtain a SS in a synchronised PN not strongly connected for the case of one token.

***Proposition** 14. Let us consider a totally synchronised SM $\langle N, M_0 \rangle$ with a unique ergodic component Er and a set of transient components $Tr_1, Tr_2, \ldots, Tr_S$. A SS for the PN, such that brings the unique token to the place $p_i \in Er$, can be determined concatenating w_1 and w_2.*

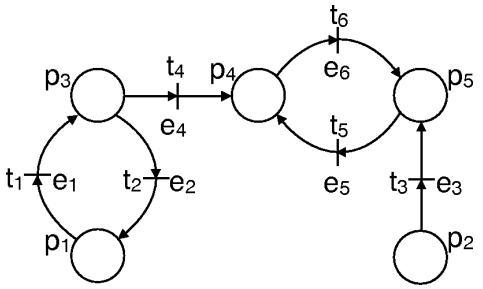

Fig. 5. An example of synchronised PN not strongly connected.

These two sequences are constructed as follows. Let $\sigma_1 = \sigma_1^1 t_1 \dots \sigma_1^S t_S$*, where the couple* (σ_1^i, t_i) *is determined as follows: let* t_i *be the transition from some* $p' \in Tr_i$ *to some* $p'' \in Er$ *such that there do not exist any* $t' \in p'^{\bullet}$ *leading to* Tr_i *such that* $f(t') = f(t_i)$*; let* σ_1^i *be the synchronizing path from the set of all places belonging to* Tr *leading to that place* p'*. Let* σ_2 *be the synchronizing path from the set of all places belonging to* Er *leading to the place* p_i*. Let* $w_1 = f(\sigma_1)$ *and* $w_2 = f(\sigma_2)$*.*

Proof: By definition of synchronizing path the input sequences corresponding to each couple (σ_1^i, t_i) make the token entering the unique ergodic component. The application of the input sequence w_2 matches with the problem already solved in proposition 8 wrt to the subnet induced by the ergodic component. □

Example *15.* Let us consider again the net in Example 5. Let the initial marking be $M_0 = [0\,1\,0\,0\,0]^T$. We want to find a SS that leads the system to the marking $M = [0\,0\,0\,1\,0]^T$. Let it be $(\sigma_1^1, t_1) = (t_1, t_4)$ and $(\sigma_1^2, t_2) = (\varepsilon, t_3)$, it holds that $\sigma_1 = t_1 t_4 t_3$. Let $\sigma_2 = t_5$ be the synchronizing path for the ergodic component and the place p_4, having ${}^{\bullet}t_6 = p_4$. It holds that $w = f(\sigma_1\sigma_2) = e_1 e_4 e_3 e_5$ is the searched SS. ■

5. Conclusion

In this paper, we have shown how Mealy machines techniques can be applied easily to the class of bounded synchronised PN, by using some arrangement. We also proposed a method that allows to determine a SS for a bounded synchronised PN by only looking at its static structure. Even in the case of multiple tokens, the existence of SS can be efficiently determined avoiding the state explosion problem.

Our approach uses synchronised PN that can have two o more transitions sharing the same event. This case introduces a nondeterminism, having a PN that in response to the same input events sequence can produce different firing sequences, reaching different markings.

A future work will be to extend our approach to synchronised PN considering the presence of *always occurring event*, the neutral event of E^*. In this case we lead with the problem of unstable markings, those markings whose outgoing transitions are receptive to the always occurring event that immediately fires.

References

David, R. and Alla, H. (2004). *Discrete, Continuous and Hybrid Petri Nets*. Springer-Verlag.

Eppstein, D. (1990). Reset sequences for monotonic automata. *SIAM J. Computing*, 19, 500–510.

G.-V. Jourdan and G.v. Bochmann (2009). On testing 1-safe Petri nets. In *Theoretical Aspects of Software Engineering, 2009. TASE 2009. Third IEEE International Symposium on*, 275 –281. doi:10.1109/TASE.2009.20.

Gaubert, S. and Giua, A. (1999). Petri net languages and infinite subsets of $\mathcal{N}^m$. *J. of Computer and System Sciences*, 59(3), 373–391.

Giua, A. and Seatzu, C. (2002). Observability of place/transition nets. *Automatic Control, IEEE Transactions on*, 47(9), 1424 – 1437. doi: 10.1109/TAC.2002.802769.

H. Zhu and X. He (2000). A theory of testing high level Petri nets. In *In Proceedings of the International Conference on Software: Theory and Practice, 16th IFIP World Computer Congress*, 443–450.

Hennie, F. (1968). *Finite-State Models for Logical Machines*. New York: John Wiley, 2 edition.

Kohavi, Z. (1978). *Switching and Finite Automata Theory*. The McGraw-Hill College, 2 edition.

Lee, D. and Yannakakis, M. (1996). Principles and methods of testing finite state machine – a survey. *Proceedings of the IEEE*, 84(8), 1090–1123.

Moore, E.F. (1956). Gedanken-experiments on sequential machines. *Automata Studies, Annals of Mathematical Studies*, (34), 129 – 153.

Murata, T. (1989). Petri nets: Properties, analysis and applications. *Proceedings of the IEEE*, 77(4), 541 –580. doi:10.1109/5.24143.

Natarajan, B.K. (1986). An algorithmic approach to the automated design of parts orienters. In *SFCS '86: Proc. of the 27th Annual Symposium on Foundations of Computer Science*, 132–142. IEEE Computer Society, Washington, DC, USA. doi: http://dx.doi.org/10.1109/SFCS.1986.5.

Pixley, C., Jeong, S.W., and Hachtel, G. (1994). Exact calculation of synchronizing sequences based on binary decision diagrams. *Computer-Aided Design of Integrated Circuits and Systems, IEEE Transactions on*, 13(8), 1024 –1034. doi:10.1109/43.298038.

Pocci, M. (2010). Finite state machines and Petri nets synchronisation toolbox. `http://www.lsis.org/poccim/SYNCH_TOOL.zip`.

Pomeranz, I. and Reddy, S. (1994). Application of homing sequences to synchronous sequential circuit testing. *Computers, IEEE Transactions on*, 43(5), 569 –580. doi: 10.1109/12.280804.

Rho, J.K., Somenzi, F., and Pixley, C. (1993). Minimum length synchronizing sequences of finite state machine. In *Design Automation, 1993. 30th Conference on*, 463 – 468.

Yamalidou, E., Adamides, E., and Bovin, D. (1992). Optimal failure recovery in batch processing using Petri net models. *Proceedings of the 1992 American Control Conference*, 3, 1906–1910.

Yamalidou, E. and Kantor, J. (1991). Modeling and optimal control of discrete-event chemical processes using Petri nets. *Computers & Chemical Engineering*, 15(7), 503 – 519. doi:DOI: 10.1016/0098-1354(91)85029-T.

Zhu, H. and He, X. (2002). A methodology of testing high-level Petri nets. *Information and Software Technology*, 44(8), 473 – 489. doi:DOI: 10.1016/S0950-5849(02)00048-4.

COLOURED PETRI NETS AS A FORMALISM TO REPRESENT ALTERNATIVE MODELS FOR A DISCRETE EVENT SYSTEM.

Juan-Ignacio Latorre[(a)], Emilio Jiménez[(b)], Mercedes Pérez[(c)]

[(a).] Public University of Navarre. Dept. of Mechanical Engineering, Energetics and Materials. Campus of Tudela, Spain
[(b)] University of La Rioja, Department of Electrical Engineering. Logroño, Spain
[(c)] University of La Rioja, Department of Mechanical Engineering. Logroño, Spain

[(a)] juaningnacio.latorre@unavarra.es, [(b)] emilio.jimenez@unirioja.es [(c)] mercedes.perez@unirioja.es

ABSTRACT
Coloured Petri nets (CPN) constitute a formalism that belongs to the paradigm of the Petri nets, used to model discrete event systems (DES). This formalism has been extensively used to represent complex systems and shows its full potential when arise a large number of subnets with the same static structure thanks to the folding process. In this paper a completely new application of the Coloured Petri nets is presented. It implies a conceptual variation in the traditional scope of use of the CPN. The coloured Petri nets will be used to represent sets of alternative Petri nets. In other words, they will represent a set of exclusive models for a single DES by means if a unique CPN. The main advantage in this application of the coloured Petri nets is that they can be used to develop efficient algorithms to solve optimization problems based on Petri net models.

Keywords: coloured Petri nets, alternatives aggregation Petri net, compound Petri net, alternative Petri net

1. INTRODUCTION

The coloured Petri nets are a broadly used formalism to model discrete event systems. They present particular interest when the real system to be modelled includes several subsystems which have the same static structure. In this case a folding procedure can be afforded in order to obtain a single subnet from the original set of subsystems with the same static structure. The subnet that results from the folding process need to include additional information which is presented as the colour attributes of every token. In this way it is possible to distinguish when a certain token present in the folded subsystem belongs or not to a certain subsystem of the original unfolded Petri net (Silva 1993, David and Alla 2005).

In this paper, it will be presented a completely new application of the coloured Petri nets, which profits from the property mentioned in the previous paragraph. This new application, which implies an important conceptual variation from the previous systems where the coloured Petri nets have been used so far, consists of the modelling of different alternative discrete event systems by means of a single coloured Petri net.

A set of discrete event systems are said to be alternative when they have the property of the exclusiveness among them. This property means that when one of the systems is chosen for being analysed, the others cannot be included in the analysis since only one of them can exist at a time in a real environment (Latorre et al. 2009c). As it has been seen, alternative DES are related to decisions. It is necessary to choose one alternative system among a set of them to define an initially undefined discrete event system. In a sense, it is possible to state that every Petri net in a set of alternative Petri nets is a model suitable for a different problem (Latorre, Jiménez and Pérez 2009a). This characteristic is very useful to reuse the model for the posing of diverse problems on a certain real system and to perform an efficient application of an optimization algorithm. As it has been seen, the conceptual leap from previous applications of CPN is important.

If the formalism of the Petri nets is used to model the original alternative discrete event systems, the result of the modelling process is a set of alternative Petri nets. This set of alternative Petri nets can be used to perform simulations and determine the quality of every one of the Petri nets regarding the achievement of a certain objective (or group of objectives). In fact, an optimization problem can be stated in order to apply a solving technique which may provide with a good solution for the problem.

The solving algorithm may have different characteristics according to the representation considered for the set of alternative Petri nets (Latorre, Jiménez and Pérez 2010a). When the information needed to define in an unambiguous way the set of Petri nets is efficiently compacted, by means for example of a folding procedure, the resulting description will not include redundant information which may lead to an efficient storage of the definition in a computer and, as a consequence, an efficient solving procedure. Coloured

Petri nets allow to obtain a single model that contains the description of every Petri net which belongs to a certain set of alternative Petri nets.

2. THE ALTERNATIVES AGGREGATION PETRI NETS

Coloured Petri nets developed to represent a set of alternative Petri nets are conceptually based in the alternatives aggregation Petri nets (AAPN).

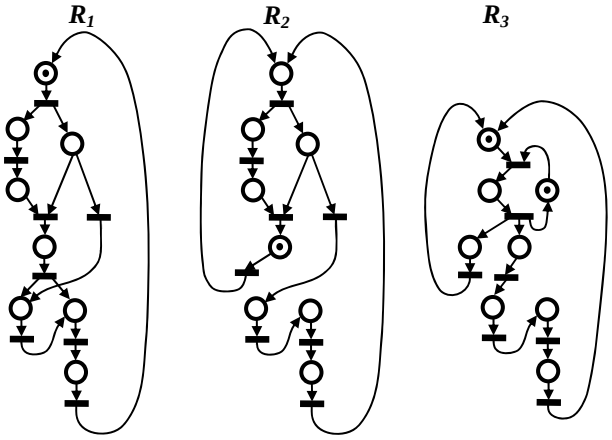

Figure 1: Simple alternative Petri nets

An AAPN is a Petri net obtained from the aggregation of Petri nets from a set of alternative Petri nets. The aggregation process of alternative PN to obtain an AAPN can be regarded as a folding procedure, in the sense that subnets with the same static structure that belong to different alternative PN are reduced to a single subnet in the AAPN. The subnets which have the same static structure are called shared subnets and they can be R-shared if the static structure and initial marking are the same in all of them or Q-shared when the static structure but not the initial marking is the same in all the cases (Latorre et al. 2009c).

In the figure 1 it can be seen a set of simple alternative Petri nets. They are alternative PN because in the example that is being presented, they are exclusive models to the same discrete event system, which behave in different ways. Nevertheless, they comply with the specifications of the DES, which allow certain freedom degrees to be specified by means of the appropriate decisions. These freedom degrees are the cause of the existence of three alternative Petri nets, any of which might be chosen as model for the system.

In order to build up an alternatives aggregation Petri net from a set of alternative Petri nets, an aggregation procedure of the different alternative PN should be performed. In fact, a specific alternative PN to be aggregated is previously divided into subnets and link transitions that connect the different subnets. The non-shared subnets are added to the AAPN and all the link transitions. All the link transitions of a certain alternative Petri net are associated to the choice variable that is related to this alternative Petri net.

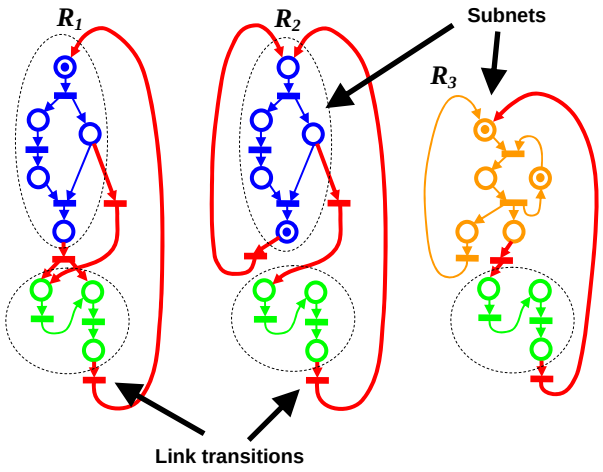

Figure 2: Decomposition in shared and non-shared subnets and link transitions.

In the figure 2 it is shown an efficient decomposition of the original set of alternative Petri nets into shared and non-shared subnets and link transitions. In fact there is a subnet that is shared by only R_1 and R_2, another subnet shared by the three alternative PN and a last subnet that belongs only to R_3. All the transitions that are not included in the subnets, because link different subnets or even a subnet with itself, are called link transitions. This decomposition is efficient because a large amount of shared subnets between the different alternative PN has been found.

The choice variables are Boolean parameters defined in a number which is equal to the cardinality of the set of alternative Petri nets and each one of them is associated to a different alternative Petri net, such that a bijection is established between the set of choice variables and the set of alternative Petri nets. The choice variables represent the information lost in the aggregation process in the same way that the attributes of the tokens (colours) represent the information that is lost in the folding procedure when a CPN is built up from a Petri net.

The resulting alternatives aggregation Petri net is a Petri net that includes in its description all the alternative models for a real discrete even system that have been aggregated. The same AAPN can be reused for the statement of different decision problems on the same real system and to perform an optimization procedure with enhanced performance.

Figure 3 shows an alternatives aggregation Petri net, which is equivalent to the original set of simple alternative Petri nets represented in the figure 1. In this net there is a set of choice variables: $S_A = \{ a_1, a_2, a_3 \}$.

The static structure of the original set of alternative Petri nets were described by means of a set of incidence matrices, while the resulting AAPN requires a single incidence matrix for an unambiguous description. In general the incidence matrix of the AAPN has larger size than any of the incidence matrices of the alternative Petri nets. Nevertheless, it is also usual that the shared subnets among the alternative Petri nets lead to an incidence matrix for the AAPN where some redundant information present in the matrices associated to the alternative Petri nets has been removed. As a consequence, the storage and operation with the incidence matrix of the AAPN may be more efficient than the handling of so many incidence matrices as alternative Petri nets are in a certain optimization problem. In other words, the AAPN help to develop efficient algorithms with enhanced performance.

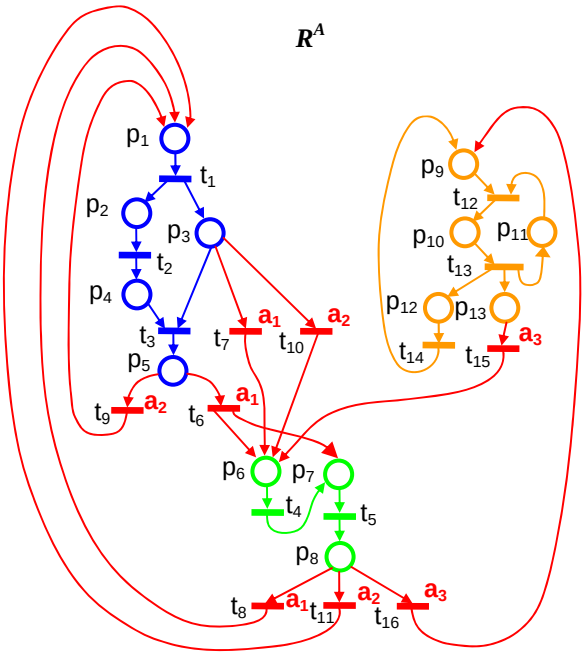

Figure 3: Alternatives aggregation Petri net

3. ALGORITHM TO TRANSFORM AN AAPN INTO A CPN

The procedure to obtain a CPN from an AAPN is almost immediate. The static structure of the AAPN and the one of its equivalent CPN are the same. Both of these Petri nets can be obtained by a process whose nature is similar: an aggregation of alternative Petri nets in the case of AAPN and the folding of different subnets in the case of a CPN. Nevertheless, it is important to realize that aggregation and folding are not the same process, since the former starts from a set of alternative models for a certain DES and the latter starts from a set of subnets that represent different subsystems of a certain discrete event system. In other words, the CPN is built up from a set of subsystems that may exist in a real environment, since the alternative Petri nets are models of systems from which only one might exist, while the rest are discarded models for a certain application.

The choice variables comply with a property of exclusiveness, because only one of them may be active at a time, meaning that a decision has been made to choose a certain alternative PN from the original set as a model for the real discrete event system. These variables also represent the information that has been lost in the process of aggregation, since a token which is present in a shared subnet of the AAPN belongs, in fact, to a certain alternative Petri net. The choice variable that is active when the token exists will point to the alternative Petri net to which it belongs.

In the translation procedure from the AAPN to the CPN, the choice variables should be transformed into the attributes of the tokens. In particular, each choice variable will lead to a choice colour. The activation of a choice variable in the original AAPN will be equivalent to the initialization of the equivalent PN with the initial marking associated to the choice variable and with all the tokens associated to the corresponding choice colour.

As it can be deduced, bijections can be defined between the set of alternative Petri nets, the set of choice variables and the set of choice colours. The decision of choosing a certain alternative Petri net as model for a real discrete event system can be done after the selection of a choice colour in an appropriate CPN model.

The exclusiveness property present in the original set of alternative Petri nets, where only one of them can be chosen as model for the original DES, and also present in the set of choice variables, where only one of them can be activated at a time, should also be present in the set of choice colours. The set of choice colours shows also the property of exclusiveness since the CPN that results from a certain AAPN has a marking with a monochrome choice colour. That is to say only one choice colour can be active at a time.

The name of choice colour implies that there is a possibility of having non-choice colours. The non-choice colours may not comply with the monochrome property (exclusiveness). In fact, the original AAPN might also be a coloured Petri net. Nevertheless, the translation process from the AAPN to the equivalent CPN adds the choice colours that should be clearly different from the other colours.

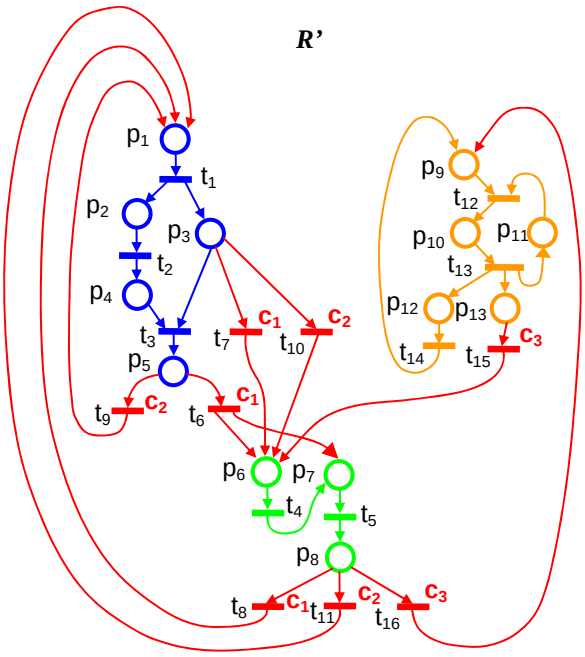

Figure 4: Coloured Petri net

The monochrome choice colour implies that the functions associated to the transitions to allow their firing, cannot change the choice colour of a token. During the evolution of a CPN, only one choice colour may exist for the tokens.

The last step in the transformation of an AAPN to a CPN is to translate the functions of choice variables associated to the transitions of the AAPN into functions of choice colours associated to the transitions of the equivalent CPN. This transformation is immediate by the substitution of the choice variables by the choice colours.

As it has been seen, three steps are included in the algorithm to transform an AAPN to a CPN: The static structure is left the same, the choice variables are translated into monochrome choice colours and the functions of choice variables are transformed into functions of choice colours.

In the figure 4, a coloured Petri net has been obtained from its equivalent alternatives aggregation Petri net. It can be noticed that the structure of both Petri nets are the same. In other words, their incidence matrices have the same components. In order to obtain the set of choice colours { c_1, c_2, c_3}, a correspondence with the set of choice variables of the AAPN has been set.

As a result of the algorithm described in this section, a coloured Petri net can be built up to describe the alternative Petri net models of a certain discrete event system, by means of monochrome choice colours and functions of choice colours associated to some transitions. The decision to choose one or another behaviour for the real discrete event system (given by the associated alternative Petri net) is performed by the activation of a certain choice colour and the deactivation of all the rest of them.

Even considering that it is possible to build up a CPN directly from a set of alternative Petri nets, the singularity of this application where a single CPN can represent a set of alternative Petri net that leads to the existence of an underlying AAPN related to the CPN has moved the authors to present in this paper the intermediate step of constructing an equivalent AAPN. The authors believe that this detailed process will help to understand the complete process and to take into account the particularities of this process of building up a CPN from a set of alternative Petri net compared to the process of constructing of a conventional CPN in a classical application where there are not any set of alternative models for the original DES.

4. REVERSE TRANSFORMATION

Given a certain CPN with monochrome choice colours, it is possible to obtain an equivalent AAPN with a direct transformation that will have the following characteristics:

1. The static structure of both nets are the same.

2. A set of choice variables should be defined in order to establish a bijection between this new set and the set of choice colours.

3. The property of exclusiveness between the choice colours, represented by making them monochrome, should be transformed into the property that only one choice variable can be active at a time, i.e. after a decision has been taken.

4. The functions of choice colours associated to some transitions should be translated into functions of choice variables, just y substitution of every choice colour by its corresponding choice variable, according to the bijection defined in 2.

The result of this reverse transformation is an alternatives aggregation Petri net that is equivalent to the original CPN. A further step can be developed in order to transform the AAPN into an equivalent set of alternative Petri nets.

5. OTHER TRANSFORMATIONS

In this paper, several representations of a set of alternative Petri nets have been presented: an alternatives aggregation Petri net and an equivalent coloured Petri net. It is possible to transform any of them into any other of them. Nevertheless, there are other representations for the original set of alternative Petri nets as the compound Petri nets that also allows to

perform transformations with the representations presented in this paper.

6. APPLICATIONS AND PROPERTIES

As it has been explained in previous sections, there are several applications and properties of the new concept presented in this paper: the use of a coloured Petri net to represent a set of alternative models for a certain discrete event system. Some of them are briefly described below:

1. Reduce the computing effort required to solve a certain optimization problem. The development of a CPN equivalent to a certain set of alternative Petri nets where there are similarities between different alternative models (shared subnets) may increase the efficiency of an optimization algorithm. This property arises as a consequence of the removal of redundant information in the description of the Petri net, mainly the incidence matrix (Latorre, Jiménez and Pérez 2010a).

2. Reuse of models. Given a certain undefined discrete event system, a set of alternative Petri nets can be developed as exclusive models. As a consequence an equivalent AAPN-CPN can be obtained from the set of alternative Petri nets. For a given DES, and hence for a given AAPN-CPN model, several different optimization algorithms can be stated, for example by means of the definition of different objectives to be achieved by the DES. In other words, by defining different objective functions it is possible to state different optimization problems and reuse the same AAPN-CPN model to represent and analyse the evolution of the same discrete event system.

3. Reuse of software. Given an optimization problem based on an AAPN as model for the original DES, it is possible to obtain the equivalent CPN and reuse the software developed for general applications of CPN in order to implement the optimization algorithm to solve it.

4. Recycle the models developed for certain alternative Petri nets. In the case of there are similarities between the alternative Petri nets, something usual in the design process of discrete event systems, it is possible to reuse the models of some alternative Petri nets and avoid the development of shared subnets that have already been created, since an equivalent AAPN-CPN may remove the redundant information. The non-shared subnets can be taken from the alternative Petri nets to the equivalent AAPN-CPN and inserted as blocks in the resulting incidence matrix or as subnets for the graphical representation.

7. CONCLUSIONS

The coloured Petri nets have been extensively used in the last years for the modelling of technological discrete event systems of very different sectors.

In this paper a conceptually new application is presented: the obtaining of a single CPN for the representation of a set of alternative Petri nets which have been developed as exclusive models for a certain discrete event system.

This new application arises from the definition of an underlying alternatives aggregation Petri net and has interesting applications and properties that are described in this paper.

The use of CPN as formalism to represent sets of alternative models allows to make the decision-taking and optimization processes based on discrete event systems easier to develop and more efficient to apply in a computer.

REFERENCES

R. David, H. Alla, “Discrete, Continuous and Hybrid Petri Nets,” Springer, Berlin. 2005

J. Heizer, B. Render, “Operations Management,” Prentice Hall. 2008.

E. Jiménez, “Techniques of advanced automation in industrial processes” “Técnicas de automatización avanzada en procesos industriales,” PhD Thesis. Ed. Univ. de La Rioja, Logroño. 2002

E. Jiménez, , M. Pérez, , J.I. Latorre, “On deterministic modelling and simulation of manufacturing systems with Petri nets”. Proceedings of European Modelling Simulation Symposium. Marseille, pp. 129-136. Marseille. 2005

E. Jiménez, , M. Pérez, I. Latorre. Industrial applications of Petri nets: system modelling and simulation. Proceedings of European Modelling Simulation Symposium, pp. 159-164. Barcelona. 2006

A. Kusiak, “Computational Intelligence in Design and Manufacturing”. Wiley-Interscience. 2000

J.I. Latorre, E. Jiménez, M. Pérez, “Comparison of optimization techniques applied to a flexible manufacturing system,” Proceedings of the 18th European Modelling and Simulation Symposium (EMSS 06). Barcelona, pp. 141-146. October 2006.

J.I. Latorre, E. Jiménez, M. Pérez, “Macro-Reachability Tree Exploration for D.E.S. Design Optimization,” Proceedings of the 6th EUROSIM Congress on Modelling and Simulation (Eurosim 2007). Ljubljana, Slovenia, September 2007.

J.I. Latorre, E. Jiménez, M. Pérez, “Decision taking on the production strategy of a manufacturing facility.

An integrated methodology," Proceedings of the 21st European Modelling and Simulation Symposium (EMSS 09). Puerto de la Cruz, Spain, vol. 2, pp. 1-7, September 2009.

J.I. Latorre, E. Jiménez, M. Pérez, E. Martínez, "The design of a manufacturing facility. An efficient approach based on alternatives aggregation Petri," Proceedings of the 21st European Modelling and Simulation Symposium (EMSS 09). Puerto de la Cruz, Spain, vol. 2, pp. 33-39, September 2009.

J.I. Latorre, E. Jiménez, M. Pérez, J. Blanco, "The problem of designing discrete event systems. A new methodological approach," Proceedings of the 21st European Modelling and Simulation Symposium (EMSS 09). Puerto de la Cruz, Spain, vol. 2, pp. 40-46, September 2009.

J.I. Latorre, E. Jiménez, M. Pérez, "A genetic algorithm for decision problems stated on discrete event systems." Proceedings of the UKSim 12th International Conference on Computer Modelling and Simulation. Cambridge, United Kingdom, March 2010.

J.I. Latorre, E. Jiménez, M. Pérez, "The alternatives aggregation Petri nets as a formalism to design discrete event systems." International Journal of Simulation and Process Modeling, Special Issue. 2010

D.Y. Lee, F. DiCesare. "FMS scheduling using Petri nets and heuristic search". Robotics and Automation. Proceedings, Volume 2, 1057 – 1062. 1992.

G. Music, "Petri net based scheduling approach combining dispatching rules and local search, " Proceedings of the 21st European Modelling and Simulation Symposium (EMSS 09). Puerto de la Cruz, Spain, vol. 2, pp. 27-32, September 2009.

M.À. Piera, M. Narciso, A. Guasch, D. Riera, "Optimization of logistic and manufacturing system through simulation: A colored Petri net-based methodology," Simulation, vol. 80, number 3, pp 121-129, May 2004

M. Silva. "Introducing Petri nets, In Practice of Petri Nets in Manufacturing" 1-62. Ed. Chapman&Hall. 1993

M. Zhou. K. Venkatesh. "Modelling, Simulation and Control of Flexible Manufacturing Systems. A Petri Net Approach", WS World Scientific, 1999

AUTHORS BIOGRAPHY

Juan Ignacio Latorre is electrical engineer. He has developed part of his professional career in the manufacturing private sector. Nowadays he is associated professor in the Public University of Navarre. He is developing his PhD thesis in optimization of manufacturing processes based on Petri net models. His research interests include automation, optimization and Petri nets.

Emilio Jiménez Macías studied Industrial Engineering (with Computer Science, Electronics and Automation specialty) by the University of Zaragoza, and in 2001 presented his PhD thesis about Industrial Automation, in the University of La Rioja, where he works presently in the Electrical Engineering Department (Coordinator of the System Engineering and Automation Group). His research areas include factory automation, modeling and simulation (Petri nets), and industrial processes.

Mercedes Pérez de la Parte received the BS degree in Telecommunications Engineering from the University of Seville in 1997. She has held research and teaching positions, since 1997 until present, at the University of Seville (Spain), at the University of Los Andes (Venezuela), and the University of La Rioja, where she is an Assistant Professor at the Mechanical Engineering Department.

MODELING AND SIMULATION OF PERIODIC SYSTEMS BY ISS CONTINUOUS PN

Emilio Jiménez [(a)]

[(a)] System Engineering and Automation Group
Electrical Engineering Department
University of La Rioja

[(a)] emilio.jimenez@unirioja.es

ABSTRACT
Infinite server semantics continuous Petri nets (ISSCPNs) is one of the most relevant timed interpretation of Continuous PNs (the relaxation into continuous models of Petri nets). Previous works comparing ISSSCPNs with Forrester diagrams and linear ordinary differential equation systems (LODES), taking into account the information delays and some methodological considerations, demonstrated that ISSCPNs permit to model any LODES when known upper and lower bounds of the state variables exists. Therefore systems with cyclic behavior or delays in the information can be modeled. These results permit analyze the modeling and simulation of cyclic systems with ISSSCPNs based on the comparison with the behavior of LODES. This type of analysis is very usual in system dynamics, in order to develop models (usually with FD) for unknown systems whose evolution have been observed. The possibility of model sinusoid functions, and the addition/substation of markings in redundant places, permits ISSCPNs model any cyclical system by Fourier decomposition, and the representation of different markings leads to very interesting graphics, which can correspond to real or approximate systems. This paper deepen into ISSCPNs expressive power, that is, the type of behaviour that they can present and the kind of systems that can be modelled with them.

Keywords: Continuous Petri nets, Forrester diagrams, relaxation of discrete event dynamic systems, positive systems, expressive power.

1. INTRODUCTION

PNs constitute a well-known *family of discrete event dynamic formalism* over the nonnegative naturals. Although PNs models are originally discrete event models, their relaxation through continuization transforms them into continuous models. At the price of losing certain possibilities of analysis, this permits to obtain some advantage, such as avoiding the state explosion problem inherent to the discrete systems and taking advantage of the extensive theory about continuous dynamic systems. Although not all PN systems allow a "reasonable" continuization [1], this relaxation is possible in many practical cases, leading to a continuous-time formalism: continuous PNs. Different timed interpretations lead to different firing/flow policies. One of the most relevant is ISSCPNs, the one that will be dealt with in this paper. Under this interpretation PNs are piecewise linear systems over the nonnegative reals.

FD, a specific modelling tool inside System Dynamics (SD), provides a graphic representation of continuous dynamic systems based on (eventually non linear) ordinary differential equation systems (ODES). They have been widely used to model complex systems with a friendly graphic representation, but they are totally equivalent to ODES. An interesting class of linear ODES are positive linear systems, whose state variables take only nonnegative values, the same as Continuous PNs. Another special class of positive linear systems are compartmental systems, which are systems composed of interconnected compartments or reservoirs.

Previous works comparing ISSSCPNs with Forrester diagrams and linear ordinary differential equation systems (LODES), taking into account the information delays and some methodological considerations, demonstrated that ISSCPNs permit to model any LODES when known upper and lower bounds of the state variables exists [10].

2. PREVIOUS DEVELOPMENTS ABOUT EXPRESSIVE POWER OF ISSCPNS

The evolution of a ISSCPN is described by the system:

$$\dot{\mathbf{m}}(\tau) = \boldsymbol{C} \cdot f(\tau)$$
$$f(\tau)[t_i] = \lambda[t_i] \cdot enab(\tau)[t_i]$$
$$\mathbf{m}(0) = \mathbf{m_0}$$

Thus a continuous Petri net under infinite servers semantics becomes a piecewise linear system. The switch between two linear systems is triggered by a change of the place giving the minimum in the expression for the enabling degree.

2.1. On positivity

Broadly speaking, positive systems are systems whose state variables take only nonnegative values. A positive system automatically preserves the non-negativity of the state variables, i.e., if non-negativity constraints on the state are added, they are redundant.

More formally, let $\sum$ (1) be a linear system:

$$\dot{\mathbf{x}}(t) = \boldsymbol{A}\,\mathbf{x}(t) + \boldsymbol{B}\,\mathbf{u}(t) \qquad (1)$$

Definition 1. [9] $\sum$ is said to be positive iff for every nonnegative initial state and for every nonnegative input its state is nonnegative. Then the positive orthand $\Re_n^+$ is a nonnegative invariant set. If $\boldsymbol{B}=\mathbf{0}$, the system is said to be uncontrolled or unforced.

Note that positivity in linear systems can depend on the basis of the input as well as on the basis of the state space. Some non-positive system can be transformed into another equivalent positive system by a basis change in the state space. This is the reason why some authors define positive systems by requiring the existence of an invariant set (without requiring, however, that such an invariant set be the positive orthand).

Theorem 1. [9] A linear system (1) is positive, iff $\boldsymbol{A}$ is a Metzler matrix and $\boldsymbol{B}$ is nonnegative (a matrix/vector is nonnegative if all its elements are nonnegative and a square matrix is *Metzler* if non-diagonal elements are nonnegative).

According to Definition 1, ISSCPNs are positive systems (the fact that the flow of a transition is proportional to its enabling degree ensures the nonnegativity of the marking). Nevertheless, the matrices $\boldsymbol{A_i}$ of the linear systems ruling the evolution of the net (recall that an ISSCPN is a piecewise linear system) can be non Metzler matrices. In a ISSCPN the switching between linear systems is triggered by a change in the place giving the minimum in the expression of the enabling degree.

The evolution of the net system in Figure 1 is driven by a linear system with matrix A_1 if $x_1 \le x_2$ and with matrix A_2 otherwise (if $x_1=x_2$ both systems are equivalent). Neither $\mathbf{A}_1$ nor $\mathbf{A}_2$ is a Metzler matrix, however the system is positive.

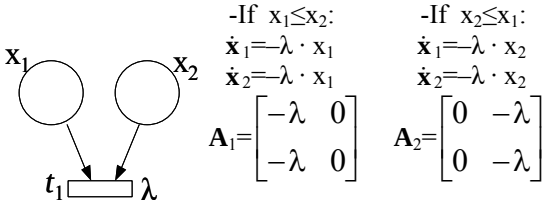

Figure 1: A ISSCPN whose associated linear systems have non Metzler matrices.

2.2. Control Arcs in PNs. Expressive power of ISSCPNs.

Control arcs will be introduced in this section. A control arc is defined on a couple {*place*, *transition*} and allows to model instantaneous control of the flow of the *transition* without modifying the marking of the *place*. It will be shown that by using control arcs any bounded LODES can be represented by an equivalent ISSCPN.

Let us describe how a *control arc* can be added to a ISSCPN. Consider an ISSCPN with a vector of internal speeds $\boldsymbol{\lambda}$ and incidence matrices **Pre** and **Post**. Let us assumed that the flow of a transition t is desired to be $\lambda[t]\cdot m[p]$ all along the evolution of the system for a given place p that is not an input place of t. In other words, we want the flow of transition t to be controlled by place p. Recall that the flow of t is $f[t]=\lambda[t]\cdot \min_{p\in \bullet t}\{\mathbf{m}[p]/\mathbf{Pre}[p,t]\}$. Therefore, in order to achieve our goal it is necessary that p is an input place of t and that it is always giving the minimum in the expression for the flow. This can be done by adding an arc going from p to t with weight k. We will asume that k is big enough to ensure that p always gives the minimum. If the internal speed of t, $\lambda'[t]$, is made k times faster ($\lambda'[t]=k\cdot\lambda[t]$) then $f[t]=\lambda[t]\cdot\mathbf{m}[p]$. In order to avoid that transition t *consumes* fluid from p, a new arc going from t to p with weight k is added to the net. This way, the flow of t is controlled by p, but the marking of p is not modified by the firing of t. Summing up, to put a control arc between $\{p,t\}$ of weight k, two arcs of weight k have to be added (from p to t and from t to p), and the internal speed of t has to be multiplied by k.

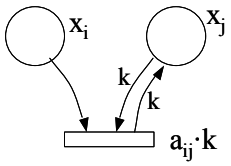

Figure 2: A control arc with weight k.

Note that in a control arc $\{p,t\}$ the weight k is assumed to be big enough to ensure the control of the transition. If the markings of the input places of t are strictly positive and the marking of p is upperbounded then such a k does always exist. However, if the marking of one of the input places tends to zero or the marking of p tends to infinity, no finite k exists such that p gives the minimum in the expression for the enalbling degree.

An *ideal control arc* is defined as a control arc with its constant k equals to infinite. The use of ideal control arcs allows to control transitions even when the marking of an input place tends to zero or the marking of p tends to infinity. Ideal control arcs represent an extension in the modelling power of ISSCPN and can be used to empty a place in finite time. They are equivalent to the *information arcs* in FD (in linear and nonnegative restricted systems).

The following lemma states that by using regular control arcs (no ideal control arcs) any LODES that has a positive and known lower and upper bounds can be modelled by an equivalent ISSCPN.

Lemma 1: For any LODES with *positive* and known lower and upper bounds there exists an ISSCPN having identical behaviour.

Proof. (see the previous work, in reference [10])

From Lemma 1, the following Proposition is immediately obtained.

Proposition 1: For any LODES whose state variables have a known lower and upper bound there exists an ISSCPN that represents the evolution of the LODES in the positive reals.

Proof: Any LODES with known lower bounds can be shifted to the positive reals by means of a change of variable. According to Lemma 1 there exists an equivalent ISSCPN for the shifted system.

Recall that by introducing ideal control arcs it is possible for a place to control a transition even if its marking stretches to infinity. Therefore the use of ideal control arcs allows to model also those LODES that are not upper bounded.

3. ODES, FD AND ISSCPNS

3.1. Behaviours types modelled with ISSCPN

Let be a general case of unforced linear ODES, $\dot{\mathbf{x}}(t) = \boldsymbol{A}\,\mathbf{x}(t)$, with dimension 2, where:

$$A = \begin{bmatrix} a11 & a12 \\ a21 & a22 \end{bmatrix}$$

The system can be represented by FD as shown in Figure 3. By ISSCPN if can be represented according to Table 1, which uses ideal control arcs in the cases with negative coefficients.

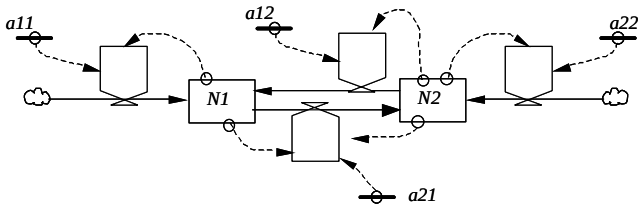

Figure 3: FD modelling a general unforced linear ODES of dimension 2.

Table 1: ISSCPN modelling general unforced linear ODES, depending on the signs of the coefficients.

	Coef. a_{ij}	Coef. a_{ii}
> 0	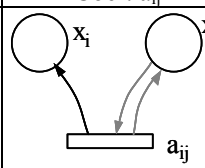	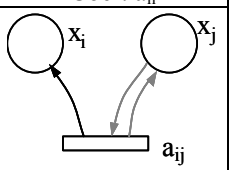
< 0	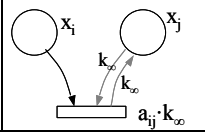	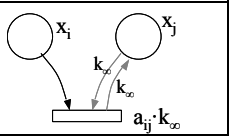

As control arcs can be used in both cases (positive or negative coefficients), the system can be represented by ISSCPN as shown in Figure 4, in which the sense of some arcs depends on the sign of the coefficient (the narrow with a + must be used with positive coefficients and viceversa).

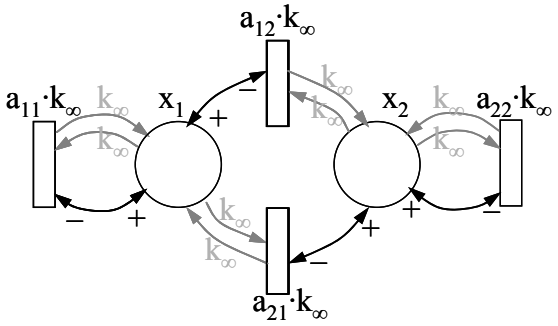

Figure 4: ISSCPN modelling a general unforced linear ODES of dimension 2.

The solution of the system is, in the general case, $e^{\mathbf{A}t} \cdot \mathbf{x}(0)$. Certain particular cases that exemplify the types of behaviour of this system are shown in Table 2. Exponential (positive and negative), linear, oscillating, hyperbolic and even sine growing behaviours can been seen.

Table 2: Examples of behaviour that can be modelled with ISSCPNs in positive systems.

A	eig(A)	e^{At}
$\begin{bmatrix} \pm a_1 & 0 \\ 0 & \pm a_2 \end{bmatrix}$	$\pm a_1, \pm a_2$	$\begin{bmatrix} e^{\pm a1 \cdot t} & 0 \\ 0 & e^{\pm a2 \cdot t} \end{bmatrix}$
$\begin{bmatrix} 0 & 0 \\ a & 0 \end{bmatrix}$	a, 0	$\begin{bmatrix} 1 & 0 \\ a \cdot t & 1 \end{bmatrix}$
$\begin{bmatrix} 0 & a \\ 1/a & 0 \end{bmatrix}$	1, –1	$\begin{bmatrix} \cosh t & a \cdot \sinh t \\ (\sinh t)/a & \cosh t \end{bmatrix}$
$\begin{bmatrix} 0 & a \\ -1/a & 0 \end{bmatrix}$	i, –i	$\begin{bmatrix} \cos t & a \cdot \sin t \\ (-\sin t)/a & \cos t \end{bmatrix}$
$\begin{bmatrix} \pm a & 0 \\ \pm b & \pm a \end{bmatrix}$	±a, ±a	$\begin{bmatrix} e^{\pm a \cdot t} & 0 \\ \pm b \cdot t \cdot e^{\pm a \cdot t} & e^{\pm a \cdot t} \end{bmatrix}$
$\begin{bmatrix} 0 & a \\ -1/a & 1 \end{bmatrix}$	$\frac{1}{2} + \frac{\sqrt{3}}{2}i, \frac{1}{2} - \frac{\sqrt{3}}{2}i$	$\frac{e^{t/2}}{\sqrt{3}} \begin{bmatrix} -\sin\frac{\sqrt{3} \cdot t}{2} + \sqrt{3}\cos\frac{\sqrt{3} \cdot t}{2} & \cdots \\ -\frac{1}{a}\sin\frac{\sqrt{3} \cdot t}{2} & \cdots \end{bmatrix}$
$\begin{bmatrix} \pm b & a \\ -1/a & \pm b \end{bmatrix}$	±b+i, ±b–i	$\begin{bmatrix} e^{b \cdot t} \cdot \cos t & a \cdot e^{b \cdot t} \cdot \sin t \\ (-\frac{1}{a} \cdot e^{b \cdot t} \cdot \sin t)/a & e^{b \cdot t} \cdot \cos t \end{bmatrix}$

The paper is based on the behaviour derived from row 4 (which is a particular case of the last row, with b=0). It is frequently presented in usual systems. Let us suppose a particular system with a material storage (St) and a staff of employees (E), whose observed real behaviour, by Jay W. Forrester [8], was one of the basis of system dynamics. The material is decreased due to the sales (S), which are assumed to be constant in time, and it is increased with the production (P), which is proportional to the number of employees. On the other hand, E varies with the contracting (C), which is proportional to the difference between the desired storage (DSt) and the present St. Figure 5 shows the FD that models this system.

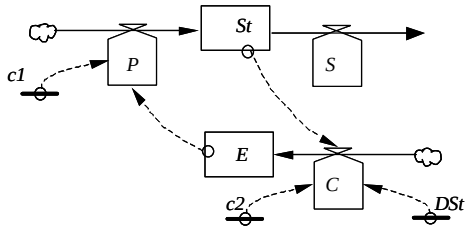

Figure 5. DF of a storage with employees system.

The differential equations system corresponding to that FD and its matrices are,

$$P(t) = c_1 \cdot E(t)$$
$$C(t) = c_2 \cdot (DSt - St(t))$$
$$dSt(t)/dt = P(t) - S$$
$$dE(t)/dt = C(t)$$

$$\boldsymbol{A}=\begin{bmatrix} 0 & c_1 \\ -c_2 & 0 \end{bmatrix} \quad \boldsymbol{B}=\begin{bmatrix} -S \\ c_2 \cdot DSt \end{bmatrix}$$

The eigenvalues of $\boldsymbol{A}$ are pure complex conjugated, independently of the values of c_1 and c_2 (due to the structure of the system), and their temporal evolution is oscillatory, sine shaped and with no damping. It can be described as:

$$St = w \cdot \sin((c_1 \cdot c_2)^{1/2} \cdot t) + DSt \quad (3)$$
$$E = w \cdot (c2/c1)^{1/2} \cdot \cos((c_1 \cdot c_2)^{1/2} \cdot t) + S/c_1$$

where *w* depends on the initial state, and it is computed as

$$w = ((St(0) - DSt)^2 + ((E(0) \cdot c_1 - S)/(c_1 \cdot c_2))^2)^{1/2}$$

So, if the storage is represented *versus* the employment, although the sales are constant a cyclic behaviour appears, with the parameters shown in Figure 6. As a curiosity, this type of behaviour (cyclic even with continuous inputs) was the origin of Forrester's studies, which were the source of System Dynamics.

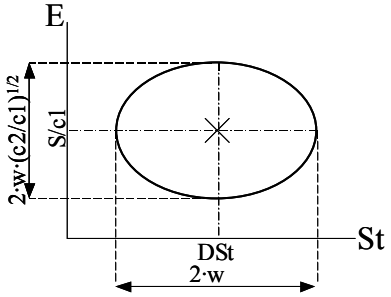

Figure 6. Behaviour of the system described in Figure 5

If St(0)=DSt and E(0)=S/c_1, then the system is stable. It is also important to emphasize that this system has only physical sense when the levels (stored elements and number of employees) have positive values, but the system of differential equations is non positive, and negative employment and storage can be reached for some initial conditions. Therefore, the constraint for non negativity (St, E≥0) must be additionally included in order to obtain a correct model.

The system with the non negativity constraint can be modelled with continuous PNs (Figure 7) but it must be taken into account that C, which can be positive or negative, must be implemented as a combination of a flow of new contracts and a flow of dismissals, both positive.

Note that two places have been used (those with unitary marking) in order to get a constant flow with ISS, and control arcs have been necessary to explicitly select the places that provide the information to the transitions with synchronizations. The system will be described by (3) whenever St≥1/k_∞ and E≥St/k_∞. Recall that k_∞ represents a *finite* constant as big we want (eventually tending to infinite).

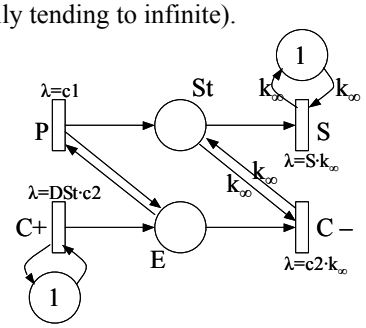

Figure 7. ISSCPN equivalent to the system in Figure 3 restricted to positive values.

It is also important to note that an appropriate value of k_∞ in the PN depends on the minimum values that St and E can reach (and then on the initial marking). For instance, if c_1=c_2=1, St(0)=9, DSt=10 and E(0)=S=12, then k_∞ does not need to be higher than 1. Figure 8 shows simultaneously the evolution of the constrained system (modelled with ISSCPN or FD with constraints) and the non restricted one (modelled with ODES or FD without constraints). Both are similar from the initial state to the first intersection with the horizontal axis (point *a* in the graphic). Figure 8a presents St versus E, and Figure 8b shows the temporal evolution of the state variables.

The choice of appropriate parameters can lead to completely positive systems, and then ideal control arcs are not needed. The model will be exactly the same as in Figure 7 by replacing the respective k_∞ for finite values k_i. An example of such type of evolution is represented in Figure 9.

The system can also be converted in a conservative PN if the complementary places of the state variables are added, as shown in Figure 10.

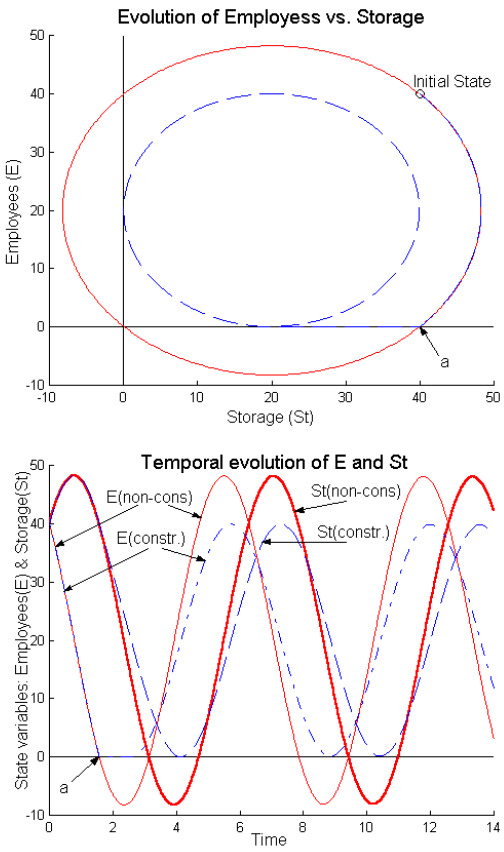

Figure 8: Evolution of the system with $c_1=c_2=1$, St(0)=E(0)=40; DSt=10, C=V=20 from constrained (broken line) and no constrained (unbroken line) models.

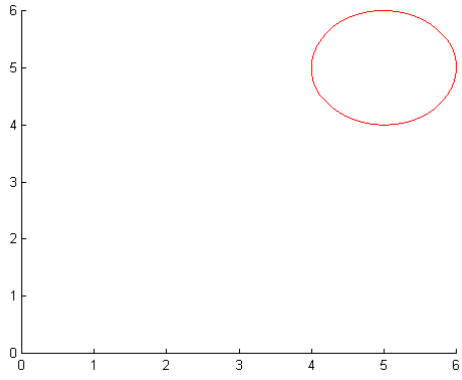

Figure 9: Evolution of the system with $c_1=c_2=1$, St(0)=4 E(0)=5; C=V=5.

Since ideal control are not used now, the system can evolution through different covertures before switching to the final coverage in which control arcs are who effectively control their transitions, as shown in Figure 11.

These coverage changes are determined by the value of the places, in the moments in which the minimum of the transitions are provided for different places, which corresponds with intersection of the curves shown in Figure 12 (intersections of red with yellow or green with blue lines).

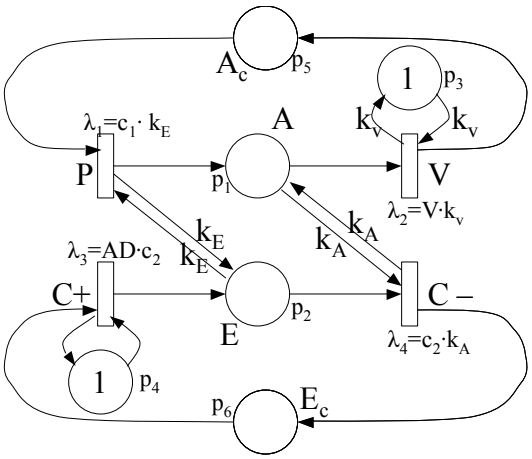

Figure 10: Conservative model equivalent to Figure 7.

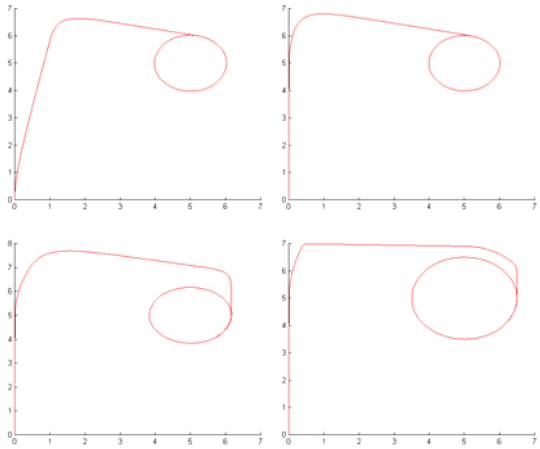

Figure 11: Different behaviours of the system depending on the parameters.

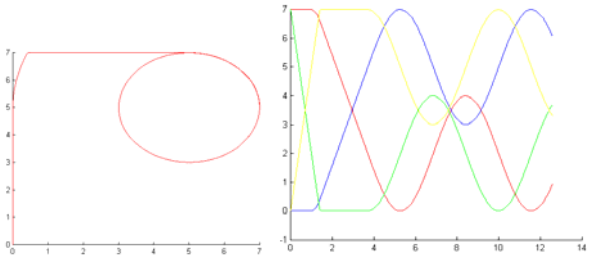

Figure 12: System evolution and temporal evolution of every variable, which permits determining the switches.

3.2. Pure systems with Petri nets

The use of control arcs occasions that the system is non-pure. A simple transformation, according to Figure 13, transforms the system into an equivalent pure PN.

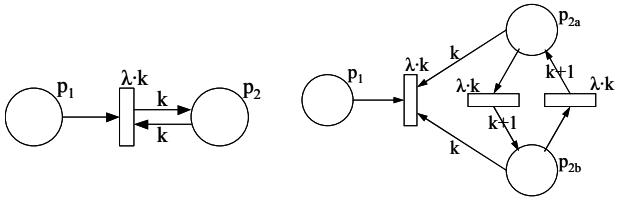

Figure 13: Control arcs modelled with pure PN.

Specifically, the example used in this paper is converted into the system in figure 14, in which the 8 arcs with weight k+1 are represented with different colour.

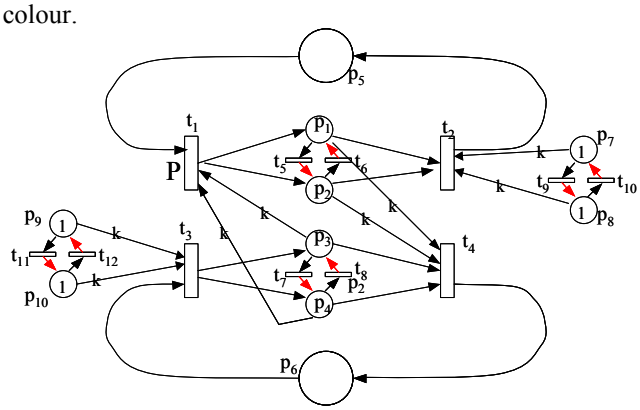

Figure 14: Conservative pure system equivalent to systems in Figures 7 and 10.

Obviously the simulation of the model in Figure 14 is exactly equal to those of the non-pure systems of Figures 7 and 10, provided that the places in which every place with control arc has been divided are exactly equals. A small difference between them can drive to stable or instable systems, as shown in Figure 15.

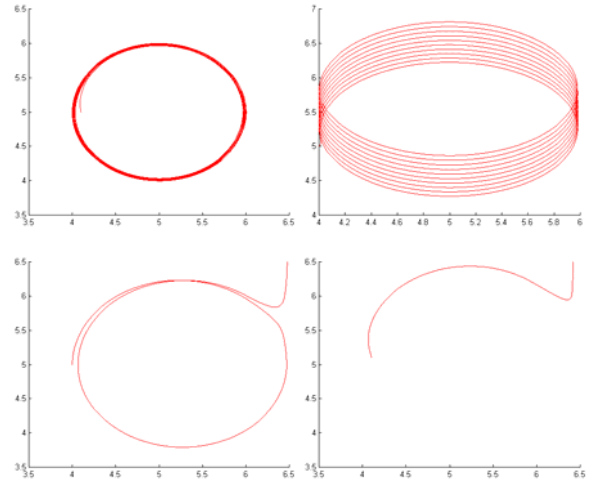

Figure 15: System evolution of model of Figure 14 with small differences in the pairs of places modelling control arcs, depending on the pairs with perturbations: a) p1-2 and p3-4, b) p7-8 c) p9-10 d) p7-8 and p9-10

4. RESULTS

A relaxed continuous view of discrete event systems, continuous Petri nets, have been considered together with Forrester Diagrams and linear ordinary differential equation systems (mainly positive systems). They have been compared in order to obtain a deeper knowledge of the expressiveness of the continuous relaxation of PNs under infinite server semantics.

Continuous Petri nets under infinite server semantics lead piecewise linear systems provided with nonnegative state and outputs (they have an internal or implicit constraint of non-negativity).

Control arcs weighted with factor *k* are an abbreviation in infinite server semantics continuous PNs, and allow to simulate bounded positive linear systems (eventually under certain transformations). But the behaviour and expressive power of infinite server semantics continuous PNs are not restricted to bounded linear positive systems. In fact, any bounded linear system (positive or not) can be shifted to the positive reals and therefore modelled by a infinite server semantics continuous PN. In particular pure oscillatory behaviours can be modelled with infinite server semantics continuous PNs.

Ideal control arcs constitute an extension for infinite server semantics continuous PNs (are the control arcs *k* weighted with factor ∞). With them its expressive power increases because they permit to simulate any positive linear system (bounded or not) or any one that can be transformed into a positive system.

The possibility of model sinusoid functions, and the addition/substation of markings in redundant places, permits ISSCPNs model any cyclical system by Fourier decomposition, and the representation of different markings leads to very interesting graphics, which can correspond to real or approximate systems.

REFERENCES

[1] M. Silva and L. Recalde, "Petri nets and integrality relaxations: A view of continuous Petri nets", *IEEE Trans. On Systems, Man, and Cybernetics*, 32(4):314-327, 2002.

[2] E. Jiménez, L. Recalde and M. Silva, "Forrester diagrams and continuous Petri nets: A comparative view", In Proc. Of the 8th IEEE Int. Conf. On Emerging Technologies and Factory Automation (ETFA 2001), Nize, pp 85-94, 2001.

[3] M. Silva and L. Recalde, "Unforced Continuous Petri Nets and Positive Systems. Positive Systems", Proc. First Multidisciplinary International Symposium on Positive Systems: Theory and Applications (POSTA 2003), 294, pp55-62, 2003

[4] T. Murata, "Petri nets: Properties, analysis and applications", Proc.of the IEEE, 77(4):541–580, 1989.

[5] M. Silva. "Introducing Petri nets", *Practice of Petri Nets in Manufacturing*, p.1–62. Ch.& H., 1993.

[6] L. Recalde and M. Silva, "PN fluidification revisited: Semantics and steady state", APII-JESA, 35(4):435-449, 2001

[7] H. Alla and R. David, "Continuous and hybrid Petri nets", *Journal of Circuits, Systems, and Computers*, 8(1):159–188, 1998.

[8] Jay W. Forrester, *Industrial Dynamics*. MIT Press, Mass, Cambridge, 1961.

[9] L. Farina and S. Rinaldi, *Positive Linear Systems. Theory and Applications. Pure and Applied Mathematics*, John Wiley and Sons, New York, 2000.

[10] Jimenez, Julvez, Recalde, Silva, Modeling and simulation of periodic systems by ISSC Petri nets, Prodeedings of the 2004 IEEE International Conference On Systems, Man & Cybernetics, pp4897-4904

ON THE SOLUTION OF OPTIMIZATION PROBLEMS WITH DISJUNCTIVE CONSTRAINTS BASED ON PETRI NETS

Juan-Ignacio Latorre[(a)], Emilio Jiménez[(b)], Mercedes Pérez[(c)]

[(a).] Public University of Navarre. Dept. of Mechanical Engineering, Energetics and Materials. Campus of Tudela, Spain
[(b)] University of La Rioja, Department of Electrical Engineering. Logroño, Spain
[(c)] University of La Rioja, Department of Mechanical Engineering. Logroño, Spain

[(a)] juaningnacio.latorre@unavarra.es , [(b)] emilio.jimenez@unirioja.es , [(c)] mercedes.perez@unirioja.es

ABSTRACT
Manufacturing facilities, chain supplies and other systems of technological interest can be usually described as discrete event systems. The Petri nets are a modeling paradigm able to cope with complex behaviour of DES. The design of this kind of systems and their efficient operation usually lead to the statement of optimization problems with disjunctive constraints. Those constraints are given by the Petri net models with variables that represent the freedom degrees of the designer or the process engineer that defines the working parameters of a production line. Disjunctive constraints are difficult to handle in optimization problems. In this paper an analysis of the disjunctive constraints is performed and an overview of four different representations for this type of constraint is developed: a set of alternatives Petri nets, a compound PN, an alternatives aggregation PN (AAPN) and a coloured Petri net (CPN). The advantages and drawbacks of every one of these representations as well as some examples of transformation algorithms are given.

Keywords: alternatives aggregation Petri net, compound Petri net, alternative Petri net, optimization.

1. INTRODUCTION

In industrial and chain supply systems it is usual to state optimization problems with disjunctive constraints when some operation or design decisions must be taken (Latorre, Jiménez and Pérez 2007). The solution procedure for those optimization problems can be afforded from different points of view. One of the possibilities, a classical approach, can be considered. In this case it is common to take into account a number of simpler problems in which the original problem can be decomposed, to solve all of them independently and to choose the best solution among them (Zhou and Venkatesh 1999). Nevertheless, a comprehensive and exhaustive analysis of the different possibilities to afford the solution of an optimization problem with disjunctive constraints has not been developed so far.

In this paper, a general view of the optimization problems with disjunctive constraints based on Petri nets is provided, with a detailed description of the disjunctive constraints and different representations of them with the purpose of analysing how a particular representation might be more suitable to solve a certain optimization problem with an enhanced performance.

On the other hand, some of the mentioned representations are associated to the classical approach of decomposition of the optimization problem into a set of simpler ones. As a consequence, a comprehensive view of the different representations of a disjunctive constraint is offered in this paper.

2. OPTIMIZATION PROBLEM WITH DISJUNCTIVE CONSTRAINTS BASED ON PETRI NETS

A design decision in an industrial or logistic problem can be associated to an optimization problem based on a disjunctive constraint. The disjunctive constraint may appear in the case a Petri net can model different alternative systems and any of them can be considered as feasible systems, which comply with the specifications given by the problem (Latorre et al. 2009c).

A disjunctive constraint shows the particular property that it is composed of a family of restrictions. Moreover, for every one of the alternative models of the system that verify the specifications of the problem, one and only one of the restrictions must be complied. For this reason an important property of every representation of the disjunctive constraint, as it will be shown in the following section, is the exclusiveness property. According to that principle, every subset of a disjunctive constraint is exclusive in the sense that it must be complied only in a single alternative or in a set of them.

3. DIFFERENT REPRESENTATIONS OF A DISJUNCTIVE CONSTRAINT

A disjunctive constraint related to an optimization problem based on a Petri net which is seen under the classical approach of dividing the original problem into

a set of simpler problems, is related to what can be called set of alternative Petri nets.

In this case a set of alternative models for the system can be considered. They have structural differences. In other words, their incidence matrices have at least a parameter which is different among them (Latorre, Jiménez and Pérez 2009a).

These alternative Petri nets are exclusive in the sense that only one of them can comply with the specifications of the problem, while the rest must be discarded after a solution procedure. Being exclusive, they verify the definition of disjunctive constraint. On the other hand, they constitute the more intuitive approach to the solution process of an optimization problem with disjunctive constraints based on Petri net, since it is very natural to interpret the problem by means of different and discrete alternative Petri net models. Nevertheless, this approach may not be the more efficient one to perform a solution procedure for the problem (Latorre, Jiménez and Pérez 2010a). This sole fact justifies the search for other representations more suitable for the solution process of other optimization problems.

In the figure 1, a set of two simple alternative Petri nets can be seen. They are simple since there is not any undefined structural parameter in them. In other words, every one of the parameters of the incidence matrices is associated to a unique value. On the other hand they are alternative for a certain system if both of them comply with the specifications and only one of them can be chosen as model for the considered system. It is necessary to choose among the two alternative PN if the system should be determined univocally.

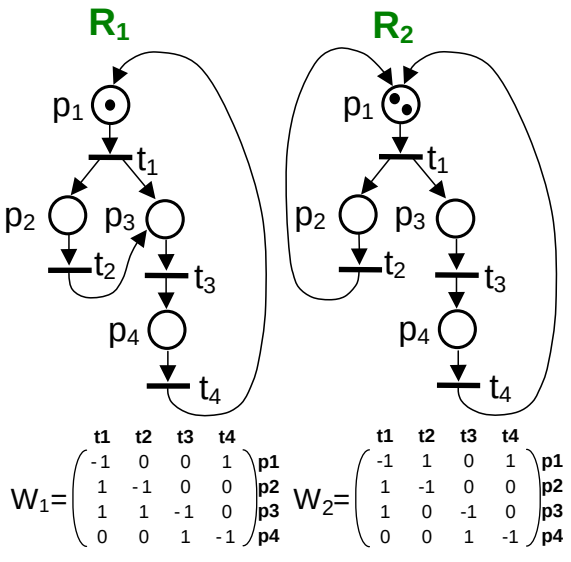

Figure 1: Simple alternative Petri net

Another representation for the disjunctive constraint implies the merging of a set or a subset of simple alternative Petri nets into a compound alternative Petri net. This merging process allows to reduce the volume of information needed to store the incidence matrices of the alternative Petri nets when there are enough similarities between them. As a result of the merging process, a particular incidence matrix for every compound alternative Petri net is obtained. In these incidence matrices some parameters are necessary to represent the different values that some elements of the matrices can have. The set of feasible values for every parameter of the incidence matrix of a compound alternative Petri net, called undefined structural parameters, is composed of elements that are exclusive. In other words, when one of these combinations of values for the undefined structural parameters of a compound Petri net is chosen, the rest are discarded. Hence, the exclusiveness of the original simple alternative Petri nets is transformed into this characteristic of the compound alternative Petri net.

In the figure 2, a compound Petri net is shown. This compound Petri net is equivalent to the set of simple alternative Petri nets of figure 1. It contains three undefined parameters. In other words, there are three variables in the Petri net: α_1, α_2 and α_3. The two first variables belong to the incidence matrix of the PN, hence they are called undefined structural parameters. The third variable is the initial marking of the place called **p1**, therefore, it is called an undefined marking parameter.

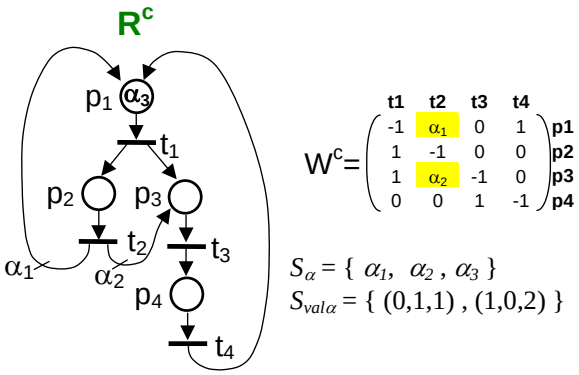

Figure 2: Compound Petri net

As it can be seen from a comparison between the set of simple alternative Petri nets in figure 1 and the compound Petri net in figure 2, both the matrix-based and the graph-based representations of the latter look simpler and seem to require less computational resources to be stored and processed by automatic calculation. Nevertheless, there is a piece of additional information that require the description of the compound Petri net that is not required by the representation of the set of simple alternative Petri nets: the set of undefined parameters, S_α, and the set of feasible combinations of undefined parameters, $S_{val\alpha}$. If the set of alternative Petri nets are not simple, that is to say if they contain undefined structural parameters, the mentioned additional information is also needed to complete the description of the set of Petri nets.

Another interesting comment on the nets of figures 1 and 2 is related to the exclusiveness property associated to the freedom degrees present in the original system. This exclusiveness is the source that creates the disjunctive constraint that make an optimization problem associated to this undefined system difficult to solve. The presence of the disjunctive constraint, due to the exclusiveness property, can be solved by means of decisions. This property is represented in the set of simple alternative Petri nets, as their name states, by the presence of different alternative models for the system. One of them should be chosen and when this is done, the system is univocally specified. On the other hand the exclusiveness property is defined in the compound Petri net by a set of feasible combinations of values for the undefined structural parameters, given by the set $S_{val\alpha}$.

Moreover, it is also possible to describe a third additional way to perform the representation of a set of simple alternative Petri nets. This new representation can be obtained from a different process of mixing the simple alternative Petri nets called aggregation. The resulting Petri net, which can also be a simple or a compound Petri net, is called alternatives aggregation Petri net. This Petri net can be obtained from a set of simple alternative Petri nets as well as from a compound Petri net.

The alternatives aggregation Petri nets can be an efficient way to represent a disjunctive constraint based on Petri nets. The property of exclusiveness that characterizes the original simple alternative Petri nets is also included in this AAPN. In this case, some choice variables are defined in order to implement the different exclusive alternative Petri nets. The choice variables verify that only one of them can and must be active as a consequence of a decision.

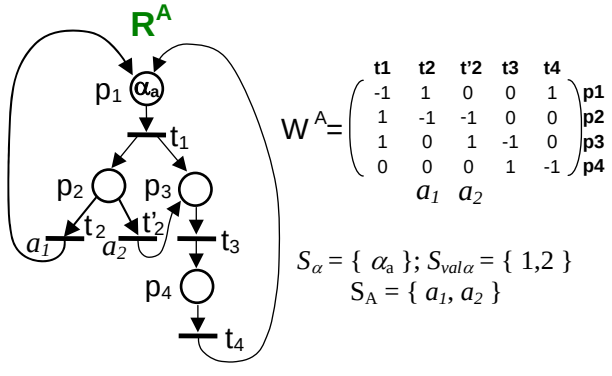

Figure 3: An alternatives aggregation Petri net

In the figure 3, an example of alternatives aggregation Petri net (AAPN) can be seen. It is equivalent to the different representations based on Petri nets shown in the figures 1 and 2. In the figure 3 there is an undefined marking parameter and a set of choice variables. Those variables are Boolean ones and verify the exclusiveness property in the sense that one of them and only one of them can be true at a time. In fact this "activation" of a single choice variable may happen after a decision on that subject has been taken. The choice variables are associated to some transitions as Booleans or Boolean functions which allow the firing of the associated transition when it is enabled and the choice function of choice variables is true.

Those choice variables can be associated to a set of choice colours linked to an equivalent Petri net. This transformation allows to develop a representation of an AAPN by means of a coloured Petri net. This last representation can be useful for the reuse of simulation and optimization software for CPN and the application of the theoretical results of the CPN to the AAPN.

4. SOLUTION ALGORITHM OF THE OPTIMIZATION PROBLEM BASED ON DIFFERENT REPRESENTATIONS FOR THE DISJUNCTIVE CONSTRAINT

Every one of the representations of a disjunctive constraint based on a Petri net allow the development of a process to obtain a solution for an optimization problem with certain particularities that can provide with an enhanced or a reduced performance according to the specific problem that is aimed to be solved.

A set of alternative Petri nets allow a solution procedure based on a set of optimization problems that can be solved independently. In fact, this approach, traditionally known as "divide and conquer", overcomes the disjunctive constraint by solving a single problem for every restriction of the family that configures the disjunctive constraint. Once every problem is solved, a choice can be done among the solutions. The chosen solution complies a restriction which is associated but none of the rest that belong to the disjunctive constraint.

This strategy of "divide and conquer" is a classical approach that can be afforded by means of independent and simple processes. The drawbacks that can be considered for this technique are the need to perform a set of different optimizations, some of which will not provide with a good solution, hence they may constitute a waste of time. On the other hand, it is necessary to develop a subsequent stage of comparison of the results of the independent optimizations to obtain the best solution for the global problem. On the other hand, a clear advantage can be found for this approach. Usually, the definition of the set of simple alternative Petri nets arises directly from the statement of the optimization problem and it is a very intuitive and natural way of representing the possible alternative models for the system to be analysed.

This idea is easy to understand when the design of a manufacturing facility is aimed. In this case, it is

possible to choose different machines to be acquired and set up. Sometimes there are different suppliers for the same stage of a certain production line. In this case the feasible combinations of different models of machines lead to a set of alternative models for the manufacturing facility that is being designed. Every one of those models is an alternative where one and only one of them must be chosen.

From the design of a manufacturing facility it is usually expected to obtain a system able to optimize certain objectives, for instance, to maximize the operational benefit and the machine utilization rate and to minimize the costs and the work in process. As a consequence, an optimization problem can be stated in order to develop the design process of the system. The feasible solutions of the optimization problems should comply with a set of constraints. In particular, these constraints define the solution space. As it can be easily deduced, every alternative Petri net constraints the values a solution can take. Moreover, any solution should only verify the constraints imposed by a single alternative Petri net, not by the rest of them. As a consequence, the set of alternative Petri nets constitutes a set of alternative constraints to the optimization problem, in other words, a disjunctive constraint.

A compound Petri net consists of a representation of a disjunctive constraint that is associated to a single incidence matrix, where in the previous case with the set of simple alternative Petri nets, a set of incidence matrices could be found. In principle, the reduction of the number of incidence matrices to be considered in the statement of the optimization problem may imply a reduction in the volume of information to be stored in the memory of the computer that would perform the solution process. This statement is especially true when the simple alternative Petri nets that are merged into a compound Petri net have similarities that reduce the size of the sets of undefined structural parameters and of feasible combination of values for those parameters.

In fact, given an optimization problem based on a Petri net, with disjunctive constraints, it is difficult to decide which representation to take for the Petri net model of the system. There are, nevertheless, certain characteristics that are more suitable for one of the representations previously mentioned. In particular, the larger the similarities between the alternative Petri nets, the more efficient a compound Petri net might be with respect to an equivalent set of alternative Petri nets.

From a given problem it may be easier to obtain one or other representation for the Petri net model of the system (a set of alternative Petri nets or a compound Petri net). The less evident representation may be obtained from the other one. In fact, it is possible to obtain any of both descriptions from the other one.

The process to obtain a set of alternative Petri nets from a compound Petri nets consists on associating an alternative Petri net to every one of the feasible combinations of values for the undefined structural parameters. This decomposition of the compound Petri net will eliminate the undefined structural parameters but it will increase the number of incidence matrices needed to represent the undefined Petri net. The exclusiveness among the feasible combination of values for the undefined structural parameters is transformed into the exclusiveness between the different alternative Petri nets.

On the other hand, the process to obtain a compound Petri net from a set of alternative Petri nets is based on a process of merging the alternative Petri nets into a single compound Petri net. This process will reduce the n incidence matrices of the alternative Petri nets into a single one with a set of undefined structural parameters.

It is interesting to notice that the set of alternative Petri nets that can be obtained from a compound Petri net is not unique, and the compound Petri net that can be built up from a set of alternative PN is neither unique. There is, in fact, a large number of Petri nets or sets of them that can be deduced from the other. Moreover, there are some interesting operations that can be performed on any representation of a disjunctive constraint of this type, also called undefined Petri net with undefined structural parameters. Those operations preserve the equivalence between the representations.

Nevertheless, it is possible to proof that given a set of alternative Petri nets, it can always be obtained a set of canonical Petri nets, which is the equivalent set of PN, where any of them presents an incidence matrix of minimal size. As a consequence it is possible to state that given a compound Petri net, the equivalent set of canonical Petri nets is unique.

Other alternative representation of an undefined Petri net with undefined structural parameters, an alternatives aggregation Petri net, will allow to develop a representation of a disjunctive constraint based on a Petri net which is associated to a single incidence matrix. It has to be noticed that any equivalent compound Petri net also presents a single incidence matrix, but the AAPN may not contain undefined structural parameters (if it is a simple AAPN) or it may contain them (if it is a compound AAPN), whereas the compound Petri net includes always variables in the incidence matrices by definition. The handling of a single incidence matrix without undefined parameters in it (that require the storage of an additional set of feasible combinations of values for them), may imply a better performance for the optimization algorithm than an equivalent compound Petri net if the size of the resulting incidence matrices are similar.

In previous paragraphs it has been explained that it is possible to develop algorithms to transform sets of alternative Petri nets into compound Petri nets and vice versa. It is also possible to perform any transformation between the AAPN and other equivalent representations of an undefined Petri net as the compound PN and sets of alternative PN. For example, the development of an equivalent AAPN from a set of alternative Petri net, can be performed from the concepts of shared subnets, link transitions and reduction and simplification rules. In more detail, a set of shared subnets is searched in the set of alternative PN. Then, an aggregation process of the non-shared subnets, related by the link transitions is done. The following step is the association of the choice variables related to the original alternative Petri nets to the link transitions provided by the corresponding alternative Petri net. Finally, reduction and simplification rules are applied in order to decrease the complexity of the functions of choice variables associated to the resulting AAPN.

The last equivalent representation of a disjunctive constraint, a coloured Petri net, will provide with a model, very similar to the original AAPN. As a consequence, the performance of the associated optimization processes is expected to be the same.

In this case, the transformation between an AAPN and an equivalent CPN is immediate. It is only necessary to relate the set of choice variables with a set of colours.

5. COMPARISON BETWEEN DIFFERENT SOLUTION PROCESSES OF AN OPTIMIZATION PROBLEM WITH A DISJUNCTIVE CONSTRAINT BASED ON A PETRI NET

The purpose of the different representations for a disjunctive constraint based on Petri nets that have been researched so far is to develop an exhaustive and comprehensive analysis of the possible ways to handle this constraint in the solution process of an optimization problem. As it has been explained in the previous section, there are significant differences in the algorithm that implements a solution process of an optimization problem regarding to the representation of the disjunctive constraint that has been considered (Latorre, Jiménez and Pérez 2010b).

The approach based on a set of simple alternative Petri nets and the one based on a compact mix of these simple alternative PN, obtained by merging (obtaining a compound PN) or aggregating the PN (leading to an alternatives aggregation Petri net), can be compared considering the following facts:

1. A set of simple alternative Petri nets usually provide with incidence matrices associated to every simple Petri net. These incidence matrices are smaller than the ones associated to a more compact equivalent representation, like a compound PN, an AAPN or a CPN.

2. When the similarities between the different simple alternative Petri nets are significant, the size of the incidence matrix of the compact representation of the disjunctive constraint is reduced dramatically. For this reason the time needed to operate with the compact incidence matrix in the solution process of the optimization problem may be less than the addition of the optimization processes of the simple alternative Petri nets which compose the complete set.

The approaches based on the compound Petri net and on the alternatives aggregation Petri nets can also be compared by the following considerations:

1. 1. As a general rule, an AAPN profits from similarities between subnets of the simple alternative Petri nets.

2. Also as a general rule, a compound Petri net profits from similarities between more distributed features of the simple Petri nets.

As a consequence, the same disjunctive constraint can lead to optimization algorithms with significantly different performance, regarding to the specific problem that is aimed to be solved.

6. CONCLUSIONS

An optimization problem based on the Petri net model of a discrete event system may contain disjunctive constraints. The time required to obtain a solution for this problem is usually an important requirement for practical applications in such a degree that the solution might not be useful if the delay time to obtain it is important.

Any reduction in the time needed to solve a problem of this kind can have important consequences in the applicability of a certain technique.

A classical approach to solve optimization problems with disjunctive constraints consists of dividing the problem into simpler ones to be solved independently and compared to choose one of the solutions as the best one.

In this paper this classical approach has been integrated in a systematic analysis of the different representations of the disjunctive constraint.

As a conclusion, it has been seen that the classical approach is associated to a set of simple alternative Petri nets.

On the other hand, a number of additional representations of the disjunctive constraints can be deduced from the systematic analysis mentioned before.

Every one of the representations found for the disjunctive constraint lead to optimization algorithms that have been presented in this paper may show very

different performances. As a consequence, the study of the best representation of a disjunctive constraint can be an important issue to obtain an efficient algorithm to solve optimization problems with disjunctive constraints based on a Petri net.

This paper describes for the first time the systematic analysis that have allow to discover the different representations of the disjunctive constraint and to analyse the possible applications in the solution algorithms of the optimization problems.

REFERENCES

R. David, H. Alla, "Discrete, Continuous and Hybrid Petri Nets," Springer, Berlin. 2005

J. Heizer, B. Render, "Operations Management," Prentice Hall. 2008.

E. Jiménez, "Techniques of advanced automation in industrial processes" "Técnicas de automatización avanzada en procesos industriales," PhD Thesis. Ed. Univ. de La Rioja, Logroño. 2002

E. Jiménez, , M. Pérez, , J.I. Latorre, "On deterministic modelling and simulation of manufacturing systems with Petri nets". Proceedings of European Modelling Simulation Symposium. Marseille, pp. 129-136. Marseille. 2005

E. Jiménez, M. Pérez, I. Latorre. Industrial applications of Petri nets: system modelling and simulation. Proceedings of European Modelling Simulation Symposium, pp. 159-164. Barcelona. 2006

A. Kusiak, "Computational Intelligence in Design and Manufacturing". Wiley-Interscience. 2000

J.I. Latorre, E. Jiménez, M. Pérez, "Comparison of optimization techniques applied to a flexible manufacturing system," Proceedings of the 18th European Modelling and Simulation Symposium (EMSS 06). Barcelona, pp. 141-146. October 2006.

J.I. Latorre, E. Jiménez, M. Pérez, "Macro-Reachability Tree Exploration for D.E.S. Design Optimization," Proceedings of the 6th EUROSIM Congress on Modelling and Simulation (Eurosim 2007). Ljubljana, Slovenia, September 2007.

J.I. Latorre, E. Jiménez, M. Pérez, "Decision taking on the production strategy of a manufacturing facility. An integrated methodology," Proceedings of the 21st European Modelling and Simulation Symposium (EMSS 09). Puerto de la Cruz, Spain, vol. 2, pp. 1-7, September 2009.

J.I. Latorre, E. Jiménez, M. Pérez, E. Martínez, "The design of a manufacturing facility. An efficient approach based on alternatives aggregation Petri," Proceedings of the 21st European Modelling and Simulation Symposium (EMSS 09). Puerto de la Cruz, Spain, vol. 2, pp. 33-39, September 2009.

J.I. Latorre, E. Jiménez, M. Pérez, J. Blanco, "The problem of designing discrete event systems. A new methodological approach," Proceedings of the 21st European Modelling and Simulation Symposium (EMSS 09). Puerto de la Cruz, Spain, vol. 2, pp. 40-46, September 2009.

J.I. Latorre, E. Jiménez, M. Pérez, "A genetic algorithm for decision problems stated on discrete event systems." Proceedings of the UKSim 12th International Conference on Computer Modelling and Simulation. Cambridge, United Kingdom, March 2010.

J.I. Latorre, E. Jiménez, M. Pérez, "The alternatives aggregation Petri nets as a formalism to design discrete event systems." International Journal of Simulation and Process Modeling, Special Issue. 2010

D.Y. Lee, F. DiCesare. "FMS scheduling using Petri nets and heuristic search". Robotics and Automation. Proceedings, Volume 2, 1057 – 1062. 1992.

G. Music, "Petri net based scheduling approach combining dispatching rules and local search, " Proceedings of the 21st European Modelling and Simulation Symposium (EMSS 09). Puerto de la Cruz, Spain, vol. 2, pp. 27-32, September 2009.

M.À. Piera, M. Narciso, A. Guasch, D. Riera, "Optimization of logistic and manufacturing system through simulation: A colored Petri net-based methodology," Simulation, vol. 80, number 3, pp 121-129, May 2004

M. Silva. "Introducing Petri nets, In Practice of Petri Nets in Manufacturing" 1-62. Ed. Chapman&Hall. 1993

M. Zhou. K. Venkatesh. "Modelling, Simulation and Control of Flexible Manufacturing Systems. A Petri Net Approach", WS World Scientific, 1999

AUTHORS BIOGRAPHY

Juan Ignacio Latorre is electrical engineer. He has developed part of his professional career in the manufacturing private sector. Nowadays he is associated professor in the Public University of Navarre. He is developing his PhD thesis in optimization of manufacturing processes based on Petri net models. His research interests include automation, optimization and Petri nets.

Emilio Jiménez Macías studied Industrial Engineering (with Computer Science, Electronics and Automation specialty) by the University of Zaragoza, and in 2001 presented his PhD thesis about Industrial Automation, in the University of La Rioja, where he works presently in the Electrical Engineering Department (Coordinator of the System Engineering and Automation Group). His research areas include factory automation, modeling and simulation (Petri nets), and industrial processes.

Mercedes Pérez de la Parte received the BS degree in Telecommunications Engineering from the University of Seville in 1997. She has held research and teaching positions, since 1997 until present, at the University of Seville (Spain), at the University of Los Andes (Venezuela), and the University of La Rioja, where she is an Assistant Professor at the Mechanical Engineering Department.

A CASE STUDY IN WORKFLOW MODELLING USING CONTROL-FLOW PATTERNS

Y. Callero[(a)], I. Castilla[(b)], R.M. Aguilar[(c)]

[(a)(b)(c)]Department of Systems Engineering and Automation, and Computer Architecture.
Universidad de La Laguna. Spain
[(a)]ycallero@isaatc.ull.es, [(b)]ivan@isaatc.ull.es, [(c)]raguilar@ull.es

ABSTRACT
Business Process Reengineering is a field where state-of-the-art powerful tools are required to obtain valid and profitable results. In this sense, Business Process Simulation is becoming one well-known instrument to analyze and return valuable solutions, although a potential user has to face the lack of a standard modelling approach. This paper introduces the most important difficulties that arise when dealing with the practical implementation of one of these approaches, the Synchronizing Workflow Models; and presents an example illustrating how these problems have been solved with the Discrete Event Simulation library, SIGHOS.

Keywords: Business Process Management, Discrete Event Simulation, Workflow Patterns, Simulation Tool, Synchronized Workflow Models, Business Process Reengineering.

1. INTRODUCTION

The workflow concept is inherently related to the notion of process, as it was originally conceived since industrialization in manufacturing and the office (Georgakopoulos, Hornick and Sheth 1995). "Processes" separate work activities into well-defined tasks, roles, rules and procedures in order to increase efficiency.

Over time, this way of working leads to a fragmentation of the business that negatively impacts on cost and on the motivation of the personnel.

In this sense, Business Process Reengineering (BPR) makes its appearance. As stated by Muthu, Whitman and Cheraghi (2006), reengineering *is the fundamental rethinking and radical redesign of business processes to achieve dramatic improvements in critical, contemporary measures of performance such as cost, quality, service and speed*. A Business Process (BP) *is a market-centred description of an organization's activities, implemented as an information process and/or a material process* (Medina-Mora, Winograd, Flores and Flores 1992).

Business Process Simulation (BPS) is an important tool within BPR. As described by Wynn, Dumas, Fidge, Hofstede and Aalst (2008), BPS is focused on the achievement of two main goals:

1. the analysis of the behaviour of a process, by means of the development of accurate simulation models;
2. the understanding of the effects of running that process through the performance of simulation experiments.

Three components describe a BPS (Wynn, Dumas, Fidge, Hofstede and Aalst 2008):

1. basic model building blocks, such as entities, resources, activities, and connectors;
2. activity modelling constructs, such as split, join, branch and assemble;
3. and advanced modelling functions, such as attributes, expressions and resource schedules.

Russell, Hofstede and Mulyar (2006) delineate the fundamental requirements that arise during business process modelling on a recurring basis and describe them in an imperative way. A pattern-based approach is used to describe these requirements. Such approach offers both a language- and technology- independent means of expression in a form that is sufficiently generic to allow for a wide variety of applications.

However, there is no generally accepted modelling technique for implementing workflow patterns as part of a simulation tool. Different notations, such as EPCs (Event-Driven Process Chain) or BPMN (Business Process Management Notation) have been posed that try to overcome the difficulties arisen when implementing such models.

Precisely, the EPC notation has served as a basis for adapting SIGHOS, a discrete event simulation library developed by the Simulation Group from the University of La Laguna, to support the use of workflow patterns in the simulation of business processes. The rest of this paper is structured as follows. The first section defines the main concepts related to

workflows modelling. Next, the methodology used to model the functionalities proposed by the control-flow patterns based on Synchronized Workflow Models is detailed. Once the strategy is explained, a practical approach is taken to present the structures designed in SIGHOS for modelling said patterns. A modelling example is presented in the next section. The last section contains a summary of the conclusions drawn from our research.

2. WORKFLOW BASICS

Having set the definition of business process, the Workflow Management Coalition (WfMC) defines "workflow" as *the partial or total automation of a business process during which documents, information or tasks are passed from one participant to another for action, according to a set of procedural* rules. (Workflow Management Coalition 1999)

There is little consensus in the workflow specification due to the lack of universal concepts for modelling business processes (Aalst, Hofstede, Kiepuszewski and Barros 2003).

One of the most widespread terminologies used to describe the concepts and general structure of a workflow is the WfMC terminology (Workflow Management Coalition 1999). The concept of "process instance" is especially important to understand the behaviour of SIGHOS models. The WfMC terminology describes a process instance as a single enactment of a process, or activity within a process, including its associated data. Each process instance is executed on a separate thread. However, if a process includes parallel activities, the corresponding process instance would include multiple concurrent threads of execution.

2.1. Control flow perspective

Among the different perspectives (control-flow, data, resource and operational) to the workflow specifications stated in (Aalst, Hofstede, Kiepuszewski and Barros 2003), this research work focuses on the control-flow perspective.

Russell, Hofstede and Mulyar (2006) studied countless practical cases involving real companies, and proposed 43 patterns which define the requirements for modelling the different scenarios defined within the control flow perspective. Many workflow definition languages, modelling tools and workflow engines have resulted from this practical approach like: BPEL (Hinz, Schmidt and Stahl 2005), XPDL (Aalst 2003), ARIS (Davis 2001), Gridant (Amin, Hategan, von Laszewski, Zaluzec, Hampton and Rossi 2004) and WW-FLOW (Kim, Kang, Kim, Bae and Ju 2000).

Kiepuszewski, Hofstede and Aalst (2003) expose the basic control flow constructs, common to most of these approaches:

- AND-Split is a point within the workflow where a single thread of control splits into two or more threads which are executed in parallel.
- AND-Join is a point in the workflow where two or more parallel executing tasks converge into a single common thread of control.
- OR-Split is a point within the workflow where a single thread of control decides on which branch to take when encountered with multiple alternative workflow branches.
- OR-Join is a point within the workflow where two or more alternative task workflow branches re-converge to a single common task as the next step within the workflow.

2.2. Theoretical foundations

Whilst the patterns proposed by Russell et al. are convenient for a practical approach, some more robust theoretical foundation is required that characterizes control flow modelling. Therefore, formal tests about expressiveness limits and properties of a model may be performed.

Petri nets have been traditionally employed to specify control flows, since activities can be seen as transitions; and causal dependencies as places, transitions and arcs. Kiepuszewski (2003) uses the properties of the Petri nets to distinguish among four different techniques employed to model control-flow patterns.

First, Kiepuszewski defines the *Standard Workflow Models* as the most "natural" interpretation of the WfMC definitions. Standard Workflow Models have the ability to create multiple concurrent instances of one activity.

Safe Workflow Models, on the contrary, never create multiple concurrent instances of an activity. Consequently, the corresponding Petri net is safe.

Intuitively, a *Structured Workflow Model* is a model where each OR-Split has a corresponding OR-Join and each AND-Split has a corresponding AND-Join, with no arbitrary cycles allowed.

Last, *Synchronizing Workflow Models* appear from a different interpretation of the WfMC definitions of basic control flow constructs. An AND-Join typically follows an AND-Split and can be seen as a construct that synchronizes a number of active threads. To synchronize that kind of construct, commercial

tools generally use a token-based technique. The semantics of Synchronizing Workflow Models can be easily captured by using Coloured Petri nets.

3. SIGHOS AND SYNCHRONIZING WORKFLOW MODELS

3.1. SIGHOS, a discrete event simulation tool

The potential of Simulation as a tool for business process modelling has not been yet recognized by much of the business community (Hlupic and Robinson 1998). However, BPS may be used to achieve a higher level of understanding when studying and analyzing businesses which are inherently complex. Not only this, simulation has several characteristics that make it appealing for business process modelling. Indeed, a process-based world view, as defined from a simulation modelling perspective, can be seen as *a time-ordered sequence of interrelated events which describe the entire experience of an entity as it flows through the system* (Balci 1988). This definition can be easily matched with the flow of entities through business processes.

SIGHOS (SIGHOS project homepage 2010) is a process-oriented discrete event simulation tool which was originally intended to simulate hospital management (Aguilar, Castilla, Muñoz, Martín and Piñeiro 2006). Being Java-based, SIGHOS takes advantage from the known benefits of using Java to implement a discrete event simulation tool (Buss 2002)(L'ecuyer and Buist 2005)(Goes, Pousa, Carvalho, Ramos and Martins 2005). Robustness, portability, and ease of implementation and documentation for programmers are some of the strengths usually associated with Java. Moreover, Java is inherently Internet- and Thread- aware, that is, the language includes in its core definition primitives to deal with network communications and concurrent programming.

SIGHOS evolved from its original conception to a broader range of applications such as call centres (Castilla, Muñoz and Aguilar 2007) by generalizing the structures employed to define processes (Castilla, García and Aguilar 2009). However, these first simple structures were not powerful enough to deal with the multiple complexities that a real business process may pose to a modeller. Thus, taking control-flow patterns as a reference, the business process modelling capacity of this tool was expanded. The difficulties arise when coping with the problems posed, by definition, by synchronizing workflow models.

3.2. Why synchronizing models?

Synchronizing Workflow Models allows the modelling of multiple instances of a process unlike Safe Workflow, Structured Workflow or Standard Workflow models as posited by Kiepuszewski (2003).

A priori, the Synchronizing Workflow Models are best suited to the SIGHOS tool since they solve the deadlock problem and efficiently allow for the problems of modelling multiple-instance patterns and loops to be overcome.

Kiepuszewski advised to use the Token-based strategy in the Synchronizing Workflow Models implementation. The goal of using this strategy is to solve the possible appearance of deadlocks during the runtime. This strategy implies that each node in the model has to propagate one or several tokens indicating the state of the outgoing threads.

3.3. Token-based strategy implemented by SIGHOS

SIGHOS adopts the token-based strategy from two basic nodes: *SingleSuccessor* or *MultiSuccessor*. The former can only be linked to a single node, while the latter may have several linked nodes.

Based on these two kinds of nodes, SIGHOS implements four basic constructs:

- *Initializer node*
- *Finalizer node*
- *Task node*
- *Structured node*

An *Initializer* is a *MultiSuccesor* node that represents a source of new tokens, so that the generation of a token involves the creation of a new thread. *AND-Split*, *OR-Split* and *Conditional* nodes are based on this node. If a true token is received, the node propagates a true token through the active outgoing branches, and a false token through the inactive ones. In case a false token is received, the node propagates a false token through each outgoing branch.

Conditional nodes are a special case of *OR-Split*. Upon receipt of a true token, the node checks each associated condition changing the resulting token value depending on the check result. Upon receipt of a false token, a false token is sent to each outgoing branch.

A *Finalizer* is a *SingleSuccesor* node that represents a sink of tokens. A token removal represents the finalization of thread execution. This node is the basis for AND-Join or OR-Join nodes. The propagation of tokens depends on the criteria present at each node for yielding flow control:

- An AND-Join node generates a new token from the confluence of incoming tokens. This node defines an acceptance value as the total amount of true tokens that it must receive through the incoming branches. When enough tokens are received, a true token is sent to the node's successor and the account of tokens is reset. This type of node has two operating modes: safe and unsafe. Using one or another operating mode affects the way the concurrent receipt of tokens through the same incoming branch is treated. In safe mode, only one token per branch and simulation timestamp is taken into account; the rest are simply discharged. In unsafe mode, all the tokens are considered and taken as valid.
- An OR-Join node simply propagates the same token which arrived to the successor. The only control that is performed affects the concurrent arrival of tokens. At that moment, the control state has to decide if all or only one thread is subsequently sent to the successors. If the criteria for yielding control is not met once every incoming branch token has been received, a false token is propagated.

A Task node is also a SingleSuccesor node and represents the execution of some kind of activity. The activity is executed upon receipt of a true token. Once the execution is complete, a true token is propagated. However, if the execution is cancelled or the node receives a false token - meaning the execution is not to be carried out - a false token is propagated.

Structured nodes are SingleSuccessor nodes which consist of one node that defines the structure's starting point, and another one that defines its end. All kind of complex branches can link such starting and end points. Only upon arrival of a true token, the control is yielded to the sub-flow contained in the structure. Otherwise, the false token is simply propagated to its successors.

3.4. Improving Synchronizing Workflow Models

One of the problems that Kiepuszewski (2003) associates with Synchronizing Workflow Models is the impossibility of handling multiple process instances without running into serious limitations. Such limitations result from his formal definition involving Petri nets. SIGHOS takes advantage from not assuming such a formal base. One goal of the tool is the conduct of efficient simulations from the standpoint of parallelism and concurrence (Castilla, García and Aguilar 2009). That is why the functional core of the tool is optimized to simulate various processes and their multiple instances without limitations. For example, with the token-based strategy, a process could have several active instances executing the same task given enough available resources. The tokens that indicate the validity of each instance are totally independent, which allows the model to be coherent.

Another important problem associated with Synchronizing Workflow Models is the control of different iterations within a loop which is solved by treating each node as a structured one. This leaves the handling of the possible arbitrary cycles that are defined in the model as the only outstanding problem. SIGHOS handles the patterns of arbitrary cycles by implementing a system of environment variables, associated with the model or defined by the user, and an expression set which allows for the conditions associated with these variables to be defined. There is also a set of user events that allows the values of these variables to be modified at different points in the model. These structures allow arbitrary cycles to be modelled, maintaining control over the possible appearance of infinite loops. On the one hand, when a true token enters one of these cycles, the set of conditions associated with this cycle will control the exit from the cycle for that token. On the other hand, when a false token enters one of these cycles, this token propagates, both to the exit branch for a cycle as well as to the branch that generates the loop. This leads to an infinite propagation of the false token, which results in an improper execution of the simulation. This undesirable situation can be solved if each false token keeps track of the nodes it has been to. Should a false token return to a node through which it has already passed, it is assumed to be immersed in a loop and deleted from the simulation since it is no longer producing relevant information.

4. CONTROL-FLOW PATTERNS SUPPORTED BY SIGHOS

This section analyzes which control flow patterns are supported by SIGHOS. Patterns are divided into categories depending on its functionality. These categories are: basic control flow patterns, advanced branching and synchronization patterns, multiple instance patterns, iteration patterns, termination patterns and trigger patterns.

Each category is discussed in a separate subsection, including an explanation about whether each specific workflow control pattern (WCP) is supported by SIGHOS or not.

4.1. Basic Control Flow Patterns

These basic patterns capture elementary aspects of process control.

Table 1. Basic control flow patterns support

Basic Control Flow Patterns	Supported by SIGHOS
WCP1: Sequence	YES
WCP2: Parallel Split	YES
WCP3: Synchronization	YES
WCP4: Exclusive Choice	YES
WCP5: Simple Merge	YES

No further explanation is required since the support of these patterns is trivial.

4.2. Advanced Branching and Synchronization Patterns

These patterns characterise more complex branching and merging concepts which arise in business processes.

Table 2. Advanced branching and synchronization patterns support

Advanced Branching and Synchronization Patterns	Supported by SIGHOS
WCP6: Multi-Choice	YES
WCP7: Structured Synchronizing Merge	YES
WCP8: Multi-Merge	YES
WCP9: Structured Discriminator	YES
WCP28: Blocking Discriminator	YES
WCP29: Cancelling Discriminator	NO
WCP30: Structured Partial Join	YES
WCP31: Blocking Partial Join	YES
WCP32: Cancelling Partial Join	NO
WCP33: Generalised AND-Join	YES
WCP37: WCP: Local Synchronizing Merge	YES
WCP38: General Synchronizing Merge	NO
WCP41: Thread Merge	YES
WCP42: Thread Split	YES

SIGHOS focuses large part of its current operating potential on the ability to represent patterns of this class. Modelling primitives are provided for almost the entire set of patterns, but three. The Cancelling Discriminator, the Cancelling Partial Join and the General Synchronizing Merge are not considered because of their non-local semantics limitations. This problem will be revisited in section 5.

4.3. Multiple Instance Patterns

These patterns describe process models including an activity with multiple active threads of execution.

Table 3. Multiple instance patterns support

Multiple Instance Patterns	Supported by SIGHOS
WCP12: Multiple Instances without Synchronization	YES
WCP13: Multiple Instances with a Priori Design-Time Knowledge	YES
WCP14: Multiple Instances with a Priori Run-Time Knowledge	NO
WCP15: Multiple Instances without a Priori Run-Time Knowledge	NO
WCP34: Static Partial Join for Multiple Instances	YES
WCP35: Cancelling Partial Join for Multiple Instances	NO
WCP36: Dynamic Partial Join for Multiple Instances	NO

SIGHOS offers the possibility of handling multiple instances as long as they are pre-defined in the model. The system is not yet able to deal with instances created dynamically during the simulation. That is why the remaining patterns in this class are not accepted, and why a process for cancelling activities has not been defined.

4.4. State-based Patterns

State-based patterns are more easily accomplished in process languages that support the notion of state. In this context, the state of a process instance is considered to include the broad collection of data associated with current execution, that is, the status of various activities as well as process-relevant working data such as activity and case data elements.

Table 4. State-based patterns support

State-based Patterns	Supported by SIGHOS
WCP16: Deferred Choice	NO
WCP17: Interleaved Parallel Routing	YES
WCP18: Milestone	NO
WCP39: Critical Section	NO
WCP40: Interleaved Routing	YES

Only 2 out of 5 patterns (the interleaved ones) are implemented in SIGHOS. The remaining patterns are beyond the scope of the library.

4.5. Cancellation and Force Completion Patterns

Several of the patterns above have variants that utilize the concept of activity cancellation where enabled or active activity instances are withdrawn. Various forms of exception handling in processes are also based on cancellation concepts.

Table 5. Cancellation and force completion patterns support

Cancellation and Force Completion Patterns	Supported by SIGHOS
WCP19: Cancel Task	NO
WCP20: Cancel Case	NO
WCP25: Cancel Region	NO
WCP26: Cancel Multiple Instance Activity	NO
WCP27: Complete Multiple Instance Activity	NO

SIGHOS does not provide any cancellation method, neither for cases nor for activity executions.

4.6. Iteration Patterns

The following patterns represent repetitive behaviour in a workflow.

Table 6. Iteration patterns support

Iteration Patterns	Supported by SIGHOS
WCP10: Arbitrary Cycles	YES
WCP21: Structured Loop	YES
WCP22: Recursion	NO

SIGHOS allows for the modelling of loops and arbitrary cycles. The recursive case is not considered.

4.7. Termination Patterns

These patterns face completion of workflows.

Table 7. Termination patterns support

Termination Patterns	Supported by SIGHOS
WCP11: Implicit Termination	YES
WCP43: Explicit Termination	NO

Being designed as an event-oriented simulator, SIGHOS directly supports the implicit termination pattern. Explicit termination, understood as a generalization of the cancellation patterns, is discharged due to the limitations in terms of non-local semantics of the library.

4.8. Trigger Patterns

Trigger patterns deal with the external signals that may be required to start certain tasks.

Table 8. Trigger patterns support

Trigger Patterns	Supported by SIGHOS
WCP23: Transient Trigger	NO
WCP24: Persistent Trigger	NO

Triggers also rely on non-local semantics which cannot be solved by the single use of tokens. Thus, their implementation goes beyond the scope of the library.

5. CONTROL-FLOW PATTERNS NOT IMPLEMENTED BY SIGHOS

As shown in the previous section, SIGHOS has been proved to be a valid tool to implement most of the patterns defined by Russell, Hofstede and Mulyar (2006). However, some patterns have not been implemented yet due to different reasons with a remarkable influence of non-local semantics (Aalst, Desel, Eichstätt-ingolstadt, Kindler and Paderborn 2002). Non-local semantics make reference to those situations where a node requires information which is not local to the node (that is, which belongs to a different part of the model) in order to take a decision on the propagation of a process instance. The token strategy introduced in section 3.2 copes with some of the problems derived from such semantics but others remain unsolved.

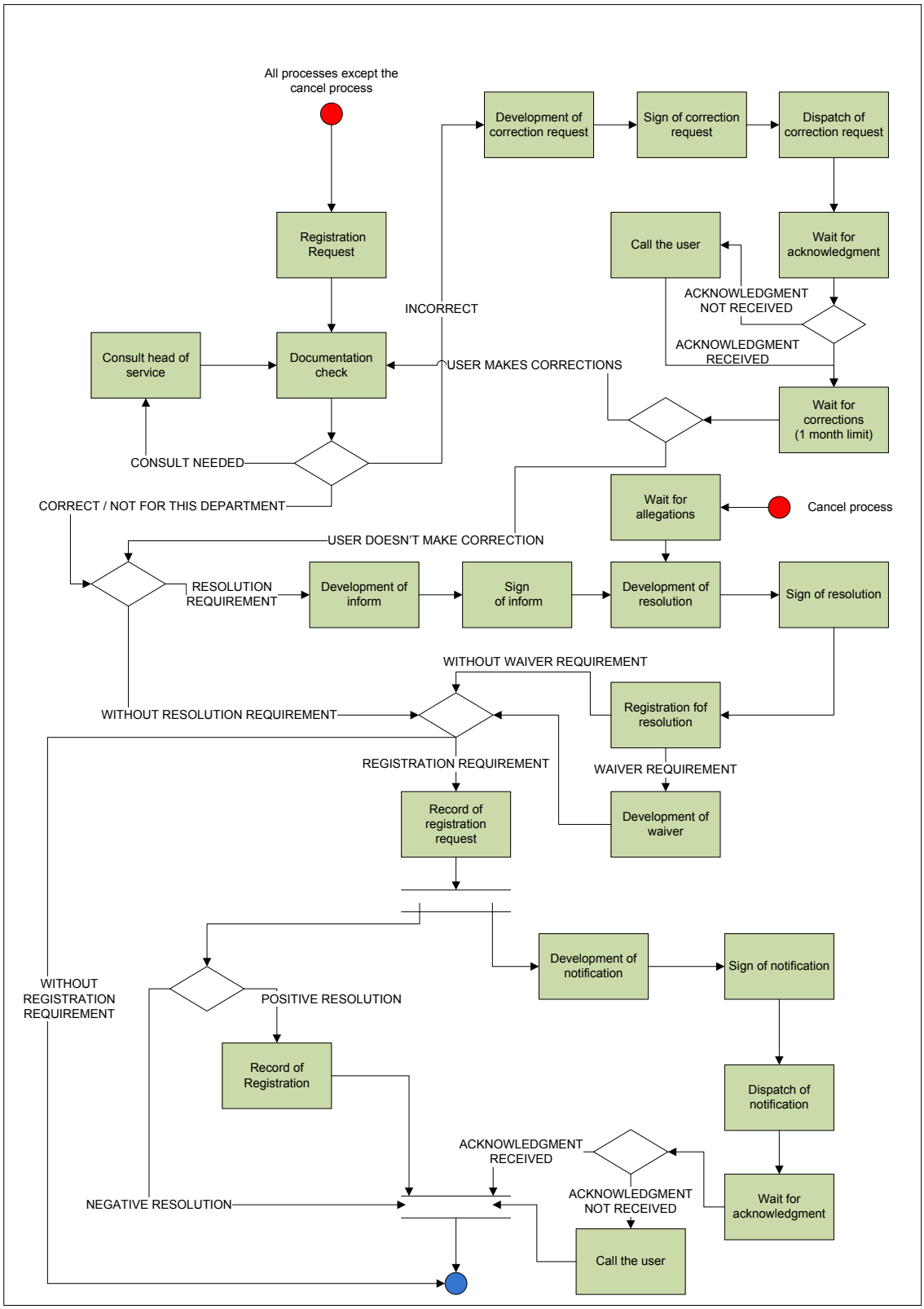

Figure 1. Registry of Associations workflow diagram

Cancellation patterns (WCP19, WCP20, WCP25, WCP26, WCP27, WCP29, WCP32 and WCP35) perfectly illustrate the problems derived from the use of non-local semantics. These patterns require explicitly breaking the execution logic of the simulator. A cancel pattern normally affects a process instance or a set of process instances. However, the process instance that activates the cancellation can be located in a completely different part of the

model. Locating such instances implies complex memory structures and an efficient search algorithm, thus increasing the memory and CPU requirements for the simulator.

6. MODELLING EXAMPLE: REGISTRY OF ASSOCIATIONS

Several civil service processes have been reorganized into electronic processes in Canary Islands government. A specific case study was described in (Callero and Aguilar 2009). Upon the basis of the workflow modelling of this case, a deeper analysis is presented in this section.

6.1. Description of the problem

Spain and the autonomous regions governments share the competences about the control of associations. The autonomous region government takes all responsibility for the establishment of different ways to set up, manage or dissolve associations. The Registry of Associations was defined to manage all of these operations.

Focusing in Canary Islands region, each province (Las Palmas and Santa Cruz de Tenerife) has its own Registry of Associations head office and its own staff. Whereas Las Palmas office has two government employees and two technicians, Santa Cruz office has three government employees and one technician. In addition, there are one head of service and one general director for the entire autonomous region. All the activities of the Registry of Associations are carried out by the described staff.

6.2. Flow modelling

The workflow of the process is shown in Figure 1. The Registry of Associations has nineteen different activities. The activities are modelled using Task Nodes.

The execution of the activities is started by a customer request but the execution flows depends on the process characteristics. Sixteen different processes can be executed in Registry of Associations, thus creating decision points to route the flow depending on the process characteristics: does the subprocess documentation needs to be corrected or consulted? Is the process resolution negative or positive?

Using Conditional nodes, associated to the environment variables, it is possible to emulate the ExclusiveChoice pattern in order to model the decision points.

Notification and registration subprocess at the end of the process are another key point in the flow of the Registry of Associations. This subprocess generates a parallel execution of tasks. One parallel branch is involved in the notification tasks and the other branch is involved in the registration tasks. Both branches are synchronized at the end of the flow.

SIGHOS Structured Nodes give to the modeller the possibility to define Structured Synchronizing Merge pattern behaviour to simulate processes like notification and registration subprocess.

7. CONCLUSIONS

Workflow technology is still under development in its traditional application areas (business process modelling and business process coordination), but also in emergent areas of component frameworks and inter-workflow, business-to-business interaction (Aalst, Hofstede, Kiepuszewski and Barros 2003).

In this paper, a practical example of an application of synchronized models for the modelling of workflow patterns has been presented.

It is clear that the token-based strategy provides an enormous freedom of design, although not all of its potential has been exploited yet. In other words, from the point of view of the developing group, the SIGHOS library can still be significantly improved in the area of modelling workflow patterns.

A modelling example has been also introduced to illustrate the use of SIGHOS and the synchronized models to simulate a real problem. Future work will further develop this model.

ACKNOWLEDGMENTS

This work is being supported by a project (reference DPI2006-01803) from the Ministry of Science and Technology with FEDER funds.

Iván Castilla is being supported by an FPU grant (ref. AP2005-2506) from the Ministerio de Educación y Ciencia of Spain.

Yeray Callero is being supported by a postgraduate grant from CajaCanarias Canary Island bank.

REFERENCES

Aalst, W. M., Desel, J., Eichstätt-ingolstadt, K. U., Kindler, E. and Paderborn, U., 2002. On the semantics of EPCs: A vicious circle. *Proceedings of the EPK 2002: Business Process Management using EPCs*, 71-80.

Aalst, W. M., Hofstede, A., Kiepuszewski, B. and Barros, A., 2003. Workflow Patterns. *Distributed and Parallel Databases*, 14, 5 - 51.

Aalst, W.M., 2003. Patterns and XPDL: A Critical Evaluation of the XML Process Definition Language, *QUT Technical report*, Brisbane.

Aguilar, R. M., Castilla, I., Muñoz, R., Martín, C. A. and Piñeiro, J. D., 2006. Verification and validation in discrete event simulation: A case study in hospital management. International Mediterranean Modeling Multiconference 2006 proceedings.

Amin, K., Hategan, M., von Laszewski, G., Zaluzec, N., Hampton, S. and Rossi, A., 2004. Gridant: A client-controllable grid workflow system. *37th Hawai'i International Conference on System Science*, 5–8.

Balci, O., 1988. The implementation of four conceptual frameworks for simulation modeling in high-level languages. *Proceedings of the 20th conference on Winter simulation - WSC '88*, 287-295.

Buss, A., 2002. Component based simulation modeling with simkit. *Proceedings of the Winter Simulation Conference*, 243-249.

Callero, Y. and Aguilar, R., 2009. Use of simulation in egovernment process development. A case study using the simulation tool SIGHOS. *21st European Modeling & Simulation Symposium proceedings*, 1, 253-260.

Castilla, I., Muñoz, R. and Aguilar, R. M., 2007. Helpdesk Modeling and Simulation with Discrete Event Systems and Fuzzy Logic. *European Modeling and Simulation Symposium (EMSS 2007) proceedings*.

Castilla, I., García, F. and Aguilar, R., 2009. Exploiting concurrency in the implementation of a discrete event simulator. *Simulation Modelling Practice and Theory*, 17, 850-870.

Davis, R., 2001. Business process modelling with ARIS: a practical guide, *Springer-Verlag London*.

Georgakopoulos, D., Hornick, M. and Sheth, A., 1995. An overview of workflow management: From process modeling to workflow automation infrastructure. *Distributed and Parallel Databases*, 3, 119-153.

Goes, L., Pousa, C., Carvalho, M., Ramos, L. and Martins, C., 2005. JSDESLib: A Library for the Development of Discrete-Event Simulation Tools of Parallel Systems. *19th IEEE International Parallel and Distributed Processing Symposium*.

Hinz, S., Schmidt, K. and Stahl, C., 2005. Business Process Management, Berlin/Heidelberg: Springer-Verlag.

Hlupic, V. and Robinson, S., 1998. Business process modelling and analysis using discrete-event simulation. *Winter Simulation Conference Proceedings*, 25, 534-548.

Kiepuszewski, B., Hofstede, A. and Aalst, W. V., 2003. Fundamentals of control flow in workflows. *Acta Informatica*, 39, 143-209.

Kiepuszewski, B., 2003. *Expressiveness and suitability of languages for control flow modelling in workflows.* Faculty of Information Technology. Queensland University of Technology.

Kim, Y., Kang, S., Kim, D., Bae, J. and Ju, K., 2000. WW-FLOW: Web-based workflow management with runtime encapsulation. *IEEE Internet Computing*, 4, 55–64.

L'ecuyer, P. and Buist, E., 2006. Simulation in java with ssj. *Proceedings of the Winter Simulation Conference*, 611-620.

Medina-Mora, R., Winograd, T., Flores, R. and Flores, F., 1992. The action workflow approach to workflow management technology. *Proceedings of the 1992 ACM conference on Computer-supported cooperative work - CSCW '92*, 281-288.

Muthu, S., Whitman, L. and Cheraghi, S. H., 2006. Business Process Reengineering: A Consolidated Methodology. *Proceedings of the 4th Annual International Conference on Industrial Engineering Theory, Applications, and Practice, 1999 U.S. Department of the Interior - Enterprise Architecture*, 8-13.

Russell, N., Hofstede, A. H. and Mulyar, N., Workflow ControlFlow Patterns: A Revised View, *BPM Center Report BPM-06-22*.

SIGHOS project homepage. Available from: http://sourceforge.net/projects/sighos/. [APR 2010]

Workflow Management Coalition, 1999. Workflow Management Coalition Terminology Glossary. *Document Number WFMC-TC-1011*.

Wynn, M., Dumas, M., Fidge, C., Hofstede, A., and Aalst, W. V., 2008. Business Process Management Workshops, Springer Berlin Heidelberg.

AUTHORS BIOGRAPHY

YERAY CALLERO was born in Haría, Lanzarote and attended the University of La Laguna, where he studied Engineering Computer Science and obtained his degree in 2008. He is currently working on his PhD with the Department of Systems Engineering and Automation at the same university. His research interests include simulation and embedded system software design.

IVÁN CASTILLA was born in La Laguna, Tenerife and attended the University of La Laguna, where he studied Engineering Computer Science and obtained his degree in 2004. He is currently working on his PhD with the Department of Systems Engineering and Automation at the same university. His research interests include parallel discrete event simulation and computer architecture.

ROSA M. AGUILAR received her MS degree in Computer Science in 1993 from the University of Las Palmas de Gran Canaria and her PhD degree in Computer Science in 1998 from the University of La Laguna. She is an associate professor in the Department of Systems Engineering and Automation at the University of La Laguna. Her current research interests are decision making based on discrete event simulation systems and knowledge-based systems, intelligent agents, and intelligent tutorial systems.

Simulation and Optimization of the Pre-hospital Care System of the National University of Mexico using Travelling Salesman Problem algorithms.

Esther Segura Pérez
Secretaría de Posgrado e Investigación, UNAM
esthersp_1976@yahoo.com.mx.

Luis Altamirano Yepez
División de estudios de Posgrado FI, UNAM
altamirano@dctrl.fi-b.unam.mx

Idalia Flores de la Mota
Secretaría de Posgrado e Investigación, UNAM
idalia@servidor.unam.mx

Keywords: simulation, travelling-salesman, optimization.

Abstract

A hybrid methodology was developed in this project, using optimization and simulation techniques to analyze efficiency in a pre-hospital healthcare system offered by Emergency Medical Technicians (TUMs) or paramedics. This healthcare is offered in the North and South of Mexico City while students are sitting their exams for admission to the National Autonomous University of Mexico. This study presents an optimization of the routes of an ambulance in charge of serving 26 security modules installed at schools where students were attending their admission exams. This optimization is done on the basis based on algorithms used to solve the travelling-salesman problem (TSP) and simulation is used to determine the scenarios where calls for the ambulance happen with a greater occurrence probability. Furthermore, the patient´s transfer route from the hospital care module is optimized with the shortest path algorithm. The pre-hospital healthcare system is formed by 11 paramedics and 5 properly equipped ambulances. Heuristic techniques were programmed with the Visual Basic 6 programming language and the simulation was executed using the Arena program.

1 Introduction

Records of the treatment of injured or sick patients go back to biblical times. During the 18th and 19th centuries different methods were used with this purpose, though it was Jean Dominique Larrey who started the first pre-hospital care system.

The National Autonomous University of Mexico (Universidad Nacional Autónoma de México UNAM) has been offering this service since 1982, using vehicles with enough capacity for a multidisciplinary team made up by both professionals and technicians to provide basic and advanced life support. Despite the fact that some studies have been carried out to improve efficiency in patient's transport times in the APH (Pre-hospital care), there is as yet little evidence of any careful study having been made on this subject either in Mexico or elsewhere. The efficiency of the APH system is measured by the system's average response time, which is the time taken by the TUMs to arrive at the scene of the accident, attend to the patient and transfer him or her to hospital if necessary. This study pioneers the use of optimization and simulation techniques to achieve greater efficiency in the system.

2 The Problem

Every year the National University of México (UNAM) organizes three admission exams for three levels: high school, undergraduate level and the open university. On each occasion there are, on average, about 114,462 applicants [6]. In order to guarantee timely medical in cases of emergency, on these occasions the Medical Services Office (DGSM) obtaining with the pre-hospital area (APH) puts a special service in place. This service has five ambulances, four of which each serve one specific area, in order to service 26 modules. The remaining ambulance supervises all the modules. The people in charge of each module require the transfer of patients for the following medical emergencies:

Faints-D, Nervous crisis-CN, Asthmatic crisis-CA, Hypoglycemia-H, Stress-induced colitis-CE, Convulsions-Co, Acute coronary syndrome- I, Metabolic problems: decompensated diabetes-DD, Traffic Accident-A, Status epilepticus –EE, Apendicitis-Ap.

Most of the patients who require the service are applicants or the people accompanying them. For this reason the aim of this research is to reduce the mortality and morbidity resulting from injuries that require medical attention. To achieve this it is necessary to optimize the access routes to the modules and from there to

the hospitals where patients will receive proper medical attention. The main index of measurement for the APH is the ambulance response time. This response time includes the call for the ambulance, the care of the patient in the module, and the patient`s transfer to a hospital. Nowadays this takes about 18 minutes.

3 Methodology

This research was developed in three phases. The first consisted of collecting, adapting and sorting the historical information, in the second phase a simulation model was designed in order to generate several scenarios and, finally, the third phase consisted of optimizing routes obtained from the simulation model. These routes were optimized using shortest route algorithms and TSP algorithms.

This project had the support of the APH people who provided the historical information about cases and average response times. These data were fitted into probabilistic functions used in the simulation model.

The scenarios focus on the module requiring the service, the causal agent, patient characteristics and whether or not the patient needs to be transferred to a hospital. Once the simulation gives the scenarios, the stage of routes optimization begins, by taking the module into account as initial input. The Dijkstra shortest route algorithm was used for this stage to find the shortest routes in each scenario.

A heuristic used in the TSP was used for the ambulance that supervises all the modules. Finally, for each scenario, the response time is taken that makes it possible to measure the performance of the APH system and be able to make good decisions.

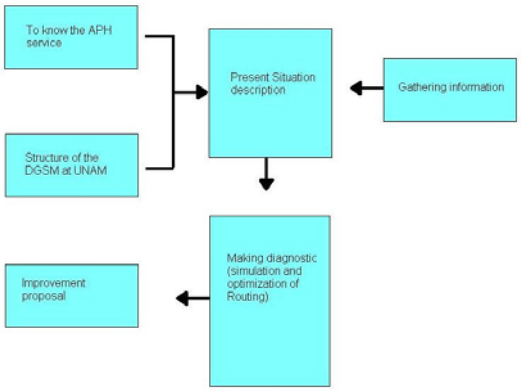

Figure 1. Proposal for improvement

4 Model design

4.1 Phase 1

Stat:Fit software was used with the historical information from the last four years in order to find the probabilistic distribution that best fits in with each module and causal agent (the source of the emergencies).

Table 1 shows the medical events for each module, the Stat:Fit software works with this information as shown in figure 2. Figure 3 shows the curve with the best fit.

This phase gives us probabilistic distribution functions that will be used in the simulation model. The table 2 shows one of the eleven tables for each module and ailment.

Ailment	Event
D	2
CN	1
CA	0
H	3
CE	1
CO	0
I	0
DD	1
A	1
EE	0
AP	0

Table 1. Number of events according to ailment.

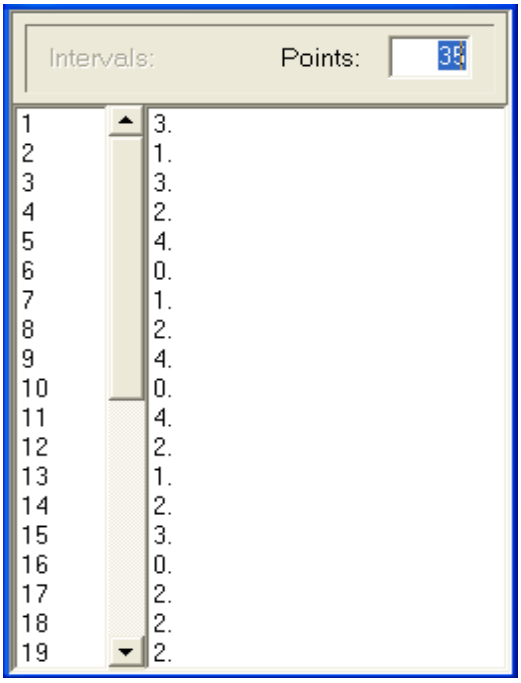

Figure 2. Example of data input for Stat:Fit.

The curve with the best fit:

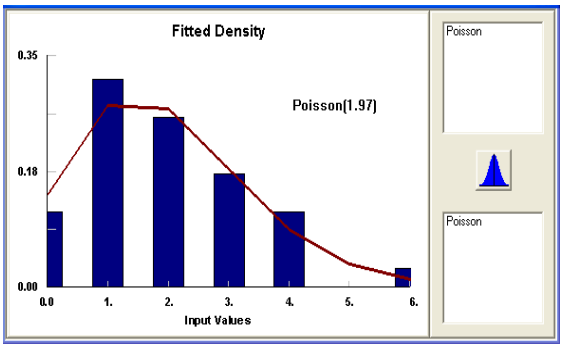

Figure 3. Discrete probability function fit.

Module	Disease	Distrubution	Parameters	
1	D	Poisson	mean	0.34
2	D	Poisson	mean	0.19
3	D	Poisson	mean	1.78
4	D	Poisson	mean	0.76
5	D	Poisson	mean	0.64
6	D	Poisson	mean	0.02
7	D	Triangular	0.32,0.62,1.98	
8	D	Poisson	mean	0.55
9	D	Triangular	0.05,0.27,1.44	
10	D	Triangular	0.01,0.6,1.00	
11	D	Poisson	mean	1.87
12	D	Poisson	mean	0.55
13	D	Poisson	mean	0.37
14	D	Poisson	mean	0.21
15	D	Poisson	mean	0.27
16	D	Poisson	mean	0.98
17	D	Poisson	mean	1.89
18	D	Poisson	mean	1.65
19	D	Poisson	mean	1.15
20	D	Triangular	0.08,0.01,1.06	
21	D	Poisson	mean	1.52
22	D	Poisson	mean	1.57
23	D	Poisson	mean	1.76
24	D	Poisson	mean	0.04
25	D	Poisson	mean	0.06
26	D	Poisson	mean	1.43

Table 2. Probability distributions for all the causal agents in one module.

4.2 Phase 2

One of the more important advantages of using a simulation model is the possibility of getting information without having to work directly in the system. In this research, the model for the APH considers each module as locations. Patients are represented by entities that enter into the module with certain probability and whose main attribute is a medical emergency.

Different scenarios are obtained from this phase that give us information about which modules need the service, the causal agent, patient characteristics and whether or not a transfer to hospital is required. The choice of hospital depends on whether or not the patient is entitled to any of the public health service schemes, such as the medical service for state employees (ISSSTE) or the medical system for private sector employees (IMSS). If neither of these is the case, he or she is transferred to a hospital that attends patients who fall outside these systems.

The simulation was done using Microsoft Excel. An example is given with five scenarios that are ready for the optimization phase.

Definition of scenarios

Table 3 shows five probable scenarios. For the sake of clarity, scenario three is described in detail and will be optimized in the Phase 3.

Scenario three shows: who asks for the APH system is people from module 26, belongs t ozone IV, causal agent five is an Appendicitis AP (a swollen appendix), the patient is a 20 years old woman, she is entitled to IMSS service and is transferred to IMSS hospital number 32.

	Scenario 1	Scenario 2	Scenario 3	Scenario 4	Scenario 5
MODULE	4	21	26	16	16
Casual Agent No.	5	11	5	4	9
Casual Agent	CN	H	AP	CA	H
Gender	F	M	M	F	F
Age	19	20	20	19	19
Insurance	NA	NA	IMSS	NA	NA
Tranfer	NO	NO	SI	NO	NO
Hospital	NA	NA	32 IMSS	NA	NA
Zone	I	III	IV	II	II

Table 3. Sample scenarios.

4.3 Phase 3

In this phase, the two problems involved with routes are solved. First the transfer of the patient to the hospital is optimized according to the scenarios given by the simulation. This optimization is done using the Dijkstra algorithm that provides the shortest route in terms of time. On the other hand the number five ambulance tour is optimized for distance, and for this case the TSP algorithms are used.

4.3.1 Optimization of the patient`s transfer time.

Transfer time is one of the more important activities for the APH system in order to lower response time. As we have already mentioned the objective is to find the shortest route in terms of time and the Dijkstra algorithm [7] allows us to find the shortest routes in a set of routes from a source vertex. In the next step, this problem is established.

Shortest Path Problem

Given a connected graph G=(V,E), a weight d:E->R^+ and a fixed vertex s in V, find the shortest path or paths from s to each vertex v in V.

Steps of the algorithm:

1. Set i=0, S_0= {u_0=s}, L(u_0)=0, and L(v)=infinity for v <> u0. If |V| = 1 then stop, otherwise go to step 2.
2. For each v in V\S_i, replace L(v) by min{L(v), L(u_i)+dv_u^i}. If L(v) is replaced, put a label (L(v), u_i) on v.
3. Find a vertex v which minimizes {L(v): v in V\S_i}, say u_i+1.
4. Let S_{i+1} = S_i cup {u_{i+1}}.
5. Replace i by i+1. If i=|V|-1 then stop, otherwise go to step 2.

For this model, vertex s is module 26 and the final vertex v is the hospital number 32. Figure 4 from the Google earth program shows a connected graph.

Figure 4. Graph with the edge lengths.

The distances between the vertex are given by the program and they represent the transfer time, so if we choose the longest distances the ambulance will take more time to arrive at the hospital. The algorithm was programmed in C language and the resulting route is given in figure 5.

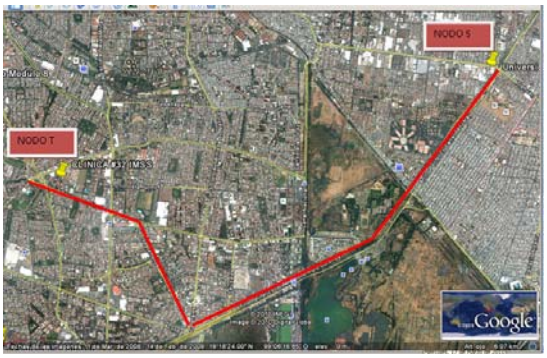

Figure 5. Resulting route.

The resulting time is 7 minutes on average with a path of 2.67 Km and considering the transfer time with the ambulance using its siren.

4.3.2 Optimization process for ambulance five.

The routing optimization for the supervision ambulance that watches the 26 modules can be established as a symmetric TSP, because the ambulance has to visit all the modules without visiting each one more than once. As it is known that the TSP is an NP-Complete problem the algorithms used to solve it are heuristics, they guarantee a good solution in the short time, but of course not an optimal one.

Consider the symmetric TSP where $c_{ji} = c_{ji} \quad \forall i, j \in V$, then the mathematical model is as follows:

$$\min Z = \sum_{i=1}^{n}\sum_{j=1}^{n} c_{ij}x_{ij}$$

$$s.a. \quad \sum_{j=1}^{n} x_{ij} = 1 \qquad \forall i = 1,...,n \quad i \neq j$$

$$\sum_{i=1}^{n} x_{ij} = 1 \qquad \forall j = 1,...,n \quad i \neq j$$

$$\sum_{i\in S}\sum_{j\in S} x_{ij} \geq 1$$

$$x_{ij} = 0,1 \qquad \forall 1 \leq i \neq j \leq n$$

Where:

c_{ij} = transfer time from site i, to site j

x_{ij} = site i is visited after visiting site j

$\min Z = \sum_{i=1}^{n}\sum_{j=1}^{n} c_{ij}x_{ij}$ = the objective function that minimizes the distance.

$\sum_{j=1}^{n} x_{ij} = 1$ It must leave from just one module

$\sum_{j=1}^{n} x_{ji} = 1$ It must enter just one module.

$\sum_{i\in S}\sum_{j\in S} x_{ij} \geq 1$ Subcircuits are not allowed

$x_{ij} = 0,1$ decision variables are binary, 1 if a module is visited, 0 otherwise.

The closest neighbor heuristic was programmed [8] to propose an initial tour that is improved with the 2-Opt technique [9]

Closest neighbor algorithm pseudocode

Start

Randomly choose a vertex j

To do $t = j$ *y* $W = V \setminus \{j\}$

While $(W \neq 0)$

To take $j \in W / c_{tj} = \min\{c_{ti} / i \in W\}$

To connect t *a* j

To do $W = W \setminus \{j\}\, t = j$

As we have already mentioned, the edge-swapping algorithm 2-Opt was used in order to improve the tour given by the closest neighbor algorithm.

2-Opt algorithm Pseudocode

Start

An initial Hamiltonian circuit is considered

For each vertex i *define a set of vertex*

$move = 1$

Label all vertex that have not been explored yet.

While (there are vertex without label)

Choose a vertex i *not explored.*

To examine all the 2-opt movements that delete 2 edges each one of them having at least one vertex $N(i)$.

If one of the examined movements shortens the length of the circuit, chose the best of them and to do $move = 1$.

Otherwise label i *as explored.*

To optimize we had to:

a) Change the geographical coordinates into Cartesian coordinates, using the terrestrial model ED50
b) Adjust the scales in order to run the algorithm.

These algorithms were programmed in Visual Basic 6, and the following results were obtained.

The optimal route consists of visiting the modules as follows: 4-2-6-3-26-20-25-13-11-19-1-22-23-18-21-12-15-14-17-9-16-10-8-5-7-4.

Applying the data to the executable program the next image is obtained that has the optimal tour visiting the 26 modules with a heuristic path of 51.7 km.

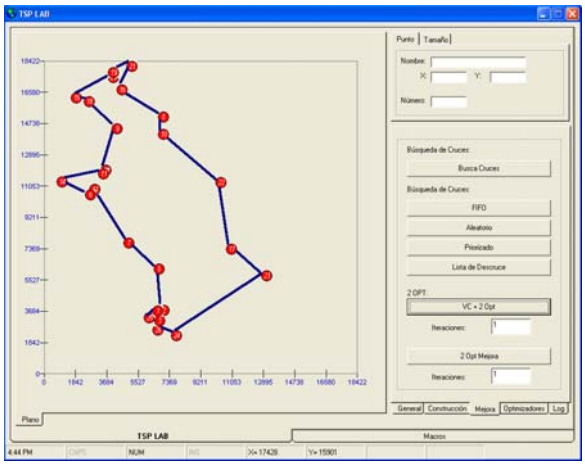

Figure 6. Optimal tour at the TSP Lab.

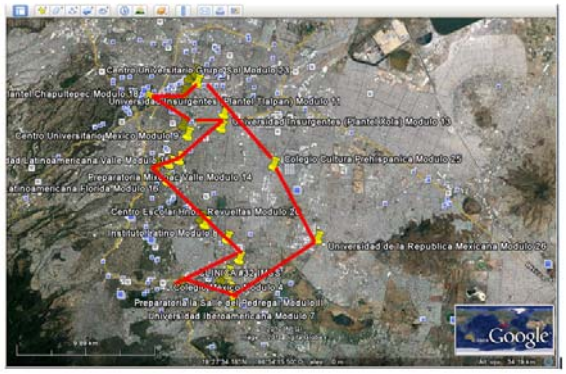

Figure 7. Route on Google Earth.

4 Conclusions

In this research we developed a simulation and worked out the transfer routes for the APH using the Dijkstra algorithm that allows us to determine the shortest route in a connected graph from a vertex s (module that requires the service) to vertex t (the hospital). With this route the response time was reduced to 8 minutes, a very important factor in the outcome for the patient. It was observed that in most cases nervous crises (CN) and stress crises are the causal agents that most often require the service.

The solution obtained by optimizing the route of ambulance five that supervises the 26 modules using an heuristic algorithm was close to the optimal obtained using an exact algorithm that requires a great deal more computational time.

Acknowledgements

We would like to thank Fernando Espinosa, Emergency Techincian level 3 from the National University of México as well to the PAPIIT Project IN100608 for their the support.

References

[1] Medina-Martínez M. Medicina de emergencia pre-hospitalaria: Su renacimiento en México. Medicina de Urgencias 2002;1(2): 57-60.

[2] (National Highway Traffic Safety Administration. Emergency Medical Services Agenda for the Future [Agenda para el futuro de los servicios médicos de emergencia]. DOT HS publicación 1996; 808: 441. US DH2.)

[3] Pinet L.M. “Atención pre-hospitalaria de urgencias en el Distrito Federal: las oportunidades del sistema de salud”. Salud Pública de México. Vol.47, No.1, enero-febrero de 2005. Pág 64-71. El texto completo en inglés de este artículo está disponible en: http://www.insp.mx/salud/47/eng
[4] Padua J.B. “Sistema médico pre-hospitalario de emergencia especializado en medicina crítica, a 10 años de operación en la ciudad de México.” Neumología y Cirugía de tórax. Vol.(4):102-108,2000.
[5] Fraga J.M. “Estatus de los técnicos en urgencias médicas en México en comparación con Estados Unidos: Se debe hacer énfasis en el entrenamiento y estado laboral.” TRAUMA, Vol.7, No.1, enero-abril, 2004. Pág.15-23.
[6]http://www.jornada.unam.mx/2009/03/30/index.php?section=sociedad&article=044n1soc
[7]http://www.alumnos.unican.es/uc900/Algoritmo.htm
[8] D. J. Rosenkrantz, R. E. Stearns, and P. M. Lewis II. An analysis of several heuristics for the traveling salesman problem. SIAM J. Comput., 6(3):563–581, 1977.
[9]G.A. Croes, "A method for solving traveling-salesman problems", Operations Research 6, 791-812. 1952.

OPTIMAL POLICIES FOR A CONGESTED URBAN NETWORK

Ciro D'Apice[(a)], Rosanna Manzo[(b)], Luigi Rarità[(c)]

[(a), (b), (c)]Department of Information Engineering and Applied Mathematics,
Via Ponte Don Melillo, 84084, Fisciano, Salerno, Italy

[(a)]dapice@diima.unisa.it, [(b)]manzo@diima.unisa.it, [(c)]lrarita@unisa.it

ABSTRACT

In this paper, we focus on car traffic simulation and optimization of a portion of the Salerno urban network in Italy. The car densities evolution is described by a fluid dynamic model. A cost functional, that measures the kinetic energy on roads, is maximized using a decentralized approach. In particular, to improve viability conditions, we apply locally optimal distribution coefficients at each 1×3 junction (one incoming road and three outgoing roads) and optimal right of way parameters at each 2×1 junctions (two incoming roads and one outgoing road). The goodness of the optimization results has been confirmed by simulations.

Keywords: conservation laws, simulation, optimization, decongestion.

1. INTRODUCTION

Urban infrastructures, as consequence of the increasing number of vehicles on road networks, are frequently characterized by a high car density, with possible birth of congestions, that cause unwished effects. The most typical ones are a reduction of cars velocities, queues formations and backward propagations, impossibility for drivers to forecast the travel times, pollution problems due to fuel consumptions. In worst cases, hard congestion levels can provoke car accidents and additional problems connected to the emergency situations management. In such a context, the problem of traffic modelling and control of cars flows assumes a great importance.

The aim of this paper is to discuss some optimization results obtained for a portion of Salerno urban network, in Italy, characterized by a heavy traffic, since it separates the centre of the city from outskirts. The topology of the network, reported in Figure 1, consists of eight roads. Each road is divided into segments, indicated by letters: Traversa Federico Romano (segments *a*, *b*, *c*), Via Parmenide (segment *d*), Via Picenza (segment *e*), Via Fiume (segment *f*), Piazza Monsignor Grasso (segment *g*), Via Trento (segments *h*, and *i*), Traversa Giuseppe Olivieri (segment *l*) and Via Davide Galdi (segment *m*). In particular, *c*, *g*, and *h* are inner road segments, while *a*, *b*, *d*, *e*, *f*, *i*, *l*, *m* external ones. Road junctions are labelled by numbers: 1 and 2 are of 2×1 type (two incoming roads and one outgoing road), 3 and 4 of 1×3 type (one incoming road and three outgoing roads).

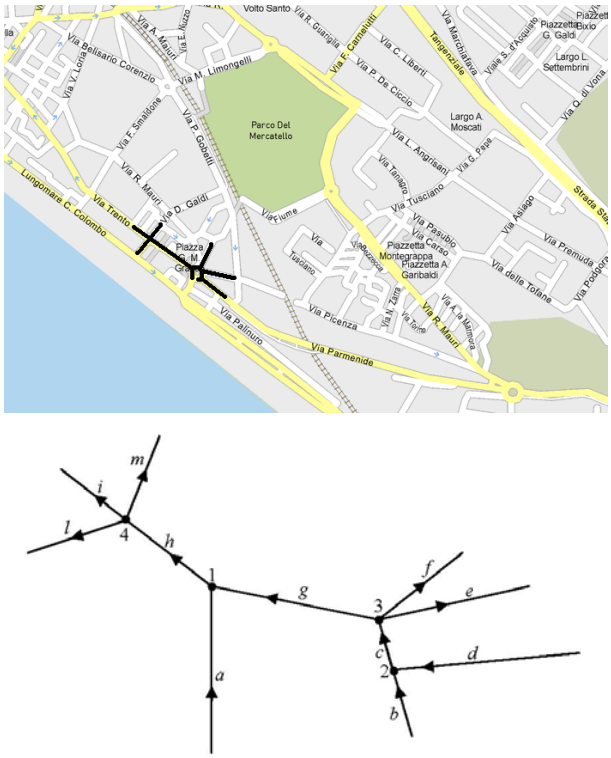

Figure 1: a portion of the real network of Salerno and its graph

For the description of traffic flows, we follow a fluid dynamic approach: the evolution of car densities is given on each road by a conservation law (Lighthill et al. 1955, Richards 1956). Dynamics at junctions is uniquely solved (Coclite et al. 2005, Garavello et al. 2006) adopting rules for the traffic distribution at nodes, the flux maximization, and the right of ways (if the number of incoming roads at nodes is greater than that of outgoing ones). Observe that the traffic evolution on the case study is captured using right of way parameters, which discriminate among priorities of incoming roads flows, in the case of 2×1 junctions, and distribution coefficients which describe the amount of traffic that, from incoming roads, is directed to outgoing ones, in the case of 1×3 junctions.

In order to improve the viability conditions, we define a cost functional, *E*, that measures the kinetic

energy of drivers on roads of the considered network. Here, we want to maximize E with respect to distribution coefficients at junctions 1×3 and right of way parameters at junctions 2×1. Some control problems have already been considered for traffic parameters of fluid dynamic models, see Gugat et al. 2005, Helbing et al. 2005 and Herty et al. 2003. In particular, in Cascone et al. 2007, Cascone et al. 2008 and Cutolo et al. 2009, different cost functionals, measuring average velocity, average travelling time, weighted and not weighted with the number of cars, flux, and kinetic energy, have been introduced and optimized for 1×2 and 2×1 junctions. Moreover, parameters of 2×2 junctions have been optimized for the fast transit of emergency vehicles in critical situations, such as accidents (Manzo et al. 2009).

The analysis of the cost functional E on complex networks is a very difficult problem, hence we follow a decentralized approach: for asymptotic E, optimal right of way parameters and distribution coefficients are found, respectively, for each 2×1 junction and each 1×3 one. For the first junctions type, we use the exact optimal solutions found in Cutolo et al. 2009; for the second one, never studied before, optimal distribution coefficients are numerically computed. The global (sub)optimal solutions for the examined network is then obtained by localization: the optimal solution is applied locally for each time at each junction.

The optimization results are tested by simulations (for numerics, see Bretti et al. 2006, Godlewsky et al. 1996, Godunov 1959, Lebacque 1996). Two different choices of distribution coefficients and right of way parameters are analyzed: optimal values given by the optimization algorithms, and random values, i.e. at the beginning of the simulation process, a random value of traffic parameters is kept constant during all simulations.

First, we consider a simple 1×3 junction to test the goodness of the numerical optimization algorithm for distribution coefficients. Then, we examine the real case study, that shows some interesting features: when random coefficients are used, hard congestions are frequent, as expected; the use of optimal traffic parameters allows a local redistribution of traffic flows at 1×3 junctions and reduction of traffic densities at 2×1 junctions, with consequent benefits in terms of roads decongestions, on the global performance of the network.

The paper is organized as follows. In Section 2, we introduce the model. Section 3 is devoted to the solutions of Riemann Problems at 2×1 and 1×3 road junctions. The cost functional, measuring the kinetic energy of cars, is presented in Section 4, where we discuss its optimization. Simulations for a single junction and for the case study are presented in Section 5. The paper ends with conclusions.

2. ROAD NETWORKS MODEL

A road network is described by a couple $(\mathtt{I},\mathtt{J})$, where $\mathtt{I}$ is the set of roads, modelled by intervals $[a_i,b_i]\subset R$, $i=1,...,N$ and $\mathtt{J}$ the set of junctions, which connect roads.

On each road, the traffic evolution is given by the conservation law (Lighthill et al. 1955, Richards 1956):

$$\rho_t + f(\rho)_x = 0, \tag{1}$$

where $\rho=\rho(t,x)\in[0,\rho_{\max}]$ is the car density, $\rho_{\max}$ is the maximal density, $f(\rho)=\rho v(\rho)$ the flux with $v(\rho)$ average velocity.

Considering $\rho_{\max}=1$ and a decreasing velocity $v(\rho)=1-\rho$, $\rho\in[0,1]$, we get the flux:

$$f(\rho)=\rho(1-\rho),\ \rho\in[0,1], \tag{2}$$

which is a strictly concave C^2 function such that $f(0)=f(1)=0$, with a unique maximum $\sigma=\frac{1}{2}$.

At junctions, traffic dynamics is found solving Riemann Problems, i.e. Cauchy Problems with a constant initial datum for each incoming and outgoing road.

Fix a junction J of $n\times m$ type (n incoming roads I_φ, $\varphi=1,...,n$, and m outgoing roads, I_ψ, $\psi=n+1,...,n+m$), and an initial datum $\rho_0=(\rho_{1,0},...,\rho_{n,0},\rho_{n+1,0},...,\rho_{n+m,0})$.

Definition. *A Riemann Solver (RS) for the junction J is a map $RS:[0,1]^n\times[0,1]^n\to[0,1]^n\times[0,1]^n$ that associates to Riemann data $\rho_0=(\rho_{\varphi,0},\rho_{\psi,0})$ at J a vector $\hat\rho=(\hat\rho_\varphi,\hat\rho_\psi)$ so that the solution on an incoming road I_φ, $\varphi=1,...,n$, is the wave $(\rho_{\varphi,0},\hat\rho_\varphi)$ and on an outgoing one I_ψ, $\psi=n+1,...,n+m$, is the wave $(\hat\rho_\psi,\rho_{\psi,0})$. We require that the following conditions hold:*

(c1) $RS(RS(\rho_0))=RS(\rho_0)$;

(c2) *on each incoming road I_φ, $\varphi=1,...,n$, the wave $(\rho_{\varphi,0},\hat\rho_\varphi)$ has negative speed, while on each outgoing road I_ψ, $\psi=n+1,...,n+m$, the wave $(\hat\rho_\psi,\rho_{\psi,0})$ has positive speed.*

If $m\geq n$, a possible RS at J can be defined by the following rules (see Coclite et al. 2005):

(A) traffic is distributed at J according to some coefficients, collected in a traffic distribution matrix $A=(\alpha_{j,i})$, $0<\alpha_{j,i}<1$, $i\in\{1,...,n\}$, $j\in\{n+1,...,n+m\}$, $\sum_{j=n+1}^{n+m}\alpha_{j,i}=1$. The $i-$th column of A indicates the percentages of traffic that, from the incoming road I_i, distribute to the outgoing roads;

(B) respecting (A), drivers maximize the flux through J.

Otherwise, if $m<n$, we need the additional rule (C), beside (A) and (B):

(C) Assume that not all cars can enter the outgoing roads, and let C be the amount that can do it. Then, p_iC cars come from the incoming road i, where $p_i\in]0,1[$ is the right of way parameter of road i, $i=1,...,n$, and $\sum_{i=1}^{n}p_i=1$.

Assuming an initial datum $\rho_0=(\rho_{\varphi,0},\rho_{\psi,0})$ and the flux function (2), the solution $\hat{\rho}$ of the RS at J is given by:

$$\hat{\rho}_\varphi\in\begin{cases}\{\rho_{\varphi,0}\}\cup\left]\tau(\rho_{\varphi,0}),1\right], & \text{if } 0\le\rho_{\varphi,0}<\frac{1}{2},\\ \left[\frac{1}{2},1\right], & \text{if } \frac{1}{2}\le\rho_{\varphi,0}\le 1,\end{cases} \tag{3}$$

$\varphi=1,...,n,$ and

$$\hat{\rho}_\psi\in\begin{cases}[0,\frac{1}{2}], & \text{if } 0\le\rho_{\psi,0}\le\frac{1}{2},\\ \{\rho_{\psi,0}\}\cup\left[0,\tau(\rho_{\psi,0})\right[, & \text{if } \frac{1}{2}<\rho_{\psi,0}\le 1,\end{cases} \tag{4}$$

$\psi=n+1,...,n+m,$

where $\tau:[0,1]\to[0,1]$ is the map such that $f(\rho)=f(\tau(\rho))$ and $\tau(\rho)\neq\rho$ if $\rho\neq\frac{1}{2}$.

3. RIEMANN SOLVERS

In this section, we consider the flux function (2) and describe the construction of Riemann Solvers at junctions, which satisfies rules (A), (B) and (C).

Fix a junction J of $n\times m$ type. We indicate the cars densities on incoming roads and outgoing ones, respectively, by:

$$\rho_\varphi(t,x)\in[0,1],\ (t,x)\in R^+\times I_\varphi,\quad \varphi=1,...,n, \tag{5}$$

$$\rho_\psi(t,x)\in[0,1],\ (t,x)\in R^+\times I_\psi,\quad \psi=n+1,...,n+m. \tag{6}$$

From condition (c2), fixing the flux function (2) and assuming $\rho_0=(\rho_{1,0},...,\rho_{n,0},\rho_{n+1,0},...,\rho_{n+m,0})$ as the initial datum of an RP at J, the maximum fluxes on roads are:

$$\gamma_\varphi^{\max}=f(\rho_{\varphi,0})H(\tfrac{1}{2}-\rho_{\varphi,0})+f(\tfrac{1}{2})H(\rho_{\varphi,0}-\tfrac{1}{2}),\quad \varphi=1,...,n, \tag{7}$$

$$\gamma_\psi^{\max}=f(\tfrac{1}{2})H(\tfrac{1}{2}-\rho_{\psi,0})+f(\rho_{\psi,0})H(\rho_{\psi,0}-\tfrac{1}{2}),\quad \psi=n+1,...,n+m, \tag{8}$$

where $H(\bullet)$ is the Heavyside function.

According to the real case study, we analyze RSs for two junction types: 2×1 and 1×3.

3.1. The case $n = 2$ and $m = 1$

Consider a junction J of 2×1 type (two incoming roads, 1 and 2, and one outgoing road, 3).

The solution to the RP at J with initial datum $\rho_0=(\rho_{1,0},\rho_{2,0},\rho_{3,0})$ is constructed in the following way. Since, from rule (B), the aim is to maximize the through traffic, we set:

$$\hat{\gamma}_3=\min\{\gamma_1^{\max}+\gamma_2^{\max},\gamma_3^{\max}\}. \tag{9}$$

Introduce the conditions:

(A1) $p\gamma_3^{\max}<\gamma_1^{\max}$;
(A2) $(1-p)\gamma_3^{\max}<\gamma_2^{\max}$.

If $\hat{\gamma}_3=\gamma_1^{\max}+\gamma_2^{\max}$, the solution to the RP is $\hat{\gamma}=(\gamma_1^{\max},\gamma_2^{\max},\gamma_1^{\max}+\gamma_2^{\max})$.

If $\hat{\gamma}_3=\gamma_3^{\max}$, we have that:

- $\hat{\gamma}=(p\gamma_3^{\max},(1-p)\gamma_3^{\max},\gamma_3^{\max})$ when A1 and A2 are both satisfied;
- $\hat{\gamma}=(\gamma_3^{\max}-\gamma_2^{\max},\gamma_2^{\max},\gamma_3^{\max})$ when A1 holds and A2 is not satisfied;
- $\hat{\gamma}=(\gamma_1^{\max},\gamma_3^{\max}-\gamma_1^{\max},\gamma_3^{\max})$ when A1 is not satisfied and A2 holds.

The case of both A1 and A2 false is not possible, since it would be $\gamma_3^{\max}>\gamma_1^{\max}+\gamma_2^{\max}$.

Once $\hat{\gamma}$ is known, from (3) and (4) we get the solution $\hat{\rho}$.

3.2. The case *n* = 1 and *m* = 3

Fix a junction *J* of 1×3 type (one incoming road, 1, and three outgoing roads, 2, 3, and 4).

For $\psi = 2,3,4$, if $\alpha_{\psi-1} \in]0,1[$, $\sum_{\psi=2}^{4} \alpha_{\psi-1} = 1$, represents the percentage of cars, which, from road 1, goes to road ψ, the fluxes solution to the RP at J are:

$$\hat{\gamma} = \left(\hat{\gamma}_1, \alpha_1\hat{\gamma}_1, \alpha_2\hat{\gamma}_1, \alpha_3\hat{\gamma}_1\right), \tag{10}$$

where

$$\hat{\gamma}_1 = \min\left\{\gamma_1^{\max}, \frac{\gamma_2^{\max}}{\alpha_1}, \frac{\gamma_3^{\max}}{\alpha_2}, \frac{\gamma_4^{\max}}{\alpha_3}\right\}, \tag{11}$$

with $\alpha_3 = 1-\alpha_1-\alpha_2$.

Notice that $\hat{\gamma}_1$ is dependent on values of α_1 and α_2. Define the variable:

$$\zeta_{i,j} = \frac{\gamma_i^{\max}}{\gamma_j^{\max}},\ i \neq j,\ i = 1,...,4,\ j = 1,...,4, \tag{12}$$

and the following sets:

$$\Omega_1 = \left\{\begin{matrix}(\alpha_1,\alpha_2)\in R^2 : \alpha_1 \le \zeta_{2,1}, \\ \alpha_2 \le \zeta_{3,1},\ \alpha_1+\alpha_2 \ge 1-\zeta_{4,1}\end{matrix}\right\}, \tag{13}$$

$$\Omega_2 = \left\{\begin{matrix}(\alpha_1,\alpha_2)\in R^2 : \alpha_1 \ge \zeta_{2,1}, \\ \alpha_2 \le \alpha_1\zeta_{3,1},\ \alpha_2 \ge 1-\alpha_1\left(1+\zeta_{4,2}\right)\end{matrix}\right\}, \tag{14}$$

$$\Omega_3 = \left\{\begin{matrix}(\alpha_1,\alpha_2)\in R^2 : \alpha_2 \ge \zeta_{3,1},\ \alpha_2 \ge \alpha_1\zeta_{3,2}, \\ \alpha_2 \ge -\alpha_1\dfrac{1}{1+\zeta_{4,3}} + \dfrac{1}{1+\zeta_{4,3}}\end{matrix}\right\}, \tag{15}$$

$$\Omega_4 = \left\{\begin{matrix}(\alpha_1,\alpha_2)\in R^2 : \alpha_1+\alpha_2 \le 1-\zeta_{4,1}, \\ \alpha_2 \le 1-\alpha_1\left(1+\zeta_{4,2}\right),\ \alpha_2 \le 1-\alpha_1\left(1+\zeta_{3,2}\right)\end{matrix}\right\}. \tag{16}$$

The open set

$$\Omega = \left\{\begin{matrix}(\alpha_1,\alpha_2)\in R^2 : 0<\alpha_1<1, \\ 0<\alpha_2<1,\ \alpha_1+\alpha_2<1\end{matrix}\right\} \tag{17}$$

is decomposed as $\Omega = \bigcup_{k=1}^{4}\Lambda_i$, where $\Lambda_1 = \Omega\cap\Omega_1$, $\Lambda_2 = \Omega\cap\Omega_2$, $\Lambda_3 = \Omega\cap\Omega_3$, and $\Lambda_4 = \Omega\cap\Omega_4$.

A unique RS is associated to each region Λ_i, $i = 1,...,4$. Precisely, we have that:

if $(\alpha_1,\alpha_2)\in\Lambda_1$, $\hat{\gamma} = \left(\gamma_1^{\max}, \alpha_1\gamma_1^{\max}, \alpha_2\gamma_1^{\max}, \alpha_3\gamma_1^{\max}\right)$,

if $(\alpha_1,\alpha_2)\in\Lambda_2$, $\hat{\gamma} = \left(\dfrac{\gamma_2^{\max}}{\alpha_1}, \gamma_2^{\max}, \alpha_2\dfrac{\gamma_2^{\max}}{\alpha_1}, \alpha_3\dfrac{\gamma_2^{\max}}{\alpha_1}\right)$,

if $(\alpha_1,\alpha_2)\in\Lambda_3$, $\hat{\gamma} = \left(\dfrac{\gamma_3^{\max}}{\alpha_2}, \alpha_1\dfrac{\gamma_3^{\max}}{\alpha_2}, \gamma_3^{\max}, \alpha_3\dfrac{\gamma_3^{\max}}{\alpha_2}\right)$,

if $(\alpha_1,\alpha_2)\in\Lambda_4$, $\hat{\gamma} = \left(\dfrac{\gamma_4^{\max}}{\alpha_3}, \alpha_1\dfrac{\gamma_4^{\max}}{\alpha_3}, \alpha_2\dfrac{\gamma_4^{\max}}{\alpha_3}, \gamma_4^{\max}\right)$.

Once $\hat{\gamma}$ is known, the solution of the RS $\hat{\rho}$ is easily found again from (3) and (4).

3.3. Examples

Consider a junction *J* of 2×1 type, an initial datum $\rho_0 = (0.25, 0.15, 0.3)$ and $p = 0.9$. From (7) and (8), the maximal fluxes on roads are:

$$\gamma_1^{\max} = 0.1875,\ \gamma_2^{\max} = 0.1275,\ \gamma_3^{\max} = 0.25. \tag{18}$$

Hence, we have that:

$$\hat{\gamma}_3 = \min\left\{\gamma_1^{\max}+\gamma_2^{\max}, \gamma_3^{\max}\right\} = 0.25,$$

and

$$\begin{aligned}\hat{\gamma} &= \left(\gamma_1^{\max}, \gamma_3^{\max}-\gamma_1^{\max}, \gamma_3^{\max}\right) = \\ &= (0.1875, 0.0625, 0.25).\end{aligned} \tag{19}$$

From (3) and (4), the density solutions are:

$$\hat{\rho} = (0.25, 0.933013, 0.5). \tag{20}$$

For a junction *J* of 1×3 type, assign the initial datum $\rho_0 = (0.4, 0.95, 0.75, 0.85)$. We get that:

$$\begin{aligned}&\gamma_1^{\max} = 0.24,\ \gamma_2^{\max} = 0.0475; \\ &\gamma_3^{\max} = 0.1875,\ \gamma_4^{\max} = 0.1275.\end{aligned} \tag{21}$$

Regions Λ_i are depicted in Figure 2. Assume $\alpha_1 = \alpha_2 = 0.3$, $(\alpha_1,\alpha_2)\in\Lambda_2$, hence:

$$\begin{aligned}\hat{\gamma} &= \left(\frac{\gamma_2^{\max}}{\alpha_1}, \gamma_2^{\max}, \alpha_2\frac{\gamma_2^{\max}}{\alpha_1}, \alpha_3\frac{\gamma_2^{\max}}{\alpha_1}\right) = \\ &= (0.1583, 0.0475, 0.0475, 0.0633).\end{aligned} \tag{22}$$

The corresponding density solutions are:

$$\hat{\rho} = (0.802, 0.95, 0.05, 0.068). \tag{23}$$

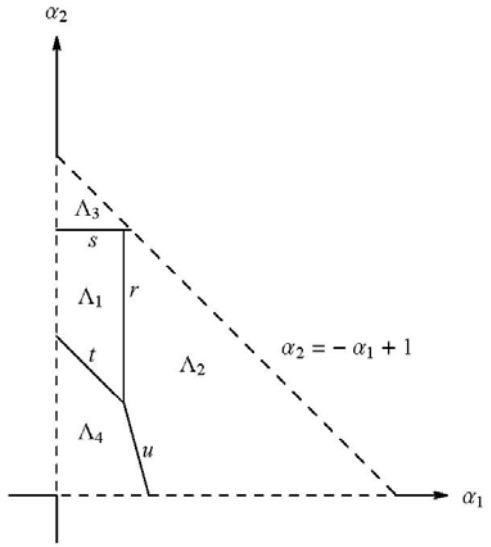

Figure 2: Decomposition of the region Ω, where $r : \alpha_1 = \zeta_{2,1}$, $s : \alpha_2 = \zeta_{3,1}$, $t : \alpha_2 = 1 - \zeta_{4,1} - \alpha_1$, and $u : \alpha_2 = 1 - \alpha_1 (1 + \zeta_{4,2})$

4. OPTIMIZATION OF ROAD NETWORKS

Consider a junction *J* of type $n \times m$ and an initial datum $\rho_0 = (\rho_{\varphi,0}, \rho_{\psi,0})$. We define the cost functional $E(t)$ as:

$$E(t) = \sum_{\varphi=1}^{n} \int_{I_\varphi} f(\rho_\varphi(t,x)) v(\rho_\varphi(t,x)) dx + \\ + \sum_{\psi=n+1}^{n+m} \int_{I_\psi} f(\rho_\psi(t,x)) v(\rho_\psi(t,x)) dx, \tag{24}$$

which measures the kinetic energy of cars travelling at the junction.

Assigned a time horizon $[0,T]$, with *T* sufficiently big, we want to maximize $\int_0^T E(t) dt$ by a suitable choice of traffic coefficients $\alpha_{\psi,\varphi} \in]0,1[$ or right of way parameters (if $n > m$) $p_\varphi \in]0,1[$, $\varphi = 1,...,n$, $\psi = n+1,...,n+m$.

4.1. The case *n* = 2 and *m* = 1

Given a junction *J* of 2×1 type, for the flux function (2) and *T* sufficiently big, the cost functional $E(T)$ assumes the form:

$$E(T) = \frac{1}{2} \sum_{i=1}^{3} \hat{\gamma}_i \left(1 - s_i \sqrt{1 - 4\hat{\gamma}_i}\right) \tag{25}$$

where, for $\varphi = 1, 2$:

$s_\varphi = -1$ if $\rho_{\varphi,0} < \frac{1}{2}$ and $\gamma_1^{\max} + \gamma_2^{\max} \le \gamma_3^{\max}$ or $\rho_{\varphi,0} < \frac{1}{2}$, $\gamma_3^{\max} < \gamma_1^{\max} + \gamma_2^{\max}$ and $p_\varphi \hat{\gamma}_3 > \gamma_\varphi^{\max}$;

$s_\varphi = +1$ if $\rho_{\varphi,0} \ge \frac{1}{2}$, or $\rho_{\varphi,0} < \frac{1}{2}$, $\gamma_3^{\max} < \gamma_1^{\max} + \gamma_2^{\max}$ and $p_\varphi \hat{\gamma}_3 < \gamma_\varphi^{\max}$;

$s_3 = -1$ if $\rho_{3,0} \le \frac{1}{2}$ or $\rho_{3,0} > \frac{1}{2}$, $\gamma_1^{\max} + \gamma_2^{\max} < \gamma_3^{\max}$;

$s_3 = +1$ if $\rho_{3,0} > \frac{1}{2}$ and $\gamma_1^{\max} + \gamma_2^{\max} \ge \gamma_3^{\max}$,

with

$$p_\varphi = \begin{cases} p, & \text{if } \varphi = 1, \\ 1 - p, & \text{if } \varphi = 2. \end{cases} \tag{26}$$

The optimal choice of right of way parameters is found analytically according to Cutolo et al. 2009 as follows.

Theorem. *Consider a junction J of* 2×1 *type. For the flux function (2) and T sufficiently big,* $E(t)$ *is optimized for the following values of p:*

1) *if* $s_1 = s_2 = +1$, *then:*
   - *(a)* $p = \frac{1}{2}$, *if* $\beta^- \le 1 \le \beta^+$ *or* $\gamma_2^{\max} = \gamma_3^{\max}$;
   - *(b)* $p \in]0, p^-]$, *if* $\beta^- \le \beta^+ \le 1$;
   - *(c)* $p \in [p^+, 1[$, *if* $1 \le \beta^- \le \beta^+$;
2) *if* $s_1 = -1 = -s_2$, *then:*
   - *(a)* $p = \frac{1}{2}$ *or* $p \in [p^+, 1[$, *if* $\beta^- \le 1 \le \beta^+$ *or* $\gamma_2^{\max} = \gamma_3^{\max}$;
   - *(b)* $p \in]0, p^-]$ *or* $p \in [p^+, 1[$, *if* $\beta^- \le \beta^+ \le 1$;
   - *(c)* $p \in [p^+, 1[$, *if* $1 \le \beta^- \le \beta^+$;
3) *if* $s_1 = +1 = -s_2$, *then:*
   - *(a)* $p = \frac{1}{2}$ *or* $p \in]0, p^-]$, *if* $\beta^- \le 1 \le \beta^+$;
   - *(b)* $p \in]0, p^-]$, *if* $\beta^- \le \beta^+ \le 1$;
   - *(c)* $p \in]0, p^-]$ *or* $p \in [p^+, 1[$, *if* $1 \le \beta^- \le \beta^+$;
   - *(d)* $p = \frac{1}{2}$ *or* $p \in [p^+, 1[$, *if* $\gamma_2^{\max} = \gamma_3^{\max}$;
4) *if* $s_1 = s_2 = -1$, *then:*

(a) $p=\frac{1}{2}$ *or* $p\in\left[p^+,1\right[$, *if* $\beta^-\le 1\le\beta^+$, *with* $\beta^-\beta^+>1$ *or* $\gamma_2^{\max}=\gamma_3^{\max}$;

(b) $p=\frac{1}{2}$ *or* $p\in\left]0,p^-\right]$, *if* $\beta^-\le 1\le\beta^+$, *with* $\beta^-\beta^+<1$;

(c) $p=\frac{1}{2}$ *or* $p\in\left]0,p^-\right]\cup\left[p^+,1\right[$, *if* $\beta^-\le 1\le\beta^+$, *with* $\beta^-\beta^+=1$;

(d) $p\in\left]0,p^-\right]$, *if* $\beta^-\le\beta^+\le 1$;

(e) $p\in\left[p^+,1\right[$, *if* $1\le\beta^-\le\beta^+$,

where

$$p^-=1-\zeta_{2,3},\ p^+=\zeta_{1,3},\qquad \beta^-=\xi_{3,1}-1,\ \beta^+=\frac{1}{\zeta_{3,2}-1}. \tag{27}$$

4.2. The case *n* = 1 and *m* = 3

For a junction *J* of 1×3 type, assuming *T* sufficiently big, the cost functional $E(T)$ becomes:

$$E(T)=\frac{\hat\gamma_1\left(1-s_1\sqrt{1-4\hat\gamma_i}\right)}{2}+ +\frac{\hat\gamma_1}{2}\sum_{\psi=2}^{4}\alpha_{\psi-1}\left(1-s_\psi\sqrt{1-4\alpha_{\psi-1}\hat\gamma_1}\right) \tag{28}$$

where

$s_1=+1$ if $\rho_{1,0}\ge\frac{1}{2}$, or $\rho_{1,0}<\frac{1}{2}$ and $\hat\gamma_1>\min\left\{\frac{\gamma_2^{\max}}{\alpha_1},\frac{\gamma_3^{\max}}{\alpha_2},\frac{\gamma_4^{\max}}{\alpha_3}\right\}$;

$s_1=-1$ if $\rho_{1,0}<\frac{1}{2}$ and $\hat\gamma_1\le\min\left\{\frac{\gamma_2^{\max}}{\alpha_1},\frac{\gamma_3^{\max}}{\alpha_2},\frac{\gamma_4^{\max}}{\alpha_3}\right\}$;

for $\psi=2,3,4$:

$s_\psi=+1$ if $\rho_{\psi,0}>\frac{1}{2}$ and, for $\psi'\ne\psi$, $\psi''\ne\psi'\ne\psi$, $\frac{\gamma_\psi^{\max}}{\alpha_{\psi-1}}\le\min\left\{\gamma_1^{\max},\frac{\gamma_{\psi'}^{\max}}{\alpha_{\psi'-1}},\frac{\gamma_{\psi''}^{\max}}{\alpha_{\psi''-1}}\right\}$;

$s_\psi=-1$ if $\rho_{\psi,0}\le\frac{1}{2}$ or, for $\psi'\ne\psi$, $\psi''\ne\psi'\ne\psi$, $\rho_{\psi,0}>\frac{1}{2}$ and $\frac{\gamma_\psi^{\max}}{\alpha_{\psi-1}}>\min\left\{\gamma_1^{\max},\frac{\gamma_{\psi'}^{\max}}{\alpha_{\psi'-1}},\frac{\gamma_{\psi''}^{\max}}{\alpha_{\psi''-1}}\right\}$.

Observe that since s_i and $\hat\gamma_i$, $i=1,...,4$, depend on the initial data, the functional (28) assumes different expressions in each region Λ_i, $i=1,...,4$, and to find the analytical optimal distribution coefficients is a huge task. Hence the values of α_1 and α_2, which optimize (28), are found numerically through the software Mathematica.

Remark. *The choice of the initial datum at J strongly influences the values of optimal* α_1 *and* α_2.

For example, if $(\alpha_1,\alpha_2)\in\Lambda_1$, $\hat\gamma_1=\gamma_1^{\max}$, *and*

$$E(T)=\frac{\gamma_1^{\max}}{2}\left(1-s_1\sqrt{1-4\gamma_1^{\max}}\right)+ +\frac{\gamma_1^{\max}}{2}\sum_{i=2}^{4}\alpha_{i-1}\left(1-s_i\sqrt{1-4\alpha_{i-1}\gamma_1^{\max}}\right) \tag{29}$$

The functional has an analytical maximum for $\bar\alpha_1=\bar\alpha_2=\frac{1}{3}$, *which is the optimal solution only if* $(\bar\alpha_1,\bar\alpha_2)\in\Lambda_1$. *Otherwise, some numerical methods are needed.*

5. SIMULATIONS

In this section, we present some simulation results in order to test the numerical algorithm for the optimization of 1×3 junctions and to analyse the effects of random and optimal choices of distribution coefficients and right of way parameters on the real case study.

5.1. Single junctions

Consider a junction of 1×3 type. Again the incoming road is labelled with 1, while outgoing roads with 2, 3, and 4. We compare different behaviours of the cost functional (28) using: optimal numerical distribution coefficients (*optimal case*); random distribution coefficients, namely parameters taken randomly when the simulation starts and then kept constant (*random case*).

The road traffic evolution is simulated using the flux function (2) in a time interval $[0,T]$, where $T=30$ min. Numerical approximations are made by the Godunov method with space step $\Delta x=0.0125$ and Δt given by the CFL condition (see Godunov 1959). We assume that, at the starting instant of simulation ($t=0$), all roads of the network are empty. Moreover, we choose the following Dirichlet boundary data: $\rho_{1,b}=0.4$, $\rho_{2,b}=0.65$, $\rho_{3,b}=0.75$, $\rho_{4,b}=0.85$.

Notice that initial conditions and boundary data are such that the network dynamics exhibits congestions on outgoing roads and optimal distribution coefficients are given by $\alpha_1=\alpha_2=\frac{1}{3}$.

Figures 3 and 4 show that, simulating the junction with optimal α_1 and α_2 values, traffic conditions are improved with respect to random cases: the optimal cost functional is higher with respect to others. In particular, although the asymptotic state is not reached (the final

T), the optimization algorithm always gives better performances than other simulation cases.

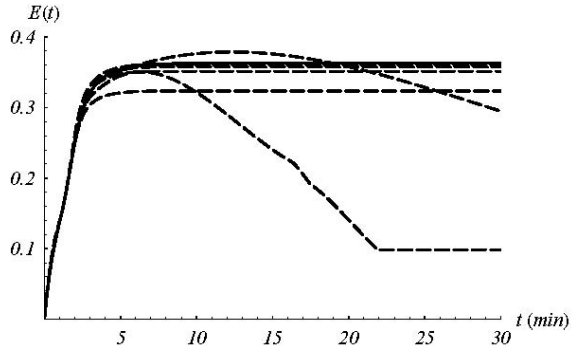

Figure 3: behaviour of $E(t)$ for optimal choice of α_1 and α_2 (solid line), and random distribution coefficients (dashed lines)

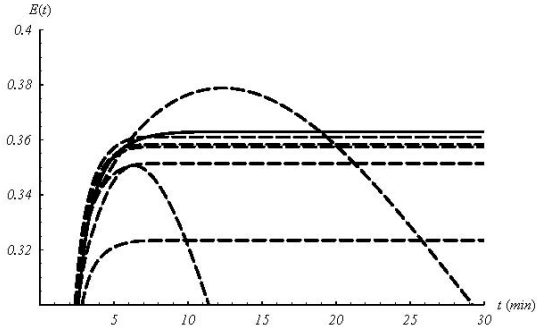

Figure 4: zoom of $E(t)$ for optimal choice of α_1 and α_2 (solid line), and random distribution coefficients (dashed lines)

5.2. Real network in Salerno

In this subsection we present some simulation results for the network of Figure 1.

The evolution of traffic flows is simulated in a time interval $[0,T]$, where $T = 100$ min, using the Godunov method with $\Delta x = 0.0125$ and $\Delta t = \Delta x / 2$. Initial conditions and boundary data for all roads are in Table 1 and are chosen so as to simulate a network with congested roads.

Again, we consider two types of simulations: optimal and random cases. Optimal right of way parameters at junctions 1 and 2 are found according to the Theorem of previous Section, while optimal distribution coefficients at junctions 3 and 4 are computed using a numerical algorithm.

Table 1: Initial conditions and boundary data for roads of the network

Road	Initial condition	Boundary data
a	0	0.3
b	0	0.3
c	0.3	/
d	0	0.4
e	0.6	0.4
f	0.7	0.9
g	0.3	/
h	0.3	/
i	0.65	0.9
l	0.75	0.9
m	0.85	0.9

In Figures 5 and 6, we report the behaviour of the cost functional $E(t)$, defined as the sum of the kinetic energy on all network roads. Notice that random simulation curves (dashed lines) are always lower than the optimal one (continuous line). Such phenomenon is easy justified: when, at road junctions of 1×3 and 2×1 types, optimal distribution coefficients and right of way parameters are, respectively, used, traffic flows are redistributed, hence allowing a congestion reduction.

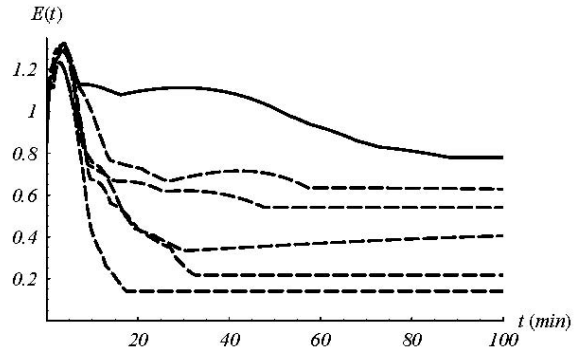

Figure 5: $E(t)$ for optimal choice of distribution coefficients (solid line) and random parameters (dashed lines)

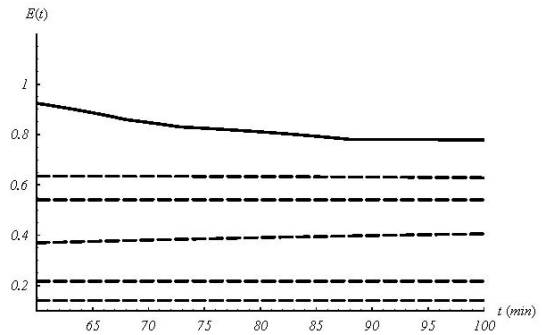

Figure 6: zoom of $E(t)$; optimal choice of distribution coefficients (solid line); random parameters (dashed lines)

6. CONCLUSIONS

In this paper, we have studied traffic flows on a portion of the Salerno urban network, in Italy.

Exact solutions for optimal right of way parameters in case of 2×1 junctions, and numerical approximations for optimal distribution coefficients in case of 1×3 junctions have been used in order to improve the viability conditions. In particular, the optimization of distribution coefficients for 1×3 junctions has been treated here for the first time.

The goodness of the optimization results has been confirmed by simulations, concluding that real benefits on traffic performances are possible.

REFERENCES

Bretti, G., Natalini, R., Piccoli, B., 2006. Numerical approximations of a traffic flow model on networks, *Networks and Heterogeneous Media* 1, 57-84.

Cascone, A., D'Apice, C., Piccoli, B., Rarità, L., 2007. Optimization of traffic on road networks. *Mathematical Models and Methods in Applied Sciences*, 17 (10), 1587-1617.

Cascone, A., D'Apice, C., Piccoli, B., Rarità, L., 2008. Circulation of traffic in congested urban areas. *Communication in Mathematical Sciences*, 6 (3), 765-784.

Coclite, G., Garavello, M., Piccoli, B., 2005. Traffic Flow on Road Networks, *SIAM Journal on Mathematical Analysis* 36, 1862-1886.

Cutolo, A., D'Apice, C., Manzo, R., 2009. Traffic optimization at junctions to improve vehicular flows, *Preprint DIIMA 57*.

Garavello, M., Piccoli, B., 2006. Traffic flow on networks, *Applied Math Series*, Vol. 1, American Institute of Mathematical Sciences.

Godlewsky, E., Raviart P., 1996. Numerical Approximation of Hyperbolic Systems of Conservation Laws, *Springer Verlag*, Heidelberg.

Godunov, S. K., 1959. A finite difference method for the numerical computation of discontinuous solutions of the equations of fluid dynamics, *Mat. Sb*. 47, 271-290.

Gugat, M., Herty, K., Klar, A., Leugeuring, G., 2005. Optimal Control for Traffic Flow Networks, *Journal of Optimization Theory and Applications* 126, 589-616.

Helbing, D., Lammer, S., Lebacque, J. P., 2005. Self-organized control of irregular or perturbed network traffic, *Optimal Control and Dynamic Games*, C. Deissenberg and R. F. Hartl eds., Springer, Dordrecht, 239-274.

Herty, M., Klar, A., 2003. Modelling, Simulation and Optimization of Traffic Flow Networks, *SIAM J. Sci. Comp.* 25, 1066-1087.

Lebacque, J. P., 1996. The Godunov scheme and what it means for first order traffic flow models, *Proceedings of the Internaional symposium on transportation and traffic theory* 13, Lyon, Pergamon Press, Oxford, 647-677.

Lighthill, M. J., Whitham, G. B., 1955. On kinetic waves. II. Theory of Traffic Flows on Long Crowded Roads, *Proc. Roy. Soc. London Ser. A.*, 229, 317-345.

Manzo, R., Piccoli, B., Rarità, L., 2009. Optimal distribution of traffic flows at junctions in emergency cases. *Submitted to European Journal of Applied Mathematics.*

Richards, P. I., 1956. Shock Wave on the Highways, *Oper. Res.*, 4, 42-51.

AUTHORS BIOGRAPHY

CIRO D'APICE was born in Castellammare di Stabia, Italy and obtained PhD degrees in Mathematics in 1996. He is associate professor in Mathematical Analysis at the Department of Information Engineering and Applied Mathematics of the University of Salerno. He is author of approximately 140 publications, with more than 80 journal papers about homogenization and optimal control; conservation laws models for vehicular traffic, telecommunications and supply chains; spatial behaviour for dynamic problems; queueing systems and networks.
His e-mail address is dapice@diima.unisa.it.

ROSANNA MANZO was born in Polla, Salerno, Italy. She graduated cum laude in Mathematics in 1996 and obtained PhD in Information Engineering in 2007 at the University of Salerno. She is a researcher in Mathematical Analysis at the Department of Information Engineering and Applied Mathematics of the University of Salerno. Her research areas include fluid – dynamic models for traffic flows on road, telecommunication and supply networks, optimal control, queueing theory, self – similar processes, computer aided learning. She is author of about 35 papers appeared on international journals and many publications on proceedings.
Her e-mail address is manzo@diima.unisa.it.

LUIGI RARITÁ was born in Salerno, Italy, in 1981. He graduated cum laude in Electronic Engineering in 2004, with a thesis on mathematical models for telecommunication networks, in particular tandem queueing networks with negative customers and blocking. He obtained PhD in Information Engineering in 2008 at the University of Salerno discussing a thesis about control problems for flows on networks. He is actually a research assistant at the University of Salerno. His scientific interests are about numerical schemes and optimization techniques for fluid – dynamic models, and queueing theory.
His e-mail address is lrarita@unisa.it.

This work is partially supported by MIUR-FIRB Integrated System for Emergency (InSyEme) project under the grant RBIP063BPH.

Simulation Model for Evaluating Scenarios in Painting Tasks Scheduling in the Automotive Industry

Idalia Flores de la Mota [(a)] Luis Altamirano Yepez [(b)]
(a) Secretaría de Posgrado e Investigación, UNAM
(b) División de estudios de Posgrado Facultad de Ingeniería, UNAM
idalia@servidor.unam.mx (a) altamirano@dctrl.fi-b.unam.mx (b)

Keywords: Simulation, Scheduling, Automotive Industry.

Abstract

The aim of this paper is to show some of the benefits of using simulation to analyze manufacturing processes, particularly those related to tasks scheduling in a paint plant in the automotive industry. Simulation can provide information about a manufacturing process because a discrete event simulation model can capture both the variability and interdependencies of system elements. We can identify four levels of planning activities: 1. Aggregate Sales and Operations Planning, 2. Aggregate Operations Planning, 3. Master production Plan and, 4. Task Scheduling.
It is in this fourth level where priority rules are used in tasks sequencing.
This paper shows a case study about an important car manufacturer's Paint Shop. We built a model in Promodel 6.0 in order to test different priority rules in scheduling painting tasks.

I. Introduction

This work is based on Miquel Angel Piera's team work about the use of simulation tools applied to manufacturing [1]. The present paper takes up a case, emphasizing the Paint Shop and built a simulation model in Promodel 6.0. The main objective is to analyze how different rules of scheduling painting tasks impact the entire system performance.

Section two shows some aspects that justify the use of simulation instead of using optimization models. In section three we will see the four levels of planning activities:

- Aggregate Sales and Operations Planning.
- Aggregate Operations Planning
- The master Production Plan
- Tasks Scheduling.

Section four describes the general operation of the plant and the fifth section describes the construction of the simulation model.

2. Simulation And Optimization

Traditional Operations Research (OR) techniques use mathematical models to solve problems involving simple or moderately complex relationships. These techniques solve deterministic and mathematical programming models, routing problems or network problems. They also solve probabilistic models such as queuing theory and decision trees. The Operations Research techniques generate quantitative results quickly without using trial and error methods. These techniques can be divided into two types: prescriptive and descriptive.

OR prescriptive techniques provide an optimal solution to a problem. These techniques include both linear and dynamic programming. They are generally applied when the only objective is to maximize or minimize a cost function.
If a system requires considering secondary objectives related to maximization or minimization, OR techniques can handle it, but the mathematical difficulty increases. Additionally, these techniques do not allow the use of random variables.

Descriptive techniques such as queuing theory provide a good estimate for basic problems like finding the expected average number of entities in a queue, or the average waiting time in it. However, when the system becomes moderately complex, the model becomes very complex and mathematically intractable. In contrast, simulation provides estimates very close to the optimal figures for complex systems, and the simulation's statistical results are not limited to one or two metrics since they provide information on all performance measures over time. Simulation is a way to reproduce the conditions of a system using a model to study its dynamics to prove or predict their behavior.

Due to the fact that simulation runs in a compressed time window, weeks of operation can be simulated in minutes or even seconds. The features that make simulation a powerful tool in decision making can be summarized as follows:

- It captures system interdependencies.
- It handles Model variability.
- It is versatile enough to model any system.
- Shows the behavior over time.
- Simulation is less costly, time-consuming and invasive than experimenting directly on the studied system.
- It provides information of various performance measures.
- Simulation is visually attractive.
- Simulation runs in compressed time, real-time or even expanded time windows.
- It captures deep details of a design.

Simulation models create a system that acts as a substitute for the real system and the gained knowledge can be transferred back to the system.

Simulation has proven to be very effective in dealing with complex problems around manufacturing decisions. Since companies make vertical and horizontal integration aiming to improve the broad performance of the entire value chain, simulation is an essential tool for effective production planning and distribution processes.

Simulation in manufacturing systems covers a wide range of applications in different time horizons, including:

- Cells Administration (seconds).
- Task Scheduling (Hours).
- Load in Resources Studies (days).
- Production Planning (Weeks).
- Process Change Studies (Months).
- System Configuration (1-2 years).
- Technology Assessment (1-2 years).

If simulation is used to make decisions in the short term, it usually requires models to be more detailed and closer to actual operations, than those used to make long term decisions. Sometimes the model is an exact replica of the real system and it even reports the current system status; for example, control applications in real time and detailed planning systems of production. If simulation is used for making long term decisions, the models may or may not be similar to current operations. The model should not be very detailed because the high-level decisions about the future are made based upon fuzzy and uncertain data.

3. Task Scheduling

Scheduling operations is an activity that takes place as a result of alignment with the supply chain's planning.

The sales and operations planning processes culminate in a high-level meeting where key decisions are made for the medium term. The ultimate goal is to reach an agreement between the various departments about the best course of action to achieve an optimal balance between supply (Capacity) and demand. The idea is to align the operational plan with the business plan.

This balance must occur both at the aggregate level and at the single product level, so the goal in planning is to generate an aggregate operations plan for the areas of Manufacturing, Logistics and Services.

The Aggregated Operations Plan aims to establish production rates by product groups or another category in the medium term. The Master Production Plan comes from the Aggregated Operation Plan. The main purpose of the aggregate plan is to specify the optimal combination of production rate level of the workforce and inventory.
Aggregate Plan's shape varies with each company. In some places it is a formal report containing objectives and planning statements; in other companies, especially the small ones, the owner can perform simple calculations of the workforce needed.

The next level of the planning process is the Master Production Plan. This is a program containing times and specified tasks. It shows the detail of how and when each piece must be worked out. The aggregate plan for a manufacturing company should specify the total volume of a particular product that will produce the next month or quarter. The master plan takes the next step and identifies the features of the product such as its quality,

color, size and style. The master plan also settles from period to period (usually on a weekly basis) how many particular products are needed and when.

The process of determining the production order in a machine or in a workplace is called sequencing or priorities sequencing. Priority rules are used for sequencing a task. Rules can be very simple and can be used for ordering only one figure like processing time, term date or arrival time. Other rules, although simple, require more data, usually to get an indicator, as the rule of the smaller time margin and the critical ratio rule.

Rule	DESCRIPTION
1. FCFS	*First-come, first-served*. Orders run in the order they arrive.
2. SOT	*Shortest operating time.* Run the job with the shortest completion time first. Often this rule is combined with a lateness rule to prevent jobs with longer times being delayed too long.
3. EDD	E*arliest due date first.* Run the job with the earliest due date first.
4. STR	S*lack time remaining*. This is calculated as the time remaining before the due date minus the processing time remaining. Orders with the shortest STR are run first.
5. STR/OP	S*lack time remaining per operation.* Orders with the shortest STR per number of operations are run first.
6. CR	*Critical rate.* This is calculated as the difference between the due date and the current date divided by the number of work days remaining. Orders with the smallest CR are run first.
7. LCFS	*Last-come, first-served.* This rule occurs frequently by default. As orders arrive, they are placed on the top of stack. The operator usually picks up the order on top to run first.
8. RANDOM	*Randm order or Whim*. The supervisors or operators usually select whichever job they feel like running.

Table 1. Priority Rules.

The following performance measures are used to evaluate priority rules:

- Due dates of customers or subsequent operations.
- Flow time.
- Work in process inventory.
- Idle time of machinery and labor.

4. Case Description

For this article's purposes the car manufacturing company's name was omitted. Also, no confidential information will be revealed.

Like many automobile manufacturing facilities, the plant begin studied is divided into three main plants: Body Shop, Paint Shop and Assembly (Trim & Chassis). There, four car models (A,B,C & D) are built.

4.1 Body Shop

In this section the main structure of the automobile is assembled. This process is achieved using three assembly lines as shown in Figure 1.

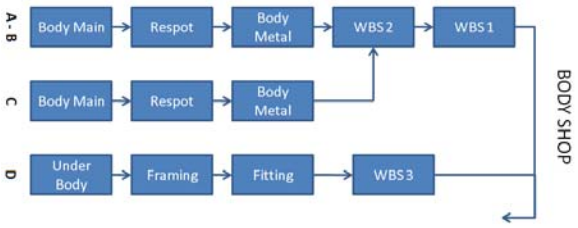

Figure 1. Body assembly lines.

There is one line for the D model and another line for C. A and B models, which are built in a shared single line.

To determine each of the sections that compound the Body Shop lines, different terminology is used. The equivalent processes are:

- Body main: Under body
- Respot: Framing
- Body metal: Fitting

In the Main and Under Body stations the bottom frame of vehicles is mounted. In

Respot or Framing stations the other structural parts are assembled. After having the entire skeleton ready, the vehicles pass through metal lines or Fitting in order to make little adjustments if needed. In this section, once the vehicle already has all its main parts, an ID is added to it in order to recognize the vehicle in the subsequent stations

Finally, vehicles go to stores WBS. In the case of the A model line, all vehicles are directed to WBS3, for the ET and HM lines, there are two stores.

WBS1, WBS2 and WBS3, represent the junction between Body Shop and Paint Shop. The first plant is responsible for filling the second plant buffers in order to pull vehicles along the marked sequence.

4.2 Paint Shop

The Paint Shop includes the paint plants P1 and P2. Both are located next to each other. This is important because part of the production line is worked out exclusively in P2. All vehicles at the beginning of the process must first pass through P2. Afterwards, some continue to P2, and the rest will be worked out in P1.

Figure 2 shows the flow of the vehicles in the Paint Shop. In P2 the initial phase of the painting process is located: the common P2. In this area a degreasing and washing process is made to the car body. Other various treatments are performed here too. All these processes are essential to each of the models produced at the plant. However, because they can be completed with some speed, they hardly become a bottleneck. All four models pass through the P2 Common.

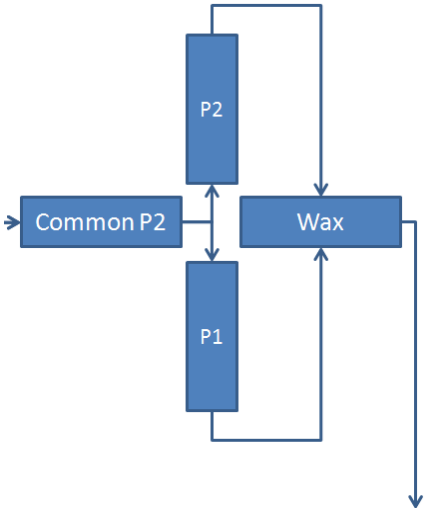

Figure 2. Paint Shop lines.

Once this initial process is made, some models are diverted to the plant P1 and others remain to finish the painting process in the plant P2. The A model must necessarily be diverted to the plant P1 because of its large volume. The other models produced can be painted in either of the two plants. However, the policy is to prioritize the work load of the plant P2. Once they reach the end of the processes P1 and P2, all vehicles are moved to the wax section. Finally the painted cars are transported to PBS stores. In this work we have used seven different colors: White, Gray, Silver, Red, Blue, Sandstone and Brown in order to

4.3 Trim & Chassis

The Paint Shop works two shifts a day. During this time they feed PBS stores for Trim & Chassis Shop. Paint and assembly lines have different speeds. Trim & Chassis Shop is working in parallel with all produced models and does not represent a bottleneck. For this reason, the Paint Shop's main objective is to produce a particular volume of vehicles for each of the models. This volume varies according to demand.

Figure 3 shows the Trim & Chassis Shop flow. There are three parallel lines where each body internal (Trim) and external (Chassis) parts are added. In this shop the lower body, the engine and main body are added.

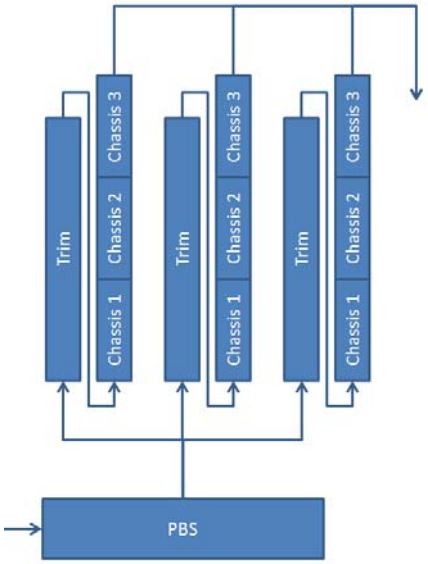

Figure 3. Trim & Chassis Shop

5. Model Design

In order to build a computer simulation model to describe the state and changes of the physical model, it is necessary to use some of the following elements: Locations, Entities, Routes, Resources, Processes, Arrivals and Variables.

Locations. They are fixed points in the system. They represent workstations or centers of attention. Its capacity is defined as the number of entities that can be addressed or processed.

Entities. They represent material, customers, documents or anything else that requires system resources to process. We have considered the four models A, B, C and D.

Routes. They represent paths from one location to another. They may represent roads, rows, or transport lines of material. The movement can be modeled in terms of time or in terms of speed and distance. Figure 4 shows the construction of the model.

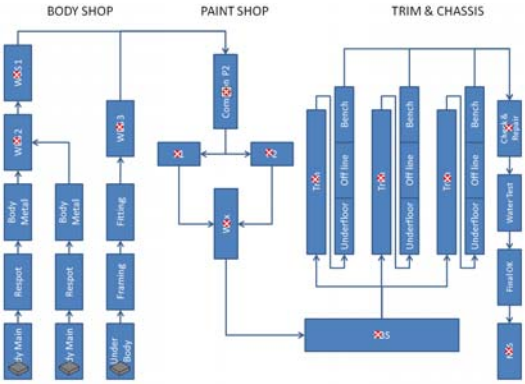

Figure 4. Model Construction.

Arrivals. The arrivals represent the first time an entity arrives to the system. In a simulation model, the time between arrivals is usually defined with a probability.

Processes. The process is defined for each entity arrival at each location, and may represent an operation or simply a timeout. In a computer simulation model, certain logic can be programmed to define the process.

Variables. Variables are reported as numerical values with relevant interest to be measured during the simulation's execution. In the studied model variables are used exclusively for counting the number of entities in a given location at a given time. Figure 5 shows an image with the model running a scenario.

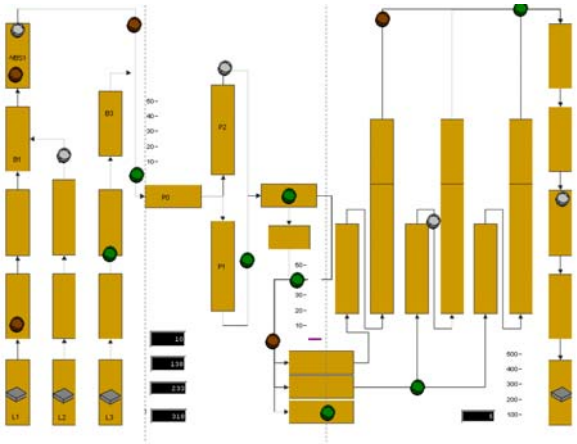

Figure 5. Model running a scenario.

6. Conclusions

Using the gathered information and following general recommendations in considering which location to simulate, the Body Shop was modeled as a processing entities group. The Paint Shop is the most important location to be modeled. Common P2 receives entities and here we can study different priority rules. Once the rules are implemented, each entity continues its process towards Wax and Trim & Chassis Shop.

To model the priority rules, the next factors were used:

- Manufacturing Lead Time was used to measure the total running time.
- Setup Color Change Time was used as remaining operation criterion.
- All operations outside the Paint Shop are the same.
- All demand must be manufactured in the same shift.

Based on the above restriction, the eight rules can be summarized in table 2:

Rule	DESCRIPTION
1. FCFS	*First-come, first-served.*
2. SOT	*Shortest operating time.*
7. LCFS	*Last-come, first-served.*
8. RANDOM	*Randm order or Whim.*

Table 2. Summarized Priority Rules.

Running a scenario for each of the 4 priority rules, we obtained the following table:

RULE	MANUFACTURING LEAD TIME
1. FCFS	7h 45 m
2. SOT	7h 13 m
7. LCFS	8h 07 m
8. RANDOM	8h 23 m

Table 3. Manufacturing Lead Time.

There we can see that the shortest operation time rule gives the best result when compared to other rules in this case.

Future Work

Currently this work is on the process of being improved by adding probability distributions and assignation rules to provide a better resemblance and description of the original system.

Acknowledgments: To the PAPIIT project IN100608, DGAPA; UNAM.

7. References

M. A. Piera, T. Guasch, V. Porcar, M. Bacardit. 2005 “Constraint Satisfaction in the Automotive Industry: A colored Petri Net Simulation Model Approach”.

G. Merkuryeva, N. Shires. 2009. “Manufacturing System Planning and Scheduling”.

Harrel. Ghosh. Bowden. 2002. *Simulation Using Promodel*. Second Edition, McGraw Hill.

M. A. Piera, A. Guasch et al. 2005 *Modelado y Simulación*. Alfa Omega.

R. B. Chase. F.R. Jacobs. N. J. Aquilano.2009. *Administración de Operaciones*, Duodécima edición, Mc Graw Hill.

METHODOLOGY FOR THE DETECTION AND PREVENTION OF FAILURES IN INDUSTRIAL PRODUCTION EQUIPMENT

Wellens A.[(a)], Esquivel J.[(b)]

[(a)]Facultad de Ingeniería, UNAM-MEXICO
[(b)] Dínamo Value Partners, MEXICO

[(a)]wann@unam.mx, [(b)] esquivelvillar@hotmail.com

ABSTRACT
This paper constitutes a methodological proposal in the area of industrial maintenance. It combines maintenance philosophies and techniques, elements of statistical process control and statistical data analysis to obtain two methodologies: the first one for the detection of chronic failures in industrial equipment and the second one to prevent sporadic failures in the same equipment.

Both methodologies are intended to be applied to production processes, as data acquisition is relatively easier than in service processes. However, they can be easily adapted to service processes as well. Their goal is to increase production equipment availability in order to improve product quality and quantity, increasing in this way the competitiveness of the company in the market.

The methodologies were applied to a cosmetics production facility with favorable results.

Keywords: failure prevention, reliability

1. INTRODUCTION

At present, the perception of management on industrial maintenance has shifted from considering it a cost to valuating the investment in maintenance of assets as a business opportunity.

The strict quality norms that have to be satisfied and the competitiveness between industries of the same type have forced the management to stop considering the maintenance department as a "fire department" to solve problems, and change its perception to a strategic unit that contributes to assure the facilities production level, including higher product quantities and qualities at lower costs.

Quality philosophies as Lean Manufacturing or TQM would have no sense in a company where the machinery presents a poor performance.

Maintenance costs are a fundamental part of the added value of whatever facility or business, and should be lowered as much as possible without failing to guarantee the availability of the productive actives. To stay competitive, facilities should consider maintenance as the fundamental pillar of management, and techniques should be developed for detection, control and execution of activities that guarantee an appropriate performance of production machinery.

The methodology for the detection of chronic failures in industrial equipment emphasizes especially on detection, as this is the main problem in solving chronic failures. Once the root cause is detected, the solution to be applied is immediate. No special analysis is needed. Although the methodology was designed for industrial equipment, it can be applied in the services area with some adaptations.

The second methodology, used to prevent sporadic failures is an alternative proposal of proactive maintenance, as it intends to identify the failure before it occurs and thus would interfere with the productive process. An inconvenience is that the major part of existing facilities (at least in Mexico) lack to have failure statistics. Some indicators, as for example mean time between failures (MTBF) should be measured as soon as the methodology is being applied to improve the results with gained experience.

2. PROPOSED METHODOLOGY

To be efficient, a productive system should achieve the equipment to operate effectively during the major time span possible (Cuatrecasas 2002). To obtain this, it is necessary to discover and eliminate factors that diminish the ideal operating conditions of the equipment. In general, six types of losses can be distinguished and these can be divided in three categories, according to the effect they have on the output of the production equipment (Figure 1). From the maintenance point of view, failures are the type of loss that has the biggest impact on the production process, as they can originate the other types of losses, such as quality defects, reduced velocity, process stops or breakdowns.

Advanced production systems pretend to optimize their efficiency through the elimination of wastes, which implies the use of the minimum possible quantity of all resources and to produce only the necessary items. Maintenance, specifically the total productive maintenance methodology, intends to use the same basic principle to optimize the process performance and output, eliminating the losses in production equipment.

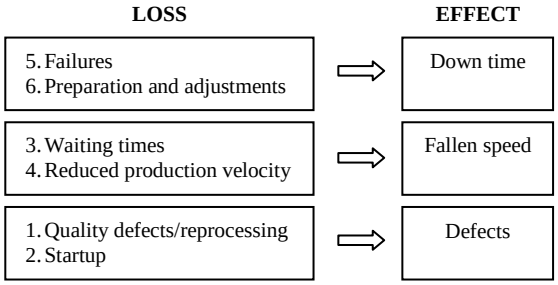

Figure 1. Types of losses and their effect on production equipment.

The aim of the proposed methodology is to reduce failures in industrial equipment. These can be of two different types:

- Chronic or continuous failures, which do not interrupt the operation of the equipment, although they reduce its performance and therefore the product quality.
- Sporadic failures, where the equipment suddenly looses one of its fundamental functions and stops operating. These failures occur unexpectedly and have to be solved urgently.

2.1. Detection of chronic failures

An appropriate diagnostic of a failure corresponds to 80% of the solution and its solution depends directly on its correct detection. An important part of chronic failures start as sporadic failures that were not solved adequately or due to the fact that they are of minor importance, were "solved" with provisional solutions, waiting for production stops or time availability to be able to propose a final solution. The main problem with this kind of solutions is that, generally, these provisional solutions will remain eternally due to the lack of time to fix them in an appropriate way, and the deficient functioning of the equipment is seen at the end as a "normal" and expected functioning.

The aim of the detection of chronic failures is to eliminate them, or, if this is not possible, to minimize their effects in the performance of the equipment. Table 1 shows the losses on which the detection of chronic failures has an effect and the corresponding aim to pursue:

Table 1: Aims of the chronic failure detection.

LOSS	AIM
Failures	Eliminate
Short stops	Reduce as much as possible
Reduced velocity	Eliminate
Quality defects	Eliminate

The following scheme summarizes the proposed methodology for the detection of chronic failures:

1. Give maintenance to the assets
2. Leave all assets functioning in normal operation
3. If an opportunity of improvement is detected (product error), then:
   - 3.1 Define the problem to solve
   - 3.2 Identify the main cause of the problem
   - 3.3 Apply the corresponding solution
   - 3.4 Compare the new performance
   - 3.5 If the new performance is better, then:
     - 3.5.1 Standardize the improvement as best practice for similar equipment
     - 3.5.2 Repeat from step 1
   - 3.6 If the new performance is not better, then:
     - 3.6.1 Start again from step 3.2, as the identified cause was not the main cause or the only one
   - 3.7 Repeat from step 1

Techniques and or methodologies as flow diagrams, checklists, histograms, Pareto diagrams and pyramids, cause-effect diagrams, dispersion diagrams, control charts, FMEA, hypothesis testing, fault tree analysis and process capacity are used to carry out the previous steps.

2.2. Prevention of sporadic failures

The prevention of sporadic failures implicates the creation of a pessimist scenario, trying this not to occur. It makes use of a *what-if* analysis considering all possible alterations the process can have, identifying its consequences.

Taking the product as the main indicator of the equipment's health, its quality characteristics can be used to deduce where the equipment is failing to produce the desired defect.

The proposed methodology to prevent sporadic failures is similar to the previous one, however, considering as second step the identification of the potential failure modes of the equipment, and looking afterwards for the main cause of each potential failure. Figure 2 indicates a flow diagram for this detection methodology.

Its main aim is to identify the potential failure modes that need to be monitored and eliminate their causes to minimize their effects. The following table shows the losses on which the detection of chronic failures has an effect as well as its corresponding aim:

Table 2: Aims of the sporadic failure detection.

LOSS	AIM
Failures	Eliminate
Long stops	Reduce as much as possible

As in the chronic failure methodology, it is important to emphasize the first step, corresponding to general maintenance. A cleaning and lubrication plan will detect minor failures, equipment ware out, bad fitting and possible fractures among others, which should be corrected before starting the prevention of sporadic failures.

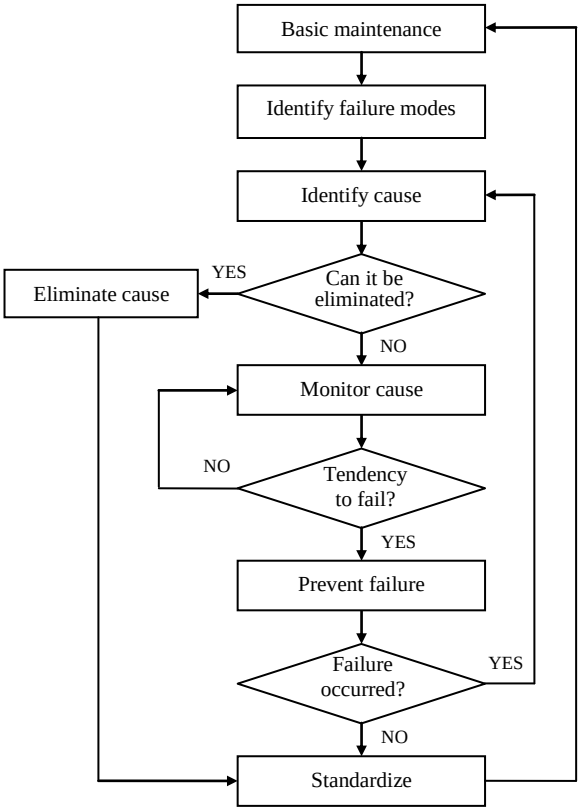

Figure 2. Proposed methodology for the prevention of sporadic failures.

3. CASE STUDY

The proposed methodology was applied at the maintenance department of a company that produces cosmetics and is characterized by direct sells per catalogue. The seller offers products which, in case of convincing a client, will be delivered at the end of the campaign, for instance two weeks. This characteristic implies that the filling equipment is changing continuously its format, and, still more important, that the products to be produced are already sold. The latter characteristic is the leading principle of the company, and demands a high availability of the production lines to avoid late delivery, money refunding and loss of clients.

To prove the effectiveness of the presented methodologies, they were applied to the production lines in charge of filling compressive tubes. Both chronic failures, on one hand in good/bad situations and on the other hand implying numerical variables, and sporadic failures were considered.

The production line for creams in cosmetic packaging tubes is composed of three workstations: manual alimentation of the tube by an operator, filling machine and transport band for inspection and packing (Figure 3).

Figure 4 shows the nomenclature of the elements of interest in cosmetic packaging tubes.

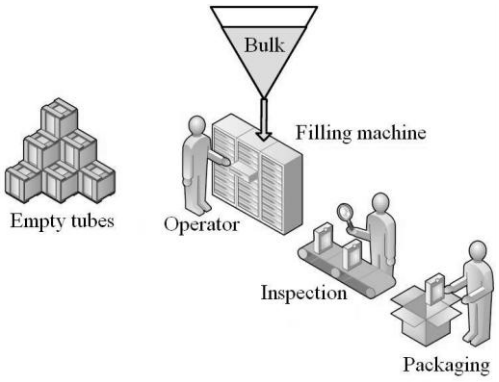

Figure 3: Tubes production line.

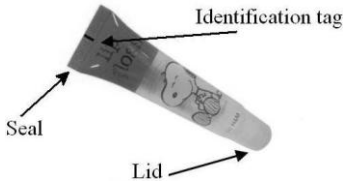

Figure 4: Cosmetic tube nomenclature.

As a first step, basic maintenance was carried out, including cleaning and lubrication of the filling machine and transport band, tightening of screws in mechanical and electrical devices and changing or repairing pieces that are in bad condition. As soon as the production line was working in normal operation, a check list was applied to a run where 5131 tubes were packed: 405 rejected pieces were detected, corresponding to a 7.9% of the run. The previous process identified both chronic and sporadic failures.

3.1. Detection of chronic failures in tube filling

The check list provided information to identify the most recurrent defect in the tubes at the end of the production line. Table 3 presents the observed defects.

Table 3: Observed defects in the production run.

Defect type	Frequency	
	Absolute	Relative
Seal	203	50.12%
Bad tag centering	116	28.64%
Product leaks	45	11.11%
Weight	41	10.13%
Total	**405**	**100.00%**

The most recurrent defect was a defective seal; this defect can be subdivided in other categories, for which the condensed information is presented in table 4.

Table 4: Observed defects in the tube seal.

Defect type in seal	Frequency	
	Absolute	Relative
Burned	126	62.07%
Bad cut	41	20.20%
With bubbles	26	12.80%
Defective	10	4.93%
Total	**203**	**100.00%**

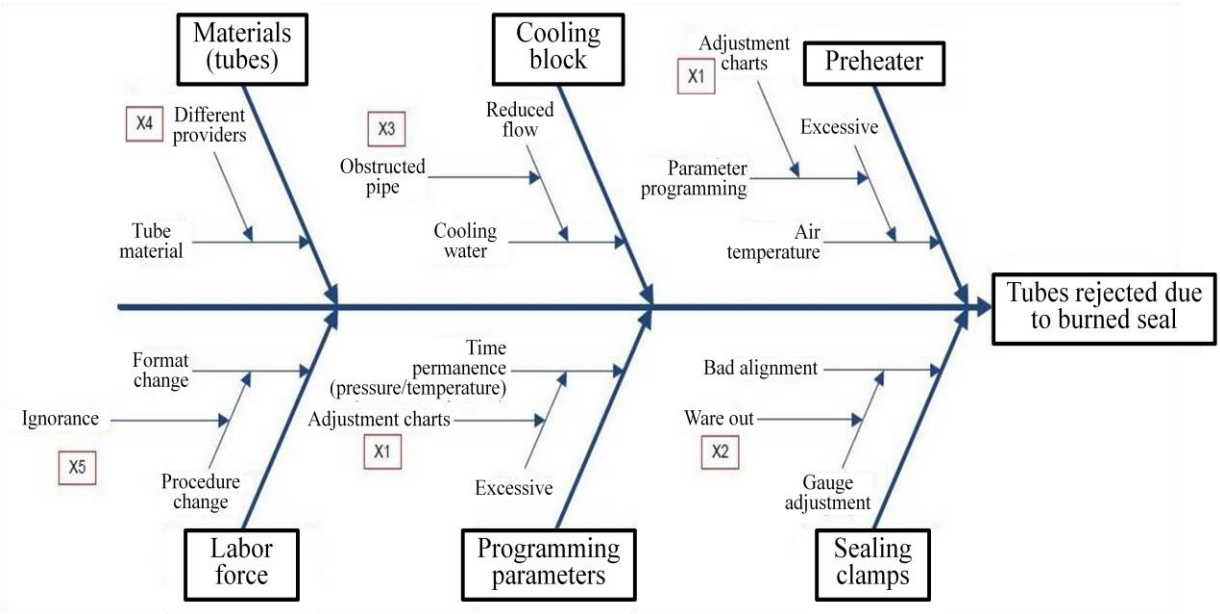

Figure 5: Cause-effect diagram for the burned seal problem.

The most important problem to reject a tube resulted to be that the seals are burned, which provides a bad aesthetic appearance. To find its cause, process maps were made, at a first level for the line, at a second level for the filling machine, and at a third and final level of the sealing mechanism. After the previous disaggregation of the process, an Ishikawa diagram was made to determine which element identified in the process map can cause the plastic seal to be burned (Figure 5).

After the diagram is finished, an AMEF table helps to determine which of the potential causes are responsible for the quality problem. For every potential cause a null hypothesis was included, and to check this hypothesis, the proposed corrective action was carried out, one at a time, and a control run was carried out to be able to quantify the number of burned seals after the corrective action. Five corrective actions were proposed, including actualization of the adjustment charts, use of only gauges and support sheets that are not worn out, to place a bypass to assure a free flow of cooling water, to buy only material of one provider and to assure that the format change is carried out according to written adjustment procedures. Carrying out the statistical procedures for null-hypothesis testing of proportions of defects before and after the corrective actions, it was found that the first three causes are significant, but the latter two are not. The corrective actions were applied provisionally in only one of the equipments to analyze its effects of the problem to be solved.

Performance of the equipment in the new conditions under normal operation was compared with the initial performance in a run with 6504 pieces produced. Table 5 summarizes the results of defects in seal in the control run.

Table 5: Observed defects in the tube seal after corrective actions.

Defect type in seal	Frequency	
	Absolute	Relative
Burned	9	8.04%
Bad cut	60	53.57%
With bubbles	28	25.00%
Defective	15	13.39%
Total	**112**	**100.00%**

As shown in table 5, the burned seal defect was reduced considerably after implementing the corrective actions. This reduction also contributes indirectly in the diminishing of total defective products, which were reduced to 360 (5.5%).

A Pareto pyramid (Wadsworth 2005) shows graphically the benefits of the proposed corrective actions (figure 6).

Figure 6: Pareto pyramid for the burned seal problem.

The previous analysis showed that the corrective actions solve almost completely the problem of burned seals, so these actions are to be made permanent in all production lines.

3.2. Weight variation of the product

The previous methodology was also applied to numerical variables, in this case the weight variation of the final product. The way to proceed is very similar, although a histogram is used instead of a Pareto diagram, summarizing weight information of 150 samples of 100 g tubes, extracted systematically (10 pieces every 30 minutes).

As lower and upper specification limits are determined respectively in 100 and 103 g, a capacity study was carried out (figure 7), indicating a potential capacity coefficient of 0.43 which corresponds to 22.8 % of pieces out of specification. Specifically, 16.5% of the tubes were found to have with weights over 103 g and although these are accepted for sale, this situation is far from optimal for the company.

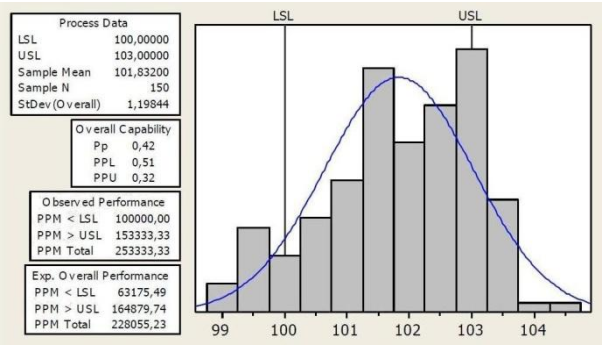

Figure 7. Process capacity for tube weights (100g).

To fill the tubes, cyclic mechanisms are used and these are synchronized with a camshaft, which provokes the tube elevator to rise and fall. The filling valve is opened and closed by one of the cams, and finally the injection of bulk product in the tube is also controlled by the camshaft. The corresponding process maps were developed, an AMEF table was made and the resulting null hypotheses were tested, again one by one, to improve the process. It was found that two significant causes for the weight variability were the ware out of the camshaft`s lining bar and an incorrect interpretation of the adjustment graphs.

After implementing the proposed corrective actions, variability could be reduced and potential capacity was determined again, turning out to be 0.73. In this case the capacity value was still not acceptable, and on one hand the Ishikawa diagram was revised again to detect possible extra causes, and on the other hand the correct implementation of corrective actions was checked. In the revision of the provisional reparation of the camshaft it was found that the welding seam was worn out somewhat, due to the fact that the camshaft was given a thermal treatment to increase its hardness. The difference in characteristics between camshaft and welding seam impedes a perfect fusion; besides, the welding seam did not have the hardness required for the stress applied to the camshaft. As the camshaft was not available in the warehouse, the maintenance department decided to work in the meantime with the repaired camshaft.

3.3. Prevention of sporadic failures in the filling line

Although products out of specification can be due to different types of errors, the camshaft problem will be presented to illustrate the case of prevention of sporadic failures, as it was repaired but still worn out. As a consequence of the previous analysis, the camshaft will be replaced as soon it is purchased, but the maintenance department wants to prevent deterioration of the shaft and thus variability of the weight of the tubes in the future.

To identify the potential failure modes, a fault tree is developed to determine which conditions will cause failures in the camshaft (figure 8). To identify the root cause, a cause-effect diagram is used were each basic event is considered as principal cause and were the top event is the problem to solve. This diagram should be developed jointly with the maintenance department.

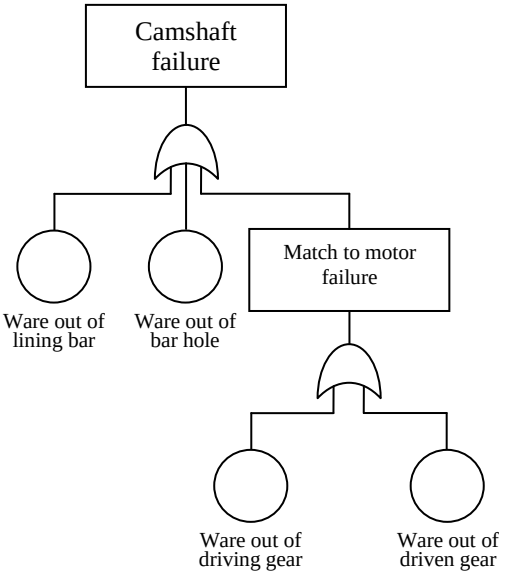

Figure 8. Fault tree for the camshaft problem.

In the cause-effect diagram, three risk conditions were detected that should be monitored or eliminated to prevent the camshaft to ware out: bad assembly, bad interpretation of provider information and non appropriate tolerance of the bar hole dimensions, the second of which is the only one that can be monitored continuously. On the other hand, a variable that can be measured is the electric current in the corresponding motor, as this is an indirect indicator of the stress that is transmitted by the camshaft. This stress generates an increment in the motor's temperature and in the coil´s current, both of which can be measured. A control diagram for these parameters was proposed to monitor possible overloading of the camshaft.

3.4. Cost/benefit analysis

A cost/benefit analysis was carried out, considering implementation costs, costs for production of defective

products, personnel training costs, salary costs for the people in charge of the implementation of the methodology and costs of the spare parts used to solve the failure. The analysis for the chronic failure in the filled tube line indicated that the implementation cost of the proposed methodologies is relatively low, and consists principally of personnel costs; however, as the level of defect products diminished drastically, these costs can easily be absorbed by the amount spilled previously in the production of defect tubes. As the number of chronic failures increases, the savings effect will be more important, as personnel costs will stay constant or increase very slightly.

Another aspect is the gain of intangible benefits, unfortunately difficult to quantify. These include reduction of the risk of late delivery, diminishing of the ambient pollution due to less defective products, sparing the company's reputation and finally the improvement of the quality concept among the personnel.

4. CONCLUSIONS

The maintenance department should be included as a strategic unit to achieve the company's aims, as an early detection and consecutive solving of failures in maintenance will improve overall efficiency in an important way. The proposed methodology is a step to achieve this.

Among advantages of the methodology the following can be mentioned:

- Changes the old paradigm that an equipment, when functioning, is necessarily working well
- Introduces the product as the main indicator of good health of the equipment and foments the register of corresponding data
- Stimulates the systematic analysis of the production equipment and their failures
- The initial investment for implementation is relatively low while the benefits are important
- The improvements are achieved on a short term

Disadvantages are:

- Its implementation is time consuming and depends on the general state of the production equipment
- It requires qualified personnel with basic knowledge in statistics, besides their technical capacities

The achievements obtained by the prevention of sporadic failures are less evident as for the detection and elimination of sporadic failures. However, this is exactly the aim of the maintenance department: its main objective should not be to repair defect equipment, but prevent its ware out and loss of functionality by detecting in a timely way chronic failures in the equipment.

REFERENCES

Cuatrecasas L., 2000. *TMP: Hacia la competitividad a través de la eficiencia de los equipos de producción*. Gestión 2000, Barcelona, España.

Wadsworth H. and Stephens, K., 2005, *Métodos de control de calidad.* Compañía editorial continental, México.

BIOGRAPHICAL NOTES

Ann Wellens is a chemical engineer with postgraduate studies in Industrial Administration (KUL, Belgium) and a master degree in Environmental Engineering (UNAM, Mexico). At the moment she is a full-time lecturer in the Systems Department of the Industrial and Mechanical Engineering Division of the National University of Mexico (UNAM). She has been working in air pollution issues for the last 15 years, dictating courses, collaborating in research projects and participating in conferences related with mathematical modeling of air pollution dispersion and statistics.

Joel Esquivel obtained his bachelor degree in Mechanical Electrical Engineering (UNAM, México) and his master degree in Industrial Engineering in the same university. He has been working as a maintenance engineer in different facilities and productive branches.

HIERARCHICAL CONSCIENT EVOLUTION

Tudor Niculiu[(a)], Maria Niculiu[(b)]

[a)] University *Politehnica* Bucureşti
[(b)] University Bucureşti

[(a)] tudor-razvan@ieee.org, [(b)] mariaoficialfac@yahoo.com

ABSTRACT
To come closer to conscience on the way to simulate intelligence by intelligent simulation, we approach simultaneously bottom-up and top-down *faith* and *intelligence*, and their intersection *conscience*. Intelligence = Consciousness × Adaptability × Intention and Faith = Intuition × Inspiration × Imagination, are the complementary parts of the human mind. *Conscience* = Consciousness × Inspiration is the link between. Simulation is the relation between function and structure. Simulation of *conscience* demands transcending from computability to simulability following philosophical goals, by integrating essential mathematical and physical knowledge. A way to begin is hierarchical simulation. *Philosophy is not a specialty but a human right*.

Keywords: Conscience, Faith, Intelligence, Simulation

1. HIERARCHIC INTELLIGENT APPROACH

Algorithms, designs, artificial systems can be computer simulated so they represent computability, top-down - construction, design, plan or bottom-up - understanding, verification, learning. The algorithmic approach is equivalent to the formal one. Knowledge and construction hierarchies can cooperate to integrate design and verification into simulation: structural object-oriented concepts handle data and operations symbolically. Hierarchy types open the way to simulate intelligence as intentioned adaptable consciousness by extending the present limits of computability. We enrich the template concept to structures and create a theoretical kernel, for self-organizing systems, based on a hierarchical formalism. This permits theoretical development as well as efficient application to different cosimulation ways of reconfigurable systems. Coexistent interdependent hierarchies structure the universe of models for complex systems, e.g., hard-soft ones. They belong to different hierarchy types, defined by simulation or knowledge abstraction levels, modules, symbols, and classes. Hierarchies correspond to the abstraction they reflect. Knowledge and construction have correspondent hierarchy types: their syntax relies on classes, their meaning on symbols and their use/ action on modules. The hierarchy types can be formalized in the theory of categories.

The hierarchical types are objects of equivalent categories (functorial isomorphic) that formally represent hierarchy types. The consciousness hierarchy type communicates to the other hierarchy types by countervariant functors, while the others intercommunicate by covariant ones. Constructive type theory permits formal simulation by generating an object satisfying the specification. Applying similar abstraction kinds to hard and soft representations and operations based on object-orientation, symbolization and structural abstraction can be extended from soft to hard. A generic type has the ability to parameterize with types a hard/ soft element. Recurrence is confined to discrete worlds while abstraction is not. All this suggests searching for understanding following mathematical structures that order algebra into topology. The alternative ways followed to extend the computability concept concentrate respectively on the mental world of the good managed by engineering, the physical world of the truth researched by science, and Plato's world of the beautiful abstractions discovered by mathematics (Penrose 1989). Knowledge bases on morphisms between real system and simulator.

Mathematics contains appropriate structures for self-referent models. The richest domain is functional analysis that integrates algebra, topology and order, e.g., contractions and fixed points in metric spaces, reflexive normed vector spaces, inductive limits of locally convex spaces, self-adjoint operators of Hilbert spaces, invertible operators in Banach algebra.

$$Simulability = Computability^{\,Continuum}$$

Natural transformations on the functors of different hierarchy types solve the correspondence problem, i.e., the association of a knowledge hierarchy to the simulation one. Intention results by human-system dialog, and completes the simulation of the intelligence. Further than modeling consciousness to simulate intelligence is the search to comprehend inspiration. A first idea is to use Lebesgue measure on differentiable manifolds and/or non-separable Hilbert spaces. Even mathematics will have to develop more philosophy-oriented to approach intuition. Evolution needs separation of faith and intelligence, understanding and using consciously more of faith's domain, and integrating them to human wisdom to be divided further to get more human.

2. FAITH AND INTELLIGENCE

Neither Intuition nor Reason arrives alone to a mathematically elementary result. As any other true art or beautiful science of the ideas or the phenomena, mathematics does not limit itself to either Intuition or Reason: these quasi-complementarities have to collaborate, and their main link is Conscience. We dare use mathematics as metaphor for relating Nature to Reality, but it is only a correct inspiring analogy. IR is an initial step in mathematics for algebra, topology, order, or their collaboration. Mathematics is for Reality just one of the favorite ways to get the Human closer.

God's ways are uncountable.
His plans are hopefully hierarchical

Society is conservative – it tries to last forever at any evolution level, using a common measure. Everything can be evaluated, although most of the essential things on that our existence bases its being are not measurable. The so-called pure Reason, i.e., the context-free Reason – most adaptable, conscious only for having, intended by the tactics of the consumption society, and totally unfaithful, gives the necessary force to stagnation or even to choosing a wrong way. Unfaithful means here that the components of the Faith (inspiration, intuition, imagination) are used separately to serve the competition for the Good that makes presently Life credible. However, the irrational of arts, particularly in mathematics, is more than reasonable, whereby the society is less than reasonable; on the contrary, it opens the way to Reality by closure to an essential and radical operation.

To master the New Power of the continuum is beyond Intuition and Reason, if they do not integrate by Conscience and future. The adaptability-based Reason cannot explain or control thoughts, even if sequential is extended to unlimited parallel/ nondeterministic. Anyway, these desired operational properties can be found mainly in the right side of the human mind. Further, the difference between continuous and nondeterministic sequential is positive. Therefore, the Reason has to be Faith-dependent completed to Intelligence. A being needs more than Intuition and Adaptability to surpass the Matter by Spirit; only the integration of Intuition and Adaptability by Conscience can explain the Human being. This inspires the thesis:

Conscience closes itself to (*knowledge* ° *simulation*)$^{-1}$
// initially Conscience = Consciousness

The idea can be formally sustained in the category theory. The essential limit of discrete computability, inherited by the computational intelligence, is generated by the necessity for self-reference to integrate the level knowledge with metalevel knowledge in Conscience modeling. A hierarchical type expressing reflexive abstraction can represent the conscient knowledge. The aspects of the Reality, and of the human mind reflecting it, have not to be neglected, although they are neither constructive nor intuitive. A way from Reason to Intelligence is to integrate Consciousness and Intention, then to integrate Intelligence and Faith to become Reality-aware.

3. FUNCTION AND STRUCTURE

Faith and Intelligence are ☯ *in Life* // Way, Truth, Life

We have to surpass the limits imposed by the above dichotomy by a unique Ideal, named *God*, constructive by continuous intelligent reconfiguration. God is in us - as faith is part of our definition, with us - by the others, and for us – spiritual evolution, first conditioned, and then assisted, to be followed by the social one. Against the danger of dichotomy, we concentrate in three different ways on the unique Reality – *Plato*: art for the art, to look for the essential Way, science with God's fear, to search for the existential Truth, engineering, to understand the Being concentrating on the Spirit in our Life.

Human among humans should reflect a strategic equilibrium, without hiding or even violating, as happens nowadays, the principle that the society has to assist unconditioned the individual, with correct continuous education, and assistance by an intelligent faith to search and research the *unknown*.

The unknown can be interpreted as a *unique God*: the absolute freedom by understanding all the necessities, and the absolute unity by closing the entire *Divide et Impera et Intellige* necessary for the Way to look for the Truth along the Life. Further, thinking while advancing, we divide twofold, as we cannot yet *Intellige* the dichotomies: *Spirit-matter* (force-substrate, function-structure, soft-hardware) ⇒ reality-nature (continuous-discrete, analog-digital), real-possible, beauty-truth (arts-science, mathematics-physics), form-contents (category-functor, representation-simulation, class-function), perspective-profoundness ⇐ *space-time* (evolution). Balance should be not in most of the dichotomies: yin-yang *can represent any dichotomy*.

Arts and sciences are equally noble, even if one appears rather spiritual and the other rather material. Their alliance is vital and shows the insolvability of the nowadays *spirit-matter* dichotomy, and of all resulted secondary dichotomies, actually functionally generated by the *space-time* dichotomy necessary to human evolution. *Reason* is an extension of natural adaptability. *Nature* is not an ephemeral context, but the matter we are built of in order to develop spiritually. The *present society* is extremely materialistic, and tries to destroy every trace of ideal. The integration experiments for the spirit-matter dichotomy failed because of their extremism.

4. HIERARCHIC INTELLIGENT SIMULATION

We extend the reconfigurability to the simulation itself. By a self-aware simulation, we get self-control of the simulation process. Therefore, we build a knowledge hierarchy corresponding to the simulation one. Expressing both simulation and knowledge hierarchies in the reference system of the basic hierarchy types (classes, symbols, modules), we create the context for a self-organized simulation. Hierarchy consists of a net that can represent any type of mathematical structure (algebraic, topological, order). It is the first step to model the Conscience.

The basic hierarchy types correspond to the fundamental partition of the real life (beauty-arts, truth-science, good-engineering), that has to be continuously integrated by philosophy (essence, existence, being). The absolute functionality is symbolized by yin-yang, while the waves suggest hierarchical levels that are increasingly structured for simulation and knowledge (Figure 1). There have to be schools to prepare the teachers of philosophy for the other humans. These schools have to develop respect for those that look for the Way on one of the three alternative paths that correspond to the fundamental partition (arts, science, engineering). As recently the essential *Divide et Impera* do not *Intellige*, the only philosophers are the masters in *arts*, e.g., mathematicians, or those that, aware or not, compose mathematically, *science* – physicists, or those that do not forget their science is a chapter of physics, or *engineering* – mostly those working in domains that attain the limits of the pure Reason. Arts are free.

Mathematics is one of the arts. Music is at least as beautiful and expressive, but mathematics does not demand an extraordinary talent, allows a reasonable dialog about it, and has well-defined reconfigurable limits of that it is aware. Mathematics has to be educated as soon as possible and not to be confounded with its handcraft (Marcus 2000). Music gets more often out of its character. Anyway, they evolved together: *Bach*, *Vivaldi*, *Haydn* were both mathematically as musically gifted, but preferred the liberty of the music to the bands of the Reason (Hofstadter 1979). Reason, as initial zone, makes mathematics more sure but less charming than the other arts that can refer directly to the Reality: music and literature. The visual arts are too Nature-dependent as seeing is the most used sense for the human. Mathematics first expressed reasonably that Reality is not completely accessible by Reason - *Pythagoras*. Mathematics school is continuous, whereby the literature and the music can generate sooner higher singular peaks: *Shakespeare*, *Beethoven*. Mathematics as the most accessible of the arts, science of the abstract ideas, and Beauty engineering, discovers and studies structure types (algebra, topology, order), relative to (construction, orientation, understanding). To science and engineering mathematics is the correct complete integration. *Art for the art* defines itself, creating the Beauty, by thesis-antithesis-synthesis, dialectic principle that governs the *evolution by closure to the inverse*.

Physics is the Science, the other natural/ social sciences are its chapters, even if they are not yet aware of it, or just try to return to their riverbed by intermediary specialties instead of integrative bridges. As any artificial system, the society is structured on natural bases, and it develops by natural laws. During the modern age, these laws were forced towards Reason, and recently they got out of control. Social laws got also less than reasonable.

Physics is essential for the constructive reconfiguration of the Faith

Physics is the paradigmatic science, art to represent the Nature - as exercise to represent the Reality, engineering of the Truth. It has to integrate the fundamental forces in a theory, and all natural/ social sciences as chapters, leading them to a real application of mathematics.

Social sciences study a universe as complex and nondeterministic as the natural one, therefore mathematics is at least as important. Recognizing the physics as the fundamental science, sciences could more directly inspire mathematics (Traub 1999). Science raises the fear of unknown and the research that is inspired by it to zones that are more abstract. It is hierarchically defined, by God's Fear, looking for the Truth; its evolution bases on qualitative leap consequent to consistent convergent quantitative accumulation. As the Reality contains abstract ideas, even if physics could explain everything as being discrete, the power of continuum cannot be forgotten. Consequently, the analog engineering has not to be neglected simulation. Physics permanently uses as alternative solutions the discrete-continuous, while the engineering just adapts intuitively to a consumption-oriented society - characteristic for primitive life.

Engineering is most frequently both art and science, being as important as arts and sciences in the partition of the Reality needed for evolution. However, it is more dangerous than its alternative approaches, of which it has to be strictly bridled: its result, called technology, is defined by its complement – so it is not superior to this; it does not impose spiritual proximity between the creator and the user so it can be applied in a complete different scope than it was generated.

Presently engineering escaped of the control of the inspiring arts, as well as of the consciousness for the science that conditions its existence. Denying the negation is not context-free. Engineering is the homonymous complement of a special science that collaborates with mathematics: this problem is solved if the sciences are integrated into physics and mathematics remains one of the arts (Niculiu 2008). Engineering (art of construction, science of simulation, technology of Good) should develop closer to mathematics: approach, integration of parts, before applying techniques, and to science: courage, multiple perspectives, and not just result-oriented.

The *yin-yang* model (Figure 2) was not randomly selected: each of the nondeterministic separated complementary pairs is functionally structured like (interface, kernel, complement's ambassador). It is formed of three tangent circles emphasizing the centers of the inner ones, retaining the essence of a dichotomy symbol that suggests a complete integration by vicinity and pointing one to another of the parts without loss of autonomy. The Chinese symbol reflects the reminding of creation as love for something else. Three circles, each tangent to the others, models a partition of something to be understood in order to get further, says Europe's center. Circle is *cerc* in our mother tongue, a perfect expression:

Cer (sky) is the infinite; *cerc* is the finite representation of infinite, by the permanent link from (never)begin to (never)end. π is the most famous real number. *Cerc* means perfection, which we permanently desire, therefore there exist integer numbers, having a perfect and beautiful theory, further searching and researching for evolution. The western Europeans attain research/ rechercher by recursive search/ chercher. Our Romanian language helps us to approach this by *cercetare*.

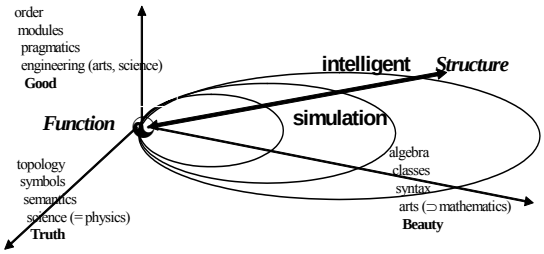

Fig. 1 Extended H-diagram

We have to be to search our essence researching our existence

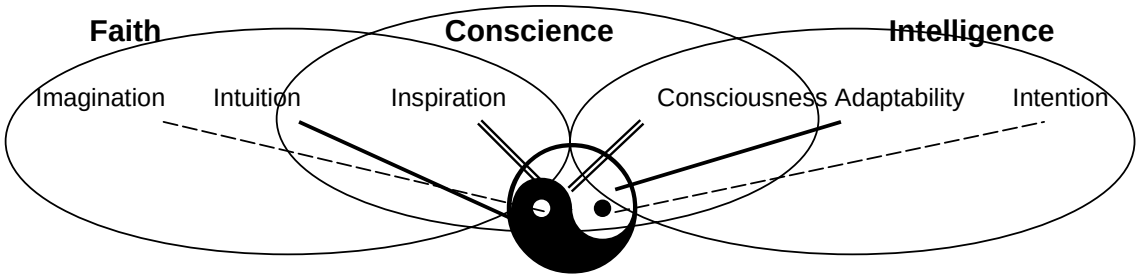

Fig. 2 Human Mind Model

Religion had to learn us about God's existence in our being. Philosophy has to learn us about essence, existence, and being. Our conscience is our representation of the essence of our existence as being.

God is in us, for ourselves, and among ourselves

Divide et Impera et Intellige has three parts as *alle guten Dinge sind drei* of the most philosophic European people. Mathematics develops by three basic structure types, integrating them. We divide our Universe in three worlds: essence, existence, and being. We divide our existence in three interdependent components: arts, science, engineering, corresponding to our beauty-loving ideas, our truth-searching efforts, and our good-oriented constructions - now exaggerated to exclusivity.

For physical or philosophical orientation, we need cardinal points.

To inspire ourselves of the most pure of the arts, we learn about cardinal numbers, although mathematics leads the way to show that nothing is pure so, without leaving anything behind, we follow the Way further. Cardinals are just numbers of elements in a set, but also for infinite sets. Nature demands the least infinity and is defined by (0, successor, induction). Adding is in Nature's definition. However, the inverse operation, subtraction, needs negative numbers. We close mathematically the Nature to an Integer that opens the physics for recognizing the limits of Reason (electrons). Meanwhile, marvelous engineering solutions for different technologies are discovered/ invented. Electronics is among the most advanced engineering sciences: it has to be practiced by the most conscient human beings. Recurrent addition is multiplication, a most important parameter for the Nature.

Mathematics closes the integers to the multiplication inverse, defining the rational numbers. These are not more than the naturals, but we can do many useful things with the Reason, from strategy to computer. *What else do we need*? say too many, forgetting that the limits of the, so-called, pure Reason are caused by the fact that it bounds itself to close the Adaptability to (discrete) sequential operations. Thanks God, neither the mathematicians, nor the physicists do accept the all-happiness (Hawking 1996). They discover in three ways (order, algebra, analysis), which assisted all of them together to think, the power of continuum and that of the patience. In this context, mathematicians and physicists means the theorem, natural laws, or even new approach discoverers, but also the engineers that understand the essential of mathematics and of physics, and bring these further by an engineering model.

A third meaning of cardinal points for an unwise use of *Divide et Impera et Intellige* as a strategy called when two fight, the third wins: intervention comes only when the fighting forces begin to get unbalanced, in favor of the less strong, not for establishing the equilibrium but for conquering all the others; the victory must be completed, so both pseudo-ally and -enemy are firmly assisted, discretely or continuously, to loose control, because of respectively all-(un)happiness. The 20th century is a too convincing example.

Presently, we talk about electronic computers, but the nowadays trend is to copy from the living Nature, emulating the advantages the living beings show, to achieve unconsciously complex duties. Vanguard domains are biotechnology and computational intelligence.

Neither intelligence nor life is well understood; remember *Zauberlehrling*. More important is that emulation is less human than simulation, so they should develop in parallel, permanently exchanging experience.

Reality does not reduce to Nature

// cardinal (IN) < cardinal (IR)

Reality extends beyond Nature and Reason, not just for the quality of the quantity, but also regarding the power of transforming operations (Turner 2009). IR closes IQ to the inverse of power rising – the first noncommutative arithmetic operation resulted by recurrence of the prior one; while power can be pursued by Reason, exponentiation shows its limits, being too complex to be computable. The Reason is the closure of the Nature relative to the primary operations, as IQ is the closure of IN to the inverse operations of + and ×. However, – as IR = $\{\lim_{n\to\infty}(q_n) |\ (q_n)\in IN\to IQ\}$, the Reason is *dense* in Reality as real numbers are the analytical closure of rationales. The density of Reason into Reality means that every real is the limit of a sequence of rationales. Therefore, we hear nowadays that if we master the Reason, Reality becomes a complexity problem, i.e., speed of convergence. The density of IQ in IR shows that between any two real numbers there is a rational one. We need to imagine that Reality >> Reason accepts that something reasonable exists between any two real objects (*nonintuitive*). Further, closing to the inclusion order, the set of all subsets of IN, IZ, IQ, or in general, of countable sets, is the uncountable IR, the power of continuum. To get to complex numbers is a matter of Imagination. Reason closes the Nature to the inverse of natural operations. Reality is the closure of the Reason to the inverse of artificial operations, or to the reasonably deducted infinite, or to an order over the Being itself. We know that if there were no cardinal number between the natural/ integer/ rational discrete and that of the real continuum, then the human logic would include the principle of the excluded tierce, what pure and simple would hurt the Human who is fond of nuances can prove that there is an intermediary level between Reason and Reality (*nonconstructive*).

There are angels between Human and God

said the wise

5. REVOLUTION BY OPENING TO EVOLUTION

The human has to enlarge, not to tear, the bands of the Reason, and to apply them to the society. The Reason has to transform into the consciously recognized limits of the Intelligence in front of the Faith that offers to the human the way to evolve beyond any limits. A reasonable society is hierarchical. Its essential architecture contains three tree-like structures for the same set of humans, therefore, interdependent: arts, science, and engineering-technology. Social hierarchies reflect only a temporary order, generated by humans, to help them concentrate on the spiritual evolution, without neglecting the material problems.

We need Consciousness to return intelligently to Faith

The hierarchical social structure can assure an optimal organization of humans among humans. The interdependence of the three social classes is not only structurally, but also functionally assured. Without giving up anything essentially human: culture, social or natural togetherness, or different approaches, humans have a lot in common: philosophic desire, comprehension of the own hierarchy in the context of the other two, free life based on understanding the necessities, constructive fear of the unknown, and especially the love for creation. Except the three cultural ways, that permanently *Divide et Impera et Intellige*, there is no other. *Intellige* is to link, to understand, and to be aware. In Latin: *intellego* = to understand, to feel, to master, to gather in mind. Artificial has a derogatory sense; however, the root of the word is art. Arts remind of liberty, as *Arts for arts*. Artificial is at first sight the complement of natural. Our ideas transfer us to places that are neither natural nor artificial. Maybe artificial means something natural created by the human being and Nature is an extension of our body. However, we feel to be superior to Nature, as to our body: we can think. Why are only humans creating arts, why do they need to know more, and why do they construct other and other natural things they have not found in the Nature? We learned the arts have to discover the Beauty that science looks for the Truth, and that engineering invents things to help us, caring for the Good. *Goethe* wrote on the theatre in Frankfurt: *Das schöne wahre Gute* because the three wonderful scopes have to be always together. He stretched the Good that is important to all natural beings, whereby for beautiful or true cares only the human being. Arts and science demand a distinct power for both development as understanding, and possibly for usefulness. The power of abstraction distinguishes us among other natural beings. Engineering is to be ingenious, not only designing engines. Any human choice to surpass the Nature by arts, to know it better by science, or to enrich it by ingenious construction, is as noble and legitimate, as to follow any selected way demands intelligence.

Artificial intelligence has an initial sense of enriching natural domains by natural extensions. Reason is an extension of the Nature. The natural language whispers: as the rational numbers are a straight extension of the natural ones, if we neglect the integers, however, you remain in a countable world as the Nature initially is. We should not be ashamed if someone that we only understand by proper preparation and that is at least so powerful as the Nature; let's remember our beautiful mother language. *Cer* (sky) suggests the infinite, and we desire to see it and to link its begin to its end, or better its never begin to its never end, and we find the *cerc* (circle). The language whispers to us again: π is not rational, it is more than this, and it is as if we listen to a symphony of *Beethoven.* We understand that the Reality of our Existence is more than the Nature of our Being, therefore, we should know them better, because only Nature can open us the way to Reality.

We wonder whether any of the alternative ways demands the same kind of intelligence, and if not, which of them should we first research (*cerceta*) in order to simulate it. Arts are free, and even when they return to Reason, as mathematics, they bring results, that could before just be seen by Intuition, to send by Inspiration and Imagination to Intelligence. Physics reaches and gets conscious - not conscient - of Reasons limits, both by the quantum theory and by the too complex phenomena, e.g., society and human. It looks like there is no difference for the intelligence that is useful to one of the ways. Intelligence is more than Reason, to make us feel as beings superior to Nature, what also means that we have to respect Nature more.

We need Conscience to link Faith to Intelligence

6. EVOLUTION CLOSING TO THE INVERSE

Intelligence allows us to consider ourselves humans, human groups, peoples, beings on the Earth, or conscious beings in the physical Universe. We also feel that there is something essential beyond the physical – the metaphysical – *Plato*. More, there is something exterior to the human intelligence, without that we could not fight the Time to evolve. We have to feel complete, even if we need education and permanent work in communication with the other humans, of the past, the present, and the future. You see now why we neglected the integers when we showed that the rational numbers are countable, i.e., they are as much as the naturals. This way, we divided the problem into two others that we do not forget to reintegrate after we have solved them - *Divide et Impera et Intellige*. We count the positive rational numbers x/y along the secondary diagonals in an odd quadrant of the coordinate system (x0y); we repeat this counting for the negative ones in an even quadrant. Finally, we count them together by jumping between quadrants for every current number. We come to the idea how to count the IQs without using *Divide et Impera et Intellige*; we have to keep in mind for harder problems, as Life, Truth, and Way.

We said *complete human* to someone complete in a context, what implicitly supposes the power to go beyond the context. This is the story of the integers (*integer* = perfect, complete): they have a beautiful complete theory, however, do not forget to build the rational numbers to feel as close as needed to any real number. Nevertheless, they realize this is not enough, rewarded by the conscience of the continuous Reality – infinitely more powerful than the discrete/ countable one. To IR, we get by the perfect circle that is beyond the power of Reason. Another way to the same scope is by the boring perfection of the square, when computing its diagonal ($\sqrt{2}$). Again and not fortuitous this alternative is due to *Pythagoras.* The beautiful natural induction tells us that the equilateral triangle and the square are but the pioneers of the regular polygon sequence that converges to the circle. Encouraged, we turn an equilateral Δ or a square about itself, obtaining the area of the circumscribed circle when the number of sides $n \to \infty$, from the areas of the n-sided polygons. However ... we wanted to approach π by a sequence of rationales, but the example is not good. Again, we hear like a sweet wind from the sea: *Alle guten Dinge sind drei*, and intuitively sense that we have to know how mathematics masters the infinite. For long time, we knew nothing of sets, but we knew too well to play the role of a calculator. We should not forget what Intuition said to Intelligence, by Imagination: we just had imagined a sequence of *algebraic irrational numbers* converging to the *transcendent* number π. We fear to be further taught what a discrete computer, instead of what an intelligent human, has to know. Perhaps not practice has to push us into evolution, but Gods fear, i.e., the scientific desire for further ascending encountered on any reached level of knowledge. Conscience attaches us to science and unfastens us of the false eternity, arrogated by some level of the evolution to freedom. To be free we have to understand all the necessities in the Reality, to escape God of any fear.

We need intelligent Faith to develop to freedom as humans among humans

7. CONCLUSIONS

We could consider just the simplifying types of hierarchy (classes, symbols, modules) and then express the construction, hoping to aim the absolute liberty, if we considered God as the simplest, totally unconstrained, essence of the Reality. However, we can simulate/ construct/ work/ live, associating knowledge hierarchies to our activities, aiming to constructive understanding of the most complex absolute necessity, by this defining God. Abstraction is the human gift for going beyond natural limits, extending pure reason to real intelligence:

God is the absolute abstraction/ the evolution goal for faith-assisted intelligence

Neither intelligence nor life are well understood, remember *Goethe*'s *Zauberlehrling*. More important is that emulation is less human than simulation, remember *Mozart*'s *Zauberflöte*. They should always develop in parallel, permanently exchanging experience, remember *Thomas Mann*'*s Zauberberg*. We have to close to the inverse of *Freedom is understood Necessity*

REFERENCES

Hawking, Stephen, 1996. *The Illustrated Brief History of Time.* Bantam Books

Hofstadter, Douglas, 1979. *Gödel, Escher, Bach, The Eternal Golden Braid*. Basic Books

Marcus, Solomon. 2000. "From Real Analysis to Discrete Mathematics and back". *Real Analysis Exchange* 25: 361-380

Niculiu, Tudor, 2008. *Object-oriented Symbolic Structural Intelligent Simulation*. Bucureşti: Matrix Publishers

Penrose, Roger, 1989. *The Emperor's New Mind*. Oxford: University Press

Traub, Joseph, 1999. Continuous Computation Model. *Physics Today,* 52: 39-43

Turner, Raymond. 2009. *Computable Models*. Springer.

THE IMPACT OF THE SIMULATION USER ON SIMULATION RESULTS: TO WHAT EXTENT HUMAN THINKING CAN BE REPLACED BY ALGORITHMS?

Gaby Neumann[(a)], Juri Tolujew[(b)]

[(a)] Technical University of Applied Sciences Wildau, Germany
[(b)] Fraunhofer Institute for Factory Operation and Automation (IFF) Magdeburg, Germany

[(a)]gaby.neumann@th-wildau.de, [(b)]juri.tolujew@iff.fraunhofer.de

ABSTRACT
In recent literature the question for how to provide simulation modellers (or users) with methods and tools for automatic trace file analysis is discussed in an increasing manner. Approaches mainly focus on formalizing simulation outcome in the context of a certain application area. They have in common the very much reduced role they give to the key actor(s) in any simulation project: the persons who build and use the simulation model. Against this background the paper reviews related work for trace file analysis with regard to its motivation, approaches and state-of-the-art. This is put into relation to simulation user needs in a particular application area, logistics, in order to discus to what extent trace file analysis helps in deriving findings, which role the user plays in receiving those results, and which kind of support is missing here and how it could be provided.

Keywords: simulation output interpretation, trace file analysis, simulation knowledge, logistics

1. INTRODUCTION

One of today's challenges consists in seeing simulation in the context of human-centred processes. In recent literature this is being addressed by, for example, providing simulation modellers (or users) with methods and tools for automatic trace file analysis in order to better cope with large amounts of simulation output data. Those approaches mainly focus on formalizing simulation outcome in the context of a certain application area.

Kemper and Tepper (2009), for example, state that in tracing a simulation model a modeller finds himself in the situation where it is unclear what properties to ask to be checked by a model checker or what hypothesis to test. They assume that cyclic behaviour of model components is always good behaviour whereas all exceptions or disturbances in this behaviour indicate errors. Therefore, the aim is to provide support by automatically identifying and removing repetition from a simulation trace in order to pay particular attention on the non-returning, progressing part of a trace. This is to be achieved by automatic trace file reduction as it is assumed that modellers do not have enough background knowledge or experience to figure out interesting parts of the trace themselves.

Wustmann, Vasyutynskyy and Schmidt (2009) assume that simulation usually aims to specify whether or not the concept of a material flow system meets formal requirements, but not how well it does it. This is said to be caused in limited methodological support and therefore strongly depend on the modelling/planning expert's experience and expertise. This is to be overcome by eliminating the user as weakest point through automatic analysis. For this an analysis tool is proposed that helps in identifying the concept's or the system's weak points, specifying their primary reasons and pointing out system immanent potential for performance increase.

Both approaches have in common the very much reduced role they give to the key actor(s) in any simulation project: the person who builds the simulation model and the person who uses the simulation model to run experiments. Instead they assume any result derived from simulation can directly and automatically be extracted from the trace file through statistical analysis, clustering or reasoning without any additional explanation by the simulating person. If this would be the case then any simulation model and any plan of experiments can be seen as objective representation of a particular part of reality and its problem situation. Any model building or experimentation activity no matter what background or intention one has would lead to the same model and to the same collection of simulation output. A particular simulation output always would lead to the same conclusions, i.e. simulation results, no matter what is being analyzed by whom and how.

If this would be the case, why do simulation projects still require human resources of certain expertise to be involved in? It is because simulation projects are not only sequences of formalizing steps that can be fully represented by more or less complex logical algorithms, but also require intuitive problem solving, combining analyzing steps and the need for creative thinking. Whereas the first can already be formalized or will be in future, the latter always remains linked to the person carrying out or contributing to or requesting simulation projects. Approaches to increase the degree of formalization in simulation, no matter if they focus on automatic model generation or automatic

trace file analysis and simulation result delivery, will always be limited by the impossibility of fully formalizing the objectives and goals of a simulation. As already concluded by Helms and Strothotte (1992) the simulation user will therefore continue to be the key factor in any simulation project.

Against this background the paper reviews related work for trace file analysis with regard to its motivation, approaches and state-of-the-art. This is put into relation to simulation user needs in a particular application area, logistics, in order to discus to what extent trace file analysis helps in deriving findings, which role the user plays in receiving those results, and which kind of support is missing here and how it could be provided. To give proof of the impact the user has on the simulation results achieved different types of users with individual background, experience and intention build individual simulation models and run simulation experiments for the same problem. Comparative analysis investigates differences and similarities of models, experiments, results and findings achieved by the different users.

2. THE USER'S ROLE IN SIMULATION

In general, simulation projects in the field of logistics – as in other fields too – are organized in the form of a service involving both, simulation experts and logistics experts with individual knowledge to be of use at certain stages of the project: Simulation experts are primarily responsible for model building and implementation steps, whereas logistics experts mainly provide application-specific knowledge for problem description, identification of input data and evaluation of results (Neumann and Ziems 2002). In order to better understand the role of the user in simulation it is worth to take a closer look at simulation knowledge sources and stakeholders for identifying which knowledge comes from where and in which form.

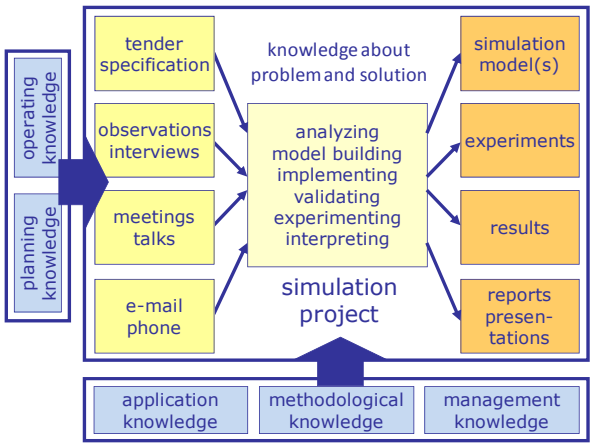

Figure 1: Sources and Evolution in Simulation Knowledge

In general, input information for a simulation project usually come with the tender specification or are to be identified and generated in the problem definition and data collection phases of the simulation (Figure 1). Here, the user decide (and bring in) what is to be taken into consideration for model building and which information is required for the investigation.

The model-building process should be seen as another important phase of collecting, evaluating and structuring information. As discussed by Neumann (2007) a simulation model is more than just a tool necessary to achieve certain objectives of experimentation and cognition. In the course of a simulation project the simulation model is developed, modified, used, evaluated and extended within an ongoing process. Therefore, it is also a kind of dynamic repository containing knowledge about parameters, causal relations and decision rules gathered through purposeful experiments. Even further, knowledge is "created" systematically through simulation based on the systematic design of experiments (including a meaningful definition of parameters and strategies) and the intelligent interpretation of results.

Simulation experiments, for example, to support logistics planning and operation might be oriented towards modifications in either functionality or structure or parameters of a model and its components or even in a combination of those variations leading to more complex fields of experiments. Experimentation efforts are directly related to the type of variation required. The latter depends on the specific design of the simulation model resulting from the underlying modelling concept of the simulation tools and the design of the conceptual model by its developer. To correctly interpret simulation output it is necessary to understand what the objectives, parameters and procedures of a certain series of experiments were and to relate this to the results and findings. Consequently, the objectives of a simulation and the questions to be answered by experiments should already be taken into consideration when designing the conceptual model. Specific opportunities and features offered by the selected simulation tool then influence transformation of the conceptual model into the computer model when it comes to model implementation.

All steps again and again require input and background information based upon the knowledge and experience of the user, i.e. the simulation expert and the domain expert. In terms of simulation target definition it is particularly necessary to understand what the domain expert expects from simulation. As this is typically specific to the application area, we continue discussions using logistics as example.

3. EXPECTED OUTCOME FROM LOGISTICS SIMULATION

In the course of a logistics simulation project both partners, logistics expert (simulation customer) and simulation expert (simulation service provider), use to face the ever challenging task to interpret numerous and diverse data in a way being correct with respect to the underlying subject of the simulation study and directly meeting its context. These data are usually produced and more or less clearly presented by the simulation

tool in the form of trace files, condensed statistics and performance measures derived from them, graphical representations or animation. Problems mainly consist in:

1. clearly specifying questions the simulation customer needs to get answered,
2. purposefully choosing measures and selecting data enabling the simulation service provider to reply to the customer's questions, or
3. processing and interpreting data and measures according to the application area and simulation problem.

To overcome these problems and give support in defining simulation goals and understanding simulation results, methods and tools are required that are easy to use and able to mediate between knowledge and understanding of the simulation customer (the logistics expert planning or operating that process and system to be simulated) and the simulation expert (the expert from the point of view of data and their representation inside computers). Within this context, it is worth thinking in more detail about what a simulation customer (the logistics expert) might look for when analyzing the outcome of simulation experiments (Neumann 2005):

- Typical events. The logistics expert specifically looks for moments at which a defined situation occurs. This kind of query can be related, for example, to the point in time at which the first or last or a specific object enters or leaves the system as a whole or an element in particular. Other enquiry might be oriented towards identifying the moment when a particular state or combination of states is reached or conditions change as defined.
- Typical phases. The logistics expert is especially interested in periods characterized by a particular situation. In this case s/he asks for the duration of the warm-up period, for the period of time the system, an element or object is in a particular state, or how long a change of state takes.
- Statements. The logistics expert looks for the global characteristics of processes, system dynamics or object flows such as process type (e.g. steady-state, seasonal changes, terminating/non-terminating), performance parameters of resources (e.g. throughput, utilization, availability), parameters of object flows (e.g. mix of sorts, inter-arrival times, processing times). This information is usually based on statistics resulting from trace file analysis and replies to either a specific or more general enquiry by the user.

When the potential interests of a simulation customer are compared, one significant difference emerges: whereas the first two aspects need specific questions formulated by the logistics expert directly at data level, the last aspect is characterized by usually fuzzy questions of principle from the more global user's point of view. Before these questions of principle can be answered, they have to be transferred to the data level by explaining them in detail and putting them in terms of concrete data (Figure 2). As result of this process of interpretation a set of specific questions is defined with each of them providing a specific part of the overall answer in which the user is interested. Questions at data level correspond to results that can be delivered directly by the simulation even if minor modifications to the simulation model should be required (Tolujew 1997). This is the kind of study also current approaches for trace file analysis support (Kemper and Tepper 2009; Wustmann, Vasyutynskyy and Schmidt 2009). To derive an answer in principle to a question of principle the respective set of specific answers needs to be processed further. These steps of additional analysis and condensing can be understood as a process of re-interpretation to transfer results from data to user level.

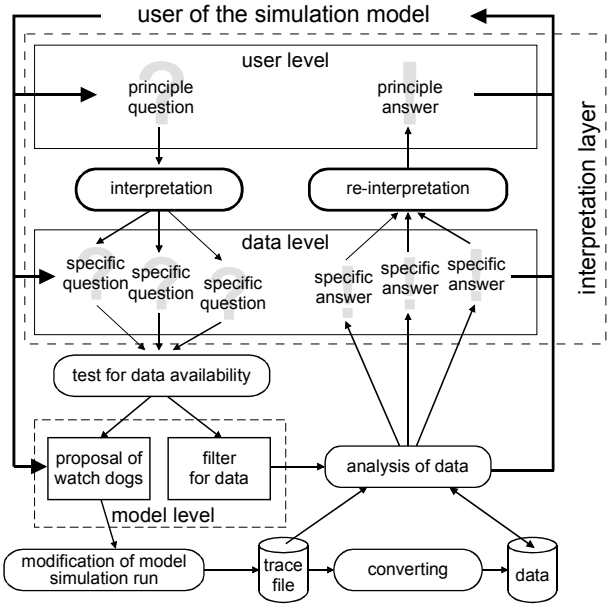

Figure 2: User-data interaction for simulation output analysis

All steps of interpretation and re-interpretation aim to link the user's (logistics expert's) point of view to that of the simulation expert. They not only require an appropriate procedure, but, even more importantly, an interpretative model representing the application area in which simulation takes place. This model needs to be based on knowledge and rules expressed in the user's individual expertise, but also in generalized knowledge of the (logistics) organization regarding design constraints or system behaviour and the experience of the simulation expert derived from prior simulations. As this knowledge might not only be of explicit nature, i.e. existing independent of a person and suitable to be articulated, codified, stored, and accessed by other persons, but also comprises implicit or tacit knowledge carried by a person in his or her mind often not being

aware of it simulation users as individuals or team need to remain involved in the steps of interpretation and re-interpretation at least. Whereas explicit knowledge might be transferred into rules and algorithms, tacit knowledge cannot be separated from its owner and therefore requires direct involvement of the knowledge holder in the interpretation process. More specifically this means support is required for translating any principle question into corresponding specific (data-related) questions as well as for deriving principle answers from a number of specific (data-related) answers. Although a set of (standard) translation rules might be known, formalized and put into the rule base already, always further questions remain that are unknown to the rule base yet. Here, the logistics expert needs support in

1. correctly formulating the right question and
2. getting the full picture from the puzzle of available data and their analysis.

One approach for enabling this could be based on viewpoint descriptions. Viewpoint descriptions were introduced into model validation as a new kind of communication and interaction between the human observer of simulation results and the computer as the simulation model using authority that was called oracle-based model modification (Helms and Strothotte 1992). Here, the principle idea is that the user presents his or her observations (in the animation) as a viewpoint description to the computer that initiates a reasoning process. This results in definition and realization of necessary changes to the simulation model in an ongoing user-computer dialogue. The main advantage of this concept lies in the reduced requirements for rule-base definition. Those aspects that easily can be formalized (e.g. typical quantitative observations or unambiguous logical dependencies) are translated into questions to the user (What is it s/he is interested in?) or various forms of result presentation (as figures or diagrams), whereas those that are non-imaginable yet or individual to the user or simply hard to formalize do not have to be included to provide meaningful support to the user. There is no need to completely specify all possible situations, views and problems in advance, because the person who deals with simulation output brings in additional knowledge, experience and creativity for coping with non-standard challenges. Even further, this way the rule-base continuously grows as it "learns" from all applications and especially from those that were not involved yet. On the other side the user benefits from prior experience and knowledge represented in the computer by receiving hints on what to look at based upon questions other users had asked or which were of interest in earlier investigations.

This approach helps in designing the interpretation layer for mediating between simulation customer and simulation model or output no matter how many data have been gathered and how big the trace file grew. Nevertheless, effectiveness and efficiency of this interpretation process depends on the availability of the right data at the right level of detail. This quite often does not only depend on the simulation model and tool used for its implementation, but also on the opportunity to aggregate data in always new ways.

4. CASE STUDY ON THE IMPACT OF THE USER

In order to demonstrate the role of the user in a simulation project and his/her impact on simulation results at both levels, the one dealing with (abstract) data and the one related to the user's point of view, the same problem description and input data can be given to different types of users for building the simulation model, running experiments and deriving simulation results. These users might vary in their domain-specific background (e.g. logistics or computing expert, engineer or management person, simulation service provider) and experience (e.g. novice or expert), but they all run the full simulation project including problem analysis, model building, implementation, validation, experimenting and interpretation. For this, it is left up to them which analysis or modelling tools or simulation package they might use. Based upon the finalized project comparative analysis can run in order to understand what findings and recommendation from the simulation have in common and what differences are caused by the individual approaches. With this, we can demonstrate what might happen if user-specific motivation and intention for simulation modelling and experiments in a particular case is not taken into consideration when deriving conclusions from statistically analyzing trace files only.

A first example of such a comparative case has been run and analysed by Neumann and Page (2006). Here, the same logistics simulation problem, namely to identify the performance limit of two different designs and two varying operational scenarios for automated stacking at high-performance container terminals has been given to two individually operating groups of students from different domains. The first group was composed of computing students from the University of Hamburg, whereas the second group was formed by logistics students from the University of Magdeburg. All students had already a certain simulation background corresponding to their educational profile.

The main differences between the approaches in both cases consist in the preparation of model implementation and the simulation models themselves. The logistics students started with a detailed analytical investigation of the system and process to gain a clear understanding of the situation and more detailed specification of the problem. From this they derived a conceptual model which they had in their minds when starting to implement the model using the DOSIMIS-3 simulation package, but they did not document it in any formalized way. Due to the fact that they were to use predefined building blocks for model implementation already representing a particular amount of functionality and logic, they had to deal with certain limitations (or at

least special challenges) in modelling and therefore in advance spent many thoughts on what really is needed to be represented in the simulation model at what level of detail. This led to a number of simplifications such as the representation of the stacking cranes' movements on the basis of a detailed understanding of the material flow backgrounds of the simulation problem.

In contrast to this the computing students focused on a very detailed representation of the stacking cranes' movements including precise tracking of the cranes' positions while moving, but they set aside representation of the storage places and individual containers. This also required detailed modelling of the cranes' management and control system and algorithms, whereas neither warehouse nor stock management was needed. Although these students had not to deal with the large number of storage locations, detailed representation of the stacking cranes required a lot of extra efforts, especially because of the complex and complicated control algorithms. Here, no limitations nor specific restrictions have been set by the simulation tool used (Java-based programming within the DESMO-J framework) and therefore the students were not forced to re-think about what really would be required to be represented in the model.

In the end both student projects produced valid and usable simulation models, but efforts for model implementation, in the course of experimentation eventually needed modification and visualization of results were quite different. Although the students were not well-experienced simulation experts which of course had an influence on the effectiveness of the model building process, those different modes of approaching and solving a simulation problem can be found in more professional simulations, too.

Results achieved from either model allowed responding to the initial question for the performance limit in terminal operation. Comparison of those results showed just some slight deviations which possibly were caused by differences in some basic technical and layout parameters, such as crane speeds and stacking module dimensions, due to different assumptions. In addition to this varying storage/retrieval strategies have been used. Although the total of these differences is consequently represented by the deviation of results, it also can be stated that results are quite similar. This finally allows concluding that despite of different modelling approaches similar simulation results could be achieved.

Nevertheless, different modelling approaches and simulation tools used resulted in very different ways of achieving the intended outcome. Simulation models were as quite individual as resulting trace files were - especially what concerns level-of-detail. Therefore, any standardized or formalized approach for trace file analysis and interpretation of output without involving the model developer (and at the same time user in this particular case) would have failed or delivered very general (rough) results only.

This first case study in an educational setting can just be the starting point for more detailed investigations on the impact a user's individual background and even personality might have on the design, implementation and use of a simulation model. In order to get a better insight and eventually derive some stereotypes that could be taken into consideration when designing the interpretation layer as shown in Figure 2, further case studies need to be run that involve professional simulation users of different backgrounds.

5. CONCLUSIONS

To understand the message of simulation results formal trace file analysis is one important step. The other one is the non-formal, more creative step of directly answering all questions that are of interest to the user (in our case the logistics expert). Precondition is to know (and understand) what the questions of the user are, but also the ability of the user to ask questions relevant to a particular problem. For the latter, the framework for trace file analysis and interpretation provides even further support: Typical questions no matter if they are of generic or specific nature help the user in identifying the problem or the questions to be asked or the aspects to be investigated. As discussed, this can be supported by the approaches for viewpoint description and defining observers or specifying analysis focus. Additionally, a pattern combining typical symptoms (i.e. visible situations or measurable characteristics) with the underlying problems causing those symptoms would be of huge benefit as this might also guide the user in truly understanding what happens in a specific material handling or logistics system.

Current approaches to trace file analysis mainly focus on deriving (standard) parameters and (typical) characteristics by use of statistical methods, clustering or reasoning. With this they provide results at data level (Figure 2) allowing basic interpretation based upon (externalized) domain-specific knowledge. This step works automatically for those aspects that can be formalized and shows limited results only for those aspects that require intuitive thinking by the user.

Against this background the paper concludes that it is necessary to see behind the simulation results by interpreting simulation output in order to understand their real message. This interpretation requires knowledge and understanding of the domain/ application area as well as mathematical and statistics skills. Trace file analysis supports preparation of interpretation steps but cannot fully replace the user who brings in objectives, motivation and focus of the simulation project as well as domain-specific experiences and competences to understand the message of simulation results. A sophisticated framework especially supports in reducing routine work like statistics calculations through incorporated powerful analysis tools and stimulating creative thinking by proposing, asking, suggesting in a really interactive communication between the simulation user and the computer.

REFERENCES

Helms, C., Strothotte, T., 1992. Oracles and Viewpoint Descriptions for Object Flow Investigation. *Proc. of the 1st EUROSIM Congress on Modelling and Simulation*, 47-53, Capri, Italy.

Kemper, P., Tepper, C., 2009. Automated trace analysis of discrete-event system models. *IEEE Transactions on Software Engineering*, vol. 35, no. 2, 195-208.

Neumann, G., 2005. Simulation and Logistics. In: Page, B., Kreutzer, W., eds. *The Java Simulation Handbook – Simulating Discrete Event Systems in UML and Java.* Aachen: Shaker, 435-468.

Neumann, G., 2007. The role of knowledge troughout the simulation lifecycle: what does a simulation model know? *Proc. of the 6th EUROSIM Congress on Modelling and Simulation*, vol. 2, TH-1-P12-5, Ljubljana, Slovenia.

Neumann, G., Page, B., 2006. Case study to compare modelling and simulation approaches of different domain experts. *Proc. of I3M 2006 - International Mediterranean Modelling Multiconference*, 517-522, Barcelona, Spain.

Neumann, G., Ziems, D., 2002. Logistics Simulation: Methodology for Problem Solving and Knowledge Acquisition. *Proc. of the 6th Multiconference on Systemics, Cybernetics and Informatics*, vol. XII, 357-362, Orlando/Florida, USA.

Tolujew, J., 1997. Werkzeuge des Simulationsexperten von morgen. *Proc. of Simulation and Animation '97*, 201-210, Magdeburg, Germany (Tools of the simulation expert of tomorrow, in German).

Wustmann, D., Vasyutynskyy, V., Schmidt, T., 2009. Ansätze zur automatischen Analyse und Diagnose von komplexen Materialflusssystemen. *Proc. of the 5th Expert colloquium of WGTL - Wissenschaftliche Gesellschaft für Technische Logistik*, 1-19, Ilmenau, Germany (Approaches for automatic analysis and diagnosis of complex material flow systems, in German).

AUTHORS BIOGRAPHY

Gaby Neumann received a Diploma in Materials Handling Technology from the Otto-von-Guericke-University of Technology in Magdeburg and a PhD in Logistics from the University of Magdeburg for her dissertation on "Knowledge-Based Support for the Planner of Crane-Operated Materials Flow Solutions". Between December 2002 and June 2009 she was Junior Professor in Logistics Knowledge Management at the Faculty of Mechanical Engineering there. In December 2009 she became full Professor on Engineering Logistics at the Technical University of Applied Sciences Wildau. Since 1991 she also has been working as part-time consultant in material handling simulation, logistics planning and specification of professional competences in certain fields of logistics. Her current activities and research interests are linked amongst others to fields like problem solving and knowledge management in logistics, logistics simulation and planning. She organises or co-organises workshops and conferences, supports international programme committees of various conferences, and has been or is being involved in a couple of research projects in these fields. Gaby Neumann has widely published and regularly presents related research papers at national and international conferences.

Juri Tolujew is a project manager in the Department for Logistics Systems and Networks at the Fraunhofer Institute for Factory Operation and Automation in Magdeburg (Germany). He received the Ph.D. in automation engineering from the University of Riga in 1976. In 2001 he received his habilitation degree in computer science from the Otto-von-Guericke University of Magdeburg. His research interests include simulation-based analysis of production and logistics systems, protocol-based methods for the analysis of processes in real and simulated systems as well as mesoscopic approaches to simulation.

Modelling Country Reconstruction based on Civil Military Cooperation

Agostino G. Bruzzone
McLeod Institute of Simulation Science Genoa- DIPTEM
University of Genoa
Via Opera Pia 15, 16145 Genova, Italy
Email agostino@itim.unige.it – URL www.itim.unige.it

Francesca Madeo, Federico Tarone
Simulation Team
Via Cadorna 2, 17100 Savona, Italy
Email {francesca.madeo, federico.tarone}@simulationteam.com – URL www.simulationteam.com

ABSTRACT

This paper provides a general overview about the use of Modeling & Simulation techniques as support to training, planning and decisions making in Country Reconstruction, after wars, natural disasters, large crisis and conflicts. In particular the authors focus on CIMIC (Civil - Military Cooperation) activities and on CIMIC process in asymmetric wars. One goal of this research is to introduce a new Conceptual Model that can connect Human Emotions (fear, trust, anger…) to something or someone in scenarios generated by Computer Generated Forces (CGF). This interest resulted from the conviction that the success of a CIMIC Operation derives from the counterinsurgents capacity in separating local population from rebels. So, the intent is to model military actions' effects (positive or not) on civilians' emotions.
In the first part of the paper current applications of IACGF (Intelligent Agents for Computer Generated Forces) are examined. In the second part, three different real cases of CIMIC operations are taken back to study CIMIC process and to identify typical phases and activities and typical actors. In the third part conceptual model is given to reproduce CIMIC operations' effects in terms of trust and gratitude toward military forces and fear or anger towards rebels or terrorists.

1. INTRODUCTION

Modelling and Simulation (M&S) are extensively used in a wide range of military applications, from development and validation of new systems and technologies to operations analysis and assessment to training support for combat situations. In military areas (Exercise, Defence Planning, Training and Education, Support to Operations), the importance of M&S is steadily increasing.
In particular, there are a lot of simulation systems good for providing training environments: Computer Aided Exercises (CAX) is a well known example. Successful results are achieved in the development of digital battlefields, by using joint and single service simulation system with different complex level and aggregation. These systems allow a reduction in cost and an increase of possible investigating scenarios.
It's important to consider into new models that [7]:

- New forms of threats to "the West" are spreading over. In fact during the 20th century, military modeling and simulation were dominated by classic "force on force" engagements, battles, and campaigns, while now peace operations, counter- terrorism, counter-narcotics, counter-proliferation, information warfare, or rules and governmental power recover for fledgling democracies and free market economies are becoming more relevant than in the past.
- New enemies for military forces are represented by paramilitary organizations, insurgencies, guerrilla forces, terrorists, drug cartels, hackers, media warriors, and ethnic or religious mobs are new enemies for military forces.
- Military missions success is increasingly influenced by religious, cultural, and humanitarian considerations that have not been part of traditional warfare.

However, the vast majority of existing models don't treat these phenomena in any reasonable way. For this reason, the use of Computer Generated Forces (CGF) is a need to support this kind of simulation. CGF are automated or semi-automated entities (such as tanks, aircraft, infantry) in a battlefield simulation that are generated and controlled by a computer system, perhaps assisted by a human operator, rather than by human participants in a simulator.
In the last years, the nature of conflicts has changed from "force to force" battles to unconventional ones, in which civilian are involved and become the key of operations success. So the necessity to evolve the existent CGF/SAF increases, with the awareness that "What's needed from defense simulations today are models which can take into account the messy decision making processes of commanders and troops in the face of incomplete, conflicting, and sometimes wrong information in an atmosphere in which the rules and constraints upon which decisions are based are neither clear nor static" [14].
In the last few years, significant advances have been made by the Computer Generated Forces (CGF) and Semi-Automated Forces (SAF) communities to make synthetic military environments more realistic.

Today, after having acquired totally or partially the capability of modularity and providing significant enhancements on main models accuracy, researchers are investigating on new interesting aspects, among which:

- Full level interoperability and real time distributed simulation
- Defining moderator (fatigue, stress,…) for human behavior models which usually represent perfect soldiers
- Enhancement (and often providing) the representation of low intensity conflict, multi-sided, without clearly identified friends, enemies or neutrals, civilians, non governmental organizations, in urban environments.

In particular there is a clear problem in CGF lack of fitness to the real operational planning, problem that requires to face the following issues: development of realistic virtual environments and at the same time CGF adaptable to the planner needs, creation of database of reusable CGF for different frameworks and implementation in the CGF of the possibility to modify its behavior based on clear and understandable parameters settings.

To overcome these limitations in current CGFs, synthetic entities are either controlled directly by a human or have their behavior managed by a human.

The lack of realism and full autonomy of synthetic entities thus limits CGF ability to replace human operators. Obviously, a more realistic way to model this kind of scenarios is needed: something that reproduces human behavior, including plausible mistakes and correct decisions.

A successful result was achieved by the authors with the development of PIOVRA (Poly-functional Intelligent Operational Virtual Reality Agents) Intelligent Agents. In fact new CGFs, able to simulate "Intelligent" behavior, filling up the gap between user requirements and current available CGF performances, were created. PIOVRA Project represents an important experience in advanced Human Behavior Modeling within an Interoperable Framework [3].

2. COUNTRY RECONSTRUCTION AND CIMIC REAL CASE STUDY

This research is mainly concentrated on the CIMIC modeling & simulation by the use of IACGF (Intelligent Agent for Computer Generated Forces) applications in asymmetric warfare contexts. Generally, the strategy of conventional warfare prescribes the conquest of the enemy's territory and the destruction of his forces. Parts in conflict have similar military power and resources and rely on tactics that are similar overall, differing only in details and execution. In asymmetric warfare, belligerents, whose relative military power differs significantly, or whose strategy or tactics differ significantly, are involved. In this case it's important that new CGF percept the presence of different ethnic civilian groups on the territory [10].

CIMIC operations are applied in the following situations [6]:

- Stabilization of an urban area where different ethnic populations, police forces, political movement agitators, terrorists and gangs act close to the military forces, trying to maintain international peace and security.
- Agitation and incidents that are directly linked with the presence and missions of the military forces on the ground
- Possible demonstrations, riots, lootings, kidnappings, murders and attack against military forces could occur.

CIMIC (Civil - Military Cooperation) activities are becoming very necessary to restore ordinary activities in a civil country. CIMIC is the military answer to new needs of operative efficacy in international operations (peacekeeping or in general Crisis Response Operations).

MoD (Ministry of Defense) defines CIMIC as follows: "The main goal of CIMIC outside national ground is to contribute to the achievement of civil objectives in all fields (justice, culture, economy, social, security…) to rebuild socio- economic tissue in the area in crisis. It is an integrated part of crisis management's processes and its role is very important during initial phases when Civil Organizations are not able to satisfy needs of local populations and institutions" [13].

CIMIC contributes mainly to:

- Restore the contact with the population, with local and international authorities
- Give support to the population
- Contribute to the economic restart.

CIMIC Operations start from basic elements that are linked to life and health**:** water (with wells building or rehabilitation), human health (with the joint medical service's support), cattle (with vet support particularly appreciated by pastoral populations such as the Afghan ones) and education. Specific and priority attention must be paid to children and women. At last economic actions are required, above all, because country stabilization goes through the restart process of its economic activities, from the lowest local level up to the national one.

In particular the solution of a crisis is the result of a comprehensive approach to ensure cooperation and coordination between civil and military. The aim is to establish two kinds of relationships: on one hand with the local authorities, with influent people, with the population, and on the other hand with the international organizations (UN, EU, the Red Cross, etc.), and the non governmental organizations that are on the theatre. CIMIC Modeling must thus represent a complex scenario where all actors (civilian and military) have not the same needs nor do they have the same centers of interest. In any case it's necessary to establish a way for sharing knowledge, experiences, researches, know-how between military

and civilian actors, scientist, consultants and humanitarian organizations [4].

Case of U.S. Army in Vietnam (1959- 1975)

The Vietnam War, also known as the Second Indochina War, was fought between the communist North Vietnam, supported by its communist allies, and the government of South Vietnam, supported by the United States and other anti-communist nations.

The Viet Cong, a lightly armed South Vietnamese communist-controlled common front, largely fought a guerrilla war against anti-communist forces in the region.

The United States entered the war to prevent a communist takeover of South Vietnam as part of their wider strategy of containment.

The United States Army entered the Vietnam War with a doctrine well suited to fighting conventional war in Europe, but worse than useless for the counterinsurgency it was about to combat. The U.S advisors in Vietnam were unprepared by nature or training to do anything except build a Vietnamese army in their own image and likeness. The U.S. military themselves learned during this period of gradual disintegration the true nature of the battle in which they were engaged. This was an unconventional, internal war of counterinsurgency rather than a conventional struggle against an external foe. It was a battle for the "hearts and minds" of the indigenous (and especially the rural) population rather than a contest to win and hold key terrain features. It was an intermeshed political-economic- military war rather than one in which political and economic issues were settled by military victory. So, new military tactics had to be developed and also new political tactics had to be devised and above all the two had to be meshed together and blended. Unfortunately, the army had neither the knowledge nor the desire to change its orientation away from conventional war. This factor conducted to the failure [16].

Case of DERB in Kosovo

Until 1989, Kosovo enjoyed a relatively independent status within the Federal Republic of Yugoslavia. However, in 1989, the Serbian leader Slobodan Milosevic forced the region under the control of Belgrade, depriving Kosovo of its former autonomy. Kosovar Albanians who made up 90 % of the population strongly opposed Milosevic's action. After the Serbian authorities struck down the opposition, the guerrilla movement Kosovo Liberation Army emerged in Albania and Nato launched Operation Allied Force by commencing air strikes on Kosovo. In this context the intent is to analyze cooperation between civilian actors and Dutch Engineering Relief Battalion (DERB). A model was developed and applied to eight civil military cooperative arrangements (see figure 1).

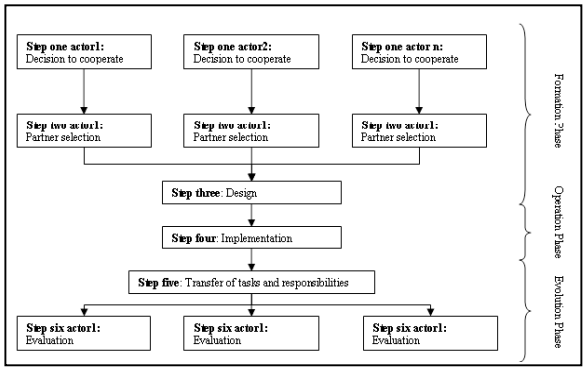

Figure 1. Process Model for civil-military cooperative arrangements in Kosovo case.

Researchers argued that the development of a cooperative arrangement is similar to a relationship between people: first two people meet, then they fall in love, next they engaged and finally they grow old together or sometimes divorce. Although not one cooperative arrangement travels the same path, a successful arrangement generally unfolds in several overlapping phases: the formation phase, the operation phase and the evolution phase.

These phases were organized in six steps:

- **Decision to cooperate.** On 11 June 1999 the assignment to form and prepare an engineering battalion was issued by the staff of the Dutch first division. A reconnaissance party, shortly followed by an advance party, was deployed in Kosovo to investigate construction sites suitable for housing the Dutch contingent over three compounds and to conduct an initial humanitarian assessment by contacting MNB South, present humanitarian organizations and the local authorities and representatives. In cooperation with the Human Resource Coordination (HRCC) and a German Cimic company, a detailed assessment was made, predominantly regarding the shelter situation. Three criteria were defined to determine priority areas in which humanitarian assistance was most needed: the degree of damage done to the villages (houses demolished at least 70 percent were considered high priority cases, small villages were top priority; the altitude of the priority areas (at an altitude from 500 meters the winter had usually started in October; the repatriation of refugees was taken into account (villages to which many former inhabitants had returned were considered priority areas).
- **Partner selection.** Based on the identified civilian actors, DERB undertook several actions in its search for appropriate partners for cooperation. These actions involved (informal) conversations between Cimic employees and representatives of humanitarian organizations. DERB implicitly used different criteria to select partners, such as partner's availability of financial means and capabilities, compatibility of personalities, compatibility of national and organization cultures.

- **Design.** After selecting a partner, DERB and the selected humanitarian partners usually concluded their agreement on cooperation verbally or by a written contract in which parties declare their intents and working plans.
- **Implementation.** The actors were involved in the actual implementation of assistance activities in several ways.
- **Transfer of tasks and responsibilities.** Most cooperative arrangements of DERB and its civilian partners ended as planned. While ending a cooperative arrangement, tasks and responsibilities were usually transferred to the civilian actors. In a few cases the military remained responsible after termination of the cooperative arrangement.
- **Evaluation.** Having transferred the tasks and responsibilities, little attention was generally paid to evaluation of the cooperative arrangement. The Dutch government evaluated the activities of the Dutch troops in Kosovo. With respect to DERB the report noticed that cooperation with humanitarian organizations and MNB South was good but lacked an integral policy [16].

Case of Algerian War of Independence (1954-62)

The war in Algeria offers most of usual characteristics of a revolutionary war. On the insurgent side, a small group of leaders aim at overthrowing the existing order. On the counterinsurgent side, a government endowed with vastly superior strength, but ideologically weak and burdened with the responsibility of maintaining law and order, reacts to stay in power. Experience shows that in this sort of war the political factors are just as important as the military ones, above all in Algeria where there was practically no military contest in the conventional sense owing to the superiority of the French armed forces in size, equipment, training and command. The insurgent leaders in Algeria were able to:

- Create and develop a strong, tested revolutionary party
- Gather around it as large as possible a popular front
- Then, and only then, proceed to open violence and initiate guerrilla warfare
- When bases have been acquired, organize a regular army and wage a war of movement, having achieved overall superiority over the opponent, launch a final annihilation campaign.

On the counterinsurgent camp, Algeria was administrated like any French metropolitan area. The territory was divided into three departments, each headed by a "prefect". The success of the FLN strategy depended on the solution of three essential problems: armament for the guerrillas, the psychological effects of their operations and control of the Moslem population. In this situation, the war could be won only if French forces succeeded in divorcing the rebels from population. There was the conviction that with psychological action the population could be manipulated. The support from population was the key to the whole problem; support meaning not sympathy or idle approval but active participation in the struggle. In any circumstances, whatever the cause, the population is split among three groups: an active minority for the cause, a neutral majority and an active minority against the cause. It's necessary to help the pro minority to emerge, assuring military's firmness of their intentions [10].

This result can be achieved by a series of well-defined political-military operations:

- Selection of the area on the basis of demographic and social characteristics (density of population, the foothold that the population offers to military action, the degree of infection, the smallest cleavage within the population, the population's access to counterinsurgent 's propaganda).
- Destruction or expulsion of the large bands
- Implanting the pacification units not in positions having a military value, but where the population lives.
- Establishing contact with the population, imposing firmly counterinsurgent's will, controlling their activities and movements so as to cut them off from the rebels, building schools and dispensaries.
- Control of the population (dividing villages in more parts, making a census of houses and families).
- Gathering intelligence, collecting information about rebels.
- Propaganda during this period.
- Destruction of the rebel cells considering that population fears the rebels more than it fears counterinsurgents and the entire population participates in the rebellion and everyone knows the members of the political cell in his village.
- Installation of provisional elected officials.
- Search for activities, defining the activist.
- Grouping and educating the activist.

3. CIMIC PROCESS ANALYSIS

Studying the described cases, the authors defined a process for CIMIC Operations. In particular they take in consideration that:

- Significant results are achieved by the Armed forces on relying on the population, with very little troops and equipment
- After the first phase of the military action, it is in the longer term that stabilization can be consolidated and made to last
- CIMIC Operations aim to gain populations trust, assisting the country and its inhabitants

So it's possible to identify a common process of leading CIMIC activities. In particular one can recognize these phases:

- **Planning phase**: education of military forces to the cultural and social attitudes of local

population, collection of knowledge and information about countries features and relevant people, propaganda towards population, selection of specific areas of interest.

- **Execution phase:** getting in touch with local population, obtaining trust by people, executing "good" actions towards people's healthy, education and security.
- **Maintenance phase**: maintenance of peace, isolating rebels and helping local population to rebuild their State.

A flow chart of CIMIC Process is represented in the following figure:

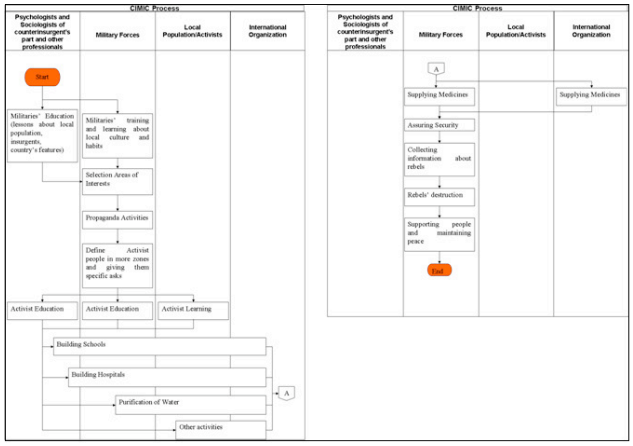

Figure 2. CIMIC Process

Activities to model are proposed as following:

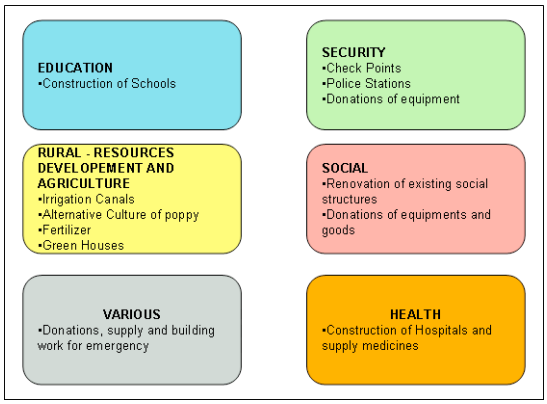

Figure 3. CIMIC Activities

4. A CONCEPTUAL MODELS TO REPRODUCE HUMAN BEHAVIORS

The conceptual model developed by the authors for this research is based on previous experience carried out in PIOVRA Project; in fact PIOVRA (Poly-Functional Intelligent Operational Virtual Reality Agents) represented the initial step forward to the creation of innovative CGF (Computer Generated Forces) able to demonstrate intelligent behavior.

The PIOVRA CGF was developed in reference to a set of features devoted to measure their capability to cooperate and compete as well as their attitude to incorporate human characteristics (i.e. fear, aggressiveness, fatigue and stress); PIOVRA CGF was tailored to reproduce population, demonstrations, ethnic groups, political parties, gangs and paramilitary forces, so a broad spectrum of entities characterizing asymmetrical warfare. Due to these reasons it is natural to consider the necessity to develop a new type of CGF, titled IACGF (Intelligent Agent for Computer Generated Forces) devoted to simulate complex behaviors. In particular, IACGF will be initially tested in CIMIC (Civil Military Co-operation) operations and will benefit of the conceptual models created for PIOVRA Project. IACGF will be focused on complex and critical applications involving both operational planning and training. The original PIOVRA CGF was driven by intelligent software agents and specific scenarios of urban disorders were used for demonstrating their capabilities. In fact the authors consider as critical the creation of the IACGF as HLA federates so that other simulation systems can be federated; therefore PIOVRA was demonstrated as an HLA federation interoperating with JTLS (Joint Theatre Level Simulator). In similar way it is expected that the new IACGF will be able to be interoperable with other simulators taking care of reproducing the factors and effects that characterise CIMIC activities; it will be useful to benefit from the legacy of PIOVRA CGF for specific aspects: i.e. the detection of different ethnic civilian groups on the territory and the relative perceptions. The use mode for the IACGF in CIMIC operational planning will include: training activities for Planners and/or Operations Commanders; in these case IACGF will operate in realistic scenarios in which the Decision Makers are able to choose among different options in presence of stochastic components and with a higher degree of uncertainty.

It is critical to be able to reproduce different basic behaviours in the units including:

- Friends
- Enemies
- Suspects (including terrorists)
- Neutrals

Obviously, dealing with CIMIC operations, it is fundamental to model realistic profiles including psychological and social modifiers as well as parameters such as stress level or level of aggregation. The capability of reproducing such behaviour is based on the use of Artificial Intelligence with special attention to the fuzzy logic applied in combining and estimating parameters based on membership functions and FAM (fuzzy allocation matrices). The approach to create IACGF for CIMIC scenario is based on OODA (Object Oriented Design and Analysis), from this point of view the following main type of objects have be defined:

- **Comportment Objects**, representing behavioural profiles corresponding to organisation, institutions, parties and group of people that define the general attitude, the characteristics of their elements (i.e. training level, social status mix, etc) and the pool of resources available

- **Action Objects**, representing units on the ground related to specific Comportment object and operating based on general task or specific orders and mutually interacting other action objects and with their comportment object.

In IACGF for CIMIC it will become very important to add social and cultural aspects (religious faith, beliefs, values, education, etc.) to psychological aspects (stress, fear, uncertainty, vulnerability, coolness). In particular, it's possible to distinguish negative emotions (anger, annoyance, unhappiness towards victims, for others, attacks and attackers, towards government) from positive ones (trust, optimism, thankfulness, relief, pride) and then to investigate theoretical links between people emotions and military actions. So, beginning from Psychological modifiers developed for PIOVRA Project and able to reproduce unit features, new elements will be added to new IACGF such as the capability to reproduce social network, creating dynamics interactions among people and among groups of people with own sociological and cultural characteristics.

With this research authors want to introduce new feelings, such as Trust or Gratitude or Recognisance, and above all to link these feelings not only with events that generate them, but also with people who are the makers of them. For instance, an explosion can generate fear in local population and, consequently, trust towards units that protect them and anger towards people responsible of the explosion. So, considering a CIMIC scenario, for instance the Disarmament Demobilization and Reintegration (DDR) of rebels, the main objective is to increase trust towards counterinsurgents and fear towards insurgents or rebels.

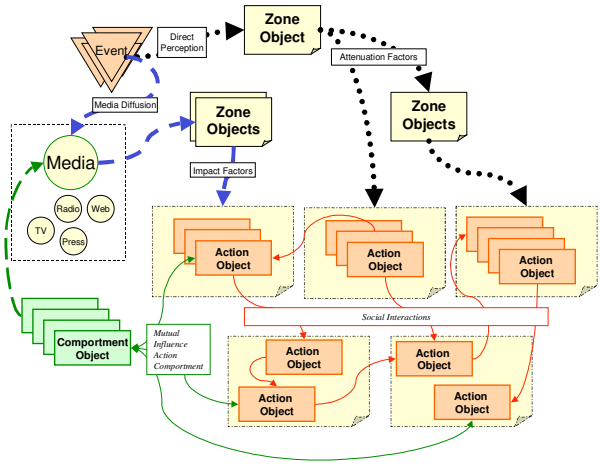

Figure 4. Fear Diffusion Model

Focusing attention on fear, this is related to events; in fact each event could generate a Risk/Danger Perception that corresponds to a *Generated Fear Level* modelled as a stochastic continuous variable between a minimum and maximum value related to the event type itself and modified by factors related to:

- Direct Perception: in this case there are attenuation factors that refer to the zone type where event happens, weather conditions and distance respect the action objects.
- Media Diffusion: in this case the factor represent the impact related to time and influence of different media
- Relata Refero: where the diffusion is going through the social network with mitigation factors due to the social communications.

The Generated Fear Level is compared with the *Action Object* properties related to social, psychological, cultural dynamic characteristics as well as its party attitudes and its current status; these elements affect the way each Action Object perceives the potential Fear generated by the event and the Human Behavior modifiers determine the reactions and are affected by different aspects such as fatigue and stress level of the unit as well as from the size/force of the Action Object respect the on-going event.

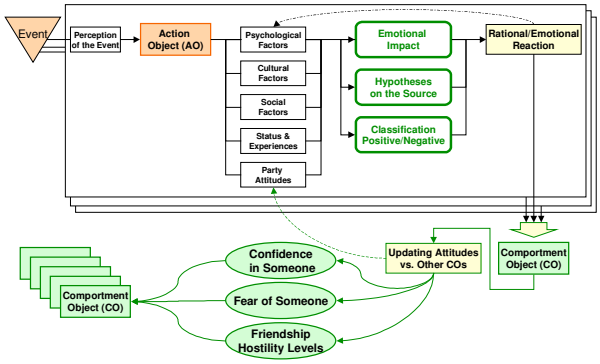

Figure 5 Event Impact Model

The reaction of the Action Object generates feedback in its own characteristics: i.e. improving or decreasing his capability to face such threats in future. In addition each Action Object generates an event assignment to a specific source to guarantee an upgrade of correspondent Comportment Object attitudes. These Attitudes are defined by membership functions applied to classes representing the attitude of a Comportment object respect another one, usually the following five classes are used:

Very hostile
Hostile
Indifferent
Friendly
Very Friendly

The element of this vector are evolving independently for each comportment object and attributed to action object and there is a mutual influence due to the event and actions during simulation run.

The computation of Comportment Objects attitudes respect another comportment object, based on the action object reactions and their perception of the event impact, is proposed the specific relations.

In fact the following relations introduce the concept of *Pool* representing the people of an action object that have been not yet instantiated in Action Objects; even these people are subjected to influence of events as an additional "special" action object.

$$A_i^{Pool_{C_{zw}}} = \frac{Ao_i^{C_{zw}} + An_i^{Pool_{C_{zw}}} \mathrm{Im}^{Pool_{C_z}}}{1 + \mathrm{Im}^{Pool_{C_z}}}$$

$$A_i^{C_{zw}}(j) = \frac{Ao_i^{C_{zw}} + An_i^{A_{jw}} \mathrm{Im}^{A_j}}{1 + \mathrm{Im}^{A_j}}$$

$$A_i^{C_{zw}} = \frac{N^{Pool_{C_z}} A_i^{Pool_{C_{zw}}} In^{Pool_{C_z}} + \sum_{j=1}^{N^{C_z}} N^{A_j} A_i^{C_{zw}}(j) In^{A_j}}{N^{Pool_{C_z}} In^{Pool_{C_z}} + \sum_{j=1}^{N^{C_z}} N^{A_j} \cdot In^{A_j}}$$

$$\sum_{i=1}^{N_{classes}} A_i^{C_{zw}} = 1$$

A_i^{Czw} Attitude element in term of i-th class (i.e. very friendly) level for the z-th Comportment Object respect the w-th comportment object after the current event

$A_i^{Pool\ Czw}$ Attitude element in term of i-th class (i.e. very friendly) level for the Pool element of the z-th Comportment Object respect the w-th comportment object after the current event

Ao_i^{Czw} Old level for i-th attitude class (i.e. very friendly) for the z-th Comportment Object respect the w-th comportment object, before current event

$An_i^{Pool\ Czw}$ New level for i-th attitude class (i.e. very friendly) for the z-th Comportment Object respect the w-th comportment object, in relation to the current event

$Im^{Pool\ Cz}$ Impact perceived by the Pool of the z-th Comportment Object of the current event

$A_i^{Czw}(j)$ Attitude element in term of i-th class (i.e. very friendly) level for the j-th Action Object belonging to the z-th Comportment Object respect the w-th comportment object after the current event

An_i^{Ajw} New level for i-th attitude class (i.e. very friendly) for the j-th Action belonging to the z-th Comportment Object respect the w-th Comportment Object in relation to the current event

Im^{Aj} Impact perceived by the j-th Action Object of the current event

$N_{classes}$ Number of classes representing attitudes

N^{Cz} Number of Action Objects of z-th Comportment Object

$N^{Pool\ Cz}$ Number of people in the Pool of the z-th Comportment Object

N^{Aj} Number of people in the j-th Action Object

$In^{Pool\ Cz}$ Influence of the Pool of the z-th Comportment Object

In^{Aj} Influence of the j-th Action Object

It is important to note that the IACGFs relate Emotions such the fear proposed in the previous example to Scenario Actors; in addition it is even important to introduce the concept of fear mitigation on medium, long term. In fact, if a negative event (i.e. explosions) recurs several times, people get used to this particular condition and fear increasing stops.

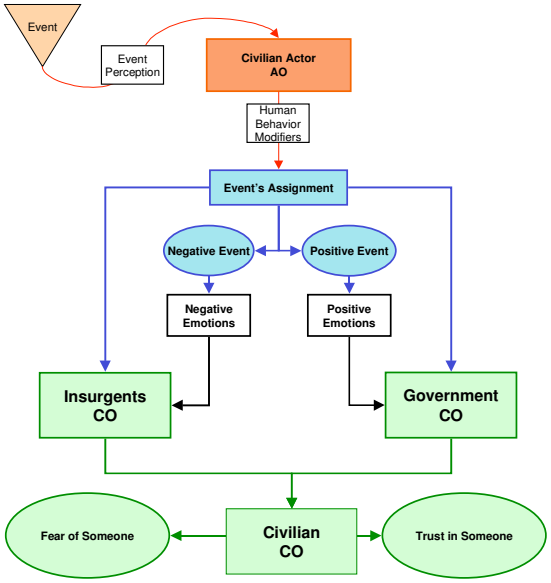

Figure 6. Fear Diffusion Micro Model

5. EXPERIMENTAL SCENARIOS

Based on previous described models it was created a simulation framework reproducing action objects belonging to different comportment objects in a town of middle size; the simulator, titled PSYOPS (Psychological Operation Simulator) was implemented in C++ for Windows ™ and its GUI is proposed in following figure.

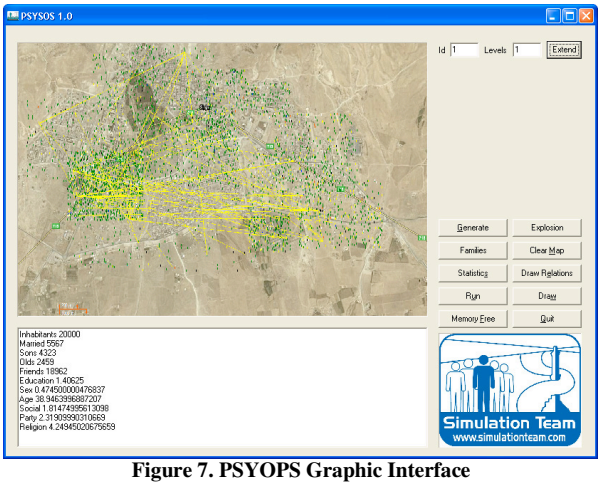

Figure 7. PSYOPS Graphic Interface

This simulator generates the population and creates stochastic social network consistent with constraints related to cultural level, age, sex, religion and social status of the inhabitants; obviously this represents an ideal framework to test the impact of critical events on the population.

Each individual in this case is an action object subjected to a set of activities around the clock corresponding to its status; agents direct the entities in term of movements (i.e. from house to work), actions (i.e. work, home activities, fun time), etc.

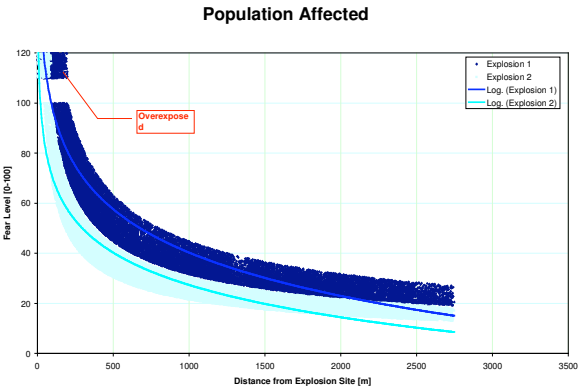

Figure 8. Fear due to Explosion

For testing diffusion in the population it was injected in the town an explosion and measured as people perceived it. The figure 8 provides a report of the fear level due to direct observation in case of two different explosions during early morning in rush hours; the results present the fear level of each individual in correspondence to its distance from explosion site considering a maximum threshold.

6. ACKNOWLEDGEMENTS

The authors are glad to thank PIOVRA & CAPRICORN Projects Sponsors: EDA (European Defence Agency), Italian and French MoD (Minister of Defence) for the support provided by these R&D initiatives.

7. CONCLUSIONS

This paper presents the initial research for the development of a new kind of Intelligent Agents devoted to simulate CIMIC Operations, taking in consideration psychological, social and cultural characteristics of units involved. In particular, starting from the successful results of previous Projects (i.e. PIOVRA), authors summarised case studies to be used in validation and verification of these simulation as well as model to attribute emotions to entities in order to consider the impact of CIMIC on the different players in complex scenarios; currently the authors are working to adapt their new IACGF to CIMIC scenarios; in this process new issues have been identified and some new models have been developed.

8. REFERENCES

1. Cinardo G. (2007) “Air Force Research Laboratory, Expert Common Immersive Theater Environment – Research and Development (XCITER&D) User’s Manual Version 1.0”, Mesa, Arizona, USA, April
2. Amico Vince, Guha R., Bruzzone A.G. (2000) "Critical Issues in Simulation", Proceedings of SCSC, Vancouver, July
3. Bocca E., Pierfederici, B.E. (2007) “Intelligent agents for moving and operating Computer Generated Forces” Proceedings of SCSC, San Diego July
4. Bruzzone A., Massei M., Caussanel J. (2006) “Survey current CGF Reporting Current Situation” PIOVRA EDA Technical Report, Genoa, Italy
5. Bruzzone A. G et al. (2004) "Poly-Functional Intelligent Agents For Computer Generated Forces", Proceedings of the 2004 Winter Simulation Conference Washington D.C., December
6. Bruzzone A., Massei M., Brandolini M. “Demonstration for human behavior modeling within civil disorder scenarios”.
7. Caussanel J., Frydman C., Giambiasi N., Mosca R. (2007) “State of art and future trend on CGF” Proceedings of EUROSIW2007, Santa Margherita, Italy, June
8. Fletcher M., (2006) “A Cognitive Agent-based Approach to Varying Behaviours in Computer Generated Forces Systems to Model Scenarios like Coalitions”, Proceedings of the IEEE Workshop on Distributed Intelligent Systems: Collective Intelligence and its Applications,
9. Galula D., (1964) “Counterinsurgency Warfare”, Praeger Security International
10. Galula D., (2006) “Pacification in Algeria 1956-1958”, Rand Corporation,.
11. Haugh, B. and Lichtblau, D., (2001) “An Information Tech-nology Support Strategy for PSYOP Impact Analysis,” IDA Paper P-3587, Institute for Defense Analyses, February
12. Haugh, B. and Lichtblau, D., (2000) “PSYOP Impact Analysis White Paper,” IDA Paper P-3060, Institute for Defense Analyses, August
13. Hue B., EMA/CPCO2J9, (2007) “What Do CIMIC Activities Bring to Stabilization1 Operations”, France, Doctrine General Military Review #12, page 29
14. Kallmeier V., Henderson S., McGuinness B., Tuson P., Harper R., Price S. Storr J. (2001) "Towards Better Knowledge: A Fusion of Information, Technology, and Human Aspects of Command and Control", Journal of Battlefield Technology, Volume 4 Number 1.
15. Lichtblau, D., et al., (2004) “Influencing Ontology,” ex-tended abstract in Behavior Representation in Modeling and Simulation Conference
16. Rietjens S.J.H., M. Bollen, (2008) “Managing Civil-Military Cooperation”, Military Strategy and Operational Art
17. Nacer A., Taylor A., Parkinson G. (2007) Comparative Analysis of Computer Generated Forces’ Artificial Intelligence, Ottawa
18. Thagard, P., (2000) Coherence in Thought and Action, Cambridge, MA: MIT Press

A METHODOLOGY FOR THE DESIGN OF SIMULATION CAMPAIGNS BASED ON POPULATION VARIANCE CHARACTERIZATION

Andrea Grassi [(a)], Elisa Gebennini [(b)], Giuseppe Perrica [(c)], Cesare Fantuzzi [(d)], Bianca Rimini [(e)]

Dipartimento di Scienze e Metodi dell'Ingegneria, Università degli Studi di Modena e Reggio Emilia
Via Amendola 2 – Pad. Morselli, 42122 Reggio Emilia, Italy.

[(a)]andrea.grassi@unimore.it, [(b)]elisa.gebennini@unimore.it, [(c)]giuseppe.perrica@unimore.it,
[(d)]cesare.fantuzzi@unimore.it, [(e)]bianca.rimini@unimore.it,

ABSTRACT

Manufacturing industrial systems are complex systems whose performance is characterized by interactions among different parts of the system as well as by stochastic phenomena affecting the operation of the parts themselves.

A key aspect in studying a complex system is the ability to model its evolution over time and, as a consequence, to identify, from a statistical point of view, the trend of the performance measures (i.e. productivity) over time. Discrete event system simulation (DESS) is certainly the widespread technique adopted to this aim.

In this paper, a methodology to characterize the trend of the variance of the population for a flow-line production system is developed. The knowledge of the relation between the variance of the population and the system run time allows the analyst to better design simulation campaigns and define warm-up period. Moreover, this result is also useful when in-field tests have to be designed to certify performances of a newly deployed system.

Keywords: simulation campaign design, transitory analysis, variance estimation, flow-line systems

1. INTRODUCTION

Manufacturing industrial systems are complex systems whose behavior is characterized by the operation of several parts (i.e. machines performing processes on products) and the interactions among the parts themselves. Frequently, stochastic phenomena affect the operational state of the machines, and, as a consequence, disruptions of production flows are stochastically propagated all over the manufacturing system.

As an example, if we refer to a production line, operative conditions of machines positioned along the line is determined by failures and repairs of the process each very machine is executing on products, while disruptive interactions between the machines are due to interruptions of the production flow.

The optimal design of a manufacturing system is related to the definition of performance targets on machines (e.g. nominal capacity, reliability parameters, etc.) and of the structure of the system (e.g. buffer location and size), so as to reach a desired performance of the whole system.

Since the behavior of the system is influenced by stochastic phenomena, performance parameters have to be computed by means of probabilistic models, aiming at providing their steady state value, or estimated by adopting methodologies able to reproduce the evolution of the system over a limited run time. Discrete event system simulation (DESS) is the widely adopted approach for that latter case.

Adopting such an approach to asses system performances, and considering that it is impossible to execute a unique infinite run, we face with the need to execute several simulation runs reproducing different histories of the system, then running the same system with different sequences of random events. Hence, the performance measured in each run represents a different individual withdrew from the population of the individuals constituting all the possible values of the system performance measured at the specified run time. The set of the individuals is then a sample withdrew from the population.

Hence, once the sample is obtained, statistical analysis methodologies have to be used to obtain an estimation of the system performance in terms of confidence interval (Law, 1983). The wider the confidence interval, the lower the precision in assessing the true value of the performance measure is.

The variance of the sample is a key factor directly influencing the amplitude of the confidence interval (Montgomery and Runger, 2007). Moreover, the variance of the population is guessed with respect to the sample variance, thus producing a further extension of the confidence interval.

If we were able to directly compute the variance of the population with respect to some characteristics of the system, we would be able to restrict the confidence interval thus obtaining better estimation. Furthermore, knowing the trend of the population variance over run time will allow us to *a priori* define the right combination of simulation run length and number of runs to execute given a desired confidence interval. This

aspect becomes very important when in-filed tests have to be deployed to certifies the performance of the system. In such a situation, system runs are executed in real time, thus there is an implicit need to reduce to a bare minimum the total time required for the test.

This paper develops a methodology to determine the trend of the population variance over run time for flow-line structured manufacturing systems. The methodology is based on some analytical considerations and is supported by experimental evidence. It is also shown how this information can be used to design simulation campaigns or in-field tests guaranteeing a specified confidence interval of the performance measure estimation.

2. METHODOLOGY DESCRIPTION

Provided that the behavior of the system is affected by stochastic phenomena, a generic performance measure is described by means of a random variable (i.e. characterized by a mean value, a variance, and a probability density function) for any finite time. All of the mean value, variance and probability density function of the performance measure vary over time. Nevertheless, we can state that, if the system is ergodic, as time tends to infinite the mean value tends to the steady state asymptotic value of the performance measure. Consequently, the variance tends to zero and the random variable degenerates to a deterministic variable.

A number of studies were carried out in years to analytically derive trends of mean value and variance over time of performance measures of some canonical systems (Kelton and Law, 1985; Li and Meerkov, 2000; Tan, 1999).

Starting from the simplest case of a single machine operating with a Bernoulli like production process (Li and Meerkov, 2000) the mean and the variance of the number of units produced after t time steps $N(t)$ can be expressed as

$$\mathrm{E}[N(t)] = t\,p \tag{1}$$

$$\mathrm{Var}[N(t)] = t\,p\,(1-p) \tag{2}$$

Defining the productivity of the machine as

$$P(t) = \frac{1}{t} N(t)\,, \tag{3}$$

we can state that the mean productivity at t is

$$\mathrm{E}[P(t)] = \frac{1}{t}\mathrm{E}[N(t)], \tag{4}$$

while its variance is

$$\mathrm{Var}[P(t)] = \frac{1}{t^2}\mathrm{Var}[\mathrm{N(t)}]. \tag{5}$$

Hence, by substituting eq. 1 and 2 in eq. 4 and 5 we can obtain

$$\mathrm{E}[P(t)] = p\,, \tag{6}$$

$$\mathrm{Var}[P(t)] = \frac{p(1-p)}{t}\,. \tag{7}$$

Let's now consider the case of a machine characterized by a deterministic production rate but affected by failure and repair phenomena represented by continuous time Markovian processes. Tan (1999) determined the number of parts produced at time t, $N(t)$, and its variance. Considering the case in which the machine has a probability $r/p+r$ to be operational at time zero, such a variance is equal to

$$\begin{aligned}\mathrm{Var}[N(t)] = {} & \frac{p\,r\,(2-p-r)}{(p+r)^3}\,t + \\ & + \frac{2\,p\,r\,(1-p-r)}{(p+r)^4}\left((1-p-r)^t - 1\right),\end{aligned} \tag{8}$$

where p and r represent the failure rate and the repair rate, respectively.

By substituting eq. 8 in eq. 5 we obtain

$$\begin{aligned}\mathrm{Var}[P(t)] = {} & \frac{p\,r\,(2-p-r)}{(p+r)^3}\,\frac{1}{t} + \\ & + \frac{2\,p\,r\,(1-p-r)}{(p+r)^4}\,\frac{\left((1-p-r)^t - 1\right)}{t^2}.\end{aligned} \tag{9}$$

Hence, we can observe that the variance of the productivity of a machine has the following form

$$\mathrm{Var}[P(t)] = \frac{K}{t} + \circ(t)\,, \tag{10}$$

where K is a parameter to be determined. Having an exact mathematical solution for K allows us to exactly know the variance of the population, otherwise K could also be determined in an experimental way by fitting the variance of a large sample with the relation

$$\overline{\mathrm{Var}}[P(t)] = \frac{K}{t}\,. \tag{11}$$

Experimental observations, realized by means of simulation campaigns, showed that eq. 10 represents a good approximation also when longer lines (i.e. lines with several machines decoupled with buffers) are considered.

Another important aspect addressed is the identification of the mass probability function of the performance measure considered, in our case $P(t)$, that changes over time. The shape of such a mass probability function is certainly not Gaussian since the value of the productivity is limited between 0 and a maximum value depending by the characteristics of the system and of the machines.

Since the productivity derives from the sum of the independent random variables representing the units produced over time, according to the central limit theorem, the mass probability function of $P(t)$ asymptotically tends to a Gaussian. Hence, from a

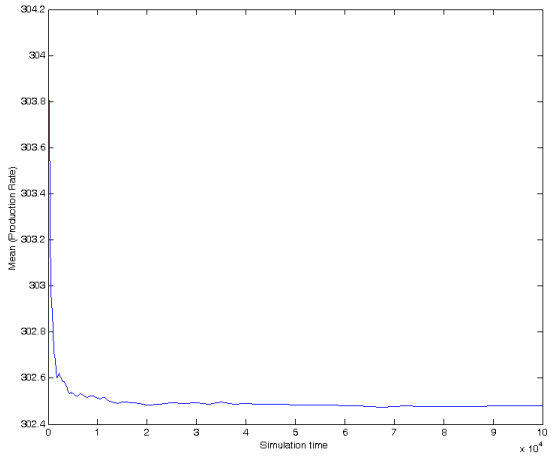

Figure 2: Mean trend.

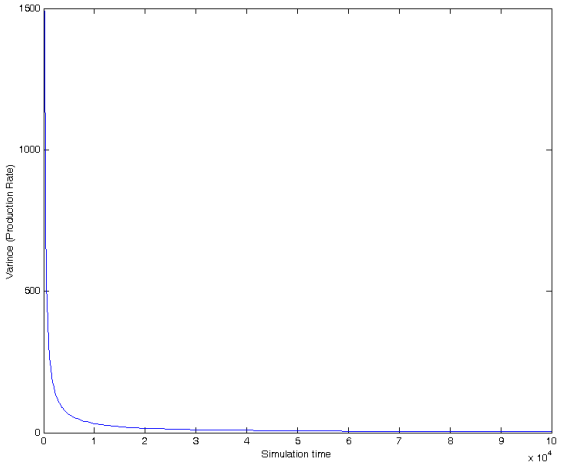

Figure 3: Variance trend.

certain time $t > t_0$ we can apply the inferential techniques explained in the next section.

3. ESTIMATION APPROACH

When dealing with simulation of stochastic processes, estimation of parameters of interest is provided in terms of confidence intervals. This approach states that the estimated range of value contains the true population parameter with a confidence of $(1-\alpha)\%$. That is, the method used to obtain this range, yields correct statements $(1-\alpha)\%$ of the time. The length of a confidence interval is a measure of precision of the estimation.

If $\overline{\vartheta}$ is the sample mean of a random sample of size n from a normal population with known variance σ^2, a $100\cdot(1-\alpha)\%$ confidence interval on ϑ is given by

$$\overline{\vartheta} - z_{\alpha/2}\frac{\sigma}{\sqrt{n}} \le \vartheta \le \overline{\vartheta} + z_{\alpha/2}\frac{\sigma}{\sqrt{n}}, \qquad (12)$$

where n is the sample size, $1-\alpha$ is the confidence level and $z_{\alpha/2}$ is the upper $100\cdot\alpha/2$ percentage point of the standard normal distribution. As it is possible to see in eq. 12, the larger the sample size, the narrower the interval is. Conversely, the larger the sample variability, the less the accuracy on the estimation is (Montgomery and Runger, 2007).

By substituting the approximate variance of eq. 11 in eq. 12 we obtain

$$\mathrm{E}[P(t)] - z_{\alpha/2}\sqrt{\frac{K}{t\cdot n}} \le \vartheta \le \mathrm{E}[P(t)] + z_{\alpha/2}\sqrt{\frac{K}{t\cdot n}}. \qquad (13)$$

4. NUMERICAL EXAMPLE

An exemplificative case study has been carried out to show how the methodology presented in this paper can be used to organize and design simulation campaigns.

Let us consider a simple production line consisting of two machines decoupled by a finite buffer (Figure 1).

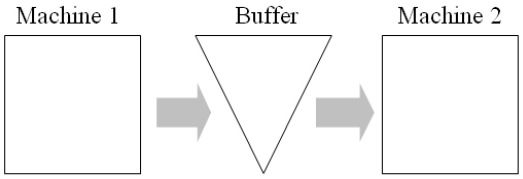

Figure 1: two-machine one-buffer line.

The input parameters of interest are as follows: production capacity (μ), failure rate (p) and repair rate (r) of each machine, and buffer size (N). The corresponding values adopted in the case study, derived from a real installation typical of the beverage/packaging field, are reported in Table 1 (where t.u. is for time unit).

Given the simulation model of such a system, a simulation campaign, consisting of 50000 runs of 10000000 time units [t.u.] length each, has been carried out. The performance measure of interest is the production rate $P(t)$ at any time instant t, i.e. the ratio between the number of produced items and the simulation time $t - t_0$. The production rate $P(t)$ has been captured at several time values over all the simulation length.

Table 1: Input Parameters

	Machine 1	Machine 2	Buffer
Capacity [itmes/t.u.]	400	400	-
Failure rate [1/t.u.]	0.01667	0.06667	-
Repair rate [1/t.u.]	0.083333	0.4	-
Size [items]	-	-	1500

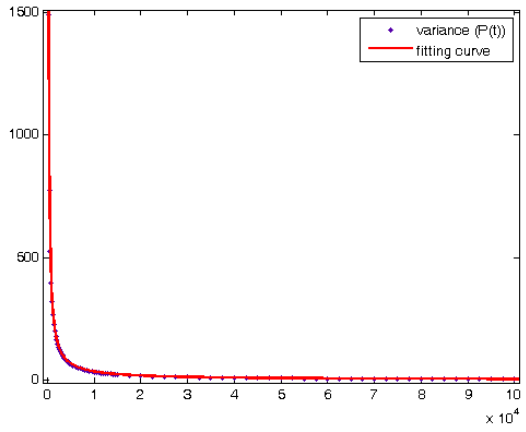

Figure 4: Fitting results.

At any capture time the sample mean $\mathrm{E}[P(t)]$ and variance $\mathrm{Var}[P(t)]$ were computed with respect to the simulated data. Figure 2 and Figure 3 depict the trend of $\mathrm{E}[P(t)]$ and $\mathrm{Var}[P(t)]$, respectively, against the simulation time *t*.

Note that the sample mean quickly approaches its steady state value. When analytical model for steady state performance computation are available, such the ones proposed in Gershwin (2002) and in Gebennini et al. (2009), the steady state value of the productivity can be conveniently *a priori* determined.

Focusing on the variance $\mathrm{Var}[P(t)]$, Figure 4 shows how the curve of $\mathrm{Var}[P(t)]$ can be properly fitted by the function reported in eq. 11. In this specific case, $K = 3 \cdot 10^5$.

In order to estimate the goodness of the fit, the R-square (i.e. the square of the multiple correlation coefficient and the coefficient of multiple determination) is computed. Specifically, its value is about 0.99, very close to 1 (i.e. the value corresponding to a perfect fit).

This result proves that the form of the approximated variance reported in eq. 11 holds also when complex lines are dealt with.

As can be seen, knowing *K* in advance for a specific system configuration allows to effectively represent the variance of the population. Practically, *K* can be determined whether by using specific analytical formula obtained in the literature, or by adopting heuristic methods (i.e. neural networks) to interpolate *K* values from a set of observations conducted with different values of system parameters.

Thus, we are provided with all the data necessary for computing the confidence interval (see eq. 13) in relation to a certain simulation time $t - t_0$ and a certain number *n* of simulation runs/repetitions. Figure 5 shows the surface representing the confidence interval half length (CI/2) for a significant range of simulation times and numbers of repetitions, i.e. the range [200,…,8000] t.u. for the simulation time and the range [1,…,30] for the number of runs. This is a useful result for dimensioning simulation campaigns by identifying isolines for any specified value of the confidence interval (Figure 6).

5. CONCLUSION

The paper presents a methodology for the design of simulation campaigns or in-field tests, specifically for identifying a trade-off between replication length and number of simulation runs to execute as a function of a specified estimation precision.

The method is based on the direct estimation of the population variance by means of a properly shaped fitting function. That shape is determined by some analytical analyses on the structure of the manufacturing system.

The trend of the population variance can be then expressed as a function of the system run time, and

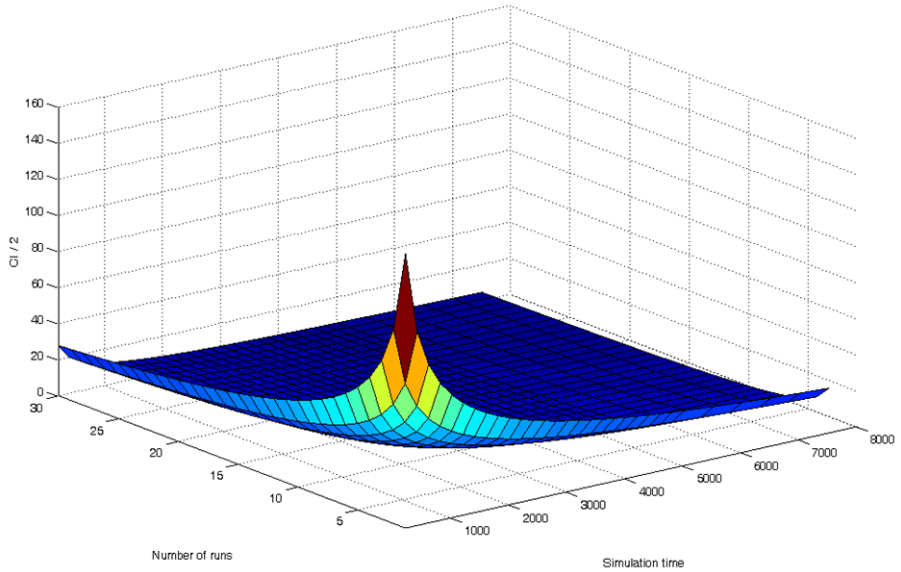

Figure 5: CI/2 surface.

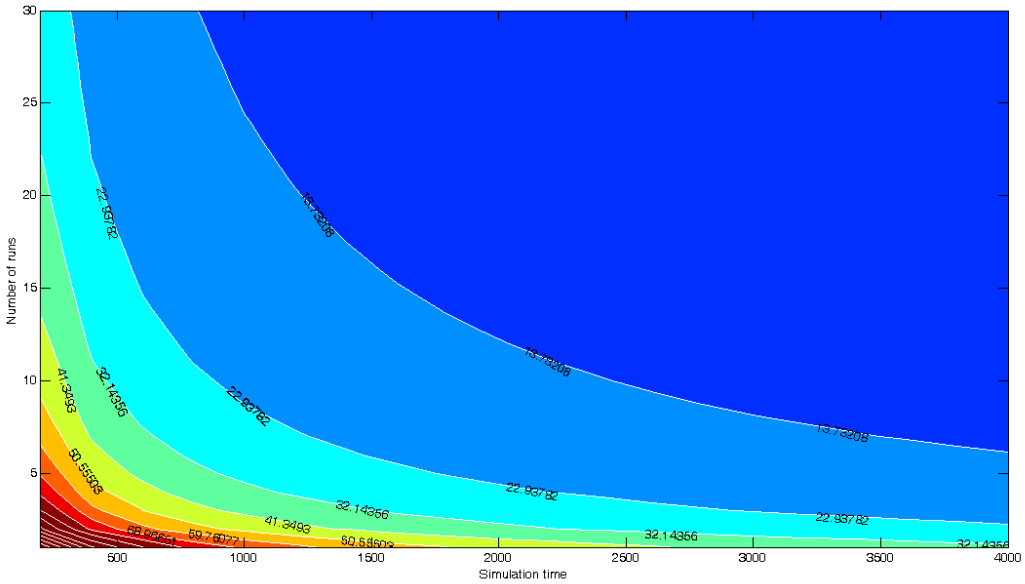

Figure 6: CI/2 contour plot.

confidence interval diagrams can be determined to find better trade-offs between the number of simulation to run and simulation length.

REFERENCES

Gebennini, E., Grassi, A., Fantuzzi, C., Gershwin, S.B., and Schick, I.C. (2009). On the introduction of a restart policy in the two-machine, one-buffer transfer line model. In *Proceedings of the 7th International Conference on Stochastic Models of Manufacturing and Service Operations*, 81–88. Ostuni, Italy.

Gershwin S.B., 2002. *Manufacturing Systems Engineering*, Massachusetts Institute of Technology. Second private printing, available via http://web.mit.edu/manuf-sys/www/gershwin.book.html

Kelton, W.D., and Law, A.M., 1985. The transient behaviour of the M/M/s queue, with implications for steady-state simulation, *Operations Research*, 33 (2), 378-396.

Law, A.M., 1983. Statistical analysis of simulation output data, *Operations Research*, 31(6), 983–1029.

Li, J., and Meerkov, S.M., 2000. Production variability in manufacturing systems: Bernoulli reliability case, *Annals of Operations Research*, 93, 299–324.

Montgomery, D.C., and Runger, G.C., 2007. *Applied Statistics and Probability for Engineers*, 4th ed. USA: John Wiley & Sons.

Tan, B., 1999. Variance of the output as a function of time: Production line dynamics, *European Journal of Operational Research*, 117, 470-484.

DATA DRIVEN TUMOR MARKER PREDICTION SYSTEM

Witold Jacak[(a)], Karin Proell[(b)], Herbert Stekel[(c)]

[(a)]Department of Software Engineering
Upper Austria University of Applied Sciences Hagenberg, Softwarepark 11, Austria
[(b)]Department of Medical Informatics and Bioinformatics
Upper Austria University of Applied Sciences Hagenberg, Softwarepark 11, Austria
[(c)] Institute of Laboratory Medicine,
General Hospital Linz, Austria

[(a)] Witold.Jacak@fh-hagenberg.at [(b)] Karin.Proell@fh-hagenberg.at [(c)] Herbert.Stekel@akh.linz.at

ABSTRACT
In this paper a system for the prediction of tumor marker values based on standard blood is presented. Several neural networks are used to learn from blood examination measurements and predict tumor markers in case these values are missing. In a post processing step the predicted values are evaluated in a fuzzy logic like style against different hypotheses and the best hypothesis is used to optimize the predicted values and its plausibility. These predicted values can then be used as input for a second system to support decision making in cancer diagnosis. A variety of experiments with tumor marker C153 show that we can get a prediction accuracy of more than 90%. Our experiments are based on hundreds of samples of up to 27 different features (blood parameters) per vector. We try to predict distinct values, classes of values and a combination of classes and values for specific marker types.

Keywords: neural network, tumor marker prediction, decision support system

1. INTRODUCTION

Tumor markers are substances produced by cells of the body in response to cancerous but also to noncancerous conditions. They can be found in body liquids like blood or in tissues and can be used for detection, diagnosis and treatment of some types of cancer. For different types of cancer different tumor markers can show abnormal values and the levels of the same tumor marker can be altered in more than one type of cancer. Examples of tumor markers include CA 125 (in ovarian cancer), CA 153 (in breast cancer), CEA (in ovarian, lung, breast, pancreas, and gastrointestinal tract cancers), and PSA (in prostate cancer). Although an abnormal tumor marker level may suggest cancer, tumor markers are not sensitive or specific enough for a reliable cancer diagnosis. But abnormally altered tumor marker values indicate a need for further medical examination.

During blood examination only a few tumor marker values are tested and for this reason the usage of such incomplete data for cancer diagnosis support needs estimation of missing marker values. Neural networks are proven tools for prediction tasks on medical data (Penny and Frost 1996). For example neural networks were applied to differentiate benign from malignant breast conditions base on blood parameters (Astion et Wilding 1992), for diagnosis of different types of liver disease (Reibnegger et al. 1991), for early detection of prostate cancer (Djavan et al. 2002; Matsui et al. 2004), for studies on blood plasma (Liparini et al. 2005) or for prediction of acute coronary syndromes (Harrison et al. 2005).

In this work we present a novel heterogeneous neural network based system that can be used for tumor marker value prediction. We use an n-dimensional vector of blood parameter values of a several hundred patients as input and train three neural networks in parallel to predict distinct values, classes of values and a combination of classes and values for specific marker types. In a post-processing step the outputs of all networks are adjusted by a fuzzy logic like decision system to obtain the most possible prediction. Unfortunately neural networks are unable to work properly with incomplete data; missing values however are a common problem in medical datasets. It may be that a specific medical procedure was not considered necessary in a particular case or that the procedure was taken in a different laboratory with the values not available in the patient record, or that the measurement was taken but not recorded due to time constraints.

In our system we use two different approaches for dealing with missing values. We reduce the input blood parameters to obtain reasonable complete sample sets. In order to train the networks with complete input blood parameters with impute on missing data values a penalty value during normalizing process.

2. GENERAL CANCER DIAGNOSIS SUPPORT SYSTEM

We focus our considerations on the design of a complex decision support system for early recognition of possibility of cancerous diseases. The system consists

* The work described in this paper was done within the Josef Ressel research center for heuristic optimization sponsored by the Austrian Research Promotion Agency (FFG).

of two components; a Tumor Marker Prediction System and a Diagnosis Support System (see Fig.1). Both systems use several heterogeneous artificial neural networks in parallel. The Tumor Marker Prediction System is in support of the Diagnosis Support System, which uses input data coming from the vector of tumor marker values $\mathbf{C} = (C_1, \ldots, C_m)$ and calculates the possibility of presence of a cancerous disease in general and the possibility of a specific tumor type in particular (tumor types are coded according to ICD 10 system).
The output values are evaluated against different hypotheses and the best hypothesis is used to optimize the predicted diagnosis and its plausibility.

An important issue for the Diagnosis Support System is data incompleteness. We need thousands of vectors of tumor markers for training and evaluation of the neural networks. Those vectors do not only contain distinct values of various marker types but also ranges of marker values, so called classes (e.g. one class for normal values, one for extreme normal values, one for beyond normal but plausible values and one for extreme values). Many of the available marker vectors consist of just a few measurements and cannot be used as training data for neural networks without further processing.

One approach to overcome this problem is to restrict the analysis only to vectors with complete data but this leads to very small sample sets. Another option is to extend the number of input values to all parameters of the blood examination, thus including also non-marker values, using a whole blood parameter vector $\boldsymbol{p} = (p_1, \ldots, p_n)$ as input. Frequently also this vector is incomplete too. For this reason the Tumor Marker Prediction System is connected ahead the Diagnosis Support System, which uses complete or partial complete blood parameter vectors $\boldsymbol{p}$ of patients to train a couple of neural networks for estimating values or classes of values for tumor markers. The output values are evaluated against different hypotheses and the best hypothesis is used to optimize the predicted value. Additionally a possibility value for estimated marker value is calculated. This Marker Value Prediction System could be also be used as a stand-alone system for a rapid estimation of marker values.

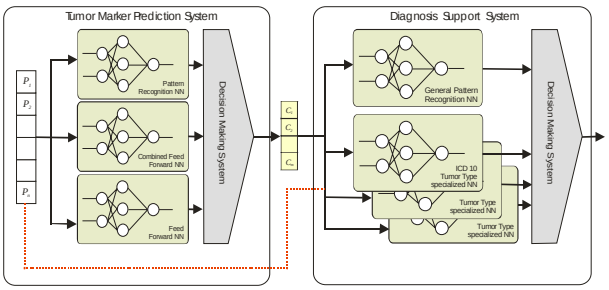

Figure 1: Architecture of Data Driven Cancer Diagnosis Support System

2.1. System for prediction of tumor marker values

Typically, the blood examination results in maximal 27 values of blood parameters such as HB, WBC, HKT, MCV, RBC, PLT, KREA, BUN, GT37, ALT, AST, TBIL, CRP, LD37, HS, CNEA, CMOA, CLYA, CEOA, CBAA, CHOL, HDL, CH37, FER, FE, BSG1, TF and about 35 tumor markers such AFP, C125, C153, C199, C724, CEA, CYFRA, NSE, PSA, S100, SCC, TPS etc. Many patient records have missing data values as many measurements did not happen being not of interest in a specific case. Different labs also may consider slightly different marker levels to be normal or abnormal. This can depend on a number of factors, including a person's age and gender, which test kit the lab uses, and how the test is done. For each parameter and marker we use the following reference ranges. (See an example in Table 1)

Table 1: Example of blood parameter ranges

CODE	Sex	Normal Lower Bound	Normal Upper Bound	Extrem Norm. Upper Bound	Over Norm. Plausible Upper Bound	Type	Unit	Age LB	Age UP
AFP	M	0	5,8	28	99	AFP (CL)	IU/ml	0	199
AFP	W	0	5,8	28	99	AFP (CL)	IU/ml	0	199
ALT	M	5	45	135	247,5	ALT (GPT)	U/l	0	199
ALT	W	5	34	102	187	ALT (GPT)	U/l	0	199
AST	M	5	35	105	192,5	AST (GOT)	U/l	0	199
AST	W	5	31	93	170,5	AST (GOT)	U/l	0	199
BSG1	M	3	8	15	55	Sinking 1h	Mm	1	199
BSG1	W	6	11	20	55	Sinking 1h	Mm	1	199
BUN	M	5	18	50	165	BUN	Mg/dl	2	16
BUN	W	5	18	50	165	BUN	Mg/dl	2	16
BUN	M	6	20	50	165	BUN	Mg/dl	19	199
BUN	W	6	20	50	165	BUN	Mg/dl	19	199

We divide the value range of marker $\mathbf{C}$ and blood parameter $\boldsymbol{p}$ into k non-overlapping intervals, called classes. In our case study we define four classes ($k = 4$): *Class 1* includes all values less than the Normal Value of marker or blood parameter, *Class 2* includes all values between Normal Value and Extreme Normal Value of marker or blood parameter, *Class 3* includes values between Extreme Normal Value and Plausible Value of marker or blood parameter and *Class 4* include all values greater than the Plausible Value.

For each class i of marker values we calculate the average value μ_i and the standard deviation σ_i. For example the respective values of marker C 153 calculated from patient data are presented in Table 2.

Table 2: C153 tumor marker parameters

Code	*Class*	μ	σ	*Min*	*Max*	*dmax*
C153	1	15,54	5,02	2	25	100
C153	2	33,59	6,73	26	50	100
C153	3	68,48	13,78	56	100	100
C153	4	162,20	321,22	101	10000	100

These classes and their limits are used for the normalizing process of parameter and marker values.

2.1.1. Architecture of marker value prediction system

The system consists of three heterogeneous parallel coupled artificial neural networks and a decision-making system based on aggregation rules.

Normalizing: The input and output values for training and testing of each network are normalized using the respective upper bound of Plausible Value. Each value of parameter or marker, which is greater than its upper bound, obtains the normalized value 1. Such a normalizing process guarantees that all values are mapped to interval [0, 1].

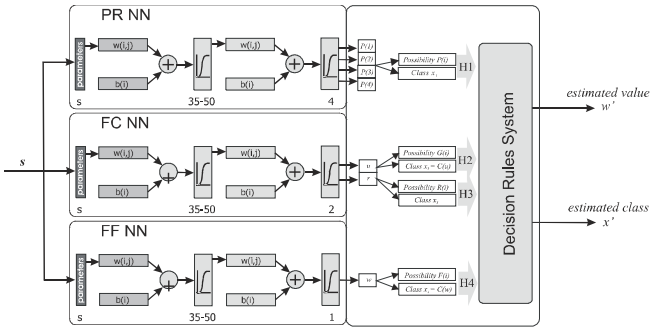

Figure 2: Neural networks based tumor marker value prediction system

Prediction System Structure: The general marker value estimation system contains of three neural networks (see Figure 2).

- Feed forward neural network (FF) with ***p*** inputs (normalized values of blood parameter vectors ***p***) and one output, normalized values of marker *C*

- Pattern recognition neural network (PR) with ***p*** inputs (normalized values of blood parameter vectors ***p***) and *k* outputs, *k*-dimensional binary vector coding classes of marker *C*

- Combined feed forward neural network (FC) with ***p*** inputs (normalized values of blood parameter vectors ***p***) and two outputs: normalized values of marker *C* (as in network FF), and normalized classes of marker *C* as:

$$NormClass^{j}(C) = j/k, \quad \text{for} = 1,...,k \qquad (1)$$

All neural networks have one hidden layer and tan-sigmoid or log-sigmoid transfer function. The output values of neural networks belong usually to the interval [0, 1].

For a given parameter vector ***p*** the three networks calculate different output data.

- The pattern recognition neural network PR produces the *k*-value vector $(P(i) \mid i = 1,..,k)$, where $P(i)$ describes the possibility (in sense of fuzzy logic) of class *i* of *C* marker connected to input parameter vector ***p***. The supposed class of marker *C* is

$$x_1 = arg(max\{P(i) | i=1,...,k\}). \qquad (2)$$

- The two output feed forward neural network FC, combined value and class training, generates two values, the value *r* interpreted as possibility of class marker *C* and value *u*, which is predicted normalized value of marker *C*.
  For value output *u* (similarly to the output of FF network) and limits of marker values we can calculate the class $x_2 = Class(u)$ to which belongs the output *u*.
  Separately we calculate the possibility vector $(G(i) \mid i = 1,...,k)$ as indirect distance to average value of each *C* marker class

$$G(i) = 1-(|u-\mu_i|/d_{max}) \text{ for } i = 1,...,k. \qquad (3)$$

  where d_{max} denotes maximal distance between values of marker *C*.
  For *r* value we calculate the possibility vector $(R(i) \mid i = 1,...,k)$ as

$$R(i) = 1-|r-i/k| \text{ for } i = 1,...,k. \qquad (4)$$

  The class of marker *C* that will be suggested is

$$x_3 = arg(max\{R(i)|i=1,...,k\}). \qquad (5)$$

- The feed forward neural network generates a normalized value *w* of marker *C*. Based on value *w* and the limits of each class we can calculate the class $x_4 = Class(w)$ to which the output of FF network belongs.
  Separately we calculate the possibility vector $(F(i) \mid i = 1,...,k)$ as indirect distance to average value of each *C* marker class

$$F(i) = 1-(|w-\mu_i|/d_{max}), \text{ for } i = 1,...,k. \qquad (6)$$

We use of the Neural Network Toolbox™ of MATLAB® for designing, implementing, visualizing, and simulating the neural networks PR, FC and FF.

2.2. Evaluation and post processing method

Based on the calculated estimation of marker values we can establish four hypotheses x_1, x_2, x_3, x_4 for determination of classes. For each hypothesis x_1, x_2, x_3, x_4 the possibility value *P*, *G*, *R*, *F* is calculated too.

These hypotheses should be verified to find the maximal possible prediction. This is done by testing a couple of aggregation functions *V* on each hypothesis possibility values. Those aggregation functions are

similar to aggregation rule in fuzzy logic decision-making system. In this experiment we use four kinds of functions *V*:

Minimum: $V(x_i) = min\{P(x_i)\ G(x_i)\ R(x_i)\ F(x_{ij})\}$ (7)

Product: $V(x_i) = P(x_i)\ G(x_i)\ R(x_i)\ F(x_i)$ (8)

Average: $V(x_i) = (P(x_i) + G(x_i) + R(x_i) + F(x_i))/4$ (9)

Count: $V(x_i) = Count\_of(x_i)$ (10)

Count is the number of identical hypothesis.

The maximal value of aggregation function determines the new predicted class. i.e.

$$x_{new} = arg\ (max\{V(xi) \mid i=1,..,4\}) \quad (11)$$

where $V(x_i) = V(P(x_i), G(x_i), R(x_i), F(x_i))$ is the evaluation function of arguments $P(x_i)$, $G(x_i)$, $R(x_i)$ and $F(x_i)$. This kind of evaluation method leads to four decision composition rules, namely *MaxMin*, *MaxProd*, *MaxAvg* and *MaxCount* known in fuzzy decision systems.

Estimation of predicted marker value: Based on such determined new class the estimation of marker value is performed. If the evaluation function *V* used in decision composition rule has a value greater than τ then the new estimated value of marker is equal to the average value of *w* and *u*. i.e.

$$w_{new} = (w + u)/2 \quad if\ V(x) > \tau \quad (12)$$
$$w_{new} = (w + u + \mu_{xnew})/3 \quad other$$

3. CASE STUDY: C 153 TUMOR MARKER

3.1. Training and Test Setup

We have taken the complete data set with 20 blood parameters from patient data: The input vector ***p*** contains complete data of following blood parameters ***p*** = (HB, WBC, HKT, MCV, RBC, PLT, KREA, BUN, GT37, ALT, AST, TBIL, CRP, LD37, HS, CNEA, CMOA, CLYA, CEOA, CBAA). We use 4427 samples as Learning Pattern Set for the neural networks system and 491 independent samples as Test Set. The datasets based on the whole data set the Pearson correlation coefficient between tumor markers and blood parameter is calculated. This correlation matrix in % is shown in Table 3:

Table 3: Correlation between tumor markers and blood parameters

Marker/ Parameter	AFP	C125	C153	C199	C724	CEA	CYFS	FPSA	NSE	PSA	PSAQ	S100	SCC	TPS
ALT	16	-10	25	19		10			31			-10		49
AST	33	13	40	27	15	27	11		49			8		36
BSG1		22	13	9	50	13	34		23	15		119	25	15
BUN		17					25	18	15		19	74	10	8
CBAA			-10									-11		
CEOA	-11		-13		-11									9
CH37	-28	-39		-23	-16	-9	-35	-11	-21				-12	-13
CHOL		-20			14		-19					-39		
CLYA	-19	-36	-20	-12	-20	-16	-15		-14	-13	-9	-35	-14	
CMOA		18			19	10							8	
CNEA		25	19		11	12	17	10	11	11		21	14	
CRP	18	32	27	17	23	23	20		41	21			11	
FE	11	-18	-29		-24	-12	-16						-11	-27
FER	15	31	31	32			35		59		14			-11
GT37	22	15	37	39	50	30			43					30
HB		-35	-38	-25		-19	-18			-15		-12	-17	
HDL	-11			-16								-151		24
HKT		-32	-36	-25		-16	-13		-8	-14			-16	
HS	-15	19		-12	-15						9			9
KREA		15	8	-9	9		14	17			21	64	10	
LD37	19	34	45	23	29	35	40		69	14		70		
MCV	17			10									-12	
PLT	-15	10	16		12		16				-11	17	12	12
RBC		-30	-31	-28		-16	-9			-12			-11	
TBIL	18	13		19	-16	12			21		9			
TF		-55	-29	-26	-28	8	-32	-20	-25				-12	34
WBC							22	11	17			24	14	

Data normalization: All data are normalized (on values [0, 1]) based on 3 classes (Normal Value, Extreme Normal Value, and Over Normal but Plausible Value). Values over Plausible value are the normalized with value 1. Data taken for learning and test process include the all four classes.

3.2. Experiments and Results

For establishing the number of neurons in a hidden layer of feed-forward networks we performed small batch set training of networks using different numbers of neurons.

The result is presented in Fig. 3.

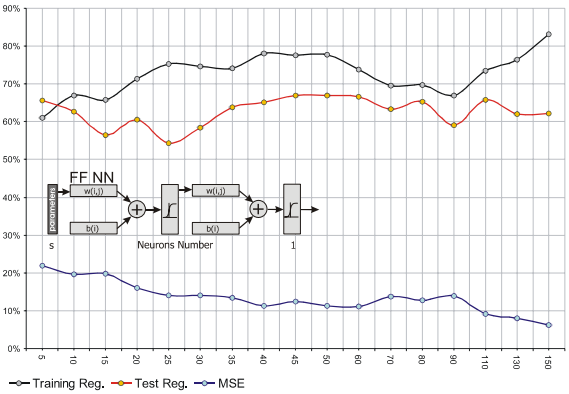

Figure 3: Test regression of neural networks with different number of neurons

The empirical test shows that best performing are networks with 40-60 neurons of hidden layer. We chose neural networks having one hidden layer with 50 neurons and tan-sigmoid activation functions. These are the neural networks settings used:

- Feed forward neural network (FF) with 20 inputs (normalized values of parameter vectors ***p***) and one output (normalized values of C153 marker)
- Pattern recognition neural network (PR) with 20 inputs (normalized values of parameter vectors ***p***) and four outputs (four dimensional binary vectors coding classes of C153 marker)
- Feed forward neural network (FC) with 20 inputs (normalized values of parameter vectors ***p***) and two outputs (normalized values of C153 marker and normalized classes of C153 with: class 1= 0,25; class 2= 0,5; class 3= 0,75; class 4=1,0)

All three neural networks were trained with Levenberg-Marquardt algorithm and a validation failure factor 6. The test outputs of all network is post processed by aggregation rules based on the decision system and finally compared with original values and classes of C153 tumor marker from test set.

The regression functions between the outputs of these three networks, post processed final estimation

and test C153 values are presented in Figure 4. It can be observed that regression of the rules based final estimation of C153 value is greater (R =0,73) than the individual estimation of separate networks (R= 0,65, R = 0,68, and R = 0,65 for PR, FC, and FF network respectively). The blue bounded area marks fatal mismatching i.e. originally large values of C153 marker and small-predicted values.

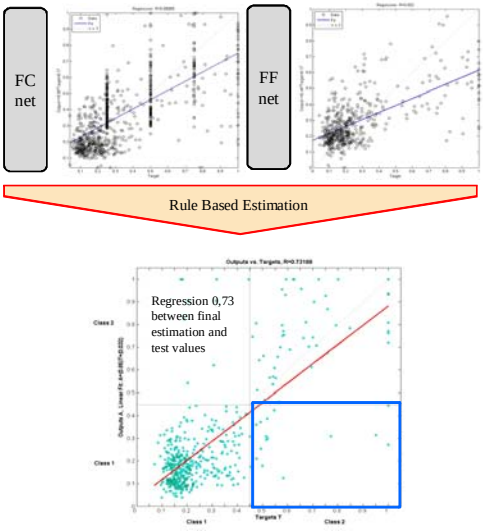

Figure 4: Results of rule based estimation system for tumor marker C153

Based on the predicted values of tumor marker C153 we calculate the matching and mismatching ratios for each class of marker. Matching and mismatching of classes between the test data of marker C153 classes and the predicted classes of different networks are presented as confusion matrixes (see Fig. 5). After post processing, we obtain 72 % matching of four classes, whereas the original networks range between 59% and 66% matching cases. The ratio of fatal mismatching is 2,9 %.

Class Net / Class Target	1	2	3	4	
1	54,8%	9,2%	0,2%	0,0%	
2	11,2%	10,0%	1,6%	0,6%	
3	0,6%	1,4%	5,9%	1,4%	
4	0,4%	0,4%	1,2%	1,0%	
Gesamt System MaxAvg	2,9%				71,7%

Confusion matrix of final estimation

Figure 5: Confusion matrix of results of Rule Based Estimation System for tumor marker C153

Additionally we have performed an experiment with a reduced number of training classes of marker C153. We merge the class 1 and class 2 of marker C153 into a new class I and class 3 and class 4 into a new class II. That means that all values of tumor marker C153 less than Extreme Normal Value of C153 determine class I and values greater than Extreme Normal Value determine class II. Normalization of blood parameters remains unchanged. Full training and test of networks was performed on input data modified in this way. The test results for those two classes are shown in separate confusion matrix tables (see Fig. 6).

Confusion matrix PR NN

Class Net / Class Target	Class I	Class II	
Class I	82,1%	8,9%	
Class II	2,4%	6,5%	
Gesamt PR Net			88,6%

Rules Based Estimation

Confusion matrix final estimation

Class Net / Class Target	Class I	Class II	
Class I	84,3%	3,3%	
Class II	2,0%	10,4%	
Gesamt System MaxAvg			94,7%

Figure 6: Confusion matrices before and after application of rules based estimation

We obtain a quite good ratio (94,7 %) of matching and the ratio of fatal mismatching is reduced to 2 %.

The dependency of quality of estimation on different composition rules is presented in Table 4. It is shown that the *MaxAvg* rule produces the best results.

Table 4: Results after application of composition rules

Rule	Confusion PR Net	Confusion FF Net	Confusion FC Value Net	Confusion FC Class Net	Confusion New Value	Confusion Two Class (Class based)	Confusion Two Class (Value based)
MaxCount	68,2	59,5	66,1	63,5	67,6	93,7	94,5
MaxAvg	68,2	59,5	66,1	63,5	**71,7**	**94,7**	**94,7**
MaxMin	68,2	59,5	66,1	63,5	68,2	89,8	94,3
MaxProd	68,2	59,5	66,1	63,5	68,0	90,2	94,5

3.2.1. Experiment with missing blood parameters values

Additionally, we have performed an experiment using vectors containing numbers of measured values from 27 to 15 (maximal 12 missing values allowed), as the number of vectors containing all 27 parameters is very small (about 160 samples). During normalization we replace the missing values with the value -1 thus resulting in input vectors containing all 27 blood parameters. We have obtained 6191 samples as Learning Pattern Set for the neural networks system and 618 independent samples as Test Set. All three neural networks were trained by Levenberg-Marquardt algorithm using a validation failure value of 6. The test outputs of all networks are post processed by the decision system based on aggregation rules and finally compared with original values and classes of C153 tumor marker from test set.

Confusion matrixes of final class estimation (Table 5) show that the final estimation method works well too with input vectors containing missing values. After post processing, we achieve 67 % matching of four classes, whereas the original networks gets between 53% and

61% matching cases. The ratio of fatal mismatching increases to 5,8 %.

Table 5: Confusion matrixes of final class estimation using input vectors with missing values and four classes

Class Net / Class Target	1	2	3	4	
1	47,1%	13,3%	0,2%	0,2%	
2	8,9%	15,0%	2,3%	0,0%	
3	0,3%	4,5%	3,7%	1,3%	
4	0,3%	0,6%	1,1%	1,1%	
Gesamt System MaxAvg	5,8%				**67,0%**

The test results for two classes are shown in a separate confusion matrix (see Table 6). We obtain in this case a good ratio (90,5 %) of matching and the ratio of fatal mismatching is reduced to 4,7 %.

Table 6: Confusion matrixes of final class estimation using input vectors with missing values and two classes

Class Net / Class Target	**Class I**	**Class II**	
Class I	82,0%	4,9%	
Class II	4,7%	8,4%	
Gesamt MaxAvg			**90,5%**

The regression functions between post processed final estimation and test C153 values are presented in Fig. 7.

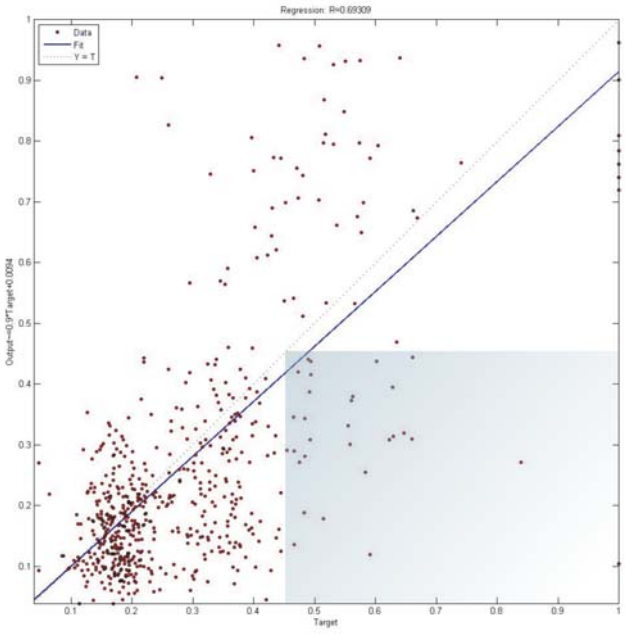

Figure 7: Regression functions between post processed final estimation and test C153 values

4. FINAL REMARKS

In this paper we focused our presentation on experiments predicting the marker C153. Similar results were obtained for marker C125, regression value 0,7865, for marker C199, regression value 0,7245 and for marker CEA, regression value 0,7225. In the next experiments we will continue testing further marker types depending on the availability of sufficient patient data. It can be expected that not all markers can be predicted with similar performance as C153.

In a further step the system will be extended by predicting combinations of markers as output of neural networks. Short tests show that such combinations can increase the quality of prediction. Moreover it is seems to be more effective to create different classes of markers as used in the recent experiment based on self-organizing maps methods. This prediction system will be an important component to the whole data driven cancer diagnosis support system.

ACKNOWLEDGMENTS

Special thanks goes to Prim. Herbert Stekel, M.D, Head of Institute of Laboratory Medicine, General Hospital Linz, Austria for providing thousands of samples of anonymous blood examination data for our experiments.

REFERENCES

Astion, M.L., Wilding P., 1992, Application of neural networks to the interpretation of laboratory data in cancer diagnosis. *Clinical Chemistry*, Vol 38, 34-38.

Djavan, B., Remzi, M., Zlotta, A., Seitz, C., Snow, P., Marberger, M., 2002, Novel Artificial Neural Network for Early Detection of Prostate Cancer. *Journal of Clinical Oncology*, Vol 20, No 4, 921-929

Harrison, R.F., Kennedy, R.L., 2005, Artificial neural network models for prediction of acute coronary syndromes using clinical data from the time of presentation. *Ann Emerg Med*.; 46(5):431-9.

Liparini, A., Carvalho, S., Belchior, J.C., 2005, Analysis of the applicability of artificial neural networks for studying blood plasma: determination of magnesium on concentration as a case study. *Clin Chem Lab Med*.; 43(9):939-46

Matsui, Y., Utsunomiya, N., Ichioka, K., Ueda, N., Yoshimura, K., Terai, A., Arai, Y., 2004, The use of artificial neural network analysis to improve the predictive accuracy of prostate biopsy in the Japanese population. *Jpn J Clin Oncol*. 34(10):602-7.

Penny, W., Frost, D., 1996, Neural Networks in Clinical Medicine. *Med Decis Making*, Vol 16: 386-398

Reibnegger, G., Weiss, G., Werner-Felmayer, G., Judmaier, G., Wachter, H., 1991, Neural networks as a tool for utilizing laboratory information: Comparison with linear discriminant analysis and with classification and regression trees. *PNAS:* vol. 88 no. 24, 11426-11430

SIMULATING COMPLEX SYSTEMS: THE CHALLENGE OF ERRATIC OUTPUT BEHAVIOR FOR DECISION SUPPORTIVE FORECASTING

Marko Hofmann [(a)], Thomas Krieger [(b)]
[(a),(b)] Universität der Bundeswehr München and ITIS GmbH
Werner-Heisenberg-Weg 39
85577 Neubiberg, Germany

[(a)] marko.hofmann@unibw.de, [(b)] thomas.krieger@unibw.de

ABSTRACT
In many complex systems a small change of the independent variables X (input) may completely change the value of the dependent variable Y (output). We call this behavior erratic and try first to find a formal definition for it. Erratic behavior can also be reproduced in corresponding simulation systems. By calibration it is even possible fine-tune the simulation to the real world data, achieving high descriptive validity. However, since the real system is highly sensitive to minor changes of the initial conditions, the simulation model must reach an equally high level of fidelity if ti comes to prediction. Even a qualitatively appropriate forecast could be of low value if the erratic behavior leads to high quantitative deviations. Unfortunately, the fidelity of simulation models is limited by many factors including available system data, money, and time. Thus, the initial conditions of the real system can only be approximated in the model input. Modeling necessarily introduces a certain amount of uncertainty with respect to the real world situation. Consequently, a tolerable level of deviation has to be defined which might be easily exceeded in the case of erratic behavior. Based on two examples we generalize this problem and try to systemize its investigation on the basis of some preliminary formal definitions. The ultimate goal of this research endeavor is the ability to assess the power of simulation-based predictions with respect to the future behavior of systems that have shown erratic behavior in the past.

Keywords: System behavior prediction, erratic and discontinuous system behavior, decision support,

1. INTRODUCTION

In complex systems the interrelation between different measurands is often erratic. Introducing a small additional amount of X (input) may completely change the value of Y (output). This behavior is sometimes even unpredictable as has been shown by chaos research. As more and more investigations on complex systems are performed using simulations it has become clear, that such erratic behavior can also be produced in corresponding simulation systems. It is, however, not obvious that real world and simulated erratic behavior are causally interconnected, since there are always many possible simulation systems (or parameterizations) that can produce such data. It is extremely seldom possible to prove that a model is isomorphic to its real world correspondent. Therefore, empirical validation seems to be of uttermost importance, especially in the context of practical decision making, decision support and risk analysis (Hofmann and Krieger, 2008).

The general goal of simulation-based decision support is to use the simulated behavior as a forecast for the real behavior. Erratic functional relations in real world systems, however, put a serious challenge to this approach. Since the real system is highly sensitive to minor changes of the initial conditions, the simulation model must reach an equally high level of fidelity. Even a qualitatively appropriate forecast could be of low value if the erratic behavior leads to high quantitative deviations. Unfortunately, the fidelity of simulation models is limited by many factors including available system data, money, and time. Thus, the initial conditions of the real system can only be approximated in the model input. Modeling necessarily introduces a certain amount of uncertainty with respect to the real world situation. Consequently, a tolerable level of deviation has to be defined. We will show that this is a question of choosing an adequate measure.

The paper will not address the issue, how sufficient observations of a real system producing erratic output are collected, although this might be the most challenging task at all. We will focus mainly on the interpretation of simulation runs and, secondary, on the conditions of a justified transfer of simulation results into reality.

The paper illustrates the challenge with two examples, and provides approaches for the formalization of “erratic behavior” of models.

2. ILLUSTRATIVE EXAMPLES

In order to illustrate the rather theoretical verbal description of the problem in the introduction the paper starts with two examples highlighting the issue. The first example is taking from military combat simulation, the second stems from evacuation simulation.

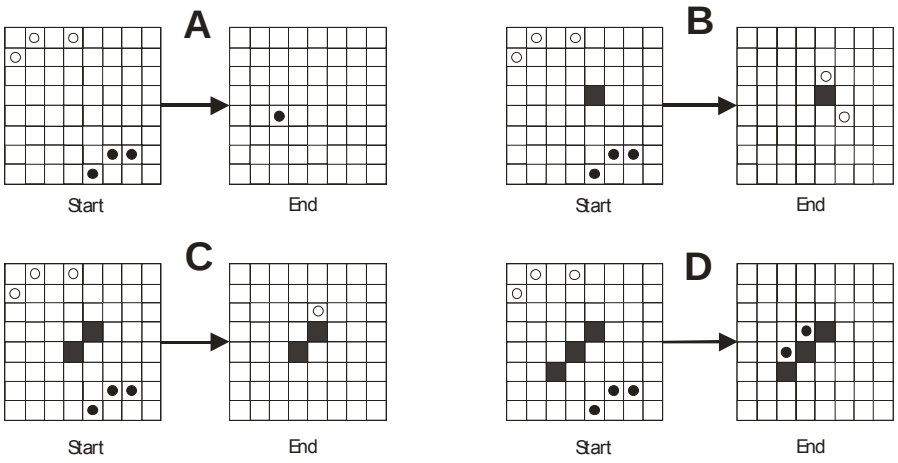

Figure 1: Sensitivity of a simplified high resolution combat simulation model towards minor changes of terrain

2.1. Military Combat Simulation

The phenomenon of unpredictably erratic output in simulation systems behavior - in the sense described above - is well known. It can, at least, be traced back to the dissertation of (Schaub, 1991), who could prove that the dependency of duel-like combat outcome from terrain representation (input variation) in high resolution combat simulation models is extremely discontinuous. His original goal was to refine an aggregated combat model (high level of abstraction) by generating context-specific effectiveness measures for it via a high resolution simulation model (low level of abstraction). He could clearly demonstrate that these measures (called "Lanchester coefficients"; they are used in almost all aggregated combat models in differential equations (Lanchester-Type models of warfare)) were highly affected by the slightest change of the terrain representation of the high resolution model (introducing a single tree representation, for example, see Figure 1). Notice that the initial positions of the troop representations (circles of different color) are identical in all four variants, and that from A to D only a single change of terrain occurs. The end states, however, differ significantly.

Schaub could trace back this effect in the model to the high sensitivity of reconnaissance and attrition processes on lines of sight, which was absolutely no contradiction to reality (which might be seen as a *qualitative concordance* of model and reality). However, the effect was much too erratic to allow sensible abstraction. Schaub concluded that Lanchester coefficients can hardly be based on high resolution models. The context-specific effectiveness measures calculated with the high resolution model output show unpredictably erratic behavior which could not be validated quantitatively by comparisons with reality.

It has to be mentioned that Figure 1 is a simplification, since it depicts high resolution combat models as deterministic models. Actually, they are stochastic models and the sensitivity effect is more appropriately visualized in Figure 2. The general problem, however, is not affected by this difference.

At least part of the challenge is simply that the resolution of the simulation model (the size of a cell) restricts depiction of reality. All terrain features must be condensed into single cell states. Thus, a group of real trees must be translated into an arrangement of cells. Due to the limits of resolution this is an underspecified transformation (see Figure 3).

Note that this is only an example, but every map (terrain representation) is limited in resolution with respect to reality. Hence, higher resolution is in most

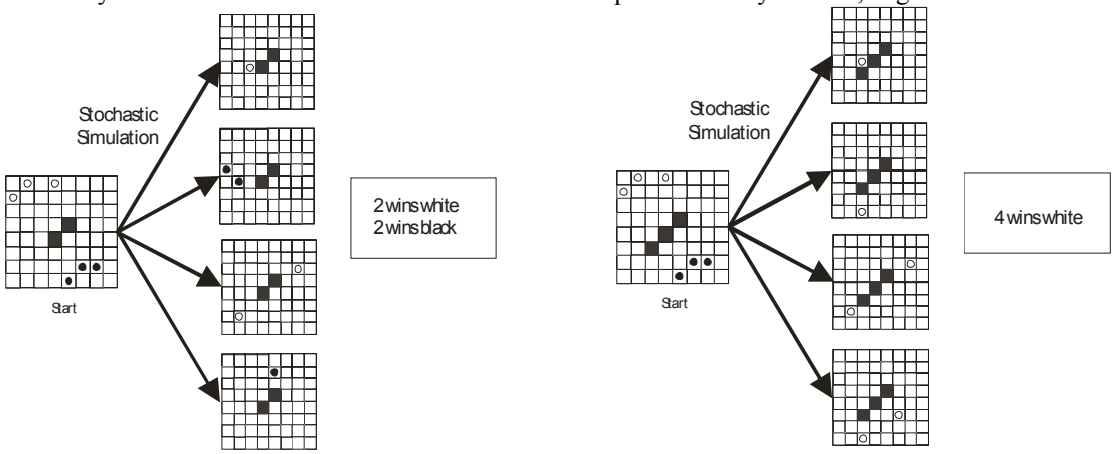

Figure 2: Stochastic combat simulation and its sensitivity to single terrain features

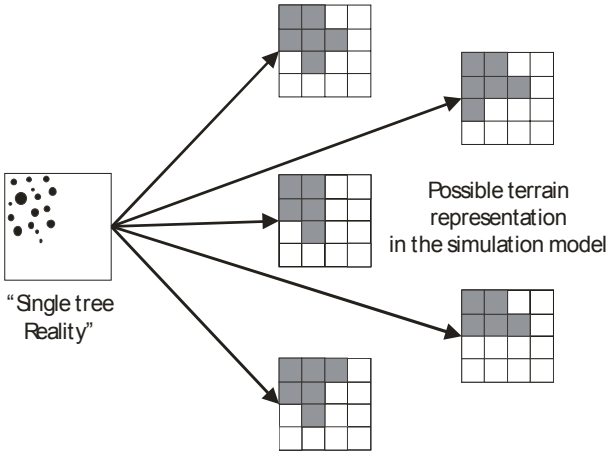

Figure 3: Uncertainty introduced into the combat simulation model by limited terrain resolution

cases only a gradual improvement, sometimes even degradation, since validation gets more and more difficult (think of the challenges of a "real time ultra high terrain representation").

Thus, we can summarize the challenge as follows: Although the erratic behavior produced by the simulation model qualitatively matches the corresponding erratic real world behavior, limits in model resolution introduce more uncertainty into the model as tolerable for such an erratic process, highly sensitive to minor changes of input.

Consequently, there is a fundamental limitation to the application of combat simulation models for decision supportive prognosis in real military conflicts.

High resolution combat simulation models are extremely complicated models when it comes to details, based on a subject not everybody is familiar with. Hence, we will use a second example to illustrate some subtleties of the problem. This second example, an evacuation simulation model, is also included to show the ubiquity of the problem.

2.2. Evacuation Simulation

Figure 4 shows two hypothetic screenshots of a simulation called ESCAPE, used for didactic purpose at the University of the Federal Armed Forces. The goal of the model is to investigate the effects of different room geometry and obstacles on the evacuation time. The lines in Figure 4 represent walls, the breaches in the walls doors, the dark squares people (agents) trying to escape through the doors of the building, the circles obstacles, and the triangle a source of danger (fire, explosion etc.). The (stochastic) model generates flight behavior of agents according to some simple movement rules, like for example:

1. If you are within a certain range of the source of danger, move in the opposite direction.
2. If you can see an outward leading door, and if there is no obstacle and no source of danger between you and the door, move towards it.
3. If you can see an internal door, and if there is no obstacle and no source of danger between you and the door, move towards it.
4. If you can see neither an internal nor external door nor a source of danger, move in line with your nearest neighbor.
5. If you can see neither an internal nor external door nor a source of danger nor any neighbor, move randomly.

The most important output parameter of the model is the total evacuation time, defined as the time from the beginning of the simulation (when the source of danger is recognized) until the departure of the last agent (see Figure 5).

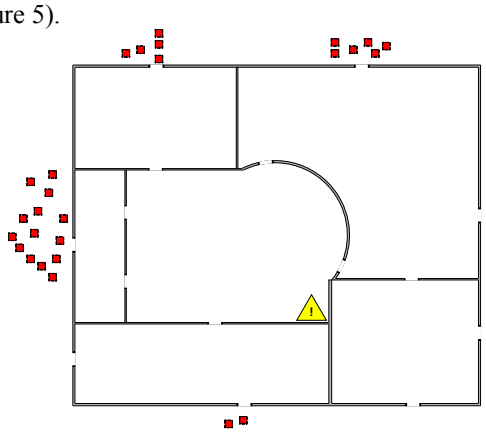

Figure 5: Final state of the ESCAPE simulation

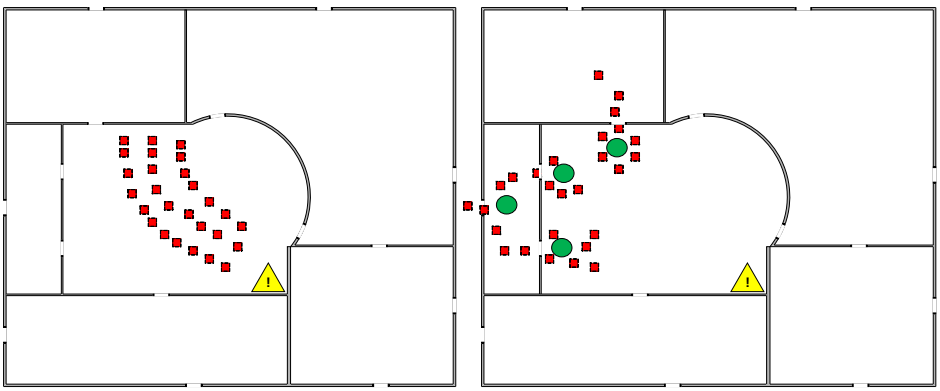

Figure 4: Example of an initial situation (left) and a simulation snapshot (right) of a slightly changed door arrangement with additional obstacles (green) in ESCAPE

The model can be modified and implemented in numerous ways. There is no single best implementation of the model and a lot of assumptions and simplifications must be made about human behavior, about textural attributes of the floors, walls, ceilings, about accidents to be considered and so on. The resolution of the models is therefore limited even with respect to crucial input parameters. The variety of reasonable assumptions and simplifications manifests itself as structural variation of the evacuation model. For example, in all models the representation of dimensions of agents and obstacles as well as their spacing is critical, and, at least to certain extent, arbitrary. For instance, the distance between columns, walls and doors and the vertical size of "persons" are closely related to the number of people who can move simultaneously. Only slight changes of these parameters in a model or slightly different modeling of geometry can cause tremendous (discontinuous) changes in total evacuation time. Consequently, there is a certain amount of irreducible uncertainty about the concordance of the real initial situation, and model input.

Evacuation time (output) is highly sensitive, both in reality and in the model, to minor changes of the location of obstacles and doors (input). The model can be calibrated in order to achieve a good qualitative concordance of model and reality, for example, with respect towards the positive effect of pillars in front of doors. However, for decision supportive prediction (designing a new building, for example) such a qualitative concordance might not suffice. Prediction of erratic real system and model behavior must match quantitatively, too.

3. GENERALIZATIONS

Based on the examples we can now try to first generalize and then formalize the concordance problem of erratic real world and corresponding model behavior.

1. Some real systems show "erratic" behavior, designating large and irregular output changes from minor input changes (Subsequently, we try to formalize this verbal description).
2. Such erratic behavior can be imitated with simulation models.
3. Using techniques of calibration concordance can be established between both erratic behaviors (for descriptive purposes, at least).
4. Due to limits of resolution the simulation cannot match the real situation perfectly.
5. Hence, deviations between both erratic behaviors are unavoidable (in predictive applications).
6. In contrast to non-erratic systems, such deviations might be substantial.
7. The concordance between reality and model is therefore often only qualitatively (A term which has to be formally defined, too).
8. For many practical decisions quantitative concordance is essential.
9. Due to the limits of model resolution erratic system behavior might lead to insufficient quantitative concordance of simulation models.

Such a verbal description might be helpful to get aware of the problem; however, it is unsatisfying with respect to further inspection and treatment of the challenge. At least three conceptual descriptions have to be stated more precisely:

First of all, "*erratic behavior*" has to be defined formally. This is obviously the most important task. Second, we need a general, formal description of the *amount of uncertainty introduced into prognosis by limited model resolution*. Third, we have to render more precisely what *qualitative concordance* actually means. All three definitions must finally be *aligned*.

In this paper we concentrate on the first task of defining the erratic/non-erratic model or system behavior in general. The task of finding corresponding measures for the second and third challenges as well as the alignment of all three definitions is postponed to later work.

4. ERRATIC FUNCTIONAL RELATIONS: IN SEARCH FOR A CLASSIFICATION SCHEME

In the first abstract of this paper we used "discontinuous" instead of "erratic"; during the elaboration of the full paper we realized, however, that the common meaning of "discontinuous" might be two narrow in capture the essence of the problem. Discontinuous is a technical term used intensively in (mathematical) calculus. It denotes a saltus in a continuous function. However, such a saltus can be large or infinitesimally small (see Figure 6, graphics A and B). Obviously, the local saltus in graphic B is much less significant with respect to the global range of Y than the saltus in graphics A. Moreover, as shown in the examples, the interpretation of simulation outputs depends on the precision of input data (besides of the general model fidelity), implying that the input X is only determined with a certain range ΔX. Within this local variation of X a significant change of Y might occur (ΔY), both in a continuous and in a discrete system (Graphics C and D of Figure 6). This change of Y has to be seen in connection with the global range of Y ($\blacktriangle Y$) over a predefined global range of X ($\blacktriangle X$).

It is self-evident, that for each application of a simulation model, a specific tolerance threshold (max ΔY) exists for the output variation ΔY, especially if caused by uncertainty of X (ΔX), and that, in general, this threshold may also depend from the global range of Y ($\blacktriangle Y$). With other words, there is always a model-purpose specific tolerable level of output uncertainty.

Formal definition of erratic behavior should reflect these considerations.

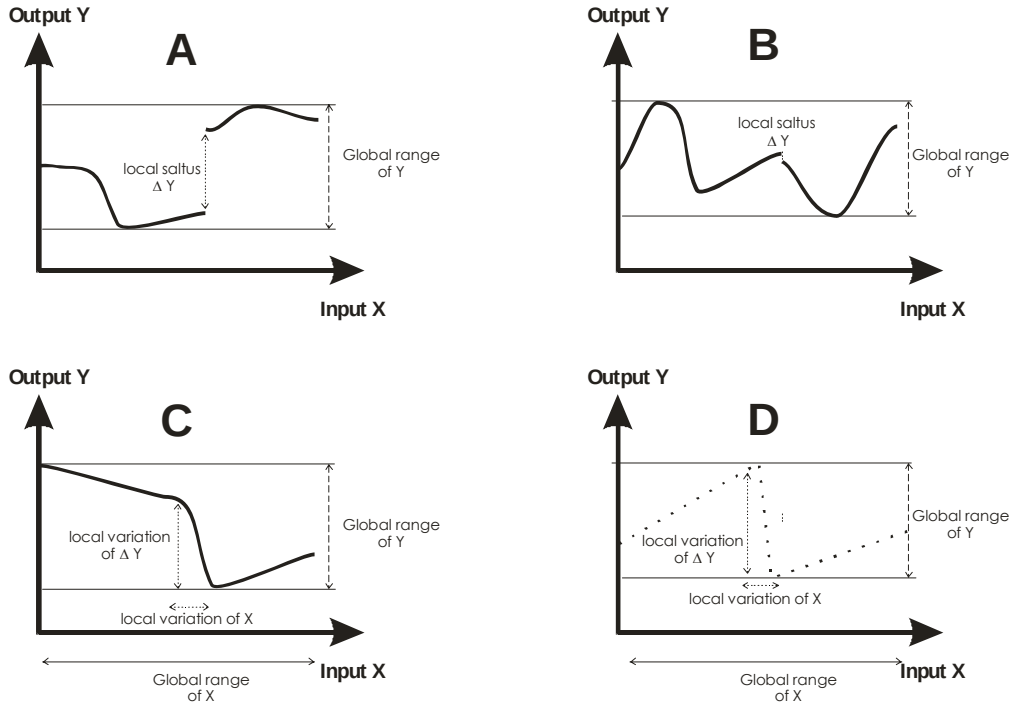

Figure 5: Erratic behaviour of output functions

5. FORMAL DEFINITIONS OF ERRATIC SYSTEM BEHAVIOR

This section is work in progress. We show the most straightforward approaches for defining erratic/non-erratic model or system behavior with mathematical formalisms. Let $f(t)$ be the system state at time t (let us assume that t is the only input parameter **x**) of system *S*. For the sake of simplicity we assume that $f(t)$ is real-valued.

First approach: We call **system S non-erratic (1)** if there exist a number $h > 0$ and a constant $K(h) > 0$ such that for all $t \in [t_0, \infty)$ the condition $|f(t+h) - f(t)| \leq K(h)$ is fulfilled. This definition assures that variations of the input **x** (here: t) smaller than h causes output variations $|f(t+h) - f(t)|$ which do not exceed a certain value $K(h)$. This limitation may help for the prognosis of future system behavior. It should be noted that that a non-erratic function may not be continuous or Lipschitz continuous functions (in the mathematical sense) at all.

This definition is extremely simple; however, at least for some applications it might be sufficient. If the data hitherto (t) gathered from a real system is non-erratic(1) it is very likely, that the deviation of a prognosis for $t+h$ will be smaller than $K(h)$.

The consideration of ▲Y (the maximal range of the output) can be easily included into the first approach by defining K(h) := (▲Y / ▲X) h.

The disadvantage of this approach is that it only considers the local behavior of the system. The common understanding of erratic behavior, however, also includes global effects. These can be taken into account with our second approach.

Second approach: Here we use the idea of the *Total Variation* of a function f and change it for our needs. For our practical purposes we simplify this concept: Let $h > 0$ be fixed and

$$V(f,t) := \sum_{i=1}^{n} |f(t+i\,h) - f(t+(i-1)\,h)|, \quad t \in [t_0, \infty).$$

Then we say that **system S is non-erratic (2)** if there exist a constant $K(h) > 0$ such that $V(f,t) < K(h)$. In this definition we consider the cumulative effect of the next n time steps starting with an arbitrary t.

The disadvantage of this definition is that substantial local deviation might not be taken into sufficient account.

Third approach: In mathematics a function is called Lipschitz continuous, if for any t_1 and t_2 in the domain of f the inequality holds:

$$\frac{|f(t_2) - f(t_1)|}{|t_2 - t_1|} \leq L, \qquad L > 0.$$

Intuitively, a Lipschitz continuous function is limited in how fast it can change. In this approach we call **system S is non-erratic (3)** if it is Lipschitz continuous. The difference $|t_2 - t_1|$ can be interpreted as time difference of two model/simulation time points or as the resolution of the formal model. In the example

of the military combat simulation $|t_2 - t_1|$ might be the size of the cells. If one considers the same model and merges 4 cells to a new cell, then Lipschitz continuity of the output function would mean, that the $|f(x) - f(y)|$ is less than $2L$.

In general -- following these lines -- one has to consider a metric d_X on the domain of f and a metric d_Y on the set of all outputs. Then Lipschitz continuity is defined as (**system S is non-erratic(4)** if)

$$\frac{d_Y(f(t_2), f(t_1))}{d_X(t_2, t_1)} \leq L, \qquad L > 0$$

for all t_1 and t_2 in the domain of f.

The major problem in practice is the specification of the strongly context depending metrics.

However, it seems to us that this definition captures most of the notion of non-erratic behavior.

The way ahead from these definitions is clear. First, one might interpret h as the irreducible *amount of uncertainty introduced by limited model resolution* (which might also be interpreted as limits of precision in practical measurement). Thus, if we can actually determine h exactly, and also find domain specific reasonable levels for $K(h)$, we might be able to judge system behavior with respect to the possibilities of making trustworthy predictions for a future $t + h$. Second, we have to construct a measure for comparing system and simulation model output behavior in order to define qualitative concordance in the light of formally defined erratic behavior. We strongly hope, that all necessary mathematical alignment can be made, and that, finally, we might be able to assess the power of simulation-based predictions with respect to the future behavior of systems that have shown erratic behavior in the past.

6. SUMMARY AND CONCLUSION

In this paper we try to illustrate, generalize, and then formalize the challenge of erratic output behavior for decision supportive simulation-based forecasting. The examples are taken from military and evacuation simulation.

We demonstrate that some real systems show "erratic" behavior, designating large and irregular output changes from minor input changes and that such erratic behavior can be imitated with simulation models. Using techniques of calibration concordance can be established between both erratic behaviors. Due to limits of resolution, however, the simulation cannot match the real situation perfectly. Hence, deviations between both erratic behaviors are unavoidable (in predictive applications). In contrast to non-erratic systems, such deviations might be substantial. The concordance between reality and model is therefore often only qualitatively. For many practical decisions, however, quantitative concordance is essential. Due to the limits of model resolution erratic system behavior might therefore lead to insufficient quantitative concordance of simulation models for predictive purposes.

Since such a verbal description is insufficient for operationalization and therefore insufficient for practical use, we have presented four possible mathematical definitions for our central concept of "erratic behavior".

Although a lot of work has still to be done to align these definitions to a formal description of the amount of uncertainty introduced into prognosis by limited model resolution, and to a formal definition qualitative concordance, we are optimistic that such alignments are possible.

If successful, we might, finally, be able to assess the power of simulation-based predictions with respect to the future behavior of systems that have shown erratic behavior in the past.

ACKNOWLEDGMENTS

The authors would like to thank the ITIS GmbH for providing the possibility to work on the problems discussed here.

REFERENCES

Hofmann, M., Krieger, Th., 2008. Great but flawed expectations: On the importance of presumptions and astonishment in model and simulation based risk management. *20th European Modeling and Simulation Symposium, September 17-19, Briatico (Italy).*

Schaub, T., 1991. Zur Aggregation heterogener Abnutzungsprozesse in Gefechtssimulations-modellen. Dissertation. Fakultät für Informatik, Universität der Bundeswehr München, Neubiberg.

AUTHORS BIOGRAPHY

MARKO HOFMANN is Project Manager at the ITIS GmbH. After his studies of computer science at the Universität der Bundeswehr München, he served two years in an army battalion staff. From 1995 to 2000 he was research assistant at the Institute for Applied System Analysis and Operations Research (IASFOR), where he got his Ph. D. in computer science. Since April 2000 he is responsible for basic research in applied computer science at the ITIS GmbH. He gives lectures in operations research, computer science and mathematics at the Universität der Bundeswehr München. He is currently finishing his habilitation.

THOMAS KRIEGER is a Research Assistant at the ITIS GmbH. He received his Diploma in Mathematics in 2000 from the Technische Universität Dresden, Germany and his Doctorate in Mathematics in 2003 from the Universität der Bundeswehr München. His research interests include Modelling and Simulation as well as Game Theory. He gives lectures in operations research, probability theory, game theory and reliability theory at the Universität der Bundeswehr München.

BEHAVIORAL VERIFICATION OF BOM BASED COMPOSED MODELS

Imran Mahmood[(a)], Rassul Ayani[(b)], Vladimir Vlassov[(c)] , Farshad Moradi[(d)]

[(a)] [(b)] [(c)]Royal Institute of Technology (KTH), Stockholm, Sweden
[(d)]Swedish Defense Research Agency (FOI), Stockholm, Sweden

[(a)]imahmood@kth.se, [(b)]ayani@kth.se, [(c)]vladv@kth.se, [(d)]farshad.moradi@foi.se

ABSTRACT

A verified composition of predefined reusable simulation components such as BOM (Base Object Model) plays a significant role in saving time and cost in the development of various simulations. BOM represents a reusable component framework and posses the ability to rapidly compose simulations but lacks semantic and behavioral expressiveness required to match components for a suitable composition. Moreover external techniques are required to evaluate behavioral verification of BOM based components. In this paper we discuss behavioral verification and propose an approach to verify the dynamic behavior of a set of composed BOM components against given specifications. We further define a Model Tester that provides means to verify behavior of a composed model during its execution. We motivate our verification approach by suggesting solutions for some of the categories of system properties. We also provide a case study to clarify our approach.

Keywords: Composability, model verification, deadlock detection, BOM, SCXML, model execution

1. INTRODUCTION

Verification is typically defined as the process of determining whether a model is consistent with its requirement specifications and whether it will satisfy the requirements of the intended application (Petty 2009). Verification is concerned with the analysis of accurate transformation of the requirements into a conceptual model. Model Verification deals with building the model right (Balci 1998) and conceptually correct. Composability on the other hand is an important term used in modeling and simulation. It is the capability to select and assemble simulation components in various combinations into simulation systems to satisfy specific user requirements (Petty & Weisel 2003). One conceptual approach to increase the efficiency and effectiveness of complex model development is, based on reusable model components (Lehmann 2004). A composeable simulation model component thus can be defined as a reusable, self-contained and independently deployed software unit that conforms to a component model (Bartholet et al. 2004), has well defined functionality and behavior and is usable in a variety of contexts (Moradi 2008). Base Object Models (BOMs) provide a framework to define and characterize these components at a conceptual level. BOM is a SISO standard and encapsulates information needed to formally represent a simulation component (Gustavson 2006).

The term Composability carries varied meanings and views in research literature that differ primarily by its different levels. It is essential to consider these different "levels" of composability, in order for them to be meaningfully composed. Medjahed et al (Brahim & Athman 2006) introduces a multilevel composability model in which the composability of Semantic Web Services is checked in four levels: Syntax, Static Semantic, Dynamic Semantic and Qualitative level. In Modeling and Simulation (M&S), these levels are also brought into consideration during the composition process of the model components. *Syntactic Composability* means that the components have the ability to fit together as is concerned with the matching of syntactic information, such as message name and number of parameters etc. *Static Semantic Composability* refers to a meaningful and computationally valid coupling of components whereas *Dynamic Semantic Composability* deals with the behavioral correctness of the composition. Composition of models becomes more challenging when models are heterogeneous in terms of their formal specifications i.e., when they have different structural and behavioral specifications (Sarjoughian 2006).

Various approaches have been developed to evaluate different levels of composability. An interesting approach has been proposed in (TEO & SZABO 2008) that deals with the Syntactic and Semantic level of composability and proposes an integrated approach for model reuse across multiple application domains. In a similar work we suggested a rule-based seven-step process (Moradi et al. 2007) to calculate the composability degree of a particular composition. It

suggests that based on a given scenario, a set of BOM components can be discovered from a BOM repository and matched to analyze their composability degree at three different levels. It was however mainly focused on Syntactic and Static Semantic level of composition. We further proposed another method in (Mahmood et al. 2009) which was mainly focused on matching the structure and behavior of the BOM components at Dynamic Semantic level. Our approach suggested in (Mahmood et al. 2009) was an elementary framework to match BOM state-machines by analyzing their structure and execute them in a runtime environment.

In this paper we revisit and extend our state-machine matching process and apply it to perform Behavioral Verification analysis on a given model composition. In this extended framework we introduce a *Model Tester* to define and compare the requirement specifications for verification and use this Tester during the model execution to verify that the behavior of components being composed match each other and that they can correctly interact with each other to meet their collective objectives. Subsequently we aim to convene our methods with Case Study scenarios in order to provide the proof of concept. Essentially behavior verification problem looks at a goal oriented correct execution of a given composition of components. Solutions to such problem would enable simulation modelers to select and compose various reusable components and verify that their composition would work correctly and satisfy their requirements and intended objectives. We summarize the primary contribution of this paper as follows:

We introduce behavioral verification of BOM based model composition and propose a model tester to represent requirement specification in form of states. We suggest using this tester with our revised state-machine matching process to verify the composed model during execution through an instrumentation technique. Based on this approach, we further suggest the design of a behavioral verification framework that takes candidate BOMs and Tester as input and perform automatic verification. We also discuss different system specification properties and as an example contribute a solution for the verification of deadlock freedom and apply it in a case study.

The rest of the paper is organized as follows: Section 2 formulates the discussion of Behavioral verification and its different methods. Section 3 contains our proposed behavioral verification process for BOM composition. Section 4 provides the details and implementation of the verification framework. A case study is presented in Sections 5 and Section 6 concludes the paper.

2. BEHAVIORAL VERIFICATION

In this section, we discuss Behavioral Verification in detail, highlight different methods for verification and describe various classes of system properties and their representation as requirement specifications. We further propose design of our model tester and its use.

As previously defined, behavioral verification is a process through which we identify that a given set of model components possess correct behavior such that when they are composed they satisfy a given criteria.

2.1. Methods of Verification

Based on the techniques used, the methods of verification can be classified into four groups: I) Informal, II) Static, III) Dynamic & IV) Formal (Balci 1998). For each group various tools and techniques have been suggested within M&S community. Informal techniques are mainly based on inspections, domain expert reasoning and comparison with the similar existing verified models. Static verification techniques primarily focus on the assessment of static model design including structural, syntax and semantic analysis. They are called static because they can be performed without the execution. Dynamic verification techniques require the execution of the model and attestation of its behavior. These techniques are based on instrumentation, abstract level execution, cause-effect graphing and reachability analysis. Formal verification techniques present high degree of difficulty while trying to prove correctness of the model using mathematical methods including induction techniques, inference models, deduction logic, predictive calculus, correction proofs, bisimulation, and model checking (Balci 1998).

In this paper our focus is on two verification methods from the Static and Dynamic groups namely Structural Analysis and Model Instrumentation. Structural Analysis is used to examine the model structure using rule-based evaluation and to verify if it adheres to the principles of Finite State Automata. Model Instrumentation involves insertion of a “Tester” instrument in the composed model to observe the behavior during abstract level execution. We refer it as Dynamic verification.

2.2. System Properties

The system properties can generally be classified into following groups (Berard & Bidoit 2001):

Reachability Properties: state that some particular situation can be reached.

Safety Properties: express that under certain conditions, something never occurs.

Liveness Properties: express that under certain conditions, something will ultimately occur.

Fairness Properties: state that under certain conditions, something will (or will not) occur infinitely often.

For each group, various cases and their solutions are commonly discussed during the verification process. Reachability and safety properties are usually the most crucial to the system correctness. Safety properties represent characteristics of the system such that undesirable event will not occur. Deadlock freeness is a special property commonly categorized as safety property however theoretically its classification as safety or liveness property is debatable (Berard & Bidoit 2001). In this paper we discuss deadlock-freeness as a safety property. We also propose solution to this common issue of verification in the later section.
For verification purposes, the composed model under consideration needs to be accompanied with a set of requirement properties described in form of a *model tester*. Figure 1 illustrates this relationship:

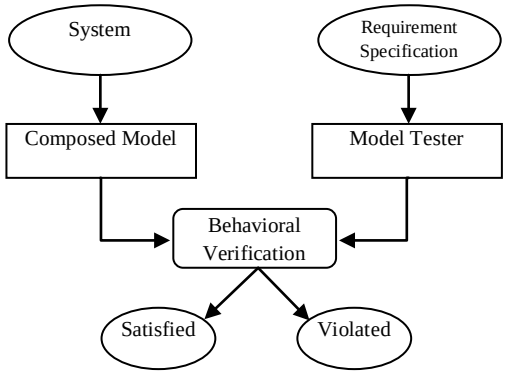

Figure 1: Behavioral Verification Relationship

2.3. Model Tester

In order to describe the requirement specifications, we define a "Model Tester". The Model Tester should be conceptualized as a tester device which is attached to the system during its execution to detect faults. The Model tester mainly consists of the specifications of behavioral properties representing desirable or undesirable situations and incidences. The Model Tester design is specified by the modeler in the form of a state-machine and consists of *good* or *bad* states that express a particular property and represent any of the families of system properties. Each state is guarded by a conditional trigger representing an event or a sequence of events (or global system change) which is sought to occur during the model execution. Good states are expected to be reached while bad states are not expected to be reached and thus the result of behavioral verification depends on the reachability (or un-reachability) of these states in the model tester.
Model tester is basically a passive component that only observes the interaction of the components of the composed model during the abstract level execution and changes its respective states once a desired or undesired behavior has been displayed by the composition hence verify the overall behavior.
Most states in the tester are exitable and are accompanied with an internal state reachability counter. Once they are reached the counter is incremented and then the tester is reset to its initial state. This is useful to record the number of times a specific behavior has been displayed by the composition and thus can be eventually utilized to collect statistics. Some states in the tester are however un-exitable and once reached halts the tester. This means either the composition has reached a successful completion of its goal(s) or it has crashed abnormally or deadlocked. Presence of such states means that the system has one or more terminating conditions.
We suggest the following general guidelines to create a Model Tester:

- A Ready state is defined to initialize the model tester in a neutral state.
- The desirable goals or objectives of a system usually expressed by reachability properties are defined as good states.
- Unwanted situations are expressed as negative reachability properties and are defined as bad states. This should be noted that Model Tester doesn't represent states of the member components of a composition; instead it contains states representing a global change or an effect of the combined behavior of the composition.
- An event or a sequence of events from the composed model is defined as condition for reaching each of these states.
- Commonly known correctness standards such as freedom of Deadlock as safety, absence of Livelock as liveness and Starvation freeness as fairness are general issues in verification process and are modeled in the tester as correctness standards depending on the domain of application whereas problems related to a specific business model are usually described as reachable properties and thus the objective of the verification is to test their satisfaction or violation.

Overall structure of the model tester is a set of good or bad states representing common safety, liveness and fairness properties and scenario specific reachability properties. The trigger to reach states of common properties is the external signal caused by the detection module integrated in the framework whereas the trigger to reach scenario specific reachability states is caused by probing the trace of the sequence of events exchange during the interaction of the members of the composition. Because for each correctness problem there are different detection algorithms and each varies based on the nature of the system however reachability can be detected by simply looking at the traces of the interaction.

The verification of the generic properties involves external solutions or integration of 3rd party model checking tools. Our proposed verification framework incorporates perpetual development and integration of similar external solutions and is open to alternatives because a variety of methodologies and techniques exists and each has its pros and cons in terms of suitability, accuracy and performance measures. Some solutions use Symbolic Model checking or Temporal Logic where as some use Graphs or Petri Nets. Our aim is to provide a generic runtime verification environment where a composed model can automatically be verified with the help of a model tester for context specific properties, while leaving the choice to the modeler to choose and integrate any external solution for system correctness verification. We however suggest a solution for deadlock detection as an example in the later section.

3. BEHAVIORAL VERIFICATION PROCESS

In this section we discuss our proposed Behavioral Verification Process and the framework in which this process has been implemented. A pre-condition for entering this process is that the components share the same semantic classes of the concepts used in the composition i.e., they have passed the static semantic matching phase as proposed in (Moradi et al. 2007).

Our proposed process is an aggregation of previously proposed state-machine matching process(Mahmood et al. 2009) with an extension of features in the framework to facilitate verification. In (Mahmood et al. 2009) we aimed to propose an initiative for developing a runtime environment for state-machine matching where as in this paper we intend to apply it for verification purpose.

Our verification process is based on a W3C compliant State-machine language and runtime environment called SCXML (State Chart Extensible Markup language) (State Chart XML (SCXML) 2009). This state-machine runtime environment has been used to perform abstract level execution of the composed model. The process consists of four steps as shown in Figure 2. First three steps in this process are preparatory and the fourth step is the execution step in which the state-machines are executed and their interaction is monitored with respect to the Model Tester. If the Model Tester doesn't reach any bad state throughout the execution and has reached all (or some) of the good states then we conclude the composition to be positively verified with respect to the given requirement specifications.

This process is briefly described as follows:

3.1. Parsing

As BOM state-machines are event driven, they are required to exchange events with each other to exit from current state and move to the next state, thus the events provide as guard to exit states. In the first step, BOM behavioral data (including state-machines, their states and corresponding events as exit conditions) of all the participating components are ingested by Parsing and their structure is loaded in the system. This step will produce a list of:

- State-machines for each component participating in the composition
- States for each state-machine
- Events (Send/Receive) of each component

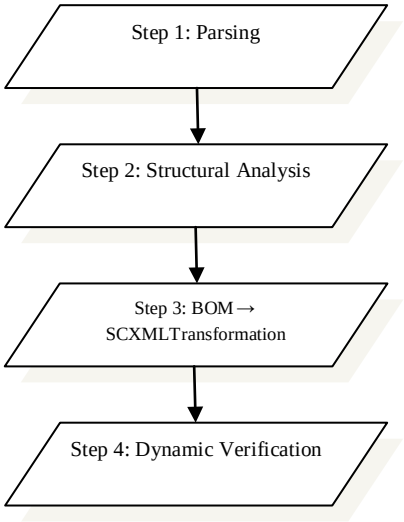

Figure 2: Behavioral Verification Process

3.2. Structural Analysis

In the second step all state-machine objects are sequentially passed through a set of Rules for structural

analysis. These rules are used to check whether a particular state-machine is structurally suitable for the composition or not. If a state-machine is verified by these rules, only then the verification process proceeds otherwise the composition becomes invalid for the given set of components.

Following is the proposed set of rules:

Rule1: Existence of Exit Condition
Each state in a state-machine must have an exit condition or otherwise it should be declared as final state.

Rule2: Existence of a sender for each receiver
In any of the participating state-machines for every Receiver waiting for an Event E there must exist a Sender that is supposed to send E.

Rule 3: Terminal Condition(optional)
If the composed model is terminating then there must exist at least one state marked as final in at least one state-machine among all the participants, such that at least one exit condition (event) leads the composed model to this state.
Violation of Rule-1 means that the execution path of a participating state-machine is broken and does not lead to a final state. Breach of Rule-2 means that there may be a situation when the state-machine will wait for an event endlessly as no corresponding sender is present to send the desired event. Rule 3 optionally evaluates the terminating condition of the model and if satisfied expresses that the model has a termination point. There may be cases where an execution is non-terminal and the system runs for an indefinite time but for simplicity we do not consider them. If all three rules are validated, we can continue to the next step.

3.3. Transformation (BOM to SCXML)
In the third step, BOM objects are transformed to SCXML format. Each state-machine will be transformed to a separate SCXML document. The term transform refers to the fact that the objects are converted from BOM to SCXML format. Here we also provide Model Tester in SCXML format so that it can also be injected in our runtime framework.

3.4. Dynamic Verification
The fourth step deals with the abstract level execution of the state-machines and their verification with respect to the model tester. In this step all components are subjected to an execution environment using verification framework. We discuss the details of our proposed Verification Framework in the next section.
In this step, all state-machines are set to their initial states. When the execution begins, each state-machine participates in a series of event exchange and as a result moves to its next state until it reaches its final state (if any, as not all members may possess final state). During this execution the verification framework uses external methods (if provided) to verify generic system properties and also monitors overall system behavior by observing events or sequence of events and trigger signals to the model tester for state change. As an example we suggested a method to detect deadlock in our framework. If the execution does not encounter any deadlock we verify that the composition satisfy the required safety property i.e. deadlock freedom. If both generic properties and context specific properties are satisfied during the entire execution time we infer that the given composition is verified with respect to behavior.

4. BEHAVIORAL VERIFICATION FRAMEWORK
In this section we discuss our proposed Behavioral Verification Framework design and its execution in detail. This framework uses SCXML to input and execute XML structure of a set of participating event driven state-machines. A finite state machine (FSM) is event driven if its inputs and outputs are modeled in the form of events or messages.

4.1. Framework Design:
Our framework consists of the following modules:

- Message Controller (MC)

This module is used as a communication platform. It is an asynchronous Message Controller used to send and receive multiple messages at a time. MC follows “Post Office” protocol and consists of an address space to accommodate each component for communication. Every component needs to register its name to be used as a unique identifier for the address so that it can be allocated with an INBOX. Each INBOX is a queue of Messages so that all the messages addressed to a component are stored in the INBOX in form of a FIFO queue and the component can process them one by one. Also there is a common OUTBOX for all outgoing messages, shared by all the components where they can place their outgoing messages addressed to each other. These outgoing messages are dispatched periodically and MC is responsible to place them in the pertaining

recipient's INBOX from where the receivers can retrieve and process them.

- **Component Executor (CE)**

A Component Executor module represents one instance of a component in the system and has a unique ID (i.e., the name of the component). Each CE has a SCXML engine object (State Chart XML (SCXML) 2009) to transact state-machine and can also communicate with the "Message Controller" to send and receive messages. CEs are implemented in form of Java Threads in order to perform parallel interaction between the components. They use SCXML document to initialize their internal SCXML engine and set the current state to their initial state. This is how a particular state-machine model is assigned to an executor thread in the system. Then an Event listener of each component is invoked and ready to fire events. Each time a suitable event is fired CE transacts its internal state-machine to the next state. A CE will stop its thread if it reaches its final state (if it has one as described by the SCXML model). If all CEs having final states are stopped, the process will successfully terminate.

- **Tester Executor (TE)**

This module is similar to Component Executor as it also has an SCXML state-machine model (representing our Model Tester) and SCXML engine. But it is passive and only receives events and changes its internal state. It also has a state reachability counter to count number of times a particular state (good or bad) has been reached. It can be modeled to have exitable or non-exitable, good or bad states. In case an exitable state if reached, the tester increments the counter and automatically resets back to the ready state to wait for any other event.

- **Event lookup Table**

This module contains a list of all the Events used in the composition and are parsed from BOM. This list of Events is accessible to each Component Executor so that being at a particular state they can locate the information of the next occurring event expected to be sent or received. This information is used to let a component either send an event to a specified recipient or wait for an event from a sender during each logical time step.

- **Monitor**

A monitor is used to observe global behavior of the composition. A monitor acts as a comparer between the member state-machines and the Model Tester. It monitors the overall execution, waits for the important exchange of events or sequences of events and fire necessary events for the Model Tester to update its state.

- **Deadlock Detector**

We propose this module as an example solution to one of the generic system property i.e., deadlock freedom.

A deadlock can be defined as: A set of components are said to be in a deadlock if each of them is waiting for an event that only another component in the same set can cause.

Deadlock is of two types: i) Total Deadlock ii) Partial Deadlock. If all components of the composition are in the waiting set then it leads to a total deadlock whereas if only some components are in the waiting set then it is a partial deadlock.

We develop deadlock detector component to observe any possible detection of deadlock and notify the monitor. This detector periodically collects the list of those components which are waiting for any event to proceed and apply our proposed deadlock detection method.

- **Deadlock Detection Method**

This method assumes a set Q of tuples of waiting components called "Receivers" which are waiting for their corresponding "Senders". This arrangement is used to establish a wait-for relationship for each waiting component.

$$Q = \{(r, s) \mid r \in \text{Receiver}, s \in \text{Sender}\}$$

Based on the information collected from the set Q, we construct a "Wait-for Graph" and fill it with vertices representing all the components from the waiting list at a particular instance of time. First a receiver will be inserted then its corresponding sender will be inserted. Then a directed edge is connected from the receiver to the sender showing "Wait-For" relation. When all the components from the waiting set have been inserted in the graph, we apply a standard Depth First Search (DFS) algorithm to find any possible cycles within the graph.

A cycle is defined as a closed loop of two or more vertices connected in a closed chain. If there exists a cycle, it means that some components are waiting for each other in a chain and thus there is a deadlock. In practice cycle detection in a Graph is done using Depth First Search (DFS) coloring algorithm. Color markers are used to keep track of which vertices have been discovered. White marks vertices that have yet to be discovered, gray marks a vertex that is discovered but still has vertices adjacent to it that are undiscovered. A black vertex is discovered vertex that is not adjacent to

any white vertices. Edges that lead to a new unvisited vertex are called Tree Edge whereas the edges that lead to an already visited vertex are called back-edges. By definition: "A directed graph G is acyclic if and only if a depth-first search of G yields no back edges". So DFS essentially detects any back-edge for finding a cycle(Skiena July, 1998). If we detect any cycle in the wait-for graph of a set of waiting components then we have found a deadlock which means there exists a cyclic chain of two or more components that are waiting for each other. If the number of waiting components in the set is equal to the total number of components participating in the composition then it will be a Total deadlock.

4.2. Framework Execution:

Figure 3 illustrate the verification framework:

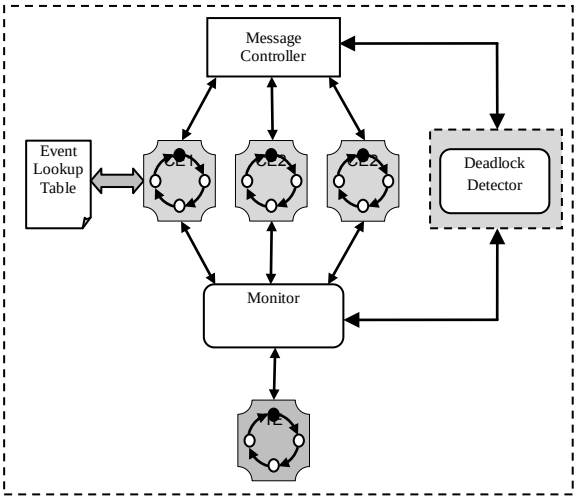

Figure 3: Behavioral Verification Framework

When the execution begins all Component Executors (CE) initialize their SCXML state-machine model objects to their initial states and also register their IDs in the Message Controller (MC) for address space allocation. When all the participating components are ready, they start dynamic interaction with each other by sending or receiving event messages using MC. Based on their current state each CE identifies the next event it is supposed to send or receive using Event Lookup table. From this table each CE can fetch information about the event which is required to exit its current state. If it is an outgoing event (i.e., the source of this event is the CE itself) then the CE will act as a Sender whereas if it is an incoming event (i.e., CE is the target of this event then it has to wait as a receiver).

In case of being a Sender a CE will prepare a message object by stamping its ID as a source, its recipient's ID as target and message parameters taken from the Event Object (previously fetched from the Event lookup table) and transmit it using Message Controller. MC will place this message in the Outgoing queue which will be dispatched in the next time generation. This CE will also fire that event in its internal state-machine and go to the next state.

If the CE is a receiver it will wait until it has received any message from the Message Controller. In case of multiple arrivals the first message from the INBOX is retrieved (as Queue is FIFO) and processed by firing the event internally and stepping to the next state. Each time there is a Sending or Receiving of an event, based on which a component transacts its state-machine to the next state, we let the system advance to next logical time step.

Deadlock detector performs its routine on each time step and checks possible deadlock occurences. In case of detection, it alerts the monitor which in turn sends a signal to the Tester Executor (TE). TE moves to the corresponding bad state and halts the execution. Monitor is also responsible to observe the behavior which corresponds to context specific reachability properties in the Model Tester and in case of finding valid sequence of events; it triggers an alert to the Model Tester. There is a performance bottleneck when we perform deadlock detection routine at each time step thus we propose to schedule them after an N interval of time where N is defined by the modeler based on the size of the composition and system resources.

The successful completion of the abstract level execution means that there is no violation of generic system properties and the context specific properties are reachable (or unreachable in case of negative reachability properties) and thus the behavior of the member components is verified.

5. CASE STUDY

In order to test our verification approach, we have considered a Restaurant Case Study. We discuss two scenarios in this case study.

5.1. Scenario A

The basic theme of the scenario is that customers arrive to a restaurant, order food, eat, pay their bills and then leave. There are 3 components in this scenario: *Customer, Waiter and Kitchen.* A sequence diagram in Figure 4 represents the pattern of interplay between these components.

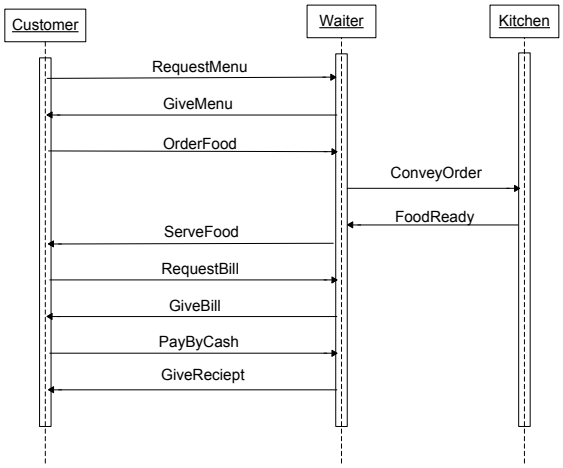

Figure 4: Restaurant sequence diagram

Figures 5, 6 & 7 represent the individual state-machines models of each component involved in the scenario. Green text with an up arrow represents a send event (as an exit condition) whereas blue text with a down arrow represents a receive event.

In the first step of the verification of composed restaurant model the state-machines are parsed from the BOMs and state-machine objects are produced. In step 2 the corresponding data is passed through structural analysis, which checks the state-machines against the rules and if passed the static analysis phase is declared as successful.

In the next step SCXML documents are generated, each representing the corresponding state-machines of the customer, waiter and kitchen components. Also a Model Tester is defined in the form of SCXML as represented by figure 8. Each SCXML document is then executed in runtime environment. When the Component-Executors are initialized to their initial states they identify their next action The first CE which is responsible to send an action in the Message controller is Customer and the action is *RequestMenu.* Waiter component is waiting for this event and as soon as it receives *RequestMenu,* it moves on the next state and Send *GiveMenu.* On receiving *GiveMenu,* the Customer starts to *OrderFood.* Thus each component sends and receives events in the same manner until the Customer component (which is the only component having a final state) reaches "Leaving" state and thus the abstract level execution is successfully completed and this is how the three BOMs are verified and validated using dynamic analysis.

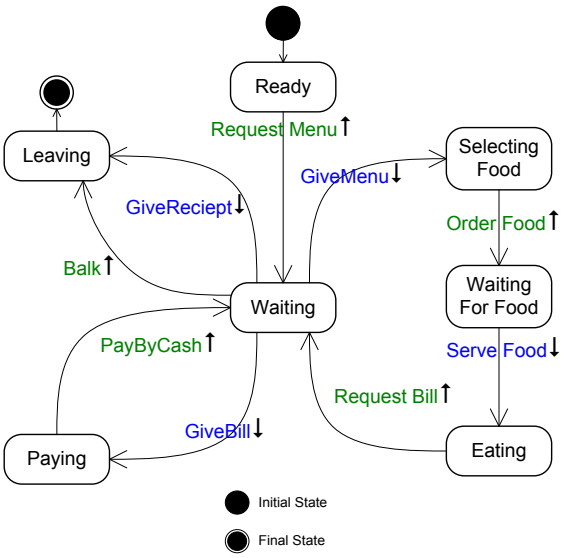

Figure 5: Customer state-machine

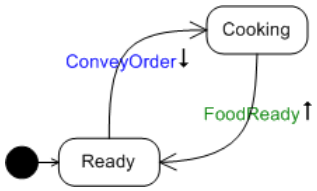

Figure 6: Kitchen state-machine

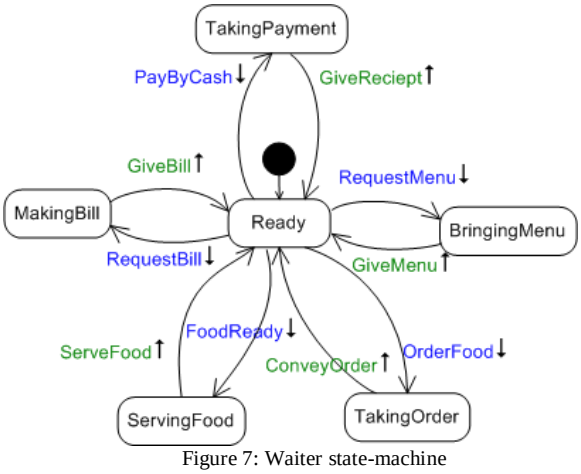

Figure 7: Waiter state-machine

Sales and Dinning are considered to be good states as they promote business. Leaving the restaurant without payment is a bad state as it incurs loss. Deadlock is a bad-state marked in gray and is un-exitable which means if reached halts the execution.

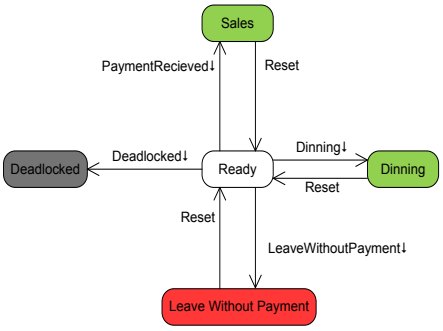

Figure 8: Model Tester

The state transition in Model Tester could occur due to a sequence of events exchange between the components e.g., in order to reach "dinning" state, the correct sequence of events is:

Customer!OrderFood → Waiter!ConveyOrder →
Kitchen!FoodReady → Waiter!ServeFood →
Customer!RequestBill → Waiter!GiveBill →
Customer!PayByCash → Waiter!GiveReciept

When this sequence is noticed by the monitor, it will fire "Dinning" event to the tester. Another sequence of events is:

Waiter!ServeFood → Customer!RequestBill→ Customer!Balk

When this sequence is noticed by the monitor, it will fire "Leave without payment" event which is a bad state because Waiter *serves food* but Customer after *requesting bill* goes to waiting state and leaves the restaurant without paying. Note the *Balk* event that can be fired from the waiting state.

If during the entire execution of the restaurant scenario, no bad states have ever been reached and the number of times the good states are reached is greater than zero, then the composed restaurant model is said to be dynamically verified in terms of behavior and with respect to the given specifications.

5.2. Scenario B

In this scenario, we modify the behavior of waiter, i.e., after taking the order, he makes a Bill and gives it to the customer and waits for the payment. Once Customer pays the bill, only then he conveys the order to the kitchen. Figure 9 represents the modified waiter.

This modification passes Structural Analysis because all the events are same only their order is changed. However when execute it in the dynamic verification step, it detects deadlock because the customer waits for the food to be served where as the waiter waits for the bill to be paid. Since two waiting components wait for each other so our deadlock detector detects a closed cycle in the wait-for graph and thus notifies the detection of deadlock to the monitor which in turn puts the Model Tester in the "Deadlocked" state and thus the composition is not verified due to deadlock.

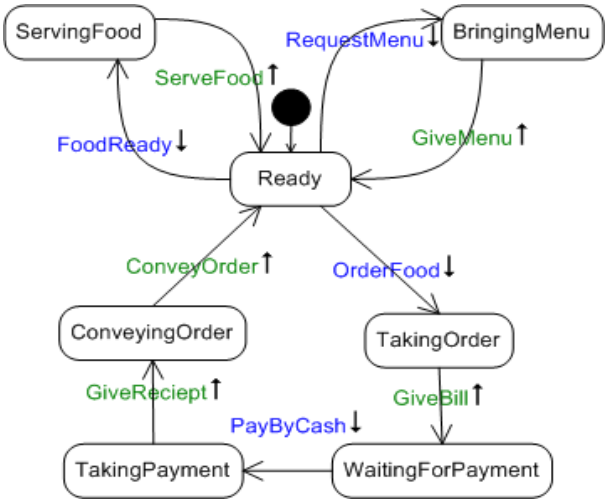

Figure 9: Waiter state-machine

6. CONCLUSIONS AND FUTURE WORK

In this paper we discussed Behavioral Verification and its different methods. We proposed a *Model Tester* to be used as an *Instrumentation Technique* for the dynamic behavioral analysis and proposed a verification framework using this technique. We also discussed different classes of the system correctness properties and suggested to represent them as good or bad states in the model tester. Deadlock Freedom being a commonly accepted correctness standard is suggested to be included in the model tester as a key requirement beside other scenario specific reachability properties. We further proposed a method to detect deadlock and implemented it as an integrated module in our verification framework. Similar modules can be developed and added to the framework to detect other safety or liveness properties thus increasing the credibility of the verification process. At the end we provided a restaurant case study as a proof of concept.

With the help of Behavioral Verification Process we can verify any BOM composition and essentially help the modeler to study and analyze the behavior using model tester which is based on system properties. These properties from different classes cover a variety of verification aspects and evaluation standards. By verifying the behavior of a set of BOM we can assert that a necessary condition in the process of BOM composition is fulfilled.

We are further interested to use formal methods such as Petri Nets and Linear Temporal Logic to verify the

composition based on more complex requirement specifications including livelock freedom and starvation freeness. We further strive to generalize our verification approach for other component frameworks such as DEVS (Discrete Event System Specification) to match and verify model compositions.

REFERENCES

Balci, O 1998, 'Verification. Validation and Testing', in *Handbook of Simulation: Principles, Methodology, Advances, Applications and Practice*, John Willey & Sons.

Bartholet, RG, Brogan, DC, Reynolds, PF & Carnahan, JC 2004, 'In Search of the Philosopher's Stone: Simulation Composability Versus Component-Based Software Design', *Simulation Interoperability Workshop*, Orlando.

Berard, B & Bidoit, M 2001, *Systems And Software Verification*, Springer.

Brahim, M & Athman, B 2006, 'A Multilevel Composability Model for Semantic Web Services', *Journal of IEEE Transactions on Knowledge and Data Engineering*, vol VOL. 17, No. 7.

Gustavson, P 2006, 'Guide for Base Object Model (BOM) Use and Implementation', Simulation Interoperability Standard Organizations (SISO).

Lehmann, A 2004, 'Component-Based Modeling and Simulation – Status and Perspectives', *Eighth IEEE International Symposium on Distributed Simulation and Real-Time Applications*.

Mahmood, I, Ayani, R, Vlassov, V & Moradi, F 2009, 'Statemachine Matching in BOM based model Composition', *13th IEEE/ACM International Symposium on Distributed Simulation and Real Time Applications*, Singapore.

Moradi, F 2008, 'Framework for Component Based Modeling and Simulation using BOMs and Semantic Web Technology', PhD Thesis, KTH/ICT/ECS AVH-08/05—SE, 2008, Stockholm.

Moradi, F, Ayani, R, Mokerizadeh, S, Shahmirzadi, GH & Tan, G 2007, 'A Rule-based Approach to Syntactic and Semantic Composition of BOMs', *11th IEEE Symposium on Distributed Simulation and Real-Time Applications*.

Petty, MD 2009, 'Verification and Validation', in *Principles of Modeling and Simulation*, John Wiley & Sons.

Petty, MD & Weisel, EW 2003, 'A Composability Lexicon', *Proceedings of the Spring Simulation*, Orlando, FL.

Sarjoughian, HS 2006, 'Model Composability', *Proceedings of the Winter Simulation Conference*.

Skiena, SS July, 1998, *The Algorithm Design Manual* , Springer.

'State Chart XML (SCXML)' 2009, W3C.

TEO, YM & SZABO, C 2008, 'CODES: An Integrated Approach to Composable Modeling and Simulation', *41st Annual Simulation Symposium*, Ottawa.

A SIMULATION MODEL TO QUANTIFY PERTURBATION EFFECTS OF AIRPORT INFRASTRUCTURES IN AIR CARGO HANDLING OPERATIONS

Miquel Angel Piera [(a)], Juan Jose Ramos [(b)], Mercedes Narciso [(c)] , Lamyae Filali [(d)]
Autonomous University of Barcelona, Department of Telecommunications and Systems Engineering.
Barcelona, Spain.
Polytechnique University of Marseile

[(a)]MiquelAngel.Piera@uab.es, [(b)]juanjose.ramos@uab.es, [(c)]mercedes.narciso@uab.es, [(d)]lamyae.filali@polytech.univ-mrs.fr

KEYWORDS
Logistics, air cargo, discrete event models, causal Models, Airports.

ABSTRACT
The optimisation and proper coordination of air cargo transport operations taking into account infrastructure capacity constraints (i.e., interactio of taxiways with pathways), as well as passenger and airline quality factors is considered nowadays a complex problem to be solved that could contribute to a better competitivity of the industrial sector.

The variety of processes, methods, individuals and organizations, in combination with a lack of methodologies to analyze the behavior of the whole airport operation as a combination of the decision taken in each subsystem (ie. handling, airline and airport managers), are one of the main risks that deals with airport and airline delays which have severe cost penalties.

In this paper, a simulation model that considers as a hard constraint the airport dwell time of low cost carriers together with uncertainties in the platform pathways to transport the cargo form the airport warehouse till the aircraft parking to load ULD pallets in the first belly has been implemented. Different policies have been implemented to minimize the handling resources required to satisfy the cargo operations for 4 European destinations.

1. INTRODUCTION

Current scenario in production and logistic fields shows globalization, needs for fast, low cost and reliable transport systems that could provide a competitive answer to fluctuations in market demands.

A particular logistic configuration that relies on an effective but also on a low cost transport system, is the well known supply chain organization, in which competitiveness and profitability require an efficient flexible transport infrastructure.

Low cost air carriers have irrupted in major airline market by offering reduced price air tickets to passengers. Originally these players focused on just serving the ‘‘visiting friends and relatives’’ and the ‘‘ethnic’’ markets, but some of them are changing to embrace more business travelers.

In order to offer competitive travel prices, routes are designed at strategical level to maximize the number of legs per day an aircraft can serve. A critical controllable aspect that can affect drastically at operational level the quality of service of these legs to be flown are the delays generated at the arrival/departure and the turn-a-round time in airports.

The growth in air travel is outstripping the capacity of the airport and air traffic control (ATC) system, resulting in increasing congestion and delays. However, a misunderstanding of the poor utilization of the available infrastructure usually leads to greater investments in additional gates, runways and extensive pavements for taxiways and aprons. In order to avoid this expensive approach, it is important to remove non-productive operations due to poor scheduling approaches.

Different kind of perturbations such as: weather, traffic congestion in some air traffic sectors, and late departures at the origin airport, leads to a typical time window predictibility around [+15 .. -15] minutes with respect to the expected arrival time for more than 40% of the landing operation along the day.

In (Zuñiga, 2010) and (Narciso 2009) two different DES models to minimize delays in the arrival procedures are described. Despite the technological advances in air navigation and the airport manager efforts, such as the well known CDM (Collaborative Decision Making) procedures to minimize delay propagations (Piera 2009), airlines feel weak to preserve route time-tables due to a lack of control on airport infrastructure priorization management rules and handling resources. This is one of the main reasons why low cost air carriers try to minimize/avoid those handling operations that could be a source of delays.

Some aspects that should be considered in a simulation model to design policies to mitigate the propagation of perturbations through the airport subsystems are those involved in the turn-a-round aircraft operation:

- The amount of baggage to be transported by the different handling companies at the different aircrafts that must share the airport pathways at a certain time window.

- The airport pathways capacity to support the movement of handling mobile resources at a certain time window.

- The physical distribution of the parking points (remote and contact points) : Bottlenecks in some pathways affects drastically the handling transport time.

From transport theory, it is well accepted that the speed of mobile handling resources (tracks, air stairs, tow, fuel tracks, buses, push backs, etc) in the airport pathways platform can be maintained around 30 km/h only if the number of resources do not exceed a certain amount of vehicles which can saturate the pathways and force a low average speed around 5 – 10 km/h. Figure 1 shows a typical airport pathway speed profile, in which the exact figure will depends on the characteristics of the airport, the distance from the terminal to the aircrafts parking positions, the interaction between the taxiways and the pathways, etc.

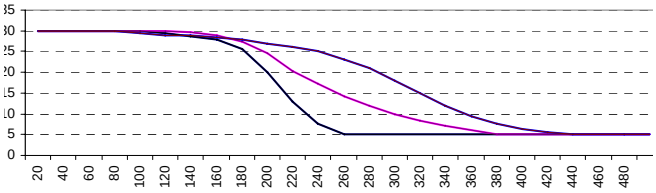

Figure 1: Speed versus Traffic in airport pathways

Despite airport managers try constantly to avoid the saturation of the platform pathways, most slots are concentrated in certain time window periods in which all aircrafts must be attended at the same time, which forces the use of all handling resources to be placed on time in order to avoid any delay in the aircraft turn-a-round time.

On the other hand, the possibility to assign contact positions (ie. fingers) instead of remote parking positions to the scheduled aircrafts is an important factor to reduce the number of mobile handling resources in the airport pathways. Note that 2 air stairs and 2 buses are mandatory to attend passengers of low cost carrier's aircrafts such as A320, B737 when they are assigned to a remote point.

The handling traffic required to attend the aircrafts for a certain period can not always be predicted since it varies according to the number of gates successfully assigned (Narciso 2009) and the amount of luggage's to be transported. On the other hand, the time required for each handling resource to reach the parking position of the aircraft depends also on the amount of mobile resources in the

pathways and the interaction between the pathways and the taxiways.

To avoid that these uncertainties could affect the aircraft dwell time in the airport, most handling companies increases the number of resources to be sure that the aircraft will be served at the right time, despite the idleness of their resources is also increased.

In this paper a simulation model that considers the number of extra handling teams to attend at the right time the load/unload cargo operation of the first belly without affecting the rest of handling operations required by the aircraft has been developed at macro level considering the different transport time perturbations.

In section II some characteristics of air cargo operations are introduced. Section III describes the main advantages and handicaps of regional and international airports to implement a low cost cargo operation. In Section IV a case study that considers 4 different destinations from Bcn airport is analyzed.

2. LOW COST CARGO COMPLEXITY

Airline charging costs to first luggage policy contributes to minimize handling operations and at the same time minimize the turn-a-round time in these airports in which luggage transport times from the terminal until the contact or remote parking point is subject of stochastic perturbations due to a lack of capacity in the airport pathways (ie. constant bottlenecks in peak hours).

As a consequence, the first belly of most low cost air carriers flies fully empty. On the other side, logistics operators (ie. OPL) tackle many loosely connected heterogeneous sets of actors, such as suppliers, factories, production firms, warehouses, distribution companies, transport and service providers, retailers, customers and so on to satisfy customer demands under a certain quality service factor and costs. Figure 2 shows a typical sequence of activities to fulfill air transport using cargo aircrafts

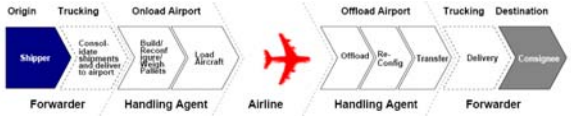

Figure 2: Air cargo activities

To be able to re-use for cargo purposes the first belly of low cost air carriers, it is very important to avoid delay propagation in the airport operations. A deep knowledge about all the events that take place and their interactions in each phase is important. Thus, by considering the Ground Phase, the turn-around handling operations can be formalized as a set of interrelated events which, properly coordinated, will satisfy the aircraft operative needs under certain service quality factors (SQF). With a proper model specification considering its interactions with the shipper the land transport and the cargo receiver, it will be possible to optimize operation efficiency through the proper management of airport re-sources (e.g. airport slots, stands and gates, check-in desks and baggage belts), considering the dynamics and costs of the cargo handling operations.

In the particular case of turn-around operations, it is easy to understand the system dynamics from a discrete event system approach, in which each operation has a certain number of preconditions, duration time estimation, and a set of post-conditions (changes in the state of airport information).

There are several characteristic of the described system that force the development of new methods (Piera 2004) to improve the air cargo operations, such as:

- A hierarchical network-based structure in which decisions at a certain level are propagated upstream and downstream.
- A large number of decision variables which increases the computational

complexity to deal with an optimal scheduling.

- Emergent dynamics appear when the system behaves as a whole and cannot always be predicted if the interaction between the different subsystems is not considered.

- Multiple performance measures use to force a trade-off solution instead of a global optimal solution.

- The stochastic nature of the arrival and departure times due to atmospheric perturbations is considered a constant source of perturbations.

3. REGIONAL AIRPORTS VS INTERNATIONAL AIRPORTS

Figure 3 shows a layout of Alguaire Airport which is located near by Lleida city in Spain. The runway capacity is below 14 operation/hour but terminal capacity constrains to a maximum of 3 operation/hour.

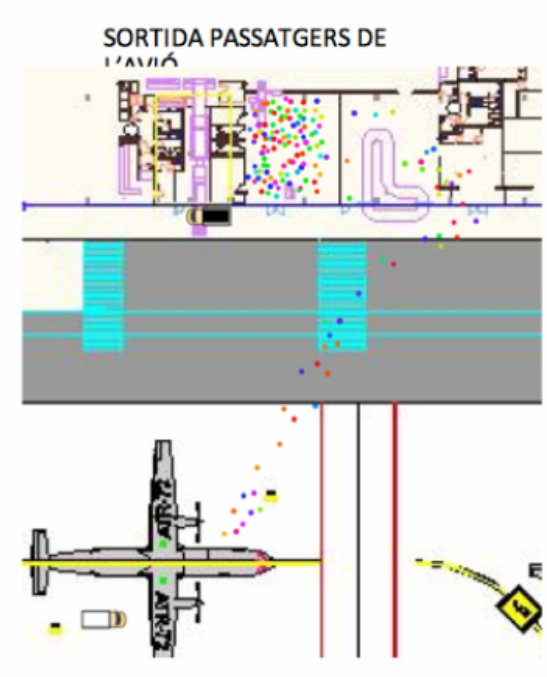

Figure 3: Aircraft parking position at a regional airport.

Now a day, there are 2 low cost carriers that operate in Alguaire airport with 2 scheduled operations in the morning and 2 in the afternoon. Aircrafts are parked just few meters from the terminal, thus passengers walk from the terminal to the aircraft, and there is no bottleneck in the airport pathways. Usually, handling movements from the terminal to the parking position are performed in less than 4 minutes.

Under these ideal operational conditions (absence of perturbations in the airport pathways), handling companies can program low cost cargo operations on the first belly just by a flexible manpower contract policy (Shangyao, 2008). From the airline point of view, the lack of perturbations in the turn-a-round time is a positive factor to sell the first belly for cargo purposes.

The first belly of an A-320 is characterized by a capacity of 12,23 mts3 and a weight constraint of 2 Tn. The extra fuel consumption for a 50 minutes flight when the first belly is full of cargo is just 50 Kg. Under similar circumstances, the extra fuel consumption for a 150 minutes flight is around 140kg. Figure 4 illustrate the extra fuel consume in Kg when the first belly is full with 2 Tn cargo. Thus for short and medium leg distances, first belly capacity can be sold at competitive prices while increasing the airline's benefits.

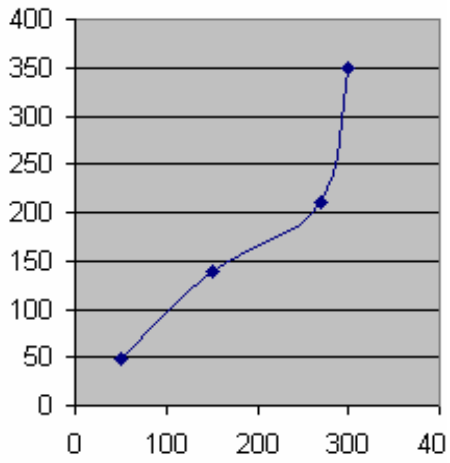

Figure 4: Extra Fuel consumption (Kg) per flight time (min.)

Despite the same costs and benefits should be obtained in international airports, the lack of confidence in preserving the turn-a-round time due to time perturbations on the airport pathways is a determinant factor for low cost carriers to prefer flying with the first belly empty instead of selling the belly capacity for cargo purposes.

Figure 5 shows the Bcn airport layout, in which it is easy to note the cargo warehouses are placed around 20 minutes from the contact parking positions in the new T1 terminal.

Figure 5: Layout of an international airport

It easy also to note that both types of perturbations can affect the cargo handling transport times from the warehouse till the parking position: platform pathway congestions and taxiway/pathways interactions. Furthermore, by considering also that the ETA use to have a perturbation described by a Uniform pdf U(-15, +30) , in order to guarantee that handling transport perturbations will not affect the aircraft turn-a-round time, a cargo handling team should be assigned during a minimum of 3 hours for just one cargo operation, which increases considerably the cost of the cargo operation.

Thus, the advantages of regional airports to support low cost cargo operations are mainly achieved due to lack of perturbations in the handling operative, however they lack of a minimum number of bellies that could be sold to transport a certain number of Tones at a regular frequency is a real handicap for low cost cargo sustainability. On the other hand, international airports can offer a competitive number of bellies, but inner logistic handling transport operations affect considerably the cost of the operation.

4. A CASE STUDY

A macro simulation model has been developed in Bcn airport using the following hypothesis and conditions:

- Only destinations with a minium of 6 flight per day has been considered, so a minimum of 12 Tn or 70 mts^3 could be managent by a transport company in order to attract the attention of freighters:
  - Frankfurt: 6 aircrafts/day
  - Paris: 22 aircraft/day
  - Brussels : 9 aircraft/day
  - Amsterdam: 6 aircraft/day

- Opportunity belly policy: Due to slot concentration in certain time periods, only those bellies that could be attended by an available handling cargo team will be considered. Thus, under this policy it is preferably to miss a belly instead of oversizing the number of cargo handling resources to load goods in all available bellies. Thus a trade-off solutions instead of a global optimal solution can be obtained using a macro simulation model.

Figure 6 shows all the programmed flights to the 4 European destinations distributed according to their ETA.

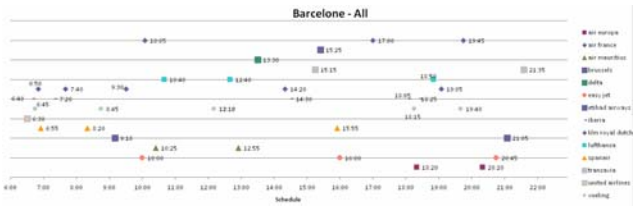

Figure 6: scheduled flights at Bcn airport

A simulation model in Arena has been developed at macro level, in which arrivals are programmed according to ETA's, and different pathways transport times are

considered to check the sensibility of the system to handling transport perturbations.

A scenario design has been considered to get a trade-off between the number of extra cargo handling teams with respect to the bellies that could be attended. The model do not considers the perturbations caused by the interation between taxiways and pathways that could appears between the cargo area till the T1 area. A shuttle system transporting ULD's from the cargo terminal to T1 has been modeled together with a cargo area in T1 where ULD's are placed waiting for its final transport to the aircraft parking position.

Figure 7 illustrates the number of aircrafts that can be attended using different number of extra cargo handling teams. Serie 1 represents the number of aircraft attended considering an average time for the cargo handling operation of 55 minutes considering the pathway travel time (go and return) and the load/unload belly operation. Serie 2 and serie 3 show the same information but considering an average time for the cargo handling operation of 65 minutes and 85 minutes respectively.

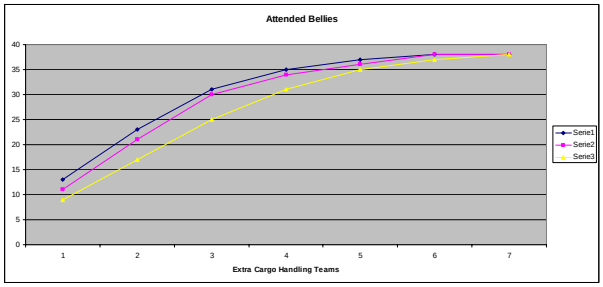

Figure 7: Bellies attended considering different handling cargo teams.

As it can be seen, a poor airport pathways capacity can affect considerably to support low cost cargo operations: increases the idleness of handling resources while at the same time affect the number of bellies that can be successfully loaded during the turn-a-round aircraft time.

According to the results obtained, a good trade-off can be obtained contracting 3 extra cargo teams, which corresponds to an average of 30 bellies per day (ie. 60 tones or 240 mts^3).

5. CONCLUSIONS

The sensitivity of the air cargo logistic systems to the constant perturbations provoked by saturation in the airport platform pathways and the interaction between taxiways and pathways has been introduceded both in regional airports and in international airports.

A simulation model to quantify how perturbations can affect the handling resources to attend cargo operations has been developed in Arena, and the results obtained illustrate the need of new logistic policies to implement low cost cargo transport operations in international airports.

REFERENCES

Narciso, Piera, Ramos, Laserna, 2009. Dynamic stand assignment to improve airport gates occupancy". EMSS'09 conference.

Piera, M.A.; Narciso, M.; Guasch, T. and Riera, 2004. Optimization of Logistic and Manufacturing Systems through Simulation: A Colored Petri Net-Based Methodology. *SIMULATION: Transactions of The Society for Modeling and Simulation International*, 80, 121-130.

Piera , MA., Ramos JJ, Robayna E., 2009. Airport Logistics Operations. "*Simulation-Based Case Studies in Logistics*". Springer.209-228.

Zuñiga, Piera, Ruiz, 2010. A TMA 4DT CD/CR causal model based in path shortening/path stretching techniques. ICRAT'10 conference.

Shangyao Y., Chia-Hung C. and Chung-Kai C. 2008. Short-term shift setting and manpower supplying under stochastic demands for air cargo terminals. Transportation (2008) 35:425–444. Springer Science+Business Media

SYSTEM DYNAMICS USE FOR TECHNOLOGIES ASSESSMENT

Egils Ginters [a], Zane Barkane [b], Hugues Vincent [c]

[a] [b] Sociotechnical Systems Engineering Institute, Vidzeme University of Applied Sciences, Cesu Street 4, Valmiera LV-4200, Latvia
[c] Thales Communications S.A. (FR), 45 rue de Villiers, 92526 Neuilly-sur-Seine Cedex, France

[a] egils.ginters@va.lv, [b]zane.barkane@va.lv, [c] hugues.vincent@thalesgroup.com

ABSTRACT
Elaboration and introduction of a new technology is a complex and expensive task therefore it is necessary to assess the set of factors influencing the future of technology during the stages of technology emergence and development. The most important parameters of assessment are acceptance and sustainability of technology. Different models exist, but mostly they are static and do not offer possibilities for dynamic assessment in real time and do not forecast the sustainability of solution. In the framework of FP7-ICT-2009-5 CHOREOS project No. 257178 a new two step methodology, Integrated Acceptance and Sustainability Assessment Model (IASAM), of socio-technical assessment has been elaborated. This model will use system dynamic simulation in STELLA environment and will take into account technical, social and financial factors, and existence of concurrent technologies for sustainability assessment.

Keywords: technology assessment, system dynamics simulation, Integrated Acceptance and Sustainability Assessment Model (IASAM),

1. INTRODUCTION

Elaboration and introduction of new technologies is a worthwhile, but complex task. It is conceivable that new approaches, during and after valorisation, will impact upon existing technologies, and will change or replace them. But, at the same time, the feedback from providers and audience (social components) will have some pressure on the approaches and technologies elaborated in the framework of the new technology, and thus will possibly ask for changes to the approaches elaborated. Indeed, critical factors for the successful introduction of any technology do not only include quality of the technical solution, but also social and financial factors, which are integral attributes of the technology assessment, because almost any system is a socio-technical one. Static approach is most typical in technology acceptance assessment. Unfortunately such approach does not offer possibilities for forecasting of viability, continuity and sustainability of the new technology in real time. In the framework of FP7-ICT-2009-5 CHOREOS project No. 257178 the new methodology Integrated Acceptance and Sustainability Assessment Model (IASAM) of socio-technical assessment has been elaborated. The methodology will take into account current tendencies of technologies development and possible future trends. It will observe qualitative parameters such as existence of technologies, financial possibilities of stakeholders and marketing skills of promoters of the new technology, ergonomic of the new technology etc.

2. TECHNOLOGY

To create an adequate system which confirms to the set of predefined criteria and ensure its operation, the designer and further operational staff (S) must implement a series of tasks.

To meet these challenges different methods and techniques exist, which are usually specified and regulated (rules, manuals, guidelines, patents, algorithms, etc.) to ensure their repeatability.

The above may be termed as the logical structure (L). However, in order to facilitate the task diverse applications (software, hardware, transport and communication facilities, equipment, machinery, etc.) can be used. Those serve as an environment of the logical structure and form a physical structure (F).

This means that any technology $(Tech)$ in freely chosen moment of time can be described as:

$$Tech = \langle L, F, S, t_0 \rangle \quad (1)$$

where L – logical structure, F – physical structure, S – social factor, but t_0 – freely chosen moment of time.

We can discuss, whether to consider social factors (staff, users, and environment) as an integral part of the technology or not. These factors create additional complexity to the technology specification, and therefore are usually ignored. This is also one of the main reasons why the sustainability of technology is unpredictable.

A technology can be developed and applied, when appropriate skills and knowledge is possessed not only

by the staff but also by the users. As well as technological, relevant social factors and circumstances exist too, and those determine the actuality of technology in use. Technology is not an unchangeable entity, because either it is changing, according to adopter's requirements, or no longer exists, that should be borne in mind when assessing any technology for sustainability and continuity.

In order to visualize the evolution of technology and its life cycle we can draw a parallel with the diagram of diffusion of innovation by Everett Rogers (Rodgers 1995) (see Figure 1).

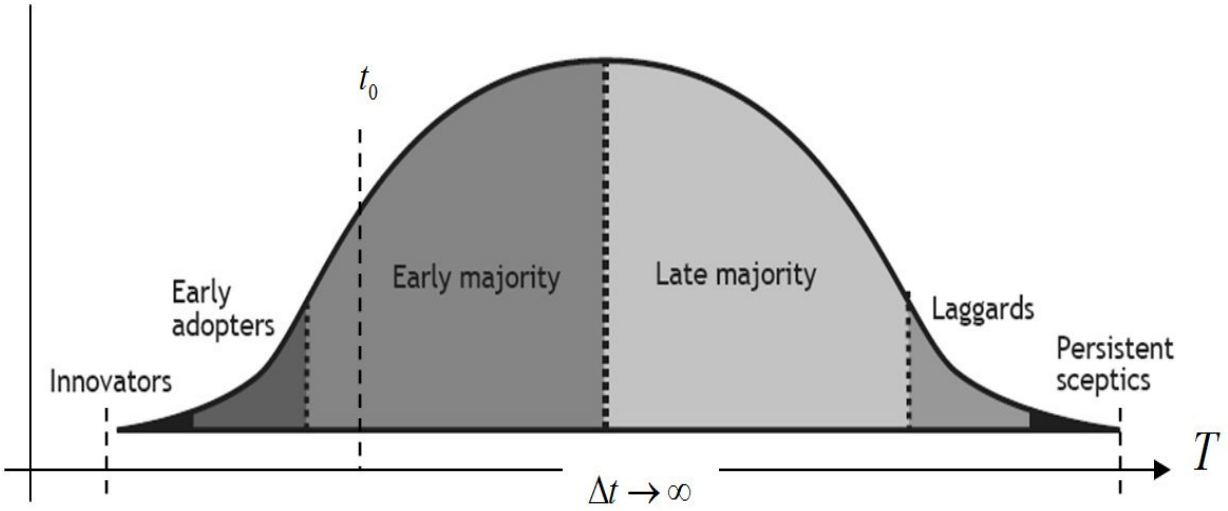

Figure 1: The Life Cycle of Technology

It shows that initially adopters are not many, but later their number is growing significantly. Once the technology has already won the public, more sceptical part of society joins, which calls for additional changes and improvements in the technology. Sooner or later the decline of the technology begins. Each developer's dream is to make a life cycle as long and profitable as possible, (to prolong the life cycle) i.e. $\Delta t \to \infty$, but not to be close to zero.

3. TECHNOLOGY ASSESSMENT

3.1. Technology Acceptance Model (TAM)

Different approaches, methods and models can be used for technology assessment. Technology Acceptance Model (TAM) (Venkatesh, Morris, Davis and Davis 2003; Lopez-Nicolas, Molina-Castillo and Bouwman 2008) was designed to predict IT acceptance and usage. It suggests that users formulate a positive attitude toward the technology when they perceive it to be useful and easy to use. TAM has been widely applied to various technologies, users and individual characteristics.

Studying virtual social networks Hossain and Silva (2009) proposed new theoretical construct that looks into the influence of social ties in an individual's acceptance process of a new technology

Pontiggia and Virili (2010) continued with the expectation that the candidate technology with a larger user network will be favoured in comparison to the one having smaller network, because users experience greater benefits with an increasing network size. Research shows that a larger user network size may push users to accept a system that could otherwise be discarded.

3.2. Task-Technology Fit (TTF)

Task-Technology Fit (TTF) model argues that a user will only adopt an information technology when it fits his/her tasks at hand and improves his/her performance. Goodhue and Thompson (1995) research identified eight factors that influence task-technology fit: data quality, locatability of data, authorization to access data, data compatibility between systems, training and ease of use, production timeliness, systems reliability, and IS developer relationship with users. Each factor is measured by interview using a seven point scale ranging from strongly disagree to strongly agree (Cane and McCarthy 2009).

Several studies (Yen, Wu, Cheng and Huang 2010) deal with integrated TAM and TTF models.

3.3. Unified theory of acceptance and usage of technology (UTAUT)

Venkatesh, Morris, Davis and Davis (2003) formulated a unified model (UTAUT) that integrates elements across the eight models – the Theory of Reasoned Action (TRA), the Technology Acceptance Model (TAM), the Motivational Model (MM), the Theory of Planned Behaviour (TPB), the Combined TAM and TPB, the Model of PC Utilization (MPCU), the Innovation Diffusion Theory (IDT), and the Social Cognitive Theory (SCT). UTAUT had four core determinants of intention and usage (performance expectancy, effort expectancy, social influence, and

facilitating conditions), and four moderators of key relationships (gender, age, experience, and voluntariness of use).

Zhou and Wang (2010) assessed mobile banking technology adoption using the task technology fit (TTF) model and the unified theory of acceptance and usage of technology (UTAUT). He found that performance expectancy, task technology fit, social influence, and facilitating conditions have significant effects on user adoption. The research considered task and technology characteristics, performance and effort expectancy, social influence and facilitating conditions used for mobile banking technology assessment. Unfortunately both models were still static and cannot be used for forecasting of sustainability of the new technology in real time.

3.4. Sustainable Assessment of Technology (SAT)

Even though modeling confirms technology acceptance by potential users, it does not verify sustainability of the technology..

The Sustainable Assessment of Technology (SAT) is a methodology elaborated by UNEP Division of Technology, Industry and Economics (DTIE) and International Environmental Technology Centre (Chandak 2007). SAT methodology integrates environmental, social and economic considerations. It focuses on environment and development together and puts them at the centre of the economic and political decision making process. SAT can be used for strategic planning and policy making, for assessing projects for funding, for assessment and comparison of alternative technologies and technology options. It is a quantitative procedure allowing sensitivity analyses and incorporation of different scenarios. SAT methodology determines three-tier assessment which incorporates screening, scoping and detailed assessment in conformity with customized criteria and indicators considering environmental, social and economic considerations. The results can be represented using star diagrams. SAT gives the possibilities for continuous improvement through Plan-Do-Check-Act (PDCA) cycle, but this process is not automatized.

Unfortunately SAT use for forecasting the situation development and changes of the technology raised by environmental, social and economic feedbacks and influence of other concurrent technologies in real time is problematic because the model is static. SAT methodology rather fits to the needs of governmental and supervision authorities aimed at analysis and planning at macro level, not at requirements of designers, promoters and adopters of new technologies.

Decision making in real time using the models mentioned above is problematic due to limited chance of getting an answer to the question “What happens if?” The existing approaches are static and mostly can be used for assessment of technology acceptance in the beginning of the life cycle. However, for real sustainability forecasting it is necessary to observe and take into account the influence of other concurrent technologies, feedbacks from social factors as well as influence the technology will create on existing technologies and how it will affect the function of designers and distributors network. To ensure convenient exploitation of the model in real time and manipulation with changing factors the system dynamics methods will be used.

4. INTEGRATED ACCEPTANCE AND SUSTAINABILITY ASSESSMENT MODEL (IASAM)

The Integrated Acceptance and Sustainability Assessment Model (IASAM) designed by Sociotechnical Systems Engineering institute at Vidzeme University of Applied Sciences consists of two phases (see Figure 2) and serves for assessment of technology acceptance and sustainability forecasting which is especially important in case of expensive and complex technology introduction.

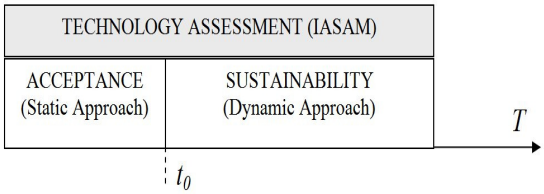

Figure 2: Technology assessment model IASAM

In acceptance phase the UTAUT model is used. Sustainability assessment structure involves a set of hierarchical models segmented in conformity with their functional role. The system dynamics simulation approach is used. The model is elaborated in STELLA environment (STELLA 2004) granting easy access to the model for the persons without specific knowledge in information technologies and mathematics. By simple graphical notation a set of differential equations are specified. Sustainability of technology (the stock in STELLA notation) is measured by the life time of the technology. At least four flows are described in the IASAM model at macro level. After that each flow and additional convertors can be specified more detailed at micro level. The main flows are Acceptance, Social impact, Finances and Expiration. The input flow Acceptance is determined by results of UTAUT and TTF use during first phase of assessment. However, Technology changes influenced by Concurrent technologies existence affect technology Acceptance (see Figure 3).

Also a feedback to Acceptance flow from Sustainability stock exists, because as long as the technology subsists in the market there are chances for its acceptance. The flow Finances characterizes possibilities the both most important actors: Stakeholders of the new technology and Adopters. If, for example, the Stakeholders have enough funding,

they can affect promoters of Concurrent technologies. Prolonging the life cycle of technology increases the technology's influence on the finances of Stakeholders and Adopters. The flow Social impact take into accounts mainly governmental factors, for example, a support for different branches of industry, and Age or Epoch factor. Latter parameter characterizes the soul or the style of the age. Is provided technology in conformity with the style of the epoch? It is very subjective parameter maybe even sophistic, but no less important than other ones.

parameters further can be specified more detailed to develop accuracy of modeling results.

5. CONCLUSIONS

Before investing significant funds in the new technology development and introduction it would be advisable to ascertain if it will be accepted by potential adopters. Some more or less widespread approaches of acceptance assessment as TTF and UTAUT exist. However, the acceptance of technology is not enough to ensure that technology will be sustainable and during

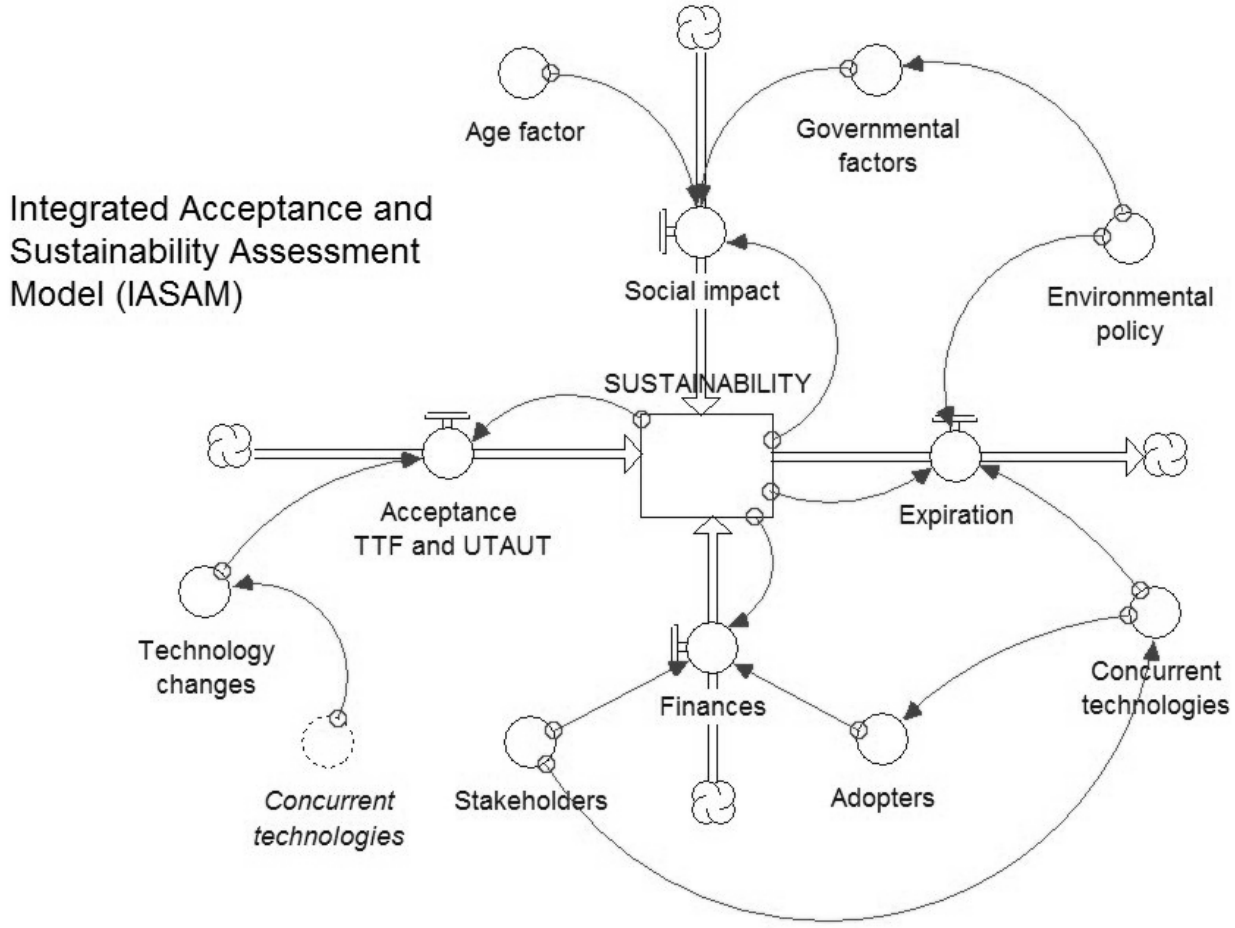

Figure 3: IASAM in STELLA notation

The Governmental factors can be affected by Environmental policy because it can be influenced not only by society but also by non-governmental sectors like Greenpeace, anti-globalization movements and other groups having different interests. The life cycle of technology is reduced by Expiration flow affected by Environmental policy and Concurrent technologies. The parameter Concurrent technologies can influence amount of Adopters.

The flows and the structure of the IASAM model are described above at macro level. Each flow and its life cycle will be able to earn back invested funding and gain the profit.

The current methods of sustainability assessment as SAT are more or less suitable for technology assessment by governmental authorities. Existing methods mainly are static and does not allow modeling and forecasting sustainability in real time.

Integrated Acceptance and Sustainability Assessment Model (IASAM) designed by Sociotechnical Systems Engineering institute at Vidzeme University of Applied Sciences allows

assessing acceptance and forecasting sustainability of the new technology in any point of the life cycle. The systems dynamic simulation approach ensures operating in real time and access to assessment process by persons without special knowledge in mathematics and modeling.

It is expected that IASAM model will be developed and validated during next three years under the framework of FP7-ICT-2009-5 CHOREOS project No. 257178. The IASAM methodology will be used as general and adaptable tool for different technologies assessment.

ACKNOWLEDGMENTS

The IASAM model described above is under development and will be tested under the framework of FP7-ICT-2009-5 CHOREOS project No. 257178 to assess future Internet technologies elaborated.

REFERENCES

An Introduction to Systems Thinking: STELLA Software, ISEEE Systems, ISBN 0-9704921-1-1, 2004.

Cane, S., McCarthy, R., 2009. Analyzing the factors that affect information systems use: a task-technology fit meta-analysis, *Journal of Computer Information Systems,* Fall 2009 108-123

Chandak S. P., 2007, Making Right Choices: A Framework for Sustainability Assessment of Technology (SAT), Available from: http://www.etvcanada.ca/forum2006/SChandak_UNEP2.pdf, 22.05.201, [accessed 28 July 2010]

Goodhue, D. L., Thompson, R. L., 1995. Task-technology fit and individual performance. *MIS Quarterly*, 34(2), 213–236.

Hossain, L., Silva, A., 2009. Exploring user acceptance of technology using social networks. *Journal of High Technology Management Research* 20 (2009) 1–18

Lopez-Nicolas, C., Molina-Castillo, F. J., Bouwman, H., 2008. An assessment of advanced mobile services acceptance: Contributions from TAM and diffusion theory models. *Information & Management*, 45(6), 359–364.

Pontiggia, A., Virili, F., 2010. Network effects in technology acceptance: Laboratory experimental evidence. *International Journal of Information Management* 30 (2010) 68–77

Robinson, L., 2009. *A summary of Diffusion of Innovations,* Available from: www.enablingchange.com.au, [accessed 28 July 2010]

Rogers, Everett M. Diffusion of Innovations. 4thed. New York: Free Press, 1995

Venkatesh, V., Morris, M. G., Davis, G. B., Davis, F.D., 2003. User acceptance of information technology: Toward a unified view. *MIS Quarterly*, 27(3), 425–478.

Yen, D.C., Wu, C.-U., Cheng F.-F., , Huang Y.-W., 2010. Determinants of users' intention to adopt wireless technology: An empirical study by integrating TTF with TAM. *Computers in Human Behavior* 26 (2010) 906–915

Zhou, T., Lu, Y., Wang, B., 2010. Integrating TTF and UTAUT to explain mobile banking user adoption. *Computers in Human Behavior* 26 (2010) 760–767

AUTHORS BIOGRAPHY

EGILS GINTERS is director of Socio-technical Systems Engineering Institute. He is full time Professor of Information Technologies in the Systems Modeling Department at the Vidzeme University of Applied Sciences. Graduated with excellence from Riga Technical University Department of Automation and Telemechanics in 1984, he got a Dr.Sc.Ing. in 1996. He is a member of the Institute of Electrical and Electronics Engineers (IEEE), European Social Simulation Association (ESSA) and Latvian Simulation Society. He participated and coordinated some of EC funded research and academic projects: e-LOGMAR-M No.511285 (2004-2006), SocSimNet LV/B/F/PP-172.000 (2004-2006), LOGIS MOBILE LV/B/F/PP-172.001 (2004-2006), IST BALTPORTS-IT (2000-2003), LOGIS LV-PP-138.003 (2000-2002), European INCO Copernicus DAMAC-HPPL976012 (1998-2000), INCO Copernicus Project AMCAI 0312 (1994-1997). His main field of interests involves: systems simulation, logistics information systems and technology assessment.

ZANE BARKANE is master student in Vidzeme University of Applied Sciences. She graduated from Riga Technical University, but now studies in Vidzeme University of Applied Sciences in study programme "Sociotechnical Systems Modeling". Her field of interests involves system analysis and technology assessment methods.

HUGUES VINCENT is working in the SC2 group where he leads the Network Centric Research and Development activities. He has more than 15 years of experience in computer science in Thales group where he worked as Software Project Leader on several Thales projects and as System Architect and System Integration Leader on the development of the command and control system of the seven regional dispatching of the French national electricity supplier (RTE-France). Subsequently, he has participated to the S4ALL project and is now leading the SemEUsE ANR project as well as the ITEmIS ANR project. He is principal investigator in the CONNECT FP7 IP FET. Also, he has been leading and working in some standard submission team in the Object Management Group (OMG), and now serves as one of the 11 members of the Architecture Board of the OMG.

A SIMULATION-BASED APPROACH TO THE VEHICLE ROUTING PROBLEM

Stefan Vonolfen[(a)], Stefan Wagner[(b)], Andreas Beham[(c)], Monika Kofler[(d)], Michael Affenzeller[(e)], Efrem Lengauer[(f)], Marike Scheucher[(g)]

[(a)(b)(c)(d)(e)] Upper Austria University of Applied Sciences, Campus Hagenberg
School of Informatics, Communication and Media
Heuristic and Evolutionary Algorithms Laboratory
Softwarepark 11, A-4232 Hagenberg, Austria

[(f)(g)] Upper Austria University of Applied Sciences, Campus Steyr
School of Management
Logistikum Research
Wehrgrabengasse 1-3, 4400 Steyr, Austria

[(a)]stefan.vonolfen@heuristiclab.com, [(b)]stefan.wagner@heuristiclab.com, [(c)]andreas.beham@heuristiclab.com, [(d)]monika.kofler@heuristiclab.com, [(e)]michael.affenzeller@heuristiclab.com, [(f)]efrem.lengauer@fh-steyr.at, [(g)]marike.scheucher@fh-steryr.at

ABSTRACT
In this work a simulation-based approach to the vehicle routing problem is presented. The simulation system is used to examine different problem environments and to optimize scenarios based on a generic domain model.

Using the simulation environment, a concrete practical transport logistic problem scenario is modeled and the simulation is coupled to the HeuristicLab optimization framework.

Keywords: vehicle routing problem, optimization, simulation

1. INTRODUCTION

The vehicle routing problem (VRP) is a well known problem in literature (for an overview, see for example Cordeau, Laporte, Savelsbergh and Vigo (2005)) and is used to model practical problem situations in transport logistics. The VRP formulation consists of a fleet of vehicles serving a set of customers with a certain demand from a single depot. There are several derivatives like the capacitated VRP with time windows (CVRPTW), or the multiple depots VRP (MDVRP).

In this work we present a simulation-based approach to vehicle routing problems. This enables the simulation and optimization of different transport logistic scenarios. Furthermore the simulation environment is a step towards online optimization. This can be performed by replacing the simulated values with real-life data.

In our approach, a simulation environment is used to examine diverse problem environments wich can be specified and simulated. The goal is to examine different practical transport logistic scenarios

Properties of the problem environment are for example the number of customers, the customer ordering behavior, the number of vehicles, the number of depots or the delivery strategy.

The simulation of a certain problem environment generates scenarios that can be optimized. For example, during a simulation run, customers make orders which results in a delivery scenario that is formulated and optimized as a VRP.

2. DOMAIN MODEL

The simulation environment is based on a generic domain model for transport logistic scenarios. Basically the domain model stores the master data and represents orders and deliveries.

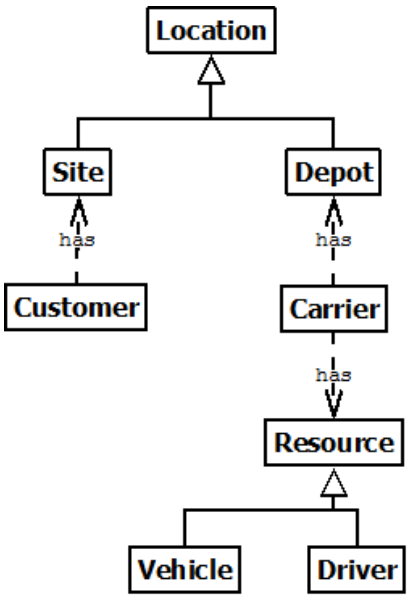

Figure 1: The master data

Figure 1 shows the model for the master data. It consists of location information. Both sites of customers

and depots of carriers have a location given in a coordinate system. The carrier has a certain set of resources which consists of drivers and vehicles.

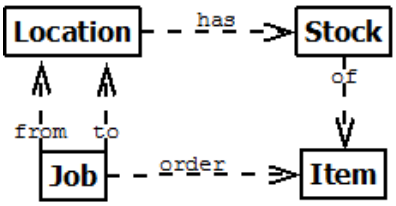

Figure 2: Orders

The representation of orders in the domain model is illustrated in Figure 2. Every location has a given stock of items. A job represents an order to deliver a certain item from a given location to another given location.

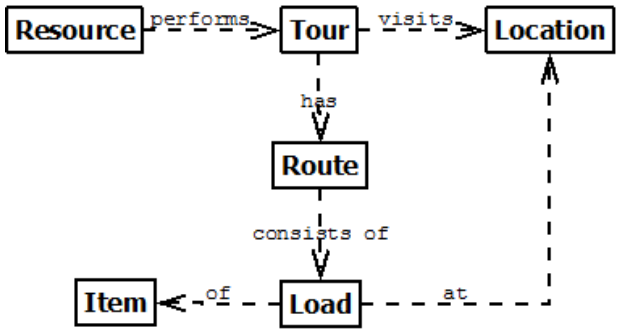

Figure 3: Deliveries

These jobs are then processed by the carrier, as shown in Figure 3. A tour visits certain locations using resources (e.g. vehicles, drivers) in no particular order. Thus, for a given tour multiple alternative routes can exist. A route is a tour where the locations are visited in a particular order. During a route multiple loads of items can be performed at certain locations.

For the classical VRP the customer makes orders (creates jobs) and provides target locations for them. The source location is determined by the depot. The model is generic enough to model other problem types like for example the dial-a-ride problem. In that case, jobs are created by the customers that specify both source and target locations in addition to a time window.

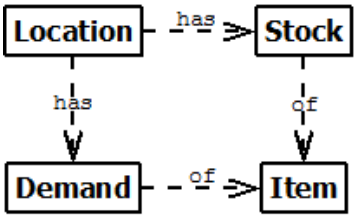

Figure 4: Vendor managed inventory extension

The domain model can also be extended to incorporate vendor managed inventory approaches. In that case a demand is calculated for every location using the current stock situation as illustrated in Figure 4. The jobs are not created by the customer, but by the carrier in that scenario.

Summarizing, because the domain model is generic, different variants of problems in the domain of transport logistics can be modeled.

3. SYSTEM ARCHITECTURE

Figure 5 illustrates the system architecture. The scenario generator creates scenarios which specify the problem environment. All master data and simulation parameters are included in a scenario specification.

The simulation loads this scenario and performs the simulation run. During a run, certain indicators and key figures can be written to a database. These indicators can be used during or after the simulation run to analyze the performance.

During the simulation run, problem instances are created for the simulation that can be optimized. In this case, VRP instances are parameterized by the simulation environment and sent to the optimization component.

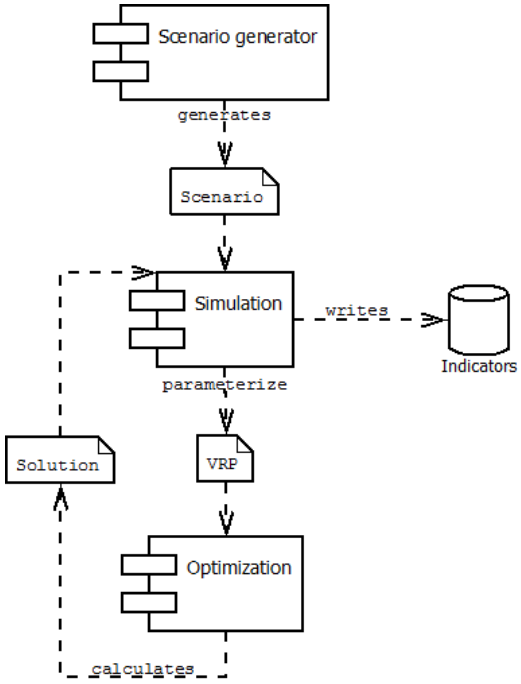

Figure 5: System Architecture

The components are examined individually in the following.

3.1. Scenario generator

As stated earlier, the scenario generator creates the problem environment. The master data is integrated into a single scenario file that can be loaded by the simulation component.

This can be achieved for example by integrating enterprise resource planning (ERP) systems or importing data from file formats like the XLS or CSV format.

Additionally, the scenario generator parameterizes the simulation run. Parameters could for example affect the customer ordering behavior or the delivery strategy.

Furthermore, the scenario generator can perform additional tasks like distance matrix generation or data preprocessing.

3.2. Simulation

To simulate the problem environment, an agent-based approach is followed. For the implementation the Repast.NET framework was used which is described by Vos (2005).

The different agents can perform certain actions at each time step of the simulation run. This enables the simulation of emergent behavior and the simulation environment can be modeled close to the actual problem scenario.

Figure 6 outlines the basic classes of the simulation environment and their relationships.

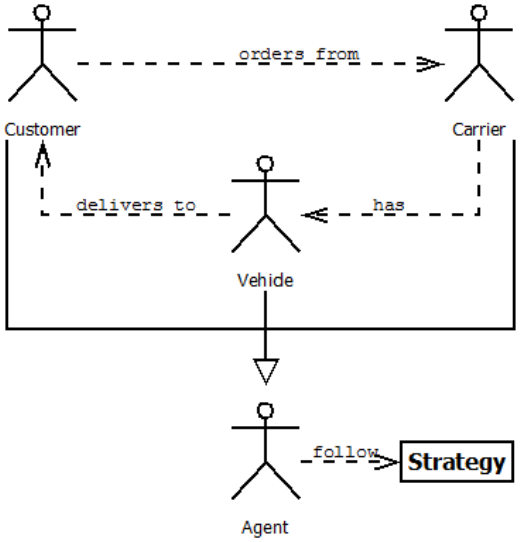

Figure 6: Simulation environment

According to the domain model, three types of agents are identified:

- Customer
- Carrier
- Vehicle

The customer agent simulates the customer behavior, like the customer ordering strategy. A customer can have inventories at different locations and the demand at each location can vary.

The delivery strategy is simulated by the carrier agent. A carrier receives orders from customers and controls a fleet of several vehicles. A carrier can have multiple depots.

The vehicle agent delivers the goods to the customer and receives orders from the carrier agent. It can choose between several alternative routes when delivering the goods to the customers, for example to avoid traffic jams.

All agents follow different strategies of performing certain actions. For example, customers could have diverse ordering strategies that can be parameterized in the scenario. Another example would be different delivery strategies by carriers.

Those strategies can be coupled to the optimization component. In that case, an optimization model like the VRP is parameterized by the agent and sent to the optimization component in order to decide what actions to perform next.

This interaction between the simulation and optimization components is defined by a generic interface. Each agent strategy can use this interface to parameterize different optimization models and use the optimization engine to make certain decisions.

3.3. Optimization

As stated before, the simulation generates scenarios by parameterizing a generic VRP model. This approach is similar to the approach followed by Beham, Kofler, Wagner and Affenzeller (2009).

The optimizer solves the problem and generates solutions for the different scenarios, which are then evaluated by the simulation. For developing the optimization solution, the extensible and generic framework HeuristicLab is used (Wagner, Winkler, Braune, Kronberger, Beham, Affenzeller 2007; Wagner 2009).

A core feature of HeuristicLab is the separation between problems and algorithms. This enables different metaheuristic optimization algorithms to be used and tested in a simulation run. As stated before, different optimization algorithms can be incorporated as strategies into the simulation environment and compared with each other.

In this particular scenario, the encoding proposed by Alba and Dorronsoro (2004) was used as a representation for the VRP, which is illustrated in Figure 8. Each route is separated by the vehicle number. The vehicles numbers start at the city count. For a VRP instance with 10 cities, the first vehicle number is 10.

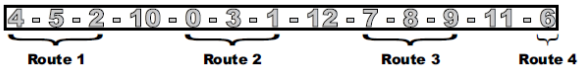

Figure 8: Problem representation (taken from Alba and Dorronsoro (2004))

Every solution is represented as a permutation, so standard permutation operators like the insertion, swap, inversion or translocation manipulation or edge recombination crossover can be used.

In order to generate solutions efficiently, so a simulation run does not take too long, a limit of one Minute was set for the optimization algorithm and the performance of several algorithms was compared. All tests were executed using HeuristicLab 3.3.0 (http://dev.heuristiclab.com) and a Core2Duo E7600 with 4 GB RAM under Windows 7 64 bit.

Different trajectory based search strategies were tested, once with a randomly generated initial solution and once generated by the push forward insertion heuristic as proposed by Thangiah (1999). As a neighborhood operator the translocation operator is used, which is described by Michalewicz (1992). The different algorithm configurations are listed in Table 1.

Table 1: Algorithm configurations

LSr (Local search with random initial solution)	
SampleSize	100
LSh (Local search with heuristic initial solution)	
SampleSize	100
SAr (Simulated annealing with random initial solution)	
StartTemperature	4000
EndTemperature	1E-06
InnerIterations	100
SAh (Simulated annealing with heuristic initial solution)	
StartTemperature	100
EndTemperature	1E-06
InnerIterations	100
TAr (Tabu search with random initial solution)	
SampleSize	500
TabuCriterion	Hard
TabuTenure	5
TAh (Tabu search with heuristic initial solution)	
SampleSize	1500
TabuCriterion	Soft
TabuTenure	50

The goal is to generate a feasible solution for the r102 instance from the Solomon benchmark library (http://www.idsia.ch/~luca/macs-vrptw/problems/welcome.htm) within one minute (250000 evaluations). This instance consists of 100 customers and is close to the test instance used in the results section. The quality value was calculated as following:

$$quality = distance + vehicles * 100 \quad (1)$$

Ten independent test runs were performed and the results are listed in Table 2.

Table 2: Algorithm Runs

Algo	Mean distance	Mean vehicles	Mean quality	Stdev quality
LSr	1786.58	22.40	4026.58	138.59
LSh	1750.71	21,40	**3890,71**	**85,59**
SAr	1780,27	21,70	3950,27	108,51
SAh	1744,94	21,80	3924,94	91,71
TAr	1815,37	22,50	4065,37	96,24
TAh	1772,59	21,30	3902,59	115,60

Basically it can be stated that the heuristic initialization improves the solution quality. The local search algorithm performs best in that configuration and has both the best mean quality and the least variation.

4. RESULTS

To validate the simulation system, a real-world scenario has been implemented and tested. The geocoding and distance matrix generation for the locations was performed using the open route service (http://www.openrouteservice.org) which is described by Neis and Zipf (2008).

The concrete scenario consists of

- One carrier
  - One depot
  - Homogenous fleet of 50 vehicles
- 84 customers
  - 1 site

There are 84 customers with one site. Each of the customer sites has a known demand that is based on real data. The customer ordering behavior is simulated by drawing from a normal distribution.

The atomic simulation step is one day, which means that the VRP model is parameterized and solved for each day.

Figure 8 shows a screen shot of a simulation run. On the left-hand side a map is displayed which shows the customer locations. Customers who have a demand in the current day are marked as red. On the right hand side several indicators are displayed. They can be used for the analysis of a simulation run. Example indicators displayed here are the traveled distance or the vehicle utilization.

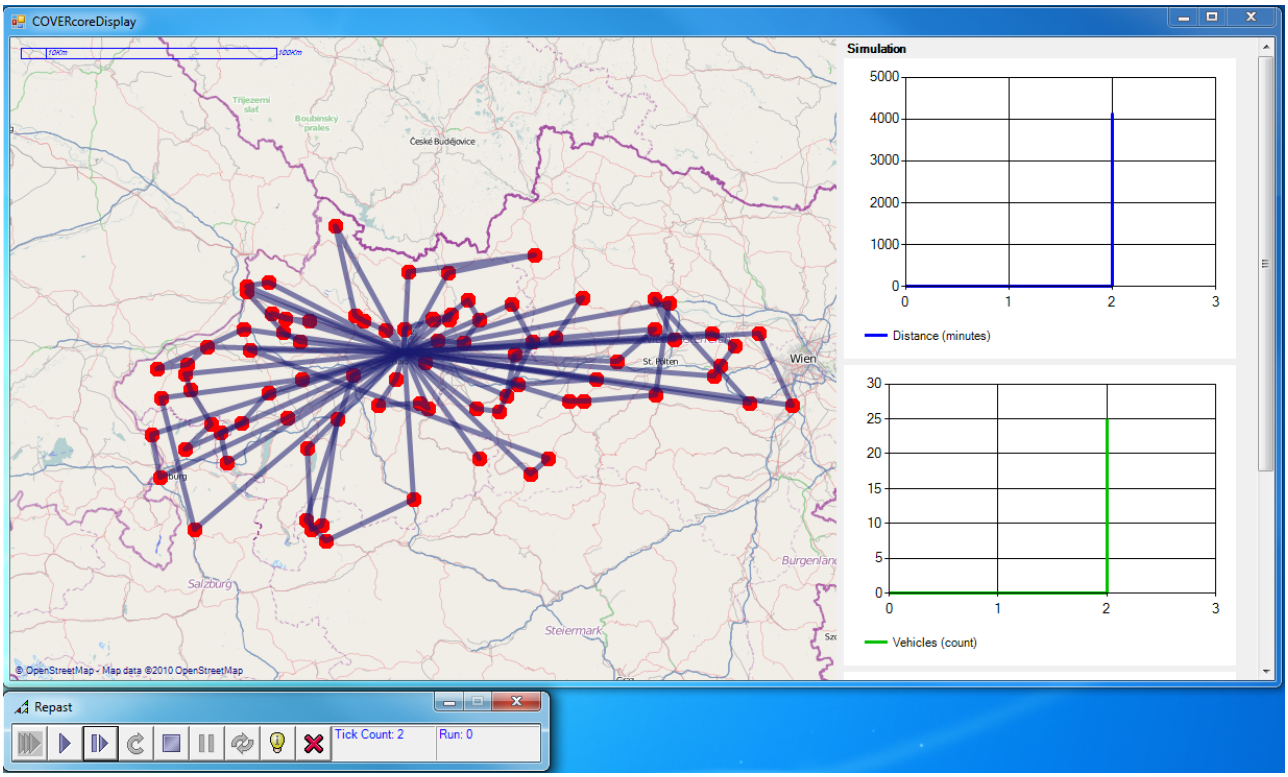

Figure 8: A simulation run

5. CONCLUSION

Concluding, a particular real-world scenario has been implemented in the simulation environment. The scenario was optimized with combination of an efficient heuristic and a metaheuristic optimizer using a permutation encoding.

In the future, different algorithms and encodings can be integrated and tested in the environment. Using the simulation system their performance for a particular scenario can be evaluated.

Additionally, different scenarios can be examined. Examples would be to examine different customer ordering behaviors, or to simulate seasonal fluctuations and evaluate how certain algorithms adapt to it.

A concrete example that will be examined is a mixed vendor-managed inventory approach to a real-world problem environment. The goal is to evaluate, how additional degrees of freedom in conjunction with fixed orders can affect the efficiency of delivery strategies.

Possible questions answered are for example:

- How much is the benefit of additional degrees of freedom in comparison to fixed orders according to costs, amount delivered and time delivered?

- In what scenarios are vendor managed inventory approaches beneficial and evaluation of mixed scenarios where some goods are ordered by the customer and some are managed by the vendor?

To sum things up, a flexible and extensible simulation system has been created that can incorporate diverse problem scenarios in the field of transport logistics as well as different algorithmic concepts to solve them and can be used to examine and compare them.

ACKNOWLEDGMENTS

The work described in this paper was done within the *Regio 13* program sponsored by the *European Regional Development Fund* and by Upper Austrian public funds.

REFERENCES

Alba, E.; Dorronsoro, B. 2004. *Solving the Vehicle Routing Problem by using Cellular Genetic Algorithms*. In: Barnhard, C.; Laporte, G. ed. *Handbooks in Operations Management & Management Science: Transportation.* Massachusetts Institute of Technology, USA. Chapter 6.

Beham A., Kofler M., Wagner S., Affenzeller M., 2009. Coupling Simulation with HeuristicLab to Solve Facility Layout Problems. *Proceedings of the 2009 Winter Simulation Conference*, pp. 2205-2217. December 13-16, Austin (Texas, USA).

Cordeau, J.-F.; Laporte, G.; Savelsbergh, M.W.P.; Vigo, D. 2005. Vehicle Routing. In: *Evolutionary Computation in Combinatorial Optimization (EvoCOP), Lecture Notes in Comput. Sci. vol. 3004*, Springer, pp. 11–20.

Neis, P., Zipf, A. 2008. *Zur Kopplung von OpenSource, OpenLS und OptenStreetMaps in OpenRouteService.org*. AGIT 2008. Symposium für angewandte Geoinformatik. Salzburg. Austria.

Michalewicz, Z. 1992. *Genetic Algorithms + Data Structures = Evolution Programs*. Springer.

Thangiah, S.R. 1999. *A Hybrid Genetic Algorithms, Simulated Annealing and Tabu Search Heuristic for Vehicle Routing Problems with Time Windows*. In: *Practical Handbook of Genetic Algorithms, Volume II: Complex Structures.* Pages 347-381.

Vos, J.R. 2005. Repast .NET: The Repast Framework Implemented in the .NET Framework. *Proceedings of the 2005 NAACSOS Conference*. June 26-28, Notre Dame (Indiana, USA).

Wagner, S.; Winkler, S.; Braune, R.; Kronberger, G.; Beham, A. 2007. Benefits of plugin-bases heuristic optimization software systems. *Computer Aided Systems Theory - EUROCAST Conference*, pp. 747-754.

Wagner, S. 2009. *Heuristic optimization software systems – Modeling of heuristic optimization algorithms in the HeuristicLab software environment*. Thesis (PhD). Johannes Kepler Univiersity, Linz, Austria.

AUTHORS BIOGRAPHY

STEFAN VONOLFEN studied Software Engineering at the Upper Austrian University of Applied Sciences, Campus Hagenberg and received his MSc in engineering in 2010. Since January 2010 he works at the Research Center Hagenberg of the Upper Austrian University of Applied Sciences. His research interests include transport logistics optimization and simulation-based optimization.

STEFAN WAGNER received his MSc in computer science in 2004 and his PhD in engineering sciences in 2009, both from Johannes Kepler University (JKU) Linz, Austria; he is professor at the Upper Austrian University of Applied Sciences (Campus Hagenberg). Dr. Wagner's research interests include evolutionary computation and heuristic optimization, theory and application of genetic algorithms, machine learning and software development.

ANDREAS BEHAM received his MSc in computer science in 2007 from Johannes Kepler University (JKU) Linz, Austria. His research interests include heuristic optimization methods and simulation-based as well as combinatorial optimization. Currently he is a research associate at the Research Center Hagenberg of the Upper Austria University of Applied Sciences (Campus Hagenberg).

MONIKA KOFLER studied Medical Software Engineering at the Upper Austrian University of Applied Sciences, Campus Hagenberg, Austria, from which she received her diploma's degree in 2006. She is currently employed as a research associate at the Research Center Hagenberg and pursues her PhD in engineering sciences at the Johannes Kepler University Linz, Austria.

MICHAEL AFFENZELLER has published several papers and journal articles dealing with theoretical aspects of evolutionary computation and genetic algorithms. In 2001 he received his PhD in engineering sciences from JKU Linz, Austria. Dr. Affenzeller is professor at the Upper Austria University of Applied Sciences, Campus Hagenberg, and head of the Josef Ressel Center *Heureka!* at Hagenberg.

EFREM LENGAUER received his PhD in economics in 2002 from JKU Linz, Austria. He is Professor of Logistics Management at the Upper Austrian University of Applied Sciences, Campus Steyr. Dr. Lengauer has published several papers dealing with transportation management and distribution network design. His research interests include heuristic optimization and simulation of logistical problems.

MARIKE SCHEUCHER received her MSc in business sciences in 2003 and her PdD in logistics in 2007, both from Johannes Kepler Univerity (JKU) Linz, Austria. She is research associate at the Logistikum.research of the Upper Austria University of Applied Sciences (Campus Steyr). Her research interests include distribution logistics, especially transport logistics.

The Web-pages of the authors as well as further information about HeuristicLab and related scientific work can be found at http://heal.heuristiclab.com/ and information about the Logistikum can be found at http://www.logistikum.at.

IMPROVEMENT ON DYNAMIC TILED TERRAIN RENDERING ALGORITHM IN LIBMINI

Liao Mingxue[(a)], Xu Fanjang[(a)], He Xiaoxin[(a)]

[(a)]Institute of Software, Chinese Academy of Sciences

[(a)]liaomingxue@sohu.com

ABSTRACT

As an open source library for large-scale terrain rendering in a continuous LOD high field, libMini takes a top-down method for static terrain rendering and achieves good performance. However, it uses the same top-down method to render elevation and texture for dynamic terrain. The method consumes a few seconds to update dynamic terrain and thus does not meet real-time requirements for rendering and leads to possible holes and gaps between adjacent terrain tiles. A millisecond-level real-time bottom-up libMini-based algorithm is proposed to render dynamic terrain while a method is presented to blend holes and gaps produced during the process of rendering dynamic tiled terrain.

Keywords: bottom-up algorithm, dynamic terrain, libMini, tiled terrain

1. INTRODUCTION

TERRAIN visualization is an important part of geographic information system, virtual battlefield environment, simulating training system, games and so on. Many algorithms are published for static terrain visualization, such as real-time continuous level of detail rendering algorithm (Lindstrom 1996), progressive meshes algorithm (Hoppe 1996), ROAM (Duchaineau 1997) and view-dependent fast real-time generating algorithm for large-scale terrain (Jin 2009). Due to the development of virtual environment simulation and increase in requirements for real-time interaction, the research on dynamic terrain visualization algorithms becomes increasingly important.

Both elevation data and image data of terrain will be changed due to interactions between 3D models and terrain in battlefield simulation or other situations, for example, explosion of thousands of bombs will force ground surfaces to collapse and will expose deep soil that takes on a different appearance from the ground surfaces and thus will pose restriction on the movement of tanks and other models in the scene. A few methods are now invented for dynamic terrain rendering.

Robert (1999) described a model of ground surfaces and explained how these surfaces can be deformed by characters in an animation. But their simulation model of ground surfaces was based on a uniform-resolution height field that cannot be extended to large-scale terrain scene.

Shamir proposed a multi-resolution dynamic meshes algorithm, which concentrates on complex geometric objects other than large-scale terrain (Shamir 2000). They used DAG (Directed Acyclic Graph) to present hierarchical structure and updated the DAG as deformations happened on objects at time steps to form T-DAG. This relatively costly T-DAG updating has a limit to on-line modifications on objects.

With an extension to ROAM and using DEXTER (Dynamic EXTEnsion of Resolution), He provided an algorithm for dynamic terrain visualization (He 2002). But their approach united with fake properties of terrain deformation and did not consider the physical model of terrain. They only dealt with relatively small scale terrain. Their terrain was divided into regions, but the continuity among the regions was not processed.

Recently, based on ROAM, Cai implemented a dynamic terrain method for rendering craters in battle-field environments (Cai 2006), but they did not address how the method runs smoothly in real-time. Exploiting the power of modern GPU, Shiben developed a system for real-time rendering and manipulation of large terrains (Shiben 2008). Their system achieves a performance of 250-microsecond terrain deformation over a block of size 1024×1024. However, the performance can be only reached with the help of GPU and thus costly.

This paper firstly proposes a real-time dynamic terrain algorithm for large-scale terrain based on libMini library (Stefan 1998). The library achieves good LOD continuity and rendering effect and has been applied well in VTP (Discoe 2005, Discoe 2009) and AquaNox game (Stefan 1998). In the library, the terrain is divided into tiles to solve the problem in large-scale data rendering. This paper also implements a dynamic terrain algorithm for elevation and image updating in the tiled terrain to eliminate holes and gaps between adjacent tiles.

2. BRIEF INTRODUCTION TO ALGORITHM OF LIBMINI

The underlying data structure of libMini algorithm for terrain rendering is basically a quadtree. The quadtree is represented by a Boolean matrix. Beginning from the

root node of the tree, if the terrain block represented by a parent node needs to upgrade its rendering detail level, we set corresponding value in the matrix to 1 and continue this way with the parents' four subnodes. A decision variable *f* with a less-than-one value in (1) tells a node to be upgraded (Stefan 1998).

$$f = \frac{l}{d \cdot C \cdot \max(c \cdot d2, 1)} \quad (1)$$

$$d2 = \frac{1}{d} \max_{i=1\ldots6} |dh_i| \quad (2)$$

In both (1) and (2), *l* is the distance to eye point, *d* is the length of the terrain block presented by the node, and *d2* is the roughness of the block. The constant *C* determines the minimum global resolution, whereas the constant *c* specifies the desired global resolution. The dh_i, which also appear in Figure 1 (Stefan 1998), are the absolute values of the differences between center elevation and average elevation of two ends of four borders and two diagonals.

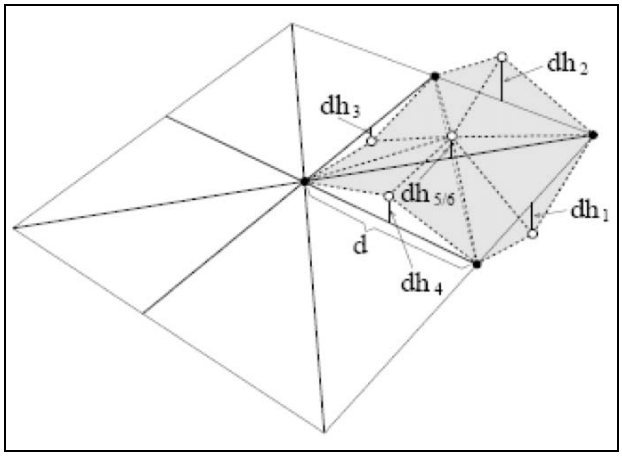

Figure 1: Definition for Variables dh_i in (2)

The major issue in rendering terrain is how to guarantee that the level difference of adjacent blocks is not greater than one in order to build a continuous mesh without holes. LibMini takes a top-down algorithm as in Figure 2 (Yang 2009) starting with highest-resolution blocks, it calculates their *d2*-values and then propagates those values to lower-resolution blocks to decide what real *d2* values of the lower-resolution blocks are.

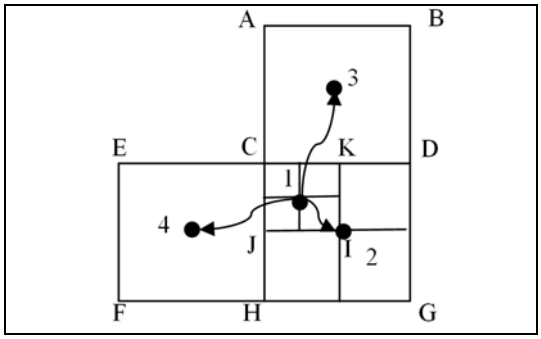

Figure 2: Process of Propagation of *d2*-values

As in Figure 2 the K (Stefan 1998) times *d2*-value is propagated from higher-resolution block CKIJ to lower ones ABCD, CEFH, and CDGH. Generally, a block in higher-resolution will propagate K times its *d2*-value to its parent block in lower-resolution and two lower-resolution blocks adjacent to its parent block. The final *d2* value of a block is the maximum of its own *d2* value and all K-times *d2* values passed to it.

According to the top-down algorithm above, if a small local part of the whole terrain changes dynamically, libMini need to calculate the new *d2*-value of the highest-resolution blocks in the local part and then to propagate the new values to lower-resolution blocks around this part. And these lower-resolution blocks also need to propagate their new *d2*-values to much-lower-resolution blocks around them. And such propagations will be continued this way up to the lowest-resolution blocks. In conclusion, a little change to any smallest part of terrain will trigger a continuous change to large-scale part of the terrain. Such changes are very time costly especially in a frequently changed terrain environment. So a smart algorithm must be designed to avoid such costly operation on dynamic terrain.

3. ALGORITHM FOR UPDATING BOTH ELEVATION AND TEXTURE

3.1. Elevation Updating

When a piece of terrain changes dynamically, the elevation of the terrain will usually be changed. Then, the changed terrain can act on the moving 3D models, such as tanks.

There are three steps to update elevation. Firstly, we use libMini API to get the highest-resolution elevation data of the changed terrain. Then, we modify the necessary part of the elevation data to demonstrate some dynamic terrain effect such as craters caused by sudden bomb explosion. At last, we build elevation data in lower resolutions with a simple interleaved method shown in Figure 30.

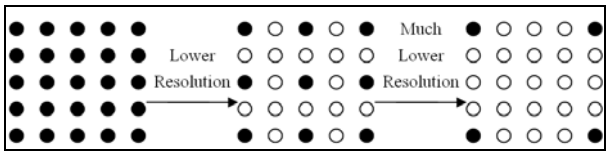

Figure 3: Simple Interleaved Method to Build Lower-resolution Data From Higher-resolution Data

After updating elevation we need to recalculate the *d2* values before rendering the new elevation. LibMini recalculates all *d2* values within about 2~3 seconds for 2048*2048 grids so that it cannot reach a real-time performance. Naturally we hope to only update a small local region where elevation is changed. However, libMini does not support such operation because using the top-down algorithm to propagate *d2* values in a local region will lead to incorrect *d2* values for lower-resolution blocks in other regions. For example, if the

old final *d2* value *x* of block CDGH in Figure 2 is set to K times the old *d2* value *y* of block CKIJ and the new *d2* value *z* of CKIJ is smaller than *y*, then the new final *d2* value of CDGH will not be updated because *x*>K*z*. In fact, if K*z* is the maximum value of all values passed to CDGH, the new final *d2* value of CDGH should have been updated to K*z*.

In conclusion, the top-down algorithm can be efficiently used for elevation update in the whole region, but not effective in a local region. Here, we devise a 2-step bottom-up algorithm to solve this problem.

Firstly all *d2* values of highest-resolution blocks in the changed local region are calculated according to a mathematical model.

Second, based on the rule of *d2*-value propagation, by a simple process of check for all higher-resolution blocks related with a lower-resolution block, it can be deduced that the *d2* value of a lower-resolution block is affected only by 12 blocks in higher resolution. As in figure 4, by checking higher-resolution blocks around block CDGH, we know its *d2*-value is affected by *d2*-values of blocks: A'K'KC, K'B'DK, DD'LI', LG'GI', GNMM', MH'HM', HF'J'J, JJ'CE', CKIJ, KDI'I, II'GM', JIM'H. The general situation is shown in figure 5 (Yang 2009). Then, a bottom-up algorithm for updating *d2*-values can be devised as below.

Bottom-up Algorithm
for each resolution ***r*** *from lower to higher*
 Evaluate block scope that need updating ***d2*** *value*
 if ***r*** *is the highest-resolution*
  for each block ***b*** *that need updating* ***d2***
   With (2) to calculate ***d2*** *of* ***b****, noted by* ***b.d2***
  endfor
 else
  for each block ***b*** *that need updating* ***d2***
   calculate ***b.d2***
   calculate $Kd2_1$, $Kd2_2$, …, $Kd2_{12}$
   $b.d2 \leftarrow max\{b.d2, Kd2_1, \ldots, Kd2_{12}\}$
  endfor
 endif
end for

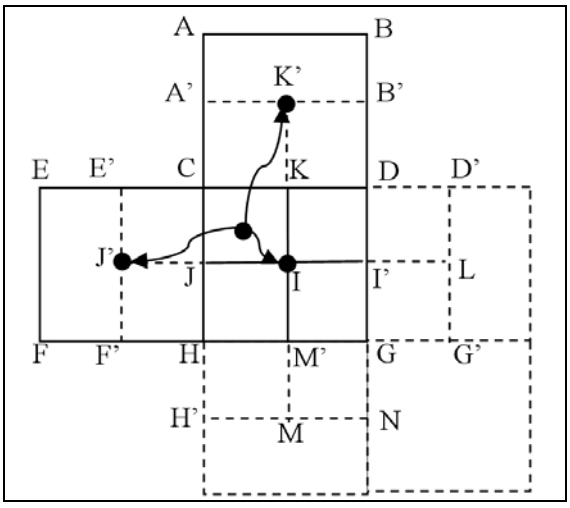

Figure 4: A Process of Finding Which *d2*-values Will Affect *d2*-value of CDGH Block

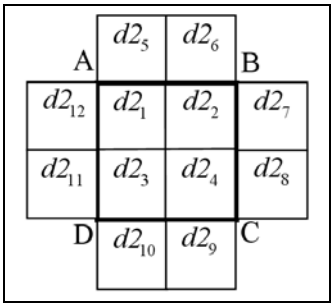

Figure 5: All 12 *d2*-values That Will Determine Lower-resolution Block ABCD's *d2* Value

For correctness of the bottom-up algorithm, we should prove a theorem given below.

Theorem 1. *The top-down algorithm in libMini for spreading* ***d2*** *values is equivalent to the bottom-up algorithm for spreading* ***d2*** *values.*

Proof. Firstly we build a discrete coordinate system with two coordinate axes ***I*** and ***J***. The starts of both ***I*** and ***J*** are 0. The ends of them are 2^n. The start point $<\boldsymbol{i}, \boldsymbol{j}>$ of blocks with resolution $2^k (\boldsymbol{n} \geqslant \boldsymbol{k} \geqslant 0)$ must be multiples of 2^k. The coordinates of a block with 2^k resolution are expressed by $[<\boldsymbol{i}, \boldsymbol{j}>, <\boldsymbol{i}+2^k, \boldsymbol{j}+2^k>]$. Figure 6 demonstrates such a coordinate system where0 the coordinate system starts with point <0, 0>, ends with point <4, 4>. The minimum resolution of blocks is 1. The maximum is 4. Figure 6 shows 16 blocks with minimum resolution, 4 blocks with 2^1 resolution, and 1 block with with 2^2 resolution. The 4 blocks with 2^1 resolution are [<0,0>,<2,2>], [<2,0>,<4,2>], [<0,2>,<2,4>] and [<2,2>,<4,4>], they all start with multiples of their resolution 2^1. Then, a 2^k resolution block may be in 4 different possible types of position as shown in (3) to (6). The 4 different types of position are shown by blocks A, B, C, D in figure 6.

$$I \equiv 0 \bmod 2^{k+1} \wedge J \equiv 0 \bmod 2^{k+1} \quad (3)$$
$$I \equiv 2^k \bmod 2^{k+1} \wedge J \equiv 0 \bmod 2^{k+1} \quad (4)$$
$$I \equiv 0 \bmod 2^{k+1} \wedge J \equiv 2^k \bmod 2^{k+1} \quad (5)$$
$$I \equiv 2^k \bmod 2^{k+1} \wedge J \equiv 2^k \bmod 2^{k+1} \quad (6)$$

Based on the top-down algorithm in libMini, the *d2* values are spread from a higher-resolution block to three lower-resolution blocks. We take a notation *top-down(b)* to indicate the blocks set containing blocks to which a higher-resolution block *b* $[<I, J>, <I+2^k, J+2^k>]$ spreads *d2* value. If the block *b* is in position (3), then the *top-down(b)* set consists of three elements as below:

(3)→*top-down(b)*=
{
$[<I, J>, <I+2^{k+1}, J+2^{k+1}>]$, (7)
$[<I, J-2^{k+1}>, <I+2^{k+1}, J>]$, (8)
$[<I-2^{k+1}, J>, <I, J+2^{k+1}>]$ (9)
}

The other three cases of *top-down(b)* are as below.

(4)→*top-down(b)*=
{
$[<I-2^k, J>, <I+2^k, J+2^{k+1}>]$, (10)
$[<I-2^k, J-2^{k+1}>, <I+2^k, J>]$, (11)
$[<I+2^k, J>, <I+2^k+2^{k+1}, J+2^{k+1}>]$ (12)
}
(5)→*top-down(b)*=
{
$[<I, J-2^k>, <I+2^{k+1}, J+2^k>]$, (13)
$[<I, J+2^k>, <I+2^{k+1}, J+2^k+2^{k+1}>]$, (14)
$[<I-2^{k+1}, J-2^k>, <I, J+2^k>]$ (15)
}
(6)→*top-down(b)*=
{
$[<I-2^k, J-2^k>, <I+2^k, J+2^k>]$, (16)
$[<I+2^k, J-2^k>, <I+2^k+2^{k+1}, J+2^k>]$, (17)
$[<I-2^k, J+2^k>, <I+2^k, J+2^k+2^{k+1}>]$ (18)
}

For any lower-resolution block $b[<I, J>, <I+2^M, J+2^M>]$, it must be a member of top-down set of a certain higher-resolution block. Let $b[<I', J'>, <I'+2^M, J'+2^M>]$ be equal to any of (7)~(18), we can get all possible higher-resolution block *B* that propagate their *d2* values to *b*. For example, let *b* be equal to (7), we have:

$$[<I',J'>,<I'+2^M,J'+2^M>]=[<I,J>,<I+2^{k+1},J+2^{k+1}>]. \quad (19)$$

From (19), we can know the relations below:

$$I=I',\ J=J',\ k=M-1. \quad (20)$$

Then *b* becomes:

$$b=[<I',J'>,<I'+2^{M-1},J'+2^{M-1}>]. \quad (21)$$

With the same method, we can get the following possible *b*:

$b=[<I', J'+2^M>,<I'+2^{M-1}, J'+2^M+2^{M-1}>]$. (22)
$b=[<I'+2^M, J'>,<I'+2^M+2^{M-1}, J'+2^{M-1}>]$. (23)
$b=[<I'+2^{M-1}, J'>,<I'+2^M, J'+2^{M-1}>]$. (24)
$b=[<I'+2^{M-1}, J'+2^M>,<I'+2^M, J'+2^M+2^{M-1}>]$. (25)
$b=[<I'-2^{M-1}, J'>,<I', J'+2^{M-1}>]$. (26)
$b=[<I', J'+2^{M-1}>,<I'+2^{M-1}, J'+2^M>]$. (27)
$b=[<I', J'-2^{M-1}>,<I'+2^{M-1}, J'>]$. (28)
$b=[<I'+2^M, J'+2^{M-1}>,<I'+2^M+2^{M-1}, J'+2^M>]$. (29)
$b=[<I'+2^{M-1}, J'+2^{M-1}>,<I'+2^M, J'+2^M>]$. (30)
$b=[<I'-2^{M-1}, J'+2^{M-1}>,<I', J'+2^M>]$. (31)
$b=[<I'+2^{M-1}, J'-2^{M-1}>,<I'+2^M, J'>]$. (32)

All possible *b* indicated by (21)~(32) is shown in figure 7. In this figure, the *d2*-value of the lower-resolution block ABCD will be affected by those of blocks (21)~(32). This figure has the same meaning as figure 5.□

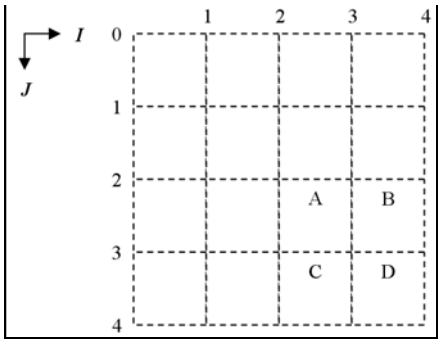

Figure 6: The Coordinate System

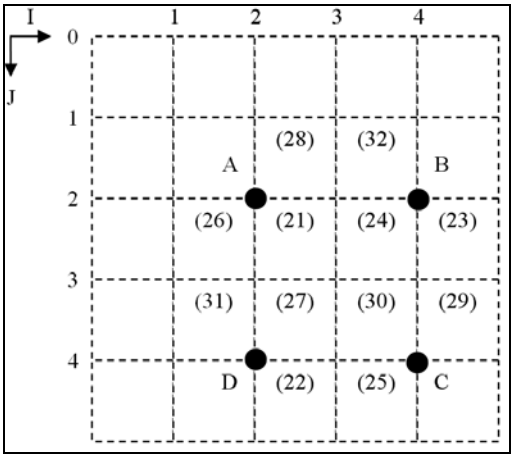

Figure 7: All Possible Higher-resolution Blocks Which *d2*-values Put on an Effect on a Specific Lower-resolution Block

Following this theorem, we can use the algorithm above to render dynamic terrain such as a terrain where groups of bombs make craters in a single tile. When the dynamic terrain crosses tiles, we should use an enhanced version of this algorithm in section 4.

3.2. Image/Texture Updating

When terrain changes dynamically, textures or images used for rendering the terrain usually need to be changed. However, we cannot change the images directly due to the fact that libMini employs S3TC (Brown 2009) algorithm to compress textures. S3TC compresses every block of 4×4 RGB or RGBA pixels into 64-bit data. Therefore, we can take four steps to update textures.

First, we calculate the image scope of the dynamically changed terrain and align it to make sure that both width and height of it are multiples of 4 and get the highest-resolution image data in this aligned scope from libMini. The second step is to decompress the aligned image and then to modify some decompressed image pixels according to the dynamical terrain model. The following step is to recompress the modified data into the form which libMini can recognize. At last, we use the modified highest resolution image to create images in other lower resolutions and reload the revised image data into memory according to the current run-time LOD.

If an image to be changed crosses n tiles (n is 1, 2 or 4), as shown in figure 8 (Yang 2009), following the 4 steps above, we need 9 steps to update the terrain image: calculate the affected areas of all tiles, align the areas, collect highest-resolution image data from all tiles, decompress them, combine the decompressed data into one image then modify the whole image according to terrain model, divide the whole image into n parts, compress each part, recalculate lower-resolution images, and in the end, rerender the images.

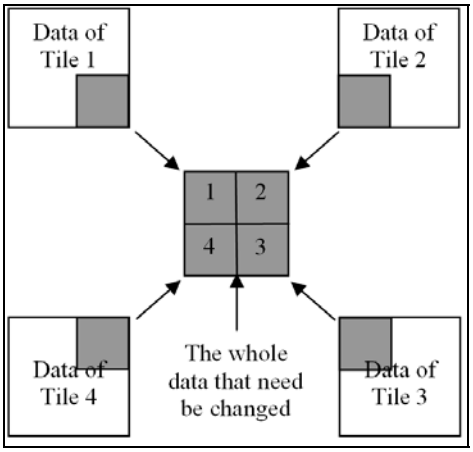

Figure 8: Processing Images Crossing Tiles

4. BLENDING BETWEEN TILES

The libMini guarantees that the difference of roughness level between two adjacent blocks within one terrain tile is less than or equal to one. It doesn't guarantee such a level difference between tiles especially when the adjacent titles change independently. As a result, there may produce holes between tiles especially when the terrain dynamically changes in the margin of tiles. The number of the influenced tiles will be 1, 2 or 4 when the terrain changes. These tiles are called target tiles. To avoid holes between target tiles, we take a 3-step blending method.

First, based on a logic coordinate system we update elevation of changed terrain to make sure that the joint elevation values of the two tiles be the same. As shown in figure 9 (Yang 2009), two lines of points covered in one ellipse are managed by two tiles. In fact, the two lines are the same. When one tile is updated on points of the same line, they may be also changed by update to the other tile. So there are two copies of elevation of the same line. In the following process of *d2* calculating the resolution levels of grids near the same line probably produce a difference greater than 1 to make holes. To keep these points the same elevation value, we treat the terrain being changed as a whole part in separate logic coordinates. After the terrain in such coordinates is updated, the elevation values of the terrain are mapped back into every tile in their coordinates.

Second, all target tiles are processed as if they were one whole tile in the process to calculate *d2*. The bottom-up algorithm in section 3.1 is used here to reduce the amount of terrain blocks to be updated. Therefore, a difference not greater than 1 of resolution level between tiles can be guaranteed and possible holes among tiles can also be eliminated.

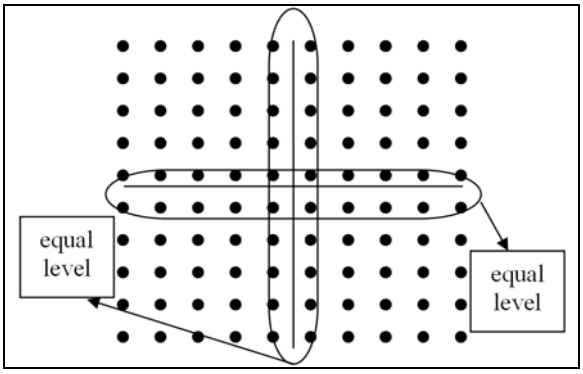

Figure 9: Keep Joint Elevation Values the Same

5. ALGORITHM PERFORMANCE AND EXPERIMENT RESULT

If the size of a terrain tile is $2^N \times 2^N$, time complexity of top-down algorithm in libMini is shown as (33) where C_1 is time for calculating *d2* and C_2 is time for passing *d2* to 3 lower-resolution blocks. We suppose that the scope of elevation data being changed is $2^n \times 2^n$, time complexity of botttom-up algorithm is shown as (34) where C_3 indicate time for indexing *d2* value of 12 higher-resolution blocks. Generally C_3 of is 4 times greater than c2. But usually *n* is about 3 and *N* is greater than 10. In conclusion, bottom-up algorithm is about 10^3 times faster than the old one and is more adaptive to situations such as war games where local changes to elevation are numerous and frequent (about 10^3/second).

$$(C_1+C_2)\sum_{k=1}^{N} 2^{2k} \approx \frac{4(C_1+C_2)}{3} 2^{2N} \quad (33)$$

$$(C_1+C_3)\sum_{k=1}^{n} 2^{2k} \approx \frac{4(C_1+C_3)}{3} 2^{2n} \quad (34)$$

We test the algorithms above on a PC with Pentium 2.8GHz CPU and 2GB memory. The programming environment is Visual Studio C++ 2005. The tested terrain consist of 16×16 tiles and each tile has 257×257 grid points and 2048×2048 pixels and dynamic terrain is created by a crater model covering about 16×16 grids. The average time to render the dynamic terrain for 1000 tests is about 1.27 milliseconds whereas the algorithm of libMini takes is 2512 milliseconds. The process of test is described below.

Firstly we build a type of crater model. The parameters of the model are defined by a quadtuple <position, direction, radius, depth> where position indicates the position of bomb explosion (the center of a crater), direction is the direction of the bomb track, and radius and depth are the radius and depth of the crater respectively.

The intersection line that a longitudinal section intersects the crater elevation plane is shown in figure

10 (Yang 2009). The numbers on this figure represent distance from the center point of the crater. If the radius of the crater is *r*, then the number 2 has the meaning of 2*r*.

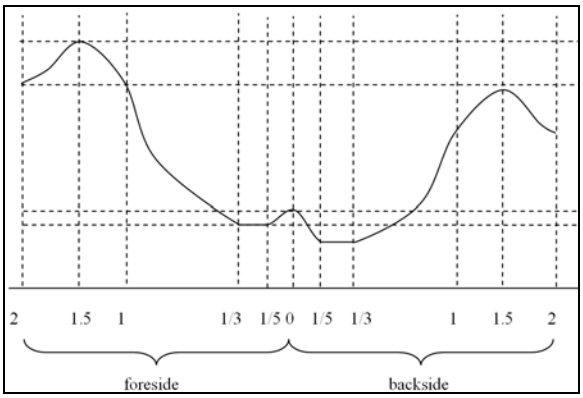

Figure 10 The Intersection Line of the Crater

Figure 11 shows how the elevation of a cross-4-tile crater is updated. To be clearer, we mark the joint part of the tiles red and the crater green. Figure 12 presents the updated crater image. Also to be clearer, one tile image left blank and the crater is lightened and marked mainly khaki.

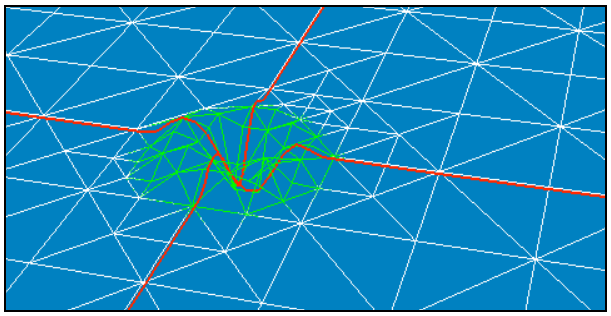
Figure 11: Update on Elevation of a Cross-4-tile Crater


Figure 12: Update on Image of a Cross-4-tile Crater

ACKNOWLEDGMENTS

The authors wish to thank associate professor Zhang Jinfang who developed a software product based on both VTP and libMini and to thank Yang Kai (Yang 2009) who implemented the algorithm of this paper.

REFERENCES

Lindstrom P., Koller D., Ribarsky W., Larry F.H., Faust N., Turner G., 1996. Real-time Continuous Level of Detail Rendering of Height Fields. *Proceedings of the 23rd Annual Conference on Computer Graphics*, pp. 109–118. August 4-9, New Orleans (LA, USA).

Hoppe H., 1996. Progressive meshes. *Proceedings of the 23rd Annual Conference on Computer Graphics*, pp. 99–108. August 4-9, New Orleans (LA, USA).

Duchaineau M., Wolinsky M., Sigeti D.E., et al, 1997. Roaming Terrain: Real-time Optimally Adapting Meshes. *Proceedings. of the 8th Conference on Visualization*, pp. 81-88. October 18-24, Phoenix (Arizona, USA).

Jin H., Lu X., Liu H., 2009. View-dependent fast real-time generating algorithm for large-scale terrain. *Proceedings of the 6th International Conference on Mining Science & Technology*, pp. 1147-1151. October, 18-20, Xu Zhou (Anhui, China).

Robert W., James F., Jessica K., 1999. Animating Sand, Mud, and Snow. *Computer Graphics Forum*, 18(1), 0-11.

Shamir A., Valerio P., Chandrajit B., 2000. Multi-resolution Dynamic Meshes with Arbitrary Deformations. *Proceedings of IEEE Visualization*, pp. 423-430. October 8-13, Salt Lake City (Utah, USA).

He Y., Cremer J., Papelis Y., 2002. Real-time Extendible-resolution Display of On-line Dynamic Terrain. *Proceedings of Graphics Interface*, pp. 27-39. May 27-29, Calgary (Alberta, Canada).

Cai X., Li F., Sun H., Zhan S., 2006. Research of Dynamic Terrain in Complex Battlefield Environments. *Lecture Notes in Computer Science*, 3942:903-912.

Shiben B., Suryakant P., Narayanan P.J., 2008. Real-time Rendering and Manipulation of Large Terrains. *Sixth Indian Conference on Computer Vision, Graphics & Image Processing*, pp. 551-559. December 16-19, Bhubaneswar (India).

Stefan R., Wolfgang H., Philipp S., Seidel H.P., 1998. Real-Time Generation of Continuous Levels of Detail for Height Fields. *Proceedings of WSCG*, pp. 315-322. February 9-13, Plzen (Czech Republic).

Stefan R., 2009. *Real-time Terrain Rendering*. Available from: http://stereofx.org/terrain.html [accessed 4 July 2010].

Discoe B., 2009. *Virtual Terrain Project*. Available from: http://vterrain.org [accessed 4 July 2010].

Discoe B., 2005. Open-Source Visualization and the Virtual Terrain Project. *Geo: Connexion International magazine*, pp. 47-50.

Brown P., 2009. *EXT_texture_compression_S3TC*. Available from: http://www.opengl.org/registry/specs/EXT/texture_compression_s3tc.txt [accessed 4 July 2010].

Yang K., 2009. *Research on Visualization of Dynamic Terrain (in Chinese)*. Thesis (Master Degree). Institute of Software, Chinese Academy of Sciences.

DEVS: AN ADD-ON FOR REACTIVE NAVIGATION

Youcef DAHMANI [(a)], Maamar El-Amine HAMRI [(b)]

[(a)] University Ibn Khaldoun B.P. 78, Zaaroura Tiaret, Algeria
[(b)] LSIS UMR CNRS 6168 University of Paul Cézanne Aix-Marseille III, France

[(a)] y@yahoo., [(b)] amine.hamri@lsis.org

ABSTRACT
This article discusses the use of the discrete event system specification (DEVS) to simulate reactive navigation. The article illustrates the utility of this formalism to combine behavioural robot navigation and systems modelling concepts.
In this work, we exploit the fuzzy logic theory in order to deal with imprecise and inaccurate robot localization. The data obtained from the localization module are presented to our DEVS model which is composed about three states representing respectively three behaviours: following left wall, following right wall and corridor following. Some modifications in Fuzzy Inference System are presented to optimize the calculus time.

Keywords: DEVS Formalism, Mobile Robots, Reactive Navigation, Fuzzy Logic Controller, Localization

1. INTRODUCTION

The mobility and the autonomy of robots pose complex problems, as regards generation of trajectory in strongly constrained and unstructured spaces. The other problem is of decision-making starting from information sensors vague or incomplete. To this end, robots need more sense, decision and technology (Michita 1999; Sergio 2000).
In this work, we use the DEVS formalism to describe three behaviours as three different states and the stimulus of each state is fired by localization distance which is given by fuzzy controller.
The DEVS (Discrete EVent system Specification) formalism was introduced by Zeigler (1976) as an abstract formalism for discrete-events modelling and simulation.
The DEVS formalism is a modelling approach based on systems theory. It's a modular and hierarchical formalism focused on state notion. DEVS is based on two types of models: atomic models and coupled models. Atomic model represents the basic behaviour of system and the coupled models are based on atomic models and/or coupled models, they represent the internal structure of the system which represent coupling between models (BISGAMBIGLIA 2008).
For the class of formalisms denoted as discrete-event (Fishwick 1995), system models are described as an abstraction level where the time base is continuous ($\Re$), but during time-span, only a finite number of relevant events occur. These events can cause the state of the system to change.

The Fuzzy logic permit to use mathematics concepts, its main advantage is the representation of the human been knowledge. The use of fuzzy logic gives good results in robot navigation without an analytical model of the environment.

2. THE DEVS FORMALISM

The DEVS (Discrete EVent Systems specifications) formalism allows two levels of description (Zeigler 2000; Glinsky 2004). At the lowest level, a basic component called atomic DEVS which describes the autonomous behaviour of a discrete-event system and at the highest level, a coupled DEVS which describes a system as coupled, hierarchical and modular model.

2.1. The atomic DEVS formalism

Formally, an atomic DEVS, which represents an atomic model, is specified by 7-tuple:
$AM=<X,S,Y,\delta_{int}, \delta_{ext},\lambda,ta>$
Where
X: input events set;
S: states set;
Y: output events set;
δ_{int}: $S\rightarrow S$: internal transition function, models the states changes caused by internal events, it describes the behaviour of a Finite State Automaton;
δ_{ext}: $Q\times S\rightarrow S$: external transition function, defines the state changes due to external events;
$Q=\{(s,e) \mid s\in S.0\leq e\leq ta(s)\}$: total states and ***e*** describes the elapsed time since the system made a transition to the current state s;
λ: $S\rightarrow Y$: output function, maps the internal state onto the output set;
ta: $S\rightarrow\Re$: time advance function, represents the lifetime of the state.

2.2. The coupled DEVS formalism

The coupled DEVS formalism describes a discrete event system in terms of a network of coupled components.
$CM=<\ ,D,\{\ \mid d\in D\},EIC,EOC,IC,select>$
Where

: set of possible inputs of the coupled model,
: set of possible outputs of the coupled model,
D : set of names associated to the model components,
| d∈D: set of the coupled model components, these components are either atomic or coupled DEVS model,
EIC: set of External Input Coupling,
EOC: set of External Output Coupling,
IC: defines the Internal Coupling,
Select: →D : function that defines priority between components.

3. FUZZY LOGIC CONTROLLER

A fuzzy logic controller permits to build control law from linguistic and qualitative description of system's behaviour via fuzzy base rules.
A fuzzy controller consists of 3 basic elements (Fig.1):
1. State interface (Fuzzification): numerical values are represented into linguistic variables with appropriate membership functions,
2. Action interface (Defuzzification): transforms the command actions into crisp values useable directly by the process which is modeled.
3. Inference engine: elaborates decisions from fired fuzzy rules, it's the core of the controller.

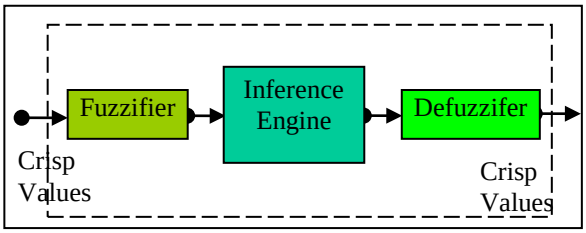

Figure 1: Fuzzy logic controller

4. MODULAR DESIGN

4.1. Robot Architecture

In the present work, the robot considered is circular having three sensors, one in front and one on each side. The sensor's orientation angle is 45° on both sides of frontal axis of the robot. For safety navigation manner, the robot is constrained by some points. The robot must move far from a safe distance, the corridor must be wide than a certain width, and the sensors have a limited scope (Fig.2)

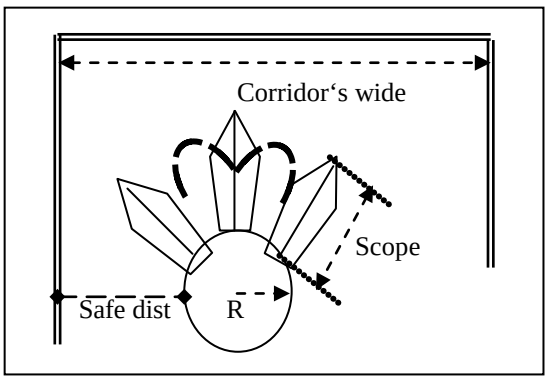

Figure 2: Structure and robot's sensor's position

4.2. Reactive Navigation in DEVS formalism

In this work, we have chosen 3 behaviours; each one represents a state (Fig.3). The transition from one state into the other is fired by external event (Table 1). This work is based on 6 events which are obtained from the localization module; this module activates the appropriate port to trigger the event. We denote Right Distance detection event (**rd**) gathered by the RD port, the Left Distance detection (**ld**) obtained via the LD port, Bilateral Distance detection (**bd**) which is gotten by by the BD port, Move to Target (**mt**) and the **end** event which are on respectively on the MT and the End ports.

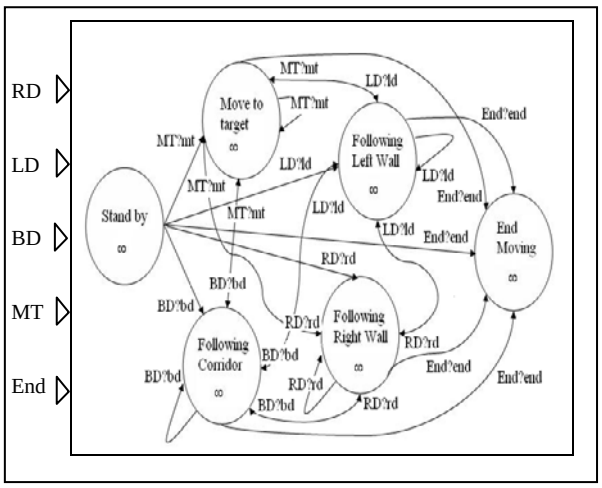

Figure 3: Reactive Navigation's DEVS model

Note that, the **bd** event is obtained if both events **rd** and **ld** are detected. **rd** and **ld** events are obtained by calculating the minimum distance between respectively, the right and frontal distance on the right sensor, and the left and frontal distance on the left gathered by the left sensor.
rd= min(right distance, frontal distance)
ld= min(left distance, frontal distance)
As illustrated on table 1, we define a following output function
δ_{ext}: Q×S→S
λ: S→Y

Table 1: Diagram of event's transitions

State / Event	Stand by	Tracking Right Wall	Tracking Left Wall	Tracking Corridor	Move to target	End Moving
rd	Tracking Right Wall	Tracking Right Wall	Tracking Right Wall	Tracking Right Wall	Tracking Right Wall	Not Available
ld	Tracking Left Wall	Tracking Left Wall	Tracking Left Wall	Tracking Left Wall	Tracking Left Wall	Not Available
bd	Tracking Corridor	Tracking Corridor	Tracking Corridor	Tracking Corridor	Tracking Corridor	Not Available
mt	Move to target	Move to target	Move to target	Move to target	Move to target	Not Available
end	End Moving	End Moving	End Moving	End Moving	End Moving	Not Available

4.3. Optimization of fuzzy controller process

The reproach of the fuzzy logic control usage is that it takes a lot of CPU time for calculations, especially for large number of fuzzy rules.

We introduce a discrete event version of Fuzzy Logic Control in order to reduce the fuzzy inference engine activity and speed up the calculation process. This idea is inspired from the works of Sheikh-Bahaei and Jamshidi (2004).

To do that, a change detector bit is added to fuzzy logic controller (Fig. 4). We define a change detector of each fired fuzzy rule, and if no change is observed on the participating linguistic terms, so we leave the rule and if rule or some other linguistic terms are hold we use the fuzzy inference method.

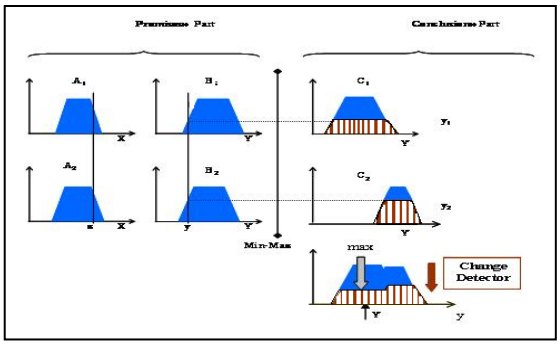

Figure 4: Proposed Fuzzy Controller

5. SIMULATIONS AND RESULTS

5.1. The Data Base Fuzzy Rules

According to our kinematics' model (Fig.5), we note θ the orientation of the robot, φ, represents the angle to the target, and α describes the deviation done by the robot when it moves (α=θ-φ).

So the structural fuzzy rules introduced by the Fuzzy logic controller are:

: **If** (θ-φ) is A **and** is B Then α is C

Where A,B and C are linguistic terms and Dx stand for Distance (right, left or frontal).

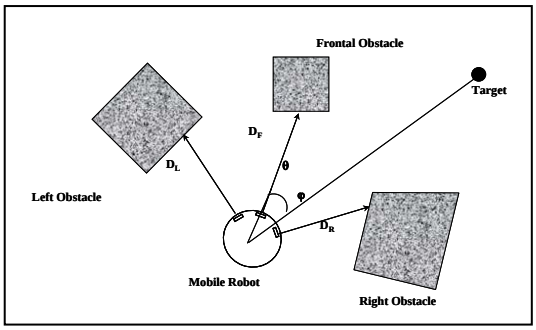

Figure 5: Cinematic of the Robot

The different variables are fuzzified as below (Fig. 6)

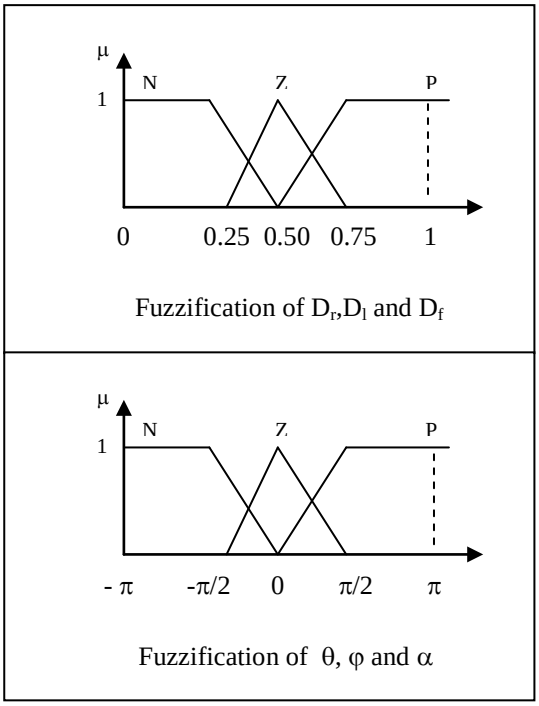

Figure 6: Input/Output Fuzzification

So, the data base fuzzy rules are described on tables 2a, 2b.

According to these rules, each behavior "state" is activated only when the change detector detects a change in the conclusion of the fired fuzzy rules.

Table 2.a: Fuzzy Data Base (Right Turn)

(θ-φ) / $\min_{(Dr,Df)}$	N	Z	P
N	P	P	P
Z	Z	Z	Z
P	N	N	N

Table 2.a: Fuzzy Data Base (Left Turn)

(θ-φ) / $\min_{(Dl,Df)}$	N	Z	P
N	N	N	N
Z	Z	Z	Z
P	P	P	P

5.2. Simulations and results

The figure 7 shows an example of a fuzzy rule implemented by these atomic models. Each atomic model has a change detector, such that each model is activated only when there is a change in the input, otherwise they are sleeping and don't take any CPU time.

We remark there is not a big difference between the two trajectories taken by the robot. But if we compare the activities between the 2 methods we found that we gain in number of iterative calculations evolving a diminution in process activity and in the other point, we decrease the number of event stimulus for the robot (see Table.3).

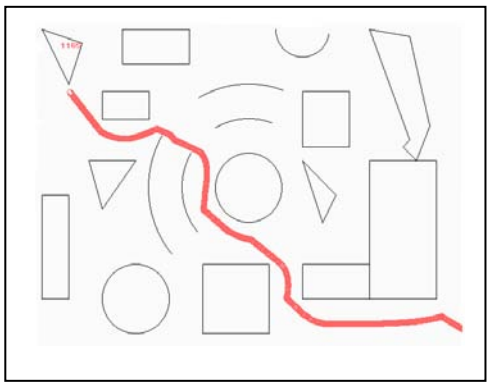

Figure 7.a: Conventional Fuzzy Navigation

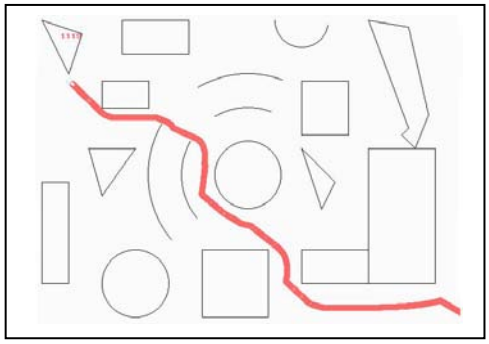

Figure 7.b: Optimized Fuzzy Navigation

The table below gives a comparison between the classic conventional fuzzy navigation and the combined discrete event one.

Table 3: Diagram of event's transitions

	Following right wall	
	Number of fuzzy iterations	RD Event call
Conventional fuzzy navigation	1765	49
Discrete Event	1119	26
	Following left wall	
	Number of fuzzy iterations	RD Event call
Conventional fuzzy navigation	814	9
Discrete Event	538	7

This result depicted on table 3 shows for the same environment, starting and ending at the same points (see Fig.7 a. and b.), the navigation process gives good results compared to the conventional fuzzy navigation.

We can see that we decrease the activity of cpu and calculation time by using the DEVS simulation. In conventional method all the fuzzy operations (fuzzification , inference, defuzzification) is done at every time step, but in Discrete Event Fuzzy Logic the calculation are done only if there is change (event) in the system.

6. CONCLUSIONS AND PERSPECTIVES

This paper has allowed us to combine fuzzy approach and DEVS formalism in reactive navigation; it gave us good results in particular for the 3 mentioned behaviours. However, the subject is not ready to be completed.

It's known that, we can always think of carrying out certain number of works, we can retain following work:

- ✓ Adding and simulating other behaviours with DEVS formalism,
- ✓ Realization of conflict behaviour in robot navigation,
- ✓ Integration of the vague concepts on all levels of robot's architecture,
- ✓ Trying this method in more complex environment.

REFERENCES

Bisgambiglia, P.A., 2008. *Approximate Modelling Approach for Discrete Events Systems: Application for Forest Fire Propagation*, PhD Thesis, University of Corse, France.

Fishwick, P., 1995. Simulation Model Design and Execution: Building Digital Worlds.

Glinsky, E. and Gabriel, W., 2004. Modeling and Simulation of Hardware/Software systems With CD++. *Information Processing and Management*, 7 (2), 147–168.

Michita, I., Kazno, H. and Tsutomu, M., 1999. Physical Constraints on Human Robot Interaction. *Proceedings of the International Joint Conference on Artificial Intelligence*, July-August, Sweden.

Sergio, U.G. and Horacio, M.A., 2000. Application of Behavior-Based Architecture for Mobile Robots Design. *Lecture Notes in Artificial Intelligence 1793, MICAI 2000: Advances in Artificial Intelligence*, pp 136-147, April 2000, Mexico.

Sheikh-Bahaei, S. and Jamshidi, M., 2004. Discrete Event Fuzzy Logic Control with Application to Sensor-Based Intelligent Mobile Robot. *Proceedings WAC*, June 28-July 1, Spain.

Zeigler, B.P., 1976. *Theory of Modeling and Simulation*, Academic Press.

Zeigler, B.P., Praehofer, H. And Kim, T.G., 2000. *Theory of Modeling and Simulation Second Edition Integrating Discrete Event and Continuous Complex Dynamic Systems*, Academic Press.

AUTHORS BIOGRAPHY

Youcef DAHMANI is lecturer of computer science at the Ibn Khaldoun University of Tiaret. He obtained his diploma of computer engineering in 1992 from U.S.T.Oran, Algeria, and the MSc degree in 1977 from university of Es Senia Oran and received the doctorate in 2006 from U.S.T.Oran. His research areas include optimization of fuzzy rules, artifial intelligence, reactive robotic systems and network security.

Maamar El-Amine HAMRI is an associate professor at Aix Marseille III university and a member of LSIS lab. His main research is the discrete event simulation. Currently his is interested to the use of simulation in IA and software engineering. He is also member of the M&S network and supervises the M&S dictionary project.

H_∞ OPTIMAL CONTROL OF DISCRETE-TIME SINGULARLY PERTURBED SYSTEMS

Mostapha Bidani[(a)], Mohamed Wahbi[(a)]

[(a)]Laboratoire de Genie electrique et Telecommunications. Ecole Hassania des travaux Publics.

[(a)]Email: bidani@scientist.com

ABSTRACT

The proposed paper provides new algorithms for solving the H_∞-optimal control of discrete-time singularly perturbed systems by using the exact decomposition scheme. In one hand, we use the bilinear transformation to generate continous-time generalized algebraic Riccati equation. On the other hand, we take advantage of the results proposed in (Hsieh and Gajic 1998), and (Bidani, Radhy and Bensassi 2002), to derive new schemes for transforming the pure-slow and pure-fast nonsymmetric discrete-time Riccati equations (NDRE) into continuous-time ones. Two scheme are based on reducing the backward into forward Hamiltonian matrix (Bidani, Radhy and Bensassi 2002). The others ones use the bilinear transformation (Lim, Gajic and Shen 1995).

Keywords: Riccati equation, H_∞ optimal control, perturbation singular.

1. INTRODUCTION

The H_∞-control problems for singularly perturbed systems have been studied in different set-up from different point of view and have witnessed a fast growth development during this twentieth century. (Pan and Bassar 1993,1994) have studied the H_∞-control problem for singularly perturbed systems via a differential game-theoretic approach. (Dragon 1993, 1996) found the boundary of the H_∞-norm for singularly perturbed systems. All these works and others consider the $O(\epsilon)$ -approximation of the two-time scale discrete generalized Riccati equation. However, it is shown through (Pan and Bassar 1993,1994), if ϵ is sufficiently small, that the attenuation disturbance coefficient of the global system $\mu(\epsilon)$ converges to $Max(\mu_s, \mu_f)$,where μ_s and μ_f design respectively the "attenuation disturbance coefficient" of the slow and fast subsystems. Thus, if ϵ is not small enough the $O(\epsilon)$ -theory, used so far, in the paper (Pan and Bassar 1993) might not produce satisfactory results.

In order to broaden the applicable systems, the development of the $O(\epsilon^k)$ -theory is a necessary requirement. Some schemes have been given; Fridman (1995, 1996) discussed the near-optimal problem of singularly perturbed systems by using a high-order accuracy controller via Sobolev's concept of decomposition (Sobolev 1984). Hsieh and Gajic (1998) proposed the exact decomposition of continuous two-time scale algebraic Riccati equation into pure-slow and pure-fast non-symmetric continuous ones.

The same problem discussed in the continuous-time systems is encountered in the discrete-time version. The main facing problem is the stiffness of the two-time scale generalized discrete Riccati equation.

In the first scheme, we are contented by interpolating the resulting two-time scale generalized discrete Riccati equation into its counterpart continuous-time version. Henceforth, our purpose in this work consists in applying the bilinear interpolation to transform the generalized algebraic discrete Riccati equation of H_∞-optimal control of discrete-time two-time scale system into the corresponding two-time scale continuous-time one. Then we use the exact decomposition of the generalized algebraic continous Riccati equation into pure-slow and pure-fast nonsymmetric continous generalized algebraic Riccati equations.

The second scheme, discussed in this paper, is based on the use of the forward Hamiltonian form. Then according to this scheme, we obtain two pure-slow and pure-fast nonsymmetric discrete generalized algebraic Riccati equations.

The third scheme, in this paper, consists in using the forward form Hamiltonian system. This way provides two nonsymmetric continous generalized algebraic Riccati equations.

In the end, we use the bilinear interpolation to transform two pure-slow and pure-fast nonsymmetric discrete generalized algebraic Riccati equations, obtained in the third scheme, to the continous-time counterpart. And this constitute the fouth scheme.

Notation :

I_n : denotes matrix identity with dimension n .

$(O)^T$: denotes the transpose of a matrix.

$\|z\|^2=\sum_{n=0}^{\infty}(z^T(n)z(n))$: denotes the l_2 -norm of sequence $\{z(n)\}$.

T_{zw} : denotes the transfer function from ω to z .

2. STATEMENT PROBLEM

Consider a system governed by the following state equation

$$x(n+1)=Ax(n)+Bu(n)+Gw(n)\ ,x(0)=0 \qquad (1)$$

$$z(n+1)=Cx(n)+Du(n) \qquad (2)$$

The matrices A, B, C and D are partitioned as :

$$A=\begin{bmatrix} I_{n_1}+\epsilon A_{11} & \epsilon A_{12} \\ A_{21} & A_{22} \end{bmatrix},\quad B=\begin{bmatrix} \epsilon B_1 \\ B_2 \end{bmatrix},\quad G=\begin{bmatrix} \epsilon G_1 \\ G_2 \end{bmatrix},$$

$$C=\begin{bmatrix} \epsilon C_1 & C_2 \end{bmatrix} \text{ and } D=\begin{bmatrix} \epsilon D_1 \\ D_2 \end{bmatrix}$$

where $x(n)\in\mathbb{R}^n$ is the state vector, $z(n)\in\mathbb{R}^p$ is the controlled output, $u(n)\in\mathbb{R}^m$ is the control vector, and $w(n)\in\mathbb{R}^l$ is the disturbance. In the sequel we assume the following :

1. (A,C) is detectable
2. (A,B) is stabilizable
3. $\begin{bmatrix} C & D \end{bmatrix}^T\begin{bmatrix} C & D \end{bmatrix}=\begin{bmatrix} CC^T & DD^T \end{bmatrix}$ and that DD^T is a positive definite matrix.

Since it is difficult to find a control strategy $u(n)$ in l^2 -norm which minimizes the H_∞-norm of T_{zw}, we are quite content to find $u(n)$ in l^2 -norm that leads to $\|T_{zw}\|_\infty<\mu$ for a given constant $\mu>\mu_0$, where μ_0 denotes the minimum in the H_∞-norm of T_{zw}.

To this end, we call for the link that exists between theH_∞-optimal control and the linear quadratic difference games theory.

We state the discrete game as the suitable scheme for finding the sequences $u^*(n)$ and $w^*(n)$ that bring J ,

$$\begin{aligned} J&=\tfrac{1}{2}\sum_{n=0}^{\infty}(z^T(n)z(n)-\mu^2 w^T(n)w(n)) \\ &=\tfrac{1}{2}(\|z\|^2-\mu^2\|w\|^2) \end{aligned} \qquad (3)$$

to a saddle-point equilibrium. $u^*(n)$ is the lower value that minimize J and $w^*(n)$ is the upper value that maximize J.

First let us introduce an Hamiltonian function as :

$$\begin{aligned} H=&\tfrac{1}{2}\big(x^T(n)C^TCx(n)+u^T(n)D^TDu(n)-\mu^2 w^T(n)w(n) \\ &+p^T(n+1)\big(Ax(n)+Bu(n)+Gw(n)\big)\big) \end{aligned} \qquad (4)$$

It can be verified that $H(x,p,u,w)$, considered as a function of two players (u^*,w^*) determined by the optimality conditions $\left(\frac{\partial H(x,p,u,w)}{\partial u}\right)_{(u,w)=(u^*,w^*)}=0$, $\left(\frac{\partial H(x,p,u,w)}{\partial w}\right)_{(u,w)=(u^*,w^*)}=0$.

The unique solution is provided by $u^*(n)=-(D^TD)^{-1}B^Tp(n+1)$, $w^*(n)=\frac{1}{\mu^2}G^Tp(n+1)$.

Then by considering the two other conditions $\left(\frac{\partial H(x,p)}{\partial x}\right)=p(n)$, $\left(\frac{\partial H(x,p)}{\partial p}\right)=x(n+1)$, it results in the corresponding Hamiltonian matrix form

$$\begin{bmatrix} x(n+1) \\ p(n) \end{bmatrix}=\begin{bmatrix} A & -\left(B(D^TD)^{-1}B^T-\frac{1}{\mu^2}GG^T\right) \\ C^TC & A^T \end{bmatrix}\begin{bmatrix} x(n) \\ p(n+1) \end{bmatrix} \qquad (5)$$

Thereafter, linearizing the co-state $p(n)$ with respect to $x(n)$, that is $p(n)=Px(n)$, we arrive to the saddle point

$$\begin{bmatrix} u^*(n) \\ w^*(n) \end{bmatrix}=-\left(\begin{bmatrix} D^TD & 0 \\ 0 & -\mu^2 I_l \end{bmatrix}+\begin{bmatrix} B & G \end{bmatrix}^TP\begin{bmatrix} B & G \end{bmatrix}\right)^{-1}\begin{bmatrix} B & G \end{bmatrix}^TPAx(n) \qquad (6)$$

where the matrix P is determined by resolving the following H_∞-algebraic Riccati equation

$$P=A^TPA-A^TP\begin{bmatrix} B & G \end{bmatrix}\left(\begin{bmatrix} D^TD & 0 \\ 0 & -\mu^2 I_l \end{bmatrix}+\begin{bmatrix} B & G \end{bmatrix}^TP\begin{bmatrix} B & G \end{bmatrix}\right)^{-1}\begin{bmatrix} B & G \end{bmatrix}^TPA+C^TC \qquad (7)$$

or equivalently

$$P=A^TP\left(I_n+\left(B(D^TD)^{-1}B^T-\mu^2GG^T\right)P\right)^{-1}A+C^TC$$

Here we should emphasis the fact that $w^*(n)$ represents the worst possible disturbance and henceforth it serves only for the design purpose. Against it $u^*(n)$ represents the optimal feedback control strategy that should be applied in practice. Therefore we should proceed by isolate $u^*(n)$ from $w^*(n)$.

To this end we use the identity $(\alpha+\delta\beta)^{-1}=\alpha^{-1}\delta(I+\beta\alpha^{-1}\delta)^{-1}$ for $\delta=\begin{bmatrix} B & G \end{bmatrix}^TP$ and $\beta=\begin{bmatrix} B & G \end{bmatrix}$ and $\alpha=\begin{bmatrix} D^TD & 0 \\ 0 & -\mu^{-2}I_l \end{bmatrix}$, we then obtain

$$u^*(n)=(D^TD)^{-1}B^TP\left(I_n+\left(B(D^TD)^{-1}B^T-\mu^2GG^T\right)P\right)^{-1}Ax(n) \qquad (8)$$

$$w^*(n)=\mu^2G^TP\left(I_n+\left(B(D^TD)^{-1}B^T-\mu^2GG^T\right)P\right)^{-1}Ax(n) \qquad (9)$$

Notice here that the computation of $u^*(n)$ is inadequate because of the existence of the matrix inverse $(D^T D)$, and this matrix $(D^T D)$ is proportional to the parameter ϵ (considered as the fast discretizing time). So to avoid this problem, we use a change of variables. Letting define the new matrix $M = P\left(I_n - \mu^{-2} G G^T P\right)^{-1}$ so that

$$P\left(I_n + \left(B(D^T D)^{-1} B^T - \mu^2 G G^T\right) P\right)^{-1} = M\left(I_n + B(D^T D)^{-1} B^T M\right)^{-1}$$

Then using the identity $(\alpha + \delta\beta)^{-1} = \alpha^{-1}\delta\left(I + \beta\alpha^{-1}\delta\right)^{-1}$,for $\alpha = D^T D$ and $\beta = B$, the expression in (8) is reduced into

$$u^*(n) = -\left(D^T D + B^T M B\right)^{-1} B^T M A x(n) \qquad (10)$$

Hence, once we apply the feedback control (10), the signal $w(n)$ becomes irrelevant for the stability analysis if $w(n) \leqslant w^*(n)$.

Notice that requirement $\left(\mu^2 I_l - G_T P G\right) > 0$ should be added to the generalized algebraic Riccati equation (7); otherwise the optimal $w^*(n)$ or the worst-case disturbance becomes unbounded which implies in turn that the stabilizing solution P of the generalized algebraic Riccati equation (7) does not exist (see for more details (Basar 1991)).

To determine the closed-loop information pattern, we call for the following theorem :

Theorem 1: *Consider the system (1)-(2) and assume that the triplet* $\left(A, B, \sqrt{C^T C}\right)$ *is stabilizable-detectable. Then the following are equivalent :*

- *There exists a feedback law* $u = K x$ *which stabilizes the system (1)-(2) and renders the* H_∞*-norm of the transfer matrix* T_{zw} *strictly less than* $\left\|T_{zw}\right\|_\infty < \mu$.
- *There exists a symmetric positive semi-definite stabilizing solution* $P \geq 0$ *satisfying the generalized algebraic Riccati equation (7) and the inequality* $\left(\mu^2 I_l - G^T P G\right) > 0$.

Moreover, one such controller is $K = -\left(D^T D + B^T M B\right)^{-1} B^T M A x(n)$ □

Proof. see **Appendix A** □

3. NEW ALGORITHMS FOR SOLVING H_∞ OPTIMAL CONTROL OF DISCRETE-TIME SINGULARLY PERTURBED SYSTEMS

3.1. First scheme

Assumption 4 : *The matrix* $(I_n + A)$ *is invertible* □

Remarque : *The assumption 4 is not a limited problem since we can make an input* $u = F x + v$ *such that* $(A + F)$*satisfies assumption 4* □

As we see the presence of a small positive parameter ϵ in matrices A, B makes the resolution of the generalized algebraic Riccati equation (7) ill-conditioned and with a way quite analogous to the partitioning in the standard regulator problem the matrix $P = P(\epsilon)$ is partitioned as : $\begin{bmatrix} P_1/\epsilon & P_2 \\ P_2^T & P_3 \end{bmatrix}$

Then, the substitution of the latter structure into the generalized algebraic Riccati equation (7) results in a more complicated equations and the reduced of the computation becomes limited. (Lim, Gajic and Shen 1995) had discussed the analogue regulator problem and they had proposed the use of a bilinear interpolation to transform the discrete-time Riccati equation into a continuous-time one. Thus, we should use the same technique to transform the generalized discrete-time Riccati equation (7) into a generalized continuous-time Riccati one.

Lemma 2 : *There exists a generalized continuous Riccati equation* $P A_c + A_c^T P + Q_c - P\left(B_c R_c^{-1} B_c - Z_c\right) P = 0$ *corresponding to the generalized discrete Riccati equation* (7).

Under the bilinear transformation, matrices A_c, B_c, Q_c, R_c *and* Z_c *are deduced as*

$$A_c = \left(I_n - 2\Phi^{-T}\right), Q_c = 2\Phi\left(C^T C\right)\left(I_n + A\right)^{-1};$$
$$\Phi = \left(I_n + A^T\right) + \left(C^T C\right)\left(I_n + A\right)^{-1}\left(B(D^T D)^{-1} B^T - \mu^2 G G^T\right);$$
$$B_c = \left(I_n - \left(I_n + A\right)^{-1}\mu^{-2} G G^T \left(I_n + A\right)^{-T} C^{-T} C\right)^{-1}\left(I_n + A\right)^{-1} B;$$

$$R_c = \frac{1}{2} D^T D + \frac{1}{2} B^T \left(I_n + A\right)^{-T} \times$$
$$\left(I_n - \left(C^T C\right)\left(I_n + A\right)^{-1}\mu^{-2} G G^T \left(I_n + A\right)^{-T}\right)^{-1}\left(C^T C\right)\left(I_n + A\right)^{-1} B;$$
$$Z_c = \frac{2}{\mu^2}\left(I_n + A\right)^{-1} G\left(I_n - \frac{1}{\mu^2} G^T \left(I_n + A\right)^{-T}\left(C^T C\right)\left(I_n + A\right)^{-1} G\right)^{-1} \times$$
$$G^T \left(I_n + A\right)^{-T}$$

□

Proof. see **Appendix B** □

To accomplish this scheme, we introduce the following requirement

$$I_l - \frac{1}{\mu^2} G^T \left(I_n + A\right)^{-T}\left(C^T C\right)\left(I_n + A\right)^{-1} G > 0 \qquad (11)$$

in order that we keep matrices $B_c R_c^{-1} B_c^T$ and Z_c positive definite. At the first glance, one see that this condition

proves the fact that the digital control is more robust than its corresponding analogy one.

Then if we consider that μ satisfies the latter requirement, the stabilizing solution P is derived from the following continuous generalized algebraic Riccati equation

$$P A_c + A_c^T P + Q_c - P\left(B_c R_c^{-1} B_c^T - Z_c\right) P = 0 \qquad (12)$$

With $\mu^2 I_l - G^T P G > 0$ and

$I_l - \frac{1}{\mu^2} G^T \left(I_n + A\right)^{-T} \left(C^T C\right) \left(I_n + A\right)^{-1} G > 0$.

But the computation of this equation is also stiff since A_c has the form $\begin{bmatrix} \epsilon A_{c11} & \epsilon A_{c12} \\ A_{c21} & A_{c22} \end{bmatrix}$ and B_c the form $\begin{bmatrix} \epsilon B_{c1} \\ B_{c2} \end{bmatrix}$ and Z_c the form $\begin{bmatrix} \epsilon^2 Z_{c11} & \epsilon Z_{c12} \\ \epsilon Z_{c12}^T & Z_{c22} \end{bmatrix}$.

To resolve this equation, we refer to the paper (Hsieh and Gajic 1998). Notice that if ϵ is not sufficiently small, we use the Schur vector method, instead of Newton iterative method, to resolve the resulting non-symmetric continuous generalized algebraic Riccati equations.

3.2. Second scheme

Using the same technique than in (Bidani, Radhy and Bensassi 2002) and by imposing $p(n) = \begin{bmatrix} p_1 / \epsilon \\ p_2 \end{bmatrix}$, with $p_1 \in \mathbb{R}^{n_1}$ and $p_2 \in \mathbb{R}^{n_2}$, and interchanging the second and the third rows in (8), we obtain

$$\begin{bmatrix} x_1(n+1) \\ p_1(n) \\ x_2(n+1) \\ p_2(n) \end{bmatrix} = \begin{bmatrix} I_{2n_1} + \epsilon T_1 & \epsilon T_2 \\ T_3 & T_4 \end{bmatrix} \begin{bmatrix} x_1(n) \\ p_1(n+1) \\ x_2(n) \\ p_2(n+1) \end{bmatrix}$$

where $T_1 = \begin{bmatrix} A_{11} & -(B_1 R^{-1} B_1^T - \frac{1}{\mu^2} G_1 G_1^T) \\ Q_1 & A_{11}^T \end{bmatrix}$,

$T_2 = \begin{bmatrix} A_{12} & -(B_1 R^{-1} B_2^T - \frac{1}{\mu^2} G_1 G_2^T) \\ Q_2 & A_{21}^T \end{bmatrix}$,

$T_3 = \begin{bmatrix} A_{21} & -(B_2 R^{-1} B_1^T - \frac{1}{\mu^2} G_2 G_1^T) \\ Q_2^T & A_{12}^T \end{bmatrix}$,

$T_4 = \begin{bmatrix} A_{22} & -(B_2 R^{-1} B_2^T - \frac{1}{\mu^2} G_2 G_2^T) \\ Q_3 & A_{22}^T \end{bmatrix}$ and

$Q = \begin{bmatrix} Q_1 & Q_2 \\ Q_2^T & Q_3 \end{bmatrix}$

On the other side, the change of the original states $\begin{bmatrix} x_1(n) \\ p_1(n) \\ x_2(n) \\ p_2(n) \end{bmatrix}$ to the new ones $\begin{bmatrix} \eta_1(n) \\ \xi_1(n) \\ \eta_2(n) \\ \xi_2(n) \end{bmatrix}$, with the help of the Chang matrix defined by

$$\begin{bmatrix} \eta_1(n) \\ \xi_1(n+1) \\ \eta_2(n) \\ \xi_2(n+1) \end{bmatrix} = K \begin{bmatrix} x_1(n) \\ p_1(n+1) \\ x_2(n) \\ p_2(n+1) \end{bmatrix} \quad \text{with}$$

$K = \begin{bmatrix} I_{2n_1} - \epsilon H L & -\epsilon H \\ L & I_{2n_1} \end{bmatrix}$, $K^{-1} = \begin{bmatrix} I_{2n_1} & -\epsilon H \\ -L & I_{2n_1} - \epsilon L H \end{bmatrix}$,

derives the pure slow and pure fast sub-Hamiltonians respectively

$$\begin{bmatrix} \eta_1(n+1) \\ \eta_2(n) \end{bmatrix} = \begin{bmatrix} a_1 & a_2 \\ a_3 & a_4 \end{bmatrix} \begin{bmatrix} \eta_1(n) \\ \eta_2(n+1) \end{bmatrix} \qquad (13)$$

$$\begin{bmatrix} \xi_1(n+1) \\ \xi_2(n) \end{bmatrix} = \begin{bmatrix} b_1 & b_2 \\ b_3 & b_4 \end{bmatrix} \begin{bmatrix} \xi_1(n) \\ \xi_2(n+1) \end{bmatrix} \qquad (14)$$

where $\begin{bmatrix} a_1 & a_2 \\ a_3 & a_4 \end{bmatrix} = I_{2n_1} + \epsilon (T_1 - T_2 L)$ and $\begin{bmatrix} b_1 & b_2 \\ b_3 & b_4 \end{bmatrix} = T_4 + \epsilon L T_2$ if the following Chang equations are satisfied

$$(I_{2n_2} - T_4) L + T_3 + \epsilon L (T_1 - T_2 L) = 0 \qquad (15)$$

$$H (I_{2n_2} - T_4 - \epsilon L T_2) + T_2 + \epsilon (T_1 - T_2 L) H = 0 \qquad (16)$$

Assumption 5 : $(I_{n_2} - A_{22})$ is non-singular through-out this paper.

Under the assumption5 or more precisely the assumption that the matrix $(I_{2n_2} - T_4)$ is non-singular, different known techniques are used to solve equations (15)(16). Here are the frame of references : the fixed point method , Newton method, the asymptotic expansion and Taylor series methods, and finally the eigenvector approach.

Therefore, the linearization of the new co-states η_2 and ξ_2 with respect to η_1 and ξ_1, respectively,

$$\begin{bmatrix}\eta_2(n+1)\\ \xi_2(n+1)\end{bmatrix}=\begin{bmatrix}P_{rs}(I_{n_1}-a_2P_{rs})^{-1}a_1 & 0\\ 0 & P_{rf}(I_{n_2}-b_2P_{rf})^{-1}b_1\end{bmatrix}\begin{bmatrix}\eta_1(n)\\ \xi_1(n)\end{bmatrix} \quad (17)$$

reduced the pure slow and pure fast sub-Hamiltonians, previously defined, to the closed-loop form of two, completely decoupled, pure slow and pure fast subsystems respectively,

$$\eta_1(n+1)=(a_1+a_2P_{rs}(I_{n_1}-a_2P_{rs})^{-1}a_1)\eta_1(n) \quad (18)$$

$$\xi_1(n+1)=(b_1+b_2P_{rf}(I_{n_2}-b_2P_{rf})^{-1}b_1)\xi_1(n) \quad (19)$$

together with two reduced-order nonsymmetric algebraic discrete-time Riccati equations :

$$P_{rs}=a_4P_{rs}a_1+a_3+a_4P_{rs}(I_{n_1}-a_2P_{rs})^{-1}a_2P_{rs}a_1 \quad (20)$$

$$P_{rf}=b_4P_{rf}b_1+b_3+b_4P_{rf}(I_{n_{12}}-b_2P_{rf})^{-1}b_2P_{rf}b \quad (21)$$

The solution P_{rs} (respt. P_{rf}) of the equation (20) (resp. (21)) is deduced from following lemmas.

Assumption 6: the fast subsystem $(A_{22}, B_2, \sqrt{Q_3})$ is stabilizable-detectable.

Let $\mu_f=inf\{\mu>0\}$ / the fast discrete-time Riccati equation (21) has a positive definite solution.

Lemma 7 : Under the assumption 6 there exists $\epsilon_1>0$ such that for any $\epsilon>\epsilon_1$ an unique solution of (21) exists.

Proof.

By using the first approximation in ϵ of b_i $(i=1,2,3,4)$, it results in

$$\begin{bmatrix}b_1 & b_2\\ b_3 & b_4\end{bmatrix}=\begin{bmatrix}A_{22} & -(B_2R^{-1}B_2^T-\frac{1}{\mu^2}G_2G_2^T)\\ Q_3 & A_{22}^{22}\end{bmatrix}$$ yielding in turn the symmetric discrete-time Riccati equation :

$$P_{rf}=Q_3+A_{22}^TP_{rf}(I_{n_2}+(B_2R^{-1}B_2^T-\frac{1}{\mu^2}G_2G_2^T)P_{rf})^{-1}A_2 \quad (22)$$

Therefore the use of Lemma 3 dictates that the unique solution P_{rf} of the equation (22) exists if the system $(A_{22}, B_2, \sqrt{(Q_3)})$ is stabilizable-detectable and the corresponding transfer matrix is inferior to certain μ_f.

To accomplish this proof, the implicit function theorem (Bidani, Radhy and Bensassi 2002) guaranteed the existence and uniqueness of the solution of equation (22) for $\epsilon\leqslant\epsilon_1$ ■

Assumption 8: The slow subsystem $(A_o, \sqrt{(B_oR_o^{-1}B_o^T)}, C_o)$ is stabilizable-detectable with

$A_o=I_{n_1}+\epsilon(A_{11}+A_{12}(I_{n_2}-A_{22})^{-1}A_{21})$, $R_o=R+D_o^TD_o$

$C_o=C_1+C_2(I_{n_2}-A_{22})^{-1}A_{21}$, $D_o=C_2(I_{n_2}-A_{22})^{-1}B_2$

and $B_o=\epsilon(B_1+A_{12}(I_{n2}-A_{22})^{-1}B_2)$ ■

Notice that **assumption 8** uses the fact that C_1 is full-rank factorization of Q_1 (i.e. $Q_1=C_1^TC_1$) and C_1 is full-rank factorization of Q_3 (i.e. $Q_3=C_2^TC_2$).

Since $A_o-\sqrt{(B_oR_o^{-1}B_o^T)}K$ is stable by hypothesis, the pair $(A_o, \frac{1}{\mu}G_o)$ is, indeed, stabilizable for $\mu>\mu_s$ where $G_o=\epsilon(G_1+A_{22}(I_{n_2}-A_{22})^{-1}G_2)$.

Lemma 9 : Under the assumption 8 there exists $\epsilon>0$ such that for any $\epsilon\leqslant\epsilon_2$ an unique solution of (20) exists.

Proof :

The proof is the same than these used in the paper (Bidani, Radhy and Bensassi 2002) the only change is that of Lemma 3 to state that the unique solution P_{rs} of the equation

$$P_{rs}=C_o^TC_o+A_o^TP_{rs}(I_{n_1}+(B_oR_o^{-1}B_o^T-\frac{1}{\mu^2}G_oG_o^T)P_{rs})^{-1}A_o$$

exists if the system $(A_o, \sqrt{(B_oR_o^{-1}B_o^T)}, C_o)$ is stabilizable-detectable and the corresponding transfer matrix is inferior to a certain μ_s. Then the use of the implicit function theorem (Bidani, Radhy and Bensassi 2002) guaranteed the existence and uniqueness of the solution of equation (20) for $\epsilon\leqslant\epsilon_2$ ■

3.3. Third scheme

Assumption 10 : The matrix A_{22} is non-singular.

Under Assumption 10, one can transform the pure-slow and pure-fast backward sub-Hamiltonians form (13)(14) into the equivalent pure slow and pure fast forward sub-Hamiltonians form, respectively, see (Bidani, Radhy and Bensassi 2002), (Lim, Gajic and Shen 1995) and (Hsieh and Gjaic 1998). Therefore the transformation of nonsymmetric algebraic discrete-time Riccati equations (20)(21) into nonsymmetric continuous-time algebraic Riccati equations are deduced straight-away,

$$P_{rs}\bar{a}_1-\bar{a}_4P_{rs}-\bar{a}_3+P_{rs}\bar{a}_2P_{rs}=0$$
$$P_{rf}\bar{b}_1-\bar{b}_4P_{rf}-\bar{b}_3+P_{rf}\bar{b}_2P_{rf}=0$$

with $\begin{bmatrix}\bar{a}_1 & \bar{a}_2\\ \bar{a}_3 & \bar{a}_4\end{bmatrix}=\begin{bmatrix}(a_1-a_2a_4^{-1}a_3) & a_2a_4^{-1}\\ -a_4^{-1}a_3 & a_4^{-1}\end{bmatrix}$,

$$\begin{bmatrix}\bar{b}_1 & \bar{b}_2\\ \bar{b}_3 & \bar{b}_4\end{bmatrix}=\begin{bmatrix}(b_1-b_2b_4^{-1}b_3) & b_2b_4^{-1}\\ -b_4^{-1}b_3 & b_4^{-1}\end{bmatrix}$$

Using permutation matrices E_1, E_2, E_3 and E_4:

$$E_1=\begin{bmatrix}I_{n_1} & 0 & 0 & 0\\ 0 & 0 & \epsilon I_{n_1} & 0\\ 0 & I_{n_2} & 0 & 0\\ 0 & 0 & 0 & I_{n_2}\end{bmatrix},\quad E_2=\begin{bmatrix}I_{n_1} & 0 & 0 & 0\\ 0 & 0 & I_{n_2} & 0\\ 0 & I_{n_1} & 0 & 0\\ 0 & 0 & 0 & I_{n_2}\end{bmatrix}$$

$$E_1=\begin{bmatrix}I_{n_1} & 0 & 0 & 0\\ a_3 & a_4 & 0 & 0\\ 0 & I_{n_2} & 0 & 0\\ 0 & 0 & b_3 & b_4\end{bmatrix},$$

$$E_1=\begin{bmatrix}I_{n_1} & 0 & 0 & 0\\ \epsilon Q_1 & (I_{n_1}+\epsilon A_{11}^T) & \epsilon Q_2 & \epsilon A_{21}^T\\ 0 & 0 & I_{n_2} & 0\\ Q_2^T & A_{12}^T & Q_3 & A_{22}^T\end{bmatrix}$$

defined as follow

$$\begin{bmatrix}x_1(n)\\ p_1(n)\\ x_2(n)\\ p_2(n)\end{bmatrix}=E_1\begin{bmatrix}x_1(n)\\ x_2(n)\\ p_1(n)\\ p_2(n)\end{bmatrix},\quad \begin{bmatrix}\eta_1(n)\\ \xi_1(n)\\ \eta_2(n)\\ \xi_2(n)\end{bmatrix}=E_2\begin{bmatrix}\eta_1(n)\\ \eta_2(n)\\ \xi_1(n)\\ \xi_2(n)\end{bmatrix}$$

$$\begin{bmatrix}\eta_1(n)\\ \eta_2(n)\\ \xi_1(n)\\ \xi_2(n)\end{bmatrix}=E_3\begin{bmatrix}\eta_1(n)\\ \eta_2(n+1)\\ \xi_1(n)\\ \xi_2(n+1)\end{bmatrix},\quad \begin{bmatrix}x_1(n)\\ p_1(n)\\ x_2(n)\\ p_2(n)\end{bmatrix}=E_4\begin{bmatrix}x_1(n)\\ p_1(n+1)\\ x_2(n)\\ p_2(n+1)\end{bmatrix}$$

Taking into account of the results used in (Bidani, Radhy and Bensassi 2002), we derive the transformation matrices $\Pi=E_2E_3K\,E_4^{-1}E_1$, $\Phi=E^{-1}E_4K^{-1}E_3^{-1}E_2$ leading thereafter to

$$\begin{bmatrix}\eta_1(n)\\ \xi_1(n)\end{bmatrix}=(\Pi_1+\Pi_2P)\,x(n),$$

$$\begin{bmatrix}\eta_2(n)\\ \xi_2(n)\end{bmatrix}=(\Pi_3+\Pi_4P)\,x(n)$$, and to

$$x(n)=(\Phi_1+\Phi_2\begin{bmatrix}P_{rs} & 0\\ 0 & P_{rf}\end{bmatrix})\begin{bmatrix}\eta_1(n)\\ \xi_1(n)\end{bmatrix}$$ and

$$P=\left(\Phi_3+\Phi_4\begin{bmatrix}P_{rs} & 0\\ 0 & P_{rf}\end{bmatrix}\right)\left(\Phi_1+\Phi_2\begin{bmatrix}P_{rs} & 0\\ 0 & P_{rf}\end{bmatrix}\right)^{-1}$$

with $\Pi=\begin{bmatrix}\Pi_1 & \Pi_2\\ \Pi_3 & \Pi_4\end{bmatrix}$, $\Phi=\begin{bmatrix}\Phi_1 & \Phi_2\\ \Phi_3 & \Phi_4\end{bmatrix}$.

4. CONCLUSION

In This paper, we have presented third scheme and fourth scheme is deduced by applying bilinear interpolation. The main facing problem to tackle is the resolution of the pure-slow and pure-fast nonsymmetric continuous generalized algebraic Riccati equations. To resolve this kind of equations, we use following the smallness of the perturbation parameter, ϵ, the iterative methods, for instance Newton method, or eigenvector and schur approach methods. As known the iterative methods are preferred for large scale systems. So, we conclude that the second scheme is not fast as the other schemes but it requires less memory.

REFERENCES

Bidani, M., Radhy, N., Bensassi, B., 2002. Optimal control of discrete-time singularly perturbed systems, *Int.J.Control* **75**, 955-966.

Pan, Z., Basar, T., 1993. H∞-optimal control of singularly perturbed systems, Part I: Perfect state measurements, *Automatica* **29**, 401-423.

Pan, Z., Basar, T., 1994. H∞-optimal control of singularly perturbed systems, Part II: Imperfect state measurements, *IEEE Trans. Automatic Control* **39**, 280-299.

Lim, M. T., Gajic, Z., Shen, X., 1995. New methods for optimal control and filtering if singularly perturbed linear discrete stochastic systems. *Proceedings of Americas Control Conference Seatle,* pp. 534-538, Washington (Wahington USA),.

Hsieh, T. H., Gajic, Z., 1998. An algorithm for solving the singularly perturbed H∞-algebraic Riccati equation, *Computers Math. Applic.* **36**, 69-77.

Fridman, E., 1995. Exact decomposition of linear singularly perturbed H∞-optimal control problem, *Kybernetica* **31**,591-599.

Fridman, E., 1996. Near-optimal H∞-control of linear singularly perturbed systems, *IEEE Trans. Automatic Control* **41**, 236-240.

Dragan, V., 1993. Asymptotic expansions for game theoretic Riccati equations and stabilization with disturbance attenuation for singularly perturbed systems, *Systems & Control Letters* **20**, 455-463.

Dragan, V., 1996. H∞-norms and disturbance attenuation for systems with fast transient, *IEEE Trans. Automatic Control* **41**, 747-750.

Basar, T., 1991. A Dynamic Games Approach to Controller Design: Disturbance Rejection in Discrete-Time, *IEEE Trans. Automatic Control* **36**, 936-952.

Goodwin G. C. and Sin, K. S., 1984. *Adaptive Filtering Prediction and Control.* Englewood Cliffs, NJ: Prentice-Hall.

Yaesh, I. and Shaked, U., 1991. A transfer Function Approach to the Problems of Discrete-Time Systems: H∞-Optimal Linear Control and Filtering, *IEEE Trans. Automatic Control* ***36, 1264-1271*** .

Sobolev, V., 1984. Integral manifolds and decomposition of singularly perturbed systems, *Systems & Control Letters* **5**, 169-179.

APPENDIX A.

In this appendix we call for an important property of linear systems, that relates the estimation of the so-called the H_∞-norm of the transform matrix of a system to the existence of solutions of an appropriate Riccati equation under stabilizability-dectectability assumption.

To this end, we consider a system described by the equation of the form

$$x(n+1)=A\,x(n)+B\,u(n) \qquad \text{(A.1)}$$

$$z(n)=C\,x(n) \qquad \text{(A.2)}$$

under the assumption that the system (A,B,C) is stabilizable-detectable, and without loss of generality, there exists a matrix T that transforms the system matrices (A,B,C) to the form

$$\tilde{A}=T^{-1}AT=\begin{bmatrix}\tilde{A}_{11} & \tilde{A}_{12}\\ 0 & \tilde{A}_c\end{bmatrix},\qquad \tilde{B}=T^{-1}B=\begin{bmatrix}\tilde{B}_1\\ 0\end{bmatrix} \quad \text{and}$$

$\tilde{C}=CT=\begin{bmatrix}\tilde{C}_1 & 0\end{bmatrix}$ where the subsystem $(\tilde{A_{11}},\tilde{B}_1,\tilde{C}_1)$ is controllable-observable and the matrix $\tilde{A}_c$ is asymptotically stable.

The matrices A, $\tilde{A}_{11}$, $\tilde{B}_1$, $\tilde{C}_1$, B and C are of dimension $n\times n$, $\bar{n}\times\bar{n}$, $\bar{m}\times\bar{n}$, $\bar{p}\times\bar{n}$, $p\times n$ and $m\times n$ respectively.

Corollary 3 (A.1) (Goodwin and Sin 1984; Yaesh, and Shaked 1991): *Given that* $T_{zw}(z)=\tilde{C}_1\left(zI_{\bar{n}}-\tilde{A}_{11}\right)^{-1}\tilde{B}_1$ *of (A.1)-(A.2) is asymptotically stable then* $\|T_{zw}\|_\infty<\mu$ *if and only if there exists a positive definite solution to the following two equations*

$$\bar{P}_1=\tilde{A}_{11}^T\bar{P}_1\tilde{A}_{11}+\tilde{C}_1^T\tilde{C}_1+\tilde{A}_{11}^T\bar{P}_1\tilde{B}_1\left(\mu^2 I_m-\tilde{B}_1^T\bar{P}_1\tilde{B}_1\right)^{-1}\tilde{B}_1^T\bar{P}_1\tilde{A}_{11}$$

and $\mu^2 I_m-\tilde{B}_1^T\bar{P}_1\tilde{B}_1>0$ ■

Since

$$T_{zw}(z)=\tilde{C}_1\left(zI_{\bar{n}}-\tilde{A}_{11}\right)^{-1}\tilde{B}_1=\tilde{C}\left(zI_{\bar{n}}-\tilde{A}\right)^{-1}\tilde{B}=C\left(zI_n-A\right)^{-1}B$$

and the fact that $P=T^{-T}\bar{P}T^{-1}$ and $\bar{P}=\begin{bmatrix}\bar{P}_1 & \bar{P}_2\\ \bar{P}_2^T & \bar{P}_3\end{bmatrix}$ we deduce from the computation that $\bar{P}=\begin{bmatrix}\bar{P}_1 & 0\\ 0 & \bar{0}\end{bmatrix}$ is the unique solution.

Then the solution of the original equation $P=A^TPA+A^TPB\left(\mu^2 I_m-B^TPB\right)^{-1}B^TPA+C^TC$ and $\mu^2 I_m-B^TPB>0$ is straight-away obtained by which implies in turn that P is a symmetric positive semi-definite solution. Therefore we can state the new version of the latter corollary.

Corollary 4 ***(A.2)****: Consider* $T_{zw}(z)=C\left(zI_n-A\right)^{-1}B$ *of (A.1)-(A.2) then* $\|T_{zw}(z)\|_\infty<\mu$ *if and only if there exists a symmetric positive semi-definite solution to the following two equations*

$$P=A^TPA+A^TPB\left(\mu^2I_m-B^TPB\right)^{-1}B^TPA+C^TC \quad \text{(A.3)}$$

$$\mu^2I_m-B^TPB>0 \quad \text{(A.4)}$$

□

Thereafter, we are now ready to proof the *Theorem 1*.

Proof. Suppose there exists a feedback law of the form $u=Kx$ that stabilizes the closed loop system :

$$x(n+1)=(A+BK)x(n)+Gw(n)\ ,x(0)$$
$$z(n)=(C+DK)x(n)$$

and renders its l_2-gain strictly less than μ or equivalently $\left\|(C+DK)\left(zI_n-(A+BK)G\right)\right\|_\infty<\mu$. Then, by Corollary A2, similar equations (A.3)-(A.4) are satisfied by some symmetric matrix $P\geqslant 0$ satisfying

$$P=(A+BK)^TP(A+BK)+(A+BK)^TPG\left(\mu^2I_l-G^TPG\right)^{-1}\times G^TP(A+BK)+(C+DK)^T(C+DK) \quad \text{or}$$

equivalently

$$P=(A+BK)^TP\left(\mu^2I_l-GG^TP\right)^{-1}P(A+BK)+(C+DK)^T(C+DK)$$

and

$$\left(\mu^2I_l-B^TPB\right)>0$$

On the other hand the representation of z in $l_2[0\quad\infty]$ conducts to $(C+DK)^T(C+DK)\equiv\left(C^TC+K^T\left(D^TD\right)K\right)$ (see assumption 3).

Denoting by $M=P\left(I_n-\mu^{-2}GG^TP\right)^{-1}$, it follows that

$$\left(I_n+\mu^{-2}GG^TP\right)^{-1}M=(C^TC)+K^T(D^TD)K+(A+BK)^TM(A+BK)$$

Then we use the identities

$$\left(I_n+\mu^{-2}MGG^T\right)^{-1}=I_n-\left(I_n+\mu^{-2}MGG^T\right)^{-1}\mu^{-2}MGG^T$$

and $\left(I_n+\mu^{-2}MGG^T\right)^{-1}\mu^{-2}MGG^TM=\mu^{-2}MG\left(I_l+\mu^{-2}G^TMG\right)^{-1}G^TM$

to obtain $M=(A+BK)^TM(A+BK)$

$$+MG\left(\mu^2I_l+G^TMG\right)^{-1}G^TM+(C)^T(C)+K^T(D)^T(D)K$$

and then $M=A^TMA+MG\left(\mu^2I_l+G^TMG\right)^{-1}G^TM$

$$-A^TMB\left(D^TD+B^TMB\right)^{-1}B^TMA+C^TC+S \quad \text{where}$$

$$S=\left(K^T+A^TMB\left(D^TD+B^TMB\right)^{-1}\right)\left(D^TD+B^TMB\right)\times\left(K+\left(D^TD+B^TMB\right)^{-1}B^TMA\right)$$

Suppose then that $u\neq u^*(S\neq 0)$, with $S>0$, we conclude according to the classical two-person zero-sum dynamic game that $(u=Kx,w^*)$ constitutes an other saddle-point and hence we can obtain for different value of K an infinity of saddle points. Contradiction (u^*,w^*) is the unique saddle point, hence $K=-\left(D^TD+B^TMB\right)^{-1}B^TMA$.

Now suppose that (7) is satisfied together with $\mu^2I_l-G^TPG>0$ by $P\geqslant 0$ and choose $K=-\left(D^TD+B^TMB\right)^{-1}B^TMA$. The generalized algebraic Riccati equation is reduced into the form

$$P=(A+BK)^TP\left(\mu^2I_m-GG^TP\right)^{-1}(A+BK)+C^TC+K^TD^TDK$$

Then by the use of **corollary A.2**, we obtain $\left\|T_{zw}\right\|_\infty<\mu$ if we prove that the pair $\left(A+BK,\sqrt{C^TC+K^TD^TDK}\right)\equiv(A+BK,C+DK)$ is detectable.

Hence suppose that v is an unstable eigenvector of $(A+BK)$ that corresponds to the unstable eigenvalue λ,

and that it belongs to the kernel of $(C+DK)$, that is $(A+BK)v=\lambda v$ and $(C+DK)v=0$.

Using the assumption that the triple (A,B,C) is stabilizable-detectable we conclude that $v=0$. Therefore the pair $(A+BK,\sqrt{C^TC+K^TD^TDK})$ is detectable. This completes the proof of Theorem ■

APPENDIX B.

Proof. : Considers the following transformations :

$A_c=I_n-2\boldsymbol{F^{-T}},Q_c=2\boldsymbol{F^{-1}}C^TC(I_n+A)^{-1}$,

$Z=GG^TS=B(D^TD)^{-1}B^T$,

$\boldsymbol{F}=(I_n+A^T)+(C^TC)(I_n+A)^{-1}(S-\mu^{-2}Z)(S-\mu^{-2}Z)\boldsymbol{F^{-1}}(I_n+A^T)$

$S_c=2(I_n+A)^{-1}(S-\mu^{-2}Z)\boldsymbol{F^{-1}}$ and

$=(S-\mu^{-2}Z)\left((I_n+A^T)^{-1}\boldsymbol{F}\right)^{-1}$.

Using the identity $(I+\delta\beta)^{-1}\delta=\delta(I+\beta\delta)^{-1}$ and the fact that

$(S-\mu^{-2}Z)=\begin{bmatrix}B & G\end{bmatrix}\begin{bmatrix}D^TD & 0\\ 0 & -\mu^2I_l\end{bmatrix}^{-1}\begin{bmatrix}B^T\\ G^T\end{bmatrix},\beta=\begin{bmatrix}B & G\end{bmatrix}$

and $\delta=\begin{bmatrix}B^T\\ G^T\end{bmatrix}$.

We obtain

$S_c=2\begin{bmatrix}B_c & G_c\end{bmatrix}\begin{bmatrix}D^TD & 0\\ 0 & -\mu^2I_l\end{bmatrix}^{-1}\times$

$\left(I_{l+m}+\begin{bmatrix}B^T\\ G^T\end{bmatrix}C^TC\begin{bmatrix}B_c & G_c\end{bmatrix}\begin{bmatrix}D^TD & 0\\ 0 & -\mu^2I_l\end{bmatrix}^{-1}\right)^{-1}\begin{bmatrix}B^T\\ G^T\end{bmatrix}$

with $\begin{bmatrix}B^T\\ G^T\end{bmatrix}=(I_n+A)^{-1}\begin{bmatrix}B & G\end{bmatrix}$.

The identity $(I+\beta)^{-1}=I-(I+\beta)^{-1}\beta$ for

$\beta=\begin{bmatrix}B^T\\ G^T\end{bmatrix}C^TC\begin{bmatrix}B_c & G_c\end{bmatrix}\begin{bmatrix}D^TD & 0\\ 0 & -\mu^2I_l\end{bmatrix}^{-1}$ yields the

equality $S_c=2\begin{bmatrix}B_c & G_c\end{bmatrix}\begin{bmatrix}D^TD & 0\\ 0 & -\mu^2I_l\end{bmatrix}^{-1}\begin{bmatrix}B^T\\ G^T\end{bmatrix}$

$-2\begin{bmatrix}B_c & G_c\end{bmatrix}\begin{bmatrix}D^TD & 0\\ 0 & -\mu^2I_l\end{bmatrix}^{-1}\times$

$\left(I_{l+m}+\begin{bmatrix}B^T\\ G^T\end{bmatrix}C^TC\begin{bmatrix}B_c & G_c\end{bmatrix}\begin{bmatrix}D^TD & 0\\ 0 & -\mu^2I_l\end{bmatrix}^{-1}\right)^{-1}\times$

$\begin{bmatrix}B^T\\ G^T\end{bmatrix}C^TC\begin{bmatrix}B_c & G_c\end{bmatrix}\begin{bmatrix}D^TD & 0\\ 0 & -\mu^2I_l\end{bmatrix}^{-1}$.

Hence using the identity :

$(I+\delta\beta)^{-1}\delta=\delta(I+\beta\delta)^{-1}$ for $\delta=\begin{bmatrix}B^T\\ G^T\end{bmatrix}C^T$ and

$\beta=C\begin{bmatrix}B_c & G_c\end{bmatrix}\begin{bmatrix}D^TD & 0\\ 0 & -\mu^2I_l\end{bmatrix}^{-1}$ we obtain

$S_c=2\begin{bmatrix}B_c & G_c\end{bmatrix}\begin{bmatrix}D^TD & 0\\ 0 & -\mu^2I_l\end{bmatrix}^{-1}\begin{bmatrix}B^T\\ G^T\end{bmatrix}$

$-2\begin{bmatrix}B_c & G_c\end{bmatrix}\begin{bmatrix}D^TD & 0\\ 0 & -\mu^2I_l\end{bmatrix}^{-1}\times$

$\left(I_p+C\begin{bmatrix}B_c & G_c\end{bmatrix}\begin{bmatrix}D^TD & 0\\ 0 & -\mu^2I_l\end{bmatrix}^{-1}\begin{bmatrix}B^T\\ G^T\end{bmatrix}C^T\right)^{-1}\times$

$C\begin{bmatrix}B_c & G_c\end{bmatrix}\begin{bmatrix}D^TD & 0\\ 0 & -\mu^2I_l\end{bmatrix}^{-1}\begin{bmatrix}B^T\\ G^T\end{bmatrix}$.

To simplify the latter expression; let us substitute $I_p+C\begin{bmatrix}B_c & G_c\end{bmatrix}\begin{bmatrix}D^TD & 0\\ 0 & -\mu^2I_l\end{bmatrix}^{-1}\begin{bmatrix}B^T\\ G^T\end{bmatrix}C^T$ by $\mathbb{R}$.

Hence, S_c is reduced into the form

$$S_c = 2B_c D^T D B_c^T C^T \mathbb{R}^{-1} C B_c D^T D B_c^T + 2B_c D^T D B_c^T C^T \mathbb{R}^{-1} C \frac{G_c G_c^T}{\mu^2} + 2B_c D^T D B_c^T C^T - 2\frac{G_c G_c^T}{\mu^2} - 2\frac{G_c G_c^T}{\mu^2} C^T \mathbb{R}^{-1} C \frac{G_c G_c^T}{\mu^2}$$
$$= 2B_c\left((D^T D)^{-1} - (D^T D)^{-1} B_c^T C^T \mathbb{R}^{-1} C B_c (D^T D)^{-1}\right) B_c^T - 2G_c\left(\frac{I_l}{\mu^2} + \frac{G_c^T}{\mu^2} C^T \mathbb{R}^{-1} C \frac{G_c}{\mu^2}\right) G_c^T + 2B_c (D^T D)^{-1} B_c^T C^T \mathbb{R}^{-1} C \frac{G_c G_c^T}{\mu^2} + 2\frac{G_c G_c^T}{\mu^2} C^T \mathbb{R}^{-1} C B_c (D^T D)^{-1} B_c^T$$

In order to compute Z_c and R_c, we introduce a matrix $\boldsymbol{L}$ such that the latter expression of S_c becomes

$$S_c = 2(B_c + G_c \boldsymbol{L})\left((D^T D)^{-1} - (D^T D)^{-1} B_c^T C^T \mathbb{R}^{-1} C B_c \times (D^T D)^{-1}\right)(B_c + G_c \boldsymbol{L})^T$$

with $\boldsymbol{L} = \frac{G_c^T}{\mu^2} C^T \mathbb{R}^{-1} C B_c \left(I_m - (D^T D)^{-1} B_c^T C^T \mathbb{R}^{-1} C B_c\right)^{-1}$.

Then by using the identity $:(I + \delta\beta)^{-1}\delta = \delta(I + \beta\delta)^{-1}$ for $\delta = \mathbb{R}^{-1} C B_c$ and $\beta = -(D^T D)^{-1} B_c^T C^T$ and the matrix $\boldsymbol{L}$ is reduced into $\boldsymbol{L} = \frac{G_c^T}{\mu^2} C^T \left(I_p - C \frac{G_c G_c^T}{\mu^2} C^T\right) C B_c$.

And Z_c is reduced into $Z_c = \frac{2}{\mu^2} G_c \left(I_l - \frac{G_c^T C^T C G_c}{\mu^2}\right) G_c^T$ by considering the fact that $\left(I_p - C\frac{G_c G_c^T}{\mu^2} C^T\right)^{-1} = \mathbb{R}^{-1} + \mathbb{R}^{-1} C B_c (D^T D)^{-1} B_c^T C^T \left(I_p - C\frac{G_c G_c^T}{\mu^2} C^T\right)^{-1}$.

The matrix $\boldsymbol{B} = B_c + G_c \boldsymbol{L}$ is computed as

$$\boldsymbol{B} = \left(I_n + \frac{G_c G_c^T}{\mu^2} C^T \left(I_p - C\frac{G_c G_c^T}{\mu^2} C^T\right)^{-1} C\right) B_c$$
$$= \left(I_n + \frac{G_c G_c^T}{\mu^2} C^T C \left(I_n - \frac{G_c G_c^T}{\mu^2} C^T C\right)^{-1}\right) B_c.$$

Henceforth $\boldsymbol{B} = \left(I_n - \frac{G_c G_c^T}{\mu^2} C^T C\right)^{-1} B_c$.

And the matrix R_c is

$$R_c = \frac{1}{2}\left((D^T D)^{-1} - (D^T D)^{-1} B_c^T C^T \mathbb{R}^{-1} C B_c (D^T D)^{-1}\right)^{-1}$$
$$= \frac{1}{2} D^T D + \frac{1}{2} B_c^T C^T \left(I_p - C\frac{G_c G_c^T}{\mu^2} C^T\right)^{-1} C B_c$$ and then by applying $:(I + \delta\beta)^{-1}\delta = \delta(I + \beta\delta)^{-1}$ for $\delta = C^T$ and $\beta = -C\frac{G_c G_c^T}{\mu^2}$, we obtain in the end

$$R_c = \frac{1}{2} D^T D + \frac{1}{2} B_c^T \left(I_n - \frac{G_c G_c^T}{\mu^2} C^T C\right)^{-1} C^T C B_c \blacksquare$$

MODULAR DRIVEN WHEELCHAIR BOND GRAPH MODELLING

A. Fakri, J.P. Vilakazi

Université Paris-Est
ESIEE Paris
Département Systèmes Electroniques
Cite Descartes
Bd Blaise Pascal – BP 99
93162 Noisy le Grand Cedex

[(a)]fakria@esiee.fr, [(b)] vilakazj@esiee.fr

ABSTRACT
Bond Graphs (BG) have become popular and are largely employed nowadays as efficient graphical description of multi-domain dynamic systems. This modelling technique is used in this paper to study the dynamics of an ordinary Manual Propelled wheelchair (MPW) and a mechatronic drive module (MDM). This electric powered mechatronic drive module is hence linked to the ordinary MPW system to obtain a modular driven manual wheelchair (MDMW). The Bond Graphs of these systems are constructed and mathematical models extracted in terms of state space differential equations. Simulation results illustrating the behaviour of some dynamic variables are also shown. This paper is aimed at providing good support for the academic field on dynamic system modelling using Bond Graph and Matlab Simulink.

Keywords**:** dynamic system, Bond Graph, modelling tools, test bed structure

1. INTRODUCTION

Improving the lives of the mobility impaired people has always been every states focus (wheelchairnet.org). The investigation on improving specifically the ordinary MPW propulsion method (which results in upper extreme injuries on long term users) has become increasingly imperative due to the growing population of the manual wheelchair users and the requirements for efficient mobility to maintain a quality of live equivalent to the general population**.**

The motivation for this work derives from attempts to employ few portable mechatronic drive modules which can be coupled when necessary to a large scale of MPW systems with the aims of improving propulsion efficiency. The engagement of such a module on MPW is illustrated on Figure 1. This yields good advantage to the system since the weight of the module is imposed on the module itself, thus prevents deformation of the structure. In the next, the modelling of such a system is presented in terms of Bond Graphs.

Currently the subject of mechatronic system design has taken a new dimension since many researchers have turned their attention to emerging technologies that allows engineers to understand multidisciplinary systems. When creating a physical device, one of the major tasks is the implementation of the model which integrates the control system, sensors and actuators dynamics in order to allow the simulation software tools to be integrated in the modelling process. The bond graph methodology is a very well suited graphical tool for modular modelling approach based on energy transfer in multi-domain systems (Karnopp, Margolis and Rosenberg 2006). We assume that the reader has some knowledge on the BG modelling method employed; therefore a brief review is given below.

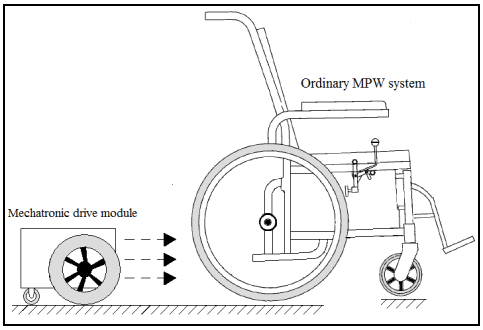

Figure 1: Manual Propelled Wheelchair (MPW) System with the Mechatronic Module

BGs represent the elementary transfer and storage of energy through different dynamic component on the system, the 0 and 1 junction are used to denote common effort and flow cases, thus permitting the extraction of balance junction dynamic equations which in turn enables derivation of mathematical models of the system. Each graphical bond carries power which is product of two variables flow and effort. Power is transferred between different domains with the use of *gyrator* and *transformer* elements. For control purposes, source of *flow* or *effort* is used as input to the system. Some part of the transferred energy is dissipated in resistive elements, Bond Graphically denoted by symbol *(R)* or stored in kinetic or potential form in respectively inertial *(I)* or capacitive (C) elements. For more information, readers may refer to (Karnopp, Margolis and Rosenberg 2006).

If properly applied, the bond graph methodology enables one to develop a graphical model that is consistent with the first principle of energy conservation without having the need to start with establishing and

reformulating equations. (Dauphin-tanguy 2000). The studied systems test bed structures are analysed and model components elaborated. Mathematical models (in terms of state space differential equations) and simulation results of these systems are also presented. In the next section, we present the decomposition of the MPW, its BG model, State space model and simulation results in an obstacle avoidance predetermined trajectory. Note that the simulation was carried out on Matlab Simulink using the BG equivalent block diagram constructed directly from the BG model; this method is presented in (Fakri, Rocaries and Carriere 1997). Section 3, presents the schematic of the mechatronic drive module, its BG model as well as simulation results in a predetermined trajectory showing behaviour of this system in open and close-loop control. Section 4 presents the whole system (MDM coupled on MPW) BG model and simulation in the same trajectory. The last section gives some conclusion and future work.

2. MANUAL PROPELLED WHEELCHAIR

2.1. Description and test bed

MPW is required in hospitals and old age institutions to transport patients who are too unwell to walk (Abel and Frank 1991).The user can manoeuvre the chair by turning the hand push rims attached to the rear wheels, as shown in Figure 1. For users who cannot operate the MPW, handles are made available for assistance from an attendant.

An illustration of an ordinary MPW test bed structure used in this modelisation is depicted on Figure 2. It essentially consists of two caster and manual rear wheels. An approach of a two wheel drive robotic system described in (Klancar, Zupancic and Karba 2007) has been applied in this modelling with the caster wheels lumped together and assumed to be imposing resistive force to the systems flow. V_{CG} and ω_{CG} represents the centre of mass velocity and inertial mass rotation, ω_l and ω_r indicates the angular velocity of the left and right wheels respectively, rear manual wheel radius and wheelchair width are represented by (***r)*** and *(Lw)* respectively. Parameter values are given in the Table. The below matrices (1) shows the kinematic mathematical model of the system, where: θ is the orientation angle, x and y shows the systems geometric position respectively:

$$\begin{bmatrix} x \\ y \\ \theta \end{bmatrix} = r \begin{bmatrix} \frac{\cos\theta}{2} & \frac{\cos\theta}{2} \\ \frac{\sin\theta}{2} & \frac{\sin\theta}{2} \\ \frac{2}{Lw} & \frac{-2}{Lw} \end{bmatrix} \begin{bmatrix} \omega r \\ \omega l \end{bmatrix} \quad (1)$$

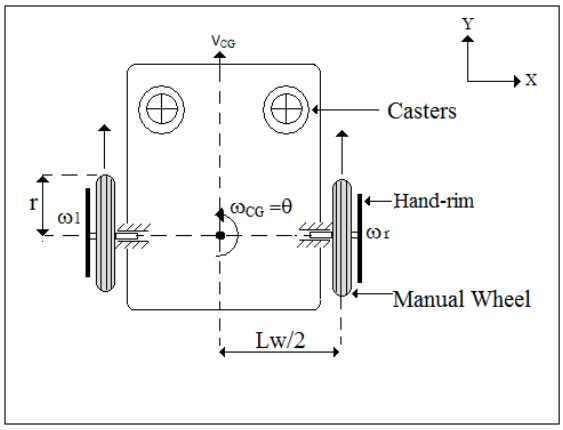

Figure 2: Top view of Manual Propelled Wheelchair (MPW) System

2.2. Bong Graph model of MPW

A remarkable feature of BGs is that an inspection of causal path can reveal information about structural control of the system behaviour. The survey of BG capabilities shows how this modelling technique serves as a core model representation, from which different information can be derived depending on purpose of the study (Gawthrop and Bevan 2007).

The test bed shown in Figure 2 is hence represented in an integral causalled BG shown in Figure 3. Where: *MSE:*τ [Nm] shows the source of effort generated from the tangential force applied by the user on the wheels, *L* [left] or *R* [right], *Jw_L* [kgm^2] is the rotational inertia of the rear wheels, *Rg* is the rear wheel to ground frictional constant, *Mt* [kg] is the total mass of the system, *Jt* [kgm^2] is the total inertial moment of the system, *Rc* is the losses on caster wheels during motion, *Rwc, Cwc* shows the wheel to structure coupling stiffness and elasticity respectively whilst *Cw and Rw* represents the rear wheels spring/damper spokes constants respectively. The non-linear *MTF* represents the energy transferred to structure depending on the applied force.

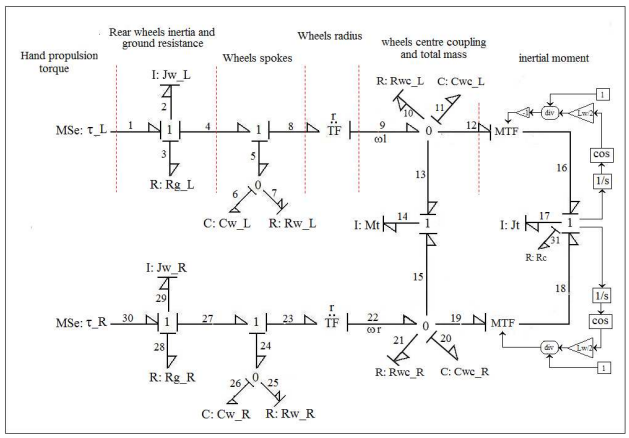

Figure 3: A Bond Graph representation of the MPW system

2.3. State Space Representation

The state space equations used by control engineers for system analysis and simulations (Klancar, Zupancic and Karba 2007; Gawthrop and Bevan 2007) are extracted directly from Figure 3. These can be used for controllability, observability and stability studies of the system. Computer software like CAMP-G, 20sim and Symbols can be used to extract these equations automatically. Equations 2 and 3 show the state space representation of MPW where *x*, *u* and *y* are the system state, input and output respectively. These equations are directly derived from the BG model in Figure 3.

$$\dot{x} = [\mathrm{A}]x + [\mathrm{B}]\mu \qquad (2)$$

$$\begin{bmatrix} e_2 \\ f_6 \\ f_{11} \\ e_{14} \\ e_{17} \\ f_{20} \\ f_{25} \\ e_{29} \end{bmatrix} = \begin{bmatrix} \dot{p}_2 \\ \dot{q}_6 \\ \dot{q}_{11} \\ \dot{p}_{14} \\ \dot{p}_{17} \\ \dot{q}_{20} \\ \dot{q}_{25} \\ \dot{p}_{29} \end{bmatrix} = [\mathrm{A}] \begin{bmatrix} p_2 \\ q_6 \\ q_{11} \\ p_{14} \\ p_{17} \\ q_{20} \\ q_{25} \\ p_{29} \end{bmatrix} + \begin{bmatrix} 1 & 0 \\ 0 & 0 \\ 0 & 0 \\ 0 & 0 \\ 0 & 0 \\ 0 & 0 \\ 0 & 0 \\ 0 & 1 \end{bmatrix} \begin{bmatrix} \tau L \\ \tau L \end{bmatrix}$$

Where:

$$\mathrm{A}=\begin{bmatrix} \frac{-Rg\_L}{JW\_L} & \frac{-1}{Cw\_L} & \frac{-k1}{Cwc\_L} & 0 & 0 & 0 & 0 & 0 \\ \frac{1}{JW\_L} & \frac{-1}{Rw\_LCw\_L} & 0 & 0 & 0 & 0 & 0 & 0 \\ \frac{k1}{JW\_L} & 0 & \frac{-Rwc\_L}{Cwc\_L} & \frac{-1}{Mt} & \frac{-1}{k2Jt} & 0 & 0 & 0 \\ 0 & 0 & \frac{1}{Cwc\_L} & 0 & 0 & \frac{1}{Cwc\_R} & 0 & 0 \\ 0 & 0 & \frac{-k2}{Cwc\_L} & 0 & 0 & \frac{1}{k3Cwc\_R} & 0 & 0 \\ 0 & 0 & 0 & \frac{-1}{Mt} & \frac{-1}{k3Jt} & \frac{-1}{Rwc\_RCwc\_R} & 0 & \frac{-k4}{Mt} \\ 0 & 0 & 0 & 0 & 0 & 0 & \frac{-1}{Rw\_RCw\_R} & \frac{1}{JW\_R} \\ 0 & 0 & 0 & 0 & 0 & \frac{-k4}{Cwc\_R} & \frac{-1}{Cw\_R} & \frac{-Rg\_R}{JW\_R} \end{bmatrix}$$

$$y = [C]\,x \qquad (3)$$

$$\begin{bmatrix} \omega_L \\ \omega R \\ VCG \\ \theta CG \end{bmatrix} = \begin{bmatrix} f_4 \\ f_{27} \\ f_{14} \\ f_{17} \end{bmatrix} = \begin{bmatrix} \frac{1}{Jw\_L} & 0 & 0 & 0 \\ 0 & \frac{1}{Jw\_R} & 0 & 0 \\ 0 & 0 & \frac{1}{Mt} & 0 \\ 0 & 0 & 0 & \frac{1}{Jt} \end{bmatrix} \begin{bmatrix} p_2 \\ p_{29} \\ p_{14} \\ p_{17} \end{bmatrix}$$

2.4. Simulation results

The general characteristics of the forces applied to the handrim during propulsion is sinusoidal and includes rapid rate of loading in the beginning of the push leading to an impact spike and followed by more gradual application and release of force. For the purpose of this study, the system was simulated with step input signals (representing the manual torque) to produce an obstacle avoidance predetermined trajectory.

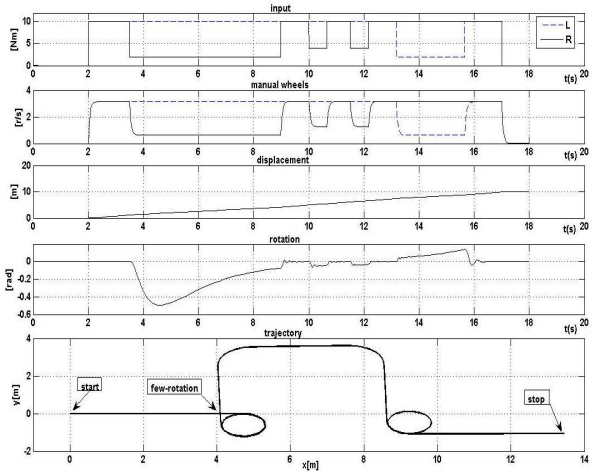

Figure 4: Manual Propelled Wheelchair Simulation Results

The main objective was to illustrate the behaviour of the MPW system without the MDM engaged on it. A combination of step signals in the range of 4 to 10Nm was applied on both wheels as depicted on Figure 4, position and orientation (with reference to the x-axis) were observed.

3. MECHATRONIC DRIVE MODULE

3.1. Description and Schematic

A typical mechatronic drive module (MDM) is depicted in Figure 5. It comprises of a direct current (DC) motor converting electric energy (from batteries in this case) into mechanical energy. Velocity reduction mechanical gears are used and the manner in which motorised wheels are coupled to the system is illustrated.

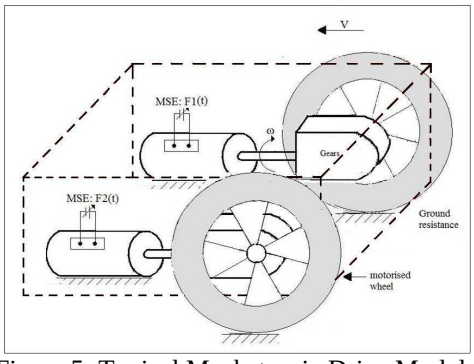

Figure 5: Typical Mechatronic Drive Module

The small values of rotational dampers and torsion springs on the shafts have been lumped together and represented by *Rs* and *Cs* respectively. This is a typical drive unit of an EPPW system.

3.2. Bond Graph model of MDM

Different components forming part of the MDM depicted on figure 5 are hence represented bond graphically in figure 6. This BG model is decomposed into four main parts, the first two representing the electric motor and the transmission gear, while the second shows the wheels inertia and the last showing the dynamics of the wheelchair structure built around the translational *Mt* and rotational *Jt* inertia. To study the dynamics of the system, the imperative outputs to be observed are i_2, ω_4, ω_{13} and v_{23} which denote the motor electric current, armature angular velocity, wheel angular velocity and the module lateral velocity or centre of mass respectively. The given state space differential equations further denotes all the outputs observed in this modelisation.

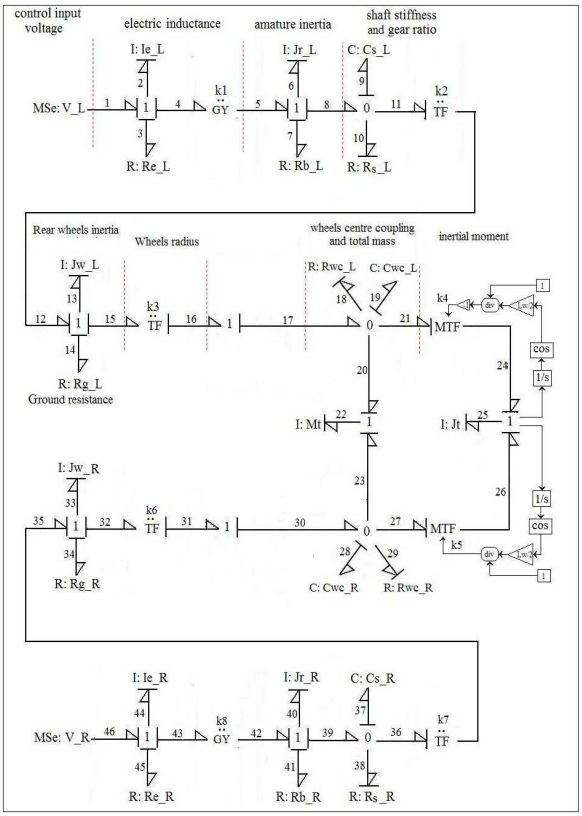

Figure 6: Bond Graph representation of MDM

3.3. State Space Representation

The equations 4 and 5 represent the state space models of the MDM system. These equations can be used for simulation, however in complex multidomain systems, the order increases and the difficulty of manual extractions of state spaces increases in proportion. This clearly denotes the difference between the Bond Graph and state space mathematical modelling.

$$\dot{x} = [A]x + [B]\mu \qquad (4)$$

$$\begin{bmatrix} e_2 \\ e_6 \\ f_9 \\ e_{13} \\ f_{19} \\ e_{22} \\ e_{25} \\ f_{28} \\ e_{33} \\ f_{37} \\ e_{40} \\ e_{44} \end{bmatrix} = \begin{bmatrix} \dot{p}_2 \\ \dot{p}_6 \\ \dot{q}_9 \\ \dot{p}_{13} \\ \dot{q}_{19} \\ \dot{p}_{22} \\ \dot{p}_{25} \\ \dot{q}_{28} \\ \dot{p}_{33} \\ \dot{q}_{37} \\ \dot{p}_{40} \\ \dot{p}_{44} \end{bmatrix} = [A] \begin{bmatrix} p_2 \\ p_6 \\ q_9 \\ p_{13} \\ q_{19} \\ p_{22} \\ p_{25} \\ q_{28} \\ p_{33} \\ q_{37} \\ p_{40} \\ p_{44} \end{bmatrix} + \begin{bmatrix} 1 & 0 \\ 0 & 0 \\ 0 & 0 \\ 0 & 0 \\ 0 & 0 \\ 0 & 0 \\ 0 & 0 \\ 0 & 0 \\ 0 & 0 \\ 0 & 0 \\ 0 & 0 \\ 0 & 1 \end{bmatrix} \begin{bmatrix} VL \\ VR \end{bmatrix}$$

Where:

$$A = \begin{bmatrix} \frac{-R_{e\_L}}{Ie\_L} & \frac{-k_1}{Jr\_L} & 0 & 0 & 0 & 0 & 0 & 0 & 0 & 0 & 0 & 0 \\ \frac{k_1}{Ie\_L} & \frac{-R_{b\_L}}{Jr\_L} & \frac{-1}{Cs\_L} & 0 & 0 & 0 & 0 & 0 & 0 & 0 & 0 & 0 \\ 0 & \frac{-1}{Jr\_L} & \frac{-1}{R_{g\_L}Cs\_L} & \frac{-1}{k_2Jw\_L} & 0 & 0 & 0 & 0 & 0 & 0 & 0 & 0 \\ 0 & 0 & \frac{1}{k_2Cs\_L} & \frac{-R_{g\_L}}{Jw\_L} & \frac{-k_3}{Cwc\_L} & 0 & 0 & 0 & 0 & 0 & 0 & 0 \\ 0 & 0 & 0 & \frac{k_3}{Jw\_L} & \frac{-1}{R_{wc\_L}Cwc\_L} & \frac{-1}{Mt} & \frac{k_4}{Jt} & 0 & 0 & 0 & 0 & 0 \\ 0 & 0 & 0 & 0 & \frac{1}{Cwc\_L} & 0 & 0 & 0 & \frac{1}{Cwc\_R} & 0 & 0 & 0 \\ 0 & 0 & 0 & 0 & \frac{k_4}{Cwc\_L} & 0 & 0 & \frac{1}{k_5Cwc\_R} & 0 & 0 & 0 & 0 \\ 0 & 0 & 0 & 0 & 0 & \frac{-1}{Mt} & \frac{-1}{k_5Jt} & \frac{-1}{R_{wc\_R}Cwc\_R} & \frac{k_6}{Jw\_R} & 0 & 0 & 0 \\ 0 & 0 & 0 & 0 & 0 & 0 & \frac{-k_{26}}{Cwc\_R} & \frac{-R_{g\_R}}{Jw\_R} & \frac{1}{k_7Cs\_R} & 0 & 0 & \\ 0 & 0 & 0 & 0 & 0 & 0 & 0 & \frac{-1}{k_7Jw\_R} & \frac{-1}{R_{g\_R}Cs\_R} & \frac{-1}{Jr\_R} & 0 & \\ 0 & 0 & 0 & 0 & 0 & 0 & 0 & 0 & \frac{-1}{Cs\_R} & \frac{-R_{b\_R}}{Jr\_R} & \frac{k_8}{Ie\_R} & \\ 0 & 0 & 0 & 0 & 0 & 0 & 0 & 0 & 0 & \frac{-k_8}{Jr\_R} & \frac{-R_{e\_R}}{Ie\_R} & \end{bmatrix}$$

$$y = [C]\,x \qquad (5)$$

$$\begin{bmatrix} iL \\ \tau L \\ \omega mL \\ \omega wL \\ VCG \\ \theta CG \\ \omega wR \\ \omega mR \\ \tau R \\ iR \end{bmatrix} = \begin{bmatrix} i_2 \\ e_6 \\ f_8 \\ f_{13} \\ f_{22} \\ f_{25} \\ f_{33} \\ f_{39} \\ e_{40} \\ i_{44} \end{bmatrix} = \begin{bmatrix} \frac{1}{Ie\_L} & 0 & 0 & 0 & 0 & 0 & 0 & 0 \\ \frac{k1}{Jr\_L} & 0 & 0 & 0 & 0 & 0 & 0 & 0 \\ 0 & \frac{1}{Jr\_L} & 0 & 0 & 0 & 0 & 0 & 0 \\ 0 & 0 & \frac{1}{Jw\_L} & 0 & 0 & 0 & 0 & 0 \\ 0 & 0 & 0 & \frac{1}{Mt} & 0 & 0 & 0 & 0 \\ 0 & 0 & 0 & 0 & \frac{1}{Jt} & 0 & 0 & 0 \\ 0 & 0 & 0 & 0 & 0 & \frac{1}{Jw\_R} & 0 & 0 \\ 0 & 0 & 0 & 0 & 0 & 0 & \frac{1}{Jr\_R} & 0 \\ 0 & 0 & 0 & 0 & 0 & 0 & 0 & \frac{k8}{Jr\_R} \\ 0 & 0 & 0 & 0 & 0 & 0 & 0 & \frac{1}{Ie\_R} \end{bmatrix} \begin{bmatrix} p_2 \\ p_6 \\ p_{13} \\ p_{22} \\ p_{25} \\ p_{33} \\ p_{40} \\ p_{44} \end{bmatrix}$$

3.4. Simulation

Illustrated in figure 7 are some of the system outputs observed during motion in a space of 20x10m^2. The system was simulated for 45s with a profile of step input signals applied on the electric motor terminals ranging from 0 to24V, with maximum value resulting into a lateral velocity of 1.8m/s, and eventually brought to stationery position at t=36.

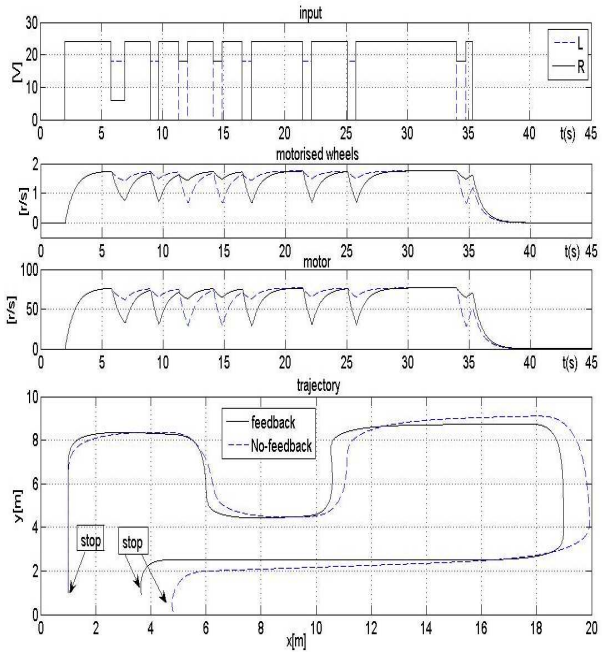

Figure 7: Mechatronic drive module simulation results

In all the graphs, the solid and dashed lines show the right and left side dynamics respectively. We can visualise that angular speeds of both the motors and wheels, follow the input profile. Rotation at the centre of mass was observed by an altering "rotation" signal (not shown). The predetermined trajectory is depicted on the lower graph with the system operating in both open and closed-loop control.

4. MODULAR DRIVEN MANUAL WHEELCHAIR

4.1. Test bed description

Ultimately, illustrated on figure 8 is the top view of an MDMW system model. The module introduces two more wheels on the existing four wheels of MPW. The module is assumed to be coupled on the same axes with the rear manual wheels as show below. *Lw/2* represents the width of MPW from centre of rotation to the centre of rear wheel. The BG and some simulations are shown in the next sections

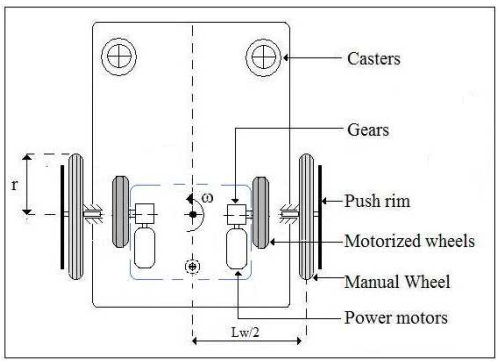

Figure 8: MDMW system

4.2. Bong Graph model

Bond graphs are based on energy exchange, and Figure 9 gives an illustration on how energy is transferred and exchanged from the voltage inputs to the MPW structure. This allows observation of different dynamic information and the system behaviour. The kinetic energy generated by the module is transmitted mechanically to the MPW system. In figure 9, the parameters *Mt and Jt* represent the translational and rotational inertia of the entire systems.

With the MDM serving as source of kinetic energy to the wheelchair system, the manual wheels of the MPW are now considered as passive. This introduces the unpreffered *derivative causality* at the manual wheels rotational inertia. The motorised and manual wheels angular velocities are observed. The following section gives the results obtained.

4.3. Simulation results

In order to observe and compare whether the MDM propels the MPW successfully, we used the same predetermined trajectory and profile of step input voltage signals (used on MDM) to the combined system. The results obtained are shown in figure 10. With more weight on the MDMW and operated in open loop control, the system displaced for 15m in 45sec instead of 32m.

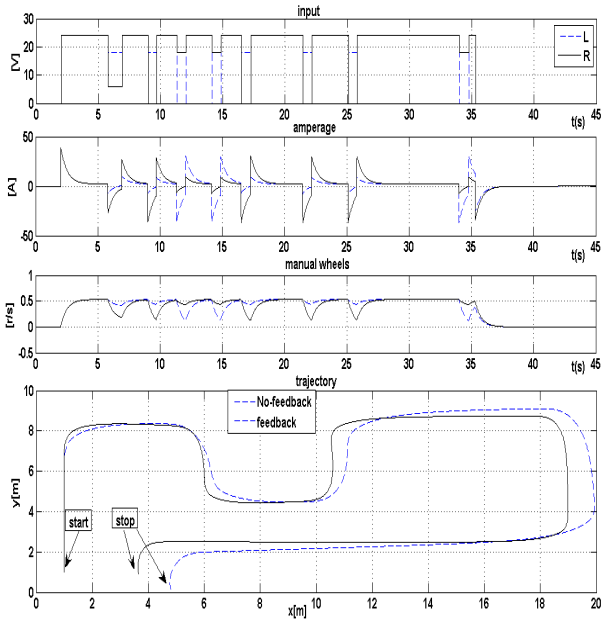

Figure 10: Modular Driven Manual Wheelchair simulation results

A local feedback from the motor's angular velocity including the PI controller was employed. Coupling stiffness increased. The system reaching the predetermined trajectory in the exact time; however more amperage consumption was noticed due to high propulsion torque required to withstand the increased translational inertia.

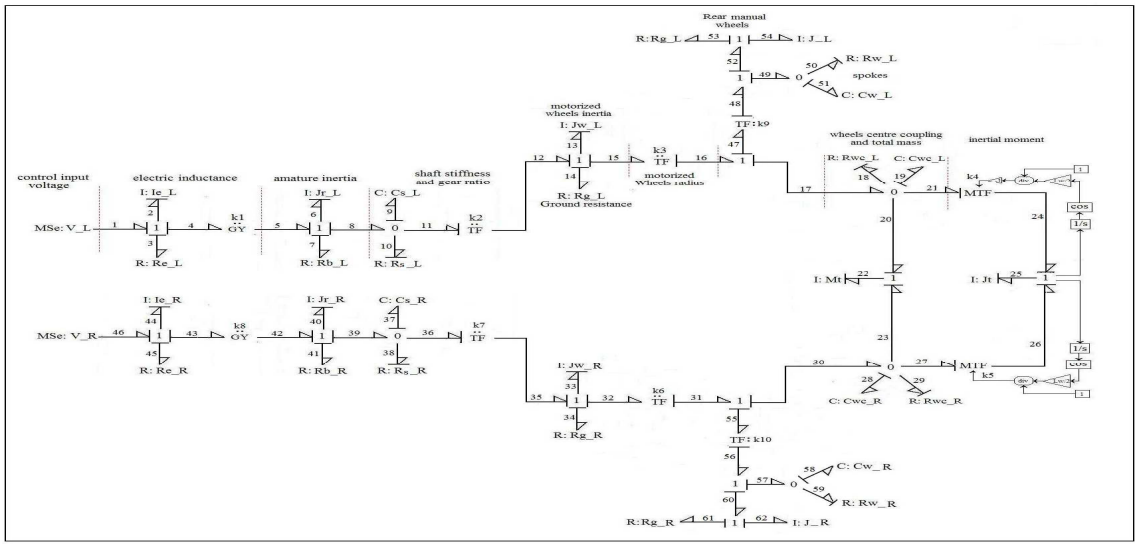

Figure 9: MDM attached to the MPW system

5. CONCLUSION AND FURTHER STUDIES

In this paper we have presented the Bond Graph modelling, analysis and simulation work of a mechatronic drive module and its coupling to the ordinary manual propelled wheelchair. The method was employed to study the different substructures and the linked systems. The models were simulated on a realistic area and can be used as a tutorial for the Bond graph studies of mobile systems.

In the near future, we will extend this work to the study of a battery and the charging system. These models will be utilised to design and implement real-time controller that can be implemented on digital control loops. We also plan to build a prototype that will be used to test the reliability functioning and to improve power efficiency management of this system.

Table: System Parameters

Parameter	Description	Value
Manual Propelled Wheelchair (MPW)		
MSe:τ	rear wheel propulsion torque (*Nm*)	*12*
Jw	rear wheel rotational inertia(*kgm²*)	*0.005*
Mt	systems mass *(kg)*	*100*
Jt	systems inertial moment *(kgm²)*	*64*
Rg	wheel to ground resistance	*0.006*
Cw	wheel spoke spring	*0.0021*
Rw	wheel spoke damper	*12*
r	rear wheel radius*(m)*	*0.30226*
Lw	wheelchair width*(m)*	*0.8*
Mechatronic Drive Module (MDM)		
Ie	electric motor inductance *(H)*	*0.0033*
Re	electric motor resistance *(Ω)*	*0.9*
Jr	rotor rotational inertia*(kgm²)*	*0.078*
Rb	motor bearing damper*(Nm-s/rad)*	*0.008*
Mt	module mass*(kg)*	*30*
Jt	module inertial moment*(kgm²)*	*7.5*
Lw	module width*(m)*	*0.6*
Cs	motor to gear shaft torsion*(Nm/rad)*	*0.00237*
Rs	motor to gear shaft damper	*11*
k_1, k_8	motor torque constant*(Nm/A)*	*0.288*
k_2, k_7	mechanical gear ration	*0.18*
k_3, k_6	motorized wheels radius*(m)*	*0.127*
MSe:L	control input voltage*(V)*	*24*
Modular Driven Manual Wheelchair (MDMW)		
J	manual wheels *(kgm²)*	*0.005*
K_9, k_{10}	manual wheels radius*(m)*	*0.30226*
Mt	combined systems total mass*(kg)*	*130*
Jt	total inertial moment*(kgm²)*	*83.5*

REFERENCES

Wheelchairnet.org, Discussion preparation for manual wheelchair propulsion. *Rehabilitation Engineering research Centre on Technology Transfer Federal Laboratory Consortium*: Mid Atlantic Region. http://www.wheelchairnet.org/ [15-04-2010].

Karnopp, D.C., Margolis, D.L., Rosenberg, R.C., 2006. *System dynamics: A Unified Approach 4th edition*. Wiley Publications.

Dauphin-Tanguy, G., 2000. *Les Bond Graphs*. Hermes edition .

Fakri, A., Rocaries, F., Carriere, A., 1997. A Simple method for the conversion of bond graph models in presentation by block diagrams. *International Conference on Bond Graph Modelling and Simulatio*, pp15-19. *ICBGM'97*. Phoenix Arizona.

Abel, E.N., Frank, T.G., 1991. *The design of an attendant propelled wheelchair*. prosthetic and orthotic inserthond.

Klancar, B., Zupancic, R., Karba, R., 2007. *Modelling and simulation of a group of mobile Robots*. Faculty of Electrical Engineering, University of Ljubljana, 1000 Ljubljana. Slovenia.

Gawthrop, P.J., Bevan, G.P., 2007. *TA Tutorial Introduction for Control Engineers. Bond Graph modeling*. IEEE Control Magazine, 24-45.

Authors Index